estec

European Space Research and
Technology Centre Keplerlaan 1
2201 AZ Noordwijk
The Netherlands

T +31 (0)71 565 6565
F +31 (0)71 565 6040 www.esa.int

Copernicus Sentinel-3 Next Generation Topography (S3NG-T) Mission Requirements Document (MRD)

Prepared by	**Earth and Mission Science Division**
Reference	**ESA-EOPSM-S3NG-MRD-3821**
Issue/Revision	**1.0**
Date of Issue	**15th October 2025**
Status	**Issued**
Document type	**Mission Requirements Document (MRD)**
Distribution	**ESA Unclassified – For Official Use**

Recommended Citation:

ESA (2025). Copernicus Sentinel-3 Next Generation Topography (S3NG-T) Mission Requirements Document (MRD), Version 1.0, 15th October 2025. European Space Agency, Noordwijk, The Netherlands, ESA-EOPSM-S3NG-MRD-3821, 327 pp.
DOI: https://doi.org/10.5281/zenodo.17454428

Approval

Title: Copernicus Sentinel-3 Next Generation Topography (S3NG-T) Mission Requirements Document		
Issue Number: 1	**Revision**: 0	**Date:** 15/10/2025

Author: Alejandro Egido (EOP-SME, Mission Scientist Phase B1/B2/C/D), Craig Donlon (previously EOP-SME, currently EOP-FA, Mission Scientist Phase 0/A) and members of the Mission Advisory Group (MAG); Remko Scharroo, Michaël Ablain, Lotfi Aouf, Sylvain Biancamaria, Bertrand Chapron, Luciana Fenoglio, Joana Fernandes, Jesús Gómez-Enri, Christine Gommenginger, Johny Johannesen, Rosemary Morrow, Estelle Obligis, Marcello Passaro, Louise Sandberg Sørensen, Andrew Saulter, Ernst Schrama, Clement Ubelmann, Rosemary Willatt.

Approved By	Signature	Date of Approval
Thorsten Fehr (EOP-SM) Head/Earth and Mission Science Division		Digitally signed by Thorsten Fehr Date: 2025.10.26 12:34:47 +01'00'
Pierrik Vuilleumier (EOP-PY) Project Manager S3NG-T		Pierrik Vuilleumier 2025.10.22 10:47:31 -07'00'
Betlem Rosich Tell (EOP-GC) Head Copernicus Ground Segment and Data Management Division	Betlem Rosich	Digitally signed by Betlem Rosich Date: 2025.10.23 17:03:13 +02'00'
Pierre Potin (EOP-E) Head of Copernicus Space Office	Pierre Potin	Digitally signed by Pierre Potin Date: 2025.10.23 09:47:11 +02'00'
Pier Bargellini (EOP-PZ) Copernicus Space Segment Programme Manager		Digitally signed by Pier Bargellini Date: 2025.10.23 09:46:26 +01'00'

Authorised By	Signature	Date of Authorisation
Rune Floberghagen (EOP-S) Climate Action, Sustainability & Science Department		Digitally signed by Rune Floberghagen Date: 2025.10.24 10:07:06 +02'00'

Change Log

Title: Copernicus Sentinel-3 Next Generation Topography (S3NG-T) Mission Requirements Document

Reason for change	Issue.	Revision	Date
Original document based on Phase-0 CDF activities.	0	1	02/03/2021
Draft version issued to S3NG-T MAG for review.	0	2	13/03/2021
Consolidation based on S3NG-T MAG formal review and discussions at MAG #1 meeting, updates from Phase A/B1 Study team, Phase A/B1 PreTEB feedback and harmonisation with draft System Requirements Document (SRD).	0	3	15/04/2021
Updated for Phase A/B1 KO based on Bidder clarifications, internal discussions and MAG inputs.	0	4	18/03/2022
Updated with corrections prior to PCR	0	4.1	14/06/2022
Updated with post PCR conclusions	0	4.2	27/09/2022
Further clarifications for Phase B1.	0	4.3	20/10/2022
Update based on Phase A/B1 outcomes, change in requirements agreed at MAG#09.	0	5	11/12/2024
Requirements consolidation with MAG post Phase A/B1.	0	6	22/04/2025
Requirements consolidation with MAG post Phase A/B1.	0	7	18/06/2025
Requirements consolidation for Phase B2/C/D ITT; Internal ESA EOP-P, EOP-G review; Document preparation for signature; first stable version.	1	0	15/10/2025

Change Record

Issue: 0	**Revision:** 4.3		
Reason for change	**Date**	**Pages**	**Paragraph(s)**
MRD-0590 revied by MAG to clarify nadir altimeter and swath altimeter characteristics for metric computations based on clarifications requested by OHB/CLS.MRD	12/06/22		Sec. 5.8.2
MRD-0960 corrected to SPE of 0.01deg (not 0.1deg) following discussion with F. Boy.	12/06/22		Sec. 6.1
MRD-1010 Note 10 added regarding ITU and Ka-band allocations with respect to AMR-C. Channel frequencies updated to be in line with ITU allocations based on inputs from Y. Soldo	12/06/22		Sec. 6.2
MRD-1040 and Table 6.2-1 Channel frequencies updated to be in line with ITU allocations based on inputs from Y. Soldo.	12/06/22		Sec. 6.2
Updated Sec. 6.2.1 with better background information and references for MRAD on-board and on-ground RFI detection on Study Manager Request.	27/07/2022		Sec. 6.2.1
Based on clarifications requested by Industry on 20/10/2022, MRD-0360 added “For the handover from S3 to S3NGT…” commensurate with MRD-0370 and clarified in Note 6 that this requirement is largely directed to the nadir altimetry part of the S3NG-T. Note 5 added in MRD-0370 to clarify the same issue for concepts other than nadir altimetry that might fly in alternative orbits.	20/10/2022		Sec 5.5.2
Based on clarifications requested by Industry on 20/10/2022, MRD-0620 and MRD-1650 updated with notes regarding the application of on-board processing and availability of full PRF data on ground for nadir altimeters	20/10/2022		Sec. 6.1 and Sec. 7.5.1.2
Based on clarifications requested by Industry on 20/10/2022, MRD-1255 added to clarify content of Level 1a nadir altimeter data. MRD-0650 Note 6 added to ensure full PRF data with no RMC processing is provided at L1a from nadir altimetry.	20/10/2022		Sec. 7.4.2 and Sec. 6.1
Based on clarifications requested by Industry on 20/10/2022, MRD-0900 clarified to 1 minute of raw data per orbit	20/10/2022		Sec 6.1
Corrected filename error for southern hemisphere sea ice mask in MRD-0070	22/10/2022		Sec. 5.1.3

Issue: 0	**Revision:** 5		
Reason for change	**Date**	**Pages**	**Paragraph(s)**
Updated Chapter 2 with current programmatic information.	11/12/24		Chapter 2
Modified and updated text in Chapter 3, with updated references and SWOT inflight results.	11/12/24		Chapter 3
MRD-0010, Requirement deleted; moved to definition section.	11/12/24		Sec. 5.0
MRD-0020, requirement deleted, specification beyond S3NGT mission scope. This requirement assumes a L3 product type, which is out of the scope of this MRD.	11/12/24		Sec. 5.0
Update of Measurement Mask names: Marine and Land Mask → Marine and Coastal Mask Hydrology Target Mask → Inland Water Mask Sea Ice Edge Mask → Sea Ice Mask Update of measurements mask definitions and specifications, MRD-0030 – MRD-0080	11/12/24		Sec. 5.1 – 5.4
Deleted requirements; redundant: MRD-200 – MRD-260	11/12/24		Sec. 5.3
MRD-340, updated commissioning phase duration to 9 months.	11/12/24		Sec. 5.5
MRD-370: modified requirement on hand-over of mission to offset uncertainty values; deleted all notes related to tandem operation phase.	11/12/24		Sec. 5.5
MRD-530: introduction of Sentinel-3 orbit specification, for S3NG-T to follow Sentinel-3 orbit ground track.	11/12/24		Sec. 5.6
MRD-560, -570: deleted, not applicable based on MRD-530	11/12/24		Sec. 5.6
Section 5.7 moved to products section. Requirements MRD-470 – MRD-520 merged with MRD-1220.	11/12/24		Sec. 5.7
Section 5.8, paragraphs on orbit selection moved to Appendices.	11/12/24		Sec. 5.8
Section 5.9.2, paragraphs on ocean sampling moved to Appendices.	11/12/24		Sec. 5.9.2
Req. MRD-590, removed notes on SWOT and other orbit considerations.	11/12/24		Sec. 5.9.2
Sec. 6.1, removed text justifying Ka-band nadir altimeter as baseline continuity for the mission; MRD-610, modified to specify Ku-band nadir looking SAR altimeter as baseline continuity. MRD-620, requirement deleted; redundant with MRD-1650.	11/12/24		Sec. 6.1
MRD-860, deleted, too low level requirement.	11/12/24		Sec. 6.1

MRD-870, rewording for clarity; notes 2 and 3 deleted as superfluous.	11/12/24		Sec. 6.1
MRD-890, -900, modified text for clarification; RAW measurements → complex altimeter echoes. Note on acquisition mask, moved to Appendix.	11/12/24		Sec. 6.1
MRD-940, -950, -990 (not applicable to SSO), -1000 (redundant with MRD-0870): deleted requirements, overspecification at MRD level.	11/12/24		Sec. 6.1
MRD-1010 consolidated frequency bands after phase A/B1.	11/12/24		Sec. 6.2
Requirements MRD-1030, -1050, -1060, -1120, -1130, -1150, -1150, -1170, and accompanying text, deleted, overspecification at MRD level; flowed down to MWR requirements in SSRD.	11/12/24		
Requirements MRD-1190, requirement deleted, overspecification, not needed by users.	11/12/24		Sec. 6.2.1
Text moved to definition section	11/12/24		Sec. 7.1
Created MRD-1220 requirement, to specify latency and availability for all data products.	11/12/24		Sec. 7.1
MRD-1320, requirement deleted, L1b specification beyond the scope of MRD, will come at later phases as part of SRD and/or GSRD.	11/12/24		Sec. 7.4
Table 7.5-1, removed TSCE and TSWE from required data prodcuts, no heritage from S3.	11/12/24		Sec. 7.5
MRD-1445, requirement created to ensure consistency between data products and operational modes.	11/12/24		Sec. 7.5
MRD-1530, requirement deleted, multimission requirement beyond the Level 2 scope of this MRD.	11/12/24		Sec. 7.5.1
MRD-1540, change of specification for drift requirement.	11/12/24		Sec. 7.5.1
MRD-1610, requirement merged with MRD-1590 (reworded).	11/12/24		Sec. 7.5.1
MRD-1630, -1640, merged with MRD-1620 (reworded).	11/12/24		Sec. 7.5.1
MRD-1700, -1710, merged with MRD-1690 (reworded).	11/12/24		Sec. 7.5.1
MRD-1760, updated specification for inland waters based on phase A/B1 results, and latest research.	11/12/24		Sec. 7.5.1
MRD-1765, reworded, removed quatitative value due to difficulty for verification.	11/12/24		Sec. 7.5.2
MRD-1790, merged with MRD-1820	11/12/24		Sec. 7.5.3
MRD-1800, requirement deleted; overspecification at MRD level.	11/12/24		Sec. 7.5.3

MRD-1810, requirement deleted. Duplicate of MRD-1850.	11/12/24		Sec. 7.5.3
MRD-1820, reworded, changed latency to NRT6H.	11/12/24		Sec. 7.5.3
MRD-1830, reworded, consolidated.	11/12/24		Sec. 7.5.3
MRD-1840, requirement deleted, merged with MRD-1465.	11/12/24		Sec. 7.5.3
MRD-1850, requirement reworded, consolidated.	11/12/24		Sec. 7.5.3
MRD-1880 to MRD-1920, and MRD-1950, moved to MRAD section as secondary mission objectives;	11/12/24		Sec. 7.5.3
MRD-1930, -1940, requirement deleted, no heritage nor traceability for requirements for the S3NGT mission.	11/12/24		Sec. 7.5.3
MRD-1960, -1970 consolidated based on MAG#09 discussions.	11/12/24		Sec. 7.5.3
MRD-1980, -1990, -2000, -2031, -2032, -2033, changed specification from goal to secondary mission objective.	11/12/24		Sec. 7.5.4
MRD-2030, requirement deleted, not a requirement.	11/12/24		Sec. 7.5.4
MRD-2031 to MRD-2034, created, from MRD-1880 to MRD-1920, and MRD-1950, as secondary mission objectives.	11/12/24		Sec. 7.5.4
MRD-2090, requirement merged with MRD-2100.	11/12/24		Sec. 7.6.1
MRD-2150, -2160, -2170, -2180, requirements deleted, not mission requirements.	11/12/24		Sec. 8.1
MRD-2250, requirement deleted, not mission requirement.	11/12/24		Sec. 7.6.1

Issue: 0	**Revision:** 6		
Reason for change	**Date**	**Pages**	**Paragraph(s)**
Modified and updated text.	22/04/25		Chapter 3
MRD-0030, modified to include large lakes.	09/04/25		Sec. 5.1.1
MRD-0070, update of Sea Ice Mask. MRD-0075, created to specify re-evaluation of SIM.	09/04/25		Sec. 5.1.3
MRD-0170, deleted requirement, not baseline continuity for S3, no traceability for this requirement.	09/04/25		
MRD-0370, -380, removed TBC from requirement, confirmation of values through science study.	09/04/25		
MRD-385, created to specify mission offset uncertainties for the key geophysical parameters over ocean.	09/04/25		

MRD-400, -430, deleted, overspecification at MRD level.	09/04/25		
MRD-880, deleted, redundant, merged with MRD-0050	09/04/25		
MRD-900, requirement reworded, notes providing acquisition mask example moved to annex.	09/04/25		
MRD-0910, removed. Redundant with MRD-0930.	09/04/25		
MRD-1070, reworded, simplified, Note 1 deleted.	09/04/25		
RFI text deleted.	09/04/25		Sec. 6.1.2
MRD-1270, deleted, now covered by MRD-1335.	09/04/25		Sec. 7.4.2
MRD-1280, deleted, overspecification at MRD level.	09/04/25		Sec. 7.4.2
MRD-1335, created.	09/04/25		Sec. 7.5
MRD-1360, removed reference to product family. MRD-1370 – MRD-1400, deleted, removed specification for products family.	09/04/25		Sec. 7.5
MRD-1465 – MRD 1510, MRD-1540 reworded for clarity.	09/04/25		Sec. 7.5.1
MRD-1520, merged with MRD-1465.	09/04/25		Sec. 7.5.1
Reworded MRD-1540 in terms of stability uncertainty.	09/04/25		Sec. 7.5.1
MRD-1820, added Note 7, to specify swath altimeter measurements.	09/04/25		Sec. 7.5.3
MRD-1860, modified as a secondary mission objective.	09/04/25		Sec. 7.5.3
MRD-2120, MRD-2220, merged and moved to MRD-2085.	09/04/25		Sec. 7.6, 8.2
MRD-2230, -2240, requirement deleted, not mission requirements.	09/04/25		Sec. 8.2

Issue: 0	**Revision:** 7		
Reason for change	**Date**	**Pages**	**Paragraph(s)**
Modified and updated text.	18/06/25		Chapter 2, 3
MRD-0030, modified to include large lakes.	18/06/25		Sec. 5.1.1
MRD-0070, update of Sea Ice Mask.	18/06/25		Sec. 5.1.3
MRD-0450, removed “full resolution”, overspecfication, not according to mission requirements. Removed Note 1.	18/06/25		Sec. 5.5.1

MRD-0530, deleted to allow some flexibility in final orbit selection.	18/06/25		Sec. 5.6
MRD-0560,-0570, -0580, reinstated.	18/06/25		Sec. 5.6
MRD-0650, Note 6 deleted, full PRF not needed, as shown in Sentinel-6 design.	18/06/25		Sec. 6.1
MRD-710, adjusted values to reflect baseline continuity. MRD-0750, Note 4-6 deleted, transponders cannot verify the requirement MRD-0760, changed specification of sigma-0, to be according a certaint wind speed value. Included reference to GPM data. MRD-780, updated specification based on current observations from Sentinel-6 and SARAL/AltiKa.	18/06/25		Sec. 6.1
MRD-0790, -0800, updated sigma-0 specification.	18/06/25		Sec. 6.1
MRD-1040, requirement deleted, overspefication at MRD level, flowed down to MWR specs in SSRD.	18/06/25		Sec. 6.2
MRD-1230, refine specification for data files.	18/06/25		Sec. 7.2
Table 7.5-1 updated, removed TBC values.	18/06/25		Sec. 7.5
MRD-1540, updated stability requirement in terms of altimeter range drift.	18/06/25		Sec. 7.5.1
MRD-1550, -1560, consolidated values for requirement based on Phase A/B1 and science studies.	18/06/25		Sec. 7.5.1

Issue: 1	**Revision:** 0		
Reason for change	**Date**	**Pages**	**Paragraph(s)**
Document clean-up, preparation for signature.	10/07/2025		All chapters
Updated the approval and authorisation signatures page according to QMS document MMAN-2050-Issue-5-0, for Mission Implementation Phase.	10/09/2025		Approval page.
Modified and updated text; editorial changes.	10/09/2025		All chapters
Included not regarding correctness and consistency of information at the time of writing.	10/09/2025		Chapter 2, 3
MRD-0040, MRD-0050, notes reworded for clarity.	10/09/2025		Chapter 5
MRD-0420, requirement deleted, not relevant to MRD.	10/09/2025		Section 5.4
MRD-0460, requirement deleted, space segment implementation, beyond MRD requirements.	10/09/2025		Section 5.5.4

MRD-540, -550, -560, -570, requirement notes simplified.	10/09/2025		Section 5.6
MRD-0590, reference to S6NG removed from requirement.	10/09/2025		Section 5.6
MRD-0980, requirement deleted.	10/09/2025		Section 6.1
MRD-1100, requirement reworded.	10/09/2025		Section 6.2
Section 7.2 and Requirement MRD-1230 reworded to avoid overspecification of ground segment implementation.	15/10/2025		Section 7.2
MRD-2060, -2070, -2080, -2085, -2110, -2130, -2150, -2160, -2170, -2180, -2190, -2200, -2210, requirements deleted, these are related to ground segment implementation, hence out of the scope of MRD.	10/09/2025		Section 7.5, Section 7.6.
MRD-2050, -2090, -2100, reworded to avoid overspecification of ground segment.	15/10/2025		Section 7.5, Section 7.6.
Rewording to clarify traceability and verification of MRD requirements.	13/10/2025		Section 1.1.3
MRD-1440, MRD-1445, MRD-1740, reworded for clarity.	13/10/2025		Section 7.4
Section 8.1 deleted, as cal/val team specification is not relevant for MRD.	13/10/2025		Section 8.1
Section 8.2 moved to Appendix.	13/10/2025		Section 8.2

Distribution

Name/Organisational Unit		
ESTEC: T. Fehr (EOP-SM) C. Rossi (EOP-SME) S. Cheli (EOP) D. Gillieron(EOP-P) P. Bargellini (EOP-PZ) P. Vuilleumier (EOP-PY) J-D. Desjonqueres (EOP-PY) J. Rancano (EOP-PYE) M. Fornari (EOP-PYP)	J. Lambin (EOP-F) P. Martimort (EOP-FM) C. Donlon (EOP-FA) S. Bras, (EOP-PES) M. Pinot-Sole (EOP-PES) **ESRIN:** R. Floberghagen (EOP-S) N. Hanowski (EOP-G) B. Rosich (EOP-GC) P. Goryl (EOP-GMQ) P. Potin (EOP-E) J. Bouffard (EOP-GM)	**European Commission:** M. Facchini (DG-DEFIS) **AT:** **Members of the S3NG-T MAG**

Members of the S3NG-T Mission Advisory Group (MAG)

Mr. M. Ablain	Magellium, France
Dr. L. Aouf	Meteo France, Toulouse, France
Dr. S. Biancamaria	LEGOS, Toulouse, France
Dr. B. Chapron	IFEMER, Brest France
Dr. L. Fenoglio	University of Bonn, Germany
Dr. J. Fernandes	University of Porto, Portugal
Dr. J. Gómez-Enri	University of Cadiz, Spain
Dr. C. Gommenginger	National Oceanography Centre, Southampton, United Kingdom
Prof. J. Johannesen	Nansen Centre, Bergen, Norway
Dr. R. Morrow	LEGOS, Toulouse, France
Dr. M. Passaro	Technical University of Munich, Germany
Dr. L. Sandberg Sørensen	DTU, Copenhagen, Denmark
Dr. A. Saulter	MetOffice, Exeter, United Kingdom
Prof. E. Schrama	TU Delft, The Netherlands
Dr. C. Ubelmann	Ocean Next, Grenoble, France
Dr. E. Obligis	EUMETSAT, Darmstadt, Germany
Dr. R. Willatt	University College London, United Kingdom

European Commission Appointed Representatives

Dr. P-Y. LeTraon	CMEMS entrusted entity representative, Mercator Ocean, France
Dr. J. Nicolas	C3S entrusted entity representative, ECMWF, United Kingdom
Dr. A. Cacciari	European Commission, Policy Officer, DG.DEFIS, Brussels Belgium

Executive Officers

Dr. A. Egido	ESA/ESTEC, Noordwijk, The Netherlands
Dr. R. Scharroo	EUMETSAT, Darmstadt, Germany

TABLE OF CONTENTS

1 INTRODUCTION

This document is the formal Mission Requirements Document (MRD) for the *Sentinel-3 Next Generation Topography* (S3NG-T) Mission.

The S3NG-T Copernicus Extension Mission provides enhanced continuity of the Copernicus Sentinel-3 radar altimetry component. It is part of the evolution of the current Copernicus Space Component (CSC) capabilities described in the CSC Long Term Scenario (ESA, 2025) to address the User Requirements expressed by the European Commission (EC).

The S3NG-T Mission Requirements Document (MRD) was an input to the European Space Agency (ESA) preparatory phase (Phase A/B1) study activities started in 2021, and to the implementation phase (Phase B2/C/D), to be kicked off tentatively Q1 2026. It is managed by the S3NG-T Mission Scientist according to the ESA Quality Management System (QMS) procedure for Mission Requirements Management (QMS-PR-MMAN-2050-EOP), and Procedure for Mission Implementation and Operations (QMS-PR-MMAN-2070-EOP).

1.1 Document and Requirement Conventions

1.1.1 Terms

The term “**To Be Confirmed**” (TBC) will be used in combination with the numerical definition of some performance parameters, the final value of which may be changed by the Agency as a result of the Definition Study engineering work.

The term “**To Be Determined**” (TBD) will be used for the numerical definition of a parameter at a later stage. Engineering assumptions shall be made in consultation with the Agency for interim numerical definitions.

Requirements marked as To Be Defined (TBD) or To Be Confirmed (TBC) indicate open issues and will be confirmed by the Mission Advisory Group (MAG) or by ESA in the course of Phase A/B1 or future Mission Phases B2/C/D/E1.

The terms “**shall**” and “**will**” denote mandatory requirements.

The term “**goal**” denotes a desirable extension to a requirement even though a commitment to such performance cannot be confirmed or verified.

The terms “**should**” and “**may**” denote requirements whose implementation shall be discussed between the Contractor and the Agency.

The term “**Note**” denotes additional information providing useful background information to a requirement.

Following the advice of the European Commission (ESA-EOPSM-EXG-MOM-3811 December 2020), definitions for the meaning of “Continuity” and “Enhanced Continuity” in terms of NG missions were agreed using three ‘levels’ as follows:

1. **Baseline continuity:** This is the minimum definition for an NG-Mission. Baseline continuity products guarantee the continuity of Level 2 products with the same coverage, revisit, performance, sampling, delivery timeliness of existing

topography parameters (e.g. SSH, Hs, Sigma0, U10 etc.). Baseline continuity is derived directly from **in-flight** performance.

2. **Enhanced continuity:** Level 2 products that meet baseline continuity **plus enhanced** revisit and effective resolution (i.e. wavelength) and/or coverage, and/or performance, and/or timeliness of existing topography parameters (e.g. SSH, Hs, Sigma0, U10, etc.) to address Copernicus User Needs.
3. **New products:** a new Level 2 product to address Copernicus User Needs providing considerable enhancement over the baseline continuity (e.g. (Directional) Wave Spectra, sea surface height gradients and river gradients. Total Surface Current Velocity measurements are considered out of scope by the European Commission).

Following this agreement, requirements for the S3NG-T are set using the following generic form:

Requirement (the verb 'shall'): baseline continuity derived from in-flight performance of the Sentinel-3 topography mission as articulated in Table 2.1.3.1.

Enhanced (the term 'goal'): specifies enhanced continuity or new products to address European Commission User Needs where goal may include a variety of product and performance aspects.

1.1.2 Requirement Numbering

Within this MRD, requirements are identified by a unique alphanumeric code with the following format:

MRD-DDDD

The digits DDDD are requirements numbers. The sequence of these numbers may contain gaps and is independent for each combination of MRD-DDDD. Some requirements are supported by explanatory comments, which are in a different style.

Assumptions are identified by a unique alphanumeric code with the following format:

ASM-DDD

where DDD follows an identical form to requirements numbering. Mission assumptions provide information on elements that are reasonably assumed to be available but outside the scope of this MRD.

Within this MRD, European Commission User Needs are identified by a unique alphanumeric code with the following format:

S3NG-T-UN-DDD

The digits DDD are requirements numbers. The sequence of these numbers may contain gaps and is independent for each combination of S3NG-T-UN-DDD. Some requirements are supported by explanatory comments, which are in a different style.

Within this MRD, European Commission Product Specification Needs are identified by a unique alphanumeric code with the following format:

S3NG-T-UN-PDD

The digits DD are requirements numbers. The sequence of these numbers may contain gaps and is independent for each combination of S3NG-T-PR-PDD. Some requirements are supported by explanatory comments, which are in a different style.

Within this MRD, Mission Objectives are split into:

Primary Objectives (PRI-OBJ-XX) that are mandatory for the success of the mission and

Secondary Objectives (SEC-OBJ-XX) that shall not drive the system design.

Paragraphs without such annotation provide information.

1.1.3 Requirements and Guidelines

Compliance with the requirements specified within this document is necessary for the success of the mission. Harmonisation of the definition of these requirements and the technical design of the mission is necessary to ensure that the mission, as eventually implemented, will be capable of compliance with the requirements.

Traceability to the requirements specified in the MRD shall be provided via suitable flow-down to lower-level specifications. Verification of MRD requirements will be achieved through verification of flowed-down requirements. The requirements in the MRD include the use of Notes that provide guidance or limitations.

Unless otherwise stated, all quantities in this MRD are specified as Total Standard Uncertainty (TSU) 1-sigma zero mean based on a Gaussian (normal) probability distribution.

2 BACKGROUND AND JUSTIFICATION

This chapter provides background information supporting the definition and justification of the MRD requirements. Please note that the information reflects the status at the time of writing (July 2025) and may not be fully up to date or consistent with the latest developments in the Copernicus Programme or the S3 NGT mission design.

Copernicus [http://www.copernicus.eu/] is a European system for monitoring the Earth in support of European policy. It includes Earth Observation satellites (notably the Sentinel series developed by ESA), ground-based measurements and, services to processes data to provide users with reliable and up-to-date information through a set of Copernicus operational services related to environmental and security issues. These include:

- Copernicus Marine Environmental Monitoring Service (CMEMS [http://marine.copernicus.eu]),
- Copernicus Land Monitoring Service (CLMS [http://land.copernicus.eu/]),
- Copernicus Atmospheric Monitoring Service (CAMS [https://atmosphere.copernicus.eu/]),
- Copernicus Security service (CMS, BS, SEA) [https://www.copernicus.eu/en/copernicus-services/security],
- Copernicus Climate Change Service (C3S) [http://climate.copernicus.eu] and,
- Copernicus emergency Service (EMS) [http://emergency.copernicus.eu].

Copernicus services provide critical information to support a wide range of applications, including environment protection, management of urban areas, regional and local planning, agriculture, forestry, fisheries, health, transport, climate change, sustainable development, civil protection and tourism. Copernicus satellite missions are designed to provide ‘upstream’ inputs to all Copernicus Services as systematic measurements of Earth’s oceans, land, ice and atmosphere to monitor and understand large-scale global dynamics. The core users and consumers of Copernicus services are policymakers and public authorities that need information to develop environmental legislation and policies or to take critical decisions in the event of an emergency, such as a natural disaster or a humanitarian crisis. The Copernicus programme is coordinated and managed by the European Commission. The development of the observation infrastructure is performed under the aegis of the European Space Agency (ESA) for the space component and of the European Environment Agency (EEA) and the Member States for a separate, but important, for the in-situ measurement component.

As set out in the ESA Program Board for Earth Observation (PBEO) paper (ESA/PB-EO(2017)31 Paris, 5 September 2017), the Copernicus Space Component (CSC) has been established as the largest and most proficient Earth Observation infrastructure in the world. With seven high-performance satellites in orbit and more than 200,000 registered Sentinel data users on the ESA/EC Copernicus data portal as well as numerous sophisticated operational services, the system has evolved at a rapid pace. In order to preserve the momentum in fulfilling user needs, the future evolution of the CSC needs to be initiated now in close cooperation with all stakeholders.

According to the Copernicus Regulation (EU Regulation No. 377/2014 dated 3 April 2014), ESA has been mandated by the EU Council and European Parliament to define *"the overall system architecture for the Copernicus space component and its evolution on the basis of user requirements, coordinated by the Commission"*. Following this rationale, ESA, in close interaction with the EC, EUMETSAT and Member States, has identified key components of a Long-Term Scenario. Evolution in the Copernicus Space Component (CSC) is taking place to meet priority user needs not addressed by the existing infrastructure, and to reinforce Copernicus services by providing new capability in the thematic domains of CO2 monitoring, polar monitoring, and agriculture/forestry monitoring. This evolution, embodied by six **Copernicus Sentinel Expansion Missions**, is synergetic with the enhanced continuity of services being targeted by the parallel development of the **Next Generation of Sentinels**.

In the context of Satellite Altimetry, it is recognised that this capability is a fundamental tool for the European Copernicus services providing measurements over the global ocean and, increasingly in the coastal zones and inland waters. Based on sustained investments started in the 1980's, Europe has gained a leading role in this domain via a long series of missions (ERS-1/-2 (e.g. Francis, 1984), TOPEX/Poseidon (Fu et al., 1994)), the Jason series (e.g. Lambin et al., 2010; Vaze et al., 2010), Envisat Radar Altimeter 2 (e.g. Zelli, 1999) CryoSat-2 (Wingham et al., 2006, Drinkwater et al, 2006) and, as part of the Copernicus system, Sentinel-3 (Donlon et al., 2011, 2016) and Sentinel-6 (Donlon et al., 2021). Currently, the topographic system is built around three observation components: sun-synchronous orbit, mid-inclination tidal-free orbit and polar orbit. A gap of sun-synchronous orbit data was experienced after the loss of Envisat in 2012 (compensated by the extensive use of CryoSat-2 over the oceans).

Europe, through the Copernicus Programme, is guaranteeing the medium/long-term continuity of both dense ground track sampling (currently sun-synchronous) and mid-inclination altimetry reference orbits via, respectively, Sentinel-3 (initiated in the Global Monitoring for Environment and Security (GMES) era, e.g. Aguirre et al., 2009) and Sentinel-6, the latter in cooperation with the US.

The Copernicus polaR Ice and Snow Topography ALtimeter mission (CRISTAL), (e.g. Kern et al., 2020), one of the Copernicus Sentinel Expansion Mission for the evolution of the current CSC, will guarantee continuity of the unique measurements of the ice-surface elevation change, successfully initiated by the CryoSat-2 mission. The aim of CRISTAL is to obtain high-resolution sea ice thickness and land ice elevation measurements and includes the capability to determine the properties of snow cover on ice so as to serve Copernicus' operational products and services of direct relevance to the polar zones.

The Sentinel-3 Next Generation Topography (S3NG-T) mission address the need for a timely extension of the current Sentinel-3 capability in terms of stability and continuity, while improving coverage, temporal revisit time, and quality of products and services.

2.1 Copernicus Services

The Copernicus services transform this wealth of satellite and in situ data into value-added information by processing and analysing the data together with numerical forecasting and prediction models. Datasets stretching back for years and decades are made comparable and searchable, thus ensuring the monitoring of changes; patterns are examined and used to create better forecasts, for example, of the ocean and the atmosphere. Maps are created from imagery, features and anomalies are identified and statistical information is extracted. These value-adding activities are streamlined through six thematic streams of Copernicus services:

The Copernicus Marine Service (CMEMS http://marine.copernicus.eu**)** leads activities in this domain. It provides regular and systematic reference information on the physical and biogeochemical state, variability and dynamics of the ocean and marine ecosystems for the global ocean and the European regional seas. The provision of data on sea surface height, sea level rise, ocean circulation, winds and waves over the ocean and sea ice derived from satellite altimetry are all fundamental inputs to CMEMS activities. The most important satellite-based observation is sea surface height (SSH) from altimetry. The SSH is an integral of the ocean interior properties and is a strong constraint for inferring the 4D ocean circulation through data assimilation. CMEMS user needs clearly articulate that continuity of the present Copernicus satellite observing system should be first guaranteed as this is mandatory for maintaining the CMEMS service. This holds, in particular for the Sentinel 6 altimeter reference mission and the twin-satellite constellation of Sentinel 3 mission. However, CMEMS capability is evolving to higher resolution forecasting and prediction models and a fundamental user need is to constrain CMEMS models with new topography observations. Today the ocean is very under sampled even when using the Copernicus and all contributing nadir-pointing altimetry missions including Jason-2/3, ESA CryoSat-2, ISRO/CNES AltiKa, NSOAS HY-2A altimeters. Multiple nadir altimeters (at least 4 altimeters) are required (this was required 10 years ago) to adequately represent ocean eddies and associated currents in models. Much higher space/time resolution (≤50 km, ≤5 days (CMEMS, 2017)) will be needed in the post 2025 time period. The enhanced continuity of Sentinel-3 altimetry is fundamental to the future evolution of CMEMS that will critically rely on the enhanced sampling characteristics of S3NG-T.

Copernicus Global Land Monitoring component of the Land Service (CGLMS, http://land.copernicus.eu/**)** leads activities in this domain. It provides geographical information on land cover to a broad range of users in the field of environmental terrestrial applications. This includes land use, land cover characteristics and changes, vegetation state, water cycle and earth surface energy variables and the terrestrial cryosphere. The Water Surface Elevation (WSE) is defined as the height of surface of continental water bodies in meters above the geoid. As a secondary objective for the mission, Sentinel-3 altimetry provides estimates of WSE for water bodies located along the satellite's ground tracks as defined at https://www.altimetry-hydro.eu/. The quality of the measurements depends on the size of the water body and on the terrain and vegetation characteristics surrounding targets. Measurements of river and lake WSE derived from

S3NG-T are a fundamental input to CGLMS's component of the Land Service and are an essential element of S3NG-T.

The Copernicus Climate Change Service (C3S, http://climate.copernicus.eu**)** leads activities in the domain of climate change. It supports society by providing authoritative information about the past, present and future climate in Europe and the rest of the World. The C3S mission is to support adaptation and mitigation policies of the European Union by providing consistent and authoritative information about climate change. C3S users include scientists, consultants, planners and policy makers, the media and the public. C3S offers free and open access to climate data and tools based on the best available science. It maintains an active dialog with users and endeavours to help them meet their goals in dealing with the impacts of climate change. C3S relies on climate research carried out within the World Climate Research Programme (WCRP) and responds to user requirements defined by the Global Climate Observing System (GCOS). It provides an important resource to the Global Framework for Climate Services (GFCS). Changes in sea level rise, ocean circulation wind and waves, sea ice and ice sheets and river and lake WSE derived from satellite topography are all fundamental inputs to C3S activities. The S3NG-T mission will provide enhanced continuity of these topography measurements in the 2030-2050 timeframe.

The Copernicus service for Security (https://www.copernicus.eu/en/copernicus-services/security) leads activities in this domain. The European Boarder and coast Guard Agency (FRONTEX, https://frontex.europa.eu/) provides the border surveillance component of the Copernicus Security Service to support the EU's external border surveillance information exchange framework (EUROSUR) by providing near real time data over land and at sea around the EU's borders. In the area of maritime surveillance, the European Maritime Safety Agency (EMSA, http://www.emsa.europa.eu/copernicus.html) operates the maritime surveillance component of the Copernicus Security Service. Copernicus Sentinel 1, 2 and 3 together with additional satellite data are combined with other sources of maritime information to monitor maritime areas of interest The European Satellite Centre (EU SatCen) provides Support to External Action (SEA) within the Copernicus Security Service. SEA assists the EU in its operations, providing decision makers with geo-information on remote, difficult to access areas, where security issues are at stake. Sentinel-3 satellite altimetry provides measurements for a variety of applications relevant to the Copernicus Security applications including sea level rise, ocean circulation, wind and waves over the ocean, sea ice parameters and monitoring of the Arctic regions. S3NG-T must enhance continuity of these measurements and provide enhanced sampling in support of Copernicus Security Services.

Copernicus Emergency Management Service (CEMS, http://emergency.copernicus.eu/**)** leads activities in this domain. It provides all actors involved in the management of natural disasters, man-made emergency situations, and humanitarian crises with timely and accurate geo-spatial information derived from satellite remote sensing and completed by available in situ or open data sources. The Copernicus EMS consists of a mapping component and an early warning component.

The mapping component of the service (Copernicus EMS - Mapping) has a worldwide coverage based on satellite imagery implemented by the European Commission DG Joint Research Centre (JRC). Copernicus EMS - Mapping can support all phases of the emergency management cycle: preparedness, prevention, disaster risk reduction, emergency response and recovery. The early warning component of the Copernicus EMS includes the European Flood Awareness System (EFAS, which provides overviews on ongoing and forecasted floods in Europe up to 10 days in advance) and the European Drought Observatory (EDO, which provides drought-relevant information and early-warnings for Europe. Global Flood Awareness System (GloFAS), Global Wildfire Information System (GWIS) and Global Drought Observatory (GDO) are used at global level. Measurements of storm surge and river and lake WSE derived from S3NG-T are a fundamental input to CEMS and are an essential element of S3NG-T.

The Copernicus Atmospheric Monitoring Service (CAMS, https://atmosphere.copernicus.eu/**)** leads activities in this domain. It provides consistent and quality-controlled information related to air pollution and health, solar energy, greenhouse gases and climate forcing, everywhere in the world. CAMS is implemented by the European Centre for Medium-Range Weather Forecasts (ECMWF). S3NG-T Measurements of atmospheric properties from microwave radiometer measurements, wind speed over the ocean and ocean waves are important inputs to CAMS – particularly for ocean-atmosphere coupling of models that are growing in maturity.

2.2 The Copernicus 2.0 Long-Term-Scenario for a Topographic Ocean and Ice Measurement Family.

As set out in the ESA Program Board for Earth Observation (PBEO) paper (ESA/PB-EO(2017)31 Paris, 5 September 2017), the Copernicus Space Component (CSC) has been established as the largest and most proficient Earth Observation infrastructure in the world. However, the future evolution of the CSC needs to be initiated now, in close cooperation with all stakeholders, to remain fulfilling evolving user needs.

The intense use and increased awareness for the potential of Copernicus have generated great expectations for an evolved Copernicus system. There is now a large set of concrete needs and requirements for the future configuration of the CSC. User and observation requirements have been identified, structured and prioritized in a continuous reflection process led by the EC. Results from EU policy analyses, consultation of Services and Member States, as well as various workshops, gap analyses, studies and task forces now provide the rationale for a ‘Long-Term Scenario’ (LTS, ESA, 2025).

Two distinct sets of expectations have emerged from the user consultation process:

1. Stability and continuity of the system, while increasing the quantity and quality of CSC products and services, lead to one set of requirements. These requirements are addressed by an ***Extension*** of the current Sentinel 1 to 6 satellite capability by providing enhanced continuity of baseline Copernicus observations.
2. Emerging and urgent needs for new types of observations constitute a second distinct set of requirements. They are addressed by a timely ***Expansion*** of the

current Sentinel satellite fleet. Both sets of expectations have been systematically reflected and integrated by ESA (as the CSC System Evolution Architect) in response to formal documented EC requirements.

The ‘Extension’ and the ‘Expansion’ components are organised around broad observation domains. The distinction between ‘Expansion’ and ‘Extension’ components is not schedule-based. The ‘Expansion’ component corresponds to the enlargement of the present measurements through the introduction of new missions to answer emerging and urgent user requirements. The ‘Extension’ component corresponds to a more progressive improvement of the current measurement capabilities, mostly by means of new generation of similar instrumentation compared to the ones currently deployed by Copernicus today.

2.2.1 Long Term Scenario Boundary Conditions

According to the Copernicus Regulation (EU Regulation No. 377/2014 dated 3 April 2014), ESA has been mandated by the EU Council and European Parliament to define *“the overall system architecture for the Copernicus space component and its evolution on the basis of user requirements, coordinated by the Commission”*. Following this rationale ESA, in close interaction with the EC, EUMETSAT and Member States, has identified key components of a Long-Term Scenario (ESA, 2020). Within the LTS, the high-level boundary conditions for the topography family of satellite mission are:

1. **Guarantee continuity of Sentinel-3 topography measurements** between 2030 – and 2050 (S3NG-T).
2. **Guarantee continuity of the Sentinel-6 reference altimetry measurements** between 2030 – and 2050 (S6NG);
3. Responding to evolving user requirements, **extend the present measurement capabilities to improve coverage and revisit** of the Copernicus Next Generation Topography Constellation (that includes S3NG-TG and S6NG);
4. Responding to evolving user requirements, **enhance the present measurement performance capabilities** within the Copernicus S3NG-T.
5. A first launch of S3NG-T satellites is not anticipated before 2034/2035.

The key driver for the launch of the Proto-Flight model of the NG missions is providing **enhanced continuity** and responding to evolving user requirements and not the mere replacement of the first generation. As such, the relevant launch dates are foreseen in the period 2030+.

2.2.2 Long Term Scenario Implementation Approach for Next Generation Copernicus Topography Measurements

The Copernicus Long Term Scenario considers the Sentinel-6 mission family as the altimeter system to maintain the reference ocean altimetric measurements, currently provided by Sentinel-6A (Donlon et al, 2021). With a planned launch date in 2025 and a nominal lifetime of 5.5 years, Sentinel-6B will be the altimeter reference mission until 2030. Considering that a one-year overlap with its successor is required to ensure accurate cross-calibration– as baselined in the current CSC-LTS (ESA, 2025) Sentinel-6C will need to be ready for launch by 2030, followed by the first Sentinel-6 Next Generation mission in 2035.

For monitoring the surface elevation of polar ice sheets, glaciers, snow – particularly at high latitudes – the CRISTAL (e.g. Kern et al., 2020) mission is assumed, to fulfil this role as an enhanced operational follow-on to the CryoSat-2 Ku-band altimetry mission (e.g. Francis, 2002) as part of the Copernicus Expansion. The S3NG-T mission will, as part of its baseline continuity mission, continue to provide measurements up to 81.5° North and South of the equator for use in synergy with CRISTAL. In Appendix VI a summary of current and future satellite altimeter missions is provided.

Several activities, including airborne campaigns, have shown that the addition of Ka-band as second frequency (with the CNES AltiKa sensor providing solid heritage) and microwave radiometer with channels optimised for the mission objectives will consolidate the data quality and open major application avenues, such as snow measurements (thanks to the different interactions at Ku-band and Ka-band), observations of inland waters and glaciers, improved coastal and polar sea/ice data. It is assumed that the CRISTAL-A satellite will be launched not earlier than end 2028 and will be replaced by CRISTAL-B, to be launched around the 2034/2035 timeframe to ensure continuity of observations.

The sun-synchronous orbit continuity after Sentinel-3C and -3D has to be guaranteed by a continuation of the topographic component of Sentinel-3 (e.g. Donlon et al, 2016). There is consensus that it is time to select a proper orbit phasing for the sun-synchronous topographic component, since historically (for ERS-1 and -2, Envisat, and Sentinel-3) a non-optimal orbit was chosen to accommodate diverging requirements from the various instruments on the platform. The key challenge remains to significantly improve the density of sampling for ocean topography to meet the requirements of sampling 50 km features every 5 days, asset out by the European Commission and CMEMS (CMEMS, 2017) and to improve sampling for Hydrology services (requested by the European Commission). This implies an optimised plan of satellite orbit and sampling capability. For this purpose, in the ESA Long Term Scenario (ESA, 2025) the Sentinel-3 Next Generation mission has been separated into separate satellite platforms for the optical component and the topography component placed in optimal orbit configurations. It is assumed that the first S3NG-T satellite would launch around 2034/2035 with 7,5 (expected extension up to 12,5) years operational lifetime and partially overlapping with the Sentinel-3C and -3D missions in order to satisfy the relevant user requirements.

The strict continuity of Sentinel-3C and -3D requires a minimum of two enhanced nadir altimeter satellites. As such, the relevant launch dates are foreseen in the period 2034/2035 to avoid any data gap with the current Sentinel-3 generation at the end of its lifetime. The enhanced continuity with improved sampling characteristics could be achieved by different mission concepts. One possible solution is based on heritage of the NASA/CNES Surface Water Ocean Topography (SWOT, Rodriguez et al, 2017; Desai et al, 2018) mission, comprising two large spacecrafts carrying an across-track swath interferometer and a nadir-looking SAR altimeter. Alternatively, a coordinated constellation of 10 to 12 miniaturised nadir-looking SAR altimeter constellation could also be considered. A more detailed explanation of these two mission concepts is provided in Appendix VII.

Nevertheless, following the S3NG-T Preliminary Concept Review (PCR) in August 2022, the decision was reached to implement the mission as a constellation of two large spacecrafts carrying a next generation nadir-looking synthetic aperture radar (SAR) altimeter that will provide the baseline continuity with the current S3 constellation, and an across-track wide swath interferometer that will provide the required enhanced sampling capabilities. This decision was confirmed at the Mission Gate Review (MGR), held at the end of Q1 2024, where inputs from the phase A/B1 intermediate System Requirements Review (ISRR) and additional analyses benefiting from the inflight experience of SWOT mission were considered to determine whether the selected mission concept was fit for purpose to meet the S3NG-T mission requirements as gathered in this MRD.

The present mission requirements document is measurement agnostic by design.

2.3 Reference Documents and Requirements Setting Approach for the S3NG-T Mission

The Copernicus programme (http://www.copernicus.eu) is user-driven and policy-driven. The Copernicus programme will be continued within similar perimeter of the Copernicus regulation, as defined in the Space regulation (COM(2018)447 final, 2018/0236 (COD) from 6 June 2018).

> *"Copernicus should build on and ensure continuity with the activities and achievements under Regulation (EU) No 377/2014 of the European Parliament and of the Council17 establishing the Union Earth observation and monitoring programme (Copernicus) as well as Regulation (EU) No 911/2010 of the European Parliament and of the Council on the European Earth monitoring programme (GMES) and its initial operations establishing the predecessor Global Monitoring for Environment and Security (GMES) programme and the rules for implementation of its initial operations".*

According to the Copernicus Regulation:

> *'The objective of Copernicus should be to provide accurate and reliable information in the field of the environment and security, tailored to the needs of users and supporting other Union policies, in particular relating to the internal market, transport, environment, energy, civil protection and civil security, cooperation with third countries and humanitarian aid' and 'Copernicus should be user-driven, thus requiring the continuous, effective involvement of users, particularly regarding the definition and validation of service requirements'*.

According to Article 48, Copernicus is broken down into four components, two of which being the data acquisition (with the space component), and the data and information processing component dealing specifically with a service portfolio ensuring delivery of information in six areas: atmosphere monitoring, marine environment monitoring, land monitoring, climate change, emergency management and security. The two other components are the data access and distribution component and a user uptake and market development component Data and information products delivered by the Copernicus programme remain subject to a free, full and open data and information policy.

"Copernicus is a user-driven programme. Its evolution should therefore be based on the evolving requirements of the Copernicus core users, while also recognising the emergence of new user communities either public or private. Copernicus should base itself on an analysis of options to meet evolving user needs, including those related to implementation, and monitoring of Union policies which require the continuous, effective involvement of users, particularly regarding the definition and validation of requirements."

The programme Article 3(9) of the Copernicus Regulation defines four groups of users and specially the core users:

1. Copernicus core users: Union institutions and bodies, European, national, regional or local authorities entrusted with the definition, implementation, enforcement or monitoring of a public service or policy;
2. research users: universities or any other research and education organisations;
3. commercial and private users;
4. charities, non-governmental organisations and international organisations.'

User interaction and user feedback play a significant role for improving the data and services' products and gaining further insight on the user needs and their possible evolution. In order to ensure the continuous and effective involvement of users, particularly regarding the definition and validation of service requirements, as well as to provide ESA with needs for space observations derived from these service requirements, the Commission services maintains continuous activities to gather user needs with various mechanism such as market uptake, interactions with users and maintenance of requirements delegated to Entrusted Entities in charge of the services, dedicated studies, workshops and working groups, of which results are shared and discussed under the governance of the Copernicus user forum. As such a major study was carried out by the Commission to collect user needs and support the analysis of observation requirements that would be needed in the future to be delivered by the evolution of the space component. The Commission conducted as well as in-depth analysis of commission services needs for policy implementation driven by Directorate General (DG) Joint Research Centre (JRC). This allowed to centralise and process all user needs in a systematic manner across all application areas and to understand their evolution since the Global Monitoring for Environment and Security (GMES) implementation groups set up during the preparation of the GMES initial operations (2010-2013) and the Copernicus programme (2014-2020).

The Commission issued in 2019 the "*Collection of user needs for the Copernicus programme Staff Working Document*" (SWD, 2019) endorsed by Commission services and synthetising this high-level expression of needs, not yet limited by possible programmatic or technical feasibility.

The implementation of Copernicus in the long-term may then better address evolving user needs benefiting of latest technological developments. As regards the next multiannual financial framework, the implementation of Copernicus will take place in accordance with the rules to be set out by the EU legislator in the future Space Programme Regulation.

The consultation of users carried out to identify user needs has been threefold, considering the existing Copernicus service portfolio as the starting point:

- user consultations made through questionnaires, interviews and workshops, Copernicus service feedback mechanisms, access to core user expert groups, consultation with ESA, EUMETSAT, Member States, participating states;
- desk studies comprising the review of existing policies (i.e. as set out in EU legislation, communications published during the current multiannual financial framework timeframe), analysis of existing solutions on the market or at research level, technical analysis of the potential of emerging space technologies (e.g. reachable with the Copernicus Expansion Missions);
- analysis of published reports from expert groups in space technologies, review of ESA, Framework Programme 7 for Research, Horizon 2020 project outcomes and market reports.

During this process, the four groups of Copernicus users have been consulted with a priority to identify the needs of core users in most of the policy areas. In this context, the needs of the Commission services have also been collected to consolidate the policy context and include needs from the public or the private sector at European or national level to comply with policies. All needs have been recorded ‘as expressed’ by users or as given in source documents. They have been stored in a database with full traceability of the information to identify which categories of users were consulted and which meetings or source documents were reviewed. User needs have been categorised whenever possible into observation requirements, product/service requirements or generic functional needs to support the formal user requirement exercise.

Since Copernicus is a user-driven programme, user needs are critical to steer and to adjust the future evolution of the programme in particular in the frame of the current Multi-annual Financial Framework of the European Union (2021-2027):

- The evolution of the Copernicus data and information products and the related services;
- The definition of the next generation of Sentinels (expected type of observation and performances);
- The requirements for additional data that could be complementary to the Sentinels and necessary for the purpose of services.

User Needs were formally provided to ESA by the European Commission (Ref. Ares(2020)1823662 - 30/03/2020) for ESA Phase-0 S3NG-T activities clearly noting in the delivery that:

> *“From the Commission perspective, the topography family should address per order ocean needs, inland water topography, coastal applications including for emergency, needs for waves products and then sea-ice products…*
>
> *Taking into account expected budgetary constraints, it is advised limiting the number of new products and at the same time finding a maximum of synergies among planned missions”.*

Notable here is the prioritization of not only sea surface topography measurements, but also inland water river and lake heights that are now elevated to Primary Mission

Objectives for S3NG-T. This position has been confirmed by the European Commission.

As clearly identified in Ref. Ares (2020)1823662 - 30/03/2020, the European Commission priorities for Copernicus are per order:

- To consider the requirements of the Copernicus service so that they can ensure the continuity of their services as of today and specifically the consistent continuity of time series and to consider the new, emerging or ad-hoc requirements expressed by the Entity entrusted for each relevant Copernicus service for the future;
- To consider areas of needs expressed by core users and their missions as expressed by the space regulation;
- To consider requirements expressed for policy implementation as stated in the Commission staff working document (SWD(2019)394, 25.10.2019);
- To comply the new priorities identified by the space strategy and the proposal for the space regulation for the next MFF (COM/2018/447 final - 2018/0236).

A compilation of the major policies and Earth observation applications supported by the Copernicus Sentinel-3 Next Generation Topography (S3NG-T) is provided in Appendix II.

To guide the development of the mission, an *ad hoc expert group* (AHEG) was convened by ESA in February -December 2020 to advise ESA during Phase-0 Studies for Copernicus Topography missions. Membership included recognised experts from the scientific user community with specific satellite altimetry competence, EUMETSAT, the European Commission and the French Space Agency, CNES. The following reference documents were provided in delivery Ref. Ares(2020)1823662 - 30/03/2020 as input to Phase-0 studies and serve as the starting point for this MRD:

- **UN-SWD**: A staff working document “Expression of User Needs for the Copernicus Programme (SWD(2019)394.pdf) that elaborates following recommendations published in the Copernicus mid-term evaluation report[1] to improve the process to gather user needs for the evolution of the Copernicus programme.
- **UN-COPURD**: Extracts of the Copernicus user requirements database (NextSpace requirements 2nd February 2018) for topography user needs analysed and prepared by DG.DEFIS separated into core user requirements and additional requirements (core-urd-SNG-topo-expert-group.xlsx, ord-SNG-topo-expert-group.xlsx, land-requirements-topography-I1.02-final.xlsx, non-core-urd-SNG-topo-expert-group.xlsx;
- **UN-NOTE**: A Summary Note prepared by DG.DEFIS highlighting specific requirements expressed by the Copernicus core services including references to CMEMS, C3S, land services detailed needs, and needs from the Emergency service, security services (Sentinel NG Topography user requirements.docx).

[1] European Commission, Directorate-General for Internal Market, Industry, Entrepreneurship and SMEs, *Interim evaluation of Copernicus, final report*, ISBN-978-92-79-71618-8, doi: 10.2873/666679, EU publications office, November 2017.

- **CMEMS(2017)**: Copernicus Marine Environmental Monitoring Service (CMEMS) requirements for the Evolution of the Copernicus Satellite Component (CMEMS, 2017).
- **C3S(2020)**:C3S in the document “EC User Requirements For The Sentinel-NG Topography Family, Inputs To ESA Ad-Hoc Expert Group” (C3S, 2020)

In Appendix III, these inputs have been used to derive numbered high-level European Commission Copernicus User Needs at system level and Product Needs. Section 3 discusses Level 2 Products and Performance in a system context and, based on European Commission User Needs, provides background and justification for S3NG-T mission requirements.

Appendix IV provides traceability between high-level European Commission Copernicus User Needs and S3NG-T Mission Requirements.

2.4 Copernicus Sentinel-3 Mission and In-Flight Performance

The Copernicus Sentinel-3 mission, part of the first generation of Copernicus satellites designed to ensure the long-term collection and operational delivery of high-quality measurements to Copernicus ocean, land, and atmospheric services. Sentinel-3 measurements are used both in their own right to monitor ocean, inland waters, sea ice and land ice parameters and as input to data assimilation systems that constrain global and regional numerical prediction models. Mission Requirements are set out in the Sentinel-3 Mission Requirements Traceability Document (MRTD, Donlon, 2011). A full description of the Sentinel-3 Mission is provided in *Donlon et al.* (2016) and a technical summary of the mission is provided in Appendix V for reference.

Assessing the uncertainties of different altimeter parameters and geophysical corrections is not straightforward. Several methods can be used to estimate these quantities that yield different results depending on the temporal and spatial scales assessed. Raynal and Labroue (2021) provide a detailed assessment of global uncertainties as part of the Sentinel-3 Mission Performance Centre (MPC) activities. They define the following spatial/temporal uncertainties:

Sub mesoscales and mesoscales uncertainty:

- White noise: this uncertainty is uncorrelated on time and is related to the instrumental measurements (altimeter).
- Short-time temporal uncertainty (< 10 days): this includes all the uncorrelated and correlated uncertainty in time for time scales < 10 days. It is important to define these uncertainties for oceanographic applications in conjunction with mesoscale or sub-mesoscale studies.

Long scale uncertainties:

- Medium temporal uncertainty (2 months – 1 year): these include all correlated temporal uncertainties at medium scales e.g. periodic signals (annual, semi-annual...). The description of these uncertainties is useful for applications requiring long time series (e.g. climate reanalyses).

- Long-term uncertainties (> 1 year): these include inter-annual and long term stability (drift) uncertainty. These are the most important for climate applications as they directly impact the global mean sea level trend.

In flight performance of the Sentinel-3A and Sentinel-3B altimetry mission is regularly reported in the scientific literature through validation activities and applications. In addition, the Sentinel-3 Mission Performance Centre (MPC) provides annual and cyclic reports available at https://sentinel.esa.int/web/sentinel/user-guides/sentinel-3-altimetry. This material is used to specify in-flight performance of Sentinel-3 that in turn, defines S3NG-T baseline continuity requirements used throughout this document.

Performance requirements for the Sentinel-3 topography mission are provided in Table 2.4-1 together with Mission Requirements set out in Donlon (2011) and set the baseline continuity performance for the S3NG-T mission.

Table 2.4-1. Copernicus Sentinel-3 topography mission performance budget (Donlon, 2011) and Sentinel-6 mission performance budget (EUMETSAT, 2018). All values are *specified for measurements integrated over 1s*, for Significant Wave Height (Hs) of 2m and for σ0 of 8dB. The specified altimeter random error assumes perfect Brown or Haynes model echoes. NRT3H is Near Real Time performance within 3 hours of acquisition, STC is short time critical within 48 hours of data acquisition for Sentinel-3 and 36 hours for Sentinel-6, NTC is non-time critical within 30 days of acquisition for Sentinel-3 and 60 days for Sentinel-6.

Quantity	Sentinel-3 Requirements (from Donlon, 2011 and S3 SRD v4.0) (NRT3H/STC/NTC)	Sentinel-3 NTC In flight Performance (S3A and S3B)	Sentinel-3 In flight Performance Sources	Sentinel-6 Requirements (from EUMETSAT, 2018)[2]	
				Requirement (NRT3H/STC/NTC)	Goal (NRT3H/STC/NTC)
Ku-band Instrument range noise (cm)	≤1.3	±0.35 ±3.45 (compared to PFAC FRM)	Mertikas et al. (2020) NTC over PFAC FRM transponder • S3A: ±0.20 ±3.45 (FRM uncertainty) • S3B: ±0.35 ±3.45 (FRM uncertainty) Long-term average (4.7 years) S3A SAR over PFAC transponder from S3MPC.CLS.APR.006: • ±1.22 (range bias: 0.64) Long-term average (2.6 years) S3B SAR over PFAC transponder from S3MPC.CLS.APR.006 • ±1.38 (range bias:-0.79) Average (22 months) S3A SAR over the ocean from Raynal and Labroue (2021): • 1.25 for wavelength 0.7- 1.0 km (following the spectral approach of Zanife et al. 2003) • 1.2 cm for >50 km >10 days for wavelength 700 m to 7 km (computed from standard deviation of the range elementary measurements)	0.8[(a)]	0.5

[2] For reference, performance requirements for the Sentinel-6 mission are also provided as a guide to the performance form current state of the art nadir pointing altimeter instruments (Poseidon-4) incorporating digital technology elements.

Ionospheric path delay (cm)	≤0.7	≤0.4 (compared to GIM)	Long-term average (4.7 years) S3A dual-frequency from S3MPC.CLS.APR.006: • ≤0.32 compared to GIM Long-term average (2.6 years) S3B dual-frequency from S3MPC.CLS.APR.006: • ≤0.31[3] compared to GIM Average (22 months) S3A SAR over the ocean from Raynal and Labroue (2021): • 1 cm (computed as the standard deviation after high pass filtering of 1Hz to remove the geophysical signal). Note • <0.1 cm filtered to 300 km (computed as the standard deviation after high pass filtering of 1Hz to remove the geophysical signal)	0.5[(b)]	0.3
Sea state bias (cm)	≤2.0[(4)]	2.0 (difficult to assess)	Average (22 months) S3A SAR over the ocean from Raynal and Labroue (2021): • SSB variability estimated to be 0.3 (computed as the standard deviation after high pass filtering of 1Hz to remove the geophysical signal)	2.0	1.0[(e)]
Dry tropospheric path delay (cm)	≤0.7	<0.1	<0.1 Average (22 months) S3A SAR over the ocean from Raynal and Labroue (2021)	0.8/0.7/0.7	0.5
Wet tropospheric path delay (cm)	≤1.4	<0.7 ±1.0	Frery et al. (2020) comparison to J3 crossovers: • S3A:0.55 ±0.78 (PLRM 3 parameter algorithm against J3) • S3B:0.56 ±0.82 (PLRM 3 parameter algorithm against J3) 2019 S3A NTC from S3MPC.CLS.APR.006: • 0.04±1.36 for SAR 5 parameter algorithm against model 2019 S3B NTC from S3MPC.CLS.APR.006: • 0.08±1.38 for SAR 5 parameter algorithm bias against model	1.2/1.2/1.0	0.8

[3] Sentinel-3B C-band range is in average 8.8 cm shorter than Sentinel-3A one: shorter C-band range implies a less negative ionosphere correction, which is consistent with the results here.

[4] Chelton (1994) considered 1% SWH for SSB uncertainty that corresponds to a 2 cm SSB uncertainty level for 2m Hs. This is considered maximum global RMS uncertainty over the open ocean.

			Average (22 months) S3A SAR over the ocean from Raynal and Labroue (2021): • 0.12		
Altimeter range noise over ocean RSS with allocations above (cm)	≤2.9			2.64/2.61/2.53	1.49
RMS radial orbit (cm)	≤10/4/3[(5)]	<0.7 (POE)	ROE Radial S3A (S3B) from CNES and ESOC GMV-GMESPOD-RSR-0015: • <1.4 (<1.3) ±0.5 (±0.6) MOE Radial S3A (S3B) from CNES and ESOC GMV-GMESPOD-RSR-0015: • <0.75 (<0.75) ±0.13 (±0.14) POE Radial S3A (S3B) from CNES and ESOC GMV-GMESPOD-RSR-0015: • <0.65 (<0.57) ±0.09 (±0.07)	5.0/2.0/1.5	3.0/1.5/1.0
Total RSS sea surface height (SSH) (cm)	≤10.4/5/4.2	<1.0 ±3.19 (PFAC FRM)	Mertikas et al. (2020) NTC over PFAC FRM ocean infrastructure: • S3A: ±0.62 ±3.19 (FRM uncertainty) S3B: ±0.75 ± 3.19 (FRM uncertainty) Average (22 months) S3A SAR over the ocean from Raynal and Labroue (2021): • 1.33 for wavelength 0.7- 1.0 km (following the white noise spectral approach of Zanife et al.2003)	5.65/3.29/2.94	3.53/2.12/1.80
Hs (dynamic range 0.5-20 m)	≤20 cm or 4%	< 10	2019: S3A (S3B) bias against ECMWF WAM model (standard deviation of difference, SDD) from S3MPC.CLS.APR.006: • ≤0.02 (≤0.02), SDD ≤0.27 (≤0.35) for Hs ≤12 m 2020: S3A (S3B) bias against ECMWF WAM model from MPC team(ref TBC): • ≤0.04 (≤0.06), SDD ≤0.25 (≤0.26) for Hs ≤12 m	15 cm ±5%[(c)]	10 cm ±5%[(c)]

[5] S3 GSRD (S3-RS-ESA-SY-0091) GSR-PDGS-PRO-080, GSR-PDGS-PRO-081. See also notes in MRD-300 regarding current performance of Sentinel-6 POD.

			2019: S3A (S3B) Bias against in situ data from S3MPC.CLS.APR.006 • <0.02 (≤0.02) SDD <0.35 (≤0.35) for Hs ≤12 m 2020: S3A (S3B) bias against in situ data from MPC team (ref TBC): • <0.12 (0.14), SDD <0.30 (0.31) for Hs ≤ 12 m Average (22 months) S3A SAR over the ocean from Raynal and Labroue (2021): • 9.7 for wavelength 0.7- 1.0 km (spectral analysis method) • 8.9 for wavelength 0.7- 1.0 km (standard deviation of Hs measurements) • 7.3 uncertainty (geographically correlated) for large scales > 50 km and < 10 days.		
Wind speed (U) (dynamic range 3 to 20 m/s)	≤2	<0.2	2019: S3A(S3B) SAR difference to in situ from S3MPC.CLS.APR.006: • ≤0.1 (-0.15), SDD ≤1.37 (≤1.38) for U_{2m} ≤ 26 m 2020: S3A (S3B) SAR difference to in situ from MPC team (ref TBC): • ≤ -0.10 (≤ -0.15), SDD ≤1.47 (1.57) for U_{2m} ≤ 26 m 2019: S3A (S3B) SAR difference to ECMWF WAM model from S3MPC.CLS.APR.006: • ≤0.14 (≤0.03), SDD ≤1.06 (≤1.05) for U_{2m} ≤ 26 m 2020: S3A (S3B) SAR difference to ECMWF WAM model from MPC team (ref TBC): • ≤0.14 (≤0.03), SDD ≤1.06 (≤1.05) for U_{2m} ≤ 26 m Average (22 months) S3A SAR over the ocean from Raynal and Labroue (2021) • 0.16 standard deviation of 1Hz after high-pass filter to account for Hs noise.	1.5[(k)]	1.0
Sigma0 (-10dB - +50 dB)[(d)]	≤ ±1, long term drift of ≤0.3dB over mission lifetime.	<0.2 ~0.3 dB stability for 2019.	2019 S3A and S3B from S3MPC.CLS.APR.006: • 1.8 Standard deviation 2016-2018 • 11.0 dB mean 2016-2018 (S3A and S3B) Average (22 months) S3A SAR over the ocean from Raynal and Labroue (2021):	0.3[(j)]	0.3

			• 0.04 dB for wavelength 0.7- 1.0 km (following the spectral approach of Zanife et al. (2003) • 0.03 dB for wavelength 700 m to 7 km (computed from standard deviation of the Sigma0 elementary measurements) • 0.14 uncertainty (geographically correlated) for large scales > 50 km and < 10 days, bias depends on the radial velocity to first order.		
Surface Water Elevation (m)	Secondary Objective: no specification	Large Rivers (≥3 km):≤0.24 m	Kittle et al (2021) 0.32 m using Sentinel-3A and Sentinel-3B datasets over the Zambezi river basin where in situ gauging stations are available. Haliki and Niedzielski (2022) obtained <0.22m (0.12 – 0.44m) uncertainty using Sentinel-3A over Polish rivers. Fenoglio et al (2022) in press 18 cm for rivers over 500m width and crossing angles ≥60°.	N/A	N/A

a. After ground processing, averaged over 1 second, for 2-meter wave height.

b. Derived from Ku- and C-band range difference, averaged over 200 km.

c. Valid for the range of 0.5 to 8 m Hs.

d. S3 SRD states: Total absolute accuracy after cross-calibration with other altimeter missions [RA-PE-020]. The long-term drift error of the sigma-0 internal calibration shall be less than 0.3dB during the mission lifetime [RA-PE-030 a]

e. Could also be expressed as 1% of Hs, to be reached at the end of the commissioning phase.

j. After cross-calibration with other altimeter missions.

k. For the range of 0.5 to 8 m Hs.

3 SCIENTIFIC JUSTIFICATION OF S3NG-T MISSION MEASUREMENT REQUIREMENTS

This chapter provides background information supporting the definition and justification of the MRD requirements. Please note that the information reflects the status at the time of writing (July 2025) and may not be fully up to date or consistent with the latest developments in the Copernicus Programme or the S3 NGT mission design.

Satellite altimetry provides an essential data set for the Copernicus services (e.g. Le Traon et al, 2019) providing measurements over the global ocean and, increasingly in the coastal zones and inland waters. Microwave radiometers supporting nadir-pointing radar altimeter payloads are also extensively used to monitor atmospheric characteristics in the troposphere (e.g. Varma et al., 2020, Quartly et al., 2019a,b).

Altimeter-derived applications span many topics, from fundamental science to operational oceanography, and a wide range of scales from regional studies to global systems and from short-term weather forecast to long-term sea level monitoring. The importance of satellite altimetry cannot be overstated in terms of the impact on operational oceanography (e.g. Munk, 2002) and climate science (e.g. IPCC, 2014, 2019). Measurements are used in a variety of applications to enable quasi-global estimates of sea level rise (e.g. Cazenave et al., 2018, Veng and Andersen, 2020), ocean sea state (e.g. Ardhuin et al., 2019, Ribal, and Young, 2019, Dodet et al., 2020), large-scale ocean and mesoscale circulation, (~30-300 km and ~5-90 day) (e.g. Chelton et al., 2007), wind speed over the ocean (e.g. Abdalla, 2012, Bushair and Gairola, 2019), estimates of sea ice thickness and volume (e.g. Laxon et al., 2003; Laxon et al., 2013; Tilling et al., 2018), mapping of land ice topography, elevation changes and mass balance (e.g. Sandberg Sørensen et al, 2018, Schröder et al, 2019; Helm et al, 2014; Otosaka et al, 2023), geodesy applications (e.g. Bloßfeld et al., 2020), ionospheric mapping (e.g. Ray, 2020) and river and lake heights estimation (e.g. Creteaux et al, 2017, Emery et al., 2018, Gao et al., 2019, Roohi et al., 2019) amongst others. In Copernicus (EU, 2014), measurements are used for operational ocean monitoring/forecasting and derivation of geostrophic ocean currents by the Copernicus Marine Environment Monitoring Service (CMEMS, e.g. LeTraon et al., 2015, 2019), wave forecasting and climatology (e.g. Campos et al., 2020, Bidlot et al., 2017, Cooper, and Forristall,1997), climate monitoring/prediction by the Copernicus Climate Change Service (C3S, Buontempo et al., 2020), numerical weather prediction (e.g. Campos et al., 2020), the study of ocean tides (e.g. Carrere et al., 2020) and gravity field mapping (Sandwell et al., 2019). Other diverse applications include sea-floor mapping (Smith and Sandwell, 1997), investigation of ocean wave-current interaction (Quilfen and Chapron, 2019), dual-frequency radar altimeter inputs to computation of rain rates (Quartly et al, 1999a, 2000), computation of integrated water vapour and cloud liquid water content (e.g., Lázaro et al (2019), computation of ocean/atmosphere gas fluxes (e.g. Frew et al., 2007, Goddijn-Murphy et al, 2013), monitoring ship traffic (Tournadre, 2014), estimating extreme waves (e.g., Alvez and Young, 2004, Hanafin et al., 2012), tracking icebergs (Tounadre et al., 2008). In addition, altimetry increasingly contributes to our understanding of the hydrological cycle by monitor variations of rivers, lakes, reservoirs and flooded regions (e.g. Crétaux et al, 2017, Emery et al., 2018, Papa et al., 2022). Escudier et al. (2017) give an extensive overview of the research and operational applications of altimetry.

Given the considerable range of applications, a sustained Sentinel-3 altimetry constellation capability is required to address operational science and societal needs.

3.1 S3NG-T and Copernicus Marine Monitoring and Prediction

Altimetry has revolutionized the understanding of large-scale ocean dynamics, i.e. the large-scale forces (pressure gradient and wind stress) that set the ocean in motion. Satellite altimetry is the most mature technique for mapping balanced geostrophic motions of the upper ocean and has led to breakthroughs in our understanding of the dynamics of large-scale (larger than roughly 200 km wavelength) oceanic circulation with, to date, unequalled views of eddy kinetic energy on a global scale. Today, a mixture of operational data in low inclination 66° orbits are available (e.g. from the Sentinel-6 satellites, Jason series, complemented by polar orbit satellites including Sentinel-3, CryoSat-2, AltiKa and HY2 series). Satellite altimeters measure Sea Surface Height (SSH), that is a combination of the marine geoid (Bruinsma et al. 2013) and an ocean component including a temporal mean sea surface height, and time-variable Sea Surface Height Anomalies (SSHA) relative to this mean.

The main balance of forces at the mesoscale and larger scales (~10 km and more) is between the Coriolis force and the pressure gradient associated with SSHA (e.g. Ducet et al., 2000; Penven et al., 2014, provides estimates of ocean current anomalies in the upper water column that are in geostrophic balance), the smaller scales (< 10 km) are dominated by ageostrophic sub-mesoscales (McWilliams 2016) with small signatures in altimetric topographic height that are not yet resolved by satellite altimetry techniques. Other unbalanced motions due to tides, internal tides and internal waves also have a signature in altimetric topographic height. Altimetric observations, particularly from missions on non-sun-synchronous orbits, provide measurements of the open-ocean and coastal tides and the phase-locked internal tides (Ray and Zaron, 2016), helping us to improve our global tidal models to better predict the ocean tides. However, non-phase locked, non-predictable internal tides and their energy cascade also have an imprint on altimetric sea surface topography over scales < 200 km (e.g. Zaron, 2017), and these are not in geostrophic balance. This mixture of balanced geostrophic flow and unbalanced SSH signals allows us to observe the different dynamics and their interactions with altimetric observations. The challenge is in separating the unbalanced component in order to calculate geostrophic currents or higher-order fields (geostrophic vorticity, strain, etc). There are difficulties when computing estimates of ocean surface geostrophic currents from altimetric SSH due to the breakdown of the geostrophic approximation towards the equator, in shallow waters, near the coast (Mulero et al., 2022; 2024), at the marginal ice zone, within sea ice regions, due to uncorrected tides or internal tides, and generally at wavelengths below ~200 km that are unresolved by today's altimetry constellation (e.g. *Dibarboure et al.,* 2014).

Altimetry is particularly important for operational models. Le Traon et al. (2017) emphasise that altimeter sea level observations are the only remotely sensed information that reflects the ocean state far below the surface because temperature and salinity variations at all depths contribute to variations in SSH. Sea level from satellite altimetry is an integral of the density structure of the ocean interior and provides a strong constraint on the 4D ocean state estimation.Because of the critical reliance on altimetry, the development of operational oceanography and operational altimetry

occurred simultaneously. The global data assimilation experiment (GODAE) was set up in 1997 after the successes of the TOPEX and ERS missions, and the main GODAE demonstration was phased with the Jason-1 and ENVISAT altimeter missions. Since then, the GODAE community (now OceanPredict, https://oceanpredict.org/) has been maintaining strong links with satellite altimetry communities and major progress has been made in developing and optimising the use of satellite altimeter data for operational oceanography.

CMEMS modelling and data assimilation systems thus highly depend on the status of the altimeter constellation. Both OSEs (Observing System Evaluations) and OSSEs (Observing System Simulation Experiments) demonstrate the major contribution of altimetry (see Le Traon et al., 2019). At least four radar altimeters are required to observe the mesoscale currents. A long-term series of a high-accuracy altimeter system (Jason/Sentinel-6 satellites) is needed to serve as a reference for the other altimeter missions and for the monitoring of climate signals notably for C3S.

The corresponding improvement of products will answer European policy needs (SWD, 2019) and will impact the different areas of benefits of CMEMS:

- maritime security and safety, including search and rescue activities;
- maritime transport through improved surface currents;
- pollution monitoring and offshore operations;
- seasonal and weather forecasting through improved ocean/wave/atmosphere coupling and representation of surface layers;
- coastal zone monitoring and forecasting;
- riverine influence in the coastal environments;
- fish egg and larvae drift modelling;
- ocean productivity (e.g. at ocean fronts).

CMEMS user needs for satellite altimetry (CMEMS, 2017) are founded on the future capability of ocean modelling systems. As CMEMS intends to evolve around 2025 to monitor and forecast the ocean at finer scale and improve the monitoring of the coastal zone, model resolution will increase by a factor of at least three (e.g., global 1/36° and regional 1/108°). Furthermore, more advanced data assimilation methods will be available. These models will be used to force downstream coastal models with a potential resolution of a few hundred meters and/or ensemble prediction approaches in the next 10-15 years.

To support such high-resolution model systems, observations are required to constrain the model solutions at the appropriate time and space scales. Since observations are likely to be limited (particularly in situ observations of full ocean depth) more advanced data assimilation and ensemble forecast methods will be required that provide probabilistic forecast capability that statistically represents the uncertainties in the relatively unconstrained forecasts. Outputs should be able to characterize, at fine scale, the upper-ocean dynamics to improve knowledge of ocean state and forecasts of ocean dynamics required as boundary conditions for nested very-high resolution regional and coastal models.

The coverage, revisit and sampling characteristics of the present satellite altimeter system (in an operational sense as opposed to ‘one-off’ scientific research missions) includes Copernicus Sentinel-3A/C; Copernicus Sentinel-3B/D; Copernicus Sentinel-

6MF followed by Copernicus Sentinel-6B and thereafter Copernicus Sentinel-6C; Jason-3; and the uncoordinated (from a system perspective) HY-2 series of NSOAS missions from China. In this form, altimetry products will not be able to provide topography products to sufficiently constrain the smaller scales of high-resolution models. The limitation is emphasised in coastal regions where the combined effects of mesoscales, wind, waves and swell, bathymetry, and tides can generate very complex small scale and high-frequency topography surfaces that are highly dynamic. This would require an assimilation of high-resolution ocean surface topography at scales of 10-50 km with an observation frequency commensurate with the physical phenomena of interest (hours to a few days at most).

While altimetry is one of the most important data sources for assimilation into operational models, to specify space time sampling requirements remains a challenge. Incorporating observations into a prediction system via data assimilation is fundamental for operational forecasting and reanalysis systems to obtain meaningful estimates of the ocean state. The accuracy of the analysis and subsequent forecasts produced by data assimilation is dependent on the accuracy and coverage of the input observations, the fidelity of the numerical model, and the quality of the data assimilation scheme itself, 3D Variation or Ensemble Optimal Interpolation (and its variants), 4D variation more advanced methods such as the Ensemble Kalman Filter for regional and shelf-seas systems are all used today (Davidson et al, 2019). As the available computational resources increase, many of the global ocean forecasting centres are developing implementations of these more advanced methods as well as hybrid ensemble/variational methods. As research advances in ocean forecasting and prediction systems (data assimilation, models, computational power, verification methods) working in tandem with the evolution and advances of the observing system will accelerate both basic and applied oceanographic research. As discussed by Davidson et al (2019) this will include:

- Optimizing observing system design using data assimilation tools.
- Adaptive/event-based observing/modelling strategies (extremes).
- Four-dimensional variational or hybrid data assimilation and optimal use of available observations.
- Model resolution (horizontal and vertical) including full tidal/mesoscale resolving and partial sub-mesoscale/internal tide resolving ensemble forecasting.

Although there is an ever-increasing drive toward higher resolution ocean model capability, the dynamics of the evolving high-resolution eddy-resolving models cannot be validated today with commensurate revisit and spatial sampling due to the lack of global observations at these finer scales (e.g. Morrow et al, 2019). The success of these developments depends on the availability of measurements within the observing system at the appropriate density to constrain the model systems at resolution commensurate with the observing system itself. Today, Sentinel-3 contributes to a small constellation of uncoordinated satellite altimeter missions from international Agencies (including Europe, USA, China, and India) on which CMEMS depends. These are homogenized using the reference altimetry time series now maintained by Sentinel-6 (e.g. Pujol et al, 2006).

3.1.1 Effective resolution of the current altimetry constellation over the ocean

Ballarotta et al. (2019, 2020) investigated the effective spatial and temporal resolution of SSH maps derived from three altimeters shown in Figure 3.1.1.1 (a). The effective resolution is defined as a 'noise-to-signal' (NSR ratio between the spectral content of mapping error and the spectral content of independent true signals (along-track and tide gauge observations)). The effective resolution is then (subjectively) defined as the wavelength above which the NSR exceeds 0.5. In other words, it corresponds to the threshold where the mapping error variance is 2 times smaller than the observed true signal variance.

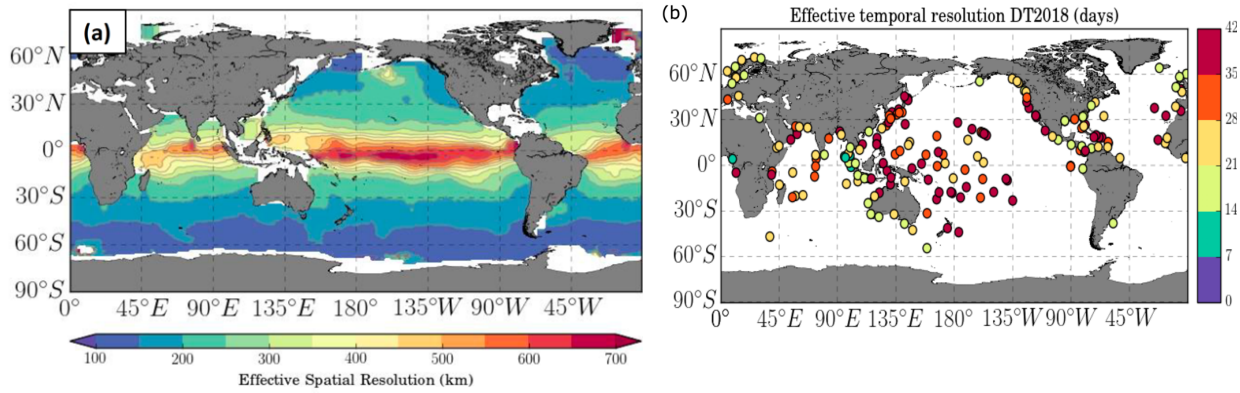

Figure 3.1.1.1. (Effective spatial resolution in km of the DUACS-DT2018 maps for (a) the Global Ocean. The resolution ranges from ~100 km wavelength at high latitudes to ~800km wavelength near the Equator, with a mean resolution at mid-latitude near 200km. (b) Effective temporal resolution in days of the DUACS-DT2018 maps (*Ballarotta et al.,* 2019).

The effective spatial resolution ranges from ~100 km wavelength at high latitudes to ~800 km wavelength in the tropical ocean, with a mean resolution at mid-latitude near 200km. The effective temporal resolution of the DUACS-DT2018 maps ranges from 13 to 49 days period (Figure 3.1.1.1(b)).The temporal resolution is heterogeneously distributed over the global ocean, particularly in the inter-tropical band where a wide range of scales are found, linked to the mixture of continental tide gauges and island tide gauges, with the latter being more representative of open-ocean conditions. At mid-to-high latitudes the temporal scales are between 14- and 28-day periods, coherent with the temporal correlation scales applied in the mapping process. The globally averaged effective temporal resolution is estimated ~28 days period. The estimation of the temporal resolution is subject to an important caveat: the estimation is based mainly on coastal locations which may be polluted by altimetry errors. Additionally, it may not be fully representative of the temporal resolution of the DUACS maps which combine various oceanic regimes (e.g., coastal, offshore high variability, offshore low variability regimes).

While these results shown in Table 3.1.1-1 are crude, they provide useful estimates of the effective spatial and temporal resolution of today's altimetry constellation. Since research missions cannot be relied on to provide an operational Copernicus altimetry

capability (particularly if no European), S3NG-T must ensure that an operational system can be implemented, operated and maintained for Copernicus services to guarantee continuity of the existing quality of altimetry measurements.

Figure 3.1.1-2 illustrates how the altimetry constellation is limited by its sampling compared to the scale of the ocean mesoscale.

Table 3.1.1-1 Summary of DUACS global SSH product spatial and temporal resolutions (*Ballarotta et al. 2019*).

Spatial Feature of interest		Temporal features of interest	
Effective Resolution (km)	**Grid Spacing (km)**	**Effective Resolution (days)**	**Grid Spacing (days)**
100-800	4-30	~28	1

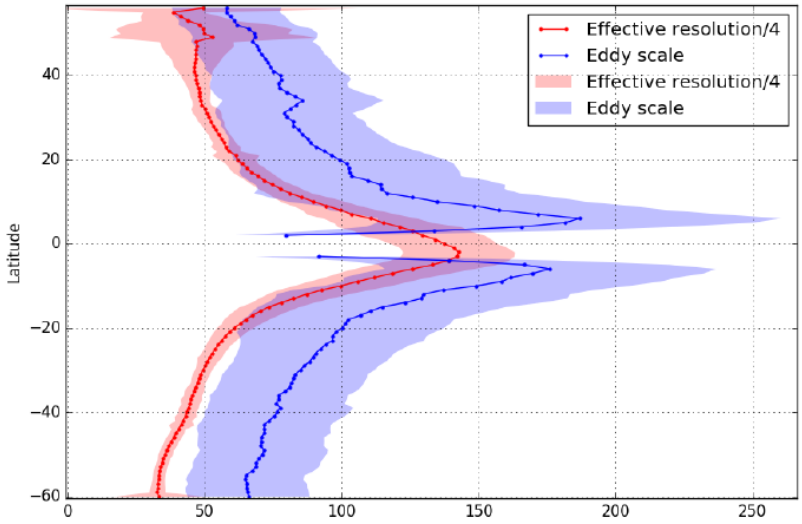

Figure-3.1.1-2. Zonally averaged eddy scale (as in Chelton et al., 2011; and computed from the DUACS-DT2018 two satellites maps) and feature radius resolution of the mesoscale structures that can be properly mapped in DUACS (i.e., derived as 0.25 × effective resolution). Units in kilometres after Chelton et al., 2011, 2014.

Against this background and to satisfy global operational oceanography ocean forecasting data assimilation needs in the 2030+ timeframe, the CMEMS (CMEMS, 2017) primary User needs are to guarantee the baseline continuity of Sentinel-3 topography capability and resolve ocean features of 50 km with a time resolution of 5 days.

3.1.2 Characteristics of ocean topography

There is a wide diversity of mechanisms affecting the ocean topography, and even dominant effects have a large geographical and temporal variability: the variability of the space/time scales of interest and their amplitude spans one or two orders of magnitude. The same applies to the scales and amplitude of the geophysical error sources. Consequently, it is not possible to define the requirements by adding up the most stringent requirements, as it would over-constrain the system. Both space/time

sampling and measurement errors need to be taken into account to define requirements for a future topography mission. Measurement sampling and resolution must be sufficient to properly constrain model assimilations, but a phenomenon does not need to be fully resolved by observations only. However, Copernicus Marine service also provides satellite high-level (Level 3 and 4) data products to users for many different applications. Measurements should be commensurate with the processes that govern their interpretation. Well-observed structures and phenomena will be captured, assimilated, and propagated by the numerical model between two observations. Resolution and precision must be high enough to not be a limiting factor for the assimilation, i.e. able to guarantee a high quality measurement of the signal of interest even if the sampling capability is not sufficient to resolve/monitor it.

The upper ocean dynamics are influenced by multiple forcing acting at the air-sea interface and by internal instabilities, and involves a continuum of variability across all space and time scales subject to small- and large-scale random perturbations and interactions. Not all of these processes have a signature in ocean surface topography which is also a surface pressure field.

Variations in surface topography can be due to large scale (>10 km) barotropic and baroclinic motions, atmospheric pressure variations, barotropic tide and internal tides. They lead to the development and co-existence of different flow patterns and phenomena that have a physical expression on the sea surface which can be measured (Chapron et al., (2017) including mesoscale and submesoscale motions, Rossby waves, Kelvin waves, surface wave and wind motion, internal waves, tidal signal, inertial gravity wave response. The most energetic components in sea level variations are from upper ocean mesoscale circulation and some smaller instabilities. These are part of an energy cascade linked to the larger general ocean circulation patterns that cause energetic vertical surface topography variations relative to a reference geoid surface.

As divergent surface wind distributions induce vertical motions, some resonance can occur. When surface waves propagate across the ocean surface, they often form series of wave groups. If the group velocity of the surface waves matches the phase velocity of an internal wave, resonant energy exchanges can thus also occur. The rate of energy transferred to internal waves is certainly much smaller than to surface waves, but the wave amplitude for a given energy density is larger by a factor, $\rho_0 \ / \ \partial\rho$ where $\partial\rho > 0$ is the difference in density across the pycnocline. The surface waves can then further be modulated in the field of orbital velocities of the internal waves. Feedback mechanisms will then contribute to modulate the internal wave field and, through interaction with the drift currents, the generation of upper ocean currents and their surface topography expressions can be altered. Furthermore, these interactions, generated by fast changes of the wave and wind stress vectors, play an important role in setting the surface mixed-layer depth (e.g., fast extreme high wind events). Small-scale mixed-layer instabilities that are energetic in winter can also have a signature in sea surface height (Sasaki et al., 2020).

Table 3.1.2-1 Summary of surface feature expressions, with typical length and time scales of interest for S3NG-T.

Feature	Surface expression height scale	Space scale	Adjustment Time scale	Comments
Open ocean circulation	0.01-2 m	100-1000 km	30-100 days	Large scale circulation patterns expressed in sea surface height.
Mesoscale circulation	0.01-1 m	30-100 km	2-7 days	Highly variable with strong dependency on geographic location (e.g. central ocean gyres have little structure compared to western boundary currents) and ocean-atmosphere dynamics. Their size and characteristics depend on latitude (Rossby radius of deformation)
Sub-mesoscale features	0.01-1 m	<1-50 km	Hours to ~3 days	Highly dynamic features depending on horizontal gradients of mesoscale dynamics, and mixed-layer processes, varies with geographic location
Sea State (Hs)	0.01-25 m	<1 – 200 km	Minutes locally, up to seasonal and interannual scales	Hs includes elements of wind sea and swell and is highly variable locally and with geographic patterns. Wind sea associated with synoptic weather patterns at larger scales
Swell waves	0.01-8 m	<1 -200 km	Hours locally, up to seasonal and interannual scales	Swell wavelength of <100 m is ideally required, Swell systems captured at larger scales
Internal waves	0.01-1 m	<1 – 20 km	Hours to days	Localised phenomena with geographical variability
Tidal signature	<11 m	<1-1000 km	Hours	Periodic diurnal, semi-diurnal signals with large geographic variability around amphidromic points with M2 typically having the largest amplitude.
Internal tides	<2+ m	<10 – 100 km	Hours – days	Periodic diurnal, semi-diurnal signals with large geographic variability with M2 typically having the largest amplitude. Generated in locations of steep ocean floor topography.
River Water Surface Elevation	<25 m	<0.1m	Hours	Depends on flood state of river
Lake Surface Water Elevation	<25+ m	1-100+ km	Days to seasonal	Depends on season and water abstraction
Sea ice freeboard	<4 m	<1 km	Days to seasonal	Depends on sea ice dynamics and geographical location
Ice sheets	<100 m	<300m	Monthly	Significant changes at ice sheet margins

A measurable ocean surface height expression must thus be considered as the cumulative results of numerous local and remote factors. Interacting with larger scale flows, the influence of these random forces on the sea surface height is not trivial, and understanding the interplay between dispersion and confinement is essential for fluid transport processes as well as mixed layer dynamics. Table 3.1.2-1 provides a summary of surface feature expressions, with typical length and time scales of interest for ocean measurements of sea surface height (elevation above a reverence datum).

Sea state impacts the noise characteristics of an SSH measurement using radar range measurements: strong variability exists depending on the geographical location, with Hs values of up to 20 meters having been recorded by radar altimeter measurements, see Figure 3.1.1-2. The orientation of the wave and swell system to the altimeter ground track introduce additional complexity exacerbated by seasonal and interannual variability, leading to spatial and temporal correlated uncertainties – particularly when using SAR techniques in the presence of swell (e.g. Rieu et al, 2021). This implies that ocean swell measurements are required to interpret altimeter measurements in the presence of swell. In the case of energetic ageostrophic features at smaller scales (tens of metres to a 10-20 km), they have much shorter lifetimes (~hours to a few days) and ideally require a staring (e.g. geostationary orbit) altimetry sensor capable of sub-hourly temporal resolution (this is not available).

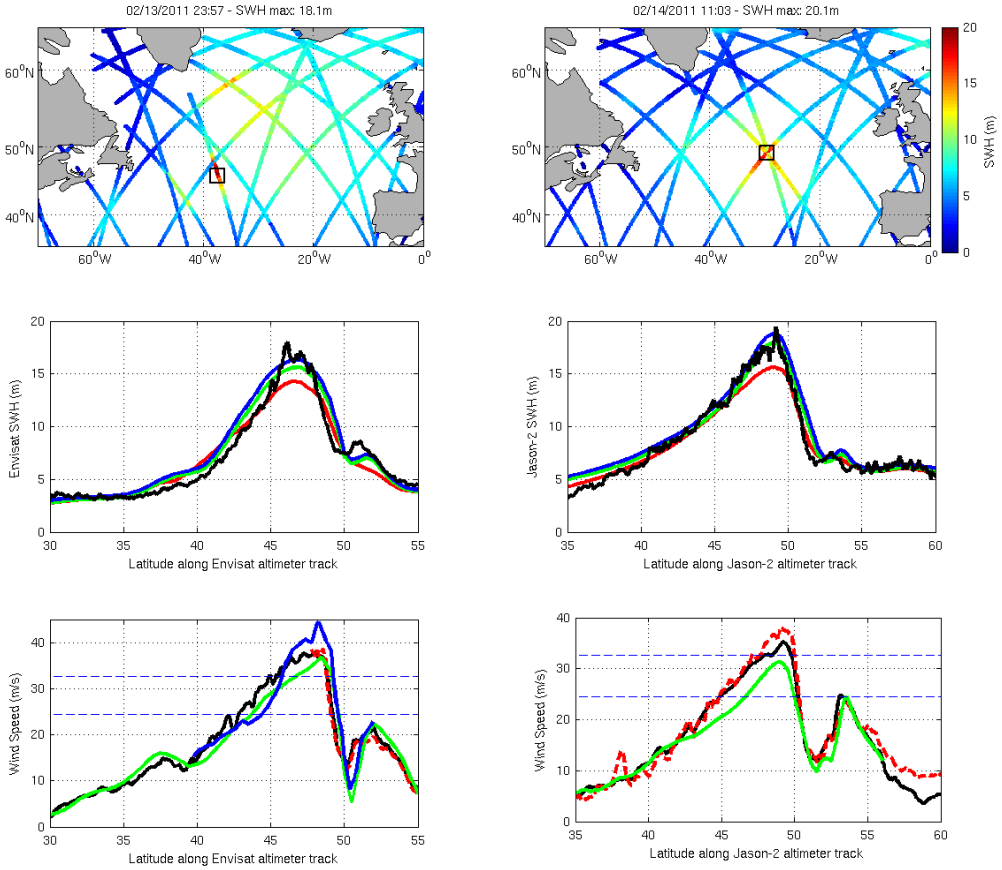

Figure 3.1.1-2 (top, left) Altimeter Hs measured by four altimeters (Jason-1, Jason-2, ERS-2, and Envisat) on 13 and (top, right) 14 Feb 2011. Such exceptional values were emphasized by Bancroft (2011) issue of MWL: "Altimetry data from 1100 UTC on the 14th [. . .] reveal seas as high as 66 ft (20.1 m), the highest the author has seen in this type of imagery." The black square in the left (right) panel indicates the location of the most extreme sea states measured during these two days by the Envisat (Jason-2) altimeter, respectively. (middle, left) Focus on the altimeter (black) Hs values estimated along the Envisat and (middle, right) Jason-2 tracks indicated by the squares boxes In the top panel above, and computed from the WW3 model forced by ECMWF (red), NCEP (green), and NCEP+10% (blue) winds. A running average has been applied to the altimeter data (~5-km resolution) to better match the resolution of the WW3 model (0.5°). (bottom, left) Wind speed from different sources interpolated on the same Envisat and (bottom, right) Jason-2 altimeter tracks. For both panels, black (green) lines give the altimeter (NCEP) wind speed. For the left (right) panel, the dashed red line gives the ASCAT scatterometer (Jason-2 radiometer) wind speed. On the left panel, the blue line gives the Oceansat-2 wind speed. All estimates have been computed at the spatial resolution of the NCEP fields. The dashed blue lines show the storm force (V ≥ 24.5 m s-1) and hurricane-force (V ≥ 32.7 m s-1) wind thresholds. A running average was again applied to the altimeter data to better match the resolution of the other data sources (~25 km). (from Hanafin et al., 2012).

3.1.3 Challenges in the coastal zone

In Europe, approximately 40% of the population lives within 50 km from the coast. Coastal zones are densely populated, exhibit high rates of inhabitant's growth and urbanization, concentrate economic assets and critical infrastructures, support green and blue economy and, therefore experience huge socio-economic and environmental changes (Geraldini et al, 2021). The Organization for Economic Co-operation and Development (OECD) note that by 2030, the 'Blue Economy' could outperform the growth of the global economy, both in terms of added value and employment. In the coming decade marine energy, marine biotechnology, coastal tourism, transport and food production sectors could offer unprecedented development and investment opportunities (EC, 2019).

A variety of International and European Union Directives relate to the coastal ocean and depend directly on the availability of ocean topography measurements.

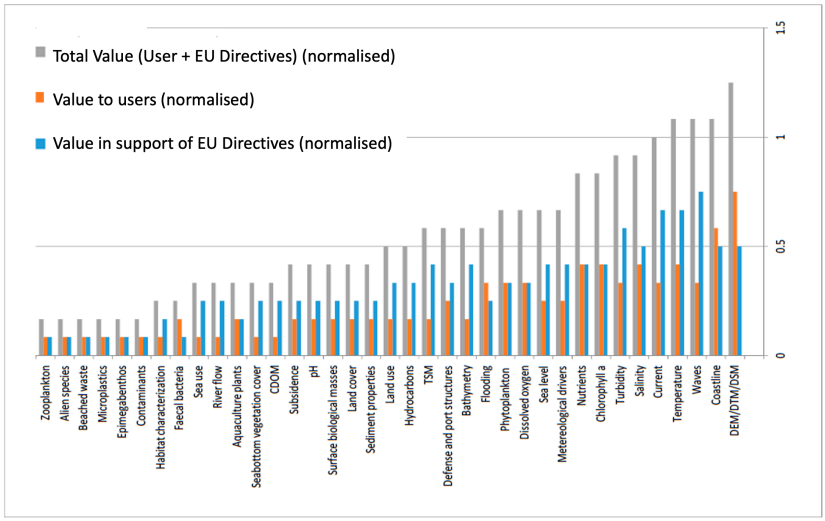

Figure 3.2-1. The most requested parameters for Coastal Ocean parameter linked to value by users and directives gathered from eighteen Institutions and Authorities in Italy (from User Needs Analysis for the Definition of Operational Coastal Services, Geraldini, 2021)

From the European Space Agency perspective, it is important to maintain a close connection to the user community and be fully aware of priorities and user needs. As an example, Geraldini et al (2021) recently provide an assessment for the importance of ocean currents, sea level, and waves for coastal applications linking their application to Maritime security (coordinated by EMSA) and the directives above for Italy. The methodology is applied to Italian institutional users, but it is scalable to the European level. Figure 3.2-1 shows that the most important variable derived from satellite altimetry, in terms of user need to address EC directives in the coastal region of Italy, is sea state (waves). Ocean currents, sea level and flooding are also highly ranked. The results provide a clear overview of the coastal user requirements, highlighting the common need of integrated information for coastal zone management (Geraldini, 2021). This example may not represent the user needs of all countries.

Coastal sea level, as observed at the shores of exposed coastlines, is strongly influenced by small scale and highly variable ocean currents and eddies, tides, and wave-induced processes (wave setup, wave runup, infra-gravity waves). Moreover, waves play an important role in sea level at the coast either directly (it has been demonstrated in CMEMS coupled wave/ocean system considering the role of wave-induced stress in improving the sea level estimate in severe storm conditions), or indirectly through their influence on the wind stress, storm surge (Marcos et al., 2019) and wave setup and runup. Therefore, coastal flood risk assessment and forecasting needs to use a wider range of wave parameters than basic significant wave height. Dodet et al. (2019) note limitations in our understanding of coastal sea-level variability due not only the lack of satellite information at the coast and the scarce frequency of co-located wave measurements in time, but also the lack of information on the wave period and direction.

Given the tremendous social, economic and biological value of coastal zones, an enhanced core monitoring of coastal zones is critical for a wide range of applications (coastal zone management, climate adaptation, coastal modelling, aquaculture, navigation and shipping, marine renewable energy, fisheries, oil spill management, search and rescue, disaster and emergency management, and academia), to respond to various policies (Marine Strategies Framework Directive (MSFD), Water Framework Directive (WFD), Bathing Water Directive (BWD), Marine Spatial Planning directive, Flood Directive, Integrated Coastal Zone Management (ICZM), Bathing Water, Common Fisheries Policy) and for resilience to climate change as expressed in the Copernicus user needs Staff Working Document.

3.2 S3NG-T and Copernicus Wave and Wind Monitoring and Prediction

Since an altimeter fundamentally measures the surface roughness characteristics (via the normalised radar backscatter) and then determines the radar range from these measurements, all satellite altimeters (nadir pointing or otherwise) inherently measure ocean waves. The radar backscatter return depends on the sea state through the mean square slope (mss) and is typically interpreted in terms of the surface wind speed through the correlation between mean square slope and surface wind (e.g. Cox and Munk, 1954).The normalised radar backscatter coefficient (Sigma0) is used to correct sea surface height measurements (via sea state bias), and derive estimates of the wind speed over the ocean at 10m height, U10.

Wave height (Hs) and wave directional spectra, $E(\varphi,\lambda)$, are of great importance for Marine Operations and Marine Emergency response (search and rescue, oil and other pollution) and fundamental to track Stokes velocities that control the dispersion and transport of marine Plastic Debris. Pollution of the seas from plastics and microplastics is one of the three major areas of the Strategy for Plastics (https://eur-lex.europa.eu/eli/dir/2019/904/oj) adopted by the Commission in 2018 and enacted into European Law on 2 July 2019; most of the proposed Actions are directly or indirectly related to marine litter, including its international dimension. In reference to the set of “maritime” requirements for the S3NG-T, the European Maritime Safety Agency (EMSA) compiled information on new/additional type of observational products that are needed

for search and rescue operations, sea surface pollution and vessel navigation/routing purposes.

Provision of wave data is a highly important component of Copernicus' mission to deliver both safety and socio-economic benefits to European citizens. Over the last decade the role of waves processes in influencing boundary exchanges between the ocean, the atmosphere, the cryosphere and land has had increased focus in terms of understanding and properly simulating the wider 'earth system', leading to a broader requirement to observe these phenomena to further develop atmosphere and ocean components of Copernicus systems. Within Copernicus, satellite derived wave information is used extensively. Within CMEMS, they are used by CMEMS Wave Thematic Assembly Centre (Wave TAC) and Monitoring and Forecast Centres (MFCs) and similarly used by analogues in National Meteorological Services and commercial forecast organisations. For marine operations downstream users have a fundamental requirement to use waves forecasts as part of any marine operational planning and execution. Typically, this is based on CMEMS services or via third parties exploiting Copernicus data. Similarly, design and renewable resource assessment projects have a primary requirement for consistent long-term datasets.

Multi-parameter requirement is in search and rescue and oil spill response activities (Christensen et al, 2018) for which EMSA are responsible. Recent research into these particle tracking problems has illustrated the need to better understand the two-way exchanges between atmosphere, wave and ocean and to better utilise the wave spectrum, for example in calculation of Stokes Drift effects (Rohrs et al, 2012). The need to continue to extend the geographic coverage of observations to higher latitudes, in order to correctly project further long-term loss of Arctic sea-ice and to stimulate research into processes driving sea ice growth/break-up/melting at ocean-ice-atmosphere interfaces, will also be important. This is critical as EMSA (and CMEMS) need access to the wind sea directional wave spectrum to estimate the Stokes drift and thereafter perform drift forecasting modelling for search and rescue, sea surface pollution (extremely important for modelling marine litter circulation) and vessel navigation/routing purposes.

Users tend to use products produced by a wave model and parameters derived from a directional wave spectrum including significant height and wave period, in their decision-making systems. Therefore, continuity and expansion are the key improvements, particularly if data are extended into the polar and coastal zones. Addressing coverage and continuity of basic Hs wave parameters ignores the growing number of more sophisticated users, such as heavy lift and pipelay marine contractors, coastal engineers and marine architects who have a clear need of wave period, direction and spectral wave information in addition to significant wave height (e.g. Lai and Slyozkin, 2014). All of these parameters can be derived from a well observed or modelled representation of the wave spectrum. Additionally, there is a need to determine swells waves for the whole of the European sea basin that can in part be resolved by Satellite altimetry (e.g. Moreau et al, 2018).

Well-calibrated and validated satellite data provide potentially more consistent baseline measurements of wave conditions over multiple decades than is achievable with current in-situ wave measurement networks, which use a variety of platform types and instrumentation with varying standards of data processing and quality control (e.g.

Durrant et al., 2010; Gemmrich et al., 2011; Timmermans et al., 2020). The importance of satellite data as a component of the observations-model mix used to underpin Copernicus and member states metocean services will only increase as new frontier regions, previously unobserved using in-situ methods, begin to be exploited (for example the Arctic). Utilising wave information to improve altimetry products is essential and well demonstrated for nadir altimetry. At high resolution, it becomes extremely challenging to separate SSH from sea state since the sea state defines the scattering surface to which a radar instrument responds and from which SSH is computed.

The so-called Sea State Bias (SSB) (e.g. Tran et al, 2010a, 2010b, 2006, Quartly et al. 2019) 'correction' is used to adjust the retrieved SSH to compensate for this effect although this remains one of the largest uncertainties in the SSH measurement. The ranging error due to ocean surface waves (the SSB) remains the largest source of uncertainty in altimeter sea surface height and sea level estimation (typically 3-5% of significant wave height). Sea state bias continues to be estimated through empirical mission-specific look-up tables based on significant wave height and wind speed, even though research indicates the critical need for new observations of wave period and directional wave spectra to finally make progress with this tenacious problem. As radar altimeters gain better sampling characteristics through unfocussed and fully focused SAR techniques (Egido & Smith, 2017) the impact of sea state becomes more challenging depending on the radar technology and geometry used. This is already apparent in moderate resolution nadir pointing altimeters such as Sentinel-3 (e.g. Boy et al., 2016, Moreau et al., 2018 amongst others) where swell systems may be detected when aligned orthogonally to the flight path of the altimeter.

Availability and quality of 2D wave spectra, wave period and wave direction information; extended coverage towards high latitudes (impact of waves on sea ice) and in coastal and shallow waters; higher temporal sampling; and observations co-located with atmospheric and ocean boundary layer parameters are all areas that will lead to an improved CMEMS service. In particular, extending the spectral domain over which wave data can be assimilated to shorter swells and maturing wind-seas should yield significant improvements in wave model predictive capabilities. Data assimilation techniques based on the use of the China France Oceanography Satellite (CFOSAT) SWIM wave directional spectra data (e.g. Hauser et al., 2020) reveal improved performance compared to traditional nadir only Hs measurements (e.g. Wang et al, 2021). CFOSAT wave products are included in the CMEMS product catalogue. Spectral and directional spectral sea state parameters are one of the most important measurements to support future evolution of CMEMS wave forecasting models, CMEMS ocean atmosphere coupled models and C3S coupled systems. This is because the exchange of heat, gas, and momentum occurs via the wave action at the sea surface. In additional, sustained global sea state observations for climate applications are clearly evident in the C3S user needs.

In reality, individual ocean surface waves are relatively small scale (order 10-100m) transitory phenomena, so the information used to describe waves more often focuses on statistics that describe the 'sea-state'; i.e. representing a population of waves sampled over a given time interval or spatial area. The most complete description of sea-state is provided via two-dimensional (frequency-direction) energy spectra, and it is the prediction of evolution of these spectra in space and time that is used as the basis

for state-of-the-art ocean wave forecast models. As a result, there is a critical demand for high quality measurement of ocean wave spectra in addition to derived parameters more normally communicated to users of wave data, such as significant wave height. However, for wave spectra there is a significant gap in observing capabilities. In-situ measurements, which are generally made at a point location, capture enough information to measure wave spectral statistics in frequency space, but will not have enough fidelity to fully represent the directional distribution of wave energy in complex cases (Ardhuin et al., 2019). Observations of wave spectra from satellites, made using a Synthetic Aperture Radar instruments such as those onboard Copernicus Sentinel-1, achieve a better two-dimensional measurement of spectral energy, but only robustly for a limited set of low frequencies (<0.08Hz, wavelengths >220m; Ardhuin et al., 2019) and with some dependency on the instrument track relative to wave direction. New capability to measure directional wave spectra from space was demonstrated recently for the first time with the Surface Waves Investigation and Monitoring (SWIM) instrument carried by CFOSAT. First results show great promise for measuring spectral properties of ocean waves in the wavelength range [70–500 m] and were shown to produce positive and significant impact in wave models when used in combined assimilation with Sentinel-1 (Hauser et al., 2020; Aouf et al., 2019).

Recent work of Altiparmaki et al (2022) demonstrated new techniques that exploit fully focused SAR processing of nadir altimeter data to provide 2D wave spectra estimates. This is a promising development for Sentinel-3 next generation topography.

Consolidating spaceborne observing capability to fill these observation gaps is needed not only to provide decision makers with near real-time observations of sea-state at high detail, but also to improve the evidence base used by models in deriving parameterisations of spectral evolution, better constrain such models through data assimilation at regional and global scales, and increase the evidence base of observed spectra that can be used in structural design studies. From a satellite observation perspective, this will involve new generation of satellites that can provide sustained measurements over the extended range of ocean wavelengths including significantly shorter wavelengths representative of high frequency wind-sea waves.

Whilst there are considerable benefits in extending the capabilities of satellites to measure the full wave spectrum, any future developments need to be mindful that, whilst general coverage of the global oceans by satellite instruments is good overall, revisit times to specific locations by individual missions (order of a week or more) remain relatively long compared to storm development timescales (order 1-2 days) and assimilation windows (order 6 hours). The issue of revisit time and coverage may be resolved through one or a combination of increased swath, level of orbit, or number of operational missions, but should also be considered in light of the application. For example, where long-period swells which cross ocean basins over timescales of days, are assimilated in global or ocean-scale wave models, the important requirement is that the swell field is sampled regularly along its track rather than repeat sampling a given point. A similar criterion is the primary requirement for measuring significant wave height in high and mid-latitude storm tracks. Conversely, when considering smaller systems such as tropical cyclones or short fetch coastal seas, revisit frequency becomes a limiting factor. Current revisit times, even with several operational missions flying, make it impossible, from satellites alone, to derive reliable statistics on extreme

wave parameters and associated impact on sea level (Marcos et al., 2019; Jiang, 2020).

In addition, the quality of wave data measured in shallow tidal waters and within a few kilometres of the coast still needs improvement. Although recent efforts in improving the processing of altimeter echoes in the coastal zone (for example through projects such as ESA COASTALT and ESA Climate Change Initiative for Sea State) have increased the number of significant wave height observations that can be correctly retrieved in the coastal zone, (Schlembach et al., 2020), implementing this in an operational context still remains a challenge. Additionally, both the revisit and data quality issues restrict the utility of satellite observations being used in real-time forecasting for regional applications in shallow shelf seas and, therefore, the impact of these data in Copernicus Marine Environment Monitoring Service (CMEMS) regional products.

The generic European Commission user needs demonstrate a potential tension between products to improve quality and extend the range of wave spectra and derived parameters retrieved versus maintaining/increasing coverage of the most commonly used significant wave height parameter. However, the clear fact is that no single or dual constellation of instruments can achieve the revisit times needed for data intensive applications such as regional wave model data assimilation. For example, a requirement provided from ECMWF is a revisit of 6 hours for a 75km x 75km grid box. The time window in this requirement is difficult to relax, since this represents a standard window for numerical weather prediction, but the required size of the revisited area will vary according to application, e.g. it is governed by the fetch areas in the region being modelled. Even with some relaxation of the spatial requirement this type of need can only be met by taking a multi-mission view. As a result, the requirement for a next generation instrument should be to optimise sampling and revisit times, at least maintaining the present contributions made by Copernicus instruments to the collective dataset. An enhanced sampling might be achieved through one, or a combination, of increased revisit time or use of multiple altimeter instruments enhancing the Sentinel-3 baseline.

There is a clear need for a next generation instrument to continue to provide directional wave spectral information and, further, to extend the range of wavelengths that can be robustly sampled to at least the limits of the SWIM instrument on CFOSAT (approximately 70 m) and, preferably, closer to the target set for the ESA EE9 SKIM concept of $\leq$30 m (Ardhuin et al., 2019). The difference between these wavelengths, when considered in wave period and associated wind speed terms are: for 70 m, approximately 7 seconds and for fully developed seas at a wind speed of 12 m/s; versus, for 30m, approximately 3.5 seconds for fully developed seas at a wind speed of 6 m/s This represents a substantial improvement in the range of sea-states that could be properly sampled by an instrument, leading not only to better estimation of the full wave spectrum but enabling use of the observations in applications requiring good specification of wind-sea, such as particle tracking, and making the observations more relevant to next generation modelling systems that will seek to directly represent the interactions between atmosphere, waves and ocean surface circulation. The shorter wavelengths are particularly important where the instrument observes regional seas with constrained fetch lengths. In terms of resolution, whilst the existing sampling

frequency of Sentinel-1 provides a target baseline, some relaxation may be preferable to widen the range of wavelengths that can be robustly observed. Any improvements in the available spectral data may also require review and update of Copernicus downstream products; for example, the addition of wind-sea components to swell partitions derived and distributed by CMEMS or, potentially, providing a 'First 5' spectral product that can be matched to the in-situ data equivalent.

For coverage, maintaining the strategy adopted by CryoSat-2 and Sentinel-3 to measure high latitudes will be increasingly important in view of the likely further diminishment of sea-ice coverage and future exploitation of the Arctic region. Similarly targeting robust retrievals of wave data at the coastline is needed. ECMWF have expressed a target proximity to the coast of 2 km, whilst a more relaxed target of 4 km could deliver a similarly high-quality coastal boundary condition and potentially reduce the difficulties in quality control involved where coastal infrastructure (e.g. major ports or coastal refinery complexes) extends from the land into the sea. However, rapid changes in sea state are known to occur within the final 1-2 km from land, invoking energetic small-scale processes (interactions with currents and shallow bathymetry) that dominate ocean-land interactions in the coastal zone.

Concerning the stability of the trend, the requirements for sea state stability should use the requirement for trend stability for regional sea level as a reference. The need on wave height trend accuracy for mean values and extremes is thus under 1 mm/year for coastal areas.

Finally, the range of sea-states that can be robustly sampled by the instrument needs to be considered. Existing altimetry carries the risk of under-sampling extreme seas in short lived storms, such as tropical cyclones, so calibration is limited for very high and phenomenal sea-states. Nevertheless, there is a strong requirement from a design perspective to limit uncertainty in the measurement of phenomenal sea-states; for example, 1-100 year return period significant wave height values in the northern North Sea of 17m or greater (Santo et al., 2016). Therefore, a target range of observation from 0.1m to over 20m significant wave height has been proposed by ECMWF. It is proposed that the objective for trends on Hs should apply to both the mean value and extreme values (up to percentile 99 and 100 year return period), given the relevance of the extreme coastal wave events for the coastal habitats and infrastructures. Based on this discussion a set of target requirements are provided in Table 3.2-1.

Table 3.2-1. Wave variable requirements for next generation Copernicus missions, based on User Needs provided by the European Commission.

Variable	Timeliness	Precision and quoted accuracy	Along-track sampling	Repeat Cycle	Spatial coverage
Significant wave height	95% of data within 3-hours	0.01m 5% or 0.1m	1-20Hz** along track	2 days	Global*, to within 4km of coast
2D wave spectra	95% of data within 3-hours	Spectra: 10% wavelength; 5 degrees direction; 10% energy	20x20km	2 days	Global

* Wave information is required to monitor coastal changes in waves due to interaction with bathymetry, setup, runup, breaking, refraction, diffraction, often happening in last hundreds of meters from coast.

** As global wave models evolve to finer resolution, a spatial resolution of 4-5 km can be expected by 2030. At this point a new standard is required when using along track Hs with better sampling than 1 Hz. 5Hz along track has been shown to better describe wave-currents interactions at the sea surface (lessons from CFOSAT mission). Note that Sentinel-3 data can already provide up to 80 Hz sampling along track in Level 1a products.

3.3 S3NG-T and Copernicus Hydrology Monitoring and Prediction

Inland water products from Copernicus are relatively new. They include inland water, wetness, snow and land ice products. Water levels are computed for lakes larger than 50 ha and intersections of major river networks. Lake water quality products and lake surface water temperature are produced according to the Global Lakes and Wetlands Database[6] (GLWD that provides water masks/classification for lakes and wetland) and the Water Framework Directive[7]. At pan-European level, Copernicus produces water and wetness products (permanent water, temporary water, permanent wetness and temporary wetness), a water and wetness probability index and water bodies' areas covered by inland water along the year. Copernicus at this stage does not provide regular information on rivers dynamics and especially on river runoff and overall hydrological dynamics, nor on under water systems. NG-TC should help to leverage substantially this gap within the Copernicus services. Moreover, the portfolio of Copernicus for hydrology and water is new and the user community is not yet fully identified. Major recognised users are the river basin authorities and agencies, regional and local authorities in charge of drinkable water, wastewaters, agencies in charge of agriculture, emergency services and hydro-meteorological administrations. It also includes private actors of the hydro-energy sector or the water transport. Communities working along the coastline where inland waters connect with the seas are also relevant. At global level, water Essential Climate Variables are produced to report to the International Global Climate Observing System program (GCOS). Considering GCOS requirements from https://gcos.wmo.int/en/essential-climate-variables/rivers/ecv-requirements Water Surface Elevation (WSE) Level is requested at ≤3 cm for Lakes, and ≤10 cm for rivers with trends of WSE levels ≤10 mm/decade.

Snow cover has a strong influence on the Earth's radiation and energy balance. Changes in snow extent tend to amplify climate fluctuations. This phenomenon needs to be well identified for the prediction of water balance, streamflow and river runoff in hydrological models used for water resource management, climate modelling and arctic/sub-arctic area monitoring. The key cryosphere parameters monitored within Copernicus are the area snow extent, snow water equivalent and lake ice extent.

Satellite radar altimetry currently provides an important source of Water Surface elevation (WSE) observations at 'virtual stations' where the altimeter ground track crosses the river centre line (Créteaux et al, 2017, Tarpanelli et al. 2020). The Sentinel-3 and Sentinel-6 missions provide, as a secondary mission objective, WSE estimates for a variety of targets and the use of such type of satellite measurements is growing

[6] https://www.worldwildlife.org/pages/global-lakes-and-wetlands-database

[7] Directive 2000/60/EC of the European Parliament and of the Council of 23 October 2000 establishing a framework for Community action in the field of water policy, OJ L 327, 22.12.2000, p. 1-73.

fast within the hydrology community. Sentinel-6 currently accommodates 31,805 targets of which 8,655 define rivers, 21,666 define lakes, 1,484 define reservoirs with no targets defined yet for glaciers. Sentinel-3A and B satellites include ~12900 virtual stations as of March 24th, 2021 (see also www.altimetry-hydro.eu). Sentinel-3 can be used to provide spatiotemporal characterization of wetlands floodplains and their connectivity to rivers and clear seasonal patterns can be seen where the satellite ground tracks cross these areas (e.g. Kittel et al., 2021). Altimeter WSE data have also been used to calibrate and refine hydrological models (e.g., Domeneghetti et al., 2014; Dubey et al., 2015; Finsen et al., 2014; Schneider et al., 2018).

Although not straightforward, rating curves establish a functional law between altimetric water height and in situ discharge observations for each river virtual station (e.g. Tarpanelli et al. 2020). Rating curves rely on knowledge of simultaneous discharge and water elevation. Rating curve might not be stable in time due to the impact of high-flow flood conditions modifying the channel form. Furthermore, in situ measurements from a river gauge are rarely located at the same location as a satellite altimeter virtual station, requiring careful consideration of the different conditions at the virtual station and the physical station.

Satellite altimetry and WSE processing techniques have steadily evolved over the last 25 years to provide a technique that is capable of resolving the height of river and lake WSE above a reference datum to an accuracy of multi decimetres at best over rivers, uncertainty could be much lower over very big lakes (e.g. Frappart et al., 2008; Medina et al., 2008; Biancamaria et al., 2017; Tarpanelli et all., 2020; Vu et al., 2018; Villadsen et al., 2016). This has important implications for successful monitoring of wetlands and floodplains with small fluctuations in WSE level (e.g., Dettmering et al., 2016). Jiang et al. (2020) evaluate a number of nadir altimeter retrackers for WSE using in situ measurements and for 26 Virtual Stations in plain areas achieved a root mean square error (RMSE) ranging from 0.12 m to 0.9 m. For 24 other virtual stations, the RMSE was over 1 m. In a following paper, Jiang et al. (2023) showed that Sentinel-3 Near real Time (NRT) products provide similar RMSE than Non Time Critical (NTC) products, when compared to in situ data at 25 locations. A recent literature review over 2018-2022 concerning altimetry over inland has been performed by Kossieris et al. (2024). They find that Sentinel-3 was used in almost half of the reviewed papers and is therefore the most used altimeter mission in the articles published between 2018-2022. Median RMSE between Sentinel-3 and in situ data on WSE ranges between a little bit more than 0.1 m to 1.4m. For some lakes, RMSE lower than 0.1m can even been obtained. This RMSE are provided for WSE anomalies (i.e. the temporal mean is removed from in situ and Sentinel-3 WSE time series), as in situ gages and Sentinel-3 tracks are not colocalized. The ability to measure river WSE depends on river width, the river reach orientation to the satellite ground track, the surrounding topographic relief, land cover (and especially the number of other water targets near the river), and features of the satellite altimeter. These aspects complicate received nadir-altimeter waveform shapes (multiple peaks) and the impact of snagging on off nadir targets. Another approach that could be applied is the fully focused SAR, which can obtain an along-track resolution of 0.5 m (Egido and Smith, 2017). This smaller footprint could differentiate different targets along-track but still be subject to across-track heterogeneous surfaces. Technically, this issue can be potentially solved by across-track interferometry if future missions can operate in SARIn mode. This has been

demonstrated for the CryoSat-2 SARIn over coastal regions and sea ice (Abulaitijiang et al., 2015; Armitage and Davidson, 2014, Di Bella, 2018; 2020; 2021). An extension to this approach could include swath InSAR altimetry to provide spatially distributed water surface elevations, but also slope and water mask and water level width in a river that are important variables for estimating river discharge (e.g. Durand et al., 2023). Swath altimetry may also provide estimates of river slopes and water extent.

With the recent increase of high-resolution spatial observations and computing performances, hydrological models are gaining global scale capabilities at constantly higher spatial resolution. Yet, despite academic efforts to make models more realistic – by adding more processes in their parameterisation for example – hydrological observations are still of priority importance, especially global scale observations. At global scales, in situ networks are heterogeneous in space and time coverage and need to be completed with satellite missions. First, such observations are necessary to characterise the model performances and identify missing processes that become non-negligible at higher resolution. Second, many previous studies (e.g. Emery et al., 2018; Leroux et al., 2016; Michailovsky et al., 2013; Munier et al., 2015) have demonstrated the added value of assimilating satellite observations into hydrological models (for instance for a better representation of the water cycle at different scales). Jiang et al. (2019) recently evaluated the value of different spatiotemporal measurement densities for hydrologic models and highlighted the benefit of high spatial distribution of CryoSat-2 data (when available) and Envisat data. While some variables of the hydrological cycle can be estimated at a low temporal frequency (groundwater level, snow cover), high spatial and temporal sampling is necessary for river height measurements, which intrinsically contain a lot of information on the hydrological processes taking place in the watershed. High spatial and temporal samplings of river height observations are required to take full advantage of assimilation techniques and to avoid potential discontinuities. Finally, assimilation techniques can be used efficiently to improve initial conditions in forecasting systems (floods and low-flows), with an expected positive impact at short to medium term for hydrology (up to few weeks).

Although the Sentinel-3 and Sentinel-6 missions have been optimised to observe oceans, considerable effort and design features are included (and are continuously evolving e.g. the Sentinel-3C/D units have a larger OLTC to support WSE monitoring) to demonstrate the retrieval of WSE from space in an operational context. Compared to early work using Jason-2 and Jason-3, Sentinel-3 provides better along track resolution in SAR mode and better coverage of water bodies using the Open-Loop Tracking Command (OLTC) that is specifically computed for land surfaces. The Sentinel-6 satellites perform even better over in-land water bodies since they combine the use of an OLTC with an altimeter operating in interleaved (open burst) mode.

3.3.1 Sentinel-3 baseline capability for Hydrology

As the user community for Copernicus WSE measurements is increasing, S3NG-T will now include WSE measurements as a primary mission objective by the European Commission (SWD, 2019). The primary driving user need over land surfaces is to provide sufficient measurements that, when used together by the next generation of operational hydrology systems within CGLMS and climate monitoring by C3S, are capable of:

- resolving river stage height for rivers having widths of ≥100m;
- lakes and reservoirs stage height with areas above 250 m x 250 m, i.e. 0.0625 km^2;
- monitoring wetlands and flooded areas.

The current time-series of the Sentinel-3 mission has demonstrated excellent feasibility for WSE measurements in an operational context and, together with other Copernicus data, provides an approach to develop operational flood forecasting and drought monitoring in support of rapid emergency response and decision-making (Tarpanelli et al. 2020). The challenge for S3NG-T is to improve the density of virtual stations and revisit time.

The Sentinel-3 altimeter tracking function aims at acquiring the echoes inside the instrument reception window. Using the Open-Loop Tracking Command (OLTC) mode, the reception window is no longer based on the analysis of previous echo position (Closed-Loop mode, or “autonomous mode”), but is defined using an a-priori elevation information, stored on-board in the OLTC tables, also called pseudo- Digital Elevation Model (DEM). The OLTC table includes a location (longitude and latitude coordinates) and an elevation value with respect to a vertical reference (e.g. geoid or ellipsoid). In the current Sentinel-3 OLTC tables, input data used for hydrology target location are:

- Contours defined in water body databases,
- Virtual Stations network (crossing between a water body and the satellite ground track),
- Global surface water mask,
- Water body databases,
- Definition of Dentinel-3 Virtual stations,
- Global and regional-to-local DEM

The OLTC hydrology targets are catalogued at the https://www.altimetry-hydro.eu/ website.

The success of the OLTC approach (especially in regions of highly variable vertical terrain especially for steep-sided river valleys and lakes in mountainous regions) relies on the definition and the accuracy of the on-board DEM stored in the OLTC. Considering the reception window width (60 meters), uncertainties in echoes centring and some margin to account for potential variations (shift of the on-ground satellite track, atmospheric propagation delays), the target elevation stored within the OLTC must have a ±10 m accuracy to ensure a correct echo acquisition. This level of accuracy is sometimes difficult to obtain in some regions where input data are not accurate enough e.g. mountainous regions), or when the water topography could have changed since the DEM has been acquired (e.g. dam built after the DEM has been made). For the OLTC memory on-board Sentinel-3 (A or B) the theoretical maximum number of virtual stations that could be included in the onboard OLTC tables is 140,000. Sentinel-3C and D have larger onboard memory for the OLTC and thus more virtual stations can be acquired.

Since the OLTC tables memory on-board Sentinel-3A and –3B is limited to 4 MBs only OLTC table points corresponding to input target location (users database) or to water surfaces are coded. An efficient compression algorithm is further applied to reduce the size of the on-board OLTC tables. Hence, the on-board OLTC tables are not optimal and are considered as a “pseudo-DEM” meaning that elevation is not defined at each

point of the satellite position along the orbit. Despite all these precautions it is not always possible to build OLTC tables that can be accommodated by the on-board memory. In this case, areas of interests (geographical patches) defined where the altimeter is operating in OLTC mode: outside these areas, the altimeter is operating in Close-Loop (autonomous tracker) which is not as efficient as Open-Loop mode for some hydrology targets. Figure 3.3.1-1 shows the locations of points in S3A OLTC table. On-board OLTC memory has been extended for Sentinel-3C and Sentinel-3D units to accommodate the growing need of the Copernicus hydrology community.

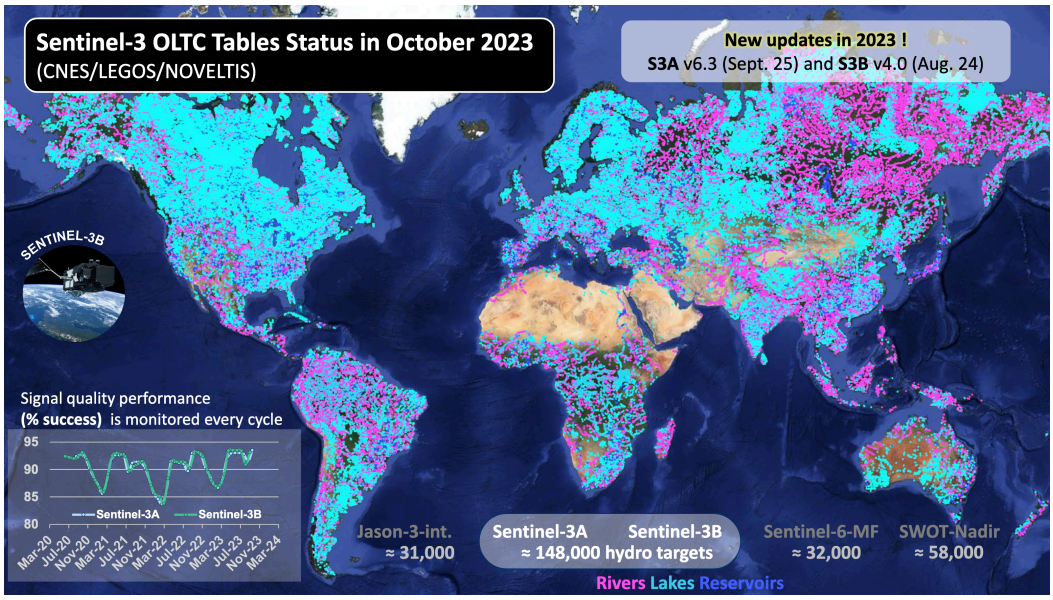

Figure 3.3.1-1 Map showing the locations of Sentinel-3A river and lakes targets within the mission OLTC facility as of September 2020. A similar map shows targets for Sentinel-3B. (https://www.altimetry-hydro.eu).

Users can enter the Sentinel-3 OLTC database to define and request hydrology target acquisitions. Since a large user base is anticipated exploiting a continuous 20+ year time series of Sentinel-3 hydrology data acquired over targets along the ground track of the satellites at the time of S3NG-T launch, maintaining continuity for the majority of these measurements, while expanding to cover more targets, is a priority for the European Commission and Copernicus.

3.3.2 Addressing Copernicus user needs for Hydrology Monitoring

The main variable of interest corresponds to water surface elevation (i.e. distance between the top of the open water surface and a reference surface, a geoid or ellipsoid).

Large and medium rivers and lakes, targeted as high priorities, have water level variations from low to high flows between a meter to several dozen metres. Therefore, to observe their seasonal variations, a vertical uncertainty around a dozen centimetres is needed, as stated in most EC users' needs (at least for the lowest vertical resolution needed, as there is also a demand for 5 cm vertical uncertainty). Of course, it is the order of magnitude of the vertical uncertainty which is important rather than its strict

value. Currently, water elevation from nadir altimeters can have RMSE compared to nearby in situ measurements between 10 cm to a few metres. However, in general, these errors are closer to multiple decimetres than only 10 cm. Thus, a vertical uncertainty between 10 cm and 15 cm after aggregating over 1 km^2 of water surface will drastically enhance the capability of Sentinel-3 and user applications. For hydrology, although WSE is the main parameter of interest, having access to sigma0 is also of interest to discriminate possible targets (especially open water).

Tourian et al. (2016) adopts an interesting approach in which WSE derived from different satellite altimetry missions is transferred to a specific virtual station using the wave travel time hydraulic concept. This improves the sampling frequency to 3–4 days (Tarpanelliet al. 2020). Although not yet demonstrated in orbit, InSAR swath altimetry could potentially estimate river surface slopes directly. Assuming sufficient measurements from several satellites to sample a flood wave, these measurements could be used to potentially track and potentially quantify long and smooth flood wave propagation in big river basins like the Amazon or the Ganges/Brahmaputra. In large to medium rivers (as small as 100 to 150 m width) such waves propagate within a river network: if this network is long enough impacts may last weeks or more from the river head to the river mouth. The first demonstration of this technique will be in 2023/24 as part of the NASA/CNES SWOT mission.

Rather than constraints on the orbit, the most important target for hydrology is the continuity of time series, i.e. to observe at least the same locations than Sentinel-3 and Sentinel-6 (potentially few kilometres up or downstream) for most virtual stations. The time sampling should not be coarser than 27 days (the smaller, the better). If two swath altimeters were deployed within the S3NG-T with appropriate orbits, they could observe 99% of the hydrology targets (lakes, reservoirs and rivers) defined within the Sentinel-3A (OLTC) table version 6.0 and Sentinel-3B OLTC table version 3.0. The 1% unobserved targets are at less than 9 km from a swath edge and at a median distance of 3.5 km. Therefore, there should be upstream or downstream observation(s) within few kilometres of these unobserved targets (although the time series at those locations would be broken).

Concerning Sentinel-3 uncertainties, Jiang et al. (2020) validated S3A SRAL SAR measurements against 50 in situ measurements over Chinese rivers. For 26 stations Root Mean Square Errors (RMSE) on the water elevation anomalies (i.e. temporal mean removed) are between 12 cm and 90 cm, for the other virtual stations RMSE is above 1 m, while Chen et al. (2023) find smaller values as in global statistics. Bogning et al. (2018) found RMSE between 20 cm and 40 cm for S3A over the Ogooué River. For 8 ice-covered very big lakes with area above 5,000 km2, Shu et al. (2020) obtained RMSE on anomalies below 10 cm, but biases (not taken into account in the RMSE) in between few cm to more than 10 cm, for S3A. However, for the remaining seven studied lakes (area below 5,000 km2) the RMSE is above 13 cm with few decimetre biases. Gao et al. (2019) found RMSE for two reservoirs in Spain of 16 cm and 28 cm for S3A. There are no performance figures available for an InSAR swath altimeter until the NASA/CNES SWOT demonstration mission flies in 2023/24 (a requirement of 10cm uncertainty for targets of 1km^2 is declared). More generally, large and medium rivers and lakes, targeted as high priorities for S3NG-T, have water level variations from low

to high flows between a meter to several dozen metres. Therefore, to observe their seasonal variations, a vertical uncertainty of ~12 cm is needed as stated in most EC users' needs (at least for the lowest vertical resolution needed, as there is also a demand for 5 cm vertical uncertainty). As mentioned, it is the order of magnitude of the vertical uncertainty which is important rather than its strict value.

Very big lakes behave as ocean surface and are the only few targets over continental surfaces where nadir altimetry can provide less than 10 cm RMSE. For such targets, ocean requirements hold. But for others, the current uncertainty is above 10 cm. This high variability in water elevation uncertainty is due to the fact that hydrology was considered as secondary objective for S3. For S3NG-T, ensuring that the instrument is designed to also observe open water on continental surfaces should enhance capability to observe inland waters. Having at least a requirement of few decimetres (in between 10 cm to 20 cm) for surface water elevations over inland waters should guarantee not just continuity of observation, but also enhance such observations.

Having a quasi-global coverage will also greatly improve the spatial sampling obtained from nadir altimeters, by leveraging the fact that nadir altimeters provide measurements only along their track. This will help to observe many water bodies currently not observed with in situ gauges or with nadir altimeters. It has been estimated that a near current constellation of nadir altimeters (AltiKa on its nominal orbit, Jason-3, Sentinel-3A and Sentinel-3B) could only observe 35% of total annual lake storage change. For rivers, S3NG-T should observe water elevation for many more watersheds than is currently the case with in-situ gauges. Moreover, providing some estimates of river slopes and lake storage change, which is difficult to do only with a limited number of nadir altimeters, will help to compute water fluxes at the continental scale, which are of prime importance for users.

The spatio-temporal sampling of water surface signatures at the scale of river networks is a crucial aspect determining the range of flow dynamics and which hydrological inverse problems can be addressed with the considered observation. Allen et al. (2018) also provide global approximation of flow wave travel time, based on gauge measurements and kinematic wave model outputs. They focus their study on celerity at bankfull flow, when waves should exhibit their peak velocity. They estimated that the global median celerity is around 1.6 m/s (with an uncertainty range of 0.7 to 3.3 m/s), the highest celerity being found in mountain regions, whereas the lowest are logically found on low slope lower part of river basins near their outlets. They also estimated that it takes 6 days (median value, with an uncertainty range of 2 to 13 days) for flow waves to propagate from the upstream part to the outlet of a basin. Of course, the smaller the basin, the shorter the propagation time. Basin sizes of big to medium basins targeted as highest priority are important and flow wave celerity in the downstream part of the basins are low (e.g. for river network length > 5,000 km, the flow celerity is estimated to be < 0.5 m/s).Therefore, a mean revisit time of around 10 days should be sufficient for such basins and will fulfil the need for few weeks to monthly products, as stated in EC documents.

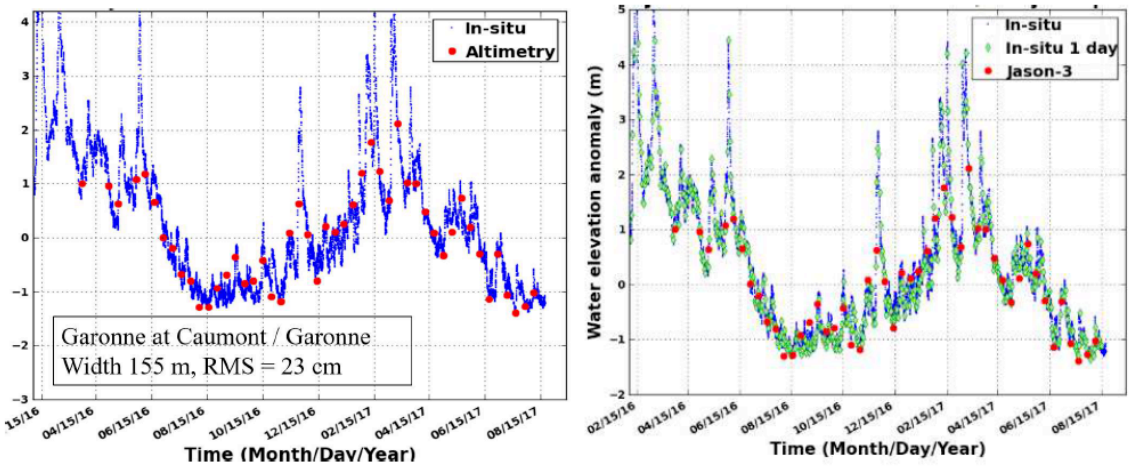

Figure 3.3.2-1. Garonne water levels observed with sampling time <15 minutes (in situ: blue), 10 days (Jason3: red), 1 day (in situ: green) (Blumstein et al, 2019).

The CNES SMall Altimetry Satellites for Hydrology (SMASH) mission (Blumstien et al., 2019) is designed to overcome current space altimetry missions low revisit frequency and complement in situ hydrology stations networks in regions where the data are sparse or inexistent. While the EC documents highlighted the need for daily, weekly and monthly time sampling, Fekete et al. (2012) highlight the need for 1-day revisit for hydrology targets in order to sample high frequency variability in river WSE, especially to better observe river flow dynamics (see Figure 3.3.2-1).

Hossain et al. (2014) have been able to design a 5 to 10-day lead-time forecasting tool in Bangladesh based on Jason-2/3 IGDR products, which are available less than a day after the measurement. Because of the vertical uncertainty of Jason-2 measurements (more than 20 cm at the virtual stations), some limitations in the space/time sampling of Jason-2/3 and some limitations in the modelling are found. This tool is used by the Bangladesh Flood Forecasting Centre operationally as a “decision support tool”, rather than directly as an official alert level forecast system.

S3NG-T measurements could be used “offline” to calibrate models or do reanalysis. For forecasting, however, a near real time product with time latency between a few hours to a few days is compulsory. Blumstien et al. (2019) state that a timeliness of 6 hours is required, which is much less than the NRT3H timeliness of Sentinel-3 today.

To conclude, the primary focus of S3NG-T for hydrology should be the medium to big rivers (> 100 m width) and lakes/reservoirs (areas above 250 m x 250 m, i.e. 0.0625 km^2) with a time sampling resolution from ~1 day (Femke et al., 2012) to monitor river dynamics and 1-10 days to monitor lake and reservoir levels leading to a decadal time series. A WSE of ≤10 cm is required. More information on these requirements is provided in next paragraphs. The rationales for these sampling capabilities are the following:

- it will provide many more observations and a continuity of observations for basins that are currently sparsely observed with in situ measurements,

- it is compliant with the resolution of regional/global hydrology models, which need observation for calibration, validation, assessing the missing physical processes and even for assimilation,
- many big basins (Amazon, Congo, Niger, Ganges/Brahmaputra, Mekong, etc.) are transboundary basins, where downstream countries do not have any information on the state of the resources upstream and therefore have fewer possibilities for forecasting floods or droughts,
- reservoirs (and even lakes) that have the most influence on river networks and associated populations living in the watershed have volume change dynamics in line with these sampling characteristics,
- it will provide key components for studying water budget at the watershed scale and/or at global scale over long time periods over a decade or even longer including the time series of past, present and future altimetry missions.

By addressing these aspects in the S3NG-T, Copernicus will be able to deliver new hydrology information to address European Policy and directives as requested in the SWD (2019).

3.4 S3NG-T and Copernicus Cryosphere Monitoring and Prediction

The Earth's cryosphere plays a critical role in our planet's radiation and sea level budgets, and several Essential Climate Variables (ECVs) are associated to the cryosphere (https://gcos.wmo.int/en/publications/gcos-implementation-plan2022). Loss of Arctic sea ice is exacerbating planetary warming owing to the ice-albedo feedback (e.g. Budyko, 1969; Serreze and Francis, 2006; Screen and Simmonds 2010), and loss of land ice is the principal source of global sea level rise (Chen et al. 2013; Horwath et al; 2022). Moreover, the high latitude seas provide fundamental ecosystem services (including fisheries management and other resources), sustains numerous indigenous communities, and due to sea-ice loss are emerging as a key area for economic exploitation. But the fragile ecosystems are subject to pressures from a growing number of maritime and commercial activities.

Sentinel-3 reaches 81.5° N and S of the equator covering sea ice and ice sheet regions. The following user needs stem from the need to maintain continuity of the current Sentinel-3 mission capability.

- Maintain ocean topography measurements from the open ocean and into the polar seas. This will contribute to the observation system for global observation of mean sea level, mesoscale and sub-mesoscale currents, wind speed and significant wave height in the Polar regions. These measurements are fundamental inputs to operational oceanography and marine forecasting services in the polar oceans.
- To support applications related to coastal and inland waters. Observation of water level at Arctic coasts as well as of rivers and lakes is a key quantity in hydrological research. Rivers and lakes not only supply freshwater for human use including agriculture but also maintain natural processes and ecosystems. The monitoring of global river discharge and its long-term trend contributes to the evaluation of global freshwater flux, which is critical for understanding the

mechanisms of global climate change. Moreover, the frozen rivers and lakes are important navigation routes in the Arctic regions, which encountered dramatic changes in the context of global warming. Their observation could help forecasting their evolutions and organizing alternative modes of transport.

- In synergy with other satellite missions, measure and monitor variability of Arctic and Southern Ocean sea-ice thickness. Seasonal sea ice cycles are important for both human activities and biological habitats. The seasonal to inter-annual variability of sea ice is a sensitive climate indicator; it is also essential for long term planning of any kind of activity in the Polar Regions. Knowledge of snow depth over sea ice is necessary to derive improved accuracy in measurements of sea-ice thickness and is also a valuable input for coupled atmosphere-ice-ocean forecast models. On shorter timescales, measurements of sea-ice thickness and information about Arctic Ocean sea state are also essential support to maritime operations and ship routing over polar oceans.
- In synergy with other satellite missions, measure and monitor the surface elevation and elevation changes of polar glaciers, ice caps and the Antarctic and Greenland ice sheets. The ice sheets of Antarctica and Greenland store a significant proportion of global freshwater volume and are important for climate change, the water cycle and contributions to sea level. Monitoring grounding line migration and elevation changes of floating and grounded ice sheet margins is important to identify and track emerging instabilities, which can negatively impact the stability of the ice sheets, leading to ice mass loss and ultimately result in accelerated future sea-level rise.

The Arctic Ocean is changing dramatically responding to significant global atmospheric warming by pan-Arctic sea-ice retreat and thinning (e.g. *Meier et al.,* 2014; *Werner et al.,* 2016). The rise in Arctic near-surface air temperatures has been more than twice as large as the global average in recent decade (e.g. *Serreze and Francis,* 2006) that is called ‘Arctic amplification’ (*Kellog,* 1975) although the underlying causes of Arctic amplification remain uncertain (e.g. *Screen and Simmonds,* 2010). Arctic amplification is the outcome of many complex and interrelated feedback mechanisms and processes (e.g. longwave radiation flux changes caused by e.g. changes in cloud type and cover, ice albedo feedbacks, changes in heat fluxes between the atmosphere and ocean due to changes in sea ice extent). It is expected that the Artic Amplification will become stronger in the near future (ref: https://doi.org/10.1016/j.gloplacha.2011.03.004).

Measurements of geophysical and societal change provide the evidence to underpin the establishment, implementation and monitoring of policy, policy decisions and their impact, not just in Europe, but across the world. In the Arctic region, several extreme concerns have been recently raised by the International Panel for Climate Change (*IPCC,* 2018):

- Warming greater than the global annual average is being experienced in many land regions and seasons, including two to three times higher in the Arctic with warming generally higher over land than over the ocean.
- Climate related risks for natural and human systems are higher for global warming of 1.5°C than at present. These risks depend on the magnitude and rate of warming, geographic location, levels of development and vulnerability, and on the choices and implementation of adaptation and mitigation options.

- There is high confidence that the probability of a sea-ice-free Arctic Ocean during summer is substantially lower at global warming of 1.5°C when compared to 2°C. With 1.5°C of global warming, one sea ice-free Arctic summer is projected per century. This likelihood is increased to at least one per decade with 2°C global warming. Effects of a temperature overshoot are reversible for Arctic sea ice cover on decadal time scales.
- Populations at disproportionately higher risk of adverse consequences of global warming of 1.5°C and beyond include disadvantaged and vulnerable populations, some indigenous peoples, and local communities dependent on agricultural or coastal livelihoods. Regions at disproportionately higher risk include Arctic ecosystems, dryland regions, small-island developing states, and least developed countries. Poverty and disadvantages are expected to increase in some populations as global warming increases; limiting global warming to 1.5°C, compared with 2°C, could reduce the number of people both exposed to climate-related risks and susceptible to poverty by up to several hundred million by 2050.
- Limiting global warming to 1.5°C compared to 2ºC is projected to reduce increases in ocean temperature as well as associated increases in ocean acidity and decreases in ocean oxygen levels. Consequently, limiting global warming to 1.5°C is projected to reduce risks to marine biodiversity, fisheries, and ecosystems, and their functions and services to humans, as illustrated by recent changes to Arctic sea ice and warm water coral reef ecosystems.

These changes may lead to dramatic consequences as discussed by *Stephen* (2018) who describes the societal impacts of a rapidly changing Arctic. Climate change and globalisation are the dominant drivers of societal impacts in the Arctic. As the climate changes, access to the Arctic is improving and, through globalisation and new economic development, a rapid transformation of the environmental and geo-political environment of the region is in progress. While there is a strong desire for sustainable development of the fragile Arctic environment at both the national and international level, significant societal impacts are inevitable.

The societal impacts of a rapidly changing Arctic are thus complex, uncertain and ambiguous. In response, the European Commission and the High Representative of the Union for Foreign Affairs and Security Policy issued to the European Parliament and the Council, on 27 April 2016, a joint communication that proposed "*An integrated European Union policy for the Arctic*". The communication highlights the strategic, environmental and socio-economic importance of the Arctic region, including the Arctic Ocean and adjacent seas. The Arctic's fragile environment is also a direct and key indicator of the climate change, which requires specific mitigation and adaptation actions, as agreed at the COP-21 held in Paris in December 2015.

To this end, the "*integrated EU Arctic policy*" has identified and is addressing three priority areas:

1. Climate Change and Safeguarding the Arctic Environment (livelihoods of indigenous peoples, Arctic environment).
2. Sustainable Development in and around the Arctic (exploitation of natural resources e.g. fish, minerals, oil and gas), "Blue economy", safe and reliable navigation (e.g. the Arctic Northern Sea Route).

3. International Cooperation on Arctic Issues (scientific research, EU and bilateral cooperation projects, fisheries management/ecosystems protection, commercial fishing).

Continuously monitoring the vast and harsh Arctic environment in such a changing world with Earth observation, navigation and communication satellites (considering the sparse population and the lack of transport links) is considered essential to the successful implementation and effective management of the Integrated EU Arctic Policy.

The existing Copernicus programme already offers operational thematic services in the fields of atmosphere monitoring, marine environment monitoring, land monitoring, climate change, emergency management and security. For example, the CMEMS Arctic – Monitoring Forecasting Centre (ARC MFC) provides accurate forecast and reanalysis products for sea ice, ocean, biology and surface waves in the whole Arctic. The system is based on a numerical ocean model assimilating in situ and satellite data. The Copernicus Atmospheric Service (CAMS) provides information products about atmospheric composition and solar radiation. Several products are of interest for the Arctic region including: monitoring and assessing the impact of emissions from fires at high latitudes (Canada, Siberia) and transport of the corresponding plumes of gases and aerosol affecting atmospheric composition in the Arctic region and monitoring and forecasting of the ozone layer, including Arctic “mini-holes” events. The Copernicus Climate Change Service (C3S) is developing new approaches to provide high-resolution regional climate-quality reanalysis over the Arctic and production of sea-ice and ice sheet Essential Climate Variables. In addition, Economic Sectoral analyses of Arctic shipping addresses the impact of climate change on ship routing issues.

A long-term programme to monitor the Earth’s polar ice, ocean and snow topography is important to both operational and scientific communities with interests in the Arctic and Antarctic. Europe has a direct interest in the Arctic due to its proximity. Changes in the Arctic environment affect strategic areas including politics, economics (e.g. exploitation of natural resources including minerals, oil and gas, fish) and security. It also has an indirect interest in the Antarctic due to the Antarctic Treaty, which permits international access in support of science. Besides economic impacts of Antarctic and Arctic changes (Whiteman et al, 2013), Europe’s interest in both Polar Regions is due to their influence on patterns and variability in global climate change, thermohaline circulation and the planetary energy balance. Last but not least, changes in the Arctic system have potential impacts on European weather, with consequences for extreme events (Francis, 2017). "An integrated European Union policy for the Arctic" (https://ec.europa.eu/environment/efe/news/integrated-eu-policy-arctic-2016-12-08_en) emphasises the strategic, environmental and socio-economic importance of the Arctic region, including the Arctic Ocean and adjacent seas. Continuously monitoring the vast and inhospitable Arctic environment with satellites (considering the sparse population and the lack of transport links) is considered essential. Following this, several guiding documents have been prepared in a European Commission-led user consultation process: Polar Expert Group (PEG) User Requirements for a Copernicus Polar Mission Phase-I report (12th June 2017), Duchossois et al. (2018a), hereafter referred to as PEG-1 report, and the Phase 2 report on Users’ requirements (31st July 2017), Duchossois et al. (2018b), hereafter referred to as PEG-2 report.

3.4.1 S3NG-T and Copernicus Sea Ice Monitoring and Prediction

Floating ice parameters are listed as the top priority for the polar mission user requirements by a collective of polar experts (Duchossois et al. 2018a,b). These parameters are selected considering the availability of existing Copernicus mission products and services of direct relevance to the Artic as well as their needs for improvement (e.g. in terms of spatial resolution, accuracy, repeat coverage, length of time series, etc) and the current level of technical and/or scientific maturity for some candidate parameters. Sea ice represents a group of variables, notably: concentration, area and extent, fast ice, thin, first- and multiyear ice, floe size, motion/drift, deformation, age, thickness, volume, snow cover/depth, freeze-up/melt time and melt pond coverage. Sea ice is thus a name for a number of variables. A critical aspect is the role of ocean waves that modify the sea ice parameters (concentration, fast ice, floe size, motion/drift, deformation, thickness, melt/freeze times). Other floating ice quantities include iceberg locations, drift and volume change as well as ice shelf thickness and extent.

Sea ice parameters from CMEMS are widely used for navigation, maritime security, coastal and marine environment, marine resources and weather and climate applications. With retreating sea ice due to global warming, we expect ice free conditions over vast areas of the Arctic Ocean. This suggests that we are no longer in a fetch limited Arctic Ocean and we will likely encounter more fully developed sea conditions. This has a huge impact for navigation and maritime safety and on the freeze/thaw regime in sea ice thickness. We can see a variety of shipping routes that will take advantage of open water conditions using routes that may even traverse the Arctic Ocean directly if sea ice conditions are thin enough. Climate models suggest that this is something to be considered in the 2030-2050 timeframe [Kim, et al., 2023].

As a secondary mission objective, Sentinel-3 provides measurements over sea ice derived from SRAL measurements along the ground track in SAR mode. Estimating Arctic-wide sea ice thickness on monthly time-scales was made routinely possible (e.g. Laxon et al. 2003, Tilling et al., 2018) with the advent of high-latitude satellite altimeters using altimeter range measurements to estimate sea ice freeboard (the height of the sea ice surface relative to local sea level).

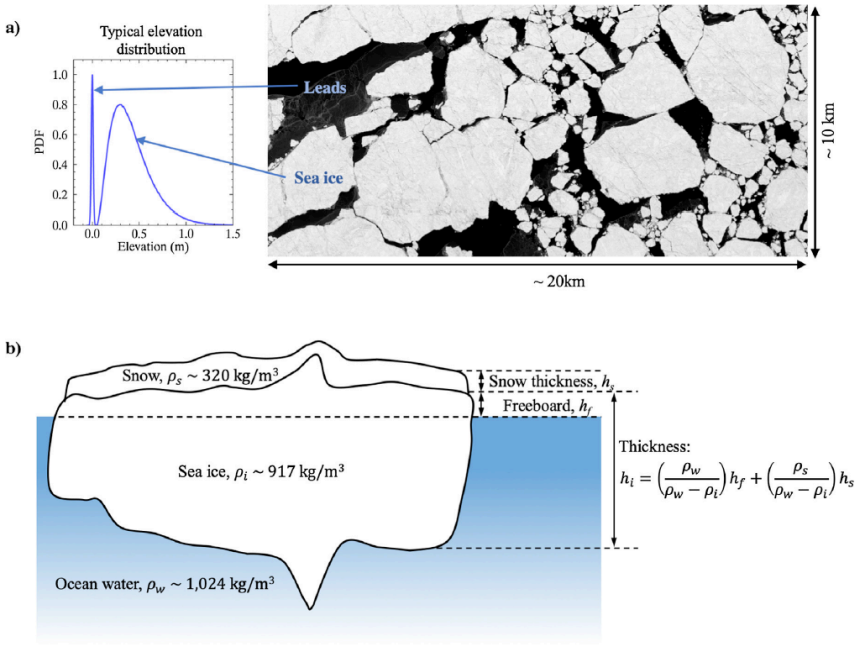

Figure 3.4.1-1 Typical elevation probability density function and spatial scales of sea ice and leads. (b) Side-profile view of sea ice (vertically exaggerated) showing the snow and sea ice layers, freeboard and thickness relations, and typical bulk densities. (from Armitage and Kwok, 2019).

Under the assumption that a sea ice floe is in hydrostatic equilibrium with the surrounding ocean, and assuming bulk values for the densities of the ice and ocean, and the density and thickness of the snow cover, freeboard can be converted to sea ice thickness. Lawrence et al (2019) derive radar freeboards from the Sentinel-3 and CryoSat-2 satellites are therefore expected to be consistent, and will provide essential continuity of the high-latitude radar altimeter time series into the 2030s. Based on 6-months of gridded data (Nov 2017 – April 2018), Lawrence et al (2021) report a mean radar freeboard for Sentinel-3A of 0.1 ±0.015 m. Mean freeboard differences between Sentinel-3A and CryoSat-2 are stable with monthly values between 0.9 cm and 1.1 cm ±0.07 cm. The standard deviation on the mean difference, which reflects the spatial variability of Sentinel-3A and CryoSat-2 differences is also stable across all months at 6.4 ±0.4 cm. The grid specifications are 1.5° longitude by 0.5° latitude grid, corresponding to grid cell dimensions of approximately 80 - 55 km at 60° latitude and 30 - 55 km at 81° latitude. A 2 cm intermission bias on sea-level anomaly, and a 1 cm offset between S3A and CS2 freeboard is attributed to different re-tracker configurations necessary for S3A when retracking leads and floes, Lawrence et al (2019). The increase in sampling resolution afforded by the combination of CryoSat-2, Sentinel-3A and Sentinel-3B data using orbit ground track files averaged over 30 days of data, shows significant improvements when using data from all three satellites. For a grid of resolution 1.5° longitude x 0.5° latitude, the addition of S3A and S3B data to the existing CS2 dataset can reduce the uncertainty on monthly gridded radar freeboard by a quarter on average (Lawrence et al., 2019). Sentinel-3 allows observations up to 81.5° latitude at ten-day frequency (only achievable with a month of CS2 data at the same resolution) allowing sub-synoptic changes both in sea ice volume evolution and

ocean circulation to be resolved. Vandemark et al. (2004) model the relationship between low-incidence Ka-band Sigma0 measurements to wind speed (via its relation to the ocean mean surface capillary wave slope variance), modified for low wind speeds to allow specular reflection. See Armitage and Ridout (2015) for details of the low-level Ka-band AltiKa processing over sea ice and Armitage and Kwok (2019) and Kacimi et al (2025) for an assessment of swath altimeter capability and performance expectations of over sea ice.

InSAR swath altimeter retrievals in the ice-covered ocean share more similarities with retrievals over inland river/lake surfaces than the open ocean: namely, mixed surface types within the swath (sea ice floes/leads vs. vegetation/river), mixed scattering behaviours from the different surfaces (bright and specular leads/rivers vs. lower backscatter sea ice floes/vegetation), and variable geometry and size of the different surfaces (see Armitage and Kwok, 2019). This means that, as for Hydrology Targets, either a performant on-board processing scheme is used or raw radar measurements with minimal on-board processing are available on-ground for further processing to retrieve sea ice parameters.

3.4.2 S3NG-T and Copernicus Ice Sheet Monitoring and Prediction

Sentinel-3 acquires data to support a range of secondary objective glaciological applications including monitoring ice sheet elevation and elevation change.

Ice sheet parameters are listed in the requirements by a collective of polar experts (Duchossois et al. 2018a,b). These parameters are selected considering the availability of existing Copernicus mission products and services of direct relevance to the Polar Regions as well as their needs for improvement (e.g. in terms of spatial resolution, accuracy, repeat coverage, length of time series, etc) and the current level of technical and/or scientific maturity for some candidate parameters. Complex surface topography over ice sheets (especially margins) complicates the echo return which diverges from its classical shape (Ray et al., 2015). This difference can range from a slight distortion of the theoretical waveform shape, to multiple superimposed reflections from distinct surfaces within the doppler beam footprint. Working with complex waveforms is one of the major challenges associated with processing radar data over regions of complex topography.

Table 3.4.2-1 Noise level and slope-related component (in degrees) of the measurement precision (from Schröder et al., 2019)

Data set	Data center	Reprocessed
Seasat	$0.21 + 1.91s^2$	$0.25 + 0.70s^2$
Geosat	$0.17 + 0.86s^2$	$0.18 + 1.16s^2$
ERS-1 (ocean)	$0.25 + 0.90s^2$	$0.09 + 0.18s^2$
ERS-1 (ice)	$0.36 + 2.37s^2$	$0.17 + 0.57s^2$
ERS-2 (ocean)	$0.23 + 0.75s^2$	$0.07 + 0.14s^2$
ERS-2 (ice)	$0.38 + 2.57s^2$	$0.15 + 0.53s^2$
Envisat	$0.17 + 1.03s^2$	$0.05 + 0.37s^2$
ICESat	$0.05 + 0.25s^2$	
CryoSat-2 (LRM)	$0.18 + 2.46s^2$	$0.03 + 1.06s^2$
CryoSat-2 (SARIn)	$0.38 + 2.01s^2$	$0.11 + 0.79s^2$

Radar altimetry measurements over the ice sheets need to be adjusted for the effects of the ice sheet surface slope, which typically ranges from 0.1° to 1.5° in Antarctica, introducing a 1.4 to 20.9 km lateral shift in the point of closest approach (Brenner et al., 1983; Levinsen et al., 2016; Remy et al., 1989, , https://doi.org/10.1016/j.rse.2006.02.026, https://doi.org/10.5194/tc-16-2225-2022) or, equivalently, a 1.2 to 274.2 m error in the estimated elevation if the measurement was assumed to be originating from nadir. Schröder et al., 2019 studied the measurement precision of Seasat, Geosat, ERS-1/2, Envisat and CryoSat-2 data over Antarctica by evaluating intra-mission crossovers between ascending and descending profiles, with a time difference of less than 31 days. They find that the precision is clearly a function of surface slope (Table 3.4.2-1).

McMillan et al (2019) show that over low-slope regions of the ice sheet interior, Sentinel-3 SRAL achieves both an accuracy and a precision of ~10 cm, with ~98% of the data validated being within 50 cm of co-located airborne measurements. Across the steeper and more complex topography of the ice sheet margin, the accuracy decreases, although analysis at two coastal sites with densely surveyed airborne campaigns shows that ~60 %–85%of validated data are still within 1 m of co-located airborne elevation measurements. Figure 3.4.2-1 shows the single cycle crossover differences as a function of slope for Sentinel-3 cycle 12 (McMillan et al, 2019).

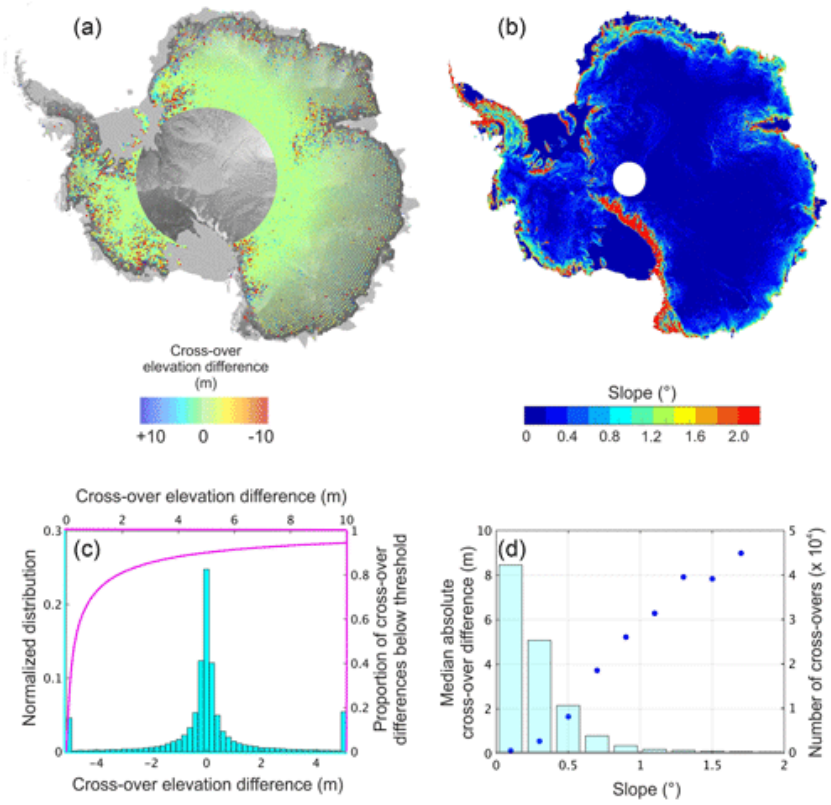

Figure 3.4.2-1: Elevation differences at orbital cross-overs for cycle 12 of the Sentinel-3A mission and comparison to the gradient of the surface slope. McMillan et al., 2019

Through analysis in three regions of the Antarctic Ice Sheet, McMillan et al (2019) demonstrate the early promise of Sentinel-3 SAR altimetry as a platform for long-term, operational monitoring of ice sheets elevation and elevation change. Sentinel-3A delay-Doppler retrievals mapping ice sheet elevation change resolve known signals of ice dynamic imbalance and to detect evidence of subglacial lake drainage activity. A recent study confirms the value of Sentinel-3 data to extent the long time series of ice sheet volume and mass change estimates (Simonsen et al., 2021).

McMillan et al (2020) note that the quartet of Sentinel-3 satellite altimeters will provide a continuous record of ice sheet elevation change. To ensure consistency of measurement between each of the four satellites, rigorous in-flight intercomparison is required. To facilitate this, Sentinel-3B was initially flown in a unique tandem formation with Sentinel-3A, enabling near instantaneous, co-located measurements to be acquired. evolution. They find that (1) there is no significant difference between S3A and S3B instrument precision, (2) that there is no significant difference between the accuracy of S3A and S3B elevation measurements, and (3) that both instruments resolve near-identical echoes of the ice sheet surface, even over complex, non-linear coastal terrain (both instruments operate with statistically equivalent accuracy and precision, even over complex ice margin terrain). Both Sentinel-3A and Sentinel-3B satellites can be used interchangeably to monitor ongoing ice sheet evolution; effectively doubling the spatial coverage of measurements available, now that Sentinel-3B has moved to its nominal orbit.

Satellite altimetry is a the key dataset used to monitor the elevation changes of the ice sheets. Users who aim at constructing longer time series of elevation changes require information on the waveform parameters. Especially in the Arctic, the temperature has been increasing (Serreze & Barry, 2011) and extreme melt event are becoming more frequent (ref). It is essential to know how the surface characteristics are changing over time and how they might affect the height retrieval from the retracker. The occurrence of surface melt is known to complicate the interpretation of elevation and elevation change, and changes in waveform characteristics can be linked to changes in the penetration of the radar signal into snow (Khvorostovsky, 2012; Slater et al., 2019; Rutishauser et al., 2023). Therefore, it is essential that waveform parameters such as the leading edge width (LeW), trailing edge slope (TeS) and especially Sigma0 are provided to the user. And it is important that the method used to derive those parameters are explicitly described in the documentation.

“closed loop” and “open-loop” tracking.

3.5 S3NG-T and Copernicus Climate Monitoring and Prediction

As the ocean warms it expands and sea level rises. This rise is further increased by the melting of ice on land, which then flows into the sea. Sea level has increased throughout the altimeter record, but recently sea level has risen at a higher rate due partly to increased melting of ice sheets in Greenland and Antarctica. In 2019, the global mean sea level reached its highest value since the beginning of the high-precision altimetry record (January 1993).

As noted by the WCRP (2017) “Coastal sea level rise is among the most severe societal consequences of anthropogenic climate change. Contemporary global mean sea level rise will continue over many centuries because of anthropogenic climate warming, with the detailed pace and final amount of rise depending substantially on future greenhouse gas emissions”. Over the coming decades, regional sea level changes and variability will significantly deviate from global mean values. The detailed sea level change along coastlines can therefore potentially be far more substantial than the global mean rise and will depend on many processes involving the ocean, the atmosphere, the geosphere and the cryosphere. Societal concerns about sea level rise originate from the potential impact of regional and coastal sea level change and associated changes in extremes on coastlines around the world, including potential shoreline recession, loss of coastal infrastructure, natural resources and biodiversity, and in the worst case, displacement of communities and migration of environmental refugees.

Local sea level rise and extreme events can have significant impacts on coastal zones. On subsiding coasts, the impacts of resulting sea level rise are already demonstrable in some coastal cities and deltas. However, there is a lack of evidence to attribute rising climate-induced sea level to coastal impacts (Cramer, W., et al., 2014, Section 3.3). By the end of the 21st century, it is very likely that a large fraction of the world’s coasts will be affected by climate-induced sea level rise (Church et al., 2013).

WCRP (2017): WCRP Grand Challenge: Regional Sea Level Change and Coastal Impacts Science and Implementation Plan Detlef Stammer, Robert Nichols, and Roderik van de Wal (co-chairs) and The GC Sea Level Steering Team Version 1.0 February 2017

From the WCRP plan:

> Available coastal sea level data can be used to assess spatial structure of variability, although resolution is limited. Until systems like SWOT are flown, developments in coastal along-track altimetry retrievals (e.g., ESA Sea Level CCI efforts, Cazenave et al., 2022) present the best prospects. The production of long-term consistent quasi-global records of sea level change and its components is possible only through high-quality continuous observations and proper uncertainties attached. To ensure this continuity, the core instruments of the current observing systems consisting of nadir satellite altimetry (TOPEX/Poseidon, Jason-1 -2 and -3, Sentinel-3A –3B and 6MF), satellite gravimetry (GRACE and GRACE-FO), ocean autonomous temperature and salinity profilers (e.g., Argo network) and tide gauges, etc., need to be maintained and replaced before their end of life. To ensure the long-term stability and accuracy, intercalibration of new core instruments against older ones needs to be taken into account in instrumental design. For observations based on multi-instruments such as satellite altimetry, the continuity of a highly accurate and stable reference mission such as the Topex/Jason series is essential to calibrate less accurate missions and achieve higher spatio-temporal resolutions. Better sea level records close to the coast would involve improvements in 1) the geophysical corrections (in particular: the wet tropospheric correction using

enhanced geophysical models or alternative measures from GNSS; improved sea-state bias correction models; and improved tidal modelling) to correct for biases and errors in the coastal region and 2) the radar measurement with new techniques such as SAR altimetry. In ice-covered regions, new retracking forms need to be developed to retrieve the radar signal that is echoed in the leads. Other ongoing efforts (e.g., development of deep Argo floats; GRACE follow-on and new gravity mission concepts like NGGM and MAGIC; improvement of the tide gauge network collocated with GPS measurements; development of new coastal in-situ measurements from high frequency radars, visible cameras, GPS reflectometry, and lidars; advanced experimental designs for specific coastal regions) need to continue over the next decade.

The sea level is particularly important because it is a core ECV identified by the WCRP as essential to estimate the impacts associated to climate change (see the WCRP Grand Challenge on regional sea level and coastal impacts) and to evaluate the current state of climate change through the constraint it provides on the estimates of the Earth Energy Imbalance (see the Earth Energy Imbalance assessment of the WCRP GEWEX core project under the GDAP section). The sea level ECV is also essential to constrain the ocean reanalyses that are a base tool to evaluate annual to decadal changes in the ocean.

To fulfil these objectives the sea level ECV needs to be accurate, highly stable, and consistent over decadal time scales. At global scale, the accuracy needed is around 5 mm and the stability around 0.3 mm/yr. At regional scale, on spatial scales of 100 km2, the accuracy needed is around 15 mm and the stability around 1.5 mm/yr.

Different amplitudes and time scales are involved in these different physical processes and the current GCOS requirement on the stability of the GMSL of ±0.3 mm/yr ([5,95]% confidence level) over a decade is probably enough to detect the current total GMSL rise and acceleration due to greenhouse gases (GHG) emissions. But it is not enough to detect a potential contribution of the permafrost thawing or to help understand the change of Earth energy imbalance, which will rather require a ±0.1 mm/yr accuracy over a decade. Longer time scales also have to be considered since, during the 21st century, potential changes in the GHG emission policies will lead to a change in the climate trajectory and thus the acceleration and the trend in forced sea level will change. These evolutions may not exceed a few tenth of mm/yr over 20-year windows (see the difference in sea level rise between the RCP2.6 scenario and the RCP 8.5 scenario along the 21st century in the IPCC SROCC report). If we want to monitor these changes to support mitigation policies, we will need an accuracy of the order of ±0.1mm/yr over 20-year windows. Reaching such a level of accuracy is a major challenge and we will have to take the most of future altimeter missions to go in this direction.

On a regional scale, the accuracy in the altimeter sea level rise estimates is above ±1 mm/yr over 10 years for regions of 1000 square km and larger (Prandi et al., 2021). This is clearly not sufficient because the expected sea level signal forced by the anthropogenic GHG emissions is at the level of [0.5-0.8] mm/yr over 10 year and longer time scales for regions of 1 000 square km and larger (Fasullo and Nerem, 2018). Thus,

the detection of the regionally forced signal requires the reduction of all sources of uncertainty in sea level estimates below this level of 0.5 mm/yr over regions of 1 000 square km.

This has been possible from October 1992 to present thanks to the spacecraft series of TOPEX/Poseidon, Jason- 1, Jason-2, and Jason-3. In the Copernicus constellation, the S6NG mission should fulfil the Copernicus objectives in terms of “sea level monitoring for climate analysis”. In order to reduce the uncertainty due to the altimeter instrument, Ablain et al. (2024), have suggested to plan a second tandem calibration phase between Jason-3 and Sentinel-6A for a few months approximately 3 years after the first tandem phase, which would allow to assess the instrumental stability between both missions with an accuracy close to ±0.1 mm/yr at the global scale and below ±0.5 mm/yr regionally. Lessons learned from Jason-3 show that it is possible to better calibrate in flight the position of the phase centres of the POD instruments (GNSS, DORIS, SLR) by changing the flying attitude of the spacecraft. When the spacecraft alternatively flies ‘forward’ and ‘backward’ (by doing flips around its yaw axis every time the solar beta-prime angle nullifies) it is possible to:

- disentangle along track the time tagging from the centre of phase POD instrument offsets.
- disentangle cross track the mis-centring of the orbit around the Earth’s centre of mass from the combined effects of mis-calibrated Solar Radiation Pressure (SRP) models and POD instrument locations.

These 2 elements enable a significant improvement of the POD performances (see the OSTST 2019 conference report). In addition, cross-track modelling errors (caused by solar radiation pressure for instance) modulate the geo-centre motion estimates along the Z (North-South) axis, thus causing spurious regional signals in the derived regional mean sea level (especially at high latitudes). Disentangling the mis-centre of the orbit around the Earth centre of mass provides an opportunity to unambiguously determine the geo-centre motion and improve significantly the validation of sea level data against independent data from GRACE and Argo at global and regional scale (through the regional and global sea level closure budget, see for example The WCRP sea level budget group (e.g. Blazquez et al. 2018, Uebbing et al. 2018)

3.6 S3NG-T and Copernicus Extreme Events, Security and Emergencies

Storms have a major impact on everyday life around the world and an improved ability to forecast, quantify and manage combined meteorological and maritime risk is essential to protect the public, property and infrastructure and to maintain a sustainable economy.

The generation and evolution of ocean waves by wind is one of the most complex phenomena in geophysics. Forecasting skill and understanding of these dynamics is critical across a wide range of oceanic applications, including maritime and coastal engineering, air-sea interactions, ocean dynamics, climate, remote sensing. However,

the generation and evolution of waves in high-wind conditions and extreme fetches remains poorly understood.

Models are widely inconsistent for large fetch/duration conditions, to a significant extent due to lack of observational guidance. Extreme storms in the North Atlantic and Pacific are seasonal and diverse in their propagation which hinders systematic in situ observations in these regions (e.g., Meucci et al., 2018; Takbash et al., 2018). Also, they usually do not provide extreme fetches. Observations of high-wind conditions with extreme fetch, however, are possible in the Southern Ocean, where these conditions occur regularly, and storms move in the same direction (West to East) throughout the year. Swell, which results from such storms in the Southern Ocean radiates into all major ocean basins, but remains poorly predicted by forecast models, both in magnitude and arrival time and not well parametrized in model (Aouf et al.2020).

More observational information is required within Copernicus to improve modelling and service capability during extreme events with respect to:

- Wave evolution at extreme fetches;
- Severe extra-tropical cyclones at extreme fetches;
- Swell dynamics and forecasting, with attention to arrival time;
- Wave-driven dispersal of floating objects (search and rescue, transport of microplastic and other pollutants);
- Wave-ice interactions in Marginal Ice Zone subject to extreme storms and waves and Non-linear wave-current interactions;
- Metocean climatology in the Southern Ocean;
- Extreme waves and wave-current interaction;
- SSH/dynamics and wave current interaction.

3.6.1 S3NG-T and Copernicus Monitoring and Prediction of Storm Surge

S3NG-T should address the following User needs for storm surge information:

Application	Variable	Required Horizontal Resolution	Required time Resolution	Required spatial Coverage	Policy context	User community
Storm Surge forecasting	Water levels at coast Hs at coast Mean wave period Mean wave direction Wave length	1/4° open ocean (22.5 km) 1m at coast	Daily for open ocean 6 hours to hourly for the near shore	Global Europe	- Directive 2014/89/EU of the European Parliament and of the Council of 23 July 2014 establishing a framework for maritime spatial planning, OJ L 257, 28.8.2014, p. 135–145 - Directive 2008/56/EC of the European Parliament and of the Council of 17 June 2008, establishing a framework for community action in the field of marine environmental policy (Marine Strategy Framework Directive), OJ L 164, 25.6.2008, p. 19–40 - report from the Commission to the European Parliament and the Council on the implementation of the Water Framework Directive (2000/I1860/EC) and the Floods Directive (2007/60/EC, Second River Basin Management Plans, First Flood Risk Management Plans and recommendations in Annex, COM/2019/95 final.	Copernicus emergency service, DG ECHO, civil protection Consistency with existing time series requested

A storm surge is a transient (a period of a few minutes to a few days) abnormally high sea level in a coastal or inland sea produced by severe atmospheric conditions. A storm surge is defined as:

$$\zeta = \text{height of observed sea level - height of predicted tide}$$

where ζ is the storm surge height, in units of meters. This equation describes the residual storm surge amplitude and may be positive (leading to flooding) or negative (leading to extreme shallow waters). It is possible to achieve a positive surge purely by advancing the tide without raising the HW level; it is really the skew surge (height at HW) that enhances flood risk. Storm surges are associated with deep atmospheric low pressure systems (Tropical Cyclone (TC) or Extra-Tropical Cyclone (ETC)) with attendant strong winds that drive seawater against the shore. In some cases, mesoscale atmospheric systems with strong squall lines may also induce storm surges (JCOMM, 2010). The water level associated with a storm surge at a given location is modified by a variety of complex interactions between the storm surge itself, local dynamic tidal characteristics, wind and swell waves, currents, and the effects of precipitation on rivers and estuaries. The tidal cycle influences a storm surge through the effects of bottom friction (dependent on current and depth) and the variation of the tide propagation speed (dependant of total water depth which the storm surge also modifies). When a deep cyclone moves towards a low lying coastal region at the same time as high astronomical tides, water levels rise rapidly and significantly.

44% of global human population are located within 150 km of the coast and eight of the ten largest cities in the world are located on the coast (e.g. Resio and Westerink, 2008). In northern Europe many coastal areas are just above or even below the mean sea level (MSL) and are particularly vulnerable to the persistent threat and impact of storm surges. The low lying North Sea shoreline is exposed to storm surges due to the high winter storm probability and storm surge residuals > 50 cm occur ~10 times every year. In the Netherlands two thirds of the population are at risk with over five million inhabitants living below sea level (e.g. Jorissen et al., 2000). In the United Kingdom, more than one million low-lying properties are at risk, corresponding to roughly five percent of the population. Other European regions also suffer from storm surges and the approximate locations of European storm surge hazard occurring are shown in Figure 3.6.1-1 although many local areas of storm surge risk are not visible in this map due to a lack of data (e.g. Schmidt-Thomé, 2006)

In the tropical regions the impacts of storm surges may be extremely severe during the hurricane/typhoon season due to the energetic nature of such large storms. This is particularly the case in regions where coastal areas are low-lying (*e.g.,* North Indian Ocean, Gulf of Mexico, and North Australia). An historical summary of deaths due to TC storm surges reveal immense numbers of fatalities but study of the table shows that in the modern era warning systems have resulted in dramatic reduction of storm surge related deaths (e.g. Swail et al., 2010) (*e.g.*, Bangladesh, 2007 where a Category 5 TC make landfall with limited mortality impact due to better preparation and warning systems). Nevertheless, tropical cyclone Nargis in 2008 caused the loss of over 146,000 lives in Myanmar and the economic impact of Hurricane Katrina for the New Orleans area in 2005 is estimated at $80 billion (Swail et al., 2010).

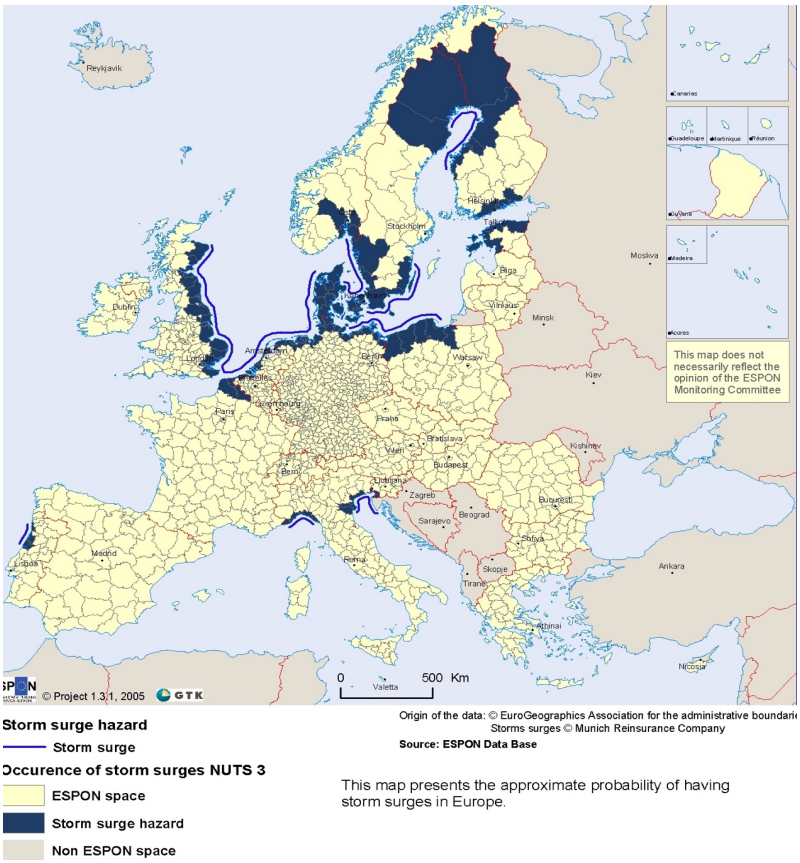

Figure 3.6.1-1. Map of approximate storm surge hazard in Europe. As storm surges are often closely linked to winter storms, the storm surge hazard area is mainly located in the areas where winter storms occur. The existing data sets do not provide enough information for a full classification of the entire EU 27+2 area. Therefore, storm surges are represented as a general hazard in areas where they might occur (Credit: Schmidt-Thomé, 2006).

For a variety of storm surge warning and coastal management applications it is often more useful to estimate the Total Water Level Envelope (TWLE) at a given location and time rather than the storm surge residual amplitude. TWLE is the combined effect of residual surge, high tide, wave setup, wave run-up, and for some regions, precipitation and river flow. TWLE may be measured directly and uniquely by satellite altimetry. An uninterrupted flow of altimeter data has accumulated since 1992 and measurements of TWLE, sea state and surface wind derived from altimetry are invaluable for monitoring coastal circulation, sea level change and their impacts in the coastal zone. In many areas (particularly in some developing Countries or regions that lack adequate in situ infrastructure), satellite altimetry measurements provide the only feasible way to retrieve regular and consistent information for coastal regions and have enormous strategic importance. Extending the capabilities of current and future satellite altimetry as close as possible to the coast, with the ultimate aim to integrate the altimetry-derived measurements of sea level, wind speed and significant wave height into coastal ocean observing systems extremely important to address these issues. Other aspects must also be addressed to optimise satellite altimetry in the coastal regions including the use of a common reference datum for *in situ* and satellite water level measurements. At

present, the datum's used in topographic and hydrographic surveying are different and common benchmark information is required for the reduction of water levels from in situ and satellite altimetry data to a common datum (*e.g.,* Rummel, 2001). This allows land-based geodetic measurements, and the oceanic mean sea surface height derived from altimetry to be used most effectively.

3.7 S3NG-T and Copernicus applications in Geodesy

For geodesy there are several interests in the S3NG-T, one is the observation of the mean sea surface and the mean dynamic topography, the other is the estimation of sea level rise, and the third is to improve the observation of tides. In addition, all efforts that relate to the modelling of precision orbits, or the definition of the reference ellipsoid are geodetic research topics. A more fundamental point is therefore, the definition of a ITRF in relation to what we discuss hereafter.

3.7.1 Mean sea surface

Observation of the mean sea surface to the best possible global resolution is a long standing challenge in geodesy. This means that the inclination should not stop at 66 degrees but continue further up to the poles. Ideally, non-repeating ground tracks are optimal implying a free drifting high inclination orbit (possibly beyond sun synchronous) as a favourite choice (examples include CryoSat-2, ERS-1, Geosat or geodetic modes of other altimeters). The real challenge is the capability of the altimeter to focus and to average out mesoscale variability on the long run. Signals such as ENSO to mesoscale can be removed by averaging. As of today, we have a long time series of measurements available since 1975-1985. Resolution both in time and space is an issue for the mean sea surface; we have low resolution mode (LRM) up to CryoSat-2 when delay Doppler SAR was introduced (now with Sentinel-3A and B, Sentinel-6A and B is likely for the future). The benefit of SAR mode is that altimetry can now reveal shorter spatial scales so that trenches, ridges, seamounts, etc., can now be detected and refined. PSD reveal the differences highlighting where we can see and cannot gain information.

Marine gravity is all about SAR mode and a free drifting orbit. Example map of free air gravity anomalies from multi-mission Altimetry provides a huge amount of information but today, we still do not know what all the features actually are in the map (and many are missing to the misfortune of submarine navigation: the USS San Francisco 8-jan-2005 crashed into an unmarked seamount). For the mean dynamic topography one needs an independent geoid, all terrestrial, marine and satellite gravity information is used, and there are assimilation solutions that combine oceanographic observed transports with altimetry and the gravity information, see for instance (LeGrand et al., 2003). It is difficult to extract a requirement from geodesy as far as the topic mean sea surface is concerned. The GOCE mission requirement was 1 cm for the geoid and 5 mgal for gravity anomalies at a resolution of 100 km (see for instance Johannessen et al. (2003) and others). But this refers to global numbers seen from the perspective of a gradiometer in orbit. Clearly it would not be enough to avoid missing a seamount during navigation at sea. Maybe the best way out for altimetry is that each mission will add knowledge to the MSS, and especially when delay Doppler altimetry is available at the

highest possible resolution, but do not specify a requirement for the MSS or the dynamic topography field or the marine gravity field.

SWOT data allows mapping 2D MSS slopes, revealing 2D features down to 8 km in wavelength, (Yu et al., 2024), not visible with 30 years of past 1D conventional altimetry. SWOT's MSS will be a starting basis for S3NG-T; the longer time series of 2D observations should better isolate the ocean and geoid components of the MSS.

3.7.2 Sea level rise

The present day estimated sea level rise is according to R.S. Nerem at the university of Colorado 3.3±0.3 mm/yr with an acceleration, estimated by different groups to be of 0.083±0.025 mm/yr^2, (Nerem et al., 2018), or 0.11±0.05 mm/yr^2, (Guerou et al., 2023). This notable disparity between the two estimates of sea level rise acceleration stems from challenges in interpreting TOPEX data and the significant uncertainties associated with it.

The long-term user requirement is 0.1 mm/yr ([5,95]% confidence level) over a decade according to (Meyssignac et al., 2023). Measuring sea level rise with a satellite altimeter puts significant constraints on the stability of the altimeter instrument including the required corrections for refraction of the radar signal and the accuracy of orbit determination which is intrinsically coupled to maintenance of the geodetic reference system. A recommended approach is to rely on SLR, DORIS, and GNSS, since maintenance of an International Terrestrial Reference System: ITRF, see also (Altamimi et al, 2016) is essential if we want to provide continuity on observing sea level rise consistently over several decades. The International Laser Ranging Service (ILRS) mechanism is necessary to tie different networks together. International Earth Rotation and Reference Systems Service (IERS) activities (global time and reference frame standards, Earth Orientation Parameter and International Celestial Reference System standards) are essential.

A long-term stable microwave radiometer is required for the wet tropospheric correction (e.g. AMR-C on Sentinel-6) and a dual frequency altimeter is required for reducing the ionospheric path delay along the altimeter to sea surface. To understand the sea level budget (ΔVolume (altimetry) = ΔMass (gravimetry) + ΔDensity (T/S profiles) we need external information on the monthly temporal gravity field, and an ARGO system of oceanic profiling floats. Both are required to understand the heat and mass terms that make up sea level rise as we see it from the altimeter instrument. Of fundamental importance is also a tide gauge network – this is a reference dataset and it must be maintained, finally we need an “Agreement” on a glacial isostatic adjustment models (currently there is no agreed reference GIA model)

3.7.3 Tides

A next generation topography constellation offers an opportunity to independently observe ocean tides. The white paper from (Arbic et al 2015) gives information on barotropic and internal tides. For barotropic tides, the M2 rms is 5 to 7 mm between 66N and 66S for deep ocean tides. On the European shelf tides are more like 3 to 5 cm

rms, but individual difference can be larger (e.g. around the UK coast). Arctic tides are noisier: 4-6 cm rms, Antarctic tides: 3-4 cm rms. Altimetry data is assimilated in various global models (FES, GOT, TPXO, EOT) which all meet high accuracy; the models can be confronted with network of independent deep-sea tide gauges. The recent SWOT swath observations on a non sun-synchronous orbit are already providing improved barotropic tides in coastal, regional and high-latitude regions (Hart-Davis et al., 2024), and global improvements are expected after many years of SWOT observations. For internal tides the surface features are smaller but can reach20 cm. near bathymetric gradients. Global models forced by the atmosphere and tides could be efficient for improving corrections for the non-phaselocked internal tides (e.g. HYCOM model, Shriver et al, 2013). While the GRACE mission requirements are stringent, inaccuracies in tide models will show up in the residuals but this can be largely resolved over time (hot spots are already improved). Tides beneath ice shelves beneath flexing ice shelves is a different topic, for details see (Padman et al, 2008).

It should be remarked that the bathymetry is a big concern for coastal regions ocean tides. Cancet et al. (2018, 2020) show great improvements in areas where we have good bathymetry

4 S3NG-T MISSION AIMS AND OBJECTIVES

4.1 S3NG-T Mission Aim

Considering the User needs expressed by the European Commission and concisely articulated in the previous sections, the **aim** of the Copernicus Next Generation Sentinel-3 Topography (S3NG-T) Mission is:

> ***To ensure continuity of Sentinel-3 in flight performance topography capability in the 2030-2050 timeframe.***

4.2 S3NG-T Objectives

Mission requirements are then derived from mission Objectives.

The primary objectives of the S3NG-T mission are to:

PRI-OBJ-1. **Guarantee continuity of Sentinel-3 topography measurements**[8] for the period 2030 to 2050 **with performance at least equivalent to Sentinel-3 in-flight performance** as defined in Table 2.4-1 ('baseline mission').

PRI-OBJ-2. Respond to evolving user requirements and **improve sampling, coverage and revisit** of the Copernicus Next Generation Topography Constellation (S3NG-T and Sentinel-6NG) to ≤50 km and ≤5 days (CMEMS, 2017) in support of Copernicus User Needs.

PRI-OBJ-3. **Enhance sampling coverage, revisit and performance for Hydrology Water Surface Elevation** measurements in support of Copernicus Services.

PRI-OBJ-4. Respond to evolving user requirements and **enhance topography Level 2 product measurement performance**.

The **secondary objectives**[9] of the S3NG-T mission are to:

SEC-OBJ-1. Provide directional wave spectrum products that address evolving Copernicus user needs.

SEC-OBJ-2. Provide new products[10] that address evolving Copernicus user needs.

[8] See definition of Topography Parameters.

[9] Secondary objectives shall not drive the system design. Examples of new products would include directional wave spectrum and topography gradients.

[10] Examples of new products with respect to those provided by Sentinel-3 today include sea surface height gradients and river reach averaged gradients, river width and water area. Total Surface Current Velocity measurements are considered out of scope by the European Commission.

5 S3NG-T MISSION REQUIREMENTS

MRD-0010 Requirement deleted.

MRD-0020 Requirement deleted.

5.1 Definition of Measurement Masks

5.1.1 Marine and Coastal Mask

In the coastal zone and over rapidly changing atmospheric moisture structures including cloud structures, precipitation and land-sea breeze (amongst other phenomena) lead to more complex atmospheric temperature, pressure and moisture structures that are significantly different from open ocean conditions. Their influence may persist for several hundred kilometers offshore. Furthermore, due to the input of freshwater from rivers and estuaries, bio-geo-chemical compounds and pollutants are more ubiquitous in this region. Natural compounds from biological decay form long-chain organic surfactants on the ocean surface in calm conditions that, together with pollutants on the ocean surface, inhibiting the growth of capillary waves (to which the radar altimeter responds) and modifying the surface emissivity (to which the microwave radiometer responds). Furthermore, these physical, bio-geo-chemical and atmospheric aspects and characteristics present a very complex sea surface topography structure and lead to specific measurement challenges compared to the open ocean.

Different Level 2 data processing techniques and algorithms are used in different regions (e.g. the open ocean, more complex coastal regions, within estuaries, etc.) and data are across a transition region that includes both land and water. A clear definition of the actual coastline and the transition zone is required. This is the purpose of the Marine and Coastal Mask. Level 1 products are anticipated as continuous half-orbit or full orbit products regardless of the surface type.

Global Self-consistent, Hierarchical, High-resolution Geography Database (GSHHG, Wessel and Smith, 1996) is a high-resolution geography data set, amalgamated from two databases: World Vector Shorelines (WVS) and CIA World Data Bank II (WDBII). The former is the basis for shorelines while the latter is the basis for lakes. The WDBII source also provides political borders and rivers. GSHHG data have undergone extensive processing and should be free of internal inconsistencies such as erratic points and crossing segments. The shorelines are constructed entirely from hierarchically arranged closed polygons. GSHHG combines the older GSHHS shoreline database with WDBII rivers and borders, available in either ESRI shapefile format or in a native binary format. Geography data are provided in five resolutions: crude(c), low(l), intermediate(i), high(h), and full(f). Shorelines are organized into four levels: boundary between land and ocean (L1), boundary between lake and land (L2), boundary between island-in-lake and lake (L3), and boundary between pond-in-island and island (L4). Datasets are in WGS84 geographic (simple latitudes and longitudes; decimal degrees). The full Resolution data set is provided at a resolution of 0.04 km.

MRD-0030 The S3NG-T Marine and Coastal Mask (MCM) shall be established according to the following specification:

- The Coastal Region is defined as 80 km on the ocean side and 20 km on the land side from the Shoreline Boundary (i.e. the Coastal Region is nominally 100 km in extent).
- All inland seas (including large lakes).
- Shoreline boundary and definition of estuaries with an estuary entrance of ≥ 2 km for rivers articulated in the Inland Water Mask.
- Open Ocean defined as all areas of open ocean water, but not part of the Coastal Region, Inland Seas and Estuaries.
- Polar Oceans including areas seasonally occupied by sea ice.

Note 1: The Shoreline Boundary separating land from ocean is defined by the Hierarchical, full-resolution (0.04 km) Shoreline (GSHHS) high-resolution dataset (Wessel and Smith, 1996) available from https://www.ngdc.noaa.gov/mgg/shorelines/gshhs.html).

Note 2: This mask is used to define the coastline and as input to different Level 2 processing schemes within the ground segment.

Note 3: Level 1 products are anticipated as continuous half-orbit or full orbit products regardless of the surface type but will depend on the ground segment concept.

Note 4: Small islands were a challenge in previous masks for Sentinel-3 and these can be addressed using other satellite data (e.g. Sentinel-2) to validate or improve on the coastal mask definition as required.

Note 5: S3NG-T-UN-022 requires a definition of the coastal zone as 24 nautical miles (44,448 km) offshore. A definition of 80 km allows a margin for an error in the coastal boundary definition. This is consistent with NG-T-UN-029 that requires the coastal zone definition to include a 12 nautical mile offshore limit.

5.1.2 Inland Water Mask

For the S3NG-T mission, a hydrology target mask will be defined to prioritise hydrology measurements. Figure 5.1.2-1 shows a Copernicus Sentinel-1 image of the Amazon River highlighting the spatial characteristics of a very large river and smaller tributaries. In this case a method to determine which hydrology targets can/should be acquired must be used based on the characteristics of targets to be observed.

Allen and Pavelsky (2018), then completed and improved by Altenau et al. (2021), used 30 years of Landsat images to create a global dataset of river widths (initially named Global River Widths from Landsat, GRWL, database and now known as SWOT River Database, SWORD) at mean annual discharge, for rivers wider than 30 m. This dataset is used to map river reaches larger than a given threshold (e.g. Figure 5.1.2.2(a) for 80 m threshold or Figure 5.1.2.2(b) for 150 m threshold). The total amount of river reaches that could potentially be observed depend on a given minimum observed river width threshold. Increasing the threshold decreases the number of observed river reaches. Also, with a large threshold, gaps appear in some rivers due to ephemeral variability. It should be reiterated that the GRWL database corresponds to river width when the

discharge reaches its averaged value. This means that during low flows, some river reaches do not flow, while during high flows, more river reaches will be wider than the threshold.

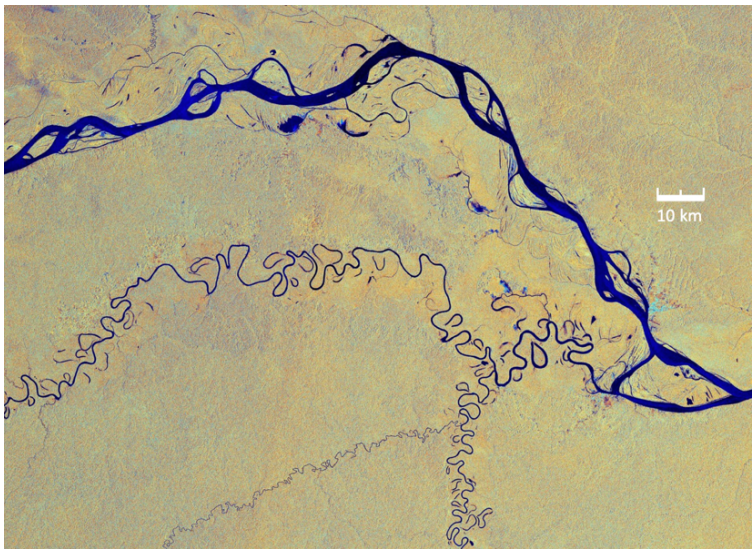

Figure 5.1.2-1. Copernicus Sentinel-1 dual-polarisation image of the Amazon River acquired on 3 March 2019. The Javari River, or Yavari River, is visible as a thinner blue line weaving through the tropical rainforest.

Figure 5.1.2-3 (a) shows the percentage of the total river lengths over Europe for which the width exceeds a given threshold. This plot shows some remarkable thresholds in mean river width variations for European rivers. If the minimum observed width is equal to 150 m, 35% of the total river lengths will be observed. This percentage increases to 40% if the minimum observed width is 100 m.

For lakes, the same approach can be followed using the CIRCA-2015 database (Sheng et al., 2016). This database contains all lakes of the globe with an area greater than 60 m x 60 m. Figure 5.1.2-3(b) shows the percentage of the total area of French lakes with an area greater than a given threshold. Contrary to rivers, the shape is quite linear and it is difficult to extract significant thresholds.

Figure 5.1.2-2(a). Rivers wider than 80 m in the GRWL database (Allen and Pavelsky, 2018). Image courtesy of S. Munier (CNRM)

Figure 5.1.2-2(b) Rivers wider than 150 m in the GRWL database (Allen and Pavelsky, 2018). Image courtesy of S. Munier (CNRM)

The primary hydrology related objective for S3NG-T is to sample water elevation of rivers greater than or equal to 100 m width and lakes/reservoirs with areas above 250 m x 250 m, i.e. 0.0625 km^2 to resolve the physical phenomena. These objectives are in concordance with the recommendations from the COSPAR (2018) report and will expand considerably the water level product from the Copernicus Global Land and Copernicus Climate Change Services. It will thus contribute to the monitoring of lake water level, lake water extent and river water level Essential Variables (EV) identified by the Group on Earth Observations (GEO) and to the Lake Water Level/Extent Essential Climate Variables (ECV) defined by the Global Climate Observing System (GCOS). They also contribute to the estimation of two main EV and ECV which characterise water fluxes on continents: lake volume change and river discharges. S3NG-T will contribute to monitoring the achievement of the United Nations Sustainable Development Goals 6 (SDG 6; Reyers et al, 2017) and the European Union Water Framework Directive (Directive 2000/60/EC).

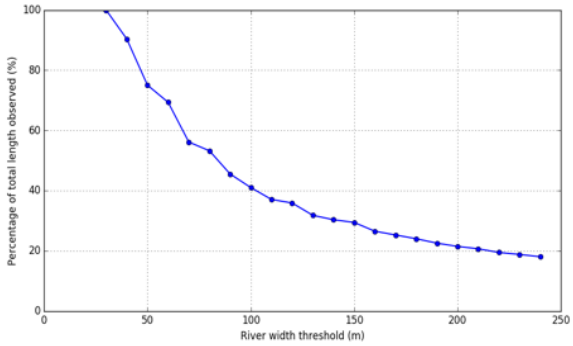

Figure 5.1.2-3(a). Percentage of total river lengths observed over Europe versus the minimum river width observed (from the GRWL database; Allen and Pavelsky, 2018). Image courtesy of S. Munier (CNRM)

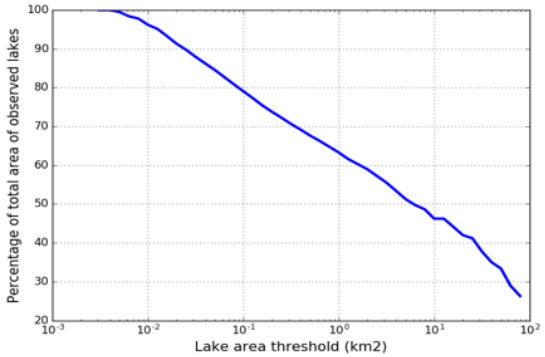

Figure 5.1.2-3(b). Percentage of total observed lake area over France versus the minimum lake area observed (from the CIRCA-2015 database, Sheng et al., 2016). Image courtesy of S. Munier (CNRM)

River and lake targets have considerable seasonal variation in terms of horizontal extent and WSE. This must be accommodated in the Inland Water Mask.

River and Lake monitoring is currently a secondary mission objective for Sentinel-3 and Sentinel-6. For Sentinel-3, hydrology ‘virtual stations’ are located at exact locations in the Sentinel-3 orbit ground track and will, but the time of the S3NG-T first launch, constitute a significant unbroken time series record of altimeter hydrology measurements. Following discussions with the European Commission, and in the interest of maximising the opportunities to measure and considerably more Hydrology targets compared to that of Sentinel-3, a target of ≥90% continuity for Sentinel-3 Hydrology targets maintained in the OLTC database (rivers, lakes and reservoirs) is defined.

MRD-0040 An Inland Water Mask (IWM) shall be established according to the following specifications:

- River width: open, non-vegetated water ≥ 0.1 km including seasonal variations
- River length: ≥ 10 km
- Open water bodies (non-vegetated water e.g. lakes reservoirs, wetlands etc) larger than 250 m x 250 m, i.e. 0.0625 km^2, (goal: 100 m x100 m).
- Estuaries with an estuary entrance of larger than 2km for rivers articulated in the Inland Water Mask.

Note 1: The S3NG-T Inland Water Mask specifies Inland Waters for the S3NG-T mission.

Note 2: The purpose of the Inland Water Mask is to minimise the downlink of data by selecting pre-defined hydrology targets.

Note 3: It is expected that some water bodies smaller than the requirement definition could be measured by S3NG-T.

Note 4: Deleted.

Note 5: River and lake seasonal variations should be accommodated in the Inland Water Mask; linked to MRD-0050.

MRD-0045 For baseline continuity, ≥90% of the hydrology targets (i.e. river, lakes and reservoirs virtual stations) included in the Sentinel-3 Open Loop Tracking Command (OLTC) shall be included (see note 1) as defined in S3NGT-OLTC-SIZING.tgz

Note 1: Reference to the Sentinel-3 OLTC in this requirement does not imply the choice of any altimeter implementation solution. Its purpose is to recognise that measurements at the virtual station targets that are maintained by the Sentinel-3 Mission will be continued by S3NG-T.

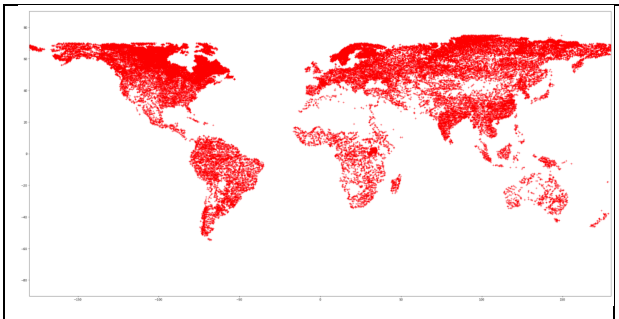

Location of 57449 S3A OLTC virtual stations as of March 2022 as specified in S3NGT-OLTC-SIZING.tgz

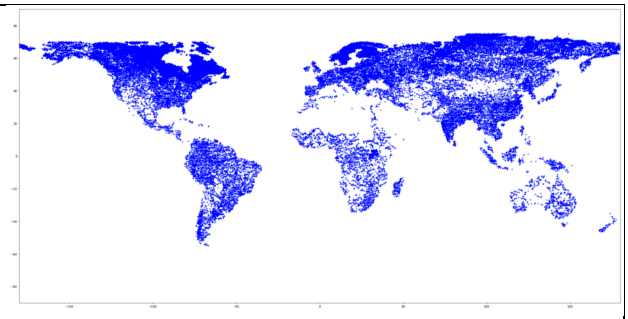

Location of 57093 S3A OLTC virtual stations as of March 2022 as specified in S3NGT-OLTC-SIZING.tgz

Note 2: For sizing purposes ESA has created a global kml map of gridded river density based on Yamazaki et al (2019), "MERIT Hydro: A high-resolution global hydrography map based on latest topography datasets", the JRC Global Surface Water Layers (Pekel et al, 2016) and ESA WorldCover (ESA, 2021). KML files are available on request from ESA in Open_Water_Density_PPP_Datasets.zip.

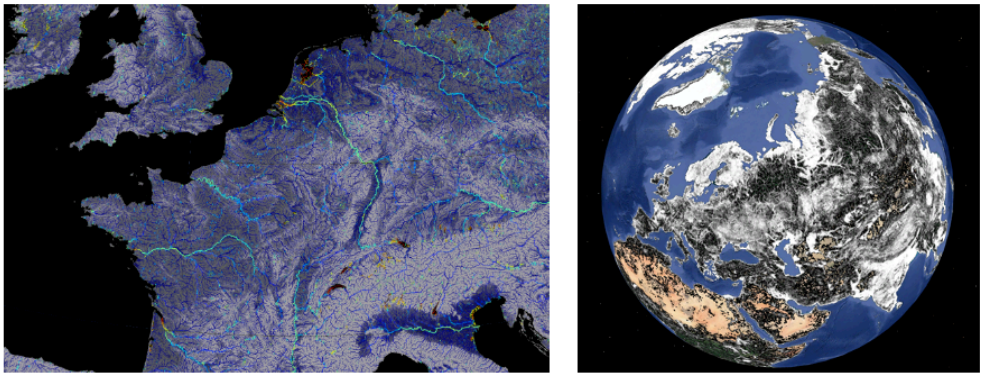

(left) Yamazaki et al (2019), "MERIT Hydro river width (right) ESA 25km river density map provided for sizing purposes.

MRD-0050 The Inland Water Mask shall be re-evaluated and uploaded to the satellite up to 4 times per year to account for seasonal variations in elevation and in horizontal extent

Note 1: This is necessary since river spatial extent and position may change seasonally.

Note 2: Depending on the concept, a more extensive and elaborate approach compared to the Sentinel-3 OLTC approach may be required (e.g. larger on-board database or regular updates of the database in-flight several times per year to address seasonal variation)

Note 3: Deleted

MRD-0060 The Inland Water Mask shall be delivered to users as an open product.

Note 1: This provides a convenient way to engage the user community in the operational management of the Inland Water Mask

5.1.3 Sea Ice Mask

For the S3NG-T, the area where sea ice can be expected is defined in a Sea Ice Mask (SIM). It is defined by the median ice extent over the period 1979-2010, based on sea ice climatology. The sea ice record to be used for the definition of the SIM is not specified to allow alignment with the operational framework of the Sentinel-3 and/or CRISTAL missions at the time of launch of Sentinel-3 NG Topo.

MRD-0070 The S3NG-T Sea Ice Mask (SIM) shall be defined as the median sea-ice extent climatology over the period 1979-2010 (TBC).

Note 1: This specification is updated to allow the use of NSIDC or OSI-SAF sea ice record to allow alignment with the current Sentinel-3 MPC and/or CRISTAL at the time of launch of S3NG-Topo.

Note 2: The following files serve as a starting point for budgeting purposes:

Northern Hemisphere: ftp://osisaf.met.no/reprocessed/ice/conc/osi-450/1979/02/ice_conc_nh_ease2-250_cdr-v2p0_197902271200.nc

Southern Hemisphre: ftp://osisaf.met.no/reprocessed/ice/conc/osi-450/2014/09/ice_conc_sh_ease2-250_cdr-v2p0_201409191200.nc

MRD-0075 The Sea Ice Mask (SIM) shall be re-evaluated and uploaded to the satellite once per month to account for monthly variations in sea ice extent.

5.1.4 Land Ice Mask

The baseline continuity definition is to cover Land Ice targets that fall on the ground track of Sentinel-3A and Sentinel-3B. As a starting point, for Greenland, surface type information from BedMachine Greenland version 3 (Morlighem et al., 2017) is used. The mask is freely available and can be accessed directly via the NASA National Snow and Ice Data Center (NSIDC). The BedMachine Greenland version 3 mask is based upon the MEaSUREs Greenland Ice Mapping Project (GIMP) Land Ice and Ocean Classification Mask, Version 1, supplemented with grounding line information (the boundary between grounded ice and floating ice tongues) based upon unpublished InSAR data (courtesy of E. Rignot and J. Mouginot). The surface type mask is shown in Figure 5.1.4-1. For Antarctica, surface type information from BedMachine Antarctica version 2 (Morlighem, 2020) is used. The mask is freely available and can be accessed directly via the NASA National Snow and Ice Data Center. The BedMachine Antarctica version 3 mask uses Grounding Lines derived using interferometric SAR data (Rignot et al., 2011). In each case, a buffer of 50 km is required to account for fluctuations in the glaciated area.

The Land Ice Mask may need to be extended to include larger regions of interest depending on the final concept selected.

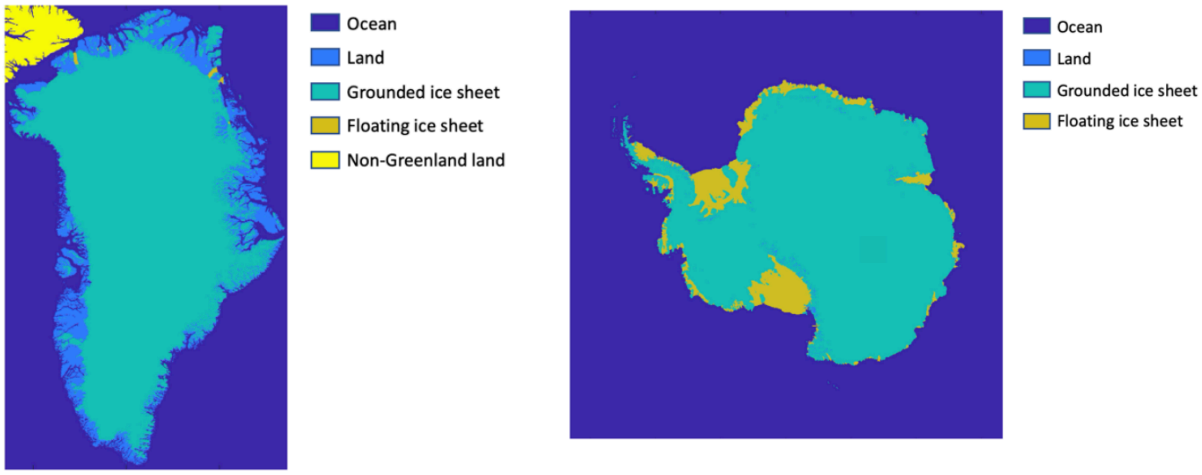

Figure 5.1.4-1 Mask for Greenland glaciers and ice cap (Rastner et al., 2012) gi_rgi05_003 available at http://glaciers-cci.enveo.at/crdp2/index.html

MRD-0080 The S3NG-T Land Ice Mask (LIM) shall be established according to the following specifications:

- Greenland and Antarctic glaciers and ice caps.
- Ice Sheets and Ice Shelves.
- Ice Sheets and Ice Shelves Margins and areas of sloping terrain up to 1.5 deg (enhanced continuity goal: 4 deg.), including a 50 km buffer.

Note 1: For baseline continuity with the Sentinel-3 Land Ice Thematic Products from the Sentinel-3 Altimeter Processing Baseline (PB), Greenland and Antarctica glaciers, ice caps, ice sheets and ice shelves should be defined according to BedMachine dataset (Morlighem, 2020). References:

Greenland: https://nsidc.org/data/idbmg4/versions/5

Antarctica: https://nsidc.org/data/nsidc-0756/versions/3:

Note 2: The Land Ice Mask may need to be extended to include larger regions of interest depending on the final concept selected.

5.2 Sentinel-3NG-T Measurement Requirements

Measurement requirements are derived for the Sentinel-3 baseline continuity mission.

MRD-0090 The S3NG-T mission shall provide measurements of elevation over ocean including open ocean, inland seas, coastal zones and from sea ice leads and polynyas.

Note 1: This requirement aims at baseline continuity with the Sentinel-3 mission.

MRD-0100 The S3NG-T mission shall provide measurements of normalised radar backscatter coefficient over ocean including open ocean, inland seas, coastal zones and from sea ice leads and polynyas.

Note 1: This requirement aims at baseline continuity with the Sentinel-3 mission.

Note 2: The limit of sea ice is defined in a Sea Ice Mask is by MRD-0070.

MRD-0110 The S3NG-T mission shall provide measurements of elevation over inland surface waters.

Note 1: This requirement aims at baseline continuity with the Sentinel-3 mission.

Note 2: Hydrology targets are defined in a Inland Water Mask is by MRD-0040.

MRD-0120 The S3NG-T mission shall provide measurements of normalised radar backscatter coefficient over inland surface waters.

Note 1: This requirement aims at baseline continuity with the Sentinel-3 mission.

Note 2: Hydrology targets are defined in a Inland Water Mask is by MRD-0040.

MRD-0130 The S3NG-T mission shall provide measurements of elevation over sea ice.

Note 1: This requirement aims at baseline continuity with the Sentinel-3 mission.

Note 2: The limit of sea ice defined in a Sea Ice Mask is by MRD-0070.

MRD-0140 The S3NG-T mission shall provide measurements of normalised radar backscatter coefficient over sea ice.

Note 1: This requirement aims at baseline continuity with the Sentinel-3 mission.

Note 2: The limit of sea ice defined in a Sea Ice Mask is by MRD-0070.

MRD-0150 The S3NG-T mission shall provide measurements of elevation over land ice.

Note 1: This requirement aims at baseline continuity with the Sentinel-3 mission.

Note 2: Land ice, polar glacier and ice sheet acquisition areas are defined in a Land Ice Mask is by MRD-0080.

MRD-0160 The S3NG-T mission shall provide measurements of normalised radar backscatter coefficient over land ice.

Note 1: This requirement aims at baseline continuity with the Sentinel-3 mission.

Note 2: Land ice, polar glacier and ice sheet acquisition areas are defined in a Land Ice Mask is by MRD-0080.

MRD-0170 Requirement deleted.

MRD-0180 The S3NG-T mission shall provide measurements of the brightness temperature at different frequencies over all surfaces.

Note 1: This requirement aims at baseline continuity with the Sentinel-3 mission.

5.3 Payload Requirements

The payload required for S3NG-T Include the following items:

A Synthetic Aperture Radar Altimeter: this instrument will make measurements to retrieve the range to the surface, ocean significant wave height (Hs) and the normalised radar backscatter coefficient (Sigma0), which has a monotonic relation to ocean wind speed (U10). Over inland water targets the altimeter determines the water surface elevation from range measurements. Sentinel-3 uses a nadir pointing synthetic aperture radar altimeter that employs delay Doppler processing to enhance the along-track resolution and reduce the measurement noise of derived measurements. Precise across-track interferometric synthetic aperture radar techniques could be considered as a means to expand coverage and revisit time of the mission.

A Microwave Radiometer: this instrument will make measurements of the brightness temperature at different frequencies across the entire altimeter footprint to determine the altimeter radar path delay due to atmospheric liquid water and water vapour load. One channel centre frequency is positioned in a water vapour emission band at (for Sentinel-3 this was at 23.8 GHz) and one where cloud-liquid water emits, i.e. in the 31.3-31.8 GHz band or in the 36-37 GHz band (for Sentinel-3 this was at 36.5 GHz, however this band is not a protected ITU-R band for Earth observation, where RFI are likely to occur). Some designs consider at channel centred at a lower frequency (Sentinel-6 used 18 GHz) that is dominated by emission from the ocean surface. A low frequency channel can be used to compensation for ocean surface emission in the water vapour band. An alternative approach uses the altimeter normalised radar backscatter coefficient as a proxy for ocean surface emission. Two radiometer channels are used by the Sentinel-3 MWR. In support of cryosphere applications, the microwave radiometer could use channels that allow snow and ice discrimination, snow depth on sea ice, sea ice concentration using channels (18.7 and 23.8, 36.5 GHz amongst others e.g. Li and Guan, 2019) although this should not drive the mission design. Ideally, consideration over inland waters would allow a better retrieval of surface water elevation if a ZPD could be implement using a radiometer measurement.

GNSS Receiver: this instrument, after processing, provides a precise orbit determination using measurements from the Galileo global navigation satellite system constellations. The instrument could also be capable of using additional GNSS constellations (e.g. GPS, Beidou, Glonass).

Laser Retroreflector: this is a passive component that reflects laser pulses fired from ground-based satellite laser ranging (SLR) stations. SLR range measurements are used in the process of precise orbit determination and (when taken near zenith) are useful as a direct range measurement during altimeter range calibration.

MRD-0190 To guarantee baseline continuity, S3NG-T shall embark a synthetic aperture nadir-pointing radar altimeter.

Note 1: This requirement aims at baseline continuity with the Sentinel-3 mission.

Note 2: An additional across-track interferometric synthetic aperture radar imaging capability could be considered to provide an enhanced capability.

MRD-0200 Requirement deleted.

MRD-0210 Requirement deleted.

MRD-0220 Requirement deleted.

MRD-0230 Requirement deleted.

MRD-0240 Requirement deleted.

MRD-0250 Requirement deleted.

MRD-0260 Requirement deleted.

MRD-0270 S3NG-T shall embark a multi-frequency microwave radiometer payload to measure upwelling brightness temperatures within the radar altimeter footprint.

Note 1: Radiometer frequencies should be selected, in accordance with the ITU allocations, so that on-ground processing of the brightness temperature measurements can provide estimates of the altimeter radar path delay range measurements due to water and water vapour in the atmosphere.

Note 2: This requirement aims at baseline continuity with the Sentinel-3 mission.

Note 3: The same antenna could be used for both the radar altimeter and the microwave radiometer as in the case of the AltiKa mission (Steunou et al, 2015).

Note 4: An enhanced solution would be required if a swath altimeter solution is embarked in addition to a nadir instrument.

Note 5: The microwave radiometer will also be used to determine sea ice and snow parameters over ocean and land surfaces within the altimeter footprint.

MRD-0280 S3NG-T shall embark a Global Navigation Satellite System GNSS receiver to receive and measure signals from the Galileo and other global navigation satellite constellations.

Note 1: This is heritage from the Sentinel-3 mission and mandatory for a topography mission.

Note 2: Darugna et al. (2022) show results from Sentinel-6 that indicate that about 80% of the GPS/Galileo with broadcast ephemerides solution differences is below 13 cm in position and 0.12 mm/s in velocity. show that decimeter level onboard orbit determination is achievable with the current navigation data.

Note 3: Depending on the quality of its products, the upcoming Galileo High Accuracy Service (HAS, https://www.gsc-europa.eu/sites/default/files/sites/all/files/E6BC_SIS_Technical_Note.pdf) might further improve such performance. It will provide orbit, clock, code and phase bias corrections, refining the GNSS orbits and clocks, which have been demonstrated to highly affect the POD accuracy and precision. However,Sentinel-6 real time onboard velocity estimation accuracy (with respect to the CNES-DORIS reference) is already less than 0.1 mm/s using Galileo only and the dynamic model without HAS (Darugna et al, 2022).

Note 4: On-board (reduced)-dynamic models integrated within the GNSS receiver will greatly assist in the computation of NRT velocities (e.g. Darugna et al, 2022, Casotto et al, 2021, Montenbruck et al, 2021;2022, Hauschild and Montenbruck, 2021).

Note 5: Use of a multi-frequency, multi-constellation approach is anticipated.

Note 6: Other GNSS constellations could be included.

MRD-0290 S3NG-T shall embark a Laser Retroreflector to return laser pulses to terrestrial Satellite Laser Ranging stations.

Note 1: This is heritage from the Sentinel-6 mission and necessary for satellite precise orbit determination and in orbit validation of satellite position.

MRD-0300 The S3NG-T mission shall embark Precise Orbit Determination (POD) instruments providing measurements of the satellite orbital position to meet mission performance.

Note 1: Sentinel-3 includes a DORIS receiver in addition to a nominal complement of GNSS (GPS on A/B models), Laser retro reflector (for off-line verification), with coarse sun sensors, and star trackers as input to the AOCS

Note 2: For Sentinel-6, using satellite laser ranging (SLR) from selected high-performance stations, < 1 cm RMS consistency between SLR normal points and Galileo enabled GNSS-based orbits is obtained, which further improves to 6mm RMS when adjusting site-specific corrections to station positions and ranging biases (Montenbruck et al, 2021).

Note 3: The Sentinel-6 Galileo enabled radial orbit component shows a bias of less than 1mm from the SLR analysis relative to the mean height of 13 high-performance SLR stations (Montenbruck et al, 2021). Sentinel-6 real time onboard velocity estimation accuracy (with respect to the CNES-DORIS

reference) is already less than 0.1 mm/s using Galileo only and the dynamic model without the use of the Galileo High Accuracy Service (HAS) (Darugna et al, 2022). Galileo GNSS-based onboard orbit determination can now reach a similar performance as the DORIS (Doppler Orbitography and Radiopositioning Integrated by Satellite) navigation system (Montenbruck et al, 2022).

5.4 Mission Lifetime Requirements

The CSC LTS (ESA, 2025) defines the baseline operation lifetime for the current and next generation Copernicus Programme.

MRD-0310 The S3NG-T shall guarantee 20 years of continuity of the Copernicus Sentinel-3 Topography mission.

Note 1: This requirement implies a series of satellites. If recurrent satellites are foreseen, these are assumed to extend the operational mission duration.

Note 2: It is assumed that Copernicus 1.0 assets (i.e. Sentinel-3, Sentinel-6) will cover the period up to 2030.

*Note 3: It is strongly advised to transition to S3*NG-T satellites before the demise of Copernicus 1.0 assets to guarantee tandem phase operations and maintain stability of the Sentinel-3 time series that is required by Copernicus Services.

Note 4: A topography reference mission capability is assumed to guarantee baseline performance that is at least equivalent to Sentinel-6 (Table 2.4-1) covering the 2030-2050 time period.

MRD-0320 The minimum design lifetime of each S3NG-T satellite shall be ≥7.5 years.

Note 1: The nominal operational lifetime of all future Sentinels is assumed to be 10 years (with the exception of Sentinel-6-NG operating in a higher orbit) as described in the ESA CSC-4 Long-term Scenario.

Note 2: This requirement includes a commissioning period of ≤9 months.

MRD-0330 Consumables (e.g. propellant) of each S3NG-T satellite shall include margins allowing an extension of the lifetime of the corresponding satellite by ≥5 years.

Note 1: The nominal operational lifetime of all future Sentinels is assumed to be 10 years (with the exception of Sentinel-6-NG operating in a higher orbit) as described in the ESA CSC-4 Long-term Scenario.

5.5 Mission Phase Requirements

5.5.1 Commissioning Phase Requirements

Following the launch of a new satellite a Commissioning phase is implemented to bring a satellite into full operational state. During this phase, the majority of ground-processing algorithms will be brought on-line. Uncertainties will be derived following dedicated calibration and validated activities to establish compliance to requirements. It is acknowledged that estimates of instrument drift will require a longer period that could extend over the mission lifetime. The approach depends on statistical analysis and by comparison with external in situ Fiducial Reference Measurements (FRM) or other satellite missions. Calibration/verification outputs will be compared with the mission requirements and the theoretical error budget specification. Typically, the commissioning phase is six months long but may be extended to accommodate Tandem phase requirements with requirements tailored to specific missions.

At the end of satellite commissioning activities, the satellite will be fully characterised and calibrated with a complete update of a Satellite System Characterisation and Calibration Data Base (SSCDB). Based on these activities the pre-launch mission performance uncertainty budget can be updated ready for operational use.

MRD-0340 The S3NG-T satellite and payload complement shall be fully commissioned in ≤ 9 months.

Note 1: This requirement is independent of any additional requirements for tandem inter-calibration activities.

MRD-0350 At the end of satellite commissioning activities, the pre-launch mission performance uncertainty budget shall be updated and delivered to users for operational use.

Note 1: The pre-launch performance estimates will be validated in flight.

Note 2: User access to the mission performance uncertainty budget is requested. L1 and L2 products will include uncertainty estimates.

Note 3: Establishing meaningful trends of uncertainties may require several years of in-flight data collection.

5.5.2 Tandem Inter-calibration Phase Requirements

Properly characterising differences between satellite instruments either as part of a series or in constellation is critical to the success of GCOS ECV activities and in turn the activities of the Copernicus Climate change Service. Recognizing that, even though satellites could be of an identical design, it is expected that differences in performance of payload instruments will exist due to subtle tolerances of materials, manufacture and pre-flight characterisation. Furthermore, as demonstrated by the very successful Jason series, Copernicus Sentinel-3 and Sentinel-6 tandem flights (Donlon et al., 2016;

2019), there are enormous benefits to conducting a Tandem flight in terms of in-flight calibrations, calibration and validation activities that will significantly enhance the early application of data from new satellites and the overall mission robustness. Noting the discussion above, it is essential that relative discrepancies between satellites are properly characterised for CDR construction and the success of the entire Copernicus topography constellation.

The main challenge is to reduce uncertainties when comparing data from different satellite missions that form a time series. When data are obtained from two satellites at different times but at the same location (i.e. in Tandem flight), there is significant correlated uncertainty:

- Uncertainty due to ocean geophysical space and time variability that complicates inter-comparison, especially in regions dominated by mesoscale structure (1-10 days, <10-50 km), which are particularly lucrative to understand inter-satellite bias;
- Uncertainty due to atmospheric space and time variability.

Both issues introduce uncertainty to the direct inter-calibration of S3NG-T instruments.

However, if a new satellite is added to a mission series resulting in more than one satellite on-orbit at the same time, by flying these satellites in tandem separated by ~30-60 seconds on the same ground track, the correlation between these uncertainties is maximized so that for all practical purposes they can be ignored: the difference between two satellite measurements is solely due to instrumental aspects. Thus, when appropriate, information learned from the commissioning and calibration of one satellite may be transferred to a second satellite with confidence. In addition, End Of Life (EOL) estimates can be established by comparing the performance of the ‘new’ satellite with the ‘old’ satellite to improve the long-term stability of the climate data records derived from Sentinel-3 and S3NG-T.

For all satellites contributing to GCOS ECV (such as Sentinel-3 see Prandi et al., 2021), and particularly those that constitute a series of follow-on satellites like Sentinel-3, the optimal duration for a tandem flight is 12 months as requested by GCOS (2016) and required by the European Integrated Policy for the Arctic (climate pillar). 12-months is considered mandatory where significant technology changes have been implemented (e.g. change from Jason class Low Resolution Mode (LRM) altimetry to Sentinel-6 Synthetic Aperture Radar (SAR) or change from nadir-only altimetry to swath altimetry). A 9-month tandem calibration phase is considered sufficient (Ablain et al, 2019) to understand the technical differences between old and new technologies.

However, for a satellite system of identical design, observing both the north and south hemisphere (and therefore a holistic view of seasonal aspects) a 6-month or less tandem flight duration may be sufficient. This excludes the additional time required for the satellite to drift towards the tandem position and towards a nominal phasing position after a tandem phase.

Should the orbit choice of S3NG-T be incompatible with a tandem flight together with Sentinel-3C or Sentinel-3D, an alternative approach based on the use near contemporaneous and collocated data will be required.

If a tandem calibration flight is not possible due to orbit incompatibility, the use of quasi simultaneous and contemporaneous crossover points of Sentinel-3C and/or Sentinel-3D within 30 minutes and ±10 km provides an alternative, less performant, approach. The objective is to detect and quantify regional and seasonal differences between satellites and fully characterise such differences in support of the Copernicus Climate Change Service (3CS).

Since the crossover technique is subject to greater uncertainty compared to the tandem calibration flight, a 12-month period is initially defined. In practice, it may be necessary to use a longer time period. However, since this has no direct impact on any operational aspect this has no impact on data availability or special operations for the mission: it is simple matching data.

MRD-0360 For the handover from S3 to S3NG-T, if the Sentinel-3C/D orbit plane is used for S3NG-T satellites, S3NG-T shall ensure a tandem calibration flight, composed of a drift phase towards a tandem configuration, followed by a tandem operation phase and completed by a second drift phase towards a nominal operational orbit position, overlapping with Sentinel-3C and/or Sentinel-3D for a duration of at least 9 months.

Note 1: Since S3NG-T satellites will be of a new design, it is imperative that the characteristics of the new system are introduced into the Sentinel-3 time series in a manner that does not introduce instability into the long time series. Sentinel-3 implemented a tandem calibration flight (see Donlon et al., 2016).

Note 2: Ideally a 12-month tandem calibration phase would allow a full analysis of seasonal uncertainties at a global level as requested by GCOS (2016). This is the basis for the 12-month tandem flight flown by Jason-3 and Copernicus Sentinel-6.

Note 3: A 9-month tandem calibration phase is considered sufficient (Ablain et al, 2019) to understand the technical differences between old and new technologies.

MRD-0370 For the handover from S3 to S3NG-T, the following offset uncertainties at global scale should be ensured for the essential ocean parameters:

- SSH offset uncertainty < 0.5 mm
- SWH offset uncertainty < 1 cm
- U10 windspeed offset uncertainty < 0.25 m/s

Note 1: Since S3NG-T satellites will be of a new design, it is imperative that the characteristics of the new system are introduced into the Sentinel-3 time series in a manner that does not introduce instability into the long time series.

Note 2: The numbers provided in this requirement for the SSH, SWH and wind speed offset uncertainty in the intermission cross-calibration represent 10% of the daily global variability of these three parameters at a global scale.

For the second satellite in the series, and for additional satellites, a tandem calibration flight at the start the new satellite lifetime naturally provides data to assess the old on-orbit satellite and effectively constitutes a second tandem for the old satellite in a single operation.

Sentinel-3 has implemented a highly successful tandem calibration phase of 5 months during Phase E1. Sentinel-6 used a 12-month Tandem phase with Jason-3 building on the previous heritage of the Jason missions.

A 6-month tandem calibration phase is considered a minimum duration based on the assumption that uncertainties can be identified over a full seasonal cycle by using coverage of both north and south hemisphere measurements. The completion of tandem calibration flight is likely to include satellite commissioning activities related to the update of the new Satellite Characterisation and Calibration Data Base (SSCDB).

MRD-0380 If a new satellite is added to the S3NG-T mission resulting in more than one satellite occupying the same orbit at the same time, a tandem calibration flight shall be flown as soon as practically possible, composed of a drift phase towards a tandem configuration, followed by a tandem operation phase of ≥ 100 days and completed by a second drift phase towards a nominal operational orbit position.

Note 1: The user needs of the Copernicus Climate Change Service is for a stable time series of measurements that comply with the Climate Monitoring Principles (GCMP, GCOS, 2003).

Note 2: The intent of the REQ is to improve bias and stability knowledge for the multi-satellite data record when a new satellite is introduced to the constellation.

Note 3: About 10 cycles (100 days) was the time length recommended to detect regional SSH biases with an uncertainty lower than ± 4 mm. Evolution of the standard deviation of the mean SSHA differences averaged per box of 1° x 3° between Jason-3 and S6-MF, according to the period length during the verification phase.

Note 4: The tandem calibration phase is flown entirely during the Phase E1 commissioning phase (i.e. tandem flight to be completed independently of In Orbit commissioning).

Note 5: A tandem calibration flight excludes the additional time required for the satellite to drift towards the tandem position and towards a nominal orbit position after a tandem phase.

MRD-0385 For S3NG-T satellites flying at the same time, the following offset uncertainties should be ensured for the essential ocean parameters:

- SSH offset uncertainty < 0.5 mm; (goal 0.25 mm)
- SWH offset uncertainty < 1 cm; (goal 0.5 cm)
- U10 windspeed offset uncertainty < 0.25 m/s; (goal 0.15 m/s).

Note 1: When a new S3NG-T satellite is added to the mission, either to operate at the same time or to take over from another, the new system shall be introduced into the Sentinel-3NG-T time series in a manner that does not introduce instability into the combined products or the long time series.

Note 2: The numbers provided in this requirement for the SSH, SWH and wind speed offset uncertainty in the intermission cross-calibration represent 10% of the daily global variability of these three parameters at a global scale.

MRD-0390 The along-track separation of S3NG-T satellites, if configured in a tandem calibration phase, shall be nominally ≤30 seconds in time apart.

Note 1: The shortest possible separation mitigates the uncertainty due to ocean geophysical space and time variability that complicates inter-comparison and inter-satellite bias; and uncertainty due to atmospheric space and time variability.

Note 2: Sentinel-3A and Sentinel-3B flew a tandem calibration phase separated by 30s in time. The Jason-3 and Sentinel-6 Tandem flight will also separate spacecraft by 30 seconds in time. The ESA FLEX mission and Sentinel-3D will fly together separated by 6-15 seconds apart.

Note 3: An along-track separation distance of up to 60s in time was used by the Sentinel-3A/B tandem calibration flight.

Note 4: Separate requirements define the tolerance for along-track drift separation.

Note 5: The achieved along-track separation between satellites depends on the launch injection that it is only known after launch.

MRD-0400 Requirement deleted.

The Sentinel-3A and B ground tracks were maintained during the tandem phase to much better than ±1 km allowing extremely useful comparisons between satellites to with 150m over ice sheets (e.g. Clerc et al, 2020) allowing detailed comparison of waveforms between Sentinel-3A and B over Antarctica (McMillan et al, 2021). An extremely high level of consistency, with close similarity of waveforms, both in terms of their magnitude and the distribution of backscattered power (i.e., waveform amplitude and shape). This consistency applies both to the waveform leading edge (corresponding to the surface return from the point of closest approach) and the trailing edge (corresponding to any subsurface and off-nadir contribution). Small shift of <100m did not appear to complicate the analysis demonstrating that the performance of both instruments is near-identical. Such a high degree of correlation in co-located waveforms acquired by both instruments, even over complex coastal terrain demonstrates that both satellites can be used interchangeably to monitor ongoing ice sheet evolution. More broadly, it also establishes the value of operating a tandem phase immediately after satellite launch and demonstrates that such operations should be performed when the Sentinel-3C and Sentinel-3D units enter service in the future (McMillan et al, 2021). Following this work, the S3NG-T ground track should be maintained to <1.0 km and ideally ±0.25 km.

MRD-0410 The relative cross-track separation of satellites, if configured in a tandem calibration phase, shall be less than or equal to ±0.5 km (goal: ±0.25 km).

Note 1: During tandem, the relative across track separation distance must be managed so that differences associated with each satellite measurement geometry are minimal.

MRD-0420 Requirement deleted.

MRD-0430 Requirement deleted.

MRD-0440 If configured in a tandem calibration phase and excluding satellite commissioning activities, data shall be acquired in nominal acquisition mode from the satellite to be commissioned throughout the Tandem flight phase.

Note 1: The principle is to assemble a dataset for analysis and establish differences between payload instruments that can be used to inter-calibrate measurements. This is best achieved by maintaining normal operations.

Note 2: The data collected will be used to transfer calibration and characterisation data collected by operational satellite(s) and using that information to understand any differences with respect to new satellites. This may accelerate the uptake and application of mission data.

5.5.3 Nominal Operations Phase Requirements

During the nominal operations phase, measurements will be continuously acquired from all payload components at full resolution except during calibration activities.

MRD-0450 During the nominal operations phase, measurements shall be continuously acquired from all payload components, except during calibration activities.

Note 1: Deleted.

MRD-0460 Requirement Deleted

5.6 Orbit Requirements

Sentinel-3 occupies a frozen sun-synchronous orbit (SSO) at 814.5 km altitude inclined to 98.65° with a 27-day repeat cycle (14+7/27 revolutions per day) and a local solar time at the descending node of 10:00 (similar to ENVISAT). This configuration satisfied a baseline requirement to provide coverage between 81.5°N and 81.5°S. This orbit has a sub-cycle at ~4 days that allows reasonable sampling of ocean mesoscale features within 10 days.

The Copernicus Sentinel-3 sun-synchronous orbit (SSO) is optimized for operational ocean applications. It was chosen as a compromise between the needs of optical missions:

- an ocean colour spectrometer requires a LTDN at high solar elevation,
- a sea surface temperature thermal infrared radiometer dedicated to Sea Surface temperature requires a LTDN at 06:00 to minimise solar warming of the surface ocean during the day,
- the topography mission required regular sampling of mesoscale (30-50 km over ~10 days) without consideration of measurement acquisition with respect to LTDN.

The final orbit choice was a frozen sun-synchronous orbit at 814.5 km altitude inclined to 98.65° with a 27-day repeat cycle (14+7/27 revolutions per day) and a local solar time at the descending node of 10:00 (similar to ENVISAT). This configuration satisfied a baseline requirement to provide coverage between 81.5°N and 82.5°S. This orbit has a sub-cycle at ~4 days that allows reasonable sampling of ocean mesoscale features within 10 days.

Two satellites operate in constellation on the same orbital plane separated by 140° in relative phase. However, this orbit choice is not fully optimised for ocean topography measurements based on a twin satellite constellation and could be improved. This is the fundamental reason for separating the Sentinel-3 mission into separate topography satellites and optical satellites.

CMEMS recommends that high inclination orbits are needed to provide requite sampling and coverage and a sun synchronous orbit (SSO) is acceptable.

MRD-0530 Deleted.

MRD-0540 If more than one satellite in-orbit simultaneously occupy the same orbital plane, the relative phase between satellites shall be configurable.

Note 1: This requirement allows any phase position in the orbit to accommodate a variable configuration satellite positioning.

Note 2: This is heritage from Sentinel-3 and necessary to allow tandem calibration flight configuration.

The rationale for maintaining a stringent satellite ground track to within ±1.0 km (ideally within ±0.25 km) to assist in consistency and performance of geophysical retrievals over ice sheets has been discussed in Sec. 5.5.1. This stringency also applies to routine operations since cross-track slopes in regions with marine geoid errors impact on the accuracy of ocean retrievals. In addition, cross track slopes may complicate retrieval of river water surface elevation estimates as discussed in Cohen et al. (2018) who demonstrate that the rivers in Version 1.0 of the 6 arc-minute Global River-Slope (GloRS) geospatial dataset have a median slope of ˜0.6m/km for 50% of the rivers. In reality, the number of larger and more mature rivers is located in areas of slowly varying terrain. In contrast, a large number of smaller width streams and tributaries dominate the headwaters of river basins typically in mountainous and hilly terrain (where slopes can reach as much as >2.6 m/km). Assuming the satellite track is maintained at ±1 km (3-sigma or 0.33km @1sigma) and noting that between each cycle the satellite will cross the river at a slightly different location within this tolerance, river slopes must be considered in terms of the water surface elevation estimation.

MRD-0550 The satellite ground track shall be maintained to be within ±1.0 km (3-sigma) (enhanced goal: ±0.25 km (3-sigma)) of the reference ground track defined at the sub-satellite point at nadir.

Note 1: Deleted.

Note 2: This requirement is linked to the performance of S3NG-T measurements over ice sheets and inland water.

Like other altimetric satellites, S3NG-T will fly at 7 km/s and cover a region of 420 km in one minute, which will effectively provide a synoptic ‘snapshot’ of SSH variations. Some of the largest signals we observe with all altimeters are ocean tides. Although high-frequency open ocean barotropic tides are now well estimated from models and altimetry (Stammer et al., 2014), there are still large errors in the coastal regions and at high latitudes > 66°, regions that are not well covered by the Jason/Sentinel-6 altimeter series.

The development of new and better tide models using hydrodynamic modelling is essential for ocean topography – particularly at higher latitudes (Quartly et al., 2018). As noted by Park et al., (1987), the choice of orbit inclination defines the coverage up to a certain latitude limit and is constrained by the desired density of coverage at the subsatellite track and by the time phasing of the repeat of the satellite's ground track as a function of inclination, which determines the aliased frequencies of the measurements of the oceanic tides. The choice of repetition period is constrained by trade-offs between temporal and spatial coverage and by the aliasing of tidal constituents. See Appendix VIII for altimeter orbit details related to tide measurement.

MRD-0560 Should alternative orbits be chosen for S3NG-T compared to the operational sun-synchronous orbit of Sentinel-3A/B, they shall minimise tidal aliasing periods M2, N2, O1, K2, P1, and Q1 ocean tidal constituents based on orbit choice and the use of ocean tide models.

Note 1: This requirement provides guidance to minimise the impact of ocean tides e.g. Parke et al., (1987), Lindsley (2011).

Note 2: Deleted.

Note 3: The aliasing of tides is a fundamental issue for altimeter sampling particularly in the aliasing band <180 days and the semi-annual/annual band

Tidal constituent	Envisat, AltiKa (35-day repeat)	Jason-3, Jason-CS/Sentinel-6 (9.9156-day)	CryoSat-2 (369-day repeat)	Sentinel-3A, -3B (27-day repeat)	IceSAT-2 (91-day repeat)
M2	94.4	62.1	112.1	157.5	55.79
S2	Infinite	58.7	Infinite	Infinite	Infinite
K1	365.25	173.1	98.1	365.25	365.25
O1	75.1	45.1	77.1	277.0	220.1

Note, the Jason satellites do not sample the Arctic because their orbital inclination is only 66°, but are included here for completeness.

Note 4: There should be no tidal aliasing at very long periods that requires an aliasing frequency >2 cycles per year.

Note 5: An ability to resolve tidal waves of close frequency and separate these signals from each other within a reasonable time of observation is important (i.e. < mission lifetime). Ideally it should be possible to separate the main tidal constituents: S2 is the principal solar semidiurnal (infinitely aliased for sun-synchronous orbits such as Sentinel-3) K1 is the main diurnal tide (luni-solar declination diurnal aliased to 365.25 days for Sentinel-3), K2 is the luni-solar declination semidiurnal, M2 is the principal lunar semidiurnal tide (aliased to 157.5 days for Sentinel-3), O1 is lunar declinational diurnal (aliased to 277 days for Sentinel-2), N2 is the larger lunar ecliptic semidiurnal.

Note 6: Deleted.

Note 7: There should be minimal aliasing at annual and semi-annual frequencies.

Note 8: Deleted.

Note 9: It may be necessary to consider other tidal constituents if the S3NG-T orbit is different from that of Sentinel-3.

MRD-0570 Should alternative orbits be chosen for S3NG-T compared to the operational sun-synchronous orbit of Sentinel-3A/B, the S3NG-T mission orbit choice shall, as much as practically possible, position aliasing frequencies of the main tidal constituents M2, N2, O1, K2, P1, and Q1 as far away from one another.

Note 1: Deleted.

Note 2: Deleted.

Note-3: Deleted.

5.7 Coverage, Revisit and Sampling Requirements

Satellite nadir altimetry coverage is indicated by ground track samples acquired over multiple days. The Sentinel-3 twin-satellite topography mission is designed to constrain global operational oceanography models at scales of ≤100 km in ≤10 days. The Sentinel-3 orbit, occupied by both satellites, has an exact repeat cycle of 27 days providing quasi global sampling with an inter-track separation distance at the Equator of 52 km after each complete orbit cycle. A primary orbit sub-cycle of approximately 4 days is at present satisfying, to first order, an ability to monitor the ocean surface mesoscale structure of ~100 km (depending on latitude). The Sentinel-3 Next Generation Topography mission is specified to provide enhanced continuity to the strict baseline measurements provided by this configuration.

The following section discusses constraints imposed on S3NG-T coverage, revisit and sampling for each of these domains.

5.7.1 Sampling and Coverage Requirements

MRD-0580 The S3NG-T mission shall provide sampling coverage between 81.5 degrees North and 81.5 degrees South

Note 1: This requirement ensures baseline continuity of the Sentinel-3 topography mission.

Note 2: This requirement does not fully address topography measurement needs in the Arctic Ocean. This may be accomplished using the planned Copernicus expansion CRISTAL mission. However, an enhanced baseline could provide measurements at higher latitudes.

5.7.2 Ocean Sampling constraints

Since the ocean remains under-sampled by the present uncoordinated altimetry constellation (e.g. Sentinel-3, Sentinel-6, AltiKa, HY Series etc), to resolve the mesoscale ocean field (10-100 km with latitude variation commensurate with the Rossby radius of deformation) it is not straightforward to specify an optimally coordinated altimetry constellation in terms of sampling, coverage, effective resolution and performance. A more thorough explanation for ocean sampling constraints is provided in Appendix IX.

The NASA/CNES SWOT mission provides a great opportunity to observe and understand the ocean energy cascade over scales from 50-200 km and < 15 days that are not well resolved with today's uncoordinated altimeter constellation, including the dynamics of mesoscale and sub-mesoscales processes and their interactions with internal tides. This legacy will be extremely useful for the S3NG-T mission.

Figure 5.8.1-3 shows the sampling characteristics of Sentinel-3 twin constellation computed in one way as a global coverage ratio defined as the percentage of the Earth's surface that can be observed within 5 days (and 10 days) assuming a nadir

altimeter with an area of influence equal to a radius of 10 km along the ground-track. Thus, the global coverage ratio can be computed by:

$$Coverage\ ratio = \frac{\sum_{i=1}^{N} Covrg(lat_i)cos(lat_i)}{\sum_{i=1}^{N} cos(lat_i)}$$

where $Covrg(lat_i)$ is the percentage of the Earth at latitude, lat_i, observed in 5 days (or 10 days), and $lat_i,\ i = 1, \dots, N$, is a sufficiently large range of latitude. Within an ocean model data assimilation system, error covariances for altimeter SSH data may use multiple length scales depending on how the model is configured. Waters et al. (2015) use 1/4° multivariate data assimilation scheme NEMOVAR (Mogensen et al., 2009, 2012) NEMO model configuration. For nadir altimeter assimilation, a high-resolution error covariance length scale is used based on the first baroclinic Rossby radius that varies latitudinally. This is of the order of a few 10-30+ km at mid latitudes. A second scale is set at ~400 km and is related to errors in barotropic processes – this larger scale is not used in our calculations here. For the coverage ratio calculations reported in this MRD, a conservative 'worst case' 10 km radius of influence is used for nadir altimeters centred at the nadir point along the altimeter ground track.

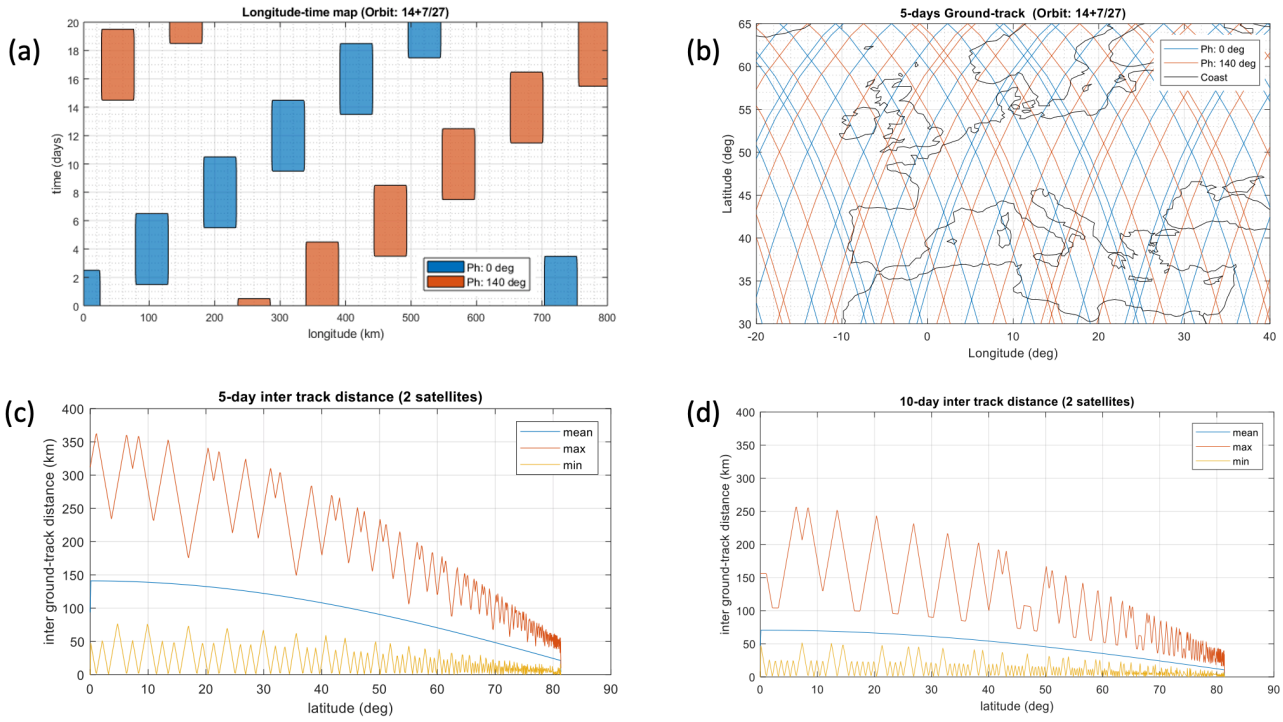

Figure 5.8.1-3. The sampling characteristics of Sentinel-3 twin constellation computed as a global coverage ratio. (a) 'Longitude-time map' that provides information regarding the spatial and temporal sampling of the constellation, in this case at equator which is a worst case scenario as sampling improves progressively at higher latitudes. Each rectangle has a height of 5 days and a width of 50 km. (b) The ground-track of the Sentinel-3 A and Sentinel-3B constellation over a period of 5 days with operational satellite position phasing of 140° on the same orbit plane. (c) 5-day ground track separation distance for 5 days as a function of latitude (d) 10-day ground track separation distance for 5 days as a function of latitude.

For the baseline continuity sampling characteristics of the Sentinel-3 twin constellation, computed as a global coverage ratio, Sentinel-3A + Sentinel-3B achieves 20.2% in 5 days and 37.1% in 10 days. If Sentinel-6 is included in the calculation, the result is 27.7% for 5 days and 42.8% for 10 days.

CMEMS (2017) provide user needs for the improvement of CMEMS required to better serve existing users and to anticipate future needs. The main areas of improvements are:

- Improved space/time resolution to better monitor and forecast the ocean at fine scale and to improve the monitoring of the coastal zone.
- Better monitoring of biogeochemical state of ocean.
- Better monitoring of the rapidly changing polar regions.

This will require major evolution of satellite observing capabilities. When moving to higher resolution, it will be fundamental to constrain CMEMS models with new observations. The sea surface height (SSH) measurements from altimetryis an integral of the ocean interior properties and is a strong constraint for inferring the 4D ocean circulation through data assimilation. Multiple nadir altimeters (at least 4 altimeters) are required (this was required 10 years ago) to adequately represent ocean eddies and associated currents in models. Much higher space/time resolution (e.g. 50 km / 5 days) will be needed in the post 2025 time period. In the post 2025 and beyond, the resolution of CMEMS models will increase by a factor of 3 (e.g. global 1/36°, regional 1/108°) and more advanced models (including coupling with the atmosphere) and data assimilation methods will be available. These models will be used to force downstream coastal models with resolution of the few hundred of meters. The resolution of current altimeter products will not be able to constrain the smallest scales of such high resolution models: the mesoscale to sub-mesoscale spectral region is difficult to interpret from altimetry alone due to the inability to disentangle the geostrophically balanced motions from its unbalanced counterpart using high-resolution along-track data. It is the combination of high resolution mesoscale structure from altimetry together with other data (for example those form near contemporaneous thermal infrared measurement's such as those from Sentinel-3 SLSTR (e.g. Donlon et al, 2012) or in the future from the Copernicus Imaging Microwave Radiometer (CIMR, (e.g. Donlon, 2020)) either in a data driven or via assimilation into ocean modes that will bring fundamental improvements in our understanding of the ocean mesoscale and their dynamics (e.g. Johannesen et al, 2018; Lacorata et al., 2019).

CMEMS thus requires a major improvement in sea surface topography space/time sampling. The objective is to resolve wavelengths of ≤50 km and time scales of ≤5 days.

MRD-0590 The S3NG-T mission shall sample the topography of the ocean surface, defined in the Marine and Coastal Mask, in space ≤50 x 50 km and in time ≤5 days (enhanced goal: ≤25 x 25 km ≤5 days). This requirement is to be evaluated using an Observation Density Map (note 3) and a supporting Coverage Ratio (note 3) metrics.

Note 1: Sentinel-3 was designed to achieve an average cross-track separation of ~50 km at 45° N and 45°S after 10-days (~100 km in 5 days) and is baseline continuity. The Coverage ratio achieves 20.2% in 5 days and 37.1% in 10 days. If Sentinel-6 is included in the calculation, the result is 27.7% (5 days) and 42.8% (10 days). Track separation at the equator for a full cycle is 52 km at the equator (worst case) using Sentinel-3A and Sentinel-3B.

Note 2: The ocean surface topography must be determined with the performances set out in Section 7.5.1 of this MRD. For this purpose, Sentinel-3 determines SSH, Hs, wind speed (Sigma0) and wet troposphere delay at the same location and time.

Note 3: This requirement must be evaluated using two metrics:

1. *Daily global ocean Observation Density maps (priority metric) and,*
2. *Daily global ocean Coverage Ratio estimates (supporting metric).*

The following assumptions should be used for all calculations: (a) a nadir altimeter having an area of influence equal to a radius of 10 km along the ground track or (b) a swath altimeter including a nadir altimeter having an area of influence equal to 65 km for each side of the swath (if no nadir altimeter is included then 20 km must be subtracted).

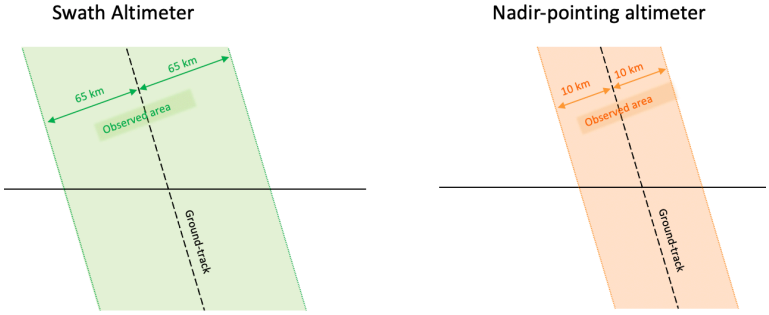

***Observation density maps** are constructed by calculating the number of observations occurring in each element of a global ocean grid of 50 x 50 km (goal 25 km x 25 km) for each day over a period of 1-5 days. If more than 33% of the box surface is observed by instrument swath then the grid box counts as observed.*

***Coverage ratio** is calculated as the average percentage of the earth surface that can be observed each day over a period of 1-5 days. The cumulative distribution of the probability (percentage of latitude weighted by cos(lat)) for which the coverage ratio is lower than x is calculated using:*

$$Coverage\ ratio = \frac{\sum_{i=1}^{N} Covrg(lat_i)cos(lat_i)}{\sum_{i=1}^{N} cos(lat_i)}$$

where $Covrg(lat_i)$ is the percentage of the Earth at latitude, lat_i, observed in a specified time period (in this case 1-5 days), and $lat_i,\ i = 1, \dots, N$, is a sufficiently large range of latitude. The percentage of latitude for which the coverage ratio is lower than 80% should be lower than 20% (TBC). The 'coverage ratio' must be adjusted to consider only measurements that are within performance requirement. For example, the impact of sea state on SSH measurement performance could be addressed by considering the probability of exceedance of Hs at a given threshold (e.g. Pe(Hs=5m).

5.7.3 Hydrology Sampling Constraints

The S3NG-T elevates Sentinel-3 hydrology measurements to primary objective.

MRD-0600 The S3NG-T altimeter shall acquire measurements over all hydrology targets defined in the S3NG-T Inland Water Mask.

Note 1: In order to optimize acquisitions over river and lake targets identified in the Inland Water Mask an on-board processor is highly desirable to reduce data rates as an alternative to continuous acquisition and downlink of measurements at full resolution over all land surfaces.

Note 2: Sufficient allocations on-board the S3NG-T spacecraft must be considered to accommodate and manage information (e.g. Inland Water Mask) necessary for acquisition and/or on-board processing of inland surface waters. This is a lesson learned from Sentinel-3A/B.

Note 3: As a lesson learned from Sentinel-3, an approach that allows regular update of information used by on-board processors should be considered (e.g. the hydrology target mask will be updated up to four times per year specified by MRD-0050).

Note 4: Hydrology sampling coverage and revisit are determined by MRD-0580 and MRD-0590 respectively.

Note 5: In the absence of a Inland Water Mask and for the purpose of system sizing up to 25% of any orbit should be allocated to Hydrology targets.

5.7.4 Cryosphere Sampling Constraints

There are no sampling constraints for sea ice or ice sheets since sampling coverage and revisit are determined by MRD-0580 and MRD-0590 respectively.

Data acquisition masks for cryosphere targets are specified in MRD-0070 and MRD-0080.

6 LEVEL 1 OBSERVATION REQUIREMENTS

6.1 Altimeter Instrument Requirements

S3NG-T is required to provide continuity of Sentinel-3 topography products at Level 2. For radar ranging several frequencies could be used within the limits of ITU regulations and, for this purpose, S-, C-, Ku and Ka-band have all been flown as elements of historical and contemporary satellite radar altimetry missions. Depending on frequency, radar range measurements are influenced by ionospheric and tropospheric path delay and some care is required to mitigate these effects. Selection of the radar frequency also influences the character of the return echoes based on the scattering properties of the target medium interacting with the radar pulse. This has a more profound impact on the measurements associated with normalised radar cross section over non-ocean surfaces that can be of benefit or detrimental depending on the purpose of the mission.

For Sentinel-3 topography, the primary mission objectives are the determination of the ocean surface height and significant wave height, the determination of river and lake/reservoir Water Surface Elevation, as well as the continuity of sea ice and ice sheet measurements.

MRD-0610 To maintain baseline continuity the S3NG-T mission shall embark a nadir looking SAR altimeter centred in Ku-band.

MRD-0620 Requirement deleted.

Accurate and well defined in-orbit calibration approaches are fundamental to the success of the S3NG-T mission. As it is not always possible to achieve complete end-to-end in orbit calibration (e.g. altimeter antenna sub-system is typically outside of the on-board calibration approach), pre-flight ground characterisation is required. Access to some on-ground characterisation information is required by the ground segment and by advanced users of S3NG-T data as part of ground processing. In addition, independent on-ground Fiducial Reference Measurements (FRM) are used during flight to monitor and assess in-orbit calibration (e.g. ground based radar transponders).

MRD-0630 On-board calibration measurements shall be used to maintain the calibration of the altimeter payload to meet requirements at any time during measurement operations.

Note 1: This requirement is to ensure full calibration of measurement data at all times and around the orbit.

Note 2: As calibration measurements are inherently noisy, sufficient measurements are required to obtain a smooth estimate of calibration evolution.

MRD-0640 All on-board calibration data and supporting engineering data required to recalibrate the altimeter measurements shall be available to users.

Note 1: Access to engineering data such as thermistor values, instrument state etc is essential to monitor the performance of the on-board calibration systems and to establish uncertainty budgets and uncertainty propagation and to re-calibrate the instrument on-ground if required as part of reanalysis.

Note 2: Supporting engineering data includes any on-board information considered necessary to reconstruct instrument calibration depending on the specific to the implementation of the on-board calibration system.

Note 3: It is anticipated that this information will be available to users via Level 1a data products.

MRD-0650 The S3NG-T baseline continuity mission shall be capable of continuous operation in fully-focused synthetic aperture radar.

Note 1: Based on the preliminary in-flight performance of Copernicus Sentinel-6 Michael Freilich Poseildon-4 altimeter (Donlon et al 2021), an open burst interleaved functionality is preferred for nadir altimetry.

Note 2: Sentinel-3 SRAL operates in SAR mode over all surfaces at Ku-band (i.e. no LRM capability is used). A fully focussed SAR mode capability, (Egido and Smith, 2017), is therefore considered the baseline for the S3NG-T mission.

Note 3: This implies the radar is operated continuously during nominal scientific measurement operations.

Note 4: Swath altimetry solutions may operate in different modes.

Note 5: Deleted.

Note 6: Deleted.

MRD-0660 The S3NG-T baseline continuity mission shall be capable of an along-track resolution better than 300 m over all target surfaces after data processing.

Note 1: This is baseline continuity for Sentinel-3.

MRD-0670 The S3NG-T baseline continuity mission nadir altimeter shall be capable of generating pulse-width limited data in parallel with SAR data.

Note 1: This requirement builds on the positive experience of Poseidon-4 interleaved mode operations aboard Sentinel-6.

Note 2: For nadir SAR enabled solutions using an open-burst continuous radar chronogram solution, both LRM and SAR data can be generated on ground.

MRD-0680 The S3NG-T baseline continuity mission altimeter shall be capable of measuring a range of surface elevation with respect to the ellipsoid to meet mission requirements.

Note 1: This allows the mission to observe the highest elevations defined in the Hydrology mission.

MRD-0690 The S3NG-T baseline continuity mission altimeter shall maintain tracking over ice surfaces, glaciers and ice sheet margins with slopes less than 1.25° (TBC).

Note 1: McMillan et al. (2021) show that both Sentinel-3A and Sentinel-3B are capable of maintaining coherent signals over ice sheet margins. See also Wingham (1995).

Note 2: Deleted, superfluous.

Note 3: High resolution on-board DEM's could be used to maintain altimeter echoes within the range window over ice margin regions.

Note 4: This requirement will be assessed based on the final configuration of the technical solution.

MRD-0700 The S3NG-T altimeter should maintain tracking over icebergs with a freeboard below 50m (enhanced goal: below 60 m (TBC)).

Note 1: For small Icebergs the analysis of CryoSat-2 SARIN data shows that 90% of the icebergs detected have a freeboard less than 60m (there are some outliers but they are rare); Antarctic icebergs tend to be quite tabular and have a freeboard slightly lower than those form Greenland.

Note 2: Tournadre et al. (2015) analyse large icebergs characteristics from altimeter waveforms analysis and provide a pdf of 5366 iceberg freeboard estimates as follows.

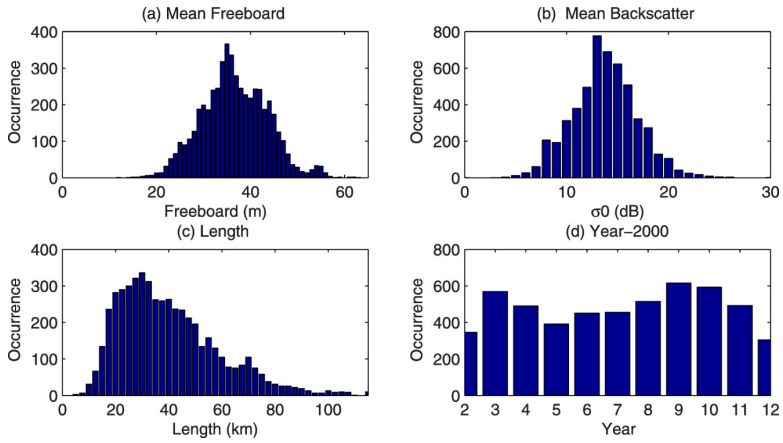

MRD-0705 The S3NG-T altimeter shall maintain tracking over water reservoirs having a surface water elevation dynamic range up to 50m (enhanced goal: up to ≤60 m (TBC))

Note 1: Inland water reservoirs have extreme variations in surface water elevation depending of reservoir capacity, that must be mostly captured by Sentinel-3A SRAL for observed reservoirs (e.g. Zhang et al. 2020).

MRD-0710 The S3NG-T baseline continuity mission altimeter range resolution shall be better than 0.5 m (enhanced goal: better than 0.3 m).

Note 1: Range resolution impacts, primarily, the ability to properly sample specular echoes, such us from hydrology targets and over sea ice leads.

MRD-0720 Orbit manoeuvres for ground track maintenance shall be scheduled to take place over areas that minimise the impact of data loss defined by the Marine and Coastal Mask and the Inland Water Mask.

Note 1: Manoeuvres may be necessary in areas that could result in data loss.

Independent on-ground Fiducial Reference Measurements (FRM) are used during flight to monitor and assess in-orbit calibration. A ground-based transponder is foreseen as part of the mission as part of the calibration and validation activities for the duration of the mission. Ground-based transponders allow verification of σ^0, range, datation, interferometry geometry among other parameters. Transponders are mandatory for Cal/Val of altimeter missions, cross-calibration of missions. Active transponders require accurate positioning (with FRM standard uncertainty) information with using GNSS and other positioning systems (e.g. DORIS beacon). A radiometer is needed to derive the wet tropospheric delay during transponder calibrations in addition to the GNSS-derived delays. As part of the Permanent Facility for Altimeter Calibration (PFAC) located in Crete, Greece (Mertikas et al., 2018, 2019), a Ku-band transponder has been established for pulse-width limited (and thus lower SNR) altimeter missions as an external calibration source (Mertikas et al., 2011; 2010) supported by with in-situ reference systems (DORIS ground station, GNSS reference points, radiometer for wet tropospheric correction, etc.). It is notable that a single Sentinel-3A and Sentinel-3B transponder pass over the PFAC during the Sentinel-3 tandem phase established a bias difference of just 1.5cm between the two altimeters. The PFAC is maintained operationally and is being upgraded with a second transponder to support Sentinel-6MF located on Gavdos Island, Western Crete as part of the ESA Sentinel-6 calibration and validation activities.

At present no Ka-band ground-based transponder exists and will need to be developed as part of the S3NG-Mission. The S3NG-T altimeter must carry appropriate functionality for use with ground-based transponders.

MRD-0730 The altimeter shall be capable of acquiring measurements from a ground-based transponder for calibration purposes.

Note 1: At this time only one European well-maintained Ku-band range transponder facility is at the disposal of Copernicus which is maintained at the PFAC in Crete. This transponder is used by Jason-2, Jasnn-3, Sentinel-6, Sentinel-3 and CryoSat-2. The location of the PFAC site is at the crossover points of Sentinel-3 and Sentinel-6 orbits. For information, the coordinates of the currently operational ESA PFAC transponder units are:

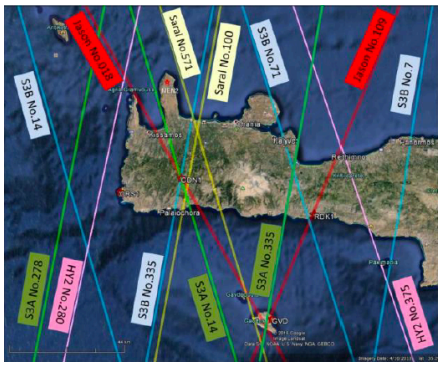

CDN1	Lat: 35.337840^0 N Lon: 23.779502^0 E	Transponder & GNSS array	S6, S3A, S3B, Jason-3, Cryosat-2	Operational
Gavdos (GVD1)	Lat: 34.838503^0 N Lon: 24.108648^0 E	Transponder & GNSS array	S6, S3A, S3B, Jason-3, Cryosat-2	

Note 2: Recent developments using Sentinel-6 using on-ground corner reflectors may provide an alternative solution for in flight calibration.

MRD-0740 It shall be possible to configure the altimeter by telecommand to acquire measurements from a ground-based transponder.

Note 1: This functionality applies only to the space segment and allows on-board settings to be fully controlled for different transponder acquisitions (e.g. gain settings) that have been used on previous missions and different.

MRD-0750 The S3NG-T baseline continuity mission shall provide range measurements with a noise floor below 0.8 cm at 1 Hz and Hs=2m (enhanced goal: ≤ 0.5 cm at ≥1 Hz and Hs=2 m) after ground processing.

Note 1: See Table 2.4-1 for in flight performance of Sentinel-3.

Note 2: Requirement is set for Sentinel-3 continuity, goal is equivalent to Sentinel-6 NTC performance.

Note 3: The upper limit depends on Significant Wave Height (Hs) that defines the noise that will increase with increasing sea state.

Note 4: Deleted.

Note 5: Deleted.

Note 6: Deleted.

The Cross-Calibrated Multi-Platform wind vector analysis (CCMP, Ricciardulli and NCAR, 2017) is a near-global, high spatial (0.25° gridded product) and temporal (6 hourly) resolution gridded dataset of surface wind vectors from 1987-present between 78° North and South of the equator. A combination of inter-calibrated satellite data from numerous microwave radiometers and scatterometers together with in-situ data from moored buoys form the basis of the analysis. A best-fit solution to all of the available observations is derived using the ECMWF ERA-Interim reanalysis winds as a first guess. The temporal record is relatively stable, and are well suited to monitor daily to interannual variability. The analysis is known to perform poorly for precipitating conditions and under high wind (>15 m/s) conditions, and is therefore not recommended for studies of global wind trends. Figure 6.1.1 shows the Probability Density Function (PDF) of the CCMP data set between 1988-2020 at a grid size of 0.25° latitude x longitude between 78° North and South of the equator.

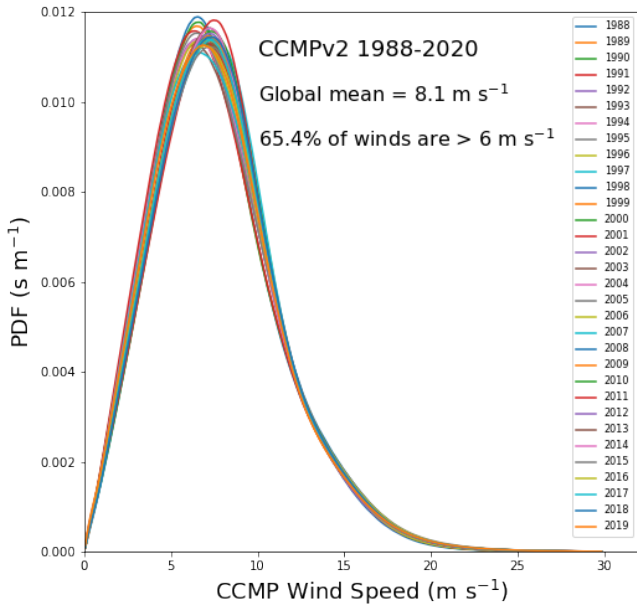

Figure 6.1-1. Probability Density Function (PDF) of global ocean wind speeds for 1988-2020 derived from the Cross-Calibrated Multi-Platform wind vector analysis (CCMP, Ricciardulli and NCAR, 2017) 0.25° gridded product) and temporal (6 hourly) resolution of surface wind vectors from 1987-present between 78° North and South of the equator. (Credit: C. Gentemann.)

MRD-0760 The nominal wind speed value over the ocean when computing the radar altimeter link budget shall be larger than 8.1 m s^{-1}.

Note 1: Figure 6.1-1 provides a PDF of the mean annual wind speed over the ocean surface.

Note 2: This wind speed value corresponds to an average nominal normalised backscatter coefficient (sigma-0) value over the ocean of 13 dB for Ku-band and 11-dB for Ka-band; see Hossan et al., 2021.

Note 3: System margins are typically added to these sigma-0 figures to achieve a minimum SNR of 11 dB as in the case of Sentinel-3 and Sentinel-6.

Note 4: Removed, note not relevant for this requirement.

MRD-0770 The nominal significant wave height (SWH) value to be assumed for any S3NG-T baseline continuity instrument calculations that depend on modelling waveforms shall be 2 metres.

Note 1: Altimeter range measurement uncertainty increases with increasing sea state.

Note 2: A mean sea state of Hs=2 m is defined based on wind speed of 8 ms-1 over the ocean at 10 m height (U10).

In terms of the atmospheric attenuation experienced by the radar, Figure 6.1-2(a) shows shows the percentiles of atmospheric attenuation at Ku-band for valid altimeter observations only from Sentinel-6 data. This mostly represents the dry, wet and liquid contributions, since large rain impacts the range and thus leads to invalid Sea Surface Height measurements. At Ku-band, the percentiles of the atmospheric attenuation computed from ERA5 is consistent with the percentile of the attenuation computed from the radiometer. The difference for large attenuation is probably due to the weak representation of rain in the model, especially for strong small convection cells responsible for large attenuation (both in amplitude and location).

Figure 6.1-2(b) shows the percentiles of atmospheric attenuation respectively at Ka-band for valid altimeter observations only, from AltiKa data. As expected, the atmospheric attenuation for valid measurements is larger at Ka-band than at Ku-band with a median at about 1 dB. At Ka-band, a bias of about 0.2 dB is observed between the atmospheric attenuation retrieved from MWR observations and computed from ECMWF or ERA5 (those latter being very similar). There are some known issues on the retrieval of the wet tropospheric correction on AltiKa and since the same approach is used for the atmospheric attenuation, the latter is most probably also impacted.

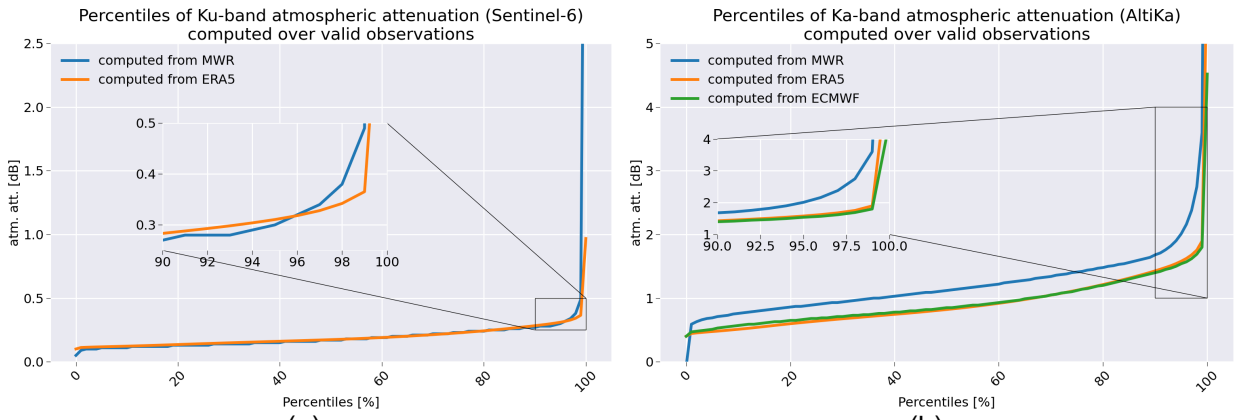

Figure 6.1: Atmospheric attenuation for valid measurements at Ku-band (a) and at Ka-band (b); courtesy, Bruno Picard.

MRD-0780 The two-way atmospheric loss shall be assumed to be 0.5 dB in Ku-band and 1 dB in Ka-band when computing the radar altimeter link budget.

Note 1: Values correspond to observed median values from Sentinel-6 and AltiKa in nominal atmospheric conditions without precipitation.

MRD-0790 The following nadir-pointing waveform model shapes shall be used for S3NG-T baseline continuity mission radiometric performance calculations:

Ocean echoes: the return echo waveform may be assumed to follow the Brown Model over ocean and some non-ocean surfaces;
Ice echoes 1: with a trailing edge slope of -0.125 dB/ns;
Ice echoes 2: with a trailing edge slope of -0.5 dB/ns;
Ice echoes 3: with a trailing edge slope yielding a total echo power equal to the total power of an ocean echo with a normalised backscatter coefficient (σ°) of 42 dB (TBC) in Ku-band and 40 dB (TBC) in Ka-band.
Specular Echo: is defined for calm water/river, lake targets and sea ice leads, and is a purely specular return with the same shape and characteristics as the radar instrument impulse response and σ° equivalent to that of the first Fresnel reflection.

Note 1: Sentinel-3 SRAL specification.

Note 2: A different Sigma0 model is required for swath altimeter solutions.

Note 3: Nadir pointing Sigma0 models for Inland Waters are TBD

Note 4: Vandemark et al. (2004) model the relationship between low-incidence Ka-band Sigma0 measurements to wind speed (via its relation to the ocean mean surface capillary wave slope variance), modified for low wind speeds to allow specular reflection

Note 5: Different echo shapes may be required for hydrology targets, ice targets and transponder

Note 6: Specular returns coming from the Fresnel zone should not account for additional margin for speckle noise.

MRD-0800 S3NG-T baseline continuity mission altimeter radiometric performances shall be met for different surfaces with echo shape characteristics and over the normalised backscatter coefficient (σ°) range as specified in Table 6.2.

Note 1: Note Deleted.

Note 2: These figures include the scattering properties of ice and the effect of slope. No further correction for surface slope is required in using the figures.

Note 3: Further adjustment for the scattering properties of ice and the effect of slope may be required.

Note 4: A comparison of backscatter values observed with AltiKa over sea ice and leads is provided in Figure 6.1.2

Note 5: Vandemark et al. (2004) model the relationship between low-incidence Ka-band Sigma0 measurements to wind speed (via its relation to the ocean mean surface capillary wave slope variance), modified for low wind speeds to allow specular reflection.

Note 6: Consideration of all figures over river and lake targets must be considered.

Note 7: A different Sigma0 model is required for swath altimeter solutions.

Table 6.1: Normalized Radar Cross Section (NRCS, sigma-0) values for different surfacesn and echo types.

Surface Type	σ° Ku-band (all TBC)	σ° Ka-band (all TBC)	σ° C-band (all TBC)
Ocean (including coastal)	Ocean echoes: 8 dB < σ° < 27 dB; Ice echoes 1: 2 dB < σ° < 42 dB. Ice echoes 2: 2 dB < σ° < 42 dB.	Ocean echoes: 6 dB < σ° < 25 dB;	Ocean echoes: 12 dB < σ° < 30 dB;
Sea ice and Icebergs	Ocean echo: 8 dB < σ° < 27 dB; Ice echoes 1: 2 dB < σ° < 42 dB; Ice echoes 2: 2 dB < σ° < 42 dB; Ice echoes 3: 42 dB < σ° < 57 dB. Specular Echoes: 42 dB < σ° < 55 dB (TBC)	Ice echoes 1, 2 and 3: 0 dB < σ° < 55 dB;	TBC
For inland ice-sheets and ice-caps	Ocean (Brown echo): 6 dB < σ° < 25 dB; Ice echoes 2: -8 dB < σ° < 40 dB; Ice echoes 3: -8 dB < σ° < 40 dB;	Ice echoes 2 and 3,: 0 dB < σ° < 40 dB;	TBC
Ice sheet margins and glaciers	Ocean echoes: 8 dB < σ° < 27 dB; Ice echoes 1: –8 dB < σ° < 42 dB; Ice echoes 2: –8 dB < σ° < 42 dB	Ice echoes 1,2,3: -10 dB < σ° < 40 dB;	TBC
Inland waters (including frozen lakes)	Ocean echoes: 8 dB < σ° < 27 dB; Ice echoes 1: -8 dB < σ° < 42 dB; Ice echoes 2: -8 dB < σ° < 42 dB; Specular Echo: 42 dB < σ° < 57 dB (TBC)	Specular Echo ($sinc^2$ response): 6 dB < σ° < 55 dB;	TBC

Figure 6.1-3(a) shows data from the AltiKa altimeter revealing a dynamic range of 5 dB to +20 dB over global ocean surfaces. Figure 6.1-3(b) shows data from the AltiKa altimeter revealing a dynamic range of 0 dB to +50 dB including for ice floes and lead areas . Specular echoes over river targets may need to be confirmed.

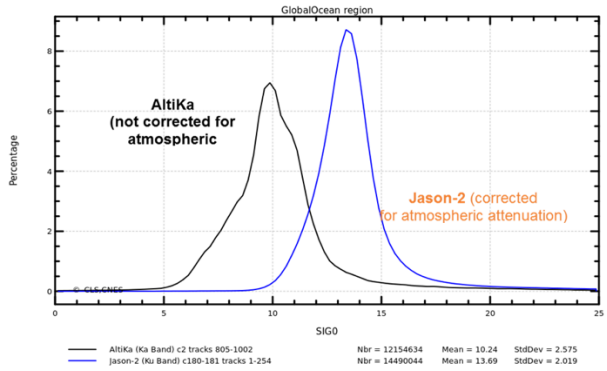

Figure 6.1-3(a). Dynamic range of AltiKa Ka-band σ^0 compared to Jason-2 Ku=band σ^0 over the global ocean (A. Guillot).

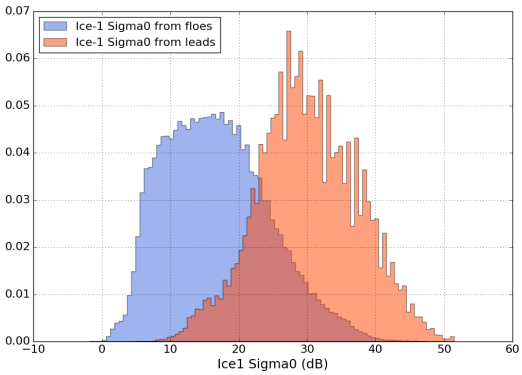

Figure 6.1-3(b). Distribution of AltiKa Ka-band σ^0 over ice floes and leads (A. Guillot).

MRD-0810 The S3NG-T baseline continuity mission dynamic range of sigma-0 shall be 0 to 55 dB at Ku band.

Note 1: Deleted.

Note 2: Specular echoes from river and lake targets may require assessment depending on the payload configuration.

MRD-0820 The S3NG-T baseline continuity mission total standard uncertainty of the sigma-0 measurement shall be better than 1dB (enhanced goal: 0.3dB), after appropriate calibration.

Note 1: Sentinel-3 SRAL specification.

MRD-0830 The S3NG-T baseline continuity mission stability in the measurement of sigma-0 shall be better than 0.3 dB per orbit at Level 1, assuming interruption of science measurements for internal calibration not more frequently than once per orbit.

Note 1: The long-term drift error of Sentinel-3 SRAL Sigma0 internal calibration is specified as less than 0.3dB during the mission life-time.

Note 2: Requirement is set equivalent to Sentinel-6 performance since S3NG-T will serve Copernicus climate service applications where stability is fundamental to the production of a climate record.

MRD-0840 The S3NG-T baseline continuity mission shall provide sigma-0 over the ocean surface with a long-term drift less than 0.5 dB (enhanced goal: 0.3 dB) after cross-calibration with other altimeter missions across the mission lifetime.

Note 1: Requirement is set for Sentinel-3 continuity, goal is equivalent to Sentinel-6 NTC performance.

Note 2: If multiple satellites are used in the S3NG-T this requirement bring homogeneity across the satellite fleet.

MRD-0850 The stability of S3NG-T baseline continuity mission NTC sigma-0 measurements shall be better than 0.3 dB during any year period.

Note 1: Requirement is set for Sentinel-3 continuity, goal is equivalent to Sentinel-6 NTC performance.

Sentinel-6 Poseidon-4 implements an on-board Range Migration Correction (RMC) algorithm that provides an efficient approach to reduce the data volume by a factor two by truncating the processed waveforms. The approach uses approximations leading to Doppler stack misalignment: a fixed RMC matrix is applied for mean altitude; mean sea surface slopes are not accounted for and the accuracy of radial velocity estimates is relatively poor compared to that available on-ground. However, on-board RMC processing can be reversed on-ground without loss of useful information so that Doppler stack misalignment can be corrected (requiring I and Q signals) and accurate SAR processing is then applied on-ground. If I and Q signals are available on-ground, all processing options are possible including: optimal sea ice processing, fully-focused SAR, SAR multi-looking, RMC stacking, pulse-pair amongst others. Simulations suggest that 64 ranges bins and 16 Doppler bands are required to achieve good performance (64 and 128 range bin noise levels are identical for range, *Hs* and σ^0). If on-board RMC is not reversible or fully configurable in flight it implies L2 processing must account for on-board errors due to assumptions and limitations of modelling - otherwise, large Hs and SSH errors are expected. This makes the L2 processing more complicated, risky and less processing options are possible.

SAR Interferometry over inland waters is complex due to the specific elevation change induced by inland topography. The NASA/CNES SWOT mission uses substantial on-board processing to reduce data rates by computing interferograms over all ocean and land surfaces that are downlinked. However, over hydrology targets a suitable on-board processing approach has not been defined and large volumes of data are downlinked from which useful measurements can be extracted on-ground. It is anticipated that on-board processing approaches could be developed for hydrology targets once SWOT in-flight data are available in the 2024/25 timeframe.

MRD-0860 Requirement Deleted.

MRD-0870 For the nadir-looking baseline continuity component of the S3NG-T mission, on-board processing algorithms shall avoid lossy compression techniques.

Note 1: Sentinel-6 implements a Range Migration compression and data truncation function on board the satellite. For the S3NG-T baseline continuity mission This means that I and Q signals must be available on ground for accurate SAR processing.

MRD-0880 Requirement merged with MRD-0050.

A dedicated mode is required to acquire raw unprocessed data to verify the on-board processors and optimize the algorithms. In addition, the on-board processing approach is likely to evolve with experience and may require complete update in flight depending on the configuration of the final concept.

MRD-0890 If on-board processing is required, a dedicated mode shall activate by telecommand to allow downlink to ground of complex altimeter echoes before onboard processing for up to 20% of an orbit within any contiguous segment of any orbit.

Note 1: As no reprocessing could be done on the ground to recover data measured before onboard processing, a set of original raw data is required to validate the onboard processing and define new on-board processing techniques that can be uploaded to the satellite.

Note 2: Lossless compression techniques may be used to minimize altimeter data rates. Lossless compression techniques are already used for Copernicus SAR imager and high-resolution optical missions.

Note 3: Superseded.

Note 4: The primary purpose of acquiring complex altimeter echoes is to confirm, monitor and potentially refine the performance of on-board processing algorithms using a prototype processor on-ground.

MRD-0900 If on-board processing is required, the geographical location of complex altimetry echoes acquisitions shall be defined by a modifiable mode mask.

Note 1: The mode mask will be refined as the mission evolves.

Note 2: An example for complex altimeter echoes acquisition mask is provided in Appendix XI.

MRD-0910 Requirement deleted.

MRD-0920 S3NG-T Level 1 and Level 2 altimeter data products time tags associated with the measurement data shall have a resolution of less than 1 microsecond (3 sigma, zero-mean) with the International Atomic Time (TAI).

Note 1: Requirement is set equivalent to Poseidon-4 performance.

MRD-0930 S3NG-T Level 1 and Level 2 altimeter products, shall have a total time-tag uncertainty (i.e. the combination of systematic and random error) less than 10 microseconds (3 sigma, zero-mean) with the International Atomic Time (TAI).

Note 1: Requirement is set equivalent to Poseidon-4 performance.

MRD-0940 Requirement deleted.

MRD-0950 Requirement deleted.

A pointing error requirement is the specification of probability that the system output of interest does not deviate by more than a given amount from the target output with a level of confidence Pc. In this context a pointing error can refer to the actual system deviation and thus performance, or the determination of the actual deviation, thus knowledge.

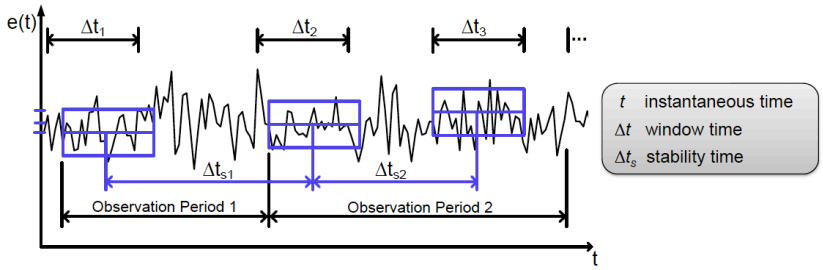

Mis-pointing of a nadir pointing satellite altimeter antenna result in significant impact on geophysical retrievals particularly for SAR altimeters (e.g. Halimi et al, 2014) since the backscatter energy within an echo has a strong dependence on mis-pointing. In particular, it modifies the slope of the waveform trailing edge and attenuates the signal – mispointing angles are used as a quality control and when mis-pointing is severe, waveforms are discarded from the final data set. Hayne (1980) explains that the mean return of an LRM waveform is the convolution of a) the average impulse response of the quasi-calm sea surface, b) the sea surface elevation distribution, and c) the radar system point-target response (transmitted pulse as affected by the receiver bandwidth). The first term a) includes the effects of the antenna beamwidth and the off-nadir pointing angle; “quasi calm” emphasizes that an incoherent surface scattering process

is assumed but that the sea surface elevation distribution is included in the surface elevation distribution. For a delay Doppler altimeter mis-pointing and its stability over shorter timescales is more critical since multiple high spatial resolution (~300m along track) measurements are focused and stacked before noise reduction; in this case, along-track mis-pointing reduces the amplitude of the multi-look echo whereas across-track mis-pointing reduces both the amplitude of the multi-look echo and the shape of the altimeter waveform (e.g. Halimi et al, 2015).

Mis-pointing can be mitigated for conventional altimetry (LRM) using the Hayne (Hayne 1980) model using a mean mis-pointing estimated over 5 s of measurement (e.g. Tournadre et al, 2011) and is an on-going area of research for delay-Doppler altimeters using generalized semi-analytical models and in future, the impact of vertical speed effect and the thermal noise (Halimi et al, 2015).

MRD-0960 The S3NG-T baseline continuity mission Absolute Performance Error (APE) for spacecraft pointing shall be below 0.2 degrees in yaw, below 0.1 degrees in pitch and below 0.1 degrees in roll (3 sigma, zero-mean) with respect to the local normal of the reference ellipsoid and with respect to the inertial reference frame.

Note 1: Ka-band pointing requirements are more stringent than at Ku-band. Specification is taken from CRISTAL.

Note 2: Absolute Performance Error (APE) is defined as the difference between the target (commanded) parameter (attitude, geolocation, etc.) and the actual parameter in a specified reference frame.

Note 3: The overall figure is to be understood as an end-to-end specification, including the satellite nadir pointing errors due to the AOCS and guidance performances, thermo-elastic effects, launch shift, 1-g release effects and altimeter antenna boresight to mechanical reference uncertainties.

Note 4: The altimeter pointing reference is the electrical boresight for the nadir looking altimeter.

Note 5: The reference ellipsoid WGS-84 should be used for calculations of position, altitude and attitude.

MRD-0970 The S3NG-T altimeter mispointing knowledge shall be computed and be made available to users.

Note 1: This is normally part of the standard products.

MRD-0980 Requirement deleted.

MRD-0990 Requirement deleted.

MRD-1000 Requirement deleted.

6.2 Microwave Radiometer Requirements

The atmosphere reduces the speed of the radar pulse, bending its trajectory and, therefore, causing a “path delay” of the altimeter signal, which would, if unaccounted for, result in a too long observed range and, therefore, too short an elevation measurement with respect to a reference ellipsoid. This effect is usually modelled into three different parts: the delay due to the dry gasses in the troposphere (mainly nitrogen and oxygen) as a “Dry tropospheric Path Delay”(DPD), the delay due to the water vapor in the troposphere as a “Wet tropospheric Path Delay”(WPD)and the delay due to the free electrons in the upper atmosphere (ionospheric path delay). To accurately monitor geophysical parameters for Earth targets, satellite altimeter measurements require an accurate determination of DPD, WPD and ionospheric path delays.

Over the ocean DTC is one of the most precise range corrections (better than 1 cm) typically derived from the ECMWF ERA interim and NCEP operational models (e.g. Fenandez et al., 2014). However, the water vapour content within the troposphere exhibits large spatial and temporal variability which is difficult to model commensurate with the space and time resolution of the altimeter measurement. Instead, dedicated microwave radiometer instruments are used to correct altimeter radar pulses for this effect.

For inland water applications, there is little information available in the literature describing path delay corrections. One of the main sources of uncertainty in inland water range measurements is the wet tropospheric correction (WTC). Currently, for most inland water bodies, except for large lakes, the main source of the WTC are NWP model outputs, which are still unable to capture the smaller scales of variability of the WTC field (certainly at the scale of along-track altimetry/scale of a river crossing). The WTC needs to be far below the WSE requirements as one of the components of the radar range equation. Historically, a requirement for WTC for inland water applications has not been set as part of the overall altimetry budget. Since the space-borne Microwave Radiometers (MWR) retrievals also depend on surface emissivity, MWR are used only over homogeneous surfaces such as large water bodies (ocean and large lakes) but have large errors over challenging transition surfaces such as those over rivers, small lakes and. in the coastal zone. Considering the current measurement capabilities, the main measurement WTC source over inland waters are dense GNSS networks, from which accurate, better than 1cm, WTC observations can be obtained (Fernandes et al. 2014;2021). Over most regions GNSS networks require densification and ground-based MWR and radiosondes are also relevant complementary sources although they are scarce. Over inland waters, the WTC must be derived from combined WTC values using a method such as GPD+ (Fernandes et al, 2021), by combining all available observations, e.g., on-board MWR and external microwave imaging radiometers (over large lakes.), GNSS and the best Numerical Weather Model (ERA5). Over most regions GNSS networks require densification. To account for the vertical variation of the water vapour, the WTC shall be provided at surface height, using mean lake levels, river profiles and the best available DEM and shall be computed at high rate (20Hz), Fernandes et al., 2014).

If tropospheric corrections are not modelled and computed properly and in a consistent manner, they limit the performance in inland water height determination. Fernandes et

al (2014) provides a very good overview of the issues and solutions. Dry tropospheric path delay corrections for inland water applications should be derived by first computing the correction at each altimeter measurement location by interpolation from sea level pressure model grids using a suitable height reduction approach. Due to its large spatio-temporal variability, the ZPD correction may be the second largest source of error over inland water regions. Over large lakes the traditional microwave radiometer derived approach can be used with confidence (if the radiometer antenna gain pattern sidelobes are well controlled to limit side-lobe contamination from land emissions). However, for smaller lakes and river reaches where a GNSS permanent ground station is available, GNSS-derived wet tropospheric corrections can be a very valuable and accurate data source, particularly, e.g., for small lakes for which the data from a single station is representative of the local wet path delay condition. In the absence of any of the previous data types, over small lakes and rivers, model-derived corrections computed at surface height, provide the highest accuracy (e.g. ECMWF ERA Interim has uncertainties of 1–3 cm in wet tropospheric correction (Fernandes et al. 2014). Several improvements hold great potential including the following:

Improvements for GPD (data combination method):

- Algorithm improvement, namely on the temporal scales of the WTC field;
- Assessment and incorporation of new WTC datasets (GNSS and imaging radiometers);
- New methods to transition current regional retrieval of the dry and wet tropospheric correction in regional approaches (e.g. HYDROCOASTAL for each region of. interest) to a global approach, covering the most relevant inland water regions.

Improvements on WTC retrievals from on-board MWR (direct methods):

- Improvement of the direct retrieval of WTC from on-board MWR, over homogeneous and transition zones;
- Over homogeneous surfaces, the goal is to improve the current retrieval algorithms (parametric and neural network approaches);
- Over transition zones, the goal is to improve the WTC retrieval, through e.g. the modelling of the land fraction in the MWR footprint.

Regional assessment (over inland water regions) of the various NWP model outputs available for the computation of the dry and wet troposphere corrections:

Such an assessment does not exist and it is necessary to identify the real needs for improvements of the WTC from model output over inland water regions.

Since space-borne Microwave Radiometers (MWR) retrievals also depend on surface emissivity, MWR are used only over homogeneous surfaces such as large water bodies (ocean and large lakes) and have large errors over transition surfaces such as those over Rivers and small lakes, as well as in the coastal zone. Considering the current measurement capabilities, the main measurement WTC source over inland waters are dense GNSS networks, from which accurate, better than 1 cm, WTC observations can be obtained. Over most regions GNSS networks require densification. Ground-based MWR and radiosondes are also relevant complementary sources but are scarce.

The Copernicus Sentinel-6 mission (Donlon et al, 2021) Advanced Microwave Radiometer for Climate (AMR-C) instrument (e.g. Brown et al., 2004; Maiwald et al., 2020) measures linear polarized brightness temperature (TB) at 18.7, 23.8 and 34 GHz. It uses an internal reference load and three noise diodes for short-term calibration, which is performed autonomously as part of the nominal measurement cycle. The three-frequencies are used to separate the three dominant components of the TB signal to estimate wet PD: total atmospheric water vapour, total integrated cloud liquid water and wind induced ocean surface roughness (e.g. Fernandes et al., 2015). The troposphere affects the altimeter radar signal at various time-space scales, from high frequency—in the vicinity of fast moving atmospheric fronts and near the coasts—to low frequency and large scales over open ocean. The relatively large ground footprint of the AMR-C 18-34 GHz channels remain the baseline inputs for Sentinel-6 to determine WP delay over the open ocean but near coastlines, the retrieval error significantly increases due to antenna beam contamination by warm landmasses (e.g. Desportes et al., 2007, Lázaro, 2019). For Jason-2/OSTM, the impact of land contamination in the measurement field of view increases rapidly ~30 km from the coastline with a minimum residual variance at 40 km (Sibthorpe et al., 2011). To support the Copernicus Sentinel-6 high resolution SAR mode from the Poseidon-4 SAR altimeter in the coastal zone, an experimental high-resolution microwave radiometer (HRMR) was developed (Kangaslahti et al., 2019) as a subsystem of the AMR-C to provide high spatial resolution measurements at 5 km resolution. HRMR includes millimetre-wave channels at 90, 130 and 168 GHz with good sensitivity in the atmospheric water vapour continuum. The HRMR has a sensitivity (NEDT) of better than 0.2 K and stability of 0.2 K for all three frequencies over 60 s. Data from these channels will extend the WP delay retrievals closer to the coast under cloud-free conditions on an experimental basis. In operation, HRMR data will not use the calibration targets of the AMR-C SCS but will be cross calibrated based on the AMR measurements over ocean targets before coastal transitions occur. See Maiwald et al (2020) for a full description of the Sentinel-6 HRMR.

It is to be noted that the 34 GHz channel of AMR-C operates outside frequency bands allocated by the ITU to Earth observations. Therefore, the use of such frequency should be avoided. The frequency bands 31.3-31.8 GHz and 36-37 GHz should be used instead.

Enhanced wet PD performance for S3NG-T can be derived using a number of additional channels with higher spatial resolution to respond to coastal regions for the nadir beam (typically at higher frequency). There is clear advantage to including the 18.7GHz (AMR-C Sentinel-6 heritage) channels. Further advantage in reducing the WTC uncertainty using higher frequency channels of the HRMR (90, 130 and 168GHz). Such channels could also provide additional capacity for precipitation screening. High frequency channels would enable rain flagging (e.g. 165 and 172GHz).

For the NASA/CNES SWOT configuration, two radiometer horns are focused on the centre of each swath to reduce wet troposphere errors.

MRD-1010 The S3NG-T baseline continuity mission shall embark a multi-channel microwave radiometer (MRAD) having channels centred at 23.8 GHz and 31.4GHz, (Enhanced continuity: one or more of 18.7 GHz, 89 GHz, 165.5 GHz and 172 GHz).

MRD-1020 Level 2 S3NG-T mission MRAD measurements for all channels shall be co-registered and near contemporaneous with the altimeter measurements after ground processing.

Note 1: This requirement allows the possibility to acquire data from different beams at different times as the satellite flies forwards.

MRD-1030 Requirement deleted.

MRD-1040 Requirement deleted.

MRD-1050 Requirement deleted.

MRD-1060 Requirement deleted.

In the coastal zone and over rapidly changing atmospheric moisture structures including cloud structures, precipitation and land-sea breeze (amongst other phenomena) lead to more complex atmospheric temperature, pressure and moisture structures that are significantly different from open ocean conditions. Their influence may persist for several hundred km offshore. Furthermore, due to the input of freshwater from rivers and estuaries, bio-geo-chemical compounds and pollutants are more ubiquitous in this region. Natural compounds from biological decay form long-chain organic surfactants on the ocean surface in calm conditions that, together with pollutants on the ocean surface, inhibiting the growth of capillary waves (to which the radar altimeter responds) and modifying the surface emissivity (to which the microwave radiometer responds). Furthermore, these physical, bio-geo-chemical and atmospheric aspects and characteristics present a very complex sea surface topography structure and lead to specific measurement challenges compared to the open ocean. At the ocean-sea ice interface, other complex phenomena arise as sea ice in the marginal ice sone is highly variable and the atmospheric structures can be very different over the ice and ocean (e.g. katabatic winds from cold dry sea ice interiors or ice sheet interiors pour out across the ocean for several hundred km). Over terrestrial hydrology targets, depending on the water body size and persistence, similar atmospheric changes may exist complicating the altimeter measurements of Water Surface Elevation.

Practically, the impact of a high performant beam efficiency can limit side-lobe contamination at L1 can be estimated and mitigated by analysing the contribution of power from the full beam (including side and other lobes) compared to the -3dB

footprint ellipse using accurate antenna gain patterns and knowledge of the brightness temperature characteristics of surrounding MRAD measurements. This requires that accurate antenna gain pattern knowledge is available for each channel and feed (if multiple feeds are employed) and a L1 data processing approach is used to adjust the -3dB measurement and compensate for side-lobe contamination.

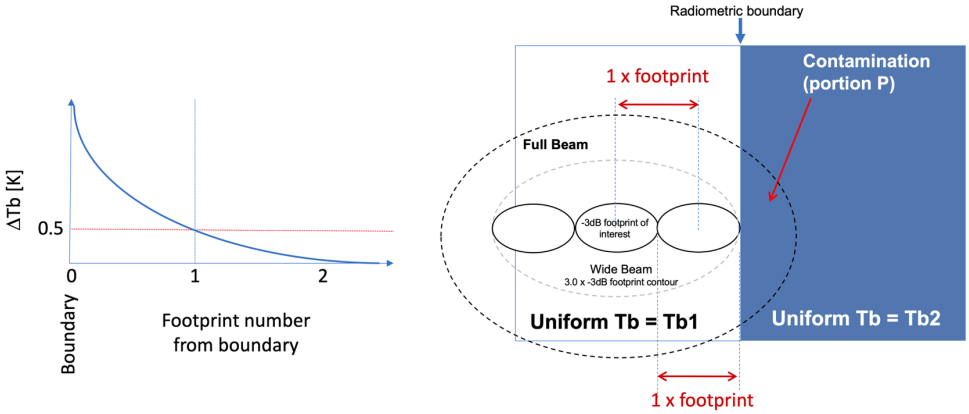

Figure 6.2-2. Schematic example of how Brightness Temperature (Tb) changes as it approaches a boundary to illustrate the meaning of MRD-1040.

Maintaining performance of MRAD at coastal and sea ice transitions is important. This is linked to the size of MRAD footprints and the quality of side-lobe compensation (a function of payload design and antenna gain pattern knowledge). When assessing the performance of MRAD at coastal and sea ice transitions and, as part of the MRAD total standard uncertainty assessment, a synthetic scene provides a powerful means to control the assumptions used (both geometrically and radiometrically). The following requirement is specified for coastal and sea ice transitions and the approach to be used to address each requirement is summarised in Figure 6.2-2.

MRD-1070 The impact of radiometric discontinuities (e.g. thermal ocean fronts, at a coastal boundary, sea ice edge or ice shelf edge etc) on S3NG-T MRAD brightness temperature measurements shall be mitigated by appropriate side-lobe compensation.

Note 1: Deleted, superfluous.

Note 2: This requirement is designed to ensure that side-lobe corrections at an appropriate level.

Note 3: This requirement implies a well-formed antenna beam and well characterised antenna side lobes and grating lobe patterns to be used in Level 1 processing.

Note 4: This requirement implies that a suitable algorithm is used to compensate for side-lobe and e.g. grating lobe contamination at Level 1.

Note 5: This requirement will be assessed theoretically by analysis.

Note 6: It is expected that the "worst case" will be in the coastal zones where there are large radiometric discontinuities (temperature, emissivity, varied terrain and elevation etc).

MRD-1080 The calibration of S3NG-T MRAD Level 1 brightness temperature in all channels shall be maintained during science measurement acquisition using an on-board calibration system.

Note 1: Options to provide reference values include hot and cold load sources (including active cold loads and noise diodes).

Note 2: The means that for all on-board calibration reference value temperatures should be reference to the International Temperature scale 1990 (ITS 1990) – see Preston-Thomas (1990)

Note 3: The reflector characteristics must be known and the reflector temperature monitored in flight.

Note 4: Vicarious calibration targets are not traceable to SI. Therefore, the on-board calibration system must be thoroughly characterised before flight and a strategy developed to periodically check calibration.

Note 5: While not strictly traceable to SI, a view of deep space, when used together with frequency-specific galactic background radiance maps, offers a practical solution.

Note 6: Active cold Load technologies provide one approach to in-flight calibration.

MRD-1090 The S3NG-T baseline continuity mission MRAD shall be capable of regularly viewing deep space as a cold calibration reference.

Note 1: Deep space is considered a reference target scene for calibration purposes (e.g. Farrar et al. 2016).

Note 2: Deleted, space segment implementation choice.

Note 3: Deleted.

Note 4: Deleted.

MRD-1100 Calibration and supporting engineering data required to recalibrate S3NG-T MRAD science measurements shall be available to users.

Note 1: Access to engineering data is essential to monitor the performance of the S3NG-T MRAD calibration systems and to re-calibrate the instrument on-ground if required as part of reanalysis.

Note 2: Supporting engineering data includes any on-board information considered necessary to reconstruct the calibration of S3NG-T MRAD and is specific to the implementation of the on-board calibration system e.g. thermistor values, scan position, feed temperature etc.

Note 3: Access to pre-flight calibration information for uncertainty budget development is required by users.

The consistency of brightness temperature retrievals from MRAD channels is important as L2 algorithms will use a combination of channels to derive measurements contained in geophysical products. In addition, depending on the implementation, MRAD may use multiple feeds each with their own characteristics in terms of calibration. The following requirements are designed to ensure that there is consistency both within a channel (regardless of the implementation used e.g. multiple feed chains) and between different bands in requirements addressing inter-channel and inter-band differences.

MRD-1110 The full antenna gain pattern shall be known and made available to users for all MRAD feeds with sufficient information to resolve all side-lobes and grating lobes.

Note 1: This information is fundamental for the proper production of Level 1 measurement data from Level 1a data because the energy from side lobes must be: (1) determined from the MRAD measurements and (2) used in Level 1 algorithms to adjust the calculated brightness temperature to compensate for these additional out of field radiance sources (3) the gain patters are required for use in the Level 1 uncertainty modelling.

Note 2: When using L1 products, users may choose to apply different method depending on the specific application.

Note 3: This information is typically derived from on-ground characterisation.

Note 4: The antenna gain pattern may vary as a function of azimuth and must be well known with cuts sufficient to resolve all side-lobes.

Note 5: The uncertainty of the antenna gain patterns will be used in the MRAD end to end uncertainty budget and performance.

MRD-1120 Requirement deleted.

MRD-1130 Requirement deleted.

Geolocation is inextricably linked to Absolute Performance Error (APE) of the instrument pointing accuracy (attitude) and the uncertainty of this parameter expressed as an Absolute Knowledge Error (AKE, see ESSB-HB-E-003, 2011). These parameters are important inputs to the L1 and L2 scientific processing systems.

Over the open ocean where no reference ground targets are available, geo-location relies on knowledge gained from instrument and platform pointing. Pointing errors may be systematic affecting all beams or may be attributable to individual beams (*Purdy et al.,* 2006). Achieving good geolocation accuracy depends on excellent knowledge of a number of in-flight parameters including beam mis-pointing, roll, pitch, yaw uncertainty and pre-launch characterisation knowledge – all depending on the implementation of MRAD. This information must also be supplemented using a variety of statistical analyses used to validate geolocation uncertainty based on the use of in-flight data, ground control points and coastline/coastline gradient analyses (e.g. *Purdy et al.* 2006) and or other methods.

It is important to select a reference location for a L1 measurement for geolocation uncertainty validation which in the case of CIMR will be beam dependent. The antenna boresight provides the position of the peak of the -3dB antenna gain and is thus the location on the Earth surface that is most representative of the signal received.

MRD-1140 The geo-location uncertainty of S3NG-T MRAD Level 1 measurement shall be better than 10% (3 sigma, zero-mean) of the footprint spatial resolution on ground, evaluated for each beam, at the antenna boresight position on ground, corresponding to mid-point for a given measurement integration interval.

Note 1: Geolocation applies to all frequencies and all polarisations.

Note 2: This requirement is to be met at L1.

Note 3: This requirement should also be considered with the colocation with the altimeter data.

MRD-1150 Requirement deleted.

MRD-1160 Requirement deleted.

MRD-1170 Requirement deleted.

6.2.1 Radio Frequency Interference (RFI) Mitigation Requirements.

RFI is an increasing problem for satellite microwave radiometers due to the introduction of 5G telecommunication networks and is a major risk to S3NG-T MRAD data quality if not addressed properly using RFI detection and mitigation strategies implemented on-board (e.g. *Kristensen et al.* 2019) and on-ground (e.g. *Uranga et al.* 2018). Due to the potentially high data rates required to mitigate RFI using time-frequency domain analysis, on-board processing is likely to be preferred. In this approach, it is important that when RFI is detected information used to detect and mitigate the RFI contamination is also sent to ground so that this can be included in reprocessing activities (potential impact on NEΔT computation) and help to identify and close unauthorised RFI signals from ground (or space) infrastructure according to ITU regulations..

MRD-1180 MRAD shall be able to detect and mitigate Radio Frequency Interference (RFI) for frequency channels below 40 GHz.

Note 1: RFI is a source of significant uncertainty in L1 products and must be clearly identified in the measurement data if they are to be scientifically useful by the operational user community.

Note 2: To support the correct verification and evolution of on-board processor RFI detection and mitigation algorithms in a changing RFI environment (e.g. 5G networks) on-ground RFI management activities and re-processing is required.

Note 3: RFI detection and mitigation could be performed on-board or as part of the ground processing depending on the available data rates and MRAD channel selection.

Note 4: RFI must be flagged in the L1 and L2 products in the LF channels.

Note 5. See figure 6.2.1-1

MRD-1190 Requirement deleted.

MRD-1200 If Radio Frequency Interference (RFI) of a measurement is detected and mitigated, relevant data generated by the RFI processor for the affected measurement shall be available to users.

Note 1: This requirement allows the performance of RFI filtering on-board to be assessed by the scientific and operational user community.

Note 2: "relevant data" would include statistical indicators such as thresholds and kurtosis, etc. Typically, a spectrogram of RFI would be down linked to ground for further processing and RFI management (ITU reporting and RFI source management).

Note 3: A diagnostic mode could be included (to be used as an example in commissioning) to downlink the data before and after RFI mitigation. This can be useful for RFI algorithm/parameters tuning.

6.3 Geodesy Requirements

The heritage Sentinel-3 mission includes a suite of instruments for POD which is extremely important for a climate quality mission. A Doppler Orbitography and Radiopositioning Integrated from Space (DORIS) sub-system is used within the NRT processing. The instrument also provides an Ultra-Stable Oscillator (USO) that provides the clock for the altimeter retrievals and positional information allowing improved altimeter surface tracking and improving coastal and inland water retrievals. For Sentinel-6 Michael Freilich, Sentinel-3C and Sentinel-3D a Global Navigation Satellite System (GNSS-POD) includes the ability to track both GPS and Galileo constellations. The GNSS-POD provides the internal reference clock pulse to all the equipment on board including the payload. The instrument provides tracking data that are used in the POD processing.

In terms of GNSS, a multi-frequency, multi-constellation approach is anticipated. Based on offline processing of Galileo dual-constellation pseudo-range and carrier phase measurements as well as broadcast ephemerides in a sequential filter with a reduced dynamic force model, navigation solutions for Sentinel-6 are extremely good with a representative position error of 10 cm (3D RMS) are achieved (Montenbruck et al, 2021; 2022, Darugna et al. 2022). For Sentinel-6, using satellite laser ranging (SLR) from selected high-performance stations, < 1 cm RMS consistency between SLR normal points and Galileo enabled GNSS-based orbits is obtained, which further improves to 6mm RMS when adjusting site-specific corrections to station positions and ranging biases (Montenbruck et al, 2021). While Galileo measurements exhibit 30–50% smaller RMS errors than those of GPS, the POD benefits most from the availability of an increased number of satellites in the combined dual-frequency solution (Montenbruck et al, 2021).

In addition, Galileo GNSS-based onboard orbit determination can now reach a similar performance as the DORIS navigation system. It lends itself as a viable alternative for future remote sensing missions (Montenbruck et al, 2022). For the radial orbit component, a bias of less than 1mm is found from the SLR analysis relative to the mean height of 13 high-performance SLR stations (Montenbruck et al, 2022).

In Sentinel-6 the Galileo enabled radial orbit component shows a bias of less than 1mm from the SLR analysis relative to the mean height of 13 high-performance SLR stations (Montenbruck et al, 2021). Sentinel-6 real time onboard velocity estimation accuracy (with respect to the CNES-DORIS reference) is already less than 0.1 mm/s using Galileo only and the dynamic model without HAS (Darugna et al, 2022). Galileo GNSS-based onboard orbit determination can now reach a similar performance as the DORIS navigation system (Montenbruck et al, 2022).

Use of the Galileo E6 code High Accuracy Service (HAS) Service is presumed (https://www.gsc-europa.eu/sites/default/files/sites/all/files/E6BC_SIS_Technical_Note.pdf). Depending on the quality of its products, the upcoming Galileo HAS service might further improve such performance. It will provide orbit, clock, code and phase bias corrections, refining the GNSS orbits and clocks, which have been demonstrated to highly affect the P2OD accuracy and precision. The Galileo HAS will be based on the free transmission of Precise Point Positioning (PPP) corrections through the Galileo E6

signal data component (E6-B) by the Galileo satellites providing improved performance compared to Sentinel-6 results of Montebruck et al (2021, 2022) and Darugna et al. (2022). By the time S3NG-T launches, the Galileo-2 system is expected to be operational with improved POD performance is anticipated.

A Laser Retro-reflector Array (LRA), is used with global satellite laser ranging stations to provide independent tracking measurements for the POD processing or POD validation.

Star-Trackers are used within the on-board Attitude and Orbit Control System (AOCS) providing attitude information (quaternions) are sensitive to platform ‘mis-pointing’ from the nominal local normal yaw steered.

MRD-1210 In addition to any on-board Attitude Orbit Control System (AOCS) solution, individual unprocessed attitude sensor data (e.g. from each star-tracker) shall be available to users.

Note 1: For example, quaternion data from star trackers with respect to the inertial reference frame is required by Users for geodesy for orbit modelling applications.

Note 2: Information on the positioning of sensors relative to CoM is required by Users

Note 3: Position, Velocity and Time information is required by users.

MRD-1215 Should multiple satellite be used to address S3NG-T mission requirements, differences between the measurements derived from individual satellites shall be known and monitored on a daily basis.

Note 1: Knowledge of differences across the constellation of satellites that comprise the S3NG-T mission is essential to avoid introducing artefacts into higher order applications (e.g. data assimilation) and products (e.g. Level 3 multi-mission maps).

Note 2: This requirement implies a need for a robust inter-calibration methodology (e.g. based on the use of Sentinel 6 as a reference, minimization of crossover differences, use of transponders, corner cube reflectors, etc.)

7 DATA PRODUCT REQUIREMENTS

The Sentinel-3 Surface Topography Mission provides Level 1 and Level 2 Near Real Time (NRT), Short-Time Critical (STC), and Non-Time Critical (NTC) data products. While these are currently delivered in discrete segments, the exact temporal or spatial extent of each product may vary depending on the processing level, geographic domain, and application needs. Future implementations may support user-driven customization of product granularity.

7.1 Product Delivery Timeliness and Availability Requirements

In alignment with the operational standards of the Copernicus ground segment for the first-generation Sentinel series, stringent requirements are established for the timeliness and availability of Near Real-Time 3-hour (NRT3H) ocean product deliveries. However, other applications, such as those focused on sea ice and inland water, may require different near real-time latencies. To address the diverse needs of these applications, the following data product latency categories are specified.

Table 7.1-1: S3NG-Topo mission latency requirements. The Timeliness specifies time elapsed from sensor acquisition to the user point of pickup. Application Domains are provided here for information only.

Latency	Timeliness and Availability	Application Domain
Near Real Time 3-hour (NRT3H)	97% of data within 3-hours	Open Ocean, Coastal Areas.
Near Real Time 6-hour (NRT6H)	97% of data within 6-hours	Inland Waters (goal), Sea Ice Freeboard.
Near Real Time 24-hour (NRT24H)	97% of data within 24-hours	Inland Waters (threshold), Sea Ice Thickness
Short Time Critical (STC)	97% of data within 36-hours	Open Ocean, Coastal Areas.
Non Time Critical (NTC)	97% of data within 30-days	All Domains.

MRD-1220 The S3NG-T mission shall provide users with Level 1 and Level 2 products within the timeliness and availability outlined in Table 7.1-1, tailored to the requirements of each specific application, as specified in subsequent requirements.

Note 1: Timeliness is defined as the time taken from measurement acquisition to delivery of a product at the user point of pickup.

Note 2: See definition of availability.

7.2 Product Format Requirements

Heritage approaches in the altimetry community and within Copernicus follow NetCDF like format (https://www.unidata.ucar.edu/software/netcdf/) for Level 1 and higher level data products (e.g. Scharroo et al, 2016) . However, given the rapid evolution of cloud-native technologies, distributed computing frameworks, and data access standards, alternative data formats offering improved scalability, interoperability, and discoverability may become more suitable by the time S3NG-T reaches operations and should not be excluded.

MRD-1230 S3NG-T Level 1 and higher-level data shall be formatted in an easily accessible format.

Note 1: At the time of writing, Network common Data format (NetCDF) is the most commonly used data product format for altimetry, see https://www.unidata.ucar.edu/software/netcdf/, which fulfil this requirement.

Note 2: Due to the fast evolution of cloud-native technologies, distributed computing frameworks, and data access standards, other data formats will become available and could be more suitable for the mission.

Note 3: At the time of writing, the most commonly used data products follow Climate and Forecast (CF) Convention, see http://cfconventions.org/, fulfil this requirement.

Note 4: At the time of writing, the current Attribute Convention for Data Discovery (ACDD) metadata convention (see http://cfconventions.org/ and http://wiki.esipfed.org/index.php/Category:Attribute_Conventions_Dataset_Discovery) or emerging frameworks such as the Spatio Temporal Asset Catalog (STAC) (STAC: SpatioTemporal Asset Catalogs), fulfil this requirement.

7.3 Level 0 Data Product Requirements

Level 0 data products contain time stamped native instrument source packets data downlinked from the spacecraft. These are typically not distributed to users.

7.4 Level 1 Data Product Requirements

7.4.1 Level 1a Data Products

L1a is the foundation product that carries all information from S3NG-T with all calibration and geolocation data available but not applied (i.e. the data remain in counts and instrument geometry and very close to a L0 product).

MRD-1240 Level 1a data products shall be produced and made available to users.

Note 1: This essential requirement provides flexibility for the ground processors and end user community because L1a products maintain data in native geometry.

Note 2: L1a products need not necessarily be produced at NRT latency.

The highest sample frequency available on ground should be available in L1a products. The intention is to provide a L1a data product that could be used as the starting point for re-processing activities.

MRD-1250 A S3NG-T Level 1a product shall contain sufficient information for any re-processing activities.

Note 1: L1a is the foundation S3NG-T product that should also contain all science and calibration data.

Note 2: The highest posting rates available from the downlinked data should be available to the user within a Level 1a product.

7.4.2 Level 1b Data Products

L1b data are derived from L1a data that are calibrated and geolocated. All engineering corrections and calibration parameters (e.g. side-lobe and grating lobe contributions, Faraday and geometric rotation corrections, calibration measurement targets, geolocation adjustment if required) are applied.

MRD-1260 Level 1b products shall be produced in instrument geometry from corresponding Level 1a data and made available to users.

Note 1: Level 1b products are the starting point for Level 2 processors.

Note 2: There should be a direct mapping from Level 1a products to corresponding Level 1b products to facilitate reanalysis activities.

Note 3: Different sampling (posting) might be considered.

MRD-1270 Requirement deleted. Now covered by MRD-1335.

MRD-1280 Requirement deleted.

MRD-1290 Total standard uncertainties and quality indicators shall be delivered for all S3NG-T measurements in Level 1b data products.

Note 1: This is critical for the L2 processor design, propagation of uncertainties in the processors, and for application of higher L2 products that are used by data assimilation systems.

Note 2: Quality indicators are typically implemented as flags and/or numerical data attached to each measurement to provide information to users on aspects related to the measurement or processing that may impact the quality of data.

MRD-1300 The methods used to generate and propagate uncertainties and quality indicators shall be coherent across product levels and documented for users in Level 1b data products.

Note 1: Deleted.

Note 2: Uncertainty estimates in higher-level products need to reflect uncertainty propagated from lower levels, if significant.

Note 3: Deleted.

MRD-1310 S3NG-T L1 baseline continuity payload products shall contain measurements at the highest sampling resolution from each payload instrument.

Note 1: Deleted.

Note 2: The choice of high resolution depends on the altimeter payload and data downlink capacity.

Note 3: MRAD high-resolution data depends on the characteristics of the payload design and data downlink capacity.

MRD-1320 Requirement deleted.

7.5 Level 2 Data Product Requirements

L2 products are generated from L1a or L1b data products using appropriate retrieval algorithms. The measurement data are converted into geophysical quantities and are combined with auxiliary input data from other sources to yield directly useful geophysical parameters (e.g. sea surface height). The output data set is a field of geophysical parameter, with associated uncertainties and processing flags. Table 7.5-1 describes L2 products produced by the S3NG-T mission.

Table 7.5-1 S3NG-T Level 2 Products – for information only (TBC, numbered requirements shall be used in case of conflict) (MCM=Marine and Coastal Mask, IWM=Inland Water Mask)

Geophysical Variables	Description	Units	Dynamic Range	Maximum Total Standard Uncertainty	Delivery Timeliness	Coverage Definition
OC-Range	Altimeter Range over ocean after retracking and all instrument corrections applied	cm		1.93 (g: 1.4)	NRT3H, STC, NTC	MCM
SSH	Sea Surface Height = altitude of satellite referenced to WGS84 reference ellipsoid - corrected ocean altimeter range – geophysical corrections	cm		3.98 (g: 2.47)	NRT3H	MCM
				3 (g: 2.08)	STC	
				2.17 (g:1.65)	NTC	
SSHA	Sea Surface Height Anomaly = altitude of satellite referenced to WGS84 reference ellipsoid - corrected ocean altimeter range – geophysical corrections - mean sea surface	cm				MCM
ADT	Absolute Dynamic Topography (ADT = SSH – geoid or ADT = SSHA + MDT) referenced to WGS84 reference ellipsoid	m				MCM
Hs (m)	Significant wave height after retracking and all instrument corrections applied	m	0.5 – 25	20 cm plus 4% Hs (g: 15 cm plus 5% Hs)	NRT3H	MCM
				20 cm plus 4% Hs (g: ≤15 cm plus 5% Hs)	STC	
				15 cm plus 4% Hs (g: ≤10 cm plus 5% Hs)	NTC	
OC-Sigma0	Normalized radar backscatter coefficient over ocean after retracking with and all instrumental corrections and atmospheric attenuation corrections applied	dB	-8 – 57	1 over mission life (g:≤0.3) After calibration	NRT3H, STC, NTC	All Masks
OC-ALT-U10		$m\ s^{-1}$	0–25	1.5 (g: ≤1.0)	NRT3H	LMM

	Altimeter derived Wind speed at 10m above the ocean surface			1.5 (g: 1.0) 1.5 (g: 1.0)	STC NTC	
RivWSE	River Water Surface Elevation above datum	cm		24[11] (g: 10)	NRT6H, (TBC), NTC	IWM
LakWSE	Lake and Reservoir Water Surface Elevation above datum	cm	0 – 50 m	24 (g: 10)	NRT6H (TBC), NTC	IWM
SI-freeboard	Sea ice freeboard	cm		≤ 3 (TBC)	NRT6H, NTC	SIM
SI-thickness	Sea ice thickness	cm		≤ 15 (TBC)	NRT24H (TBC), NTC	SIM
SI-SSH	SSH over areas of sea ice (see OC-SSH)	cm		≤ 3 (TBC)	NRT3H, STC, NTC	SIM
Iceberg	Iceberg detection over ≤25 km (TBC)grid	m	0 – 60m		NTC	LMM
SIED	Sea Ice Edge is a surface classification product that assigns ocean grid cells to sea-ice classes (e.g. Open Water, Very Open Drift Ice, Open Drift Ice, Closed Ice, etc.). See Aaboe et al. (2018).	Class		(TBC) %	NRT6H, STC, NTC	SIM
SITY	Ice type is provided as a number of defined categories (typically new ice, first year ice, second year ice, multi-year ice, fast ice) according to specific spectral signatures	Class		(TBC) %	NRT6H, STC, NTC	SIM
SIC	Sea Ice Concentration	%		(TBC) %	NRT6H, STC, NTC	SIM
SnowDp	Snow Depth on sea ice	m		(TBC) %		SIM
IS-Elevation	Elevation over ice sheets	m		2	NTC	LIM
RainAtt	Altimeter derived Rain Attenuation	dB				
PRECIP	Precipitation rate over ocean	mm//hr	0.1-100 (TBC)	80% (TBC)	NRT3H, STC, NTC	LMM
MRAD-CLW	MRAD derived Cloud Liquid Water	kg m^2		(TBC)	NRT3H, STC, NTC	LMM
MRAD-WV	MRAD derived Water vapour	kg m^2		(TBC)	NRT3H, STC, NTC	LMM
MRAD-WPD	Wet tropospheric Path Delay derived from the on-board radiometer and valid over ocean surfaces only.	m		(TBC)	NRT3H, STC, NTC	LMM
MRAD-ATT	Atmospheric attenuation of Sigma0 from MRAD	dB		(TBC)	NRT3H, STC, NTC	LMM
DWSP	Directional Wave Spectrum (secondary product)			(TBC)	NRT3H, STC, NTC	LMM
Others (TBD)						

[11] Haliki and Niedzielski (2022) obtained <0.22m (0.12 – 0.44m) using Sentinel-3A over Polish rivers.

MRD-1330 S3NG-T Level 2 data products shall be made available to users.

Note 1: See definition of product levels.

Note 2: Different sampling (posting) must be considered. The highest posting rates available from the downlinked data should be available to the user or clearly linked with the corresponding Level 1b data.

MRD-1335 S3NG-T Level 2 data products shall be derived from Level 1b data products, auxiliary data and other S3NG-T Level 2 data products as needed.

Note 1: See definition of product levels.

MRD-1340 Total standard uncertainties and quality indicators shall be delivered for all S3NG-T measurements in the Level 2 data products.

Note 1: This is critical for the L2 processor design and for uptake of Level 2 products by data assimilation systems [AD-2].

Note 2: Standard Total Uncertainties are expected to be propagated from Level 1 to Level 2.

Note 3: Quality indicators are typically implemented as flags and/or numerical data attached to each measurement to provide information to users on aspects related to the measurement or processing that may impact the quality of data.

MRD-1350 The methods used to generate and propagate uncertainties shall be coherent across product levels and documented for users for all Level 2 data products.

Note 1: This is critical for the L2 processor design and for uptake of L2 products by data assimilation systems [AD-2].

Note 2: Uncertainty estimates in higher-level products need to reflect uncertainty propagated from lower levels, if significant.

Note 3: Quality indicators are typically implemented as flags and/or numerical data attached to each measurement to provide information to users on aspects related to the measurement or processing that may impact the quality of data (e.g. track inclination respect to the coast)

MRD-1360 Various S3NG-T Level 2 geophysical data product types shall be established for the different foreseen applications or domains.

Note 1: The primary foreseen applications or domains for S3NGT are open ocean, coastal areas, estuaries, inland water bodies, sea ice and land ice.

Note 2: The final content of the Level 2 geophysical data products will be defined in future mission development phases.

MRD-1370 Requirement deleted.

MRD-1380 Requirement deleted.

MRD-1390 Requirement deleted.

MRD-1400 Requirement deleted.

MRD-1410 S3NG-T Level 2 products, independent of delivery timeliness, shall be as consistent as possible in content, format, and derivation.

Note 1: The final content of a Level 2 products will be defined in future mission development phases.

MRD-1420 Quality flags shall be defined and included in S3NG-T in all data product files.

Note 1: The list and definition of quality flags depends on the final altimeter design.

MRD-1430 All corrections to the altimeter measurements shall be included in S3NG-T Level 2 data product files.

Note 1: Corrections typically include: instrumental corrections on the altimeter range, radar propagation corrections, geophysical corrections (e.g. inverse barometer/DAC, internal/pole/solid Earth/ocean tides), environmental variables (e.g. atmospheric parameters, wind speed, TEC, precipitation, etc.)

Note 2: The list of corrections depends on the final altimeter design.

MRD-1440 Level 2 geophysical variables shall mitigate systematic offsets at the boundaries of S3NG-T data products.

Note 1: It is recognised that different data processing and data formats may be required for the different application domains. However, this requirements is aimed at achieving, as much as possible, Level 2 geophysical variable consistency at product boundaries (e.g. at the coastal ocean and open ocean boundary or SSH between open ocean and sea ice leads).

MRD-1445 Level 2 measurements between different altimeter operating modes and application domains shall mitigate systematic offsets at product boundaries.

Note 1: It is recognised that different data processing and data formats may be required for the different application domains. However, this requirement is aimed at achieving, as much as possible, Level 2 geophysical variable consistency at product boundaries between different operating modes and application domains (e.g. at the coastal ocean and open ocean boundary or SSH between open ocean and sea ice leads).

7.5.1 Ocean Product Requirements

MRD-1450 The S3NG-T Level 2 nadir altimetry products shall contain measurements averaged at 20 Hz (enhanced goal: 80 Hz) and 1 Hz time intervals.

Note 1: 1 Hz measurement is a standard used by satellite altimetry and provides continuity with Sentinel-3

Note 2: The S3NG-T MAG requested improved measurement sampling frequency compared to Sentinel-3 which provides Level 1a posting of 80 Hz and a Level 1b posting of 20 Hz.

MRD-1460 The following reference data shall be included in S3NG-T ocean data product files:

- Ocean depth (bathymetry) is given as negative values; land elevation as positive values;
- Height of the geoid above the reference ellipsoid (WGS84) computed from the model with a correction to refer the value to the mean tide system i.e. includes the permanent tide (zero frequency);
- Mean sea surface height above reference ellipsoid (WGS84);
- Distance to the coastline (derived from the Marine Land Mask);
- Others (TBD).

Note 1: Reference data is used to compute geophysical quantities

Note 2: The list of reference depends on the final altimeter design.

7.5.1.1 Sea Surface Height Requirements

Table 7.5.1.1-1 specifies the total standard uncertainty (TSU) for the 1-Hz Level 2 sea surface height measurements and provides an apportionment to its main contributors. These figures are based on Sentinel-3A and Sentinel-3B in-flight performance (See Table 2.4-1 for in flight performance of Sentinel-3) and are adjusted based on anticipated S3NG-T developments.

Table 7.5.1.1-1. Total Standard Uncertainty (TSU) budget for S3NG-T SSH estimation. All data specified for a 1 Hz integration time at Hs=2 m. (all values in cm, 1-sigma zero mean)

Parameter (cm)	NRT3H		STC		NTC	
	REQ	GOAL	REQ	GOAL	REQ	GOAL
Range noise	≤0.8	≤0.5	≤0.8	≤0.5	≤0.8	≤0.5
Ionospheric path delay	≤0.5	≤0.3	≤0.4	≤0.3	≤0.3	<0.3
Sea State Bias	≤2.0	≤1.5	≤2.0	≤1.5	≤1.5	≤1.0
Dry tropospheric path Delay	≤0.7	≤0.5	≤0.7	≤0.5	≤0.5	≤0.5
Wet tropospheric path delay	≤1.2	≤1.0	≤1.2	≤0.7	≤0.7	≤0.7
TSU altimeter range measurement noise	≤2.61	≤1.96	≤2.59	≤1.82	≤1.93	≤1.44
Radial orbit (RSS)	≤3.0	≤3.0	≤1.5	≤1.0	≤1.0	≤0.8
TSU sea surface height (SSH) measurements	≤3.98	≤2.47	≤3.00	≤2.08	≤2.17	≤1.65

MRD-1465 The total standard uncertainty (TSU) of the 1-second along-track averaged sea surface height (SSH) measurements over the ocean surface shall be less than the values specified in Table 7.5.1.1-1 for the prescribed data latencies.

Note 1: This requirement may be validated by intercomparison with other altimeter missions or independent in situ measurements.

Note 2: The altimeter range noise depends on Hs. For NTC products estimates (e.g. Sentinel-6 suggests uncertainties of 1.2 cm at 1 m Hs, 1.5 cm at 2 m Hs, 2.4 cm at 5 m Hs, and 3.2 cm at 8 m Hs.

Note 3: The total RSS for sea surface height shall be met by any satellite instrument concept regardless of retrieval technique.

Note 4: Deleted. Not relevant.

Note 5: For a swath altimetry concept, the 1-Hz along-track averaged measurement should be translated to a pixel size equivalent to the nadir altimeter footprint, that is, ~6.6 km along-track by ~7.5. km across-track

Note 6: For a swath altimetry concept, systematic errors, not apportioned in Table 7.5.1.1-1, should also be included in the TSU of the sea surface height measurements.

MRD-1470 The contribution of the ionospheric path delay to the total standard uncertainty budget of the 1-second averaged altimeter range measurements over the ocean surface shall be less than the values specified in Table 7.5.1.1-1.

Note 1: A dual frequency nadir looking altimeter should be able to meet this requirement based on Sentinel-3, Sentinel-6 and AltiKa inflight performance.

Note 2: Ka-band is much less affected by the ionosphere than Ku-band. The attenuation due to the ionosphere is proportional to the inverse of the frequency squared, so the attenuation in Ka-band is about seven times lower than in Ku-band. (Steunou et al., 2015). AltiKa attains an ionospheric correction of 0.3cm (Verron et al 2015) that is the same as Sentinel-6 Ku-band NTC performance

Note 3: Requirement is set for Sentinel-3 continuity, goal is equivalent to Sentinel-6 NTC performance.

Note 4: To be assessed using different techniques including comparison to GIM and other models (e.g. Zhao et al., 2021).

A Sea State Bias correction is designed to compensate for the impact of sea state effects in the altimeter range estimate within the altimeter footprint. It includes three components: electromagnetic (EM) bias and skewness bias, (Gaspar et al., 1994). For a nadir altimeter like Sentinel-3, re-tracker bias includes the impacts of the waveform retracking algorithm used. The SSB correction varies from a few centimetres to a few decimetres depending on different sea states, and thus playing an important role in reducing SLA noise (Labroue et al., 2006). SSB corrections use U10 and Hs derived from altimeter Sigma0 measurements. Pires et al. (2016) and Tran et al. (2006) highlight the use of wave period to improve the SSB correction. In the coastal regions, SSB is more challenging due to the variable characteristics of Hs. Since understanding of the mechanisms causing the SSB is limited, there is scant theoretical modelling of the SSB correction (Peng et al., 2020). More advanced techniques may be required for swath altimeter solutions.

Note that the use of a SAR Ka-band nadir pointing altimeter would potentially enable better sensitivity to surface roughness providing a means to analyse and reduce the impact of sea state on SSH measurements (e.g. smaller footprint compared to Ku-band instruments, vertical wave velocity, resonance with smaller waves to ˜8 m) depending on the instrument configuration. This is important since sea state is a major uncertainty term in altimetry measurements from space.

New techniques of SSB must be developed to reduce this uncertainty ideally based on measurements. For example, use of fully-focused SAR altimeter data, measurement pulse correlations (e.g. Egido and Smith 2019) and off-nadir or nadir-pointing microwave radiometer measurements having sensitivity to surface ocean roughness (e.g. Tran et al., 2002; Tran and Chapron, 2006). The directional wave spectrum (e.g. from CFOSAT) may help improve knowledge of SSB and lead to new approaches.

MRD-1480 The contribution of the sea state bias to the total standard uncertainty budget of the 1-second averaged altimeter range measurements over the ocean surface shall be less than the values specified in Table 7.5.1.1-1.

Note 1: Progress toward more advanced Sea State Bias correction is required to improve radar altimeter measurements regardless of the technical concept.

Note 2: This requirement may be validated by intercomparison with other altimeter missions, independent in situ sea state data and wave model outputs.

Note 3: wave spectral information be available from S3NG-T (MRD-1650), these estimates may be used in the determination of the SSB correction.

Atmospheric losses on the radar altimeter signal increase rapidly with frequency and at Ka-band they are larger than at Ku-band. A drawback of the use of Ka-band is that the attenuation of the signal due to liquid water (rain and clouds), that can be significant notably in the tropical regions. This is a constraining factor since limitation of the altimeter link budget imposes an attenuation of the signal. At Ka-band, Tournadre et al. (2009) suggest a 3dB atmospheric loss for the AltiKa mission. The CRISTAL mission sues a value of 1 dB at Ka-band.

Tournadre et al. (2009) note that for light rain and/or cloud liquid water content even for small rain cells and/or clouds, can significantly distort the echo waveform and degrade the accuracy of the geophysical parameters inferred by waveform analysis. The Sentinel-3 dual frequency altimeter (Ku- and C-band) uses differential attenuation to detect and flag precipitation that would not be possible for a single frequency Ka-band altimeter. Clouds and rain are characterized by sharp coherent along-track fluctuations of the off-nadir angle and a Matching Pursuit (MP) flagging algorithm has been developed and implemented for AltiKa based on the analysis of these fluctuations. Comparison to simulated operational dual-frequency flag shows that the MP flag performs better in detecting range errors and waveforms distortion, while its performances are inferior in detecting samples attenuated by rain. However, in-orbit AltiKa data show that the MP algorithm exceeds expectation and rain had little influence on data availability and quality (Verron et al 2020).

MRD-1490 The contribution of the dry tropospheric path delay to the total standard uncertainty budget of the 1-second averaged altimeter range measurements over the ocean surface shall be less than the values specified in Table 7.5.1.1-1.

Note 1: Deleted..

Note 2: Dry tropospheric path delay corrections are typically derived from numerical weather prediction models (e.g. Fernandez et al, 2021).

Note 3: Requirement is set for Sentinel-3 continuity, goal is equivalent to Sentinel-6 NTC performance.

Note 4: This requirement could be met using validated atmospheric model outputs.

Note 5: This requirement assumes use of improved ECMWF model in line with the ECMWF 2021-2030 Strategy (https://www.ecmwf.int/sites/default/files/elibrary/2021/ecmwf-strategy-2021-2030-en.pdf)

MRD-1500 The contribution of the wet tropospheric path delay to the total standard uncertainty budget of the 1-second averaged altimeter range measurements over the ocean surface shall be less than the values specified in Table 7.5.1.1-1.

Note 1: See Table 2.4-1 for in flight performance of Sentinel-3.

Note 2: Wet tropospheric path delay measurements should be derived from microwave radiometer instruments that are part of the S3NG-T payload.

Note 3: Requirement is set for Sentinel-3 continuity, goal is equivalent to Sentinel-6 NTC performance.

Note 4: For inland waters, GNSS may be the best source for wet path delay retrieval (Fernandes et al., 2014; Vieira et al., 2018). In addition, GNSS plays a major role in filling the gap left by MWR in coastal regions.

Note 5: This requirement could be validated using satellite sounder measurements, radiosonde profiles and atmospheric model outputs.

The Sentinel-3 orbit is provided by the Copernicus POD Service (e.g. Fernandez et al, 2015) that continues to evolve (e.g. Peter et al, 2020).

MRD-1510 At any point in the orbit, the contribution of the radial (ellipsoid normal) orbit position and velocity to the total standard uncertainty budget of the 1-second averaged altimeter range measurements over the ocean surface shall be less than the values specified in Table 7.5.1.1-1.

Note 1: It is assumed that the Copernicus POD Service will provide orbit information.

Note 2: Relativistic and ellipsoidal clock corrections should be accounted for.

Note 3: Results of the Sentinel-3A and Sentinel-3B latest Copernicus POD Service (Regular Service Review) can be found at https://sentinel.esa.int/web/sentinel/technical-guides/sentinel-3-altimetry/pod/documentation

MRD-1520 Requirement merged with MRD-1465.

MRD-1530 Requirement deleted.

MRD-1540 The surface elevation measurement drift of the S3NG-T mission altimeter system shall be below 0.5 mm/yr (TBC) over a 5 year period (TBC).

Note1: This requirement refers to the residual drifts after calibration of known instrumental effects.

Note 2: This requirement includes contributions of the S3NG-T altimeter, MWR, and POD suite. Contributions beyond the S3NG-T mission scope, such as ocean internal variability, ITRF geo-centre motion, gravity field trends, etc., are excluded.

Note 3: It is anticipated that Sentinel-6NG will provide the reference mission for global and regional mean sea level.

Note 4: This requirement may be verified with the use of transponders and/or corner reflectors.

MRD-1550 For scales smaller than 1000 km S3NG-T SSH measurements shall have a total standard uncertainty below 1.7 cm (TBC) after inflight calibration for typical sea state values of 2 m.

Note 1: This equates to a time scale of < ~3 minutes and addresses random noise and high-frequency correlated uncertainties.

Note 2: Separation between long- and short-scale uncertainties for end-to-end performance can be useful depending on the final technical concept.

MRD-1560 For scales larger than 1000 km and smaller than 40000 km (TBC) S3NG-T SSH measurements shall have a total standard uncertainty below 1.4 cm (TBC) after inflight calibration for typical sea state values of 2 m.

Note 1: This equates to a time scale of > ~3 minutes and addresses low frequency systematic uncertainties.

Note 2: Separation between long- and short-scale uncertainties for end-to-end performance can be useful depending on the final technical concept.

Sea level anomaly is an essential variable for oceanic operational system as it gives outstanding information both on the small scales dynamics and climate change.

MRD-1570 The S3NG-T mission shall provide Level 2 sea surface height anomaly measurements.

Note 1: Sea surface height anomaly = altitude of satellite - corrected ocean altimeter range - geophysical corrections - mean sea surface

MRD-1580 The S3NG-T mission shall provide Level 2 absolute dynamic topography measurements after ground processing.

Note 1: The Absolute Dynamic Topography (ADT = SSH – geoid) cannot be directly measured by altimetry but can be derived from subtracting the Geoid to the altimetric Sea Surface Height (SSH) or, alternatively, from adding the MDT to the altimetric SLA:

Note 2: This requirement implies application of a very high-resolution geoid for the S3NG-T mission

7.5.1.2 Sea State Requirements

The sea surface wave field exhibits a very complex and highly dynamic moving surface (both vertically and horizontally) that impacts the quality of radar ranging with Hs varying from a few cm to considerably more than 20 m (e.g. Hanafin et al, 2021). , see Figure 7.5.1.2-1).

MRD-1590 The S3NG-T mission shall provide Level 2 significant wave height, Hs, measurements for all sea surface height estimates provided by the altimeter payload.

Note 1: Hs is a baseline requirement for continuity of Sentinel-3 measurements.

Note 2: See Greilier et al. (2016). The term significant wave height is historical as this value appeared to be well correlated with visual estimates of wave height from experienced observers. It can be shown to correspond to the average 1/3rd highest waves (H1/3).

Note 3: Swell is known to impact altimeter SSH measurements through aliasing (e.g. Moreau et al, 2018; Rieu et al, 2021) when orthogonal to the satellite ground track. Directional wind sea waves and swell estimates would help to monitor and mitigate these issues.

Note 4: Spectral and directional spectral sea state parameters are the most important measurements to support future evolution of CMEMS wave forecasting models and CMEMS ocean atmosphere coupled models and C3S coupled systems since the exchange of heat, gas, and momentum occurs via the waves. Furthermore, at high resolution, it becomes extremely challenging to separate SSH for sea state since the sea state defines the scattering surface to which a radar instrument responds. This is already seen in moderate resolution nadir pointing altimeters (e.g. Boy et al., 2016, Moreau et al., 2018, amongst others)Note 5: This requirement ensures that sufficient information is available to interpret SSH measurements and apply sea state bias corrections. SSB corrections use U10 and Hs derived from altimeter Sigma0 measurements.

Note 6: Pires et al. (2016) and Tran et al. (2006) highlight the use of wave period to improve the SSB correction.

Note 7: In the coastal regions, SSB is more challenging due to the variable characteristics of Hs (Peng et al. 2020)

MRD-1600 The S3NG-T mission shall provide Level 2 significant wave height, Hs, up to 20 m (enhanced goal: 25 m (TBC)).

Note 1: This dynamic range includes Hs for extreme sea states.

Note 2: The Sentinel-3 SRAL specification is 0-20m

Note 3: This requirement may need to be validated for different dynamic range due to the limited number of extreme sea state reference measurements (extreme sea states are local phenomena and wave buoys, typically used to validate altimeter Hs do not function well in these conditions). Because of this, Sentinel-6 validated Hs over a range of only 0.5-8m.

Note 4: Since Hs is used as part of the sea state bias estimation, all range measurements form the altimeter must be accompanied by an estimate of Hs.

Note 5: The standard deviation/variance of the significant wave height measurement should be included in the Hs products to assist in SSB determination to capture gradient changes.

MRD-1610 Merged with MRD-1590.

MRD-1620 The S3NG-T mission shall provide Level 2 significant wave height, Hs, with a total standard uncertainty for 1-Hz measurements (or equivalent pixel size) below 15 cm plus 5% Hs in the range of 0.5 to 8 m (enhanced goal 0.5 - 15 meters).

Note 1: This is baseline continuity from Sentinel-3.

Note 2: Requirement is set for Sentinel-3 continuity, enhanced goal is equivalent to the Sentinel-6 requirement.

Note 3: This requirement may be validated by intercomparison with other altimeter missions or independent in situ measurements.

Note 4: Extreme sea states as seen in radar altimeters today (e.g. Hanafin et al., 2021) are local phenomenon and reference in situ wave buoys, typically used to validate altimeter Hs, do not function well in these conditions. As measurements are likely to be scarce for extreme sea states, validation of Hs measurements outside in the range of 0.5 to 8 m is considered sufficient for each satellite commissioning activities.

MRD-1630 Merged with MRD-1620.

MRD-1640 Merged with MRD-1620.

User needs for maritime Surveillance and from European Maritime Safety Agency (EMSA) request new/additional products that are needed for search and rescue operations, sea surface pollution (including marine plastic debris) and vessel navigation/routing purposes. Only through wave induced flows can such activities lead to successful outcomes since the Stokes drift is fundamental to the ocean surface

dynamics and is completely different to the geostrophic flows inferred from SSH. Because of this, these products are also fundamental to the future evolution of Copernicus Wave Forecasting and coupled ocean-atmosphere model capability in the 2030 timeframe. Finally, many European directives and policies, particularly in the coastal zone, require at least Hs and ideally wave directional spectra for their successful implementation and monitoring of policy impact.

MRD-1650 As a Secondary Mission Objective, the S3NG-T mission shall be capable of producing Level 2 Wave Directional Spectrum, E(k,φ), estimates. Variation of wave energy in directions should have a directional resolution of ≤ 15° (enhanced goal: 10°) for wavelengths longer than 100 m (enhanced goal: 50 m). The uncertainty should be ≤ 10% for energy and wavelength quantities for Hs in the range of 0.5 to 8 m (enhanced goal 0.5 - 15 meters).

Note 1: A 2D directional spectrum can be provided from nadir altimetry as explained by Altiparmaki et al. (2022). Should the directional wave spectrum not be feasible, a 1D wave spectrum should be provided.

Note 2: This is a fundamental data product for many Copernicus applications in support of many European directives and policies.

Note 3: Spectral and directional spectral sea state parameters are the most important measurements to support future evolution of CMEMS wave forecasting models and CMEMS ocean atmosphere coupled models and C3S coupled systems since the exchange of heat, gas, and momentum occurs via the waves. Furthermore, at high resolution, it becomes extremely challenging to separate SSH from sea state since the sea state defines the scattering surface to which a radar instrument responds. This is already seen in moderate resolution nadir pointing altimeters (e.g. Boy et al., 2016, Moreau et al, 2018 amongst others). CMEMS already make use of CFOSAT/SWIM directional wave spectrum measurements.

Note 4: This requirement is significant for the improvement of ocean/waves coupled systems managed by CMEMS-MFCs. Accounting of directional wave energy leads to better parametrization of wind-waves growth in the wave model for storm events.

Note 5: This requirement is relevant for better estimate of wave forcing into CMEMS ocean models (e.g. Wang et al, 2021) including wave-induced stress, Stokes drift and wave breaking induced turbulence for upper ocean layer mixing, marine debris (e.g. plastic, oil radioactive) tracking, and search and rescue.

Note 6: As a Secondary Mission Objective, the S3NG-T Level 2 swell number for partition i, Hs(i), of the unambiguous directional wave spectrum E(k,φ) should have a combined uncertainty of ≤30 cm or ≤10 (TBC)% whichever is greater.

Note 7: As a Secondary Mission Objective, the S3NG-T Level 2 peak period for partition i, Tp(i), of the unambiguous directional wave spectrum E(k,φ) should have a combined uncertainty of ≤1 s if Hs(i) ≥ 30 cm.

Note 8: As a Secondary Mission Objective, the S3NG-T Level 2 mean direction for partition i, φm(i), of the unambiguous directional wave spectrum E(k,φ) should have a combined uncertainty of ≤10° if Hs(i) ≥ 30 cm.

Note 9: As a Secondary Mission Objective, the S3NG-T Level 2 directional spread for partition i, σsi, of the unambiguous directional wave spectrum E(k,φ) should have a combined uncertainty of ≤15° if Hs(i) ≥30 (TBC)cm.

Note 10: See Caudal et al., (2014).

Note 11: The priority is to support wave forecasting models and coupled ocean-atmosphere models used by Copernicus applications.

MRD-1660 As a Secondary Mission Objective, the S3NG-T Level 2 Wave Directional Spectrum, E(k,φ), data products shall be made available to users at NRT3H, STC and NTC data latencies.

Note 1: This is a fundamental data product for many Copernicus applications in support of many European directives and policies.

MRD-1670 As a Secondary Mission Objective, the S3NG-T Wave Directional Spectrum products shall consist of (TBC):

1. Unambiguous directional wave spectrum E(k,φ);
2. αu(k, φi) wavenumber function;
3. ασ(k,φi) wave direction function;
4. Cross spectrum C'uσ (k,φ);
5. Hs, Significant Wave Height;
6. Hsi, swell number for partition i;
7. Tpi, peak period for partition i;
8. φm,i, mean direction of partition i;
9. Uncertainty estimates for each measurement;
10. Other relevant information (TBD).

Note 1: The exact content of wave directional spectrum products depends on the final implementation of S3NG-T.

Note 2: A wave product is available from Sentinel-1 data sets but has a long-wave cut-off at ~150m and thus does not address wind seas that are necessary for wave modelling and coupled ocean-atmosphere models in the 2030 time frame.

Note 3: The priority is to support wave forecasting models and coupled ocean-atmosphere models used by Copernicus applications.

Note 4: Ideally, uncertainty should be less than 5-10% for Hs, wavelength and direction, in 2030 we should expect less than 7%.

7.5.1.3 Wind Speed at 10m over the ocean (U10) Requirements

Wind speed over the ocean is a standard output from satellite altimeters such as Sentinel-3.

MRD-1680 The S3NG-T mission Level 2 wind speed measurements at 10 m height (U10) dynamic range shall be 2 – 25 m/s.

Note 1: This requirement may need to be validated for different dynamic range due to the limited number of extreme U10 measurements (extreme U10 are local phenomena and buoys, typically used to validate altimeter U10 do not function well in these conditions).

MRD-1690 The S3NG-T mission shall provide Level 2 wind speed measurements at 10 m height (U10) with a total standard uncertainty below 1.5 m/s (Enhanced goal: below 1.0 m/s (TBC)).

Note 1: This is baseline from Sentinel-3

Note 2: This requirement applies to all data latencies.

MRD-1700 Requirement merged with MRD-1690.

MRD-1710 Requirement merged with MRD-1690.

MRD-1720 The S3NG-T mission shall provide Level 2 wind speed measurements at 10 m height (U10) for all sea surface height estimates provided by the altimeter payload.

Note 1: This requirement ensures that sufficient information is available to interpret SSH measurements and apply sea state bias corrections. SSB corrections use U10 and Hs derived from altimeter Sigma0 measurements.

MRD-1730 The S3NG-T mission shall provide normalised radar cross section (sigma0) measurements for all measurements within the altimeter footprint.

Note 1: This requirement ensures that sufficient information is available to interpret SSH measurements and apply sea state bias corrections. SSB corrections use U10 and Hs derived from altimeter Sigma0 measurements.

7.5.1.4 Specific requirements for the Coastal Ocean

MRD-1740 The S3NG-T mission shall maintain continuity of open ocean topography measurements and those provided in the coastal ocean.

Note 1: It is recognised that different data processing and data formats may be required between the open ocean and coastal zone. However, Level 2 geophysical variable systematic offsets should be mitigated as much as possible to achieve consistency of the open ocean and coastal area application domains.

MRD-1750 The S3NG-T mission shall generate Level 2 SSH,Hs and U10 products down to 3 km (enhanced goal: down to 0.5 km) from the coastal boundary defined in the Marine and Coastal Mask.

7.5.2 Inland Water Product Requirements

MRD-1760 The S3NG-T mission shall provide Level 2 Water Surface Elevation for an area of 1 km^2 within the Inland Water Mask with the following total standard uncertainty (TSU) and data latencies:

- TSU below 24 cm at NRT3H;
- TSU below 15 cm at STC (goal NRT12H);
- TSU below 10 cm (goal 5 cm) at NTC.

Note 1: Sentinel-3 in flight performance taken from Table 2.4.-1. Haliki and Niedzielski (2022) obtained <0.22m (0.12 – 0.44m) uncertainty using Sentinel-3A over Polish rivers. Include here Jeremey Aublanc 2024 paper. Requirement is also in line with results from Sentinel-3 latest Land Thematic Product reprocessing BC005 Validation Report, available online at: Sentinel-3 Altimetry Land Full Mission Reprocessing Campaign - Validation Report.

Note 2: Hydrology was a secondary mission objective for Sentinel-3. For S3NG-T hydrology has been elevated to a Primary mission Objective by the European Commission. This requirement aims at achieving at NRT equivalent performance than Sentinel-3 in NTC, which in itself represents an enhancement in the continuity.

Note 3: Enhanced goal at NTC is taken from S3NG-T-UN-P24, S3NG-T-UN-P25 (goal ≤ 5 cm). S3NG-T-UN-P26 requests ≤ 3 cm and S3NG-T-UN-P27 and S3NG-T-UN-P29 request ≤ 50 cm.

Note 4: For the verification of this requirement it is assumed that the WSE is constant within the 1km^2 water body.

Note 5: This requirement applies to water bodies where the full river reach or lake with an area >1km2 can be observed without any source of error like obstruction by vegetation, dark water, layover, etc.

MRD-1765 The S3NG-T mission shall provide Level 2 river discharge estimates for medium to large rivers with a width larger than 3 km within the Inland Water Mask.

Note 1: Requirement addresses cover EC river discharge user need S3NG-T-UN-024, S3NG-T-UN-034 S3NG-T-UN-047, S3NG-T-UN-078, S3NG-T-UN-09.

Note 2: Anh and Aries (2019) obtain river discharge with RMSE of 4-11% using a neural net approach for the Amazon.

Note 3: See Dubey et al (2015), Emery et al (2018), Fekete et al (2012), Revel et al (2021), Tarpanelli et al (2020), Durand et al. (2023).

Note 4: To derive discharge accurate knowledge of the river channel form and its variation is required. The choice of rivers with known characteristics will be established during later phases of the Mission.

Note 5: The total standard uncertainty for the river discharge product shall be characterised.

7.5.3 Cryosphere Product Requirements

7.5.3.1 Sea ice parameters

Sea ice freeboard, which is the portion of the floating ice that is above sea level, is estimated from the elevation difference between altimeter radar echoes backscattered from sea ice and those from the ocean surface within sea ice leads. Sea ice freeboard is converted to sea ice thickness using published estimates for the density of sea ice, ocean water, and snow, assuming hydrostatic equilibrium of the sea ice in the ocean and, by estimating the depth of snow accumulated on the ice surface (e.g., Laxon et al., 2013; Ricker et al., 2014; Tilling et al., 2018). Sea ice freeboard (not including snow cover) is typically only 5–20% of its thickness (Alexandrov et al., 2010), uncertainties in measurements of sea ice freeboard increase by a factor of ~10 when converted to thickness. Following Landy et al. (2020), the principal sources of systematic uncertainty for sea ice thickness estimates are (i) partial wave penetration into the snowpack on multi-year ice (MYI), for instance, due to metamorphic snow features (ii) snow depth on sea ice and (iii) density estimates (iv) partial penetration of the radar pulse into the snowpack on first year ice (FYI_, for instance due to brine wicking-induced snow basal salinity (v) sea ice density estimates (vi) sea level bias resulting from off-nadir ranging to leads and low along-track lead densities and (vii) sea ice surface roughness. The uncertainties for retracker/roughness-based remain a challenge and the ensemble of uncertainty sources may be correlated. Estimates for individual component uncertainties for CryoSat-2 Ku-band SAR interferometry range from 7–32% over FYI and from 8–30% over MYI. Systematic uncertainties introduced in the retracking step have the potential to bias sea ice thickness estimates up to 20% over FYI and up to 30% over MYI, with regional patterns depending on the ice surface roughness. For FYI with a thickness of 2m, this translates into an uncertainty of around 40 cm, and for MYI

with a thickness of 3 m, an uncertainty of around 90 cm. See Landy et al. (2020) for a thorough discussion on these aspects.

The snow depth and density climatology of Warren et al. (1999) remains state -of-the-art to derive sea ice thickness estimate (e.g. Tilling et al., 2018) but is identified as a primary source of ice thickness error for altimeter estimates (Ricker et al., 2014, Brackmann-Folgmann and Donlon, 2019) due to spatiotemporal variations in snow properties, including density, grain size and basal salinity (Nandan et al., 2017). Ricker et al. (2014) suggested that sea ice surface roughness may also represent a significant source of ice thickness uncertainty in empirical retracking algorithms. The raw range measurement between the altimeter and target is only approximate, so the radar waveform must be “retracked” to accurately identify the mean sea ice or ocean scattering surface, represented by a point on the waveform's leading edge (Quartly et al., 2019). Landy et al. (2019) suggest that power thresholds should realistically change depending on sea ice properties, principally surface roughness at the scale of the radar footprint. However, even if waveform classifications and geophysical corrections are equal, different retracking algorithms still have a significant impact on the measured sea ice freeboard varying by 4–6 cm with the freeboard pattern, and asymmetry between FYI and MYI zones varying considerably (Landy et al., 2020). Sea ice freeboard bias increases as the sea ice surface becomes rougher (i.e., the standard deviation of elevations), up to 20 cm for a surface roughness of 0.5 m (Landy et al., 2019) leading to a worst case sea ice thickness bias of ≤2 m (Landy et al., 2020).

Ricker et al. (2017) notes that CryoSat-2 sea ice thickness retrievals from altimetry are limited to ~0.5 m. Landy et al. (2019; 2020) use the Lognormal Altimeter Retracker Model (LARM) algorithm model simulations to show that smooth newly-formed sea ice, with a roughness height σ of only 1–3 cm, should produce radar echoes with a retracking point of >95% (Landy et al., 2019) highlighting that a roughness-based correction would need to be removed from the retracked sea ice floe elevations to accurately resolve the freeboards of thinner ice floes (Laforge et al., 2020). Assuming high (>95%) tracking thresholds over sea ice and >98% over sea ice leads, a theoretical lower detection bound on the ice freeboard retrieval of approximately 2.5 cm with verification of 2–3 cm covering large areas that, in the absence of snow cover, suggests a minimum detectable ice thickness of ~0.25 m. As the Arctic sea ice is increasingly dominated by thin FYI, it will become “smoother” although such regions when in compression can readily deform and ridge, lock ocean swell wave signatures into the surface (Ardhuin et al 2015) and lead to locally higher roughness.

Compared to Ku-band, Ka-band, has a lower radar penetration of snow and ice targets due to much higher volume scattering that is around ten times less than for Ku-band. This means that height estimates will differ from Ku-band measurements since Ka-band corresponds to a much thinner surface layer over snow and ice (< 3 cm for snow on sea ice and <1 m for continental ice) providing improved measurements.

Based on 6-months of gridded data (Nov 2017 – April 2018), Lawrence et al (2019) report a mean radar freeboard for Sentinel-3A of 0.1 ±0.015 m. Mean freeboard differences between Sentinel-3A and CryoSat-2 are stable with month-to-month values between 0.9 cm and 1.1 cm ±0.07 cm. The standard deviation on the mean difference, which reflects the spatial variability of Sentinel-3A and CryoSat-2 differences is also stable across all months at 6.4 ±0.4 cm. The grid specifications are 1.5° longitude by

0.5° latitude grid, corresponding to grid cell dimensions of approximately 80 - 55 km at 60° latitude and 30 - 55 km at 81° latitude. Armitage and Ridout (2015) and Guerreiro et al (2016) discuss Ka-band (AltiKa) retrievals of sea ice in the Arctic highlighting residual errors in sea ice thickness estimates due to different Ka- and Ku-band scattering from the air-snow interface and within the snow pack (the impact of liquid water brine pockets within the snow and ice influence their radar scattering properties). The degree to which satellite radar altimeters are affected by snow surface and volume scattering has been estimated by Armitage and Ridout, (2015) suggesting that Ku-band echoes penetrate to the ice surface over FYI and penetrate the majority of the snow layer over MYI, while Ka-band echoes are scattered from roughly the midpoint of the snow layer over for both FYI and MYI ice types.

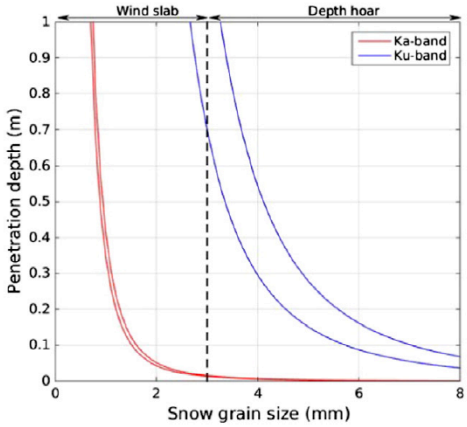

Figure 7.5.3.1-1. Theoretical radar penetration depth (m) as a function of snow grain size at Ka-band (red) and Ku-band (blue) frequencies. The two lines at each frequency represent the minimum and maximum penetration depth for different densities and air temperatures. The corresponding size distribution of wind slab grains and depth hoar crystal according to field observations is indicated (from Guerreiro et al (2016))

The essential step in estimating freeboard from an altimeter is to distinguish between echoes originating from leads and those originating from sea ice floes. The sea surface height anomaly measured over leads within the sea ice is interpolated underneath sea ice floes, and the floe elevation relative to the interpolated sea surface height is termed the radar freeboard (e.g. Laxon et al. (2013), Armitage and Ridout (2015)). Guerreiro et al (2016) suggest, that the radar penetration depth at Ka and Ku-band frequencies demonstrates that the main return echo at Ku-band penetration should originate from a region close to the snow/ice interface while at Ka-band, the maximum penetration depth should be smaller than 5 cm for snow grains larger than 2 mm (see Figure 7.5.3.1-1). They conclude that the simultaneous use of SARAL-AltiKa and CryoSat-2 altimeters to retrieve sea ice freeboard and corresponding altimetric snow depth (ASD) could significantly improve sea ice volume estimates at pan-Arctic scale up to 81.5° leading to the basis of a dual-frequency solution for the CRISTAL Mission. In the context of S3NG-T measurements over sea ice, the use of CRISTAL and other altimeter missions (e.g. HY2) in synergy is assumed. The Sentinel-3 mission is also providing sea ice products operationally of excellent quality, consistent with CryoSat-2, helping extend and improve Arctic sea ice monitoring (Gregory, et al., 2021; Lawrance, et al., 2021).

MRD-1770 The S3NG-T shall provide measurements of the sea ice parameters referenced in the requirements in this Section for the area within the S3NG-T Sea Ice Mask.

Note 1: See MRD-060 for definition of the S3NG-T Sea Ice Mask.

MRD-1780 The S3NG-T shall maintain continuity and consistency in sea surface height measurements between ice free oceans and leads in ice covered oceans.

Note 1: This requirement acknowledges the use of different retrievals of SSH from ice leads and the need for consistency with open ocean SSH measurements.

MRD-1790 Requirement merged with MRD-1820.

MRD-1800 Requirement deleted.

MRD-1810 Requirement deleted.

MRD-1820 The S3NG-T mission shall provide Level 2 sea ice freeboard estimates at a resolution of ≤ 25 km with a total standard uncertainty below 3 cm (2 cm goal) under favourable sea ice conditions, at NRT6H data latency.

Note 1: NRT6H data latency is compatible with specifications for the CRISTAL Copernicus Expansion Mission.

Note 2: The minimum freeboard to be retrieved is 3 cm.

Note 3: To be assessed as an average over a 1-month period on a 1.5° longitude by 0.5° latitude grid.

Note 4: Because of the roughness of the ice floe surfaces averaging will be required to obtain a useful measurement.

Note 5: This requirement applies for "favourable sea ice conditions", i.e. winter months in which the ice is free of melt ponds and rain.

Note 6: This is Sentinel-3 baseline in-flight performance at NTC.

Note 7: In this context, segments for a swath altimeter can also be considered as 25 km x 25 km areas – see Armitage and Kwok (2019) for a full discussion.

MRD-1830 The S3NG-T mission shall provide Level 2 sea ice freeboard estimates across all seasons.

Note 1: Performance under more challenging conditions, i.e. summer months, shall be assessed.

MRD-1840 Requirement deleted; merged with MRD-1465.

MRD-1850 The S3NG-T mission shall provide Level 2 sea ice thickness estimates with horizontal resolution and availability identical to freeboard estimates, at NRT24H data latency, or better.

Note 1: User requirement goals range from 1 cm to 5 cm (transport/navigation) to 25 cm (meteorology).

Note 2: NRT24H data latency is compatible with specifications for the CRISTAL Copernicus Expansion Mission.

Note 3: See thin ice requirement note (Note 2) in MRD-1820.

Note 4: Sea ice density influences the calculation of sea ice thickness from freeboard. Thus uncertainty in density estimate, expected to be derived from an external source, will contribute to the sea ice thickness uncertainty.

Note 5: Snow depth estimates on sea ice are needed to improve the accuracy of both the sea ice freeboard retrieval and subsequent derivation of sea ice thickness. Snow depth estimates could potentially be derived from co-temporal observations at Ku- and Ka-band, microwave radiometer measurements.

Note 6: This requirement could be validated using CRISTAL measurements.

MRD-1860 As a secondary mission objective, the S3NG-T mission should be able to detect icebergs at a horizontal resolution (gridded product) of ≤25 km.

Note 1: Considering the sampling by a nadir altimeter, the requested resolution cannot be achieved everywhere. Altimetry will be used in synergy with other high-resolution data such as SAR imagery.

Note 2: It has been demonstrated that small icebergs, with areas in the range 0.5 to 30 km2, have a significant signature in the noise part of high-resolution altimeter waveforms, that can be analysed to determine their distribution. RD7. Also, large iceberg (B17a) ~40x30 km detection compare literature e.g. RD6.

Note 3: The distribution of iceberg freeboard is required to set the altimeter tracking window size. As a starting point an extreme example is iceberg A68 that had a 30m freeboard. Based on this an initial figure of 35m could be considered.

MRD-1870 The S3NG-T mission shall be able to derive monthly products of sea ice distribution and volume at ≤ 25 km resolution (gridded product).

Note 1: The current capability from altimetry is 100 km resolution, every month.

MRD-1880 Requirement deleted.

MRD-1900 Requirement moved to MRAD Level 2 products section.

MRD-1910 Requirement merged with MRD-1900

MRD-1920 Requirement merged with MRD-1900.

MRD-1930 Requirement deleted.

MRD-1940 Requirement deleted.

MRD-1950 Requirement moved to MRAD Level 2 products section.

7.5.3.2 Ice sheet parameters

MRD-1960 The S3NG-T shall provide Level 2 measurements of Land ice parameters for the targets defined by the S3NG-T Land Ice Mask at STC and NTC data latencies. To maintain baseline continuity, land ice parameters include:

- land ice surface elevation,
- surface type classification (floating / grounded ice),
- Radar backscatter coefficients (Sigma-0)
- Other waveform parameters

Note 1: Waveforms parameters refer to, but are not exclusive to, leading edge width, leading edge slope, trailing edge slope,

MRD-1970 The S3NG-T shall provide Level 2 measurements of Land ice surface elevation with a total standard uncertainty of ≤ 2 m over ice sheet interiors where slopes are ≤1.5° averaged over a 1-month period on a 1.5° longitude by 0.5° latitude grid, at NTC data latencies.

Note 1: Major changes in surface elevation are observed at outlet glaciers and boundaries of Greenland and Antarctica. In these regions, monthly to seasonal maps of surface elevation are needed.

Note 2: Wingham (1995) suggest that the ice elevation estimates are limited by sampling – SAR approaches are thus preferred.

7.5.4 MRAD Product Requirements

7.5.4.1 Atmospheric products

MRD-1980 As a secondary mission objective, the S3NG-T mission should provide Level 2 estimates of precipitation rate (liquid phase only, mm/h) over the Marine and Coastal Mask at a spatial resolution of ≤ (TBC) km (goal TBC km), between 0.1 (TBC) and 100 (TBC) mm/h with a standard total uncertainty ≤ 80% (TBC) at 1 (TBC) mm/h or ≤ 50% (TBC) above 10 (TBC) mm/h.

Note 1: Validation of this product is usually performed by inter-comparison with other products over ocean, due to the paucity of in-situ measurements. Usually, biases are observed among various products. For example, the CIMR-derived product, the bias in instantaneous rain rates should not exceed 80% at 1 mm /h or 50% at 10 mm/h.

Note 2: Water vapor, cloud liquid water, and precipitation estimates should be retrieved simultaneously to ensure consistency between products. Their retrievals are highly interdependent and should not be tempted separately.

MRD-1990 As a secondary mission objective , the S3NG-T mission should provide Level 2 estimates of cloud liquid water (kg m-2) over the Marine and Coastal Mask at a spatial resolution of ≤ (TBC) km (goal = TBC km), with a standard total uncertainty ≤ (TBC) %.

Note 1: See Jacob et al (2019).

Note 2: Water vapor, cloud liquid water, and precipitation estimates should be retrieved simultaneously to ensure consistency between products. Their retrievals are highly interdependent and should not be tempted separately.

MRD-2000 As a secondary mission objective, the S3NG-T mission should provide Level 2 estimates of total column water vapour(kg m-2) over the Marine and Coastal Mask at a spatial resolution of ≤ (TBC) km (enhanced goal: (TBC) km), with a standard total uncertainty of ≤10 (TBC) % (with a minimum uncertainty of ≤ TBC kg m^{-2}).

Note 1: Water vapor, cloud liquid water, and precipitation estimates should be retrieved simultaneously to ensure consistency between products. Their retrievals are highly interdependent and should not be tempted separately.

MRD-2010 The S3NG-T mission shall provide atmospheric attenuation of the normalised radar backscatter coefficient, for all frequencies of the altimeter system, at Level 2 at a spatial resolution of ≤ (TBC) km

(enhanced goal: (TBC) km), with a standard total uncertainty of ≤ (TBC) % (with a minimum uncertainty of ≤ (TBC) dB).

Note 1: The radar signal is attenuated by rain, cloud liquid water, and water vapor in the atmosphere augmented by the backscatter from rain drops via volume scattering. Spatial variability of attenuation sources within the altimeter footprint complicates compensation algorithms.

Note 2: Because of the nonlinearity of attenuation relations, the impact of clouds/rain depends more on the cloud/rain variability within the altimeter footprint than on the mean characteristics, which makes correction using coincident rain or cloud data difficult. Small rain cell and small dense clouds can thus strongly distort the waveforms and lead to erroneous geophysical parameter estimates (see (e.g. Tournadre et al. 2009a, 200b, 2015).

Note 3: Atmospheric attenuation a is frequency dependent. The high attenuation due to atmospheric cloud liquid water at Ka-band is a drawback. In addition, Ka-band is significantly affected by precipitation. However, AltiKa shows that ground processing is able to mitigate these impacts (e.g. Tournadre et al. 2009a, 200b, 2015) to a level that where they are not considered a measurement constraint.

Note 4. This depends on the final design choice of S3NG-T.

MRD-2020 S3NG-T shall provide atmospheric path delay at Level 2 for all measurements within the altimeter footprint at a spatial resolution ≤ (TBC) km (enhanced goal: (TBC) km), with a total standard uncertainty according to specification in requirement MRD-1500.

Note 1: Deleted.

7.5.4.2 Other Level 2 MRAD Products

MRD-2030 Requirement deleted.

MRD-2031 As a secondary mission objective, the S3NG-T mission should provide Level 2 estimates of Sea Ice Edge Detection (SIED).

Note 1: Sea Ice Edge is a surface classification product that assigns ocean grid cells to sea-ice classes (e.g. Open Water, Very Open Drift Ice, Open Drift Ice, Closed Ice, etc.). See Aaboe et al. (2018).

Note 2: The SIED product is a refined ice/no-ice mask, that can be used for navigation and used masking sea-ice signal in other products and/or satellite missions (e.g. IR-radiometer-based SSTs, OC products, etc.).

Note 3: The uncertainty specification assumes a confidence matrix is used to discriminate the sea-ice classes when compared to SAR and Scatterometer data (e.g. Aaboe et al, 2016).

Note 4: An alternative uncertainty characterization of the SIED product is the mean distance to SAR/ice-chart sea-ice edge, expressed in in km (Aaboe et al, 2016). In this case, the requirement would be < 10 km.

Note 5: Ice type is provided as a number of defined categories (typically new ice, first year ice, second year ice, multi-year ice, fast ice) according to specific spectral signatures.

Note 6: This requirement will benefit from a combination of microwave radiometer data with scatterometer and SAR data from other satellite missions.

Note 7: Uncertainty assumes a confidence matrix is used to discriminate FYI from MYI when compared to SAR and Scatterometer data (e.g. Zhang et al, 2019).

The main sources of uncertainty in sea ice thickness retrievals are associated with inadequate knowledge of the snow layer depth and the radar interaction with the snow pack (e.g. Armitage and Ridout, 2015).

Snow lying on top of sea ice plays an important role in the radiation budget because of its high albedo, the Arctic freshwater budget, and influences the Arctic climate: it is fundamental climate variable. Importantly, accurate snow depth (SD) products are required to convert satellite altimeter measurements of ice freeboard to sea ice thickness (SIT). Due to the harsh environment and challenging accessibility, in situ measurements of snow depth are sparse. The quasi-synoptic frequent repeat coverage provided by satellite measurements offers the best approach to regularly monitor snow depth on sea ice. A number of algorithms are based on satellite microwave radiometry measurements and simple empirical relationships (for a review see *Braakmann-Folgmann and Donlon*, 2019). Reducing their uncertainty remains a major challenge.

Snow depth on sea ice has been estimated using a combination of AMSR-E or AMSR-2 brightness temperatures (e.g. using 18.7 and 36.5, GHz) using a spectral gradient approach (e.g. *Markus et al.,* 2006; *Comiso et al.,* 2003). Although the method is confounded in the presence of snow melt water and sensitive to the ice roughness below, potentially this can allow direct snow measurements to replace the Warren snow climatology (*Warren et al.,* 1999). Several studies investigated the uncertainty bounds of the microwave SD retrieval in the Arctic and Antarctic (e.g. *Markus et al.,* 2006; *Stroeve et al.,* 2006) and the current retrieval methods have a Scientific Readiness Level (SRL) of 4 or higher. In the Arctic, the traditional 19/37 GHz gradient ratio retrieval, however, is limited to first-year ice. Recently, the method was extended to work over multiyear ice in spring and more reliable over first-year ice by inclusion of the 6.9 GHz channels (*Rostosky et al.,* 2018).

Maass et al. (2013, 2015) and *Zhou et al,* (2018) proposed the use of L-band radiometer data for snow depth retrieval over thicker Arctic sea ice, where the sensitivity of L-band measurements towards ice thickness shift to snow depth. Similarly, it was demonstrated by *Rostosky et al.* (2018) that the use of C-band in combination with Ku-band has retrieval skills over thicker old ice.

The performance and uncertainty of the Snow Depth retrieval is well quantified by several studies (e.g., *Markus et al.,* 2006; *Stroeve et al.,* 2006; *Rostosky et al.,* 2018). This method can be considered mature. However, due to the high variability of snow properties (e.g., layering, ice lenses, liquid water content, salinity) and the underlying

sea ice (e.g., roughness, salinity) conceptually there are significant uncertainties (RMSD approx. 10 cm) for the retrieved SD.

Kilic et al. (2018b) describe an approach to estimate the snow depth, the snow-ice interface temperature, and the effective temperature of Arctic sea ice using AMSR2 and Ice Mass Balance buoys data. At low microwave frequencies, the sensitivity to the atmosphere is low, and it is possible to derive sea ice parameters due to the penetration of microwaves in the snow and ice layers. The snow depth over sea ice is estimated with an error of 5.1 cm, using a multilinear regression of 6, 18, and 36 GHz vertical polarisation data.

Braakmann-Folgmann and Donlon (2019) explore a new approach to retrieve snow depth on sea ice from multi-frequency satellite microwave radiometer measurements using a neural network approach. Neural networks have proven to reach high accuracies in other domains and excel in handling complex, non-linear relationships. using airborne snow depth measurements from Operation Ice Bridge (OIB) campaigns and compare them to products from three other established snow depth algorithms. Neural networks outperform other algorithms in terms of accuracy when compared to the OIB data. The estimated snow depth covers the full range of measured OIB snow depths and our approach works over both FYI and MYI without requiring a map of ice types to distinguish between both.

MRD-2032 As a secondary mission objective, the S3NG-T mission should provide Level 2 snow depth estimates over sea ice in freezing conditions at 25 km resolution, co-located and contemporaneous to sea ice freeboard estimates.

Note 1: Microwave radiometer channels with appropriate geometry that can measure terrestrial snow cover include 18.7 and 36.5 GHz, both polarizations although algorithms are not mature

Note 2: Minimum retrieval snow depth should be 0.05 m (in line with MRD-280).

Note 3: Dry snow refers to snow with liquid water content of less than 2 %.

Note 4: An uncertainty goal of 5 cm over 25 km orbit segments for snow on sea ice thickness will enable fulfilling the freeboard and thickness requirements.

A large number of SIC retrieval algorithms from microwave radiometer observations exist, using most of the available frequency channels. The development of SIC algorithms from microwave radiometer data is an active field of research, and by the time CIMR flies other approaches might have matured further. One of these is multi-variate optimal estimation (OE) that combines more frequency channels, and relies less on ancillary input.

Algorithms combining Ka-band (~19 GHz) and Ku-band (~37 GHz) frequency channels are by far the most common because of long time availability (SMMR, SSM/I, SSMIS, AMSR-E/2), relative moderate noise levels compared to near 90 GHz algorithms, and spatial resolution. Examples are the *Comiso,* (1995) Bootstrap algorithm, the NASA

Team algorithm (*Cavalieri,* 1991), the Bristol algorithm (*Smith,* 1996), the OSISAF algorithm (*Andersen et al.,* 2006), the SICCI2 algorithms (*Lavergne et al.,* 2018), mostly developed for SSM/I and being applied to SMMR, SSM/I, SSMIS, and AMSR-E and AMSR2 data. These algorithms are used operationally at many processing centres, such as EUMETSAT OSISAF (feeding into CMEMS), U.S. NSIDC, JAXA, CMA, etc. These SIC products are used to initialize operational global and regional model forecasts, e.g. at ECMWF, at CMEMS and at national meteorological and marine forecasting centre.

Having Ka-band (18.7GHz) and Ku-band (36.5GHz) would ensure that this type of algorithm can be used to derive SIC at a high accuracy (<5%). A generic form for a SIC algorithm is expressed by:

$$C(\vec{T}) = \frac{\hat{v} \cdot (\vec{T} - <\vec{T}^W>)}{\hat{v} \cdot (<\vec{T}^I> - <\vec{T}^W>)} \qquad \text{(Eqn. 6.3.1.1)}$$

where $C(T)$ is the sea-ice concentration computed from T (an n-dim vector of L1b Tb, for example $T=[T_{18.7V}, T_{36.5V}, T_{36.5H}]$ triplet for a 3D algorithm like Bristol or SICCI2). $<T^W>$ and $<T^I>$ are respectively the open water and consolidated sea-ice mean signature, i.e. the water and ice tie-points. v is a unit vector holding the coefficients of the algorithms.

MRD-2033 As a secondary mission objective, the S3NG-T mission should provide Level 2 sea ice concentration (SIC) products at a spatial resolution of ≤ (TBC) km and a standard total uncertainty of ≤ (TBD)%.

Note 1: The target standard total uncertainty of ≤5% is realistic for homogeneous scenes, and non-melting surface conditions. In regions of high gradient (e.g. the marginal ice zone) and under surface melt conditions, the standard total uncertainty will be larger.

Note 2: High resolution (e.g. 5-10 km) microwave radiometer channels channel at 18.7 and 36.5 GHz are optimal channel for sea ice concentration measurements (e.g. Ivanova et al., 2015). See also Zabolotskikh, (2019).

Note 3: SIC can be estimated from along-track or swath altimeter measurements

Note 4: The best performance SIC products will be obtained when S3NG-T data are used together with other satellite measurements including scatterometer, SAR and optical data to help e.g. resolve melt water ponds during summer amongst other issues.

7.6 User Service Requirements

MRD-2040 Users shall have access to the generated mission data products and all relevant information, including pre-launch characterisation and auxiliary data, to allow the mission data products exploitation,.

Note 1: This implies the development of a comprehensive an extensive Mission and Product Handbook (S3NG-T MPH) for the different level of products and access to detailed descriptions of the algorithms used at the different levels

Note 2: The S3NG-T MPH should include e.g. data quality information, system anomalies, planning for upcoming operations, production performance, product descriptions, changes in production baseline (processor update/reprocessing campaign) etc.

Note 3: The S3NG-T MPH should include a catalogue of the mission data products

Note 4: Any significant change in the data generation or processing should be communicated to all data users in a timely manner. A timely manner means when a chance is known it is communicated well in advance of that change.

Note 5: A catalogue of all mission data product files should be maintained, storing all relevant identification information and be available to the users. This is essential to services and users in the operational domain that wish to perform reanalyses.

Note 6: It should be possible for users to access mission data products stored in the historical archive.

Note 7: Access to pre-launch characterisation data is required by the user community for processing activities in support of total standard uncertainty derivation for all products and climate applications.

MRD-2050 The user shall be able to search for mission data products using various search criteria and visualise their contents to enable interactive usage.

Note 1: This could be a web-based service.

MRD-2060 Requirement deleted.

MRD-2070 Requirement deleted

MRD-2075 Users shall be able to access to Level 1 and Level 2 ATBD documents.

Note 1: This is required to implement and manage the S3NG-T uncertainty budget throughout the mission.

MRD-2080 Requirement deleted

MRD-2085 Requirement deleted.

7.6.1 Reprocessing Requirements

MRD-2090 It shall be possible to reprocess data products starting at L0, L1 and L2.

Note 1: Reprocessing is a fundamental part of the S3NG-T mission.

Note 2: While L1a products are considered the nominal starting point for re-processing, a capability to reprocess data from L0 may be required in the future as part of dedicated climate reprocessing activities (which has been historically found to be the case for many missions).

Note 3: It is expected that L0 data will be retained in the archive for climate data stewardship and future reprocessing if required by the Copernicus Climate Change Service

Note4: This requirement implies that all necessary calibration and engineering data is also retained and archived for future reprocessing campaigns.

MRD-2100 It shall be possible to reprocess all Level 1 and Level 2 data on a regular basis according to algorithm, validation and data processing evolution.

Note 1: At the time of writing, altimetry missions are typically reprocessed every 1 to 2 years.

MRD-2110 Requirement deleted

MRD-2120 Requirement deleted

MRD-2130 Requirement deleted

7.7 Calibration and Validation Requirements

Calibration and validation will, primarily, be carried out during the commissioning and verification phases of the mission. *Calibration* addresses aspects of the measurement system, which need to be addressed in the generation of the level 1b data products. Since they are concerned with the conversion from the instruments' measurement quantities into standard physical units, they may be addressed by many techniques. The geolocation accuracy is to be quantified and -if possible- improved as part of the Calibration step. *Validation*, is a term used in the context of the conversion of these instrument measurements into the geophysical quantities. Validation is concerned with the characterisation of uncertainty in the L1 and L2 parameters. Commonly, this is achieved by suitable analysis of the Level 2 data themselves, often in combination with *Fiducial Reference Measurements (see Appendix I for definitions)*.

During the assessment and the verification phase of the mission (the first 6-12 months after launch), the majority of ground-processing algorithms and all critical output quantities and associated errors will be calibrated and validated (though some elements such as instrument drift require a much longer period that could extend to the mission lifetime). This is typically done through statistical analysis and by comparison with external measurements from in-situ equipment or other satellite missions. The calibration/verification outputs will be compared with requirements and expected error budget specifications. The parameters to be verified include altimeter range, associated corrections, sea surface height/sea level anomaly, orbit, wind speed (from σ^0) and Hs. In addition to the biases, the calibration process will provide an estimation of the individual drifts of the measurement system components alone. Instrument calibrations will be monitored at least each cycle throughout the life of the mission to determine if the measurement system is meeting its requirements.

Transponders and corner reflectors are FRMs for altimetry as they allow verification of σ^0, range, datation, interferometry geometry among other parameters. These are mandatory for Cal/Val activities and cross-calibration of missions. Both transponders and corner reflectors need to be supported by accurate positioning (with FRM standard uncertainty) information, using GNSS and other positioning systems (e.g. DORIS beacon). Additionally, a collocated radiometer is also desired to derive the wet tropospheric delay during transponder calibrations in addition to the GNSS-derived delays.

MRD-2140 A ground-based transponder and/or corner reflector(s) network shall be implemented as part of the S3NG-T mission baseline for long-term calibration and validation activities throughout the mission lifetime.

Note 1: Deleted.

MRD-2150 Requirement deleted.

MRD-2160 Requirement deleted.

MRD-2170 Requirement deleted.

MRD-2180 Requirement deleted.

7.8 Operational Performance Monitoring Activities

In addition to Calibration and Validation activities, the overall performance of the mission will be monitored throughout Phase E2. Monitoring will be performed at several levels: at the level of the satellite and its payload instruments, at the level of the basic quality of data products and monitoring to enable the underlying quality of the data to be assessed.

MRD-2190 Requirement deleted.

MRD-2200 Requirement deleted.

MRD-2210 Requirement deleted.

7.9 User Software Requirements

MRD-2220 Requirement merged with MRD-2085.

MRD-2230 Requirement deleted.

MRD-2240 Requirement deleted.

MRD-2250 Requirement deleted.

8 REFERENCES

Aaboe, S., Breivik, L.-A., Eastwood, S., 2016. Global Sea Ice Edge and Type Validation Report, v2.1, http://osisaf.met.no/docs/osisaf_cdop2_ss2_valrep_sea-ice-edge-type_v2p1.pdf

Aaboe, S., Breivik, L.-A., Sørensen, A., Eastwood, S. and Lavergne, T., 2018. Global Sea Ice Edge and Type Product User's Manual, v2.3, http://osisaf.met.no/docs/osisaf_cdop3_ss2_pum_sea-ice-edge-type_v2p3.pdf

Abdalati, W. et al., 2010. The ICESat-2 Laser Altimetry Mission, in Proceedings of the IEEE, vol. 98, no. 5, pp. 735-751, doi: 10.1109/JPROC.2009.2034765.

Abdalla, S., 2012. Ku-Band Radar Altimeter Surface Wind Speed Algorithm, Marine Geodesy, 35:sup1, 276-298, DOI: 10.1080/01490419.2012.718676

Ablain, M., Dorandeu, J., Le Traon, P.-Y., and Sladen, A., 2006. High resolution altimetry reveals new characteristics of the December 2004 Indian Ocean tsunami, Geophys. Res. Lett., 33, L21602, doi:10.1029/2006GL027533.

Ablain, M., Cazenave, A., Valladeau, G., and Guinehut, S., 2009. A new assessment of the error budget of global mean sea level rate esti- mated by satellite altimetry over 1993–2008, Ocean Sci., 5, 193– 201, doi:10.5194/os-5-193-2009.

Ablain, M., Philipps, S., Picot, N. and Bronner, E., 2010. Jason-2 global statistical assessment and cross-calibration with Jason-1, Mar. Geod., 33(S1), 162–185, doi:10.1080/01490419.2010.487805.

Ablain, M., Cazenave, A., Larnicol, G., Balmaseda, M., Cipollini, P., Faugère, Y., Fernandes, M. J., Henry, O., Johannessen, J. A., Knudsen, P., Andersen, O., Legeais, J., Meyssignac, B., Picot, N., Roca, M., Rudenko, S., Scharffenberg, M. G., Stammer, D., Timms, G., and Benveniste, J., 2015. Improved sea level record over the satellite altimetry era (1993–2010) from the Climate Change Initiative project, Ocean Sci., 11, 67–82, doi:10.5194/os-11-67- 2015, 2015.

Ablain, M., Meyssignac, B., Zawadzki, L., Jugier, R., Ribes, A., Spada, G., Benveniste, J., Cazenave, A., and Picot, N., 2019. Uncertainty in satellite estimates of global mean sea-level changes, trend and acceleration, Earth Syst. Sci. Data, 11, 1189–1202, https://doi.org/10.5194/essd-11-1189-2019, 2019.

Ablain, M., Lalau, N., Meyssignac, B., Fraudeau, R., Barnoud, A., Dibarboure, G., Egido, A., and Donlon, C. J.: Benefits of a second tandem flight phase between two successive satellite altimetry missions for assessing the instrumental stability, EGUsphere [preprint], https://doi.org/10.5194/egusphere-2024-1802, 2024.

Abulaitijiang,A., O.B. Andersen, L. Stenseng, 2015. Coastal sea level from inland CryoSat-2 interferometric SAR altimetry Geophys. Res. Lett., 42, 1841-1847, 10.1002/2015GL063131.

Aguirre M., Baillion Y., Berruti B., Drinkwater M., 2009. Operational Oceanography and the Sentinel-3 System. In: Olla P. (eds) Space Technologies for the Benefit of Human Society and Earth. Springer, Dordrecht. https://doi.org/10.1007/978-1-4020-9573-3_4

Aires, F., Prigent, C., Rossow, W. B., & Rothstein, M., 2001. A new neural network approach including first guess for retrieval of atmospheric water vapor, cloud liquid water path, surface temperature, and emissivities over land from satellite microwave observations. Journal of Geophysical Research: Atmospheres, 106(D14), 14887-14907.

Alexandrov, V., Sandven, S., Wahlin, J., and Johannessen, O. M.2010. The relation between sea ice thickness and freeboard in the Arctic, The Cryosphere, 4, 373–380, https://doi.org/10.5194/tc-4-373-2010, 2010.

Allen, G. H. T. M. Pavelsky, 2018. Global extent of rivers and streams. Science, 361, 585-588, doi:10.1126/science.aat0636.

Allen, G. H., David, C. H., Andreadis, K. M., Hossain, F., and Famiglietti, J. S., 2018. Global estimates of river flow wave travel times and implications for low-latency satellite data. Geophysical Research Letters, 45, 7551–7560. https://doi.org/10.1029/2018GL077914

Allen, T., 2001. GANDER – a constellation of miocrosats designed to reduce risks at sea, Space Policy, 17, 61-64.

Alpers, W. R., Ross, D. B., and Rufenach, C. L., 1981. On the detectability of ocean surface waves by real and synthetic aperture radar, J. Geophys. Res., 86(C7), 6481– 6498, doi:10.1029/JC086iC07p06481.

Altamimi, Z., Rebischung, P., Métivier, L., and Collilieux, X., 2016. ITRF2014: A new release of the International Terrestrial Reference Frame modeling nonlinear station motions, J. Geophys. Res. Solid Earth, 121, 6109– 6131, doi:10.1002/2016JB013098.

Altiparmaki, O., M. Kleinherenbrink, M. Naeije, C. Slobbe, and P. Visser, P., 2022, SAR altimetry data as a new source for swell monitoring. Geophysical Research Letters, 49, e2021GL096224. https://doi.org/10.1029/2021GL096224

Alves, J. H. G. M., Young, I. R., 2004. On estimating extreme wave heights using combined Geosat, TOPEX/Poseidon and ERS-1 altimeter data. Appl Ocean Res 25(4):167–186

Andela, N., Liu, Y.Y., van Dijk, A.I.J.M., de Jeu, R.A.M., & McVicar, T.R., 2013. Global changes in dryland vegetation dynamics (1988-2008) assessed by satellite remote sensing: comparing a new passive microwave vegetation density record with reflective greenness data. Biogeosciences, 10, 6657-6676

Andersen, S., R. Tonboe, L. Kaleschke, G. Heygster, and L. T. Pedersen, 2006. Intercomparison of passive microwave sea ice concentration retrievals over the high-concentration Arctic sea ice, J. Geophys. Res., 112, C08004, doi:10.1029/2006JC003543.

Anh, D. and F. Aires, 2019. River Discharge Estimation based on Satellite Water Extent and Topography: An Application over the Amazon, J. Hydrometerology, DOI: 10.1175/JHM-D-18-0206.1

Anthes, R.A., Bernhardt, P.A., Chen, Y., Cucurull, L., Dymond, K.F., Ector, D., Healy, S.B., Ho, S.-P., Hunt, D.C., Kuo, Y.-H., Liu, H., Manning, K., McCormick, C., Meehan, T.K., Randel, W.J., Rocken, C., Schreiner, W.S., Sokolovskiy, S.V., Syndergaard, S., Thompson, D.C., Trenberth, K.E., Wee, T.-K., Yen, N.L. and Zeng, Z., 2008. The COSMIC/FORMOSAT-3 mission: early results. Bulletin of the American Meteorological Society, 89, 313– 333

Aouf, L., A. Dalphinet, D. Hauser, L. Delaye, C. Tison, B. Chapron, L. Hermozo and C. Tourain, 2019. On The assimilation of CFOSAT wave data in the wave model MFWAM: Verification phase. IGARSS 2019-2019 IEEE International Geoscience and Remote Sensing Symposium, IEEE.

Aouf, L., Hauser, D., Chapron, B., Toffoli, A., Tourain, C., & Peureux, C., 2021. New directional wave satellite observations: Towards improved wave forecasts and climate description in Southern Ocean. Geophysical Research Letters, 48, e2020GL091187. https://doi.org/10.1029/2020GL091187

Arbic, B. K.; Lyard, F., Ponte, A., Ray, R. D., Richman, J. G., Shriver, J. F., Zaron, E. and Zhao, Z., 2015. Tides and the SWOT mission: Transition from Science Definition Team to Science Team. Civil and Environmental Engineering Faculty Publications and Presentations. 336. http://archives.pdx.edu/ds/psu/16710

Arbic, B.K., et al., 2018: A primer on global internal tide and internal gravity wave continuum modeling in HYCOM and MITgcm. In "New Frontiers in Operational Oceanography", E. Chassignet, A. Pascual, J. Tintoré, and J. Verron, Eds., GODAE OceanView, 307-392, doi:10.17125/gov2018.ch13.

Ardhuin, F., Collard, F., Chapron, B., Girard-Ardhuin, F., Guitton, G., Mouche, A., and Stopa, J. E. (2015), Estimates of ocean wave heights and attenuation in sea ice using the SAR wave mode on Sentinel-1A. Geophys. Res. Lett., 42, 2317– 2325. doi: 10.1002/2014GL062940.

Ardhuin, F., Stopa J. E., Chapron, B., Collard, F., Husson, R., Jensen, R., Johannessen, J., Mouche, A., Pasaro, M., Quartly, G., Swail, V., and Young, I., 2019, Observing Sea States, Frontiers in Marine Science, 6, 124-, https://www.frontiersin.org/article/10.3389/fmars.2019.00124

Ardhuin F., Brandt P., Gaultier L., Donlon C., Battaglia A., Boy F., Casal T., Chapron B., Collard F., Cravatte S., Delouis J-M., De Witte E., Dibarboure G., Engen G., Johnsen H., Lique C., Lopez-Dekker P., Maes C., Martin A., Marié L. Menemenlis D., Nouguier F., Peureux C., Rampal P., Ressler G., Rio M-H., Rommen B., Shutler J. D., Suess M., Tsamados M., Ubelmann C., van Sebille E., van den Oever M., Stammer D., 2019. SKIM, a Candidate Satellite Mission Exploring Global Ocean Currents and Waves, Frontiers in Marine Science, 6, 209-, DOI=10.3389/fmars.2019.00209

Armitage, T. W. K and R. Kwok, 2019. SWOT and the ice-covered polar oceans: An exploratory analysis, Advances in Space Research, ISSN 0273-1177, https://doi.org/10.1016/j.asr.2019.07.006.

Armitage, T. W. K., and Ridout, A. L., 2015. Arctic sea ice freeboard from AltiKa and comparison with CryoSat-2 and Operation IceBridge, Geophys. Res. Lett., 42, 6724– 6731, doi:10.1002/2015GL064823.

Armitage, T.W.K., M.W.J. Davidson, 2014. Using the interferometric capabilities of the ESA CryoSat-2 mission to improve the accuracy of sea ice freeboard retrievals IEEE Trans. Geosci. Remote Sens., 52, 529-536, 10.1109/TGRS.2013.2242082

Auriol, A. and Tourain, C., 2010. DORIS System: the new age, in DORIS Special Issue: Precise Orbit Determination and Applications to the Earth Sciences, P. Willis (Ed.), Advances In Space Research, 46(12):1484-1496, DOI:10.1016/j.asr.2010.05.015

Backus GE, Gilbert JF, 1967. Numerical applications of a formalism for geophysical inverse problems. Geophys. J. R. Astron. Soc. Jul; 1967 13(1–3):247–276.

Backus GE, Gilbert JF, 1968. Resolving power of gross Earth data. Geophys. J. R. Astron. Soc. Oct; 1968 16(2):169–205.

Bai, Y., , Y. Wang , Y. Zhang, C. Zhao and G. Chen, 2020. Impact of OceanWaves on Guanlan's IRA Measurement Error, Remote Sens. 2020, 12, 1534; doi:10.3390/rs12101534

Ballarotta, M., C. Ubelmann, M.-I Pujol, G. Taburet, J.-F. Legeais, Y. Faugere, A. Delepouille, D. Chelton, G. Dibarboure, N. Picot and the DUACS team, 2019. On the resolution of ocean altimetry maps, Ocean Sci., 15, 1091–1109, 2019, https://doi.org/10.5194/os-15-1091-2019

Ballarotta, M., Ubelmann, C., Rogé, M., Fournier, F., Faugère, Y., Dibarboure, G., Morrow, R., & Picot, N., 2020. Dynamic Mapping of Along-Track Ocean Altimetry: Performance from Real Observations, Journal of Atmospheric and Oceanic Technology, 37(9), 1593-1601. Retrieved Apr 4, 2021, from https://journals.ametsoc.org/view/journals/atot/37/9/jtechD200030.xml

Bancroft, G., 2011: Marine weather review—North Atlantic area, January to June 2011. Mariner's Weather Log, 55, 13–26.

Bao, M. 1999. A nonlinear integral transform between ocean wave spectra and phase image spectra of a cross-track interferometric SAR. In Proceedings of the IEEE 1999 International Geoscience and Remote Sensing Symposium. IGARSS'99 (Cat. No.99CH36293), Hamburg, Germany, 28 June–2 July 1999; IEEE: Piscataway, NJ, USA, 1999; Volume 5, pp. 2619–2621.

Bauer, P., and R. Bennartz, 1998. Tropical Rainfall Measuring Mission microwave imaging capabilities for the observation of rain clouds, Radio Sci., 33(2), 335–349, doi:10.1029/97RS02049

Baur, M. J., Jagdhuber, T., Feldman, A.F., Akbar, R., Entekhabi, D., 2019. Estimation of relative canopy absorption and scattering at L-, C- and X-bands, Remote Sensing of Environment, Volume 233, 111384, https://doi.org/10.1016/j.rse.2019.111384.

Bell, S., (1999), Measurement Good Practice Guide No. 11 (Issue 2) A Beginner's Guide to Uncertainty of Measurement, National Physical Laboratory, UK, available from http://publications.npl.co.uk/npl_web/pdf/mgpg11.pdf

Bender, M. A., T. P. Marchok, C. R. Sampson, J.A. Knaff, and M. J. Morin, 2017: Impact of Storm Size on Prediction of Storm Track and Intensity Using the 2016 Operational GFDL Hurricane Model. Wea. Forecasting, 32, 1491–1508, https://doi.org/10.1175/WAF-D-16-0220.1

Bergadà, M. P. Brotons, Y. Camacho, L. Díez, A. Gamonal, J. Luis García, R. González, A. Pacheco, and M. Ángel Palacios, 2010. Design and development of the Sentinel-3 Microwave Radiometer, Proc. SPIE, Vol. 7826, 78260M doi:10.1117/12.864575

Biancamaria, S., Durand, M., Andreadis, K. M., Bates, P. D., Boone, A., Mognard, N. M., et al. (2011). Assimilation of virtual wide swath altimetry to improve Arctic river modeling. Remote Sensing of Environment, 115(2), 373–381. https://doi.org/10.1016/j.rse.2010.09.008

Bidlot J. R., 2017. Twenty-one years of wave forecast verification. ECMWF Newsletter 150:31–36

BIPM, 1995. Comptes rendus de la 20e reunion de la Conference generale des poids et mesures. Available online at /http://www.bipm.org/en/CGPM/db/20/S.

Blazquez, A., B Meyssignac, J. M. Lemoine, E Berthier, A Ribes, A Cazenave, 2018. Exploring the uncertainty in GRACE estimates of the mass redistributions at the Earth surface: implications for the global water and sea level budgets, Geophysical Journal International, Volume 215, Issue 1, October 2018, Pages 415–430, https://doi.org/10.1093/gji/ggy293

Bloßfeld, M., Zeitlhöfler, J., Rudenko, S. Dettmering, D., 2020.Observation-Based Attitude Realization for Accurate Jason Satellite Orbits and Its Impact on Geodetic and Altimetry Results. Remote Sens. 2020, 12, 682.

Blumstein, D., A. Guérin, A. Lamy, A. Couhert, A. Piquereau, B. Palacin, F. Rouzies, A. Mallet, S. Biancamaria, S. Le Gac, T. Amiot, P. Maisongrande, S. Cherchali, S. Coutin-Faye, 2019. SMASH: A Constellation of Small Altimetry Satellites Dedicated to Hydrology, presented at the 6th Workshop on Advanced RF Sensors and Remote Sensing Instruments, ARSI'19 & 4th Ka-band Earth Observation Radar Missions Workshop, KEO'19

Bokhorst, S., Pedersen, S.H., Brucker, L. et al., 2016. Changing Arctic snow cover: A review of recent developments and assessment of future needs for observations, modelling, and impacts, Ambio, 45: 516. https://doi.org/10.1007/s13280-016-0770-0

Bonaduce, A., Benkiran, M., Remy, E., Le Traon, P. Y., and Garric, G (2018). Contribution of future wide-swath altimetry missions to ocean analysis and forecasting. Ocn. Sci. 14, 1405–1421. doi: 10.5194/os-14-1405-2018

Bonnefond, P., Exertier, P., Laurain, O., Guinle, T., Féménias, P., 2019. Corsica: A 20-Yr Multi-Mission Absolute Altimeter Calibration Site, Advances in Space Research, Special Issue « 25 Years of Progress in Radar Altimetry », doi : 10.1016/j.asr.2019.09.049.

Bonnefond, P., Exertier, P., Laurain, O., Menard, Y., Orsoni, A., Jeansou, E., Haines, B., Kubitschek, D., Born, G., 2003. Leveling Sea Surface using a GPS catamaran, Special Issue on Jason-1 Calibration/Validation, Part 1, Mar. Geod., Vol. 26, No. 3-4, 319-334, doi: 10.1080/714044521.

Bonnefond, P., Haines, B.J., Watson, C., 2011. In situ Absolute Calibration and Validation: A Link from Coastal to Open-Ocean Altimetry. Springer Berlin Heidelberg, Berlin, Heidelberg. chapter 11. pp. 259–296, doi:10.1007/978-3-642-12796-0_11.

Bonnefond, P.; Laurain, O.; Exertier, P.; Boy, F., Guinle, T., Picot, N., Labroue, S., Raynal, M., Donlon, C., Féménias, P., Parrinello, T., Dinardo, S., 2018. Calibrating the SAR SSH of Sentinel-3A and CryoSat-2 over the Corsica Facilities. Remote Sens. 2018, 10, 92.

Boy, F., Desjonqueres, J.D., Picot, N., Moreau, T., Raynal, M., 2016. CryoSat-2 SAR-mode over oceans: Processing methods, global assessment, and benefits. IEEE Trans. Geosci. Remote Sens. 2016, 55, 148–158.

Boy, F., et al., 2018. Early results from Sentinel-3B commissioning phase, Ocean Surface topography Science Team, 2018, Ponta Delgarda, Portugal.

Brackmmann-Folgmann, A. and C. Donlon, 2019. Estimating Snow Depth on Arctic Sea Ice using satellite Microwave Radiometry and a Neural Network, submitted to Cryosphere discussions, February 2019.

Brenner, A. C., Bindschadler, R. A., Thomas, R. H., & Zwally, H. J., 1983. Slope-induced errors in radar altimetry over continental ice sheets. Journal of Geophysical Research, 88(C3), 1617–1623.

Brown, G. S., 1977. The average impulse response of a rough surface and its applications. IEEE Transactions on Antennas and Propagation,25(1), 67–74.

Brown, S., 2006. AMR Beam Matching Algorithm, JPL technical document, 12 October 2006.

Brown, S., 2013. Maintaining the Long-Term Calibration of the Jason-2/OSTM Advanced Microwave Radiometer Through Intersatellite Calibration," in IEEE Transactions on Geoscience and Remote Sensing, vol. 51, no. 3, pp. 1531-1543, March 2013, doi: 10.1109/TGRS.2012.2213262.

Brown, S., Desai, S., Keihm, S. and Lu, W., 2009. Microwave radiometer calibration on decadal time scales using on-earth brightness temperature references: Application to the TOPEX microwave radiometer. J. Atmos. Oceanic Technol., 26: 2579–2591.

Brown, S., Ruf, C., Keihm, S. and Kitiyakara, A., 2004. Jason microwave radiometer performance and on-orbit calibration. Marine Geodesy, 27(1-2), pp.199-220.

Brucker, L., and T. Markus, 2013. Arctic-scale assessment of satellite passive microwave-derived snow depth on sea ice using Operation IceBridge airborne data. Journal of Geophysical Research-Oceans 118: 2892–2905.

Brun, E., Vionnet, V., Decharme, B., Peings, Y., Valette, R., Karbou, F., and Morin, S., 2013. Simulation of northern Eurasian local snow depth, mass and density using a detailed snowpack model and meteorological reanalyses. J. Hydrometeorol., 14, 203–219.

Buontempo, C., Hutjes, R., Beavis, P., Berckmans, J., Cagnazzo, C., Vamborg, F., Thépaut, J.-N., Bergeron, C., Almond, S, Amici, A., Ramasamy, S., Dee, D., 2020. Fostering the development of climate services through Copernicus Climate Change Service (C3S) for agriculture applications, Weather and Climate Extremes, 27, https://doi.org/10.1016/j.wace.2019.100226.

Bushair, M.T., Gairola, R. M., 2019. A combined passive–active microwave retrieval of ocean surface wind speed from SARAL-AltiKa microwave radar altimeter and radiometer. Meteorol Atmos Phys 131, 1205–1212, https://doi.org/10.1007/s00703-018-0631-4

Calle, D., Cancela, S., Carbonell, E., Rodríguez, I., Tobías, G., Fernández-Hernández, I., "First Experimentation Results with the Full Galileo CS Demonstrator," Proceedings of the 29th International Technical Meeting of the Satellite Division of The Institute of Navigation (ION GNSS+ 2016), Portland, Oregon, September 2016, pp. 2870-2877. https://doi.org/10.33012/2016.14728

Camargo, C. M. L., Riva, R. E. M., Hermans, T. H. J., Slangen, A. B. A., 2020. Exploring Sources of Uncertainty in Steric Sea-Level Change Estimates. Journal of Geophysical Research: Oceans, 125, e2020JC016551. https://doi.org/10.1029/2020JC016551

Campos, R.M., Alves, J.G., Penny, S.G. et al., 2020. Global assessments of the NCEP Ensemble Forecast System using altimeter data. Ocean Dynamics 70, 405–419, https://doi.org/10.1007/s10236-019-01329-4

Cancet M., Andersen O., Abulaitijiang A., Cotton D., Benveniste J., 2019. Improvement of the Arctic Ocean Bathymetry and Regional Tide Atlas: First Result on Evaluating Existing Arctic Ocean Bathymetric Models. In: Mertikas S., Pail R. (eds) Fiducial Reference Measurements for Altimetry. International Association of Geodesy Symposia, vol 150. Springer, Cham. https://doi.org/10.1007/1345_2019_85

Cancet, M., Bijac, S., Chimot, J., Bonnefond, P., Jeansou, E., Laurain, O., Lyard, F., Bronner, E., Féménias, P., 2013. Regional in situ validation of satellite altimeters: Calibration and cross-calibration results at the Corsican sites, Advances in Space Research, Volume 51, Issue 8, 15 April 2013, Pages 1400-1417, ISSN 0273-1177, http://dx.doi.org/10.1016/j.asr.2012.06.017.

Carayon, B. et al., 2015. Miniaturized altimeter an innovative concept of miniaturized altimeter for constellations, 2015 IEEE International Geoscience and Remote Sensing Symposium (IGARSS), Milan, Italy, 2015, pp. 1231-1233, doi: 10.1109/IGARSS.2015.7325995.

Carrea, L., Embury, O. and Merchant, C. J. (2015) Datasets related to in-land water for limnology and remote sensing applications: distance-to-land, distance-to-water, water-body identifier and lake-

centre co-ordinates. Geoscience Data Journal, 2 (2). pp. 83-97. ISSN 2049-6060 doi: https://doi.org/10.1002/gdj3.32

Carrere, L., Arbic, B. K., Dushaw, B., Egbert, G. D., Erofeeva, S. Y., Lyard, F., Ray, R. D., Ubelmann, C., Zaron, E., Zhao, Z., Shriver, J. F., Buijsman, M. C., and Picot, N., 2020. Accuracy assessment of global internal tide models using satellite altimetry, Ocean Sci. Discuss., https://doi.org/10.5194/os-2020-57, in review.

Carrieres, T., Buehner, M., Lemieux, J., and Toudal Pedersen, L. (Eds.). 2017. Sea Ice Analysis and Forecasting: Towards an Increased Reliance on Automated Prediction Systems. Cambridge: Cambridge University Press. doi:10.1017/9781108277600

Casotto, S., Bardella, M., Sciarratta, M., Darugna, F., Grenier, A., Zoccarato, P., Pietro G., (2021): GNSS-Based Dual-Constellation and Dual-Frequency Real-Time Reduced-Dynamics P2OD for LEO Satellites, ION GNSS+ 2021 Conference, St. Louis, Missouri, September 20-24

Cavalieri, D. and C. Parkinson, 2012. Antarctic sea ice variability and trends, 1979-2010, Cryosphere, vol. 6, p. 881, Jun. 2012.

Cavalieri, D. J., J. P. Crawford, M. R. Drinkwater, D. T. Eppler, L. D. Farmer, R. R. Jentz, and C. C. Wackerman, 1991. Aircraft active and passive microwave validation of the sea ice concentration from the Defence Meteorological Satellite Program Special Sensor Microwave Imager, J. Geophys. Res., 96(C12), 21,998– 22,008

Cavalieri, D.J., T. Markus, A. Ivanoff, et al. 2012. A comparison of snow depth on sea ice retrievals using airborne altimeters and an AMSR-E simulator. IEEE Transactions on Geoscience and Remote Sensing 50: 3027–3040.

Cazenave, A, Palanisamy, H., Ablain, M., 2018. Contemporary sea level changes from satellite altimetry: What have we learned? What are the new challenges?, Advances in Space Research, 62, 1639-1653, https://doi.org/10.1016/j.asr.2018.07.017.

Cazenave, A. et al, 2018. Global sea-level budget 1993–present WCRP Global Sea Level Budget Group, Earth Syst. Sci. Data, 10, 1551–1590, 2018 https://doi.org/10.5194/essd-10-1551-2018

Cazenave A., Gouzenes Y., Birol, F., Leger F., Passaro M., Calafat F.M., Shaw A., Nino F., Legeais J.F., Oelsmann J., Restano M., Benveniste J.: Sea level along the world's coastlines can be measured by a network of virtual altimetry stations. Communications Earth and Environment (Nature Portfolio), 3(1), 10.1038/s43247-022-00448-z, 2022

CCI, Climate Change Initiative Coastal Sea Level Team (the), 2020. Coastal sea level anomalies and associated trends from Jason satellite altimetry over 2002-2018, Nature Scientific Data, in press, 2020.

Chambers, D. P., Ries, J. C., Urban, T. J., 2003. Calibration and verification of Jason-1 using global along-track residuals with TOPEX, Mar. Geod., 26(3&4), 305–317, doi:10.1080/714044523.

Chapron, B., Johnsen, H. & Garello, R., 2001. Wave and wind retrieval from SAR images of the ocean. Ann. Télécommun. 56, 682–699. https://doi.org/10.1007/BF02995562

Chelton, D. B., 1994. The sea state bias in altimeter estimates of sea level from collinear analysis of TOPEX data, J. Geophys. Res., 99(C12), 24995– 25008, doi:10.1029/94JC02113.

Chelton, D. B., Schlax, M. G., Samelson, R. M., de Szoeke, R. A., 2007. Global observations of large oceanic eddies, Geophys. Res. Lett., 34, L15606, doi:10.1029/2007GL030812.

Chelton, D. B., Schlax, M. G., Samelson, R. M., Farrar, J. T., Molemaker, M. J., McWilliams, J. C., et al. 2019. Prospects for future satellite estimation of smallscale variability of ocean surface velocity and vorticity. Prog. Oceanogr. 173,256–350. doi: 10.1016/j.pocean.2018.10.012

Chen X, et al. 2017. The increasing rate of global mean sea-level rise during 1993- 2014. Nat Clim Change 7:492–495

Chen, J. L., C. R. Wilson, and B. D. Tapley, (2013). Contribution of ice sheet and mountain glacier melt to recent sea level rise. Nature Geoscience, 6(7), 549.Meier et al., 2014

Chen J., L. Fenoglio, K. Kusche, K. Liao, H. Uyanik, Z.A. Nazdir, Y. Lou (2023) Evaluation of Sentinel-3A altimetry over Songhua river basin, J. of Hydrology, https://doi.org/10.1016/j.jhydrol.2023.129197.

Cheng, L., Abraham, J., Trenberth, K.E. et al.2021. Upper Ocean Temperatures Hit Record High in 2020. Adv. Atmos. Sci. (2021). https://doi.org/10.1007/s00376-021-0447-x

Cipollini, P. & Co-Authors, 2010, The Role of Altimetry in Coastal Observing Systems, in Proceedings of OceanObs'09: Sustained Ocean Observations and Information for Society (Vol. 2), Venice, Italy, 21-25 September 2009, Hall, J., Harrison D.E. & Stammer, D., Eds., ESA Publication WPP-306. available from https://abstracts.congrex.com/scripts/jmevent/abstracts/FCXNL-09A02a-1716477-1-cwp4b04_cipollini.pdf

Clerc, S.; Donlon, C. Borde, F. Lamquin, N. Hunt, S.E. Smith, D. McMillan, M. Mittaz, J. Woolliams, E., Hammond, M., Banks, C., Moreau, T., Picard, B., Raynal, M., Rieu, P., Guérou, T., 2020. A. Benefits and Lessons Learned from the Sentinel-3 Tandem Phase. Remote Sens. 2020, 12, 2668.

Close, S., T. Penduff, S. Speich, J.-M. Molines, 2020. A means of estimating the intrinsic and atmospherically-forced contributions to sea surface height variability applied to altimetric observations, Progress in Oceanography, 184, https://doi.org/10.1016/j.pocean.2020.102314.

CMEMS, 2017. Copernicus Marine Environmental Monitoring System (CMEMS) requirements for the Evolution of the Copernicus Satellite Component, available from https://marine.copernicus.eu/sites/default/files/media/pdf/2020-10/CMEMS-requirements-satellites.pdf

CNES, 2006. OSTM/Jason-2 science and operational requirements, TP3-J0-SP-188-CNES Mar 6, 2006 available from CENTRE NATIONAL D'ÉTUDES SPATIALES, Toulouse, France.

Cohen, S., T. Wan, Md Tazmul Islam, J. P. M. Syvitski, 2018, Global river slope: A new geospatial dataset and global-scale analysis, J. Hydrology, 563, 1057-1067, https://doi.org/10.1016/j.jhydrol.2018.06.066

Comiso, J. C., and R. Kwok, 1996. Surface and radiative characteristics of the summer Arctic sea ice cover from multisensor satellite observations, J. Geophys. Res., 101(C12), 28397–28416, doi:10.1029/96JC02816.

Cooper, C. K., Forristall, G. Z., 1997. The use of satellite altimeter data to estimate extreme wave climate. J Atmos Ocean Technol 14(2):254–266.

Couderc, V. 2015. Jason-3 System Requirements, TP4-J0-STB-44-CNES v 1.3, Centre Nationale d'Etudes Spatiales, Toulouse, 2015.

Couhert, A, L. Cerri, JF. Legeais, M. Ablain, N. P. Zelensky, B. J. Haines, F. G. Lemoine, W. I. Bertiger, S. D. Desai, M. Otten, 2015. Towards the 1 mm/y stability of the radial orbit error at regional scales, Advances in Space Research 55 (2015) 2–23

Crétaux, J.-F., K. Nielsen, F. Frappart, F. Papa, S. Calmant, J. Benveniste, 2017. Hydrological applications of satellite altimetry: rivers, lakes, man-made reservoirs, inundated areas. In: Stammer, D., Cazenave, A. (Eds.), Satellite Altimetry Over Oceans and Land Surfaces, Earth Observation of Global Changes. CRC Press, 2017.

Crétaux J.-F. et al., 2018. Absolute calibration or validation of the altimeters on the Sentinel-3A and the Jason-3 over Lake Issykkul (Kyrgyzstan). Remote Sensing, 10, 1679, doi:10.3390/rs10111679

Cullen, R., Davidson, M. W. J., Drinkwater, M. R., Francis, C. R., Haas, C., Hawley, R. L., Mavrocordatos, C.M., Morris, E. M., Rack, W., Ratier, G., Viau, P. and Wingham, D. J., 2006.'ESA's new range of radar altimeters for the extraction of geophysical parameters from land, sea ice and ocean surfaces' Proc. Radar Altimeter Symposium, Venice March 2006.

de Rosnay, P., J. Muñoz-Sabater, C. Albergel, L. Isaksen, S. English, M. Drusch, J.-P. Wigneron: "SMOS brightness temperature forward modelling and long term monitoring at ECMWF", Remote Sensing of Environment, 237 (Feb 2020) https://doi.org/10.1016/j.rse.2019.111424

Deltacommissie 1961 Report Delta Committee Parts 1–6. The Hague, Staatsdrukkerij en Uitgeverijbedrijf. (In Dutch, with extensive English summaries.)

Darugna, F., Casotto, S., Bardella, M., Sciarratta, M., Zoccarato, P., Giordano, P., (2022): Sentinel-6A GPS and Galileo Dual-Frequency Real-Time Reduced-Dynamics P2OD, NAVITEC 2022, 5-7 April, Noordwijk, the Netherlands

Desai, S., Rodriguez, E., Fernandez, D. E., Peral, E., Chen, C. W., Bleser, J.-W. De, and Williams, B. (2018). Surface water and Ocean topography mission (SWOT) science requirements document (Technical Report JPL D-61923). Pasadena, CA: Jet Propulsion Laboratory, California Institute of Technology. Retrieved from https://swot.jpl.nasa.gov/docs/D-61923_SRD_Rev_B_20181113.pdf

Desportes, C., Obligis, E. and Eymard, L., 2007. On the wet tropospheric correction for altimetry in coastal regions. IEEE Trans. Geosci. Rem. Sens., 45(7): 2139–2149.

Dettmering, D., Schwatke, C., Boergens, E., and Seitz, F. 2016. Potential of ENVISAT radar altimetry for water level monitoring in the Pantanal wetland, Remote Sens., 8, 596, https://doi.org/10.3390/rs8070596.

Dibarboure, G., Boy, F., Desjonqueres, J. D., Labroue, S., Lasne, Y., Picot, N., Poisson, J. C., Thibaut, P., 2014. Investigating Short-Wavelength Correlated Errors on Low-Resolution Mode Altimetry. J. Atmos. Oceanic Technol., 31, 1337–1362, https://doi.org/10.1175/JTECH-D-13-00081.1.

Dibarboure, G., C. Renaudie, M.-I. Pujol, S. Labroue, N. Picot, 2012. A demonstration of the potential of CryoSat-2 to contribute to mesoscale observation, Advances in Space Research, Volume 50, Issue 8, 1046-1061,https://doi.org/10.1016/j.asr.2011.07.002.

Dibarboure, G., Lamy, A., Pujol, M.-J., Jettou, G., 2018, The drifting phase of SARAL: Securing stable ocean mesoscale sampling with an unmaintained decaying altitude. Remote Sensing 10(7), 1051. https://doi.org/10.3390/rs10071051

Di Bella, A., H. Skourup, J. Bouffard, and T. Parrinello, “Uncertainty reduction of Arctic sea ice freeboard from CryoSat-2 interferometric mode,” *Adv. Space Res.*, vol. 62, no. 6, pp. 1251–1264, Sep. 2018.

Di Bella, A., M. Scagliola, L. Maestri, H. Skourup, and R. Forsberg, “Improving CryoSat-2 SARIn L1b products to account for inaccurate phase difference: Impact on sea ice freeboard retrieval,” *IEEE Geosci. Remote Sens. Lett.*, vol. 17, no. 2, pp. 252–256, Feb. 2020.

Di Bella, A.; Kwok, R.; Armitage, T.W.K.; Skourup, H.; Forsberg, R. Multi-peak Retracking of CryoSat-2 SARIn Waveforms Over Arctic Sea Ice. *IEEE Trans. Geosci. Remote Sens.* **2021**, *59*, 3776–3792.

Dieng H., Cazenave A., Meyssignac B. and Ablain M., 2017. New estimate of the current rate of sea level rise from a sea level budget approach, Geophys. Res. Lett., 44, doi:10.1002/2017GL073308.

Dodet, G., Piolle, J.-F., Quilfen, Y., Abdalla, S., Accensi, M., Ardhuin, F., Ash, E., Bidlot, J.-R., Gommenginger, C., Marechal, G., Pasesaro, M., Quartly, G., Stopa, J., Timmermans, B., Young, I., Cipollini, P., and Donlon, C., 2020. The Sea State CCI dataset v1: towards a sea state climate data record based on satellite observations, Earth Syst. Sci. Data, 12, 1929–1951, https://doi.org/10.5194/essd-12-1929-2020, 2020.

Domeneghetti, A., Tarpanelli, A., Brocca, L., Barbetta, S., Moramarco, T., Castellarin, A., and Brath, A.2014. The use of remote sensing-derived water surface data for hydraulic model calibration, Remote Sens. Environ., 149, 130–141, https://doi.org/10.1016/j.rse.2014.04.007,.

Donlon, C. J, R. Cullen, L. Giulicchi, P. Vuilleumier, C. R. Francis, M. Kuschnerus, W. Simpson, A. Bouridah, M. Caleno, R. Bertoni, J. Rancaño, E. Pourier, A. Hyslop, J. Mulcahy, R. Knockaert, C. Hunter, A. Webb, M. Fornari, P. Vaze, S. Brown, J. Willis, S. Desai, J-D Desjonqueres, R. Scharroo, C. Martin-Puig, E. Leuliette, A. Egido, W. H. F. Smith, P. B., S. Le Gac, N. Picot, and G. Tavener, 2021. The Copernicus Sentinel-6 Mission: Enhanced Continuity of Satellite Sea Level Measurements from Space, Rem. Sens. Env., Rem. Sens. Env. 258, https://doi.org/10.1016/j.rse.2021.112395

Donlon, C. J, Minnett, P., Fox, N. Wimmer, W., 2015. Strategies for the Laboratory and Field Deployment of Ship-Borne Fiducial Reference Thermal Infrared Radiometers in Support of Satellite-Derived Sea Surface Temperature Climate Data Records, in Zibordi., G,. Donlon C., Parr A., (Eds.), 2015. Optical Radiometry for Oceans Climate Measurements, Vol. 47 Experimental Methods in Sciences, Elsivier, 697 pp., ISBN: 9780124170117

Donlon, C. J., 2011, The Sentinel-3 Mission Requirements Traceability Document (MRTD), version 1, EOP-SM/2184/CD-cd, available from http://download.esa.int/docs/EarthObservation/GMES_Sentinel-3_MRTD_Iss-1_Rev-0-issued-signed.pdf

Donlon, C. J., 2015b. Optimised phasing of Sentinel-3A, B, C and D to best serve the need of the Copernicus Marine Environment Monitoring Service (CMEMS), European Space Agency Technical Not, EOP-SM/2896/CD-cd, V4.1, available from the European Space Agency, Noordwijk, the Netherlands.

Donlon, C. J., K. S. Casey, I. S. Robinson, C. L. Gentemann, R. W. Reynolds, I. Barton, O. Arino, J Stark, N. Rayner, P. LeBorgne, D. Poulter, J. Vazquez-Cuervo, E. Armstrong, H. Beggs, D. Llewellyn Jones, P. J. Minnett, C. J. Merchant, R. Evans, 2009. The GODAE High Resolution Sea Surface Temperature Pilot Project (GHRSST-PP), Oceanography, Volume 22, Number 3, 34-45.

Donlon, C. J., M. Martin, J. D. Stark, J. Roberts-Jones, E. Fiedler and W. Wimmer, 2012. The Operational Sea Surface Temperature and Sea Ice analysis (OSTIA), Remote Sensing of the Environment, 116, 140-158, doi: 10.1016/j.rse.2010.10.017.

Donlon, C. J., O'Caroll, A., Smith, D., Scharroo, R., Bourg, L., Kwiatowska, E., Merchant, C., Sathyendranath, S., Labrue, S., Larnicol, G., 2016. Scientific Justification for a Tandem mission between Sentienl-3A and and Sentinel-3B during the E1 commissioning Phase, European Space Agency Technical Not, EOP-SM/3057/CD-cd, V4.2, available from the European Space Agency, Noordwijk, the Netherlands.

Donlon, C., Berruti, B., Buongiorno, A., Ferreira, M.-H., Féménias, P., Frerick, J., Goryl, P., Klein, U., Laur, H., Mavrocordatos, C., Nieke, J., Rebhan, H., Seitz, B., Stroede, J., and Sciarra, R., 2012. The Global Monitoring for Environment and Security (GMES) Sentinel-3 mission, Remote Sens. Environ., 120, 37–57, 2012.

Donlon, C., Scharroo, R., Willis, J., Leuliette, E., Bonnefond, P., Picot, N., Schrama, E., Brown, S., 2019. Sentinel-6A/B/Jason-3 Tandem Phase Configurations, JC-TN-ESA-MI-0876 V2.0, 8 July 2019, available from the European space agency, Noordwijk, the Netherlands.

Dorandeu, J., Ablain, M., and Le Traon, P.-Y., 2003. Reducing Cross- Track Geoid Gradient Errors around TOPEX/Poseidon and Jason-1 Nominal Tracks: Application to Calculation of Sea Level Anomalies, J. Atmos. Ocean. Tech., 20, 1826–1838.

Drinkwater, M.R., D.G. Long, D.S. Early, 1994. Enhanced Resolution Scatterometer Imaging of Southern Ocean Sea Ice, In Earth Observation Quarterly, 43, 4-6,.

Drinkwater, M., Francis, R., Ratier, G., & Wingham, D. (2004). The European Space Agency's Earth Explorer Mission CryoSat: Measuring variability in the cryosphere. Annals of Glaciology, 39, 313-320. doi:10.3189/172756404781814663

Du, J., J. S. Kimball and L. A. Jones, 2015. Satellite Microwave Retrieval of Total Precipitable Water Vapor and Surface Air Temperature Over Land From AMSR2, in IEEE Transactions on Geoscience and Remote Sensing, vol. 53, no. 5, pp. 2520-2531, doi: 10.1109/TGRS.2014.2361344

Dubey, A. K., Gupta, P. K., Dutta, S., and Singh, R. P., 2015. An improved methodology to estimate river stage and discharge using Jason-2 satellite data, J. Hydrol., 529, 1776–1787, https://doi.org/10.1016/j.jhydrol.2015.08.009.

Dubois, P. and Chapron, B. 2018. Characterization of the ocean waves signature to assess the Sea State Bias in wide-swath interferometric altimetry. In Proceedings of the IGARSS 2018–2018 IEEE International Geoscience and Remote Sensing Symposium, Valencia, Spain, 22–27 July 2018; IEEE: Piscataway, NJ, USA, 2018 pp. 3789–3792.

Ducet, N., Le Traon, P. Y., Reverdin G., 2000. Global high-resolution mapping of ocean circulation from TOPEX/Poseidon and ERS-1 and 2, J. Geophys. Res., 105, 9,477–19,498.

Duchossois G., P. Strobl, V. Toumazou, S. Antunes, A. Bartsch, T. Diehl, F. Dinessen, P. Eriksson, G. Garric, M-N. Houssais, M. Jindrova, J. Muñoz-Sabater, T. Nagler, O. Nordbeck, User Requirements for a Copernicus Polar Mission - Phase 1 Report, EUR 29144 EN, Publications Office of the European Union, Luxembourg (2018) ISBN 978-92-79-80961-3,doi:10.2760/22832,JRC111067 https://ec.europa.eu/jrc/en/publication/user-requirements-copernicus-polar-mission-0

Duchossois G., P. Strobl, V. Toumazou, S. Antunes, A. Bartsch, T. Diehl, F. Dinessen, P. Eriksson, G. Garric, K. Holmlund, M-N. Houssais, M. Jindrova, M. Kern, J. Muñoz-Sabater, T. Nagler, O. Nordbeck, E. de Witte, User Requirements for a Copernicus Polar Mission - Phase 2 Report EUR 29144 EN, Publications Office of the European Union, Luxembourg (2018). ISBN 978-92-79-80960-6, doi:10.2760/44170, JRC111068. https://ec.europa.eu/jrc/en/publication/user-requirements-copernicus-polar-mission

Dufau, C., Orsztynowicz, M., Dibarboure, G., Morrow, R., & Le Traon, P. Y., 2016. Mesoscale resolution capability of altimetry: Present and future. Journal of Geophysical Research: Oceans, 121(7), 4910-4927.

Durand, M., Gleason, C. J., Pavelsky, T. M., Prata de Moraes Frasson, R., Turmon, M., David, C. H., et al., 2023. A framework for estimating global river discharge from the Surface Water and Ocean Topography satellite mission. Water Resources Research, 59, e2021WR031614. https://doi.org/10.1029/2021WR031614

EC, 2019. European Commission. Directorate General for Maritime Affairs and Fisheries and the Joint Research Centre. The EU Blue Economy Report 2019. Publ. Off. Eur. Union 2019

Egido, A., Smith, W. H. F., 2019. Pulse-to-pulse correlation effects in high PRF Low-Resolution Mode altimeters. IEEE Trans. Geosci. Remote Sens. 2019, 57, 2610–2617.

Emery, C. M., Paris, A., Biancamaria, S., Boone, A., Calmant, S., Garambois, P.-A., and Santos da Silva, J., 2018. Large-scale hydrological model river storage and discharge correction using a satellite altimetry-based discharge product, Hydrol. Earth Syst. Sci., 22, 2135–2162, https://doi.org/10.5194/hess-22-2135-2018, 2018.

Eppler, D., L. Farmer, A. Lohanick, M. Anderson, D. Cavalieri, J. Comiso, P. Glorsen, C. Garrity, T.Grenfell, M. Hallikainen, et al., 1992. Passive microwave signatures of sea ice. In Microwave Remote Sensing of Sea Ice, in Carsey, F.D., Ed.; American Geophysical Union: Washington, DC, USA, 1992; doi:10.1029/GM068p0047.

ESA, 2012. Sentinel-2: ESA's Optical High-Resolution Mission for GMES Operational Services, (ESA SP-1322/2 March 2012) available form ESA/ESTEC, Noordwijk, The Netherlands)

ESA, 2018. Jason CS/Sentinel 6 analysis of on-board RMC processing, JC-TN-ESA-MI-0769, v1 rev. 2 August 2018, available form European Space Agency, Noordwijk, the Netherlands.

ESA, 2019, Earth Explorer 9 candidate Mission SKIM Report for Mission Selection, ESA-EOPSM-SKIM-RP-3550, version 1.0, 21 June 2019, available from https://www.skim-ee9.org/Docs-refs

ESA, 2025, "" Copernicus Space Component (CSC) Long Term Scenario, ESA/PB-EO(2025)30 Paris, 14 May 2025.

ESA, 2020. Sentinel-6 Mission Performance Working Group cal/val concept Plan,JC-TN-ESA-MI-0500 available from ESA/ESTEC Noordwijk, the Netherlands.

ESA, 2021, ESA-WorldCover, 2020. Worldwide Land Cover Mapping: VITO NV.2021, https://esa-worldcover.org/en

Escudier, P, Fellous J-L., 2008. The Next 15 Years of Satellite Altimetry Ocean Surface Topography Constellation, User Requirements Document, CEOS, available from http://ceos.org/observations/documents/Satellite_Altimetry_Report_2009-10.pdf

ESSB-HB-E-003 working group, 2011. ESA Pointing error engineering handbook, ESSB-HB-E-003, version 1, 19th July 2011.

EU, 2014. Regulation (EU) No 377/2014 of the European Parliament and of the Council of 3 April 2014 establishing the Copernicus Programme and repealing Regulation (EU) No 911/2010 Text with EEA relevance available from https://eur-lex.europa.eu/legal-content/EN/TXT/?uri=CELEX%3A32014R0377

EUMETSAT, 2017. Sentinel-3 SRAL Marine User Handbook, EUM/OPS-SEN3/MAN/17/920901, v1A, 12 December 2017.

EUMETSAT, 2018. Sentinel-6 End User Requirements Document (EURD), version 3E, EUM/LEO JASCS/REQ/12/0013.

EUMETSAT, 2019. Sentinel-6 System Requirements Document (SRD) v3C, EUM/LEO-JASCS/SPE/12/0039v3F, available from EUMETSAR, Darmstadt, Germany.

Farrar, S., D. Draper, L. Jones and F. Alquaied, 2016. Advantages of Calibration Attitude Manoeuvres for spaceborne microwave radiometer missions, 2016 14th Specialist Meeting on Microwave Radiometry and Remote Sensing of the Environment (MicroRad), Espoo, 2016, pp. 186-190, doi: 10.1109/MICRORAD.2016.7530531.

Fekete, B. M., U. Looser, A. Piertoniro, R. D. Robarts, 2012. Rationale for monitoring discharge on the ground, J. Hydrometeorology, 13, 1977-1986.

Fernandes, M. J., Lázaro, C., Ablain, M., Pires, N., 2015. Improved wet path delay PDs for all ESA and reference altimetric missions, Remote Sensing of Environment, 169, 50-74, https://doi.org/10.1016/j.rse.2015.07.023.

Fernandes, M.J., Lazaro, C., Nunes, A.L., Scharroo, R., 2014. Atmospheric corrections for altimetry studies over inland water. Remote Sens. 6 (6), 4952–4997. https://doi.org/ 10.3390/rs6064952.

Fernandez, J., Escobar D., Ayuga F., et al., 2015. Copernicus POD service operations. In: Proceedings of the Sentinel-3 for Science Workshop, 2-5 June 2015, Venice, Italy, (ESA SP-734). ESA Communications, ESTEC, Noordwijk, The Netherlands.

Fernandez, M., 2019. Copernicus POD Regular Service Review Jun - Sep 2019 Copernicus Sentinel-1, -2 And -3 Precise Orbit Determination Service (SENTINELSPOD) GMV-GMESPOD-RSR-0015

Fernandez, M. J., C. Lazaro and t. Vireira, 2021. On the role of the troposphere in satellite Altimetry, Rem. Sens. Env., 252, https://www.sciencedirect.com/science/article/pii/S0034425720305228

Finsen, F., Milzow, C., Smith, R., Berry, P., and Bauer-Gottwein, P., 2014. Using radar altimetry to update a large-scale hydrological model of the Brahmaputra river basin Flemming Finsen, Christian Milzow, Richard Smith, Philippa Berry, Hydrol. Res., 45, 148–164, https://doi.org/10.2166/nh.2013.191

Fowler, C., W. Emery, and M. Tschudi, 2013. Polar Pathfinder Daily 25 km EASE-Grid Sea Ice Motion Vectors. Version 2. (daily and mean gridded field), NASA DAAC at the Natl. Snow and Ice Data Cent., Boulder, Colo., USA.

Francis, C. R, 1984. The ERS-1 Radar Altimeter: an overview, in SA ERS-1 Radar Altimeter Data Prod. p 9-16 (SEE N85-12419 03-43), available from the European Space Agency, Noordwijk, the Netherlands.

Francis, C. R, 2002. Design of the CryoSat system, IEEE International Geoscience and Remote Sensing Symposium, Toronto, Ontario, Canada, 2002, pp. 1759-1761 vol.3, doi: 10.1109/IGARSS.2002.1026245.

Francis, J. A. 2017. Why Are Arctic Linkages to Extreme Weather Still up in the Air?, Bulletin of the American Meteorological Society, 98(12), 2551-2557. Retrieved Mar 9, 2021, from https://journals.ametsoc.org/view/journals/bams/98/12/bams-d-17-0006.1.xml

Frappart, F., Papa, F., Famiglietti, J. S., Prigent, C., Rossow, W. B., and Seyler, F. 2008. Interannual variations of river water storage from a multiple satellite approach: A case study for the Rio Negro River basin, J. Geophys. Res., 113, D21104, doi:10.1029/2007JD009438.

Frery M-L, Siméon M, Goldstein C, Féménias P, Borde F, Houpert A, Olea Garcia A. 2020. Sentinel-3 Microwave Radiometers: Instrument Description, Calibration and Geophysical Products Performances. Remote Sensing. 2020; 12(16):2590. https://doi.org/10.3390/rs12162590

Frew, N. Glover, M., Bock, D. M., McCue, S. J., 2007. A new approach to estimation of global air-sea gas transfer velocity fields using dual-frequency altimeter backscatter, J. Geophys. Res., 112, C11003, doi:10.1029/2006JC003819

Fu, L.-L., Christensen, E. J., Yamarone, C. A., Lefebvre, M., Ménard, Y., Dorrer, M., and Escudier, P., 1994. TOPEX/POSEIDON mission overview, J. Geophys. Res., 99(C12), 24369– 24381, doi:10.1029/94JC01761.

Fu, L., Haines, B. J., 2013. The challenges in long-term altimetry calibration for addressing the problem of global sea level change, Adv. Space. Res., 51, 1284-1300, 2013.

Gao Q, Makhoul E, Escorihuela MJ, Zribi M, Segui PQ, Garcia P, Roca M, 2019. Analysis of Retrackers' Performances and Water Level Retrieval over the Ebro River Basin Using Sentinel-3. Remote Sensing, 11(6), 718, https://doi.org/10.3390/rs11060718

Garbe, J., Albrecht, T., Levermann, A. et al. 2020. The hysteresis of the Antarctic Ice Sheet. Nature 585, 538–544. https://doi.org/10.1038/s41586-020-2727-5

Gaspar, P., Ogor, F., Le Traon, P.Y., Zanife, O.Z., 1994. Estimating the sea state bias of the TOPEX and POSEIDON altimeters from crossover differences. J. Geophys. Res. Oceans 99 (C12), 24981–24994.

GCOS, 2003, The Global Observing System for Climate: Climate Monitoring Principles, available from https://gcos.wmo.int/en/essential-climate-variables/about/gcos-monitoring-principles

GCOS, 2016. The Global Observing System for Climate: Implementation Needs, GCOS-200: available from https://library.wmo.int/opac/doc_num.php?explnum_id=3417

GCOS, 2011. Systematic observation requirements for satellite-based data products for climate, 2011 Update. Supplemental details to the satellite-based component of the "Implementation Plan for the Global Observing System for Climate in Support of the UNFCCC (2010 Update)" , United Nations Environment Programme , International Council For Science, December 2011 GCOS – 154

Gemmrich, J., B. Thomas and R. Bouchard, 2011. Observational changes and trends in northeast Pacific wave records., Geophysical Research Letters 38(22).

Geraldini, S.; Bruschi, A.; Bellotti, G.; Taramelli, A. 2021. User Needs Analysis for the Definition of Operational Coastal Services. Water, 13, 92. https://doi.org/10.3390/w13010092

Gilbert, S., 1986, The Thames Barrier. Thomas Telford Ltd. 30 June 1986. 216 pages. ISBN 0-727-70249-1.

Girard-Ardhuin, F.; Ezraty, R., 2012. Enhanced Arctic Sea Ice Drift Estimation Merging Radiometer and Scatterometer Data. IEEE Trans. Geosci. Remote Sens., 50, 2639–2648.

Goddijn-Murphy, L., Woolf, D.K., Chapron, B., Queffeulou, P., 2013. Improvements to estimating the air–sea gas transfer velocity by using dual-frequency, altimeter backscatter, Remote Sensing of Environment, 139, 1-5, https://doi.org/10.1016/j.rse.2013.07.026.

Gommenginger, C. P., B. Chapron, A. Hogg, C. Buckingham, B. Fox-Kemper, L. Eriksson, F. Soulat, M.-H. Rio, C. Ubelmann, F. Ocampo-Torres, B. Buongiorno Nardelli, D. Griffin, P. Lopez-Dekker, P. Knudsen, O. Andersen, L. Stenseng, N. Stapleton, W. Perrie, N. Violante-Carvalho, J. Schulz-Stellenfleth, D. Woolf, J. Isern-Fontanet, F. Ardhuin, P. Klein, A. Mouche, A. Pascual, X. Capet, D. Hauser, A. Stoffelen, R. Morrow, L. Aouf, O. Breivik, L.-L. Fu, J. Johannessen, Y. Aksenov, L. M. Bricheno, J. Hirschi, A. C. H. Martin, A. P. Martin, G. Nurser, J. Polton, J. Wolf, H. Johnsen, A. Soloviev, G. Jacobs, F. Collard, S. Groom, V. Kudryavstev , J. Wilkin, V. Navarro, A. Babanin, M.

Martin, J. Siddorn, A. Saulter, T. Rippeth, B. Emery, N. Maximenko, R. Romeiser, H. Graber, A. Alvera Azcarate, C. Hughes, D. Vandemark, J. da Silva, P.-J. van Leeuwen, A. Naveira-Gabarato, J. Gemmrich, A. Mahadevan, J. Marquez, Y. Munro, S. Doody and G. Burbidge, 2019. Developing new spaceborne observations of submesoscale ocean dynamics and small scale atmosphere-ocean processes in coastal, shelf and polar seas., OceanObs'2019, Frontiers in Marine Science 6(457): 1.

Gommenginger, C. P., Martin-Puig, C., Amarouche, L., and Raney, K., 2013. SAR Mode Error Budget Study: Review of State of Knowledge of SAR Altimetry over Ocean, EUMETSAT Ref. EUM/RSP/REP/14/749304, version 2.2, Darmstadt, Germany, 2013.

Gommenginger, C. P., Martin-Puig, C., Dinardo, S., Cotton, P. D., and Benveniste, J., 2012. Improved altimetric performance of CryoSat-2 SAR mode over the open ocean and the coastal zone, Presented at the European Geosciences Union General Assembly, Vienna, Austria, 22–27 April 2012, 2012.

Gommenginger, C. and M. Srokos,

Gommenginger, C. P., Srokosz, M. A., Challenor, P. G., and Cotton, P. D., 2003. Measuring ocean wave period with satellite altimeters: A simple empirical model, Geophys. Res. Lett., 30, 2150, doi:10.1029/2003GL017743, 22.

Gommenginger, C., Martin-Puig, C., A., Laiba Raney, R. K., 2013. Review of state of knowledge for SAR altimetry over ocean. Report of the EUMETSAT JASON-CS SAR mode error budget study (EUMETSAT Reference, EUM/RSP/REP/14/749304, Version 2.2) Southampton, GB. National Oceanography Centre 57pp.

Greenwald, T. J., Bennartz, R., Lebsock, M., and Teixeira, J., 2018. An uncertainty data set for passive microwave satellite observations of warm cloud liquid water path. Journal of Geophysical Research: Atmospheres, 123(7), 3668-3687.

Gregory, W., Lawrence, I. R., and Tsamados, M.: A Bayesian approach towards daily pan-Arctic sea ice freeboard estimates from combined CryoSat-2 and Sentinel-3 satellite observations, The Cryosphere, 15, 2857–2871, https://doi.org/10.5194/tc-15-2857-2021, 2021.

Grenfell, T. C., Barber, D. G., Fung, A. K., Gow, A. J., Jezek, K. C., Knapp, E. J., Nghiem, S. V., Onstott, R. G., Perovich, D. K., Roesler, C. S., Swift, C. T., and Tanis, F., 1998. Evolution of electromagnetic signatures of sea ice from initial formation to the establishment of thick first year ice, IEEE T. Geosci. Remote, 36, 1642–1654, 1998.

Grenfell, T. C., Cavalieri, D. J., Comiso, J. C., Drinkwater, M. R., Onstott, R. G., Rubinstein, I., Steffen, K., and Winebrenner, D. P., 1992. Considerations for microwave remote sensing of thin sea ice, in: Microwave Remote Sensing of Sea Ice, edited by: Carsey, F. D., American Geophysical Union, Washington, D.C., doi:10.1029/GM068p0291.

Gross, R., Beutler, G., Plag, H.-P., 2009. Integrated scientific and societal user requirements and functional specifications for the GCOS. In: Plag, H.-P., Pearlman, M. (Eds.), Global Geodetic Observing System: Meeting the Requirements of a Global Society on a Changing Planet in 2020. Springer.

Guerreiro, K., Fleury, S., Zakharova, E., Kouraev, A., Rémy, F., and Maisongrande, P., 2017. Comparison of CryoSat-2 and ENVISAT radar freeboard over Arctic sea ice: toward an improved Envisat freeboard retrieval, The Cryosphere, 11, 2059-2073, https://doi.org/10.5194/tc-11-2059-2017, 2017.

Guerreiro, K., S. Fleury, E. Zakharova, F. Rémy and A. Kouraev, 2016. Potential for estimation of snow depth on Arctic sea ice from CryoSat-2 and SARAL/AltiKa missions, Remote Sensing of Environment 186 (2016) 339–349

Haines, B., Desai, S., Born, G., 2010. The Harvest Experiment: calibration of the climate data record from TOPEX/Poseidon, Jason-1 and the Ocean Surface Topography Mission", Mar. Geod., 33 (Suppl. 1), pp. 91–113http://dx.doi.org/10.1080/01490419.2010.491028, 2010.

Haines, B., Desai, S.D., Kubitschek, D., Leben, R.R., 2020. A brief history of the harvest experiment: 1989–2019. Advances in Space Research URL: http://www.sciencedirect.com/science/article/pii/S0273117720305718, doi: 10.1016/j.asr.2020.08.013

Haliki, M. and T. Niedzielski, 2022, The Accuracy of the Sentinel-3A altimeter over Polish rivers, J. Hydrology, 606, 12,735, https://doi.org/10.1016/j.jhydrol.2021.127355

Halimi, A. Mailhes, C., Tourneret, J.-Y., Thibaut, P., and Boy, F., 2014. A semi-analytical model for delay/Doppler altimetry and its estimation algorithm, IEEE Trans. Geosci. Rem. Sens., 52, 4248–4258, https://doi.org/10.1109/TGRS.2013.2280595, 2014.

Halimi, A., C. Mailhes, J. Tourneret, F. Boy and T. Moreau, 2015. Including Antenna Mispointing in a Semi-Analytical Model for Delay/Doppler Altimetry, in IEEE Transactions on Geoscience and Remote Sensing, vol. 53, no. 2, pp. 598-608, Feb. 2015, doi: 10.1109/TGRS.2014.2326177.

Hamlington, B. D., Frederikse, T., Nerem, R. S., Fasullo, J. T., Adhikari, S., 2020. Investigating the acceleration of regional sea level rise during the satellite altimeter era. Geophysical Research Letters, 47, e2019GL086528. https://doi.org/10.1029/2019GL086528

Hanafin, J. A., and Coauthors, 2012. Phenomenal Sea States and Swell from a North Atlantic Storm in February 2011: A Comprehensive Analysis. Bull. Amer. Meteor. Soc., 93, 1825–1832, https://doi.org/10.1175/BAMS-D-11-00128.1.

Hanjsek, I., G. Parrella, H. Rott, T. Nagler, C. Derksen and J. Lemmetyinen, 2017. Identification of needs and requirements for a space mission on snow mass. Technical Note 1, v1.2. ESTEC Contract No. 4000118310/16/NL/FF/gp.

Hart-Davis, M. G., Andersen, O. B., Ray, R. D., Zaron, E. D., Schwatke, C., Arildsen, R. L., et al. (2024). Tides in complex coastal regions: Early case studies from wide-swath SWOT measurements. *Geophysical Research Letters*, 51(20), e2024GL109983. https://doi.org/10.1029/2024GL109983

Hasselmann, K.; Raney, R.K.; Plant, W.J.; Alpers, W.; Shuchman, R.A.; Lyzenga, D.R.; Rufenach, C.L. Tucker, M.J. 1985. Theory of synthetic aperture radar ocean imaging: A MARSEN view. J. Geophys. Res. Oceans 90, 4659–4686.

Hauschild, A. and O. Montenbruck, 2021, Precise real-time navigation of LEO satellites using GNSS broadcast ephemerides, NAVIGATION, Journal of the Institute of Navigation, vol. 68, no. 2, pp. 419–432.

Hauser, D., C. Tourain, L. Hermozo, D. Alraddawi, L. Aouf, B. Chapron, A. Dalphinet, L. Delaye, M. Dalila and E. Dormy, 2020. New Observations From the SWIM Radar On-Board CFOSAT: Instrument Validation and Ocean Wave Measurement Assessment EEE Transactions on Geoscience and Remote Sensing, vol. 59, no. 1, pp. 5-26, Jan. 2021, doi: 10.1109/TGRS.2020.2994372.

Hayne, G. S., 1980. Radar altimeter mean return waveforms from near-normal-incidence ocean surface scattering. IEEE Trans. Antennas Propag., AP-28, 687–692.

Healy, B, Polichtchouk, I., Horányi, A., 2020. Monthly and zonally averaged zonal wind information in the equatorial stratosphere provided by GNSS radio occultation. Q J R Meteorol Soc. 2020; 1– 10. https://doi.org/10.1002/qj.3870

Hein, G. W, Pany, T., 2002. Architecture and Signal Design of the European Satellite Navigation System Galileo – Status Dec. 2002, Journal of Global Positioning Systems, Vol. 1, No. 2: 73-84

Helm, V., Humbert, A., and Miller, H.: Elevation and elevation change of Greenland and Antarctica derived from CryoSat-2, The Cryosphere, 8, 1539–1559, https://doi.org/10.5194/tc-8-1539-2014, 2014.

Hernández-Carrasco, I., López, C., Hernández-García, E., and Turiel, A., 2011. How reliable are finite-size lyapunov exponents for the assessment of ocean dynamics? Ocean Model. 36, 208–218. doi: 10.1016/j.ocemod.2010.12.006

Heygster, G., Huntemann, M., Ivanova, N., Saldo, R., and Pedersen, L. T., 2014. Response of passive microwave sea ice concentration algorithms to thin ice, Proceedings Geoscience and Remote

Sensing Symposium (IGARSS), 2014 IEEE International, 13–18 July, Quebec City, QC, 3618–3621, doi:10.1109/IGARSS.2014.6947266.

Hilburn, K. A., Meissner, T., Wentz, F. J., and Brown, S. T., 2016. Ocean vector winds from WindSat two-look polarimetric radiances. IEEE Trans. Geosci. Remote Sens. 54, 918–931. doi: 10.1109/TGRS.2015.2469633

Hilburton, H and F. J. Wentz, 2008. Inter-calibrated Passive Microwave Rain Products from the Unified Microwave Ocean Retrieval Algorithm (UMORA), J. Applied Met. And Climatology, 778-794, DOI: 10.1175/2007JAMC1635.1

Ho, S.-P., Anthes, R.A., Ao, C.O., Healy, S.B., Horanyi, A., Hunt, D., Mannucci, A.J., Pedatella, N., Randel, W.J., Simmons, A., Steiner, A., Xie, F., Yue, X. and Zeng, Z., 2019. The COSMIC/FORMOSAT-3 radio occultation mission after 12 years: accomplishments, remaining challenges, and potential impacts of COSMIC-2. Bulletin of the American Meteorological Society. https://doi.org/10.1175/BAMS-D-18-0290.1

Hollmann, R., and Co-authors, 2013. The ESA Climate Change Initiative: Satellite Data Records for Essential Climate Variables, Bull. Amer. Meteor. Soc., 94, 1541–1552 doi: http://dx.doi.org/10.1175/BAMS-D-11-00254.1, 2013.

Horwath, M., Gutknecht, B. D., Cazenave, A., Palanisamy, H. K., Marti, F., Marzeion, B., Paul, F., Le Bris, R., Hogg, A. E., Otosaka, I., Shepherd, A., Döll, P., Cáceres, D., Müller Schmied, H., Johannessen, J. A., Nilsen, J. E. Ø., Raj, R. P., Forsberg, R., Sandberg Sørensen, L., Barletta, V. R., Simonsen, S. B., Knudsen, P., Andersen, O. B., Ranndal, H., Rose, S. K., Merchant, C. J., Macintosh, C. R., von Schuckmann, K., Novotny, K., Groh, A., Restano, M., and Benveniste, J.: Global sea-level budget and ocean-mass budget, with a focus on advanced data products and uncertainty characterisation, Earth Syst. Sci. Data, 14, 411–447, https://doi.org/10.5194/essd-14-411-2022, 2022.

Hossan, A.; Jones, W.L. Ku- and Ka-Band Ocean Surface Radar Backscatter Model Functions at Low-Incidence Angles Using Full-Swath GPM DPR Data. Remote Sens. 2021, 13, 1569. https://doi.org/10.3390/rs13081569.

Huang, Y., S. Huang and J. Sun, 2018. Experiments on navigating resistance of an icebreaker in snow covered level ice, Cold Regions Science and Technology, v152, 1-14, https://doi.org/10.1016/j.coldregions.2018.04.007.

Huess, V., Andersen, O. B., 2001. Seasonal variation in the main tidal constituent from altimetry. Geophys. Res. Lett., 28, 567–570, https://doi.org/10.1029/2000GL011921.

Huntemann, M., Heygster, G., Kaleschke, L., Krumpen, T., Mäkynen, M., and Drusch, M., 2014. Empirical sea ice thickness retrieval during the freeze-up period from SMOS high incident angle observations, The Cryosphere, 8, 439-451, https://doi.org/10.5194/tc-8-439-2014.

IPCC, 2018. Global Warming of 1.5°C, SR15 available from http://www.ipcc.ch/report/sr15/

IPCC, 2014. Climate Change 2014: Synthesis Report. Contribution of Working Groups I, II and III to the Fifth Assessment Report of the Intergovernmental Panel on Climate Change [Core Writing Team, R.K. Pachauri and L.A. Meyer (eds.)], 2014, IPCC, Geneva, Switzerland, 151 pp.

IPCC, 2019. IPCC Special Report on the Ocean and Cryosphere in a Changing Climate [H.-O. Pörtner, D.C. Roberts, V. Masson-Delmotte, P. Zhai, M. Tignor, E. Poloczanska, K. Mintenbeck, A. Alegría, M. Nicolai, A. Okem, J. Petzold, B. Rama, N.M. Weyer (eds.), available online at https://www.ipcc.ch/srocc/download-report/

ITU, 2016, Radio Regulations, Edition 2016, available from https://www.itu.int

Ivanova, N., Johannessen, O. M., Pedersen, L. T., and Tonboe, R. T., 2014. Retrieval of Arctic sea ice parameters by satellite passive microwave sensors: a comparison of eleven sea ice algorithms, IEEE T. Geosci. Remote, 52, 7233–7246, 2014.

Ivanova, N., Pedersen, L. T., Tonboe, R. T., Kern, S., Heygster, G., Lavergne, T., Sørensen, A., Saldo, R., Dybkjær, G., Brucker, L., and Shokr, M., 2015. Inter-comparison and evaluation of sea ice

algorithms: towards further identification of challenges and optimal approach using passive microwave observations, The Cryosphere, 9, 1797-1817, https://doi.org/10.5194/tc-9-1797-2015.

Jacob, M., Ament, F., Gutleben, M., Konow, H., Mech, M., Wirth, M., and Crewell, S.: Investigating the liquid water path over the tropical Atlantic with synergistic airborne measurements, 2019. Atmos. Meas. Tech., 12, 3237–3254, https://doi.org/10.5194/amt-12-3237-2019.

Jayles, C., Berthias, J.-P., Laurichesse, D., Nordine, S., Cauquil, P., Tavernier G., 2002. DORIS-DIODE: two-years results of the first European Navigator, Advances in Space Research, Volume 30, Issue 2, 301-306, doi: 10.1016/S0273-1177(02)00299-5

Jayles, C., J.P. Chauveau, F. Didelot, A. Auriol and C. Tourain, 2016. DORIS System and Integrity Survey, Adv. In Space Research 58 (2016) 2691-2706, http://dx.doi.org/10.1016/j.asr.2016.05.032

Jayles, C., Nhun-Fat, B., Tourain, C., 2006. DORIS: system description and control of the signal integrity, J Geod, 80: 457–472, DOI 10.1007/s00190-006-0046-8

JCGM, 2008, Evaluation of measurement data — Guide to the expression of uncertainty in measurement JCGM 100:2008, GUM 1995 with minor corrections, First edition September 2008, available from http://www.bipm.org/utils/common/documents/jcgm/JCGM_100_2008_E.pdf

JCOMM, 2010, Storm Surge User Guide, Version 4B, available from the JCOMM Secretariat, http://www.jcomm.info/

Jiang, H., 2020. Evaluation of altimeter undersampling in estimating global wind and wave climate using virtual observation. Remote Sensing of Environment 245: 111840.

Jiang, L., K. Nielsen, S. Dinardo, O. B. Andersen, P. Bauer-Gottwein, 2020, Evaluation of Sentinel-3 SRAL SAR altimetry over Chinese rivers, Remote Sensing of Environment, 237, 111546, https://doi.org/10.1016/j.rse.2019.111546.

Jiang, L., Y. Zhao, K. Nielsen, O. Andersen, P. Bauer-Gottwein, 2023. Near real-time altimetry for river monitoring-a global assessment of Sentinel-3. Environmental Research Letters, 18(7), 074017, doi:10.1088/1748-9326/acdd16

Johannessen, J. J., G. Balmino, C. Le Provost, R. Rummel, R. Sabadini, H. Sünkel, C. C. Tscherning, P. Visser, P. Woodworth, C. W. Hughes, P. LeGrand, N. Sneeuw, F. Perosanz, M. Aguirre-Martinez, H. Rebhan, M. R. Drinkwater, 2003. The European Gravity Field and Steady-State Ocean Circulation Explorer Satellite Mission: Impact in Geophysics, Surveys in Geophysics, Vol. 24, 2003, pp. 339-386

Johannessen, J. A., B. Chapron, F. Collard, M. . -H. Rio, G. Quartly and C. Donlon, 2018, Advances in Surface Current Observations From Space: The Globcurrent Case, IGARSS 2018 - 2018 IEEE International Geoscience and Remote Sensing Symposium, 2018, pp. 153-156, doi: 10.1109/IGARSS.2018.8519451.

Johnson, J. T., et al., 2020, Real-Time Detection and Filtering of Radio Frequency Interference Onboard a Spaceborne Microwave Radiometer: The CubeRRT Mission," in IEEE Journal of Selected Topics in Applied Earth Observations and Remote Sensing, vol. 13, pp. 1610-1624, doi: 10.1109/JSTARS.2020.2978016.

Johnston, G., Riddell, A., Hausler, G., 2017. The international GNSS service. In: Teunissen, Peter, J.G., Montenbruck, O. (Eds.), Springer Handbook of Global Navigation Satellite Systems, first ed. Springer International Publishing, Cham, Switzerland, pp. 967–982, doi: 10.1007/978-3-319-42928-1.

Jorissen, R, Litjens J. and A. Mendez Lorenzo, 2000, Flooding risk in coastal areas. Risks, safety levels and probabilistic techniques in five countries along the North Sea coast. The Hague, Ministry of Transport, Public Works and Water Management, 61pp.

JPL Internal Document (2018). SWOT calibration/validation plan. JPL D-75724, available online at: https://swot.jpl.nasa.gov/system/documents/files/2244_2244_D-75724_SWOT_Cal_Val_Plan_Initial_20180129u.pdf (last accessed 08 April 2021)

Kaleschke, L., Maaß, N., Haas, C., Hendricks, S., Heygster, G., and Tonboe, R. T., 2010. A sea-ice thickness retrieval model for 1.4 GHz radiometry and application to airborne measurements over low salinity sea-ice, The Cryosphere, 4, 583–592, doi:10.5194/tc-4- 583-2010, 2010.

Kaleschke, L., X. Tian-Kunze, N. Maaß, A. Beitsch, A. Wernecke, M. Miernecki, Gerd Müller, B. H. Fock, A. M.U. Gierisch, K. H. Schlünzen, T. Pohlmann, M. Dobrynin, S. Hendricks, J. Asseng, R. Gerdes, P. Jochmann, N. Reimer, J. Holfort, C. Melsheimer, G. Heygster, G. Spreen, S. Gerland, J. King, N. Skou, S. Schmidl Søbjærg, C. Haas, F. Richter, and T. Casal, 2016. SMOS sea ice product: Operational application and validation in the Barents Sea marginal ice zone, Rem. Sen. of Env., 180, 264-273, https://doi.org/10.1016/j.rse.2016.03.009.

Karvonen, J., 2017., Baltic Sea Ice Concentration Estimation Using SENTINEL-1 SAR and AMSR2 Microwave Radiometer Data, in IEEE Transactions on Geoscience and Remote Sensing, vol. 55, no. 5, pp. 2871-2883.
doi: 10.1109/TGRS.2017.2655567

Kazumori, M., 2012. A retrieval algorithm of atmospheric water vapor and cloud liquid water for AMSR-E, Eur. J. Remote Sens., vol. 45 pp. 63–74, doi: 10.5721/EuJRS20124507.

Keihm, S. J., Janssen, M. A., Ruf, C. S., 1995. TOPEX/POSEIDON microwave radiometer (TMR): III. Wet troposphere range correction algorithm and pre-launch error budget, IEEE Trans. Geosci. Remote Sensing, 33, 147-161.

Kellogg W.W., 1975. Climate Change and the Influence of Man's Activities on the Global Environment. In: Singer S.F. (eds) The Changing Global Environment. Springer, Dordrecht.
https://doi.org/10.1007/978-94-010-1729-9_2

Kern, M., Cullen, R., Berruti, B., Bouffard, J., Casal, T., Drinkwater, M. R., Gabriele, A., Lecuyot, A., Ludwig, M., Midthassel, R., Navas Traver, I., Parrinello, T., Ressler, G., Andersson, E., Martin-Puig, C., Andersen, O., Bartsch, A., Farrell, S., Fleury, S., Gascoin, S., Guillot, A., Humbert, A., Rinne, E., Shepherd, A., van den Broeke, M. R., and Yackel, J., 2020. The Copernicus Polar Ice and Snow Topography Altimeter (CRISTAL) high-priority candidate mission, The Cryosphere, 14, 2235–2251, https://doi.org/10.5194/tc-14-2235-2020.

Kern, S., Khvorostovsky, K., Skourup, H., Rinne, E., Parsakhoo, Z. S., Djepa, V., Wadhams, P., and Sandven, S., 2015. The impact of snow depth, snow density and ice density on sea ice thickness retrieval from satellite radar altimetry: results from the ESA-CCI Sea Ice ECV Project Round Robin Exercise, The Cryosphere, 9, 37–52, doi:10.5194/tc-9-37-2015.

Kern, S., Rösel, A., Pedersen, L. T., Ivanova, N., Saldo, R., and Tonboe, R. T., 2016. The impact of melt ponds on summertime microwave brightness temperatures and sea-ice concentrations, The Cryosphere, 10, 2217–2239, https://doi.org/10.5194/tc-10-2217-2016, 2016.

Kilic, L., C. Prigent, F. Aires, G. Heygster, V. Pellet, and C. Jimenez, 2020. Ice Concentration Retrieval from the Analysis of Microwaves: A New Methodology Designed for the Copernicus Imaging Microwave Radiometer. Remote Sens., 12, 1060.

Kilic, L., Prigent, C., Boutin, J., Meissner, T., English, S., & Yueh, S., 2019. Comparisons of ocean radiative transfer models with SMAP and AMSR2 observations. Journal of Geophysical Research: Oceans, 124, 7683– 7699. https://doi.org/10.1029/2019JC015493

Kilic, L., Tonboe, R. T., Prigent, C., and Heygster, G, 2018b, Estimating the snow depth, the snow-ice interface temperature, and the effective temperature of Arctic sea ice using Advanced Microwave Scanning Radiometer 2 and Ice Mass Balance buoys data, The Cryosphere Discuss., https://doi.org/10.5194/tc-2018-223, in review, 2018.

Kiliszek, D. and K. Kroszczyński, 2020. Performance of the precise point positioning method along with the development of GPS, GLONASS and Galileo systems, Measurement, 164, https://doi.org/10.1016/j.measurement.2020.108009.

Kim, YH., Min, SK., Gillett, N.P. *et al.* Observationally-constrained projections of an ice-free Arctic even under a low emission scenario. *Nat Commun* **14**, 3139 (2023). https://doi.org/10.1038/s41467-023-38511-8

Kittel, C. M. M., Jiang, L., Tøttrup, C., and Bauer-Gottwein, P. 2021. Sentinel-3 radar altimetry for river monitoring – a catchment-scale evaluation of satellite water surface elevation from Sentinel-3A and Sentinel-3B, Hydrol. Earth Syst. Sci., 25, 333–357, https://doi.org/10.5194/hess-25-333-2021, 2021.

Knaff, J. A., C. R. Sampson, and K. D. Musgrave, 2018. Statistical tropical cyclone wind radii prediction using climatology and persistence: Updates for the western North Pacific, Wea. Forecasting, doi: 10.1175/WAF-D-18-0027.1.

Kontu, A., J. Lemmetyinen, J. Pulliainen, J. Seppänen, and M. T. Hallikainen, 2014. Observation and modeling of the microwave brightness temperature of snow-covered frozen lakes and wetlands. IEEE Trans Geosci. Remote Sensing, 52(6), 3275-3288.

Kossieris, S., V. Tsiakos, G. Tsimiklis, A. Amditis, 2024. Inland Water Level Monitoring from Satellite Observations: A Scoping Review of Current Advances and Future Opportunities. Remote Sensing, 16(7), 1181, doi:10.3390/rs16071181

Kramer, H. J., 2015. FormoSat-7/COSMIC-2 (Constellation Observing System for Meteorology, Ionosphere and Climate), available at: https://directory.eoportal.org/ (last access: 24 March 2016), 2015.

Kremp, and E. Rudolph, 2010, Development of an OPerational Tide Model for the Elbe Estuary-OPTEL, Storm Surges Congress, Hamburg, Germany, 13–17 September 2010, SSC2010-60-1, available from http://meetingorganizer.copernicus.org/ssc2010/meetingprogramme

Kristensen, S. S., N. Skou, S. S. Søbjærg and J. E. Balling, "Developments of RFI Detection Algorithms and Their Application to Future European Spaceborne Systems," IGARSS 2019 - 2019 IEEE International Geoscience and Remote Sensing Symposium, 2019, pp. 4451-4454, doi: 10.1109/IGARSS.2019.8900091.

Kristensen, S. S., S. S. Søbjærg, E. Balling and N. Skou, (2022), RFI Detection and Mitigation Processor for the Copernicus Imaging Microwave Radiometer Satellite, RFI2022, 14-18th April 2022, https://events.ecmwf.int/event/258/contributions/2880/attachments/1561/2800/RFI2022_Kristensen.pdf

Kruopis, N., J. Praks, A. Arslan, H. Alasalmi, J. Koskinen and M. Hallikainen, 1999. Passive microwave measurements of snow-covered forests in EMAC'95. IEEE Trans Geosci Remote Sensing, 37, 2699-2705.

Kudryavtsev, V., Yurovskaya, M., Chapron, B., Collard, F., and Donlon, C., 2017. Sun glitter imagery of surface waves. part 1: directional spectrum retrieval and validation. J. Geophys. Res. 122, 369–1383. doi: 10.1002/2016JC012425

Kursinski, E.R., Hajj, G.A., Schofield, J.T., Linfield, R.P. and Hardy, K.R., 1997. Observing Earth's atmosphere with radio occultation measurements using the Global Positioning System. Journal of Geophysical Research, 102, 23429– 23465

Kurtz, N.T., Farrell, S.L., Studinger, M., Galin, N., Harbeck, J.P., Lindsay, R., Onana, V.D., Panzer, B., Sonntag, J.G., 2013. Sea ice thickness, freeboard, and snow depth products from Operation IceBridge airborne data. Cryosphere 7:1035–1056. http://dx.doi.org/ 10.5194/tc-7-1035-2013.

Kwok, R., G. F. Cunningham, M. Wensnahan, I. Rigor, H. J. Zwally, 2009. Thinning and volume loss of the Arctic ocean sea ice cover: 2003-2008, J. Geophys. Res. Oceans, vol. 114, 2009, Art. no. C07005. doi: 10.1029/2009JC005312.

Kwok, R., Schweiger, A., Rothrock, D. A., Pang, S. & Kottmeier, C. 1998. Sea ice motion from satellite passive microwave imagery assessed with ERS SAR and buoy motions. J. Geophys. Res. 103, 8191–8214.

Labroue, S., Gaspar, P., Dorandeu, J., Mertz, F., Tran, N., Zanife, O.Z., Femenias, P., 2006. Overview of the improvements made on the empirical determination of the sea state bias correction. Am. J. Agric. Econ. 614, 77.

Lacorata, G. , R. Corrado, F. Falcini, R. Santoleri, 2019, FSLE analysis and validation of Lagrangian simulations based on satellite-derived GlobCurrent velocity data, Remote Sensing of Environment, 221, 136-143, https://doi.org/10.1016/j.rse.2018.11.013.

Laforge, A., S. Fleury, S. Dinardo, F. Garnier, F. Remy, J. Benveniste, J. Bouffard, J. Verley, 2020. Toward improved sea ice freeboard observation with SAR altimetry using the physical retracker SAMOSA+, Advances in Space Research, https://doi.org/10.1016/j.asr.2020.02.001.

Lamb, H.H. and Frydendahl, Knud, 1991. Historic Storms of the North Sea, British Isles and Northwest Europe, Cambridge University Press, ISBN 9780521375221

Lambin, J., Morrow, R., Fu, L.-L., Willis, J. K., Bonekamp, H., Lillibridge, J., Perbos, J., Zaouche, G., Vaze, P., Bannoura, W., Parisot, F., Thouvenot, E., Coutin-Faye, S., Lindstrom, E., and Mignogno, M., 2010. The OSTM/Jason-2 Mission, Marine Geodesy, 33, 4–25, https://doi.org/10.1080/01490419.2010.491030, 2010.

Lambin, J., Morrow, R., Fu, L.-L., Willis, J. K., LEuliette, E., Lillibridge, L. and H. Bonekamp, H., 2011. Jason-3 Mission Requirements Document, issue 1, available from CNES, Toulouse, France.

Landy, J. C., Petty, A. A., Tsamados, M., & Stroeve, J. C., 2020. Sea ice roughness overlooked as a key source of uncertainty in CryoSat-2 ice freeboard retrievals. Journal of Geophysical Research: Oceans, 125, e2019JC015820. https://doi.org/10.1029/2019JC015820

Landy, J. C.M., Tsamados and R. K. Scharien, 2019. A Facet-Based Numerical Model for Simulating SAR Altimeter Echoes From Heterogeneous Sea Ice Surfaces, in IEEE Transactions on Geoscience and Remote Sensing, vol. 57, no. 7, pp. 4164-4180, July 2019, doi: 10.1109/TGRS.2018.2889763.

Lahtinen., J. et al., (2019). Real-Time RFI Processor for Future Spaceborne Microwave Radiometers, in IEEE Journal of Selected Topics in Applied Earth Observations and Remote Sensing, vol. 12, no. 6, pp. 1658-1669, doi: 10.1109/JSTARS.2019.2910640.

Lavergne, T., 2016a. Low Resolution Sea Ice Drift Product User's Manual, Ocean & Sea Ice SAF GBL LR SID — OSI-405-c, Version 1.8 — July 2016 available from http://osisaf.met.no/docs/

Lavergne, T., 2016b. Ocean & Sea Ice SAF Algorithm Theoretical Basis Document for the OSI SAF Low Resolution Sea Ice Drift Product GBL LR SID — OSI-405-c Version 1.3 — May 2016.

Lavergne, T., R. Tonboe and L. Pendersen, 2020. CIMR Sea-Ice Concentration Algorithm Theoretical Basis Document (ATBD) v4 - January 2020, Deliverable D-60 from the CIMR Mission Requirement Consolidation study (CIMR MRC), Contract 4000125290/18/NL/AI, available from the European Space Agency, Noordwijk, the Netherlands.

Lavergne, T., Sørensen, A. M., Kern, S., Tonboe, R., Notz, D., Aaboe, S., Bell, L., Dybkjær, G., Eastwood, S., Gabarro, C., Heygster, G., Killie, M. A., Brandt Kreiner, M., Lavelle, J., Saldo, R., Sandven, S., and Pedersen, L. T., 2019. Version 2 of the EUMETSAT OSI SAF and ESA CCI sea-ice concentration climate data records, The Cryosphere, 13, 49-78, https://doi.org/10.5194/tc-13-49-2019,.

Lavergne, T.; Eastwood, S.; Teffah, Z.; Schyberg, H.; Breivik, L.A. 2010. Sea ice motion from low-resolution satellite sensors: An alternative method and its validation in the Arctic. J. Geophys. Res. Oceans, doi:10.1029/2009JC005958.

Lawrence, I. R., T. W.K. Armitage, M. C. Tsamados, J. C. Stroeve, S. Dinardo, A. L. Ridout, A. Muir, R. L. Tilling, A. Shepherd, 2021. Extending the Arctic sea ice freeboard and sea level record with the Sentinel-3 radar altimeters, Advances in Space Research, https://doi.org/10.1016/j.asr.2019.10.011

Laxon, S., Peacock, N. & Smith, D. 2003. High interannual variability of sea ice thickness in the Arctic region. Nature 425, 947–950. https://doi.org/10.1038/nature02050

Laxon, S.W.; Giles, K.A.; Ridout, A.L.; Wingham, D.J.; Willatt, R.; Cullen, R.; Kwok, R.; Schweiger, A.; Zhang, J.; Haas, C.; Hendricks, S.; Krishfield, R.; Kurtz, N.; Farrell S.; Davidson, M., 2013. CryoSat-2 estimates of Arctic sea ice thickness and volume. Geophys. Res. Lett., 40, 1-6. doi:10.1002/grl.50193.

Lázaro, C., Fernandes, M. J., Vieira, T., and Vieira, E., 2019. A coastally improved global dataset of wet tropospheric corrections for satellite altimetry, Earth Syst. Sci. Data Discuss., https://doi.org/10.5194/essd-2019-171

Le Gac, S.; Boy, F.; Blumstein, D.; Lasson, L.; Picot, N., 2019. Benefits of the Open-Loop Tracking Command (OLTC): Extending conventional nadir altimetry to inland waters monitoring. Adv. Space Res. 2019.

Le Roy, Y., Deschaux-Beaume, M., Mavrocordatos, C., Borde, F., 2009. SRAL, A radar altimeter designed to measure a wide range of surface types, Geoscience and Remote Sensing Symposium,2009 IEEE International,IGARSS 2009, DOI: 10.1109/IGARSS.2009.5417636

Le Traon P-Y, Antoine D, Bentamy A, Bonekamp H, Breivik LA, Chapron B, Corlett G, Dibarboure G, DiGiacomo P, Donlon C, Faugère Y, Font J, Girard-Ardhuin F, Gohin F, Johannessen JA, Kamachi M, Lagerloef G, Lambin J, Larnicol G, Le Borgne P, Leuliette E, Lindstrom E, Martin MJ, Maturi E, Miller L, Mingsen L, Morrow R, Reul N, Rio MH, Roquet H, Santoleri R, Wilkin J, 2015. Use of satellite observations for operational oceanography: recent achievements and future prospects. J Oper Oceanogr 8(S1):12–27

Le Traon P-Y, Reppucci A, Alvarez Fanjul E, Aouf L, Behrens A, Belmonte M, Bentamy A, Bertino L, Brando VE, Kreiner MB, Benkiran M, Carval T, Ciliberti SA, Claustre H, Clementi E, Coppini G, Cossarini G, De Alfonso Alonso-Muñoyerro M, Delamarche A, Dibarboure G, Dinessen F, Drevillon M, Drillet Y, Faugere Y, Fernández V, Fleming A, Garcia-Hermosa MI, Sotillo MG, Garric G, Gasparin F, Giordan C, Gehlen M, Gregoire ML, Guinehut S, Hamon M, Harris C, Hernandez F, Hinkler JB, Hoyer J, Karvonen J, Kay S, King R, Lavergne T, Lemieux-Dudon B, Lima L, Mao C, Martin MJ, Masina S, Melet A, Buongiorno Nardelli B, Nolan G, Pascual A, Pistoia J, Palazov A, Piolle JF, Pujol MI, Pequignet AC, Peneva E, Pérez Gómez B, Petit de la Villeon L, Pinardi N, Pisano A, Pouliquen S, Reid R, Remy E, Santoleri R, Siddorn J, She J, Staneva J, Stoffelen A, Tonani M, Vandenbulcke L, von Schuckmann K, Volpe G, Wettre C and Zacharioudaki A, 2019. From Observation to Information and Users: The Copernicus Marine Service Perspective. Front. Mar. Sci. 6:234. Doi: 10.3389/fmars.2019.00234

Le Traon, P.Y.; Nadal, F.; Ducet N. 1998. An improved mapping method of multisatellite altimeter data; J. Atmos. Oceanic Technol., 15, 522-534.

Ledley, T. S., 1991. Snow on sea ice: Competing effects in shaping climate. Journal of Geophysical Research, 96, 17,195–17,208. https://doi.org/10.1029/91JD01439.

Lee, S.-M., B.-J. Sohn, and S.-J. Kim, 2017. Differentiating between first-year and multiyear sea ice in the Arctic using microwave-retrieved ice emissivities. J. Geophys. Res. Atmos., 122, 5097-5112, doi: 10.1002/2016JD026275.

Legeais, J.-F., Ablain, M., Zawadzki, L., Zuo, H., Johannessen, J. A., Scharffenberg, M. G., Fenoglio-Marc, L., Fernandes, M. J., Andersen, O. B., Rudenko, S., Cipollini, P., Quartly, G. D., Passaro, M., Cazenave, A., and Benveniste, J. 2018. An improved and homogeneous altimeter sea level record from the ESA Climate Change Initiative, Earth Syst. Sci. Data, 10, 281–301, https://doi.org/10.5194/essd-10-281-2018.

LeGrand, P., Schrama, E. J. O., and Tournadre, J., 2003. An inverse estimate of the dynamic topography of the ocean, Geophys. Res. Lett., 30, 1062, doi:10.1029/2002GL014917, 2.

Leighton, T.G., Coles, D.G.H., Srokosz, M., White, P. R. and Woolf, D. K, 2018. Asymmetric transfer of CO2 across a broken sea surface. Sci Rep 8, 8301. https://doi.org/10.1038/s41598-018-25818-6

Lemmetyinen, J., A. Kontu, J-P. Kärnä, J. Vehviläinen, M. Takala, and J. Pulliainen, 2011. Correcting for the influence of frozen lakes in satellite microwave radiometer observations through application of a microwave emission model. Remote Sens. Environ., 115(12), 3695-3706.

Leppäranta, M. 1983. A growth model for black ice, snow ice and snow thickness in subarctic basins. Hydrology Research, 14(2), 59–70.

Leuliette, E. W., Steven Nerem, R., and Mitchum, G. T., 2004. Calibration of TOPEX/Poseidon and Jason Altimeter Data to Construct a Continuous Record of Mean Sea Level Change, Mar. Geod., 27, 79–94, doi:10.1080/01490410490465193.

Levinsen, J. F., Simonsen, S. B., Sorensen, L. S., & Forsberg, R. 2016. The impact of DEM resolution on relocating radar altimetry data over ice sheets. IEEE Journal of Selected Topics in Applied Earth Observations and Remote Sensing, 9(7), 3158–3163.

Li, L., Chen, H. and Guan, L. 2019. Retrieval of Snow Depth on Sea Ice in the Arctic Using the FengYun-3B Microwave Radiation Imager, J. Ocean Univ. China 18, 580–588 (2019). https://doi.org/10.1007/s11802-019-3873-y

Li, L., P. Gaiser, M. Albert, D. Long, and E. Twarog, 2008. WindSat passive microwave polarimetric signatures of the Greenland ice sheet, IEEE Trans. Geosci. Remote Sens., vol. 46, no. 9, pp. 2622–2631.

Li, S., H. Shen, Y. Hou, Y. He & F. Bi, 2018, Sea surface wind speed and sea state retrievals from dual-frequency altimeter and its preliminary application in global view of wind-sea and swell distributions, International Journal of Remote Sensing, 39:10, 3076-3093, DOI: 10.1080/01431161.2018.1433889

Lindsley, R. D., 2011. Fitting Tidal Constituents to Altimeter Data, Utah space grant consortium, 2011 conference available at https://digitalcommons.usu.edu/spacegrant/2011/Session3/2/

Liu, Y and P. Minnett, 2016. Sampling errors in satellite-derived infrared sea-surface temperatures Part I: Global and Regional MODIS fields, Rem. Sens. Env., 177, 48-64, http://dx.doi.org/10.1016/j.rse.2016.02.026

Liu, Y.Y., van Dijk, A.I.J.M., de Jeu, R.A.M., Canadell, J.G., McCabe, M.F., Evans, J.P., & Wang, G. 2015. Recent reversal in loss of global terrestrial biomass. Nature Clim. Change, 5, 470-474

Liu, Y.Y., van Dijk, A.I.J.M., McCabe, M.F., Evans, J.P., and de Jeu, R.A.M., 2013. Global vegetation biomass change (1988–2008) and attribution to environmental and human drivers. Global Ecology and Biogeography, 22, 692-705

Long D. G, Daum D. L., 1998. Spatial resolution enhancement of SSM/I data. IEEE Trans. Geosci. Remote Sens. Mar; 1998 36(2):407–417.

Long, C. S., Fujiwara, M., Davis, S., Mitchell, D.M. and Wright, C.J., 2017. Climatology and interannual variability of dynamic variables in multiple reanalyses evaluated by the SPARC Reanalysis Intercomparison Project (S-RIP). Atmospheric Chemistry and Physics, 17(23), 14593– 14629

Long, D. G., 2016. Optimum Image Formation for Spaceborne Microwave Radiometer Products, IEEE, Tras. Geosci. Rem. Sens., 54(5(, 2763-2779, doi:10.1109/TGRS.2015.2505677

Long, D. G., 2017. Polar Applications of Spaceborne Scatterometers, in IEEE Journal of Selected Topics in Applied Earth Observations and Remote Sensing, vol. 10, no. 5, pp. 2307-2320. doi: 10.1109/JSTARS.2016.2629418.

Lorente, P.; Sotillo, M.G.; Aouf, L.; Amo-Baladrón, A.; Barrera, E.; Dalphinet, A.; Toledano, C.; Rainaud, R.; De Alfonso, M.; Piedracoba, S.; Basañez, A.; García-Valdecasas, J.M.; Pérez-Muñuzuri, V.; Álvarez-Fanjul, E. 2018. Extreme Wave Height Events in NW Spain: A Combined Multi-Sensor and Model Approach. Remote Sens., 10, 1.

Lorell, J., Colquitt, E., and Anderle, R. J., 1982. Ionospheric correction for SEASAT altimeter height measurement, J. Geophys. Res., 87(C5), 3207– 3212, doi:10.1029/JC087iC05p03207.

Lu, J., G. Heygster and G. Spreen, 2018. Atmospheric Correction of Sea Ice Concentration Retrieval for 89 GHz AMSR-E Observations, in IEEE Journal of Selected Topics in Applied Earth Observations and Remote Sensing, vol. 11, no. 5, pp. 1442-1457. doi: 10.1109/JSTARS.2018.2805193.

Łyszkowicz, A. B., Bernatowicz, A., 2017. Current state of art of satellite altimetry. Geod. Cartogr., 66, 259–270, https://doi.org/10.1515/geocart-2017-0016.

Budyko M. I., 1969. The effect of solar radiation variations on the climate of the Earth, Tellus, 21:5, 611-619, DOI: 10.3402/tellusa.v21i5.10109

Maass, N., Kaleschke, L., Tian-Kunze, X., Tonboe, R.T., 2015. Snow thickness retrieval from L-band brightness temperatures: a model comparison. Ann. Glaciol. 56 (69), 9–17.

Madsen, K. S., Høyer, J. L., Fu, W., Donlon, C., 2015. Blending of satellite and tide gauge sea level observations and its assimilation in a storm surge model of the North Sea and Baltic Sea, J. Geophys. Res. Oceans, 120, 6405– 6418, doi:10.1002/2015JC011070.

Maekynen, M., Cheng, B., and Similae, M., 2013. On the accuracy of thin-ice thickness retrieval using MODIS thermal imagery over Arctic first-year ice, Ann. Glaciol., 62, 87–96, doi:10.3189/2013AoG62A166.

Maiwald et al., 2020. Completion of the AMR-C Instrument for Sentinel-6, in IEEE Journal of Selected Topics in Applied Earth Observations and Remote Sensing, vol. 13, pp. 1811-1818, 2020, doi: 10.1109/JSTARS.2020.2991175.

Maiwald, F. et al., 2016. Reliable and Stable Radiometers for Jason-3, in IEEE Journal of Selected Topics in Applied Earth Observations and Remote Sensing, vol. 9, no. 6, pp. 2754-2762, June 2016, doi: 10.1109/JSTARS.2016.2535281.

Marks, K. M., and W. H. F. Smith, 2021, Comparison of Stacked Sentinel-3 A&B and AltiKa Repeat Cycle Data. Earth and Space Science, 8, e2021EA001892. https://doi.org/10.1029/2021EA001892

Markus, T., D. Cavalieri, A. Gasiewski, M. Klein, J. Maslanik, D. Powell, B. Stankov, J. Stroeve and M. Sturm, 2006. Microwave Signatures of Snow on Sea Ice: Observations. IEEE Trans. Geosci. Remote Sens., 44, 3081-3090. doi:10.1109/TGRS.2006.883134

Matevosyan, H., Lluch, I., Poghosyan A., Golkar, A., 2017. A Value-Chain Analysis for the Copernicus Earth Observation Infrastructure Evolution: A Knowledgebase of Users, Needs, Services, and Products," in IEEE Geoscience and Remote Sensing Magazine, vol. 5, no. 3, pp. 19-35, Sept. 2017, doi: 10.1109/MGRS.2017.2720263.

Mätzler, C., E. Schanda, and W. Good, 1982. Towards the definition of optimum sensor specifications for microwave remote sensing of snow. IEEE Trans. Geosci. Remote Sens., GE-20, 57-66.

Maykut, G. A, 1978. Energy exchange over young sea ice in the central Arctic. Journal of Geophysical Research, 83, 3646–3658. https://doi.org/10.1029/JC083iC07p03646

McMillan M, A. Shepherd, A. Muir, J. Gaudelli, A.E. Hogg R. Cullen, 2017. Assessment of CryoSat-2 interferometric and non-interferometric SAR altimetry over ice sheets, Advances in Space Research, doi: 10.1016/j.asr.2017.11.036

McMillan M, A. Shepherd, A. Sundal, K. Briggs, A. Muir, A. Ridout, A. Hogg, and D. Wingham 2014. Increased ice losses from Antarctica detected by CryoSat-2, Geophysical Research Letters, 41, pp.3899-3905. doi: 10.1002/2014GL060111

McMillan, M., Muir, A., Shepherd, A., Roca, M., Aublanc, J., Thibaut, P., ... & Benveniste, J., 2019. Sentinel-3 Delay-Doppler altimetry over Antarctica. The Cryosphere, 13(2), 709-722.

Meier, W. N., J. S. Stewart, Y. Liu, J. Key and J. A. Miller, 2017. Operational Implementation of Sea Ice Concentration Estimates From the AMSR2 Sensor, in IEEE Journal of Selected Topics in Applied Earth Observations and Remote Sensing, vol. 10, no. 9, pp. 3904-3911. doi: 10.1109/JSTARS.2017.2693120

Meier, W.N., Hovelsrud, G.K., van Oort, B.E., Key, J.R., Kovacs, K.M., Michel, C., Haas, C., Granskrog, M.A., Gerland, S., Perovich, D.K., Makshtas, A., Reist, J.D., 2014. Arctic sea ice in transformation: A review of recent observed changes and impacts on biology and human activity. Rev. Geophys. 52 (3), 185e217.

Meissner, T. and F. J. Wentz, 2012. The emissivity of the ocean surface between 6 and 90 GHz over a large range of wind speeds and earth incidence angles," IEEE Trans. Geosci. Remote Sens., vol. 50, no. 8, pp. 3004–3026.

Meissner, T. and F. Wentz, 2002. An updated analysis of the ocean surface wind direction signal in passive microwave brightness temperatures, IEEE Trans. Geosci. Remote Sens., vol. 40, no. 6, pp. 1230–1240.

Meissner, T., L. Ricciardulli, and F.J. Wentz, 2017/ Capability of the SMAP Mission to Measure Ocean Surface Winds in Storms. Bull. Amer. Meteor. Soc., 98, 1660–1677,https://doi.org/10.1175/BAMS-D-16-0052.1

Ménard, Y., Fu, L.-L., 2001. Jason-1 Mission, Jason-1 science plan, AVISO newsletter 8, AVISO altimetry edition, Ramonville St. Agne, France, 2001.

Meredith, M. , A. Sundfjord, S. Henson, A. Meijers, E. Murphy, R. Bellerby, M. Daase, F. Cottier, M. Belchier, M. Chierici, I. Ellingsen, S. Falk-Petersen, S. Hill, P. Holland, G. Tarling, P. Trathan, J. Turner, J. Wilkinson, L. Batchellier, L. Capper, J. Oliver, 2018, The State of the Polar Oceans 2018: Making Sense of Our Changing World, United Kingdom Foreign and Commonwealth Office as part of the UK-Norway Memorandum of Understanding on Polar Research and Cultural Heritage, available from www.gov.uk/government/publications/uk-norway-memorandum-of-understanding-on-polar-research-and-cultural-heritage

Merkouriadi, I., B. Cheng, R. M. Graham, A. Rosel and M. A. Granskog, 2017. Critical role of snow on sea ice growth, J. Geophys. Res. Lett., 44, 10,479–10,485. https://doi.org/10.1002/2017GL075494

Mertikas S, Donlon, C., Féménias, P., Mavrocordatos, C., Galanakis, D., Tripolitsiotis, A., Frantzis, X., Kokolakis, C., Tziavos, I. N., Vergos, G., Guinle, T., 2018. Fifteen Years of Cal/Val Service to Reference Altimetry Missions: Calibration of Satellite Altimetry at the Permanent Facilities in Gavdos and Crete, Greece, Remote Sensing, https://www.mdpi.com/2072-4292/10/10/1557 .

Mertikas S, Tripolitsiotis A, Donlon C, Mavrocordatos C, Féménias P, Borde F, Frantzis X, Kokolakis C, Guinle T, Vergos G, Tziavos IN, Cullen R. 2020. The ESA Permanent Facility for Altimetry Calibration: Monitoring Performance of Radar Altimeters for Sentinel-3A, Sentinel-3B and Jason-3 Using Transponder and Sea-Surface Calibrations with FRM Standards. Remote Sensing. 2020; 12(16):2642. https://doi.org/10.3390/rs12162642

Mertikas S. P., Donlon, C., Cullen, R., Tripolitsiotis A., 2019. Scientific and Operational Roadmap for Fiducial Reference Measurements in Satellite Altimetry Calibration & Validation, International Association of Geodesy Symposia, Chap 61. https://doi.org/10.1007/1345_2019_61

Mertikas S.P. , C. J. Donlon, P. Femenias, C. Mavrocodatos, D. Galanakis, T. Guinle, F. Boy, A. Tripolitsiosis, V. Fantzis, I. N. Tziovos, and G. F. Vergos, 2019. Absolute Calibration of Sentinel-3A and Jason-3 Altimeters with Sea-Surface and Transponder Techniques in West Crete, Greece. In: Mertikas S., Pail R. (eds) Fiducial Reference Measurements for Altimetry. International Association of Geodesy Symposia, vol 150. Springer, Cham. https://doi.org/10.1007/1345_2019_63

Mertikas, S. P, Ioannides, R. T., Tziavos, I. N., Vergos, G. S., Hausleitner, W., Frantzis, X, Tripolitsiotis, A., Partsinevelos, P. and Andrikopoulos, D., 2010b. Statistical Models and Latest Results in the Determination of the Absolute Bias for the Radar Altimeters of Jason Satellites using the Gavdos Facility, Marine Geodesy, 33, S1, 114-149 2010b.

Mertikas, S. P., Daskalakis, A., Koutroulis, Ef., Tripolitsiotis A., Partsinevelos, P., 2011. Preparatory works for the altimeter calibration of the Sentinel-3 mission using the dedicated calibration site in Crete and Gavdos, Proc. SPIE 8175, Remote Sensing of the Ocean, Sea Ice, Coastal Waters, and Large Water Regions 2011, 81750U (October 07, 2011); doi:10.1117/12.899133;http://dx.doi.org/10.1117/12.899133, 2011.

Mertikas, S. P., et al., 2010. Statistical models and latest results in the determination of the absolute bias for the radar altimeters of Jason satellites using the Gavdos facility, Mar. Geod. (Suppl. 1), pp. 114–149http://dx.doi.org/10.1080/01490419.2010.488973.

Mertikas, S.P., Donlon, C., Femenias, P., Cullen, R., Galanakis, D., Frantzis, X., Tripolitsiotis, A., 2019. Fiducial Reference Measurements for Satellite Altimetry Calibration: The Constituents. International Association of Geodesy Symposia, Chap 56. https://doi.org/10.1007/1345_2019_56

Mertikas, S.P., Ioannides, R. T., Tziavos, I. N., Vergos, G. S., Hausleitner, W., Frantzis, X., Tripolitsiotis, A., Partsinevelos, P., Andrikopoulos, D., 2010. Statistical Models and Latest Results in the Determination of the Absolute Bias for the Radar Altimeters of Jason Satellites using the Gavdos facility, Marine Geodesy, 33: 1, 114-149, http://dx.doi.org/10.1080/01490419.2010.488973.

Meyssignac, B., Ablain, M., Guérou, A. et al. How accurate is accurate enough for measuring sea-level rise and variability. Nat. Clim. Chang. 13, 796–803 (2023). https://doi.org/10.1038/s41558-023-01735-z

Mitchum, G, 1998. Monitoring the stability of satellite altimeters with tide gauges, J. Atmos. Ocean. Tech., 15, 721-730.

Moesinger, L., Dorigo, W., Jeu, R. de, Schalie, R. van der, Scanlon, T., Teubner, I., Forkel, M., 2019. The Global Long-term Microwave Vegetation Optical Depth Climate Archive VODCA. Earth System Science Data Discussions 1-26. https://doi.org/10.5194/essd-2019-42.

Mogensen KS, Balmaseda MA, Weaver A, Martin MJ, Vidard A. 2009. NEMOVAR: A variational data assimilation system for the NEMO ocean model. ECMWF News, 120: 17–21.

Mogensen KS, Balmaseda MA, Weaver A. 2012. The NEMOVAR ocean data assimilation system as implemented in the ECMWF ocean analysis for System 4', Technical report 668. ECMWF, Reading, UK.

Montenbruck, O., Hackel, S., Wermuth, M. et al. 2021, Sentinel-6A precise orbit determination using a combined GPS/Galileo receiver. J Geod 95, 109, https://doi.org/10.1007/s00190-021-01563-z

Montenbruck, O., Kunzi, F. & Hauschild, 2022, A. Performance assessment of GNSS-based real-time navigation for the Sentinel-6 spacecraft. GPS Solut 26, 12, https://doi.org/10.1007/s10291-021-01198-9

Montenbruck, O., Steigenberger, P. & Hugentobler, U., 2015, Enhanced solar radiation pressure modeling for Galileo satellites. J Geod 89, 283–297, https://doi.org/10.1007/s00190-014-0774-0

Moreau, T., Tran, N., Aublanc, J., Tison, C., Le Gac, S., Boy, F., 2018. Impact of long ocean waves on wave height retrieval from SAR altimetry data, Advances in Space Research, 62, Issue 6, 1434-1444, https://doi.org/10.1016/j.asr.2018.06.004.

Morrow Rosemary, Fu Lee-Lueng, Ardhuin Fabrice, Benkiran Mounir, Chapron Bertrand, Cosme Emmanuel, d'Ovidio Francesco, Farrar J. Thomas, Gille Sarah T., Lapeyre Guillaume, Le Traon Pierre-Yves, Pascual Ananda, Ponte Aurélien, Qiu Bo, Rascle Nicolas, Ubelmann Clement, Wang Jinbo, Zaron Edward D., 2019. Global Observations of Fine-Scale Ocean Surface Topography With the Surface Water and Ocean Topography (SWOT) Mission, Frontiers in Marine Science, 6, 232-, DOI=10.3389/fmars.2019.00232

Morrow, R., Blurmstein, D., and Dibarboure, G., 2018. Fine-scale Altimetry and the Future SWOT Mission. New Frontiers In Operational Oceanography. Available from http://purl.flvc.org/fsu/fd/FSU_libsubv1_scholarship_submission_1536170512_b3d57dea

Mouginot, J., B. Scheuchl, and E. Rignot. 2017. MEaSUREs Antarctic Boundaries for IPY 2007-2009 from Satellite Radar, Version 2. [Indicate subset used]. Boulder, Colorado USA. NASA National Snow and Ice Data Center Distributed Active Archive Center. https://doi.org/10.5067/AXE4121732AD

MPC, 2020: Sentinel-3 Mission Performance Centre Sentinel-3 STM Annual Performance Report 2019 based on in-flight data up to and including 2018, S3MPC.CLS.APR.006, Issue 1, available from http://copernicus.eu/web/sentinel/user-guides/sentinel-3-altimetry

MPC, 2021: Sentinel-3 Mission Performance Centre Sentinel-3 STM Annual Performance Report 2020 based on in-flight data up to and including 2019, S3MPC.CLS.APR.008, Issue 1.1, available from http://copernicus.eu/web/sentinel/user-guides/sentinel-3-altimetry

Mulero-Martínez, R., J. Gómez-Enri, R. Mañanes, M. Bruno, Assessment of near-shore currents from CryoSat-2 satellite in the Gulf of Cádiz using HF radar-derived current observations. Remote Sensing of Environment. 10.1016/j.rse.2021.112310, 2021.

Mulero-Martinez, R., J Gómez-Enri, L De Oliveira Júnior, E Garel, P Relvas, R Mañanes, Spatiotemporal variability of the coastal circulation in the northern Gulf of Cadiz from Copernicus Sentinel-3A satellite radar altimetry measurements. Advances in Space Research. 10.1016/j.asr.2024.02.054, 2024.

Munk, W, 2002. Testimony of Walter Munk to the U.S Commission on Ocean Policy, San Pedro, California 18 April 2002, available from https://govinfo.library.unt.edu/oceancommission/meetings/apr18_19_02/munk_statement.pdf

Munk, W., 1966 Abyssal recipes. Deep-Sea Res., 13 (1966), pp. 707-730

Nandan, V., Geldsetzer, T., Yackel, J., Mahmud, M., Scharien, R., Howell, S., … Else, B., 2017. Effect of snow salinity on CryoSat-2 Arctic first-year sea ice freeboard measurements. Geophysical Research Letters, 44, 10,419– 10,426. https://doi.org/10.1002/2017GL074506

Naoki, K., Ukita, J., Nishio, F., Nakayama, M., Comiso, J. C., and Gasiewski, A., 2008. Thin sea ice thickness as inferred from passive microwave and in situ observations, J. Geophys. Res., 113, C02S16, doi:10.1029/2007JC004270.

Narvekar, G. Heygster, T. J. Jackson, G. Macelloni, R. Bindlish, and J. Notholt, 2010. Passive polarimetric microwave signatures observed over Antarctica, IEEE Trans. Geosci. Remote Sens., vol. 48, no. 3, pp. 1059–1075.

Narvekar, P. S., G. Heygster, and R. Tonboe, 2020. Analysis of WindSat Measured Passive Fully Polarimetric Measurements Over Arctic Sea Ice, IUP, Univ. Bremen, Bremen, Germany, Final Rep. Danish Meteorol. Inst., Tech. Rep. [Online]. Available: http://www.iup.uni-bremen.de/iuppage/psa/documents/WindSatArcticReplong.pdf

NASA, 2011. OSTM End of Prime Mission Report, NASA Headquarters, Washington, DC, USA, 2011.

Nerem, R. S., Beckley, B. D., Fasullo, J. T., Hamlington, B. D., Masters, D., & and Mitchum, G. T., 2018. Climate-change–driven accelerated sea-level rise detected in the altimeter era. Proceedings of the National Academy of Sciences, 115(9), 2022–2025, 2018.

Ngan T., F. Girard-Ardhuin, R.Ezraty, H. Feng, and P. Féménias, 2009. Defining a Sea Ice Flag for Envisat Altimetry Mission, IEEE Geoscience and Remote Sensing Letters, Vol. 6, No. 1, Jan 2009

Nielsen K., O.B. Andersen, H. Ranndal, 2020. Validation of Sentinel-3A based lake level over US and Canada. Remote Sensing, 12, 2835, doi:10.3390/rs12172835

Nouël F, Bardina J, Jayles C, Labrune Y, Truong B., 1988. DORIS: a precise satellite positioning Doppler system, Astrodynamics 1987, Soldner JK, Misra AK, Lindberg RE, Williamson W (eds), vol 65, Adv Astron Sci, American Astronautical Society, Springfield, pp 311–320

NRC, 2004. Climate Data Records from Environmental Satellites, , Committee on Climate Data Records from NOAA Operational Satellites; Board on Atmospheric Sciences and Climate; Division on Earth and Life Studies; National Research Council, 150pp, ISBN: 978-0-309-09168-8, DOI: 10.17226/10944

Olmedo, E., I. Taupier-Letage, A. Turiel, and A. Alvera-Azcárate, (2018), Improving SMOS Sea Surface Salinity in the Western Mediterranean Sea through Multivariate and Multifractal Analysis. Remote Sens., 10, 485.

Otosaka, I., Shepherd, A., & McMillan, M., 2019. Ice Sheet Elevation Change in West Antarctica From Ka-Band Satellite Radar Altimetry. Geophysical Research Letters, 46, 13135– 13143. https://doi.org/10.1029/2019GL084271

Otosaka, I. N., Shepherd, A., Ivins, E. R., Schlegel, N.-J., Amory, C., van den Broeke, M. R., Horwath, M., Joughin, I., King, M. D., Krinner, G., Nowicki, S., Payne, A. J., Rignot, E., Scambos, T., Simon, K. M., Smith, B. E., Sørensen, L. S., Velicogna, I., Whitehouse, P. L., A, G., Agosta, C., Ahlstrøm, A. P., Blazquez, A., Colgan, W., Engdahl, M. E., Fettweis, X., Forsberg, R., Gallée, H., Gardner, A., Gilbert, L., Gourmelen, N., Groh, A., Gunter, B. C., Harig, C., Helm, V., Khan, S. A., Kittel, C., Konrad, H., Langen, P. L., Lecavalier, B. S., Liang, C.-C., Loomis, B. D., McMillan, M., Melini, D., Mernild, S. H., Mottram, R., Mouginot, J., Nilsson, J., Noël, B., Pattle, M. E., Peltier, W. R., Pie, N., Roca, M., Sasgen, I., Save, H. V., Seo, K.-W., Scheuchl, B., Schrama, E. J. O., Schröder, L., Simonsen, S. B., Slater, T., Spada, G., Sutterley, T. C., Vishwakarma, B. D., van Wessem, J. M., Wiese, D., van der Wal, W., and Wouters, B.: Mass balance of the Greenland and Antarctic ice sheets from 1992 to 2020, Earth Syst. Sci. Data, 15, 1597–1616, https://doi.org/10.5194/essd-15-1597-2023, 2023.

Ovando, A., Martinez, J. M., Tomasella, J., Rodriguez, D. A., and von Randow, C., 2018. Multi-temporal flood mapping and satellite altimetry used to evaluate the flood dynamics of the Bolivian Amazon wetlands, Int. J. Appl. Earth Obs. Geoinf., 69, 27–40, https://doi.org/10.1016/j.jag.2018.02.013.

Owe, M., De Jeu, R., & Walker, J., 2001. A methodology for surface soil moisture and vegetation optical depth retrieval using the microwave polarization difference index. IEEE Transactions on Geoscience and Remote Sensing, 39, 1643-1654.

Owe, M., De Jeu, R., Holmes, T., 2008. Multisensor Historical Climatology of Satellite-Derived Global Land Surface Moisture. Journal of Geophysical Research. 113. 10.1029/2007JF000769.

Padman, L., Erofeeva, S. Y., and Fricker, H. A., 2008. Improving Antarctic tide models by assimilation of ICESat laser altimetry over ice shelves, Geophys. Res. Lett., 35, L22504, doi:10.1029/2008GL035592.

Papa, F., Crétaux, J.-F., Grippa, M., Robert, E., Trigg, M., Tshimanga, R. M., Kitambo, B., Paris, A., Carr, A., Fleischmann, A. S., de Fleury, M., Gbetkom, P. G., Calmettes, B., Calmant, S., 2023. Water Resources in Africa under Global Change: Monitoring Surface Waters from Space. Surveys in Geophysics, 44(1), 43-93, doi:10.1007/s10712-022-09700-9

Park, E., 2020. Characterizing channel-floodplain connectivity using satellite altimetry: Mechanism, hydrogeomorphic control, and sediment budget, Remote Sens. Environ., 243, 111783, https://doi.org/10.1016/j.rse.2020.111783, 2020.

Parke, M. E., Stewart, R. H., Farless, D. L., and Cartwright, D. E., 1987. On the choice of orbits for an altimetric satellite to study ocean circulation and tides, J. Geophys. Res., 92(C11), 11693– 11707, doi:10.1029/JC092iC11p11693.

Passaro, M., Cipollini, P. Vignudelli, S. Quartly, G. D., Snaith, H. M., 2014. ALES: A multi-mission adaptive subwaveform retracker for coastal and open ocean altimetry, Remote Sensing of Environment, 145, 73-189, https://doi.org/10.1016/j.rse.2014.02.008.

Paţilea, C., Heygster, G., Huntemann, M., and Spreen, G.: Combined SMAP–SMOS thin sea ice thickness retrieval, The Cryosphere, 13, 675–691, https://doi.org/10.5194/tc-13-675-2019, 2019.

Pavlis, C. E, Mertikas, S. P. and the GAVDOS Team, 2004. The GAVDOS Mean Sea Level and Altimeter Calibration Facility: Results for Jason-1, Marine Geodesy 27, 631-655.

Pearson, C., P. Moore and S. Edwards, 2020. GNSS assessment of sentinel-3A ECMWF tropospheric delays over inland waters, Advances in Space Research, 66, 2827–28

Pedersen, L. T., Saldo, R., Ivanova, N., Kern, S., Heygster, G., Tonboe, R., Huntemann, M., Ozsoy, B., Ardhuin, F., and Kaleschke, L., 2018. Reference dataset for sea ice concentration, https://doi.org/10.6084/m9.figshare.6626549.v3.

Pekel, J-F., A. Cottam, N. Gorelick, A. S. Belward, 2016, High-resolution mapping of global surface water and its long-term changes. Nature 540, 418-42. (doi:10.1038/nature20584)

Peng, F and X. Deng, 2020. Improving precision of high-rate altimeter sea level anomalies by removing the sea state bias and intra-1-Hz covariant error, Remote Sensing of Environment,251, 112081, https://doi.org/10.1016/j.rse.2020.112081.

Peral, E., E. Rodríguez, and D. Esteban-Fernández, 2015. Impact of surface waves on swot's projected ocean accuracy. Remote Sensing , 7 (11) , 14 509–14 529.

Perovich, D. K., 1996. The optical properties of sea ice (no. MONO-96-1). Hanover, NH: Cold regions research and engineering lab.

Peter, H., J. Berzosa, M. Fernández, J. Fernández, P. Féménias. Copernicus POD Service – Evolution in Sentinel-3 Orbit Determination. OSTST-2020. 19-23 October 2020. Virtual meeting.

Phalippou, L., Caubet, E., Deemster, F., Richard, J., Rys, L., Deschaux-Beaume, M., Francis, R., and Cullen, R., 2012. Reaching sub-centimeter range noise on Jason-CS with the Poseidon-4 continuous SAR interleaved mode, Ocean Surface Topography Science Team 2012, Venice, Italy, 27–28 September 2012, available at: http://www.aviso.oceanobs.com/en/user-corner/science-teams/ostst-swt-science-team/ostst-2012-venice.html (last access: 24 March 2016), 2012.

Phalippou, L., Deemster, F., 2013. Ocean SAR altimetry from SIRAL2 on CryoSat-2 to Poseidon-4 on Jason-CS, presented at the SAR Altimetry EGM, NOC, Southampton, united Kingdom, 26 June 2013.

Picard, G., L. Brucker, A. Roy, F. Dupont, M. Fily, and A. Royer, 2013. Simulation of the microwave emission of multi-layered snowpacks using the dense media radiative transfer theory: the DMRT-ML model. Geosci Model Devel, 6, 1061-1078.

Pires, N., Fernandes, M.J., Gommenginger, C., Scharroo, R., 2016. A conceptually simple modeling approach for Jason-1 sea state bias correction based on 3 parameters exclusively derived from altimetric information. Remote Sens. 8 (7), 576.

Pitcher L.H. et al. 2020. Advancing field-based GNSS surveying for validation of remotely sensed water surface elevation products. Frontiers in Earth Science, 8, 278, doi:10.3389/feart.2020.00278

Poe, G. A., 1990. Optimum interpolation of imaging microwave radiometer data, IEEE Trans. on Geoscience and Remote Sensing, GE-28, pp. 800-810.

Ponte R. M., M. Carson, M. Cirano, C. M. Domingues, S. Jevrejeva, M. Marcos, G. Mitchum R. S. W. van de Wal, P. L. Woodworth, M. Ablain, F. Ardhuin, V. Ballu, M. Becker, J. Benveniste, F. Birol, E. Bradshaw, A. Cazenave, P. De Mey-Frémaux., F. Durand, T. Ezer, L. Fu, I. Fukumori, K. Gordon, M. Gravelle, S. M. Griffies, W. Han, A. Hibbert, C. W. Hughes, D. Idier, V. Kourafalou, C. M Little, A. Matthews, A. Melet, M. Merrifield, B. Meyssignac, S. Minobe, T. Penduff, N. Picot, C. Piecuch, R. C. Ray, L. Rickards, A. Santamaría-Gómez, D. Stammer, J. Staneva, L. Testut, K. Thompson, P. Thompson, S. Vignudelli, J. Williams, S. D. P. Williams, G. Wöppelmann, L. Zanna, and X. Zhang, 2019. Towards Comprehensive Observing and Modeling Systems for Monitoring and Predicting Regional to Coastal Sea Level, Front. Mar. Sci., 6, 437-, DOI=10.3389/fmars.2019.00437

Ponte A.L., Klein P, 2015. Incoherent signature of internal tides on seal level in idealized numerical simulations. Geophys. Res. Lett., 42: 1520–1526. doi: 10.1002/2014GL062583.

Prandi, P., Meyssignac, B., Ablain, M. et al. 2021. Local sea level trends, accelerations and uncertainties over 1993–2019. Sci Data 8, 1 (2021). https://doi.org/10.1038/s41597-020-00786-7

Preston-Thomas, H, 1990. The International Temperature Scale of 1990 (ITS-90), Metrologia 27, 107 (1990).

Prigent, C., C. Jimenez & P. Bousquet, J, 2019. Satellite-derived global surface water extent and dynamics over the last 25 years (GIEMS-2), Journal of Geophysical Research: Atmospheres.

Prigent, C., Jimenez, C., & Aires, F., 2016. Toward "all weather," long record, and real-time land surface temperature retrievals from microwave satellite observations. Journal of Geophysical Research Atmospheres, 121(10), 5699-5717.

Prigent, C., Matthews, E., Aires, F., and Rossow, W. B., 2001. Remote sensing of global wetland dynamics with multiple satellite data sets. Geophysical Research Letters, 28(24), 4631- 4634.

Prigent, C., Papa, F., Aires, F., Jimenez, C., Rossow, W. B., and Matthews, E., 2012. Changes in land surface water dynamics since the 1990s and relation to population pressure. Geophysical Research Letters, 39(8).

Pujol, M.-I., Y. Faugère, G. Taburet, S. Dupuy, C Pelloquin, M. Ablain, N. Picot, 2016. DUACS DT2014: the new multi-mission altimeter dataset reprocessed over 20 years. Ocean Sci. Discuss., doi:10.5194/os-2015-110.

Pulliainen, J., 2006. Mapping of snow water equivalent and snow depth in boreal and sub-arctic zones by assimilating space-borne microwave radiometer data and ground-based observations. Remote Sens. Environ., 101, 257-269.

Pulliainen, J. and M. Hallikainen, 2001. Retrieval of Regional Snow Water Equivalent from Space-Borne Passive Microwave Observations, In Remote Sensing of Environment, Volume 75, Issue 1, Pages 76-85, ISSN 0034-4257, https://doi.org/10.1016/S0034-4257(00)00157-7.

Pulliainen, J. T., J. Grandell, and M. T. Hallikainen, 1999. HUT Snow Emission Model and its Applicability to Snow Water Equivalent Retrieval. IEEE Trans. Geosci. Remote Sens., 37(3), 1378-1390.

Purdy, W., P. Gaiser, G. Poe E. Uliana, T. Meissner, and F. Wentz, 2006. Geolocation and pointing accuracy analysis for the WindSat sensor, IEEE TGRS, vol. 44(3), pp 496-505.

Quartly, G. D., 2009. Improving the intercalibration of σ0 values for the Jason-1 and Jason-2 altimeters, IEEE Geosci. Rem. Sens. Lett., 6(3), 538–542, doi:10.1109/LGRS.2009.2020921.

Quartly, G. D., Legeais, J.-F., Ablain, M., Zawadzki, L., Fernandes, M. J., Rudenko, S., Carrère, L., García, P. N., Cipollini, P., Andersen, O. B., Poisson, J.-C., Mbajon Njiche, S., Cazenave, A., and Benveniste, J., 2017. A new phase in the production of quality-controlled sea level data, Earth Syst. Sci. Data, 9, 557–572, https://doi.org/10.5194/essd-9-557-2017, 2017.

Quartly, G. D., Rinne, E., Passaro, M., Andersen, O. B., Dinardo, S., Fleury, S., Guerreiro, K., Guillot, A., Hendricks, S., Kurekin, A. A., Müller, F. L., Ricker, R., Skourup, H., and Tsamados, M. 2018. Review of Radar Altimetry Techniques over the Arctic Ocean: Recent Progress and Future Opportunities for Sea Level and Sea Ice Research, The Cryosphere Discuss. [preprint], https://doi.org/10.5194/tc-2018-148, 2018.

Quartly, G. D., Srokosz, M. A., and Guymer, T. H., 1999b. Global precipitation statistics from dual-frequency TOPEX altimetry, J. Geophys. Res., 104(D24), 31489– 31516, doi:10.1029/1999JD900758.

Quartly, G. D., Srokosz, M. A., Guymer, T. H., 1999a. Changes in oceanic precipitation during the 1997–98 El Niño, Geophys. Res. Lett., 27, https://doi.org/10.1029/1999GL011311

Quartly, G.D.; Nencioli, F.; Raynal, M.; Bonnefond, P.; Nilo Garcia, P.; Garcia-Mondéjar, A.; Flores de la Cruz, A.; Crétaux, J.-F.; Taburet, N.; Frery, M.-L.; Cancet, M.; Muir, A.; Brockley, D.; McMillan, M.; Abdalla, S.; Fleury, S.; Cadier, E.; Gao, Q.; Escorihuela, M.J.; Roca, M.; Bergé-Nguyen, M.; Laurain, O.; Bruniquel, J.; Féménias, P.; Lucas, B., 2020. The Roles of the S3MPC: Monitoring, Validation and Evolution of Sentinel-3 Altimetry Observations. Remote Sens. 12, 1763.

Quilfen, Y., Chapron, B., 2019. Ocean surface wave-current signatures from satellite altimeter measurements. Geophysical Research Letters, 46, 253– 261. https://doi.org/10.1029/2018GL081029

Quilfen, Y., Prigent, C., Chapron, B., Mouche, A. A., and Houti, N., 2007. The potential of QuikSCAT and WindSat observations for the estimation of sea surface wind vector under severe weather conditions, J. Geophys. Res., 112, C09023, doi:10.1029/2007JC004163.

Quilfen, Y., J. Piollee and B. Chapron, 2021, Towards improved analysis of short mesoscale sea level signals from satellite altimetry, Earth Syst. Sci. Data Discuss. [preprint], https://doi.org/10.5194/essd-2021-352

Rahmstorf S., 2002. Ocean circulation and climate during the past 120,000 years, Nature volume 419, pages 207–214.

Raney, R. K and D. L Porter, 2001. WITTEX: An Innovative Three-Satellite RadarAltimeter Concept, IEEE Trans. Geosci. Rem. Sens., 39, 2387-

Raney, R. K., 1998. The delay/Doppler radar altimeter, IEEE Trans. Geosci. Rem. Sens., 36, 1578–1588, https://doi.org/10.1109/36.718861.

Rasmussen, E., and J. Turner, Eds., 2003. Polar Lows. Cambridge University Press, 612 pp.

Rastner, P., Bolch, T., Mölg, N., Machguth, H., Le Bris, R., Paul, F., 2012. The first complete inventory of the local glaciers and ice caps on Greenland. The Cryosphere, 6, 1483-1495. (doi:10.5194/tc-6-1483-2012)

Ray C. et al., 2015. SAR Altimeter Backscattered Waveform Model, in IEEE Transactions on Geoscience and Remote Sensing, vol. 53, no. 2, pp. 911-919, Feb. 2015, doi: 10.1109/TGRS.2014.2330423.(2020)

Ray, C., Martin-Puig, C., Clarizia, M. P., Ruffini, G., Dinardo, S., Gommenginger, C. and Benveniste, J., 2015. SAR Altimeter Backscattered Waveform Model, IEEE Trans. Geosci. Remote Sens., 53(2), 911–919, doi:10.1109/TGRS.2014.2330423.

Ray, R. D., 2020. Daily harmonics of ionospheric total electron content from satellite altimetry, Journal of Atmospheric and Solar-Terrestrial Physics, 209, 105423, https://doi.org/10.1016/j.jastp.2020.105423.

Ray R.D. and Zaron E.D., M2 internal tides and their observed wavenumber spectra from satellite altimetry, J. Phys. Oceanogr., 46:1, 3-22, doi: 10.1175/JPO-D-15-0065.1, 2016.

Raynal, M and S. Labroue, 2021. S3MPC – S3A STM Error Budget, S3MPC.CLS.TN.006 6, issue 1.0.

Reale, F.; Pugliese Carratelli, E.; Di Leo, A.; Dentale, F., 2020. Wave Orbital Velocity Effects on Radar Doppler Altimeter for Sea Monitoring. J. Mar. Sci. Eng., 8, 447.

Recchia, L., Scagliola, M., Giudici, D., Kuschnerus, M., 2017. An Accurate Semianalytical Waveform Model for Mispointed SAR Interferometric Altimeters, IEEE Geoscience And Remote Sensing Letters, Vol. 14, No. 9, 1537.

Remy, F., Mazzega, P., Houry, S., Brossier, C., & Minster, J., 1989. Mapping of the topography of continental ice by inversion of satellite altimeter data. Journal of Glaciology, 35(119), 98–107.

Resio, D. and J. Westerink, 2008, Modelling the Physics of Storm Surges, Physics Today, 61(9), 33-38

Reul, N., B. Chapron, E. Zabolotskikh, C. Donlon, A. Mouche, J. Tenerelli, F. Collard, J.F. Piolle, A. Fore, S. Yueh, J. Cotton, P. Francis, Y. Quilfen, and V. Kudryavtsev, 2017. A New Generation of Tropical Cyclone Size Measurements from Space. Bull. Amer. Meteor. Soc., 98, 2367–2385, https://doi.org/10.1175/BAMS-D-15-00291.1

Reul, N., B. Chapron, E. Zabolotskikh, C. Donlon, Y. Quilfen, S. Guimbard, and J. F. Piolle, 2016. A revised L-band radio-brightness sensitivity to extreme winds under tropical cyclones: The five year SMOS-storm database. Remote Sens. Environ., 180, 274–291, doi:https://doi.org/10.1016/j.rse.2016.03.011.

Reul, N., J. Tenerelli, B. Chapron, D. Vandemark, Y. Quilfen, and Y. Kerr, 2012b. SMOS satellite L-band radiometer: A new capability for ocean surface remote sensing in hurricanes, J. Geophys. Res., 117, C02006, doi:10.1029/2011JC007474.

Reul, N., J. Tenerelli, J. Boutin, B. Chapron, F. Paul, E. Brion, F. Gaillard, and O. Archer, 2012a. Overview of the first SMOS sea surface salinity products. Part I: Quality assessment for the second half of 2010, IEEE Trans. Geosci. Remote Sens., 50(5), 1636–1647, doi:10.1109/TGRS.2012.2188408.

Revel, M., Ikeshima, D., Yamazaki, D., & Kanae, S., 2021. A framework for estimating global-scale river discharge by assimilating satellite altimetry. Water Resources Research, 57, e2020WR027876. https://doi.org/10.1029/2020WR027876

Ribal, A., Young I. R., 2019. 33 years of globally calibrated wave height and wind speed data based on altimeter observations. Nat-Sci Data 6(77):1–15

Ricciardulli, L., and NCAR (National Center for Atmospheric Research Staff, Eds), 2017. The Climate Data Guide: CCMP: Cross-Calibrated Multi-Platform wind vector analysis. Retrieved from https://climatedataguide.ucar.edu/climate-data/ccmp-cross-calibrated-multi-platform-wind-vector-analysis.

Ricciardulli, L., Meissner, T., and Wentz, F., 2012. Towards a climate data record of satellite ocean vector winds, Proceedings of the 2012 IEEE International Geoscience and Remote Sensing Symposium (Munich: IEEE).

Richard, J., V. Enjolras, L. Rys, J. Vallon, I. Nann and P. Escudier, 2008. Space Altimetry from Nano-Satellites : Payload Feasibility, Missions and System Performances, IGARSS 2008 - 2008 IEEE International Geoscience and Remote Sensing Symposium, Boston, MA, USA, 2008, pp. III - 71-III - 74, doi: 10.1109/IGARSS.2008.4779285.

Richter, F., M. Drusch, L. Kaleschke, N. Maaß, X. Tian-Kunze, and S. Mecklenburg, 2018. Arctic sea ice signatures: L-band brightness temperature sensitivity comparison using two radiation transfer models, The Cryosphere, 12, 921-933, https://doi.org/10.5194/tc-12-921-2018.

Ricker, R., Hendricks, S., Helm, V., Skourup, H., and Davidson, M., 2014. Sensitivity of CryoSat-2 Arctic sea-ice freeboard and thickness on radar-waveform interpretation, The Cryosphere, 8, 1607–1622, https://doi.org/10.5194/tc-8-1607-2014.

Ricker, R., Hendricks, S., Kaleschke, L., Tian-Kunze, X., King, J., and Haas, C. 2017. A weekly Arctic sea-ice thickness data record from merged CryoSat-2 and SMOS satellite data, The Cryosphere, 11, 1607–1623, https://doi.org/10.5194/tc-11-1607-2017.

Rieu, R., T. Moreau, E. Cadier, M. Raynal, S. Clerc, C. Donlon, F. Borde, F. Boy, C. Maraldi, 2021. Exploiting the Sentinel-3 tandem phase dataset and azimuth oversampling to better characterize the sensitivity of SAR altimeter sea surface height to long ocean waves, Advances in Space Research, 67, Issue 1, 253-265, https://doi.org/10.1016/j.asr.2020.09.037.

Rio, M.-H., Santoleri R., 2018. Improved global surface currents from the merging of altimetry and Sea Surface Temperature data, Remote Sensing of Environment, ISSN 0034-4257, https://doi.org/10.1016/j.rse.2018.06.003.

Rio, M., Santoleri, R., Bourdalle-Badie, R., Griffa, A., Piterbarg, L., and Taburet, G., 2016. Improving the Altimeter-Derived Surface Currents Using High-Resolution Sea Surface Temperature Data: A Feasability Study Based on Model Outputs, Journal of Atmospheric and Oceanic Technology, 33(12), 2769-2784.

Roberts, J. et al., 2016. Evolution of South Atlantic density and chemical stratification across the last deglaciation, PNAS (2016). DOI: 10.1073/pnas.1511252113

Robinson, W. D., C. Kummerow, and W. S. Olson, 1992. A technique for enhancing and matching the resolution of microwave measurements from the SSM/I instrument, IEEE Trans. Geosci. Remote Sens., 30, 419-429, 1992.

Rodriguez, E. and E. J. Martin, 1992. Theory and design of interferometric synthetic aperture radars. IEE Proc. Radar Signal Process., 139, 147–159.

Rodriguez, E., D. Esteban-Fernandez, E. Peral, C. W. Chen, J. De Bleser, and B. Williams, 2017, Wide-Swath Altimetry - A Review, in Stammer, D and Cazanave, A (Eds), Satellite Altimetry over Oceans and Land Surfaces, CRC Press, eBook ISBN9781315151779

Roohi, Sh, Amini, A., Voosoghi, B., Battles, D., 2019. Lake Monitoring from a Combination of Multi Copernicus Missions: Sentinel-1 A and B and Sentinel3A. J Hydrogeol Hydrol Eng 8:3.

Rossiter, J. R., 1953, The North Sea Storm Surge of 31 January and 1 February 1953., Phil. Trans. R. Soc. Lond. A, 246:371-400;doi:10.1098/rsta.1954.0002.

Rostan, T., D. Ulrich, S. Riegger and A. Østergaard, 2016. MetoP-SG SCA wind scatterometer design and performance, IEEE International Geoscience and Remote Sensing Symposium (IGARSS), Beijing, 2016, pp. 7366-7369. doi: 10.1109/IGARSS.2016.7730921

Rostosky, P., Spreen, G., Farrell, S. L., Frost, T., Heygster, G., and Melsheimer, C., 2018. Snow depth retrieval on Arctic sea ice from passive microwave Radiometers - Improvements and extensions to multiyear ice using lower frequencies. Journal of Geophysical Research: Oceans, 123. https://doi.org/ 10.1029/2018JC014028.

Roy, A., A. Royer, J.-P. Wigneron, A. Langlois, J. Bergeron, and P. Cliché, 2012. A simple parameterization for a boreal forest radiative transfer model at microwave frequencies. Remote Sens. Environ., 124, 371-383.

RSM, Risk Management Solutions, 2003. The 1953 U.K. Floods, 50 - year Retrospective, 2003 available from http://www.rms.com/Publications/1953_Floods_Retrospective.pdf

Rubino, R.; Duffo, N.; González-Gambau, V.; Corbella, I.; Torres, F.; Durán, I.; Martín-Neira, M, 2020. Deriving VTEC Maps from SMOS Radiometric Data. Remote Sens., 12, 1604.

Ruf, C., 1998. Constraints on the polarization purity of a Stokes microwave radiometer, Radio Science, Volume 33, 6, Pages1 617-1639.

Ruf, C., Keihm, S. and Janssen, M. A., 1995. TOPEX/Poseidon microwave radiometer (TMR): I. Instrument description and antenna temperature calibration. IEEE Trans. Geosci. Remote Sens., 33(1): 125–137.

Rummel R., 2001, Global unification of height systems with GOCE. Proceedings of the IAG Symposia, Vol. 123, Sideris (ed.), Gravity, Geoid and Geodynamics. Springer Verlag ISBN 3-540-42469-5.

Sakov, P., Counillon, F., Bertino, L., Lisæter, K. A., Oke, P. R., and Korablev, A., 2012. TOPAZ4: an ocean-sea ice data assimilation system for the North Atlantic and Arctic, Ocean Sci., 8, 633-656, https://doi.org/10.5194/os-8-633-2012.

Sampson, C., and A. Schrader, 2000. The automated tropical cyclone forecasting system (Version 3.2). Bull. Amer. Meteor. Soc., 81(6), 1231-1240, doi: 10.1175/1520-0477(2000)081

Sandberg Sørensen, L., Simonsen, S. B., Forsberg, R., Khvorostovsky, K., Meister, R., and Engdahl, M. E.: 25 years of elevation changes of the Greenland Ice Sheet from ERS, Envisat, and CryoSat-2 radar altimetry, Earth Planet. Sci. Lett., 495, 234–241, https://doi.org/10.1016/j.epsl.2018.05.015, 2018.

Sandwell, D. T., Harper, H., Tozer, B., Smith, W. H.F., 2019. Gravity field recovery from geodetic altimeter missions, Advances in Space Research, https://doi.org/10.1016/j.asr.2019.09.011.

Santos-Ferreira, A.M.; da Silva, J.C.B.; Magalhaes, J.M.; Amraoui, S.; Moreau, T.; Maraldi, C.; Boy, F.; Picot, N.; Borde, F., 2022, Effects of Surface Wave Breaking Caused by Internal Solitary Waves in SAR Altimeter: Sentinel-3 Copernicus Products and Advanced New Products. Remote Sens., 14, 587. https://doi.org/10.3390/rs14030587

Sanò, P.; Panegrossi, G.; Casella, D.; Marra, A.C.; D'Adderio, L.P.; Rysman, J.F.; Dietrich, S. 2018. The Passive Microwave Neural Network Precipitation Retrieval (PNPR) Algorithm for the CONICAL Scanning Global Microwave Imager (GMI) Radiometer. Remote Sens. , 10, 1122.

Sasaki, H., Kida, S., Furue, R., Aiki, H., Komori, N., Masumoto, Y., Miyama, T., Nonaka, M., Sasai, Y., and Taguchi, B., 2020. A global eddying hindcast ocean simulation with OFES2, Geosci. Model Dev., 13, 3319–3336, https://doi.org/10.5194/gmd-13-3319-2020.

Savage, A.C., B.K. Arbic, M.H. Alford, J.K. Ansong, J.T Farrar, D. Menemenlis, A.K. O'Rourke, J.G. Richman, J.F. Shriver, G. Voet, A.J. Wallcraft, and L. Zamudio, 2017. Spectral decomposition of internal gravity wave sea surface height in global models, J. Geophys. Res., 122, doi:10.1002/2017JC013009

Scharroo, R., 2018. Sentinel-6 End-User Requirements Document, EUM/LEO-JASCS/REQ/12/0013, v3E available from EUMETSAT, Darmstadt, Germany.

Scharroo, R., Bonekamp, H., Ponsard, C., Parisot, F., von Engeln, A., Tahtadjiev, M., de Vriendt, K., and Montagner, F., 2016. Jason continuity of services: continuing the Jason altimeter data records as Copernicus Sentinel-6, Ocean Sci., 12, 471–479, https://doi.org/10.5194/os-12-471-2016.

Scharroo, R., Leuliette, E. W., Lillibridge, J. L., Byrne, D., Naeije, M. C., Mitchum, G. T., 2013. RADS: Consistent multi-mission products, in Proc. of the Symposium on 20 Years of Progress in Radar Altimetry, Venice, 20-28 September 2012, Eur. Space Agency Spec. Publ., ESA SP-710, p. 4 pp., 2013.

Scharroo, R., Lillibridge, J. L., Smith, W. H. F., Schrama, E. J. O., 2004. Cross-calibration and long-term monitoring of the microwave radiometers of ERS, TOPEX, GFO, Jason, and Envisat, Mar. Geod., 27(1- 2), 279–297, doi:10.1080/01490410490465265.

Scharroo, R., Smith, W. H. F., Lillibridge, J. L., 2005. Satellite altimetry and the intensification of Hurricane Katrina, Eos Trans. AGU, 86(40), 366– 366, doi:10.1029/2005EO400004.

Scherllin-Pirscher, B., Steiner, A.K. and Kirchengast, G., 2014. Deriving dynamics from GPS radio occultation: three-dimensional wind fields for monitoring the climate. Geophysical Research Letters, 41(20), 7367– 7374

Schmidt-Thomé, P, 2006. The spatial effects and management of natural and technological hazards in Europe, European Spatial Planning Observation Network (ESPON), ISBN/ISSN. 9516909183, available from http://www.preventionweb.net/english/professional/publications/v.php?id=3621

Schmitt, A.U., L. Kaleschke, 2018. A Consistent Combination of Brightness Temperatures from SMOS and SMAP over Polar Oceans for Sea Ice Applications. Remote Sens., 10, 553.

Schneider, R., Godiksen, P. N., Villadsen, H., Madsen, H., and Bauer-Gottwein, P., 2017. Application of CryoSat-2 altimetry data for river analysis and modelling, Hydrol. Earth Syst. Sci., 21, 751–764, https://doi.org/10.5194/hess-21-751-2017.

Schneider, R., Ridler, M. E., Godiksen, P. N., Madsen, H., and Bauer-Gottwein, P., 2018. A data assimilation system combining CryoSat-2 data and hydrodynamic river models, J. Hydrol., 557, 197–210, https://doi.org/10.1016/j.jhydrol.2017.11.052.

Schröder, L., Horwath, M., Dietrich, R., Helm, V., Broeke, M. R., and Ligtenberg, S. R., 2019. Four decades of Antarctic surface elevation changes from multi-mission satellite altimetry. The Cryosphere, 13(2), 427-449.

Schulz-Stellenfleth, J.; Lehner, S. 2001. Ocean wave imaging using an airborne single pass across-track interferometric SAR. IEEE Trans. Geosci. Remote Sens. 39, 38–45.

Scott, K. A., E. Li and A. Wong, 2014. Sea Ice Surface Temperature Estimation Using MODIS and AMSR-E Data Within a Guided Variational Model Along the Labrador Coast," in IEEE Journal of Selected Topics in Applied Earth Observations and Remote Sensing, vol. 7, no. 9, pp. 3685-3694, doi: 10.1109/JSTARS.2013.2292795

Screen, J. A. and Simmonds, I. 2010. The central role of diminishing sea ice in recent Arctic temperature amplification. Nature 464, 1334–1337.

Serreze, M. C. and Francis, J. A., 2006. The Arctic amplification debate. Clim. Change 76, 241–264.

Seung-Bum, Kim, Frank J. Wentz, and Gary S. E. Lagerloef, 2011. Effects of Antenna Cross-Polarization Coupling on the Brightness Temperature Retrieval at L-Band, IEEE Trans. Reosci. Re. Sens., 49, 5, 1637-

Sheng Y., C. Song, J. Wang, E. A. Lyons, B. R. Knox, J. S. Cox and F. Gao, 2016. Representative lake water extent mapping at continental scales using multi-temporal Landsat-8 imagery. Remote Sensing of Environment, 185, 129-141, doi:10.1016/j.rse.2015.12.041.

Sibthorpe, A., Brown, S., Desai S. D., Haines, B J., 2011, Calibration and Validation of the Jason-2/OSTM Advanced Microwave Radiometer Using Terrestrial GPS Stations, Marine Geodesy, 34:3-4, 420-430, DOI: 10.1080/01490419.2011.584839

Simonsen, S. B., Barletta, V. R., Colgan, W. T., and Sørensen, L. S., 2021. Greenland Ice Sheet Mass Balance (1992–2020) From Calibrated Radar Altimetry. Geophysical Research Letters, 48(3), e2020GL091216.

Sippel, S. J., S. K Hamilton, J. M. Melack, B. J. Choudery, 1994. Determination of inundation area in the Amazon River floodplain using the SMMR 37 GHz polarization difference, Rem. Sens. Env. 48, 70-76

Smirnova, J.E., Zabolotskikh, E.V., Bobylev, L.P. et al., 2016. Statistical characteristics of polar lows over the Nordic Seas based on satellite passive microwave data, Izv. Atmos. Ocean. Phys. 52: 1128. https://doi.org/10.1134/S0001433816090255

Smith, D. M., 1996. Extraction of winter total sea-ice concentration in the Greenland and Barents Seas from SSM/I data, International Journal of Remote Sensing, 17:13, 2625-2646, DOI: 10.1080/01431169608949096

Smith, W. H. F., R. Scharroo, V. V. Titov, D. Arcas, and B. K. Arbic, 2005. Satellite Altimeters Measure Tsunami, Oceanogray 18(2):11–13, DOI: 10.5670/oceanog.2005.62

Smith, W. H., Sandwell, D. T., 1997. Global Sea Floor Topography from Satellite Altimetry and Ship Depth Soundings, Science, 277, 1956-1962 DOI: 10.1126/science.277.5334.1956

Soldo, Y., D. M. Le Vine, P. de Matthaeis and P. Richaume, 2017. L-Band RFI Detected by SMOS and Aquarius, in IEEE Transactions on Geoscience and Remote Sensing, vol. 55, no. 7, pp. 4220-4235, July 2017. doi: 10.1109/TGRS.2017.2690406

Soldo, Y., D. M. Le Vine and E. Dinnat, 2019. SMAP Observations of the Fourth Stokes Parameter At L-Band, IGARSS 2019 - 2019 IEEE International Geoscience and Remote Sensing Symposium, Yokohama, Japan, pp. 8407-8410, doi: 10.1109/IGARSS.2019.8900153.

Spreen, G., L. Kaleschke, and G. Heygster, 2008. Sea ice remote sensing using AMSR-E 89-GHz channels, J. Geophys. Res., 113, C02S03, doi:10.1029/2005JC003384.

Stammer, D., R. D. Ray, O. B. Andersen, B. K. Arbic, W. Bosch, L. Carrère, Y. Cheng, D. S. Chinn, B. D. Dushaw, G. D. Egbert, S. Y. Erofeeva, H. S. Fok, J. A. M. Green, S. Griffiths, M. A. King, V. Lapin, F. G. Lemoine, S. B. Luthcke, F. Lyard, J. Morison, M. Müller, L. Padman, J. G. Richman, J. F. Shriver, C. K. Shum, E. Taguchi and Y. Yi, 2014. Accuracy assessment of global barotropic ocean tide models, Rev. Geophys., 52, 243– 282, doi:10.1002/2014RG000450.

Stephen, K, 2018. Societal Impacts of a rapidly changing Arctic, Current Climate Change Reports 4:223–237, https://doi.org/10.1007/s40641-018-0106-1

Steunou, N., Desjonquères, J. D., Picot, N., Sengenes, P., Noubel J., Poisson J. C., 2015. AltiKa Altimeter: Instrument Description and In Flight Performance, Marine Geodesy, 38:sup1, 22-42, DOI: 10.1080/01490419.2014.988835

Stewart, K. D., Hogg, A. M., England, M. H., and Waugh, D. W., 2020. Response of the Southern Ocean overturning circulation to extreme Southern Annular Mode conditions. Geophysical Research Letters, 47, e2020GL091103. https://doi.org/10.1029/2020GL091103

Stogryn, A., (1978), Estimates of brightness temperatures from scanning radiometer data, IEEE Trans. on Antennas Propagation, AP-26, pp. 720-726.

Stroeve, J. C., M. C. Serreze, M. M. Holland, J. E. Kay, J. Malanik, andA. P. Barrett, 2012. The Arctic's rapidly shrinking sea ice cover: A research synthesis, Climatic Change, vol. 110, nos. 3–4, pp. 1005–1027.

Stroeve, J.C., T. Markus, J. A. Maslanik, D. J. Cavalieri, A. J. Gasiewski, J. F. Heinrichs, J. and M. Sturm, M., 2006. Impact of Surface Roughness on AMSR-E Sea Ice Products. IEEE Trans Geosci. Re, Sens., 44 (11), 3103-3117. doi:10.1109/TGRS.2006.880619

Sturm, M., and R. Massom, 2010. Snow on sea ice. In D. Thomas and G. Dieckmann (Eds.), Sea ice (2nd ed), (pp. 153–204). Oxford, UK: Wiley-Blackwell.

Sumata, H., T. Lavergne, F. Girard-Ardhuin, N. Kimura, M. A. Tschudi, F. Kauker, M. Karcher, and R. Gerdes 2014. An intercomparison of Arctic ice drift products to deduce uncertainty estimates, J. Geophys. Res. Oceans,119,4887–4921, doi:10.1002/2013JC009724

Svendsen, E., K. Kloster, B. Farrelly, O. M. Johannessen, J. A. Johannessen, W. J. Campbell, P. Gloersen, D. Cavalieri, and C. Matzler, 1983. Norwegian remote sensing experiment: Evaluation of the NIMBUS 7 Scanning Multichannel Microwave Radiometer for sea ice research, J. Geophys. Res., 88(C5), 2781 – 2791.

Svendsen, E., Matzler, C., and Grenfell, Th., 1987. A model for retrieving total sea ice concentration from a spaceborne dual-polarized passive microwave instrument operating near 90 GHz, Int. J. Remote Sens., 8, 1479–1487.

Swail, V. & Co-Authors, 2010, Storm Surge, in Proceedings of OceanObs'09: Sustained Ocean Observations and Information for Society (Vol. 2), Venice, Italy, 21-25 September 2009, Hall, J., Harrison D.E. & Stammer, D., Eds., ESA Publication WPP-306. available from https://abstracts.congrex.com/scripts/jmevent/abstracts/FCXNL-09A02a-1753729-1-cwp3c04.pdf

Swift, C.T., D.J. Cavalieri, P. Gloersen, H.J. Zwally, N.M. Mognard, W.J. Campbell, L.S. Fedor, S. Peteherych, 1995. Observations of the Polar Regions from Satellites using Active and Passive Microwave Techniques, in Saltzman, B (Ed.), Advances in Geophysics, 27, 335-392, https://doi.org/10.1016/S0065-2687(08)60409-4.

Taburet, N., Zawadzki, L., Vayre, M., Blumstein, D., Le Gac, S., Boy, F., Raynal, M., Labroue, S., Crétaux, J.-F., Femenias, P., 2020. S3MPC: Improvement on Inland Water Tracking and Water Level Monitoring from the OLTC Onboard Sentinel-3 Altimeters. Remote Sens. 2020, 12, 3055.

Takala M., K. Luojus, J. Pulliainen, C. Derksen, J. Lemmetyinen, J.-P. Kärnä, J. Koskinen and B. Bojkov, 2011. Estimating northern hemisphere snow water equivalent for climate research through assimilation of space-borne radiometer data and ground-based measurements. Remote Sensing of Environment, 115, 3517-3529.

Takala, M., J. Pulliainen, S. Metsämäki and J. Koskinen, 2009. Detection of Snowmelt Using Spaceborne Microwave Radiometer Data in Eurasia From 1979 to 2007. IEEE Transactions on Geoscience and Remote Sensing, 47 (9), 2996-3007.

Tarpanelli, A. S. Camici, K. Nielsen, L. Brocca, T. Moramarco, J. Benveniste, 2020, Potentials and limitations of Sentinel-3 for river discharge assessment, Advances in Space Research, ISSN 0273-1177, https://doi.org/10.1016/j.asr.2019.08.005.

Tedesco, M., and J. Jeyaratnam, 2016. A new operational snow retrieval algorithm applied to historical AMSR-E brightness temperatures. Remote Sens., 8, 1037; doi: 10.3390/ns8121037.

Teubner, I.E., Forkel, M., Jung, M., Liu, Y.Y., Miralles, D.G., Parinussa, R., van der Schalie, R., Vreugdenhil, M., Schwalm, C.R., Tramontana, G., Camps-Valls, G., Dorigo, W., 2018. Assessing the relationship between microwave vegetation optical depth and gross primary production. International Journal of Applied Earth Observation and Geoinformation 65, 79–91.https://doi.org/10.1016/j.jag.2017.10.006

Tian-Kunze, X., Kaleschke, L., Maaß, N., Mäkynen, M., Serra, N., Drusch, M., and Krumpen, T. 2014. SMOS-derived thin sea ice thickness: algorithm baseline, product specifications and initial verification, The Cryosphere, 8, 997-1018, https://doi.org/10.5194/tc-8-997-2014.

Tietsche S., M. A. Balmaseda, P. de Rosnay, H. Zuo, X. Tian-Kunze, and L. Kaleschke, 2018. Thin sea ice in the Arctic: comparing L-band radiometry retrievals with an ocean reanalysis. The Cryosphere, 12, 2051-2072, doi: 10.5194/tc-2017-247

Tilling R.L., A. Ridout, A. Shepherd 2016. Near-real-time Arctic sea ice thickness and volume from CryoSat-2, Cryosphere, 10, pp.2003-2012. doi: 10.5194/tc-10-2003-2016

Tilling, R. L., Ridout, A., Shepherd, A., 2018. Estimating Arctic sea ice thickness and volume using CryoSat-2 radar altimeter data, Advances in Space Research, 62, 6, 1203-1225, https://doi.org/10.1016/j.asr.2017.10.051.

Timmermans, B., C. Gommenginger, G. Dodet and J. R. Bidlot, 2020. Global Wave Height Trends and Variability from New Multimission Satellite Altimeter Products, Reanalyses, and Wave Buoys. Geophysical Research Letters 47(9): e2019GL086880.

Tonboe, R. T., Eastwood, S., Lavergne, T., Sørensen, A. M., Rathmann, N., Dybkjær, G., Pedersen, L. T., Høyer, J. L., and Kern, S., 2016. The EUMETSAT sea ice concentration climate data record, The Cryosphere, 10, 2275-2290, https://doi.org/10.5194/tc-10-2275-2016.

Tonboe, R., G. Dybkjaer and J. L. Hoeyer, 2011. Simulations of the snow covered sea ice surface temperature and microwave effective temperature, Tellus A: Dynamic Meteorology and Oceanography, 63:5,1028-1037, DOI: 10.1111/j.1600-0870.2011.00530.x

Tournadre J., N. Bouhier, F. Girard-Ardhuin, F. Remy, 2016. Antarctic icebergs distributions 1992-2014 . Journal Of Geophysical Research-oceans , 121(1), 327-349 http://doi.org/10.1002/2015JC011178.

Tournadre, J., 2014. Anthropogenic pressure on the open ocean: the growth of ship traffic revealed by altimeter data analysis. Geophys Res Lett 41:7924–7932

Tournadre, J., Bouhier, N., Girard-Ardhuin, F., and Rémy, F. 2015, Large icebergs characteristics from altimeter waveforms analysis, J. Geophys. Res. Oceans, 120, 1954– 1974, doi:10.1002/2014JC010502.

Tournadre, J., Chapron, B., and Reul, N. 2011. High-Resolution Imaging of the Ocean Surface Backscatter by Inversion of Altimeter Waveforms, Journal of Atmospheric and Oceanic Technology, 28(8), 1050-1062.

Tournadre, J., Lambin-Artru, J., Steunou, N., 2009a.Cloud and Rain Effects on AltiKa/SARAL Ka-Band Radar Altimeter—Part I: Modeling and Mean Annual Data Availability, in IEEE Transactions on Geoscience and Remote Sensing, vol. 47, no. 6, pp. 1806-1817, June 2009, doi: 10.1109/TGRS.2008.2010130.

Tournadre, J., Lambin-Artru, J., Steunou, N., 2009b. Cloud and rain effects on ALTIKA/SARAL Ka-band radar altimeter Part II: Definition of a rain/cloud flag. IEEE Trans. Geosci. Remote Sens. 47 (6), 1818–1826.

Tournadre, J., Whitmer, K., and Girard-Ardhuin, F., 2008. Iceberg detection in open water by altimeter waveform analysis, J. Geophys. Res., 113, C08040, doi:10.1029/2007JC004587.

Tran, N., Labroue, S., Philipps, S., Bronner, E., Picot, N., 2010a. Overview and update of the sea state bias corrections for the Jason-2, Jason-1 and TOPEX missions. Mar. Geod. 33 (S1), 348–362.

Tran, N., Vandemark, D., Chapron, B., Labroue, S., Feng, H., Beckley, B., Vincent, P., 2006. New models for satellite altimeter sea state bias correction developed using global wave model data. J. Geophys. Res. Oceans 111 (C9).

Tran, N., Vandemark, D., Labroue, S., Feng, H., Chapron, B., Tolman, H., Picot, N., 2010b. Sea state bias in altimeter sea level estimates determined by combining wave model and satellite data. J. Geophys. Res. Oceans 115 (C3).

Tran, N., Vandemark, D., Ruf, C. S., Chapron, B., 2002. The dependence of nadir ocean surface emissivity on wind vector as measured with microwave radiometer, in IEEE Transactions on Geoscience and Remote Sensing, vol. 40, no. 2, pp. 515-523, Feb. 2002, doi: 10.1109/36.992827.

Tran, N.; Chapron, B., 2006. Combined Wind Vector and Sea State Impact on Ocean Nadir-Viewing Ku- and C-Band Radar Cross-Sections. Sensors, 6, 193-207. https://doi.org/10.3390/s6030193

Tsang, L., C.-T. Chen, A. T. C. Chang, J. Guo, and K.-H. Ding, 2000. Dense media radiative transfer theory based on quasi-crystalline approximation with applications to microwave remote sensing of snow. Radio Sci., 35(3), 731 - 749.

Tsang, L., J. A. Kong, and R. T. Shin, 1985. Theory of Microwave Remote Sensing. New York: Wiley.

Tsutsui, H.; Maeda, T., 2017. Possibility of Estimating Seasonal Snow Depth Based Solely on Passive Microwave Remote Sensing on the Greenland Ice Sheet in Spring. Remote Sens., 9, 523.

UNESCO, 1985. The international system of units (SI) in oceanography, UNESCO Technical Papers No. 45, IAPSO Pub. Sci. No. 32, Paris, France.

Uranga, E., A. Llorente, R. Oliva, A. de la Fuente, E. Daganzo and Y. Kerr, "Monitoring of Smos Rfi Sources in the 1400-1427mhz Passive Band," IGARSS 2018 - 2018 IEEE International Geoscience and Remote Sensing Symposium, 2018, pp. 1241-1244, doi: 10.1109/IGARSS.2018.8517676.Vihma, T., (2014), Effects of Arctic sea ice decline on weather and climate: A review, Surveys Geophys., vol. 35, no. 5, pp. 1175–1214.

Valladeau, G., Legeais, J. F., Ablain, M., Guinehut S., Picot N., 2012. Comparing Altimetry with Tide Gauges and Argo Profiling Floats for Data Quality Assessment and Mean Sea Level Studies, Marine Geodesy, 35:sup1, 42-60, DOI: 10.1080/01490419.2012.718226

Vandemark, D., Chapron, B., Sun, J., Crescenti, G.H., Graber, H.C., 2004. Ocean wave slope observations using radar backscatter and laser altimeters. J. Phys. Oceanogr. 34, 2825–2842.

Varma, A. K., Mangalsinh N. R., Piyush, D. N., 2020. Precipitation measurement from SARAL AltiKa and passive microwave radiometer observations, International Journal of Remote Sensing, 41:23, 8948-8964, DOI: 10.1080/01431161.2020.1797214

Vaze, P., Neeck, S., Bannoura, W., Green, J., Wade, A., Mignogno, M., Zaouche, G., Couderc, V., Thouvenot, E., Parisot, F., 2010. The Jason-3 Mission: completing the transition of ocean altimetry from research to operations, Proc. SPIE 7826, Sensors, Systems, and Next-Generation Satellites XIV, 78260Y (13 October 2010); https://doi.org/10.1117/12.868543

Veng, T., Andersen, O. B., 2020. Consolidating sea level acceleration estimates from satellite altimetry, Advances in Space Research, https://doi.org/10.1016/j.asr.2020.01.016.

Vergara, O., R. Morrow, I. Pujol, G. Dibarboure and C. Ubelmann, 2019, Revised global wave number spectra from recent altimeter observations. Journal of Geophysical Research: Oceans, 124, 3523– 3537. https://doi.org/10.1029/2018JC014844

Verkhoglyadova, O.P., Leroy, S.S., Ao, C.O., 2014. Estimation of winds from GPS radio occultations. Journal of Atmospheric and Oceanic Technology, 31(11), 2451– 2461

Verron, J., Pascal Bonnefond, Ole Andersen, Fabrice Ardhuin, Muriel Bergé-Nguyen, Suchandra Bhowmick, Denis Blumstein, François Boy, Laurent Brodeau, Jean-François Crétaux, Mei Ling Dabat, Gérald Dibarboure, Sara Fleury, Florent Garnier, Lionel Gourdeau, Karen Marks, Nadège Queruel, David Sandwell, Walter H.F. Smith, E.D. Zaron, 2020. The SARAL/AltiKa mission: A step forward to the future of altimetry, 2020; Advances in Space Research, https://doi.org/10.1016/j.asr.2020.01.030.

Verron, J., Bonnefond, P., Aouf, L., Birol, F., Bhowmick, S.A., Calmant, S., Conchy, T., CreÅLtaux, J.F., Dibarboure, G., Dubey, A.K., Fauge`re, Y., Guerreiro, K., Gupta, P.K., Hamon,M., Jebri, F., Kumar, R., Morrow, R., Pascual, A., Pujol, M.I., ReÅLmy, E., ReÅLmy, F., Smith, W.H.F., Tournadre, J., Vergara, O., 2018. The benefits of the Ka-Band as Evidenced from the SARAL/AltiKa altimetric mission: scientific applications. Remote Sens. 10 (2), 163. https://doi.org/10.3390/rs10020163.

Verron, J., Picot, N., (Eds.), 2015. The SARAL/AltiKa Satellite Altimetry Mission. Marine Geodesy 2015, 38 (S1).

Vieira, T., Fernandes, M.J., Lazaro, C., 2018. Analysis and retrieval of tropospheric corrections for CryoSat-2 over inland waters. Adv. Space Res. 62 (6), 1479–1496. https://doi.org/10.1016/j.asr.2017.09.002.

Vignudelli, S., Kostianoy, A. G., Cipollini, P., Benveniste, J., 2011. Coastal Altimetry, Springer, 2011. ISBN: 978-3-642-12795-3

Vihma, T., 2014. Effects of Arctic sea ice decline on weather and climate: A review, Surveys Geophys., vol. 35, no. 5, pp. 1175–1214.

Villadsen, H., Deng, X., Andersen, O. B., Stenseng, L., Nielsen, K., and Knudsen, P. 2016. Improved inland water levels from SAR altimetry using novel empirical and physical retrackers, J. Hydrol., 537, 234–247, https://doi.org/10.1016/j.jhydrol.2016.03.051

Vincent, P.; Steunou, N.; Caubetq, E.; Phalippou, L.; Rey, L.; Thouvenot, E.; Verron, J. 2006. AltiKa: a Ka-band Altimetry Payload and System for Operational Altimetry during the GMES Period. Sensors 2006, 6, 208-234. https://doi.org/10.3390/s6030208

Vu, P. L., Frappart, F., Darrozes, J., Marieu, V., Blarel, F., Ramillien, G., Bonnefond, P., and Birol, F., 2018. Multi-satellite altimeter validation along the French Atlantic coast in the southern Bay of Biscay from ERS-2 to SARAL, Remote Sens., 10, 93, https://doi.org/10.3390/rs10010093.

Wagner, K. W., K. K. Schroeder, and J. T. Black, 2021. Distributed space missions applied to sea surface height monitoring, Acta Astronautica 178 (2021) 634–644

Wagner, W. G. Lemoine, and H. Rott, 1999. A Method for Estimating Soil Moisture from ERS Scatterometer and Soil Data. Rem. Sens. of Env., vol.70, 191-207.

Walker, N.; Partington, K.; Van Woert, M.; Street, T. , 2006. Arctic sea ice type and concentration mapping using passive and active microwave sensors. IEEE Trans. Geosci. Remote Sens. 44, 3574–3584.

Walsh, E. J., 1982. Pulse-to-pulse correlation in satellite radar altimeters, Radio Sci., 17(4), 786– 800, doi:10.1029/RS017i004p00786.

Wang, J. K., Aouf, L., Dalphinet, A., Zhang, Y. G., Xu, Y., Hauser, D., and Liu, J. Q. (2021). The wide swath significant wave height: An innovative reconstruction of significant wave heights from CFOSAT's SWIM and scatterometer using deep learning, Geophysical Research Letters, 48, e2020GL091276. https://doi.org/10.1029/2020GL091276

Warren, S. G., Rigor, I. G., Untersteiner, N., Radionov, V. F., Bryazgin, N. N., Aleksandrov, Y. I., and Colony, R. (1999), Snow depth on Arctic sea ice, J. Climate, 12, 1814–1829.

Watanabe, M., G. Kadosaki, Y. Kim, M. Ishikawa, K. Kushida, Y. Sawada, T. Tadono, M. Fukuda, M. Sato 2011. Analysis of the sources of variation in L-band backscatter from terrains with permafrost, IEEE Trans. Geosci. Remote Sens., 50 (1) , pp. 44-54

Waters, J., Lea, D.J., Martin, M.J., Mirouze, I., Weaver, A. and While, J., 2015. Implementing a variational data assimilation system in an operational 1/4 degree global ocean model. Q.J.R. Meteorol. Soc., 141: 333-349. https://doi.org/10.1002/qj.2388.

Watson C.S., White, N., Church, J., Burgette, R., Tregoning, P., Coleman R., 2011. Absolute Calibration in Bass Strait, Australia: TOPEX/Poseidon, Jason-1 and OSTM/Jason-2, Marine Geodesy, 34:3-4, 242-260, doi: 10.1080/01490419.2011.584834.

WCRP Global Sea Level Budget Group (the), 2018. Global sea level budget, 1993-present, Earth System Science Data, 10, 1551-1590, https://doi.org/10.5194/essd-10-1551-2018,

Wentz F. J. and T. Meissner, 2007. Supplement 1: Algorithm theoretical basis document for AMSR-E ocean algorithms, Remote Sens. Syst., Santa Rosa, CA, USA, Tech. Rep. 051707.

Wentz F. J. and T. Meissner, 2016. Atmospheric absorption model for dry air and water vapor at microwave frequencies below 100 GHz derived from spaceborne radiometer observations, Radio Sci., vol. 51, no. 5, pp. 381–391.

Wentz, F. J., 1997. A well-calibrated ocean algorithm for special sensor microwave/imager, J. Geophys. Res., vol. 102, no. C4, pp. 8703–8718.

Werner, K., M. Fritz, N. Morata, K. Keil, A. Pavlov, I. Peeken, A. Nikolopoulos, H. S. Findlay, M. Kędra, S. Majaneva, A. Renner, S. Hendricks, M. Jacquot, M. Nicolaus, M. O'Regan, M. Sampei, C. Wegner, 2016. Arctic in Rapid Transition: Priorities for the future of marine and coastal research in the Arctic, Polar Science, 10, 364-373, https://doi.org/10.1016/j.polar.2016.04.005.

Werner, K., M. Fritz, N. Morata, K. Keil, A. Pavlov, I. Peeken, A. Nikolopoulos, H. S. Findlay, M. Kędra, S. Majaneva, A. Renner, S. Hendricks, M. Jacquot, M. Nicolaus, M. O'Regan, M. Sampei, C. Wegner, (2016), Arctic in Rapid Transition: Priorities for the future of marine and coastal research in the Arctic, Polar Science, Volume 10, Issue 3, 364-373, https://doi.org/10.1016/j.polar.2016.04.005.

Wessel, P., and W. H. F. Smith, 1996. A global, self-consistent, hierarchical, high-resolution shoreline database, J. Geophys. Res., 101(B4), 8741–8743, doi:10.1029/96JB00104.

Whiteman, G., Hope, C. and Wadhams, P. 2013. Vast costs of Arctic change. Nature 499, 401–403. https://doi.org/10.1038/499401a

Wiebe, H., G. Heygster and L. Meyer-Lerbs, 2008. Geolocation of AMSR-E Data. IEEE Trans. Geosci. and Remote Sensing 46(10), p. 3098-3103, doi:10.1109/TGRS.2008.919272.

Wiesmann, A., and C. Mätzler, 1999. Microwave emission model of layered snowpacks. Remote Sens. Environ., 70(3) 307 - 316.

Wilheit, T.T. and A. T. C. Chang, 1980. An algorithm for retrieval of ocean surface and atmospheric parameters from the observations of the scanning multichannel microwave radiometer. Radio Sci. 15, 525–544.

Wingham, D. J., Francis, C. R., Baker, S., Bouzinac, C., Brockley, D., Cullen, R., de Chateau-Thierry, P.. Laxon, S.W., Mallow, U., Mavrocordatos, C., Phalippou, L., Ratier, G., Rey, L., Rostan, F., Viau, P., Wallis, D.W., 2006. CryoSat: A mission to determine the fluctuations in Earth's land and marine ice fields, Advances in Space Research, 37, Issue 4, 841-871, https://doi.org/10.1016/j.asr.2005.07.027.

Wingham, D., 1995. The limiting resolution of ice-sheet elevations derived from pulse-limited satellite altimetry. Journal of Glaciology, 41(138), 413-422. doi:10.3189/S0022143000016282

WMO, 2017. Sea-Ice Information Services in the World, Edition 2017 (last revision 2017-08-02), WMO-No. 574 available from http://www.jcomm.info/index.php?option=com_oe&task=viewDocumentRecord&docID=9607

Xie, J., Counillon, F., Bertino, L., Tian-Kunze, X., and Kaleschke, L., 2016. Benefits of assimilating thin sea ice thickness from SMOS into the TOPAZ system, The Cryosphere, 10, 2745-2761, https://doi.org/10.5194/tc-10-2745-2016, 2016.

Yamazaki D., D. Ikeshima, J. Sosa, P.D. Bates, G.H. Allen, T.M. Pavelsky. MERIT Hydro: A high-resolution global hydrography map based on latest topography datasets Water Resources Research, vol.55, pp.5053-5073, 2019, (https://doi.org/10.1029/2019WR024873

Ye Y. and G. Heygster, 2016b. Arctic Multiyear Ice Concentration Retrieval from SSM/I Data Using the NASA Team Algorithm with Dynamic Tie Points. In: Lohmann G., Meggers H., Unnithan V., Wolf-Gladrow D., Notholt J., Bracher A. (eds) Towards an Interdisciplinary Approach in Earth System Science. Springer Earth System Sciences. Springer, Cham., https://doi.org/10.1007/978-3-319-13865-7_12

Ye, Y., M. Shokr, G. Heygster, and G. Spreen, 2016a. Improving Multiyear Sea Ice Concentration Estimates with Sea Ice Drift. Remote Sens. 2016, 8, 397.

Yu, Y., Sandwell, D. T., Dibarboure, G., Chen, C., & Wang, J. (2024). Accuracy and resolution of SWOT altimetry: Foundation seamounts. Earth and Space Science, 11, e2024EA003581. https://doi.org/10.1029/2024EA003581

Yueh, S. H., 1997. Modeling of wind direction signals in polarimetric sea surface brightness temperatures, IEEE Trans. Geosci. Remote Sens., vol. 35, no. 6, pp. 1400–1418.

Yueh, S. H., 2000. Estimates of Faraday rotation with passive microwave polarimetry for microwave remote sensing of Earth surfaces, IEEE Trans. Geosci. Remote Sens., vol. 38, no. 5, pp. 2434–2438.

Yueh, S. H., R. West, W. J. Wilson, F. K. Li, E. G. Njoku and Y. Rahmat-Samii, 2001. Error sources and feasibility for microwave remote sensing of ocean surface salinity, in IEEE Transactions on Geoscience and Remote Sensing, vol. 39, no. 5, pp. 1049-1060,. doi: 10.1109/36.921423

Yueh, S. H., W. J. Wilson, S. J. Dinardo, and S. V. Hsiao, 2006. Polarimetric microwave wind radiometer model function and retrieval testing for WindSat, IEEE Trans. Geosci. Remote Sens., vol. 44, no. 3, pp. 584–596.

Yueh, S., W. Tang, A. Fore, A. Hayashi, Y. T. Song, and G. Lagerloef, 2014. Aquarius geophysical model function and combined active passive algorithm for ocean surface salinity and wind retrieval, J. Geophys. Res. Oceans, 119, 5360–5379, doi:10.1002/2014JC009939.

Zabolotskikh, E. and B. Chapron, 2017. Improvements in Atmospheric Water Vapor Content Retrievals Over Open Oceans From Satellite Passive Microwave Radiometers, in IEEE Journal of Selected Topics in Applied Earth Observations and Remote Sensing, vol. 10, no. 7, pp. 3125-3133. doi: 10.1109/JSTARS.2017.2671920

Zabolotskikh, E. V., 2019. Review of Methods to Retrieve Sea-Ice Parameters from Satellite Microwave Radiometer Data, Izvestiya, Atmospheric and Oceanic Physics, 2019, Vol. 55, No. 1, pp. 109–127.

Zabolotskikh, E. V., Mitnik, L. M., and Chapron, B., 2013. New approach for severe marine weather study using satellite passive microwave sensing, Geophys. Res. Lett., 40, 3347– 3350, doi:10.1002/grl.50664.

Zabolotskikh, E., G. Irina, A. Myasoedov and . Chapron, 2016. Detection and study of the polar lows over the arctic sea ice edge, IEEE International Geoscience and Remote Sensing Symposium (IGARSS), Beijing, 2016, pp. 7705-7707. doi: 10.1109/IGARSS.2016.7731009

Zanifé, O. Z., P. Vincent, L. Amarouche, J. P. Dumont, P. Thibaut & S. Labroue, 2003. Comparison of the Ku-Band Range Noise Level and the Relative Sea-State Bias of the Jason-1, TOPEX, and Poseidon-1 Radar Altimeters. Special Issue: Jason-1 Calibration/Validation, Marine Geodesy, 26:3-4, 201-238, DOI: 10.1080/714044519

Zaron, E. D. 2017. Mapping the nonstationary internal tide with satellite altimetry, J. Geophys. Res. Oceans, 122, 539–554, doi:10.1002/2016JC012487.

Zaussinger, F., Dorigo, W., Gruber, A., Tarpanelli, A., Filippucci, P., Brocca, L. (2019). Estimating irrigation water use over the contiguous United States by combining satellite and reanalysis soil moisture data. Hydrology and Earth System Sciences 23, 897–923. https://doi.org/10.5194/hess-23-897-2019

Zawadzki L., Ablain, M., 2016. Accuracy of the mean sea level continuous record with future altimetric missions: Jason-3 vs. Sentinel-3a, Ocean Sci., 12, 9–18, 2016 www.ocean-sci.net/12/9/2016/ doi:10.5194/os-12-9-2016

Zelli, C, 1999. ENVISAT RA-2 advanced radar altimeter: Instrument design and pre-launch performance assessment review, Acta Astronautica, 44, Issues 7–12, 323-333, https://doi.org/10.1016/S0094-5765(99)00063-6.

Zhang, Z., Y. Yu, X. Li, F. Hui, X. Cheng and Z. Chen, 2019. Arctic Sea Ice Classification Using Microwave Scatterometer and Radiometer Data During 2002–2017, IEEE Transactions on Geoscience and Remote Sensing, vol. 57, no. 8, pp. 5319-5328, Aug. doi: 10.1109/TGRS.2019.2898872

Zhang, X., Jiang, L., Kittel, C. M. M., Yao, Z., Nielsen, K., Liu, Z., et al., 2020, On the performance of Sentinel-3 altimetry over new reservoirs: Approaches to determine onboard a priori elevation. Geophysical Research Letters, 47, e2020GL088770. https://doi.org/10.1029/2020GL088770

Zhao, J., Hernández-Pajares, M., Li, Z. et al.2021. Integrity investigation of global ionospheric TEC maps for high-precision positioning. J Geod 95, 35. https://doi.org/10.1007/s00190-021-01487-8

Zhao, Z., 2019. Mapping internal tides from satellite altimetry without blind directions. Journal of Geophysical Research: Oceans, 124, 8605– 8625. https://doi.org/10.1029/2019JC015507

Zheng, J., T. Geldsetzer, and J. Yackel, 2017. Snow thickness estimation on first-year sea ice using microwave and optical remote sensing with melt modelling, In Remote Sensing of Environment, Volume 199, 2017, Pages 321-332, ISSN 0034-4257, https://doi.org/10.1016/j.rse.2017.06.038.

Zhou, L., Xu, S., Liu, J., and Wang, B., 2018. On the retrieval of sea ice thickness and snow depth using concurrent laser altimetry and L-band remote sensing data, The Cryosphere, 12, 993-1012, https://doi.org/10.5194/tc-12-993-2018.

APPENDIX I DEFINITION OF TERMS

Absolute Dynamic Topography: the mean sea surface height with respect to the geoid

Absolute Performance Error (APE): difference between the target (commanded) parameter (e.g. attitude, geolocation etc) and the actual parameter in a specified reference frame (ESSB-HB-E-003, 2011).

Absolute Knowledge Error (AKE): difference between an actual parameter (e.g. attitude, geolocation etc.) and the known (measured or estimated) parameter in a specified reference frame (ESSB-HB-E-003, 2011).

Across track direction: direction orthogonal to the projection of the spacecraft velocity on the tangent plane to the Earth at the geodetic sub-satellite position

Along track direction: direction parallel to the projection of the spacecraft velocity on the tangent plane to the Earth at the geodetic sub-satellite position.

Altitude: the satellite altitude is the shortest distance from the satellite centre of mass to the Earth surface.

Ancillary Data: data acquired on-board in support of the observation data, both for the instrument and the platform, such as calibration and timing data.

Auxiliary Data: supporting data sets provided outside the Space Segment data stream used to apply corrections to the Space Segment sensor data. Examples include: previously derived calibration parameters, ground control data, NWP data, or external imager data.

> **Instrument Ancillary data**: data generated on-board by the instrument in support of the observation data, such as calibration, timing for each line acquisition, compression ratio, data validity flag (e.g. nominal detector temperature), needed to process the measurement data on ground.
>
> **Platform Ancillary data**: data acquired on-board by the platform in support of the observation data, such as orbit position, velocity and time, attitude (generated by the AOCS sensors) needed to process measurement data on ground. Depending on timing constraints (NRT1H, NRT3H product or not), these data will be post-processed on-ground to improve the accuracy of orbit and attitude restitution.

Ascending Node Crossing (ANX): the latest crossing of the equator by the satellite going from South to North.

Availability: the probability that the space segment (including the link to the ground segment) provides all the required data with their nominal quality and within the specified timeliness.

> Note 1: All sources of unavailability after acquisition of the operational orbit and commissioning, validation and initial calibration shall be considered. Examples are planned and unplanned orbital excursions (e.g. manoeuvres required for orbit control and maintenance if incompatible with image acquisition), atmospheric effects (e.g. leading to space-to-ground link outages), single event upsets due to cosmic ray effects, time spent in safe mode.

Note 2: The space segment availability covers the instrument itself and all on-board elements needed to support the instrument, including the satellite data chain and the downlink transmission.

Note 3: The availability of ground segment is assumed to be 100%.

Bandwidth: difference between the upper and lower frequencies in a continuous set of frequencies.

Beam Efficiency (η_{be}): the ratio between the received power (including co- and x-polar radiation) in the main beam and the total received power (including co- and x-polar radiation) over the full sphere:

$$\eta_{be} = \frac{\int_0^{2\pi}\int_0^{\theta_1} (|E_{co}(\theta,\varphi)|^2 + |E_x(\theta,\varphi)|^2)\, sin\theta d\theta d\varphi}{\int_0^{2\pi}\int_0^{\pi} (|E_{co}(\theta,\varphi)|^2 + |E_x(\theta,\varphi)|^2)\, sin\theta d\theta d\varphi}$$

where θ_1 equal to 2.5 x θ_{3dB} footprint are the electric field co-polar and cross-polar components.

Brightness temperature (Tb): a measurement of microwave radiation radiance traveling upward from the top of the atmosphere (TOA) to the satellite, expressed in units of the temperature of an equivalent black body.

Note 1: Tb is the fundamental parameter measured by a microwave radiometer. TOA Tb is specific to a satellite implementation and refers to the measurement made in a specific frequency band, at a given polarization, with a specific instrument viewing the earth using a specific geometry. For clarity this includes all emission, reflection and scattering processes and Faraday rotation effects at the antenna.

Calibration: CEOS define Calibration as: “the process of quantitatively defining a system’s responses to known, controlled signal inputs”. Calibration includes aspects of the measurement system which need to be addressed in the generation of all level 1b data products. Since level 1b algorithms and associated products take care of the conversion from the instruments’ measurement quantities (engineering units) into standard physical (SI) units, they may be addressed by many techniques. Examples of calibration are the compensation for internal path delay in computing the apparent echo range, phase or power measurement from an altimeter, or compensating for gain and linearity in generating brightness temperature as measured by a microwave radiometer. Calibration parameters are applied during the generation of the level 1b data products. Pre-launch estimates will be available (and initially used) but, as far as possible, improved estimates need to be established in-orbit. Furthermore, the uncertainty associated with these calibration parameters will be characterised in-orbit.

Calibration Mode: mode of operation defined to support the in-flight characterisation of the payload.

Calibration key data: required for processing the Level 0 to Level 1b data. Since the characteristics of the instrument can (and will) change over the mission, the calibration key data will change along with it. At launch, the calibration key data will consist of the data that is derived from on-ground calibration. During the mission the calibration key data will be updated with in-flight calibration data and adapted to match new insights in the instrument's performance.

Calibration key data set: a set of data products that contains the calibration key data for a given orbit. The calibration key data set can consist of several files containing the actual data, for example in HDF or NetCDF format, and a descriptive file, for example in XML, that specifies, which parameter can be found in which data file.

Characterisation: the direct measurement, or analytical derivation from measurement, of a set of technical and functional parameters, over a range of conditions (e.g. temperature) to provide data necessary for calibration, ground processor initialisation and verification. Characterisation can be performed either before launch on-ground and/or in-flight. In-flight, at least all those parameters have to be determined that may have varied since on-ground characterisation or which have not been measurable on-ground. In-flight characterisation may be based either on data derived from facilities built into the instrument (internal calibration) and/or on external sources (external calibration).

Commissioning: verification and validation activities conducted after the launch and before the entry in operational service either on the space segment only or on the overall system (including the ground segment).

Coastal Zone: (see coastal region)

Coastline Boundary: boundary separating land from ocean defined by the Hierarchical, full-resolution (0.04 km) Shoreline (GSHHS) high-resolution dataset (Wessel and Smith (1996) available from https://www.ngdc.noaa.gov/mgg/shorelines/gshhs.html).

Coastal Region: includes all small islands is defined as 2*the largest microwave radiometer footprint size or 50 km (TBC) [S3NG-T-UN-022] (whichever is largest) on both sides of the Coastline Boundary (i.e. the Coastal Region is nominally 100 km in extent).

Coverage: geographical area systematically acquired over the earth surface.

Cross-Polarisation: radiation orthogonal to the desired polarisation (e.g. the cross-polarisation of a vertically polarised antenna is the horizontally polarised field).

> Note 1: Cross- polarisation power refers to the total power received in cross-polarisation in the main beam of the antenna, divided by the total power received by the antenna (in co- and cross- polarisations).

Cycle: one full completion of an orbit repeat period. A cycle starts at the equator when combined with orbit numbers, at the southern rollover point in when combined with pass numbers.

Data Latency: the time interval from data acquisition by the instrument to delivery as Level 1b data product at the user segment interface.

Dynamic range: range of brightness temperatures within which requirements are to be met.

Effective Field of View (IFOV): -3dB region of an antenna gain pattern projected onto and swept over the Earth Surface for a measurement integration time.

End Of Life (EOL): this event occurs at the end of the system in-orbit lifetime.

Fiducial Reference Measurement (FRM): the suite of independent ground measurements that provide the maximum Scientific Utility and Return On Investment for a satellite mission by delivering, to users, the required confidence in data products, in the form of independent validation results and satellite measurement uncertainty estimation, over the duration of the mission. The defining mandatory characteristics of an FRM are:

- Have documented evidence of SI traceability via inter-comparison of instruments under operational-like conditions.
- Are independent from the satellite retrieval process.
- Include an uncertainty budget for all FRM instruments and derived measurements is available and maintained, traceable where appropriate to SI ideally directly through an NMI
- Are collected using measurement protocols and community-wide management practices (measurement, processing, archive, documents etc.) are defined and adhered to.
- FRM uncertainties should be fit for purpose (i.e. be of a magnitude that is relevant to the application e.g. “Validation of satellite derived TSCV 0.1 ms^{-1} or better”).

First-year Ice: Sea ice of not more than one winter’s growth, developing from young ice; thickness 0.3 m - 2 m, and sometimes slightly more in areas where deformation and ridging have occurred. May be subdivided into thin first-year ice, medium first-year ice and thick first-year ice.

Floating Ice: Any form of ice floating in water. The principal kinds of floating ice at the sea surface are sea ice which is formed by the freezing of sea water at the surface, lake ice and river ice formed on rivers or lakes and glacier ice in ice shelves (ice of land origin).

Floe: Any relatively flat piece of sea ice 20 m or more across. Floes are subdivided according to horizontal extent (giant, vast, big, medium, small).

Freeboard: Sea ice freeboard is the distance between the interpolated local sea surface and the ice-air interface or, in the case of snow layer, to ice-snow interface.

Glacier Ice: Ice in, or originating from, a glacier, whether on land or floating on the sea as icebergs, bergy bits or growlers.

Glacier: A mass of ice predominantly of atmospheric origin, usually moving from higher to lower ground. A seaward margin of a glacier that is aground, the rock basement being at or below sea-level, is termed an ice wall. The projecting seaward extension of a glacier, which is usually afloat, is termed a glacier tongue. In the Antarctic, glacier tongues may extend over many tens of kilometres.

Geo-location: worst-case spatial sample localisation (to zero mean 1-sigma knowledge error) knowledge expressed in geodetic coordinates within a Level 1B image product.

Geo-location Accuracy: difference between the estimated barycentre position of any spatial sample and its true position projected onto the WGS84 reference Earth ellipsoid.

Geometrical Coverage time: represents the time required to perform systematic acquisition of a given area disregarding precipitation and possibly under different observation conditions (in particular varying measurement geometry).

Geometrical Revisit time: represents the period for systematic acquisition of the same area disregarding precipitation and under the same observation conditions.

Goal: a non-mandatory but highly desirable requirement, the implementation of which shall be studied to allow for an assessment of the system impacts. The implementation or not of the goal requirements will be decided by the Agency after analysis of the implications.

Half Power Beam-width (HPBW): angle at which the antenna's power radiation pattern is at half its maximum value.

Height: The elevation of the actual surface observed above the reference ellipsoid.

Horizontal Polarisation (H): electric field is perpendicular to the plane of incidence.

Housekeeping Telemetry: refers to all non-science TM that is generated on-board, either on a periodic basis (Periodic Housekeeping TM) or as on-board events, or on request (report of parameters and tables, dump of memories, dump of data, etc.)

Ice Shelf: A floating ice sheet of considerable thickness with freeboard of 5 - 60 m or more above sea-level, attached to the coast or a glacier. Usually of great horizontal extent and with a level or gently undulating surface. Nourished by annual snow accumulation at the surface and often also by the seaward extension of land glaciers. Limited areas may be aground. The seaward edge is termed an ice front.

Iceberg: A massive piece of ice of varying shape, protruding more than 5 m above sea level, which has broken away from a glacier or an ice shelf, and which may be afloat or aground. Icebergs by their external look may be subdivided into tabular, dome-shaped, sloping and rounded bergs.

Ice Cover: Floating ice covering a water area regardless of its age, concentration, mobility and other characteristics. This is the most general notion, usually requiring further specification. The ice cover boundaries are the ice edge and the coastline.

Ionospheric path delay: also called the ionospheric bias correction, compensates for the free electrons in the Earth's ionosphere slowing a radar pulse. Solar control of the ionosphere leads to geographic and temporal variations in the free electron content, which can be modelled, or measured.

Image: ensemble of data acquired over a two-dimensional scene with equal number of spatial samples in the cross and along track direction. The number of spatial samples in cross track is defined by the instrument swath and spatial sampling interval.

Image Navigation: the knowledge of the relationship between a spatial sample in instrument coordinates and the corresponding point on the Earth, given by latitude and longitude coordinates.

> Note 1: In general, Image navigation refers to the methods employed to obtain that knowledge. Image navigation accuracy is a measure of how well that relationship is known. Image registration is an indication as to how well that navigation knowledge is maintained and controlled over time.

Image swath: maximum distance on ground between the positions of two spatial samples belonging to the scan line or row.

Inland seas: shallow sea that covers central areas of continents during periods of high sea level that result in marine transgressions. Modern inland seas include: the Marma Sea, Baltic Sea, White Sea, Black Sea, Hidson Bay (including James Bay), Seto Inland Sea, Caspian Sea.

In-Orbit Lifetime: period of time between the beginning of the in-orbit commissioning and the end of the delivery of data by the satellite.

Integration time: time it takes for the instrument scan mechanism to scan across the angular distance corresponding to the footprint ellipse minor axis.

Instrument Field of View (FOV): the angle subtended at the satellite nadir point between the most extreme position on the left-hand part of the instrument swath and the most extreme position on the right-hand part of the instrument swath.

Instantaneous Field of View (IFOV): -3dB region of an antenna gain pattern projected onto the Earth Surface where the measurement integration time is zero.

Inter-channel spatial co-registration: maximum equivalent ground distance between the positions of all pairs of spatial samples acquired in two channels and related to the same target on Earth.

Inter-channel temporal co-registration: maximum time interval between the acquisitions of channels related to the same target on Earth.

Inter-channel radiometric accuracy: unknown bias error (difference between measured value and true value) of the ratio of radiances measured in two channels and associated to the same target on Earth. The inter-channel radiometric accuracy shall be demonstrated by averaging a sufficiently large number of samples such that the residual temporal variation does not dominate the calculation.

Lead: A more than 50 m wide rectilinear or wedge-shaped crack, from several kilometres to several hundreds of kilometres in length. At below freezing temperatures, new, nilas and young ice forms at the surface of leads.

Main Beam: angular region within 2.5 times the ellipse representing the 3dB angular contour of the antenna pattern (see Full Beam for schematic). This ellipse is referred to as the “3dB contour Ellipse”.

> Note 1: The ellipse representing the 3dB angular contour of the antenna pattern is defined as in the following:
>
> Note 2: The major axis is defined by the straight-line segment connecting the two points at maximum distance lying on the 3dB contour;
>
> Note 3: The minor axis is a segment, orthogonal to the major axis, and passing through the centre of the major axis. Its length is the maximum distance between any two points lying on the 3dB contour along the direction orthogonal to the major axis.

Nadir: nadir direction is defined as the line from the centre of the satellite reference frame that is perpendicular to the reference ellipsoid tangent.

Near Real-Time (NRT): information or data available within a few seconds (typically reserved for activities on-board the spacecraft).

Near-Real-Time-3-Hour (NRT3H): products are available in less than 3 hours at the point of user pickup after data acquisition by the satellite. NRT3H products are used for operational applications such as sea ice services, operational oceanography and meteorology, and in support of operational hydrology users.

Nominal Operational Lifetime: the time in orbit over which the performance has to be met with a given satellite availability and excluding the time necessary for the execution of LEOP and commissioning.

Non-Time-Critical (NTC): products are available in less than 30 days at the point of user pickup after data acquisition by the satellite. NTC rely on the availability of auxiliary of the highest quality. NTC is linked to the delivery timeliness of the Copernicus POD Service and application of precise orbit ephemeris (POE) from the Copernicus POD Service (CPOD) is applied. NTC products are consolidated products as they are generated using the most precise auxiliary information available and target climate users

Short Time Critical (STC): products are available at the user point of pickup no later than 36 hours from measurement acquisition. STC is linked to the delivery timeliness of the Copernicus POD Service and application of medium orbit ephemeris (MOE) from the Copernicus POD Service (CPOD) is applied. STC products are used for operational applications such as sea ice services, operational oceanography and meteorology.

Old Ice: Sea ice which has survived at least one summer's melt; typical thickness up to 3m or more. It is subdivided into residual first-year ice, second-year ice and multi-year ice.

Orbit: one full revolution of the satellite starting and ending at an ascending node.

NOTE 1: a satellite orbit can be specified in two ways: absolute orbit and relative to a specific orbit cycle. The orbit numbers are specified at the sensing start time and sensing stop time of the product.

Orbit sub-cycle: Orbital sub-cycles are defined as a period of near-repeat for Earth remote-sensing satellites. A sub-cycle corresponds to the time needed to collect a coverage that is globally homogeneous and such that the ground-track difference at the equator after N days between the ascending node crossing longitude and the initial one is smaller than X km, see also Dibarboure et al (2018).

Out-of-band rejection: the minimum level of suppression of a signal outside of specified channel.

Pass: spans half an orbital revolution and is either ascending (South-North) or descending (North-South). This means that a pass always starts at the turnover point, i.e. the passing near the South or North Pole. The pass number represents the number of passes since the beginning of the mission (absolute) or since the beginning of the cycle (relative). Odd pass numbers are ascending, even are descending.

Payload: see instrument

Payload Data Ground Segment (PDGS): elements of the ground segment that perform the functions of data processing, archiving and distribution to the users. They normally

also perform the long-term calibration and control the quality and status of the instrument(s) and data products.

Platform: parts of the satellite that provide the functionalities and resources required to operate the instrument and to control and monitor the satellite.

Polarisation sensitivity: assuming measurement of a stable, spatially uniform, linearly polarized scene, the polarization sensitivity is defined as:

$$P = \frac{S_{\max} - S_{\min}}{S_{\max} + S_{\min}}$$

where S_{max} and S_{min} are the maximum and minimum sample values obtained when the polarization is gradually rotated over 180 deg.

Precision: difference between one result and the mean of several results obtained by the same method, i.e. reproducibility (includes random uncertainties only).

NOTE: Precision describes the spread of these measurements when repeated. A measurement that has high precision has good repeatability. The statistical standard deviation derived from a number of repeated measurements may serve as a measure of precision.

Product level definitions: the concept of product levels, and the definitions thereof, have been codified by CEOS (Committee on Earth Observation Satellites). The CEOS definitions are the basis for the product levels defined in these requirements, with appropriate modifications since the original definitions were formulated with imaging sensors in mind. Data downlinked from the satellite consist of a serial stream of data bits embedded within a framework of transfer frames appropriate for the purpose. This level of data, which may be temporarily archived at the reception station, is not readable by a general-purpose computer and not included in the set of product level definitions.

Level	Description
L0	Reconstructed, unprocessed instrument and payload data at full resolution, with any and all communications artefacts (e.g., synchronization frames, communications headers, duplicate data) removed.
L1a	L0 data reconstructed, unprocessed instrument data at full resolution, time-referenced, and annotated with ancillary information, including radiometric and geometric calibration coefficients and geo-referencing parameters (e.g., platform ephemeris) computed and appended but not applied to the data.
L1b	Level 1a data that have been quality controlled and reformatted but not resampled All radiometric and spectral calibration have been applied to provide top-of-atmosphere spectral brightness temperatures (Tb) in units of Kelvin. Geometric information is computed, appended but not applied. Preliminary pixel classification is included in the product.
L2	Derived geophysical variables at the same resolution and location as Level 1 source data.
L2P	Mono-mission Level 2 altimeter products with enhanced geophysical corrections and biases accounted for so that they can easily be combined with Level 2P data from other altimeter missions.

L3	Variables mapped on uniform space-time grid scales, usually with some completeness and consistency. L3U (Uncollated) product are from gridded individual satellite swath data. L3C (generally referred to as L3) collate several swaths from an instrument (e.g. daily composite).
L4	Results from analyses of lower-level data (e.g., variables derived from multiple measurements) typically using an analysis technique (e.g. optimal estimation) or a model.

Within these general definitions several distinct products may be defined at each level, containing different levels of detail in the parameters provided.

Radiometric accuracy: see Absolute radiometric accuracy.

Radiometric resolution: smallest change of radiometric sensitivity that can be measured.

Radiometric Sensitivity (NEΔT): smallest value of input brightness temperature or radiance that can be detected in the system output for an integration time that is compliant with each individual radiometer footprint along the conical scan direction.

NOTE: The sensitivity requirement applies to calibrated radiances and is applicable throughout the dynamic range. System noise, gain variations and calibration noise shall be taken into account when calculating the sensitivity. In case of multiple beams for single channel the definition and the associated requirements for NEΔT applies to each individual footprint and related integration time. The following formula shall be used:

$$NE\Delta T = (T_{SYS} + T_{scene})\sqrt{\left(\frac{1}{B\tau}\right) + \left(\frac{\Delta G}{G}\right)^2 + \left(\frac{1}{BN\tau_C}\right)}$$

where TSYS is the receiver noise temperature (including antenna losses), Tscene is the scene temperature, B is the bandwidth, τ is the integration time ΔG/G is the receiver gain variation, τc is the calibration target integration time and N is the number of calibration cycles averaged.

Radiometric Stability: degree to which radiometric accuracy remains constants over time.

NOTE: Changes in radiometric stability, also known as drift, can be due to components aging, decrease in sensitivity of components, and/or a change in the signal to noise ratio, etc. Radiometric stability is quantified as the standard deviation of measurement differences when viewing an invariant and homogeneous calibration target(s) over a defined period of time and of such magnitude that NEΔT is insignificant, with the system operating within its dynamic range.

Range: one-way distance from the satellite to the target surface.

Relative Pointing Error (RPE): angular separation between the instantaneous pointing direction and the short-time average pointing direction at a given period.

Reference Altitude: the difference between the mean semi-major axis of a circular orbit having the orbital period specified by the repeat cycle and the Earth's equatorial radius.

The satellite altitude differs from the reference altitude, depending on the satellite's location along its orbit.

Residual first-year Ice: First-year ice that has survived the summer's melt and is now in the new cycle of growth. It is 30 to 180 cm thick depending on the region where it was in summer. After 1 January (in the Southern hemisphere after 1 July), this ice is called second-year ice.

Revisit time: time between two consecutive possible observations of a same target within the specified incidence angle range.

Sample: measurement made during a fraction of the L1b integration time.

Satellite or Spacecraft: refers to each one of the independently flying elements of the space segment. It comprises all hardware to be placed into Earth orbit with the exception of the launch vehicle. The satellite is composed of the platform and the instrument.

Sea Ice: Ice, which has originated from the freezing of sea water. It presents the main kind of floating ice encountered at sea.

Sea Ice Concentration: The ratio of the area of ice features to the total area of a sea part (zone) delineated on the chart, expressed in tenths. The total concentration includes all stages of development and the partial concentration includes areas of ice of specific age or arrangement which comprise only part of the total concentration. Written as the ratio of sea ice to water, either a fraction (8/10) or percentage (80%) of sea ice coverage.

Sea Ice Extent: Total area covered by some amount of sea ice at a given time, including open water between floes.

Sea ice thickness: Sea ice thickness is the vertical thickness of the floating ice, converted from freeboard assuming hydrostatic equilibrium, and excludes the snow layer on top. The thickness over an area or orbit segment is the average thickness excluding ice free areas.

Second-year Ice: Old ice which has survived only one summer's melt; typical thickness up to 2.5 m and sometimes more. Because it is thicker than first-year ice, it has a larger freeboard. Ridged features as a result of melting during the preceding summer attain a smoothed rounded shape. In summer, numerous melt ponds of extended irregular shape form on its surface. Bare ice patches and melt ponds are usually greenish-blue.

Sea Surface Height Anomaly: (SSHA) the difference between the long-term average sea surface height, i.e. the MSS, and the ocean height actually observed by the satellite.

Sea Surface Salinity: Sea Surface Salinity (SSS) is expressed according to the Practical Salinity Scale (UNESCO, 1985) defined as conductivity ratio: a seawater sample of Practical Salinity 35 has a conductivity ratio of 1.0 at 15°C and 1 atmosphere pressure, using a potassium chloride (KCl) standard solution containing a mass of 32.4356 grams of KCl per Kg of solution. Thus SSS is ratio quantity and has no physical units. The use of PSU or PSS as a physical unit for SSS is incorrect. However, the use of PSS to indicate that the PSS scale has been used is appropriate.

Side Lobe: lobes of local maxima in the far field radiation pattern that are not the main beam (see Full beam for schematic).

NOTE: Multiple side lobes may exist in any given antenna gain pattern and the peak side lobe is the largest magnitude side lobe.

Signal to Noise Ratio: ratio of signal power to the noise power.

Significant wave height (Hs or incorrectly, SWH): the mean of the highest third of the waves; instead of Hs the notation H1/3 is also often used. Hs represents well the average height of the highest waves in a wave group. The significant wave height can also be computed from the wave energy.

Spatial Resolution: see footprint_size.

Spatial Sampling Distance (SSD): distance between the centre of adjacent footprint samples on the Earth's surface.

Sub-Satellite Point (SSP): the point on the Earth's reference ellipsoid that intersects the nadir direction.

Swath width: the across-track ground which is imaged and over which the performance requirements are met.

System Gain: the overall gain of the instrument channel (from the antenna aperture to the instrument output).

Topography parameters: the collective suite of measurements derived from Sentinel-3 including ocean parameters, river and lake parameters, sea ice parameters, ice sheet parameters and atmospheric parameters. These parameters have different time and space scales and can be inter-related.

Total Standard Uncertainty: From *Bell* (1999) accuracy (or rather inaccuracy) is not the same as uncertainty. Unfortunately, usage of these words is often confused. Correctly speaking, 'accuracy' is a qualitative term (e.g. one could say that a measurement was 'accurate' or 'not accurate'). Uncertainty is quantitative. When a 'plus or minus' figure is quoted, it may be called an uncertainty, but not an accuracy.

For Sentinel-3 ARA is not used in the traditional manner but instead we calculate the Total Standard Uncertainty (which is a zero mean "1-sigma" total uncertainty). The strength of this approach is that each component of the total standard uncertainty can be validated (which is not the case for ARA which implies a reference of "truth"). It is noted that this approach, while consistent with international agreements on uncertainty specification (JCGM, 2008), it is different compared to other formulations (e.g. as for the MetOp-SG(B) MWI) that do not include NE∆T/NESZ as part of the absolute radiometric accuracy definition. Four components of Total Standard Uncertainty are: NE∆T or NESZ, Lifetime radiometric stability, orbital stability and beginning of life uncertainty. The total standard uncertainty for a single measurement (in one channel) is the combination of uncertainty from random and systematic effects. These correctly combine in quadrature:

$$u_{total} = \sqrt{u_{random}^2 + u_{systematic}^2} \qquad \text{(Eqn. 4.2.10.1)}$$

Channel NE∆T addresses the uncertainty from random effects in the instrument.

The stability requirements limit the excursions of the calibration from "truth" on slower timescales: the orbit stability requirement constrains the drift of the calibration on orbital

timescales; the lifetime stability constrains the degree of drift of calibration over the mission lifetime; and one further component is required to obtain the total standard uncertainty, namely the beginning of life uncertainty of pre-launch calibration knowledge ($u_{pl\text{-}cal}$) e.g. derived from ground characterisation). In particular, $u_{pl\text{-}cal}$ implies a rigorous pre-launch characterisation of the instrument (and thus links to the calibration and validation plans). This is consistent with the definition of all quantities as zero mean 1-sigma standard deviations in the MRD requirements. Therefore, the requirements adhere to the formulation of Total Standard Uncertainty. As an example, for Microwave Radiometry, TSU can be expressed as:

$$u_{total}^2 \cong u_{NE\Delta T}^2 + u_{orbit-stability}^2 + u_{lifetime-stability}^2 + u_{pl-cal}^2 \text{(Eqn. 4.2.10.2)}$$

Interpretation of total standard uncertainty, NE∆T, orbital stability and the lifetime stability as uncertainty components is consistent with the definition of all of them as zero mean **1-sigma** standard deviations in the MRD requirements.

Uncertainty: the closeness of agreement between the result of a measurement and a true value of a measurand as follows:

- **Uncertainty (of measurement):** parameter, associated with the result of a measurement, that characterizes the dispersion of the values that could reasonably be attributed to the measurand.
- **Standard Uncertainty:** uncertainty of the result of a measurement expressed as a standard deviation
- **Type A evaluation (of uncertainty):** method of evaluation of uncertainty by the statistical analysis of series of observations
- **Type B evaluation (of uncertainty):** method of evaluation of uncertainty by means other than the statistical analysis of series of observations
- **Combined standard uncertainty:** standard uncertainty of the result of a measurement when that result is obtained from the values of a number of other quantities, equal to the positive square root of a sum of terms, the terms being the variances or covariances of these other quantities

Validation: confirmation, through the provision of objective evidence, that the requirements for a specific intended use or application have been fulfilled.

NOTE: CEOS definition is the process of assessing by independent means the quality of the data products (the results) derived from the system outputs.

Validation typically focusses on Level 2 data products after conversion of instrument measurements into geophysical quantities. Validation results in the end-to-end characterisation of the uncertainty of geophysical parameters (SSH, Hs and wind speed) derived from the calibrated altimeter echoes (which are termed retrieval errors) and in the ground processing system and algorithms that are implemented. Validation is a core component of a satellite mission (and should be planned for accordingly) starting at the moment satellite instrument data begin to flow until the end of the mission. Without adequate validation, the geophysical retrieval methods, algorithms, and geophysical parameters derived from satellite measurements cannot be used with confidence and the return on investment for the satellite mission is reduced. In addition, meaningful

uncertainty estimates cannot be provided to users. Once on-orbit, the uncertainty characteristics of (a) the satellite instruments (i.e. altimeter, microwave radiometers, GNSS, etc.) established during pre-launch laboratory calibration and characterisation activities and (b) the end-to-end instrument measurements (e.g. microwave brightness temperature, radar power and backscatter) from which geophysical measurements (e.g. SSH) are retrieved, can only be assessed via independent calibration and validation activities.

Verification: confirmation, through the provision of objective evidence, that the specified requirements have been fulfilled.

Vertical Polarisation (V): electric field is parallel to the plane of incidence.

Water Surface Elevation (WSE): height of surface of continental water bodies in meters above the geoid.

Wide Beam: angular region 3.0 times the ellipse representing the 3dB angular contour described by the antenna pattern (see Full Beam for schematic).

Wave peak period: Tp, the wave period with the highest energy.

Wave Spectrum: The energy density spectrum of a sea state, generally designated by *E(f).*

Wide Beam Efficiency: the ratio of total (cross- and co-polarised) power received by an antenna within its wide beam to the total power received from the full sphere, assuming isotropic and unpolarised illumination of broadband noise such as thermal radiation.

APPENDIX II MAJOR POLICIES AND EARTH OBSERVATION APPLICATIONS SUPPORTED BY THE S3NG-T MISSION

Table II-1: Summary major policies and EO applications supported by the S3NG-T mission.

Policies Directives	Applications	User Requirements	User entities
EU Integrated Policy on the Arctic	Climate Change and the Arctic Environment, sustainable development in the Arctic, International cooperation on Arctic matters,	Monitoring of floating sea ice and ocean surface parameters with high spatial resolution to support sustainable development and environmental security, cooperation and long-term monitoring of societal impacts in the Arctic Environment. Enhance the safety of navigation in the Arctic.	Arctic States, EC, ESIF[20], UN, UNCLOS[21], ECGFF[22], ACGF[23], TEN-T[24], OSPAR, GEOCRI.
Water Framework Directive—2000/60/EC.	Water rights management, Water pricing, Ground water abstraction limits, Protection of inland and coastal water surfaces. Available online: https://eur-lex.europa.eu/legal-content/EN/TXT/?uri=celex:32000L0060.	Monitoring of water use from field scale to irrigation system level for enforcing sustainable water abstraction for agricultural production	EEA; national and river basin management authorities, coastal communities
Marine Strategy Framework Directive—2008/56/EC. **SWD/2020/62 final** **SWD/2020/61 final** **SWD/2020/60 final**	Available online: https://eur-lex.europa.eu/legal-content/EN/TXT/?uri=CELEX%3A32008L0056 SWD- Background document for the Marine Strategy Framework Directive on the determination of good environmental status and its links to assessments and the setting of environmental targets Accompanying the Report from the Commission to the European Parliament and the Council on the implementation of the Marine Strategy Framework Directive (Directive 2008/56/EC) SWD - Review of the status of the marine environment in the European Union Towards clean, healthy and productive oceans and seas Accompanying the Report from the Commission to the European Parliament and the Council on the	Good environmental status, pollutions, protected areas,	Coastal authorities; energy sector, blue economy sector, Rregional sea conventions

[20] European Structural and Investment Funds

[21] UN Convention on the Law of the Sea (UNCLOS)

[22] European Coast Guard Functions Forum (ECGFF)

[23] Arctic Coast Guard Forum (ACGF)

[24] trans-European Network for Transport (TEN-T)

	implementation of the Marine Strategy Framework Directive (Directive 2008/56/EC) SWD - Key stages and progress up to 2019 Accompanying the Report from the Commission to the European Parliament and the Council on the implementation of the Marine Strategy Framework Directive (Directive 2008/56/EC)		
UN Sustainable Development Goals	Water use efficiency and management, Sustainable agricultural production	Reporting on the SDG 6.4 for increase water-use efficiency across all sectors and ensure sustainable withdrawals.	National statistical offices, UNEP, UN Statistics
UN Framework Convention on Climate Change	Risk management and climate change adaptation	Mitigating water scarcity impacts related to climate change or extreme weather calamities	Insurance providers; farmers; national water authorities
COM/2020/788 final **European climate pact**	Communication from the Commission to the European Parliament, the Council, the European Economic and Social Committee and the Committee of the regions European Climate Pact		
COM/2020/562 final **2030 Climate ambition**	Communication from the commission to the European parliament, the council, the European economic and social committee and the committee of the regions Stepping up Europe's 2030 climate ambition Investing in a climate-neutral future for the benefit of our people		
COM/2020/329 final **Atlantic marine strategy**	Communication from the commission to the European parliament, the council, the European economic and social committee and the committee of the regions A new approach to the Atlantic maritime strategy – Atlantic action plan 2.0 An updated action plan for a sustainable, resilient and competitive blue economy in the European Union Atlantic area		
SWD/2020/140 final **Atlantic action plan 2.0**	Commission staff working document accompanying the document communication from the commission to the European parliament, the council, the European economic and social committee and the committee of the regions A new approach to the Atlantic maritime strategy – Atlantic action plan 2.0 An updated action plan for a sustainable, resilient and competitive blue economy in the European Union Atlantic area		
Convention for the Protection of the Marine Environment	OSPAR work areas: biological diversity & ecosystems, hazardous substances & eutrophication, human	Marine biodiversity indicator remote sensing, need for higher accuracy	OSPAR contracting parties, Users of nautical charts and sailing

of the North-East Atlantic (the 'OSPAR Convention')	activities, offshore industry, radioactive substances, cross cutting issues. https://www.ospar.org/about	of measurements and classification, continuity of data sources	directions in high risk/ prohibited areas, more general users of the coastline, Fishermen etc.
Northern Dimension policy framework	Thematic partnerships related to environment (NDEP), public health and social well-being (NDPHS), transport and logistics (NDPTL), and culture (NDPC). The Northern Dimension policy aims at providing a common framework for the promotion of dialogue and cooperation, strengthening stability, well-being and intensified economic cooperation, promotion of economic integration and competitiveness and sustainable development in Northern Europe. https://eeas.europa.eu/diplomatic-network/northern-dimension_en	Arctic coastal zone monitoring, satellite hydrographic monitoring and assessment of environmental trends along the arctic coast.	Regional and sub-regional organizations and commissions in the Baltic and Barents area, the sub-national and local authorities, non-governmental organizations and other civil society organizations (including notably indigenous peoples' organizations), universities and research centres, business and trade union communities, etc.
European Maritime Transport Policy	Maritime Safety and Security; Digitalisation and Administrative Simplification; Environmental Sustainability and Decarbonisation; Raising the Profile and Qualifications of Seafarers and Maritime Professions and; EU Shipping: A stronger global player. https://ec.europa.eu/transport/themes/strategies/2018_maritime_transport_strategy_en	Floating sea ice and ocean surface parameters to be monitored with high spatial resolution.	Shipping operators, Maritime transport industry, CLIA[25] , EBA[26], ECSA[27], EMPA[28], ETF[29], Interferry, and WSC[30]
IMO International Code for ships operating in polar waters (Polar Code)	The Polar Code is intended to cover the full range of shipping-related matters relevant to navigation in waters surrounding the two poles – ship design, construction and equipment; operational and training concerns; search and rescue; and, equally important, the protection of the unique environment and eco-systems of the polar regions. http://www.imo.org/en/MediaCentre/HotTopics/polar/Pages/default.aspx	Improved knowledge on sea ice and other hazards for polar navigation. In particular sea ice thickness and concentration forecasting.	European Community Ship owners' Association (ECSA), ship operators
EUR-Lex: **Integrated Coastal Zone Management—ICZM**	https://eur-lex.europa.eu/legal-content/EN/TXT/?uri=CELEX%3A32002H0413.	Integrated coastal zone management,	

[25] Cruise Lines International Association (CLIA)

[26] European Boatmen's Association (EBA)

[27] European Community Shipowners' Association (ESCA)

[28] European Maritime Pilots Association (EMPA)

[29] European Transport Workers' Federation (ETF)

[30] World Shipping Council (WSC)

	Protection of marine biodiversity http://ec.europa.eu/environment/marine/eu-coast-and-marine-policy/marine-strategy-framework-directive/index_en.htm	
EUR-Lex: **Urban Waste Water Treatment Directive—91/271/EEC**	Available online: https://eur-lex.europa.eu/legal-content/EN/TXT/?uri=CELEX%3A31991L0271.	Water management
EUR-Lex: **Integrated Pollution Prevention and Control—2010/75/EU**	Available online: https://eur-lex.europa.eu/legal-content/EN/TXT/?uri=CELEX%3A32010L0075.	
EUR-Lex: **Habitats Directive—92/43/EEC**.	Available online: https://eur-lex.europa.eu/legal-content/EN/TXT/?uri=celex%3A31992L0043	protected species, inland waters
EUR-Lex: **Birds Directive—2009/147/EC**.	Available online: https://eur-lex.europa.eu/legal-content/EN/TXT/?uri=CELEX%3A32009L0147	Protected species, inland waters
EUR-Lex: **Bathing Waters Directive—2006/7/EC**.	Available online: https://eur-lex.europa.eu/legal-content/EN/TXT/?uri=celex%3A32006L0007	Water quality
EUR-Lex: **Floods Directive—2007/60/EC**.	Available online: https://eur-lex.europa.eu/legal-content/EN/TXT/?uri=CELEX%3A32007L0060	Flood prevention, early warning and emergency management
EUR-Lex: **Directive on Safety Rules and Standards for Passenger Ships 2009/45/EC.**	Available online: https://eur-lex.europa.eu/legal-content/en/TXT/?uri=CELEX:32009L0045	Inland shipping
EUR-Lex: **Directive on Specific Stability Requirements for ro-ro Passenger Ships—2003/25/EC**.	Available online: https://eur-lex.europa.eu/legal-content/GA/TXT/?uri=CELEX:32003L0025	shipping
Maritime Spatial Planning Directive—2014/89/EU.	Directive 2014/89/EU of the European Parliament and of the Council of 23 July 2014 establishing a framework for maritime spatial planning, OJ L 257, 28.8.2014, p. 135–145.Available online: https://eur-lex.europa.eu/legal-content/EN/TXT/?uri=celex%3A32014L0089	
Common Fisheries Policy, 1224/2009 and repealing Council Regulations (EC) No 2371/2002 and (EC) No 639/2004 and Council Decision 2004/585/EC, OJ L 354, 28.12.2013, p. 22–61.	Regulation (EU) No 1380/2013 of the European Parliament and of the Council of 11 December 2013 on the Common Fisheries Policy, amending Council Regulations (EC) No 1954/2003 and (EC) No 1224/2009 and repealing Council Regulations (EC) No 2371/2002 and (EC) No 639/2004 and Council	

	Decision 2004/585/EC, OJ L 354, 28.12.2013, p. 22–61.	
International Maritime Organization, International **Convention for the Safety of Life at Sea**,, 1974, (SOLAS),	International Maritime Organization, International Convention for the Safety of Life at Sea, 1974, (SOLAS), available at http://www.imo.org/en/about/conventions/listofconventions/pages/international- convention-for-the-safety-of-life-at-sea-(solas),-1974.aspx.	
International Maritime Organization, International Convention for the Prevention of Pollution from Ships (MARPOL),	International Maritime Organization, International Convention for the Prevention of Pollution from Ships (MARPOL), 1973, available at http://www.imo.org/en/about/conventions/listofconventions/pages/international-convention-for-the- prevention-of-pollution-from-ships-(marpol).aspx.	
Directive (EU) 2019/904, **reduction of Plastics**	Directive (EU) 2019/904 of the European Parliament and of the Council of 5 June 2019 on the reduction of the impact of certain plastic products on the environment, OJ L 155, 12.6.2019, p. 1–19.	Water pollution by plastics, drift modelling
A **European Strategy for Plastics** in a Circular Economy Marine Litter	Communication from the Commission to the European Parliament, the Council, the European Economic and Social Committee and the Committee of the Regions, COM/2018/028 final. Directorate-General Joint Research Centre MSFD Technical Subgroup on Marine Litter, Guidance on Monitoring of Marine Litter in European Seas, JRC scientific and policy reports, 2013, available at http://publications.jrc.ec.europa.eu/repository/bitstream/JRC83985/lb-na-26113-en-n.pdf. Directorate-General Joint Research Centre MSFD GES Technical Subgroup on Marine Litter, Riverine Litter Monitoring - Options and Recommendations, JRC scientific and policy reports, 2016, available at http://ec.europa.eu/environment/marine/good-environmental-status/descriptor-	

	10/pdf/MSFD_riverine_litter_monitoring.pdf.
Monitoring, reporting and verification of **carbon dioxide emissions from maritime transport**	Regulation (EU) 2015/757 of the European Parliament and of the Council of 29 April 2015 and amending Directive 2009/16/EC, OJ L 123, 19.5.2015, p. 55–76.
Integrated European Policy for the Arctic	Joint Communication to the European Parliament and the Council *An integrated European Union policy for the Arctic*, JOIN/2016/021 final.
Climate Action Policy	European Commission, *Climate action, 2050 long-term strategy*, available at https://eur- lex.europa.eu/legal-content/EN/TXT/PDF/?uri=CELEX:52018DC0773&from=EN.
Council Regulation (EU) 2016/369 of 15 March 2016 on the **provision of emergency support within the Union** OJ L 70, 16.3.2016.	Emergency Support Provision
European **Directive on flood Risks**	Directive 2007/60/EC of the European Parliament and of the Council of 23 October 2007 on the assessment and management of flood risks, OJ L 288, 6.11.2007, p. 27–34.
United Nations, ***International Strategy for Disaster Reduction***	United Nations, *International Strategy for Disaster Reduction,* General Assembly, Sixtieth session, Agenda item 52 (c), 05-49930, Resolution adopted by the General Assembly on 22 December 2005 [on the report of the Second Committee (A/60/488/Add.3)] 60/195, 2 March 2006, see https://undocs.org/A/RES/60/195.
Council Directive 2008/114/EC **European critical infrastructures and the assessment of the need to improve their protection**	Council Directive 2008/114/EC of 8 December 2008 on the identification and designation of European critical infrastructures and the assessment of the need to improve their protection, OJ L 127, 16.5.2019, p. 34–79.

Space Strategy for Europe, COM/2016/0705	Communication from the Commission to the European Parliament, the Council, the European Economic and Social Committee and the Committee of the Regions *Space Strategy for Europe*, COM/2016/0705 final

APPENDIX III EUROPEAN COMMISSION COPERNICUS USER NEEDS FOR TOPOGRAPHY MEASUREMENTS TO SUPPORT COPERNICUS

The European Commission UN-SWD provides extensive guidance on User needs for Marine environment, Maritime affairs and fisheries. The following extracts relate to topography aspects are used to derive high-level user needs to be addressed by the S3NG-T Mission. These are identified as *[S3NG-T-UN-xxx:<Requirement text>].*

III.1 Copernicus user needs for policy implementation

III.1.1 Marine environment

Policy context

As summarised in a recent publication of the European Parliament, 'Ocean governance and blue growth Challenges, opportunities and policy responses, from March 2019, it is widely recognised that oceans offer new opportunities for sustainable economic growth while being seriously at threat because of climate change and biodiversity loss.

In 2018, the Marine Strategy Framework Directive (MSFD) will start its second 6-year cycle with a need to further enhance the actions to be taken to achieve the good environmental status of oceans, and strengthen cross linkages to other policies that help protect marine ecosystems and manage the anthropogenic pressures affecting them. Indicators and data sources used for the implementation of the Marine Strategy Framework Directive *[S3NG-T-UN-001: S3NG-T should provide ocean observations to support the development of the GES indicators with consistent time series over time: sea level, wave height, ocean circulation]* at regional, national and EU level could also be considered *[S3NG-T-UN-002: S3NG-T should provide ocean products at regional and coastal scales to support national reporting including connectivity between rivers and ocean]* to shape the contribution of Europe to the ongoing UN world ocean assessment started in 2016.

Reducing plastics, the loss of fishing gears and marine litter is also high on the maritime affairs agenda. On top of the Marine Strategy Framework Directive, this topic has been introduced in several legislations: the plastics strategy, the waste legislation, and recently in the circular economy action plan. *[S3NG-T-UN-003: S3NG-T should provide estimates of ocean circulation and Total Surface Current Velocity that together with models, would monitor the source, ocean transport, degradation and fate of floating marine plastic debris]*.

Building on a widely shared understanding that the ocean governance framework needs to be reinforced, the European Commission and the EU's High Representative published on 10 November 2016 a joint Communication related to the 'International Ocean Governance' proposing actions for safe, secure, clean and sustainably managed oceans in Europe and around the world, also stressing that a better understanding about the oceans is necessary to achieve these objectives. This is an integral part of the EU's response to the United Nations' 2030 agenda for sustainable development, for the implementation of the sustainable development goal 'Life below water'. *[S3NG-T-UN-004: S3NG-T should maintain and improve satellite altimetry measurements to better understand the ocean at global scale to support the 6 topics of IOG: pollution, climate, blue economy, security, fisheries, marine protected areas.]*

Under the G7 umbrella science working group in the 2016 Tsukuba communiqué, the Commission, together with France, Germany, Italy and other major countries, agreed to the development of an international initiative called the 'Future of Seas and Oceans'. This initiative aims at enhancing global sea and ocean observation to better monitor inter alia climate change and marine biodiversity. *[S3NG-T-UN-005: S3NG-T should enhance global observations (performance and sampling) of ocean topography measurements and contribute to climate change monitoring*].

Environmental Policy context

Copernicus contributes to the monitoring of the state and dynamics of oceans needed under the Marine Strategy Framework Directive, the Maritime Spatial Planning Directive and other European and international environmental legislations, as well as to the understanding of the oceans' role in accentuating or mitigating climate changes *[S3NG-T-UN-006: S3NG-T including S6 NG-T should contribute to the continuity of ocean climate records]*.

The sustainable development goal 14 dedicated to ocean health 'Life below Water', is part of the 2030 agenda of the United Nations with 10 targets and indicators on which to report. The Intergovernmental Panel on Climate Change special report '*Climate Change, the Oceans and Cryosphere*' confirms the crucial significance of future changes in the ocean to ecosystem health and human well-being. 19 (over 54 in total) essential climate variables[88] have been established by the global climate observing system programme (GCOS) to monitor the ocean climate. *[S3NG-T-UN-007: the duration of the S3NG-T missions should be of sufficient duration to confidently establish and monitor future ocean changes by contributing to the GCOS and SDG reporting]*

User communities

Ocean products are used by a significant large community of public bodies (e.g. national hydrological, weather or marine services, environmental agencies, ministries of transport, fisheries, operational maritime authorities for ports, coastguards), but also a significant research community involved in oceans, climate, Earth science or biology. The user base is equally balanced with the private sector acting in blue economy especially interested in ocean physics: energy, shipping, tourism, fisheries and aquaculture. *[S3NG-T-UN-008: S3NG-T data products should be made available to operational applications public user communities, scientific user communities and commercial user communities]*.

Evolving user needs

The Copernicus marine portfolio is in a continuous process of improvement to extend forecast periods, increase the resolution of observations based on satellite data and modelling. The higher the resolution is, better decision-making for example for ship routing is reliable. Public authorities need that the ocean features are better described in resolution and dynamics and the performances of the portfolio is improved to implement maritime spatial planning by 2021, report on the 11 descriptors for good environmental status by 2020 and address coastal challenges. Therefore, the following improvements are needed *[S3NG-T-UN-009: The S3NG-T should increase the resolution of topography observations in time and space to address maritime spatial planning at coast, implementation of the 11 GES indicators at coast, ship routing in complementarity to meteorological services]*:

- improving the description of ocean physics by (1) improving horizontal resolution to at least 1/36° for the global ocean and at least double this resolution in regional seas *[S3NG-T-UN-010: S3NG-T should provide sufficient density, revisit and coverage sampling to support ocean models at a horizontal resolution of 1/36° globally] [S3NG-T-UN-011: S3NG-T should provide sufficient density, revisit and coverage sampling to support ocean models at a horizontal resolution of 1/72° regionally]* (2) improving in treatment of closed or marginal seas with high dynamics at sub-mesoscale, linked to interactions with the atmosphere, ice, waves and winds *[S3NG-T-UN-012: S3NG-T should provide topography measurements of sea-ice, wave and wind products in closed and marginal seas]* (3) better addressing coastal areas and hydrological systems especially in areas of greatest human activity and hence pressure on the marine environment or European economic zones of interest including for overseas territories *[S3NG-T-UN-013: S3NG-T should enhance measurements in the coastal ocean]* (4) better addressing uncertainties to ensure high-quality datasets *[S3NG-T-UN-014: S3NG-T should provide uncertainty estimates in all products]*;
- understanding the dynamics of the biological component of the ocean in terms of 'fauna and flora' (because of the marine species being either exploited or to be protected) and how this marine living component behaves in relation to the ocean state, climate change and the man-made pressures (e.g. transport, pollution, fisheries, etc.) and in particular the plankton-to-fish links; *[S3NG-T-UN-015:S3NG-T should provide topography measurements (i.e. sea surface height, ocean currents, sea state etc) of ocean state in support of the biological ocean component].*
- better understanding environmental changes over the poles with a refined monitoring of sea-ice conditions and changes in continental ice, glaciers or permafrost, land-ice/snow and sea-ice interface improving real-time observation and short-term forecasts, but also long-term projections to best predict impacts of climate change; *[S3NG-T-UN-016:S3NG-T should provide measurements to monitor sea ice conditions and changes] [S3NG-T-UN-017:S3NG-T should provide topography measurements to monitor continental ice condition and changes] [S3NG-T-UN-018:S3NG-T should provide topography measurements to measure glacier conditions and changes] [S3NG-T-UN-019:S3NG-T should provide measurements to monitor land-ice/snow and sea-ice interface/snow conditions and changes*] *[S3NG-T-UN-020: S3NG-T should provide measurements with a delivery timeliness to support applications in the polar regions in near real time for short-term forecasts and climate scales]*
- in addition, integrating these various components into a full consistent overview of the ocean dynamics both at short term (with real-time observations and forecasts) to support daily applications but also in time to contribute to the analysis of climate change at global and regional scale and its impacts, and constituting a reference system. *[S3NG-T-UN-021:S3NG-T should provide measurements tailored to Copernicus Services for integration with climate models]*

III.1.2 Coastal management

UN-SWD articulates the following User Needs for coastal Management.

In 2017 and 2018, as requested by the Copernicus User Forum and Committee, the Copernicus run dedicated consultations with experts and user workshops to discuss the evolution of Copernicus services to address coastal zones. Copernicus already delivers a full suite of real time observation, forecasts and climate records scaled for the EU regional sea basins specific ocean features. However, the performances of such products are not representative enough of coastal phenomena heavily influenced by land and rivers (area of the continental shelf and up to 24 nautical miles from coastline in terms of territorial waters and contiguous zone). *S3NG-T-UN-022: S3NG-T should ensure that the definition of the coastal zone will include a limit of 24 nautical miles offshore] [S3NG-T-UN-023:S3NG-T should provide measurements with improved performance compared to sentinel-3 over the coastal ocean] [S3NG-T-UN-024:S3NG-T should provide estimates of river discharge into the coastal ocean]*

Policy context

Coastal areas are key places of significant human activities such as tourism, economic activities, fisheries, offshore operations, industrial port areas, cities growth. These are also areas potentially vulnerable to many risks such as storm surges, flooding, erosion or climate change impacts such as sea level rise. *[S3NG-T-UN-025:S3NG-T should provide measurements supporting storm surge monitoring complementary of meteorological products] [S3NG-T-UN-026:S3NG-T should provide measurements in support of flood mapping and management] [S3NG-T-UN-027:S3NG-T should provide products in support of coastal erosion monitoring and management] [S3NG-T-UN-028:S3NG-T should provide measurements of sea level rise]* Coastal development can be at the expense of natural systems (e.g. wetlands, beaches and dunes) that normally act as buffer between the sea and the land, leading to a conflict between protecting socio-economic activity and sustaining the ecological functioning of coastal zones in Europe.

Integrated coastal zone management have been subject to policy making in 2002 but then have been further developed through the existing directives in force: the Marine Strategy Framework Directive, Maritime Spatial Planning Directive, the Water Framework Directive, and the common fisheries policy (addressing specifically territorial coastal fishing within 12 Nautical miles). *[S3NG-T-UN-029:S3NG-T should ensure that the definition of the coastal zone will include a limit of 12 nautical miles offshore]* The description of the coastal environmental status is made through the quality elements established by the Water Framework Directive and the 11 descriptors (Annex 1 of Marine Strategy Framework Directive) for assessing the good environmental status.

User community

The coastal community is dominated by local public actors - regions, department, town councils, community of communes - in charge of their coastline, bathing waters, drinkable waters and utilities such as ports, dams but also local mobility, urban planning, tourism development and nature protection. The private sector is also important, operating at coast for civil works, water operations, sanitation, energy, short sea shipping and tourism. Most of these actors, when searching for information at sea, rely on national institutes in charge of hydrology and oceanography, most of them operating coastal ocean modelling capacities to monitor the shore for coastal erosion or marine ecosystems and fish exploitation. [*S3NG-T-UN-030:S3NG-T should provide topography measurements in support of coastal ocean modelling]*

Evolving needs

The needs for coastal environmental monitoring is mainly to monitor and understand the trends in spatial extent of vulnerable coastal ecosystems including to climate change, to understand anthropogenic pressures on the condition of such systems, as well as the interactions with shallow coastal waters. Pressures could be identified/characterised along four geographical areas that need different approaches: land (terrestrial part of coast e.g. up to 10 km inland from shoreline), transitional waters (according to the nomenclature of Water Framework Directive), coastal waters (according to the nomenclature of Water Framework Directive) up to marine waters. [*S3NG-T-UN-031:S3NG-T should recognize definitions of transitional waters (according to the nomenclature of Water Framework Directive), coastal waters (according to the nomenclature of Water Framework Directive) and to marine waters]*

Coastal land pressures on ecosystems, as defined by the 2018 report on 'the Mapping and Assessment of Ecosystems and their Services Report' are characterised by five main drivers to be considered in land use and land change: habitat change, climate change, invasive species, over-exploration, and pollution and nutrient enrichment.

Users need information that is representative of the dynamics of the coasts. This requires that the information is complementary and consistent from the land to the sea and vice-versa, being also tuned to much higher resolution to observe and predict coastal sub-mesoscale dynamics including surges, tides and fine resolution water quality phenomenon (e.g. blooms, sediment transport, turbidity) that could affect, for example, fisheries, aquaculture, coastal erosion, dam resistance to surges. *[S3NG-T-UN-032:S3NG-T should ensure consistency between land and ocean products] [S3NG-T-UN-033:S3NG-T should provide measurements to observe coastal sub-mesoscale dynamics]*

Coastal communities mainly develop their own coastal ocean models to describe at best specifics of their areas of interest, given that their capacities can be well initialised or forced with accurate upstream information. As such, they need boundary conditions compatible of their high-resolution (1 km) description of the ocean behaviour (coming from the open ocean or regional seas) and the hydrological inputs coming from the land (like rivers, estuaries or ice melt). [*S3NG-T-UN-034:S3NG-T should provide hydrological inputs (e.g. discharge estimates) to the coastal ocean from rivers, estuaries and ice melt]*

To better link with the land, they also need an improved access and better accuracy of the digital elevation model. The coastal topography and bathymetry are unanimously being asked by national coastal services. [*S3NG-T-UN-035: S3NG-T should provide estimates of bathymetry in the coastal ocean]* Land-sea interactions could be dynamically observed with respect to erosion or accumulation, sediment transport, concentration of pollutants at high-resolution (less than 1km) like chemicals but also floating plastic debris (Marine Directive for Litter). In order to develop solutions for resilience to climate change effects like coastal floods, storm surges, sea level rise, climate records of coastal products should be given due consideration [*S3NG-T-UN-036:S3NG-T should provide topography measurements to support climate adaptation applications in the coastal zone]*.

III.1.3 Fisheries and aquaculture

UN-SWD articulates the following User Needs for Fisheries and Aquaculture.

Copernicus operates a significant suite of real-time ocean observations and biogeochemical ocean forecasts to support activities related to fisheries, support to sustainable best practising, fisheries control and fish stock planning. [*S3NG-T-UN-037: S3NG-T should provide topography measurements in support of biogeochemical and ecological forecasts (e.g. sea state, winds, ocean currents)]* Such products are used regularly and from recent statistics of use of the program, this user demand is growing significantly. A dedicated study was carried out in 2018 to address this sector of activity in cooperation with Directorate-General for Maritime Affairs and Fisheries.

Policy context

To provide for the sustainability of fisheries in EU waters and the EU fleet worldwide, the Common Fisheries Policy Regulation (CFP) has defined a set of harmonised provisions to manage the EU fleet and their fishing activities to keep fish stocks at healthy levels, for managing European fishing fleets and for conserving fish stocks. To ensure the sustainability of fisheries and aquaculture in the waters around our continent, the EU CFP set fishing quotas per exploited species and regional limitations of fishing effort. Similar mechanisms are also negotiated internationally, in particular within Regional Fisheries Management Organisations (RFMO) to which the EU is a contracting party.

Access to accurate and verified data and parameters is of upmost importance to provide for a proper management and control of fishing and aquaculture activities. *[S3NG-T-UN-038: S3NG-T should provide ocean products at global scale and regional scale for EU policy implementation, support to RFMOs, at coastal scale to support aquaculture].*

User Community

The fishery industry is for most of it living near the coastline, where about half of the world population resides. The artisanal and coastal fisheries industry is a major source of revenue for the local markets, tourism and population. At larger scale, the industrial fisheries and fish processing industry generate important value when dealing with some major pelagic species like tuna, herrings or mackerels or anchovy.

In parallel, fisheries control is managed at national level, at sea or when landing, by public authorities and controlled at European level by the European Fisheries Control Agency (EFCA).

[S3NG-T-UN039: S3NG-T should support policy implementation by European Fisheries Control Agency (EFCA) and EU Member States sustainable fisheries management and reporting]. [S3NG-T-UN-040: S3NG-T ocean products (e.g. geostrophic currents, waves, winds) should be available to support industrial and coastal fisheries].

Evolution of User needs

EU public authorities and Regional Fisheries Management Organisations (RFMOs) need mainly information and tools for the following:

- identify favourable ocean conditions at sea (e.g. planktons, temperature) to best plan annual or seasonal fishing activities; [*S3NG-T-UN-041: S3NG-T should provide topography measurements in support of fisheries applications]*
- perform fish / marine ecosystem stock assessment to support the definition of time-area closure schemes to fishing based on habitats particularly centred on fish reproduction, and multi-annual plans, the definition of quotas and effort limitation

helping ensuring the sustainability of fish populations and the fishery profitability; [*S3NG-T-UN-042: S3NG-T should provide topography measurements in support of seasonal and annual fish stock assessment]*

- tools to monitor and control the fishing activity and production at sea including detecting and deterring unregulated and illegal fishing, mapping and control of aquaculture sites;
- tools to better anticipate or understand the impacts of fisheries on the environment and the man-made pressures on fisheries and marine ecosystems especially incidental bycatch and physical disturbance to the sea-floor;
- long-time series of information to monitor at long-term the impact of climate change on fish stocks and especially on recruitment and support food security related policies. [*S3NG-T-UN-043: S3NG-T should provide topography measurements in support of long-term climate impacts on fisheries (e.g. sea level rise, ocean currents)]*

The fisheries and aquaculture industry need

- information of low-pressure grounds for fishing and suitable aquaculture farm sites while remaining within the protective limits and regulations;
- monitoring information of the ocean health and ocean conditions influencing the stocks and the production, water quality and possible pollution at sea (e.g. harmful algae blooms, plankton-to-fish links, oil, land chemical pollutants, atmospheric inputs of nutrients, etc.);
- information to optimise fisheries activities while steaming and fishing and securing operations at sea.

In particular, this requires more dynamic and fine scale information of physical and biogeochemical ocean variables such as temperature, thermocline, oceanic thermal and productivity fronts, content in chlorophyll, nutrients or first stage of the food web elements (like nektons), and the implications of climate change. Near real-time information is needed to guide fishermen outside of active nurseries or habitat of protected species. However, time series and forecasts are also particularly relevant for planning activities and developing environmental scenarios of fish stocks assessment based on modelling. [*S3NG-T-UN-044: S3NG-T should provide topography measurements at different time scales :near real time, daily to monthly and climate scales].* [*S3NG-T-UN-045: S3NG-T should provide topography measurements to support model based products for fisheries applications].*

The list of expected water quality and biogeochemistry variables is significant with new products linked to pollutants, eutrophication, productivity of oceanic fronts and algae species differentiation with toxicity information, distribution of nutrients and functional types of plankton, plankton biomass, phenology, suspended sediments but also environmental parameters such as bathymetry, seabed habitats, river discharges, winds and waves. [*S3NG-T-UN-046: S3NG-T should provide topography measurements (e.g. wind, wave SSH, ocean currents) in support of monitoring suspended sediments]*

While the current list of ocean products available in Copernicus is satisfactory and fit for purpose for offshore aquaculture and fisheries (mostly industrial), users consulted during

workshops ask for more ‘closer-to-shore products’ in real-time and at finer scale for small-scale fisheries and aquaculture activities taking place in the near shore and coastal areas but also in lakes and inland waters. [*S3NG-T-UN-047: S3NG-T should provide river discharge measurements aquaculture activities in the coastal ocean activities]* [*S3NG-T-UN-048: S3NG-T should provide topography measurements close to shore area].* The area of interest is pan-European but also global given the extensive coverage of exclusive economic zones from European Member States and areas managed by Regional Fisheries Management Organisations (RFMO). [*S3NG-T-UN-049: S3NG-T should provide topography measurements in support of fisheries and aquaculture in the pan-European context including the exclusive economic zones of European Member states]*

Needs for fisheries control specially in terms of combating illegal, unreported and unregulated fishing practices by the European Fisheries Control Agency (EFCA) and its stakeholders fall under the Maritime Surveillance area.

III.1.4 Maritime Spatial Planning

UN-SWD articulates the following User Needs for Marine spatial Planning.

Information needed for maritime spatial planning ranges from environmental information (e.g. habitats, seabed, sediments, bathymetry, and coastline) to datasets mapping human activities (e.g. fishing, aquaculture, shipping, energy, cables and pipelines). Copernicus delivers already part of the environmental information especially through long-time series of ocean products necessary to produce atlas. However, such data are mainly at regional sea basin scale and not enough detailed at coastal level. Man-made activities are not directly mapped and monitored in Copernicus even though satellite observation can be useful to identify shipping lanes, fisheries and aquaculture grounds. [*S3NG-T-UN-050: S3NG-T should provide measurements in support of aquaculture and fisheries spatial planning at coastal scale]*

Policy context

Competition for maritime space – for renewable energy equipment, aquaculture and other uses – has highlighted the need to manage waters more consistently. Maritime spatial planning (MSP) works across borders and sectors to ensure human activities at sea take place in an efficient, safe and sustainable way. In 2014, the Directive for Maritime Spatial Planning in Europe was adopted to reduce conflicts, encourage investment (blue economy), increase cross-border cooperation and protect the environment.

The Directive lists the 11 relevant mandatory areas of intervention and data to be collected and mapped, that should be addressed by Member States and updated at least every 4 years.

User community

Member States have to implement maritime spatial planning. If regional local authorities, cities, environmental agencies are most of the time in charge of it, its implementation requires the contribution of many institutes specialised in marine science, biology or water management. The private sector, association of industries and foundations are also part of the elaboration of plans.

Evolving needs

The Commission set up a platform to support all EU Member States in the implementation of the directive by 2021. In this framework, studies have been performed to identify data gaps. Copernicus and EMODNET (the marine knowledge information system from the Directorate-General for Maritime Affairs and Fisheries) provide many data sources for maritime spatial planning especially for human activities. On the Copernicus side, progress is needed to fit with expected resolution for coastal mapping.

Needs related to siting human activities such as aquaculture farms or marine renewable energies plants are described in each sector of interest: energy, maritime transport, marine environmental monitoring and fisheries and aquaculture. [*S3NG-T-UN-051: S3NG-T should provide topography measurements of waves, winds and ocean surface currents to support applications in energy, maritime transport, marine environmental monitoring]*

One important need lies in the obligation to consider land-sea interactions for which it would be useful if Copernicus delivers land-sea consistent data and information products as indicated for coastal management. [*S3NG-T-UN-052: S3NG-T should provide consistent information from the open ocean to the coastal ocean]*

At sea, the oil and gas industry is mainly interested in oil slicks detection and met-ocean conditions. Higher resolution solving sub mesoscale dynamics and vertical mixing / diffusivity, could lead to improved forecasting capacity of the production*. [S3NG-T-UN-053: S3NG-T should provide measurements in support of sub-mesoscale dynamics] [S3NG-T-UN-054: S3NG-T should provide measurements in support of vertical mixing and diffusivity in the ocean]* Future deep-sea exploration and exploitation need deeper ocean modelling down to 5000 or 7000 meters with improved global modelling and relevant in-situ measurements. Inland/coastal water information: density, salinity, plumes, seabed mapping and bathymetry with coastal resolution including interferences with watersheds, estuaries, tides and waves, intrusion of unsalted waters at sea (for oil and gas on continental shelves and in large estuaries), [*S3NG-T-UN-055: S3NG-T should provide topography information on the interactions between inland waters, estuaries and costal ocean]* information on sea ice and continental ice are needed for most oil and gas extraction areas on the continental shelf *[S3NG-T-UN-056: S3NG-T should provide information on sea ice and continental ice]* This industry is also accountable for possible pollution impacts on the marine environment and marine life. They need products that could enable them to detect and fight against possible accidental oil pollution, but also simulate biogeochemical impacts that could affect the living environment (e.g. plankton, fish stocks, marine mammals, corals). [*S3NG-T-UN-057 S3NG-T should provide new products (e.g. wave, wind and current) in real time in support of oil spill pollution]*

III.1.5 Arctic policy and polar areas

UN-SWD articulates the following User Needs in Polar Regions.

Copernicus addresses the poles with:

- a dedicated Arctic ocean monitoring and forecasting centre in charge of observing, forecasting sea ice conditions and maintain related long-time series of arctic changes; [*S3NG-T-UN-058: S3NG-T should provide information on sea-ice over the Arctic]*
- cryosphere monitoring on land for lake ice extent, snow cover and snow parameters; [*S3NG-T-UN-059: S3NG-T should provide topography measurements*

of lake surface ice] [*S3NG-T-UN-060: S3NG-T should provide measurements of snow cover and snow parameters]*

- climate records and climate projections delivered for international reporting on seven essential climate variables related to sea-ice and glaciers; [*S3NG-T-UN-061: S3NG-T should provide measurements to support ECV for sea ice]* [*S3NG-T-UN-062: S3NG-T should provide measurements to support ECV for glaciers]*
- maritime surveillance services monitoring shipping and fishing in the Arctic for maritime safety purposes[*S3NG-T-UN-063: S3NG-T should provide topography products in support of Arctic maritime safety]*.

Policy context

The Arctic's fragile environment is also a direct and key indicator of climate change, which requires specific mitigation and adaptation actions as agreed with the global agreement reached during the COP-21 held in Paris in December 2015. To this end, the integrated EU Arctic policy has identified three priority areas:

- climate change and safeguarding the Arctic environment (livelihoods of indigenous peoples, Arctic environment);
- sustainable development in and around the Arctic (exploitation of natural resources e.g. fish, minerals, oil and gas), blue economy, safe and reliable navigation (e.g. North East Passage);
- international cooperation on arctic issues (scientific research, EU and bilateral cooperation projects, fisheries management / ecosystems protection, commercial fishing).

User community

All categories of users from the public to the private sector are considered in the frame of the Arctic policy up to the citizen and indigenous population.

Evolving needs

In the frame of Copernicus, a polar expert group has been set up to assess the interest and define high-level mission requirements for future space missions dedicated to the monitoring of the poles in a context of climate change and aligning with the Arctic policy. The experts held several workshops, collated and analysed documents to establish the users' needs synthesised in Polar Expert Group Reports I, II and III.

Domains of interest expressed by users range from meteorology, climatology, hydrology, oceanography, ecology, natural and industrial hazards, emergency response, energy, transport, infrastructure management to security and climate change adaptation and mitigation. Therefore, data and information products are needed related to the atmosphere, ocean, fresh waters, land surface and vegetation but also specific products linked to the poles such as permafrost and soils, sea ice including icebergs and ice shelves, ice sheets, glaciers and ice caps, plus seasonal snow. [*S3NG-T-UN-064: S3NG-T should provide topography measurements of seasonal snow cover]*

The expert group established a summary list of variables to support as many needs as possible ordered by priority of interest:

- floating ice variables including sea ice extent / concentration / thickness / type / ridge / drift velocity, thin sea ice distribution, iceberg detection / volume change and drift, ice shelves thickness and extent. These parameters are necessary for operational services (navigation, marine operations) as well as to climate modelling; [*S3NG-T-UN-065: S3NG-T should provide topography measurements of sea ice thickness]* [*S3NG-T-UN-066: S3NG-T should provide topography measurements of sea ice concentration]* [*S3NG-T-UN-067: S3NG-T should provide topography measurements of sea ice [thickness] distribution]* [*S3NG-T-UN-068: S3NG-T should provide topography measurements to monitor icebergs]*
- glaciers, caps and ice sheets parameters including extent / calving front / grounding line / surface elevation and surface elevation change / surface velocity / mass balance and mass change / melt extent to monitor climate change and sea level rise; [*S3NG-T-UN-069: S3NG-T should provide topography measurements of ice sheet elevation]* [*S3NG-T-UN-070: S3NG-T should provide topography measurements of glacier elevation]* [*S3NG-T-UN-071: S3NG-T should provide topography measurements to support ice mass balance estimates]* [*S3NG-T-UN-072: S3NG-T should provide topography measurements of ice sheet mass change estimates]* [*S3NG-T-UN-073: S3NG-T should provide topography measurements of sea level rise]*
- sea level / sea level anomaly parameters to have a better description of oceanic large scale and mesoscale circulation/variability and currents for marine forecasting; [*S3NG-T-UN-074: S3NG-T should provide topography measurements of sea level in polar regions]* [*S3NG-T-UN-075: S3NG-T should provide topography measurements of sea level anomalies in polar regions]* [*S3NG-T-UN-076: S3NG-T should provide topography measurements of ocean currents in polar regions]* [*S3NG-T-UN-077: S3NG-T should provide topography measurements of significant wave height in polar regions]*
- all weather sea surface temperature (SST) for climate modelling, mesoscale analysis, oceanic predictions and as climate change indicator;
- surface albedo as major determinant for the energy balance between atmosphere and surface, crucial for many application domains including climate, meteorology, numerical weather modelling, hydrology and more;
- surface fresh water (river run-off and discharge, river and lake ice thickness) as an important resource for the supply of water to populations as well as for transport activities and impact on ocean changes / climate modelling; [*S3NG-T-UN-078: S3NG-T should provide topography estimates of river discharge in polar regions]*
- snow (extent/fraction and snow equivalent water, melt extent both on land and sea-ice) important for many applications in hydrology, meteorology, water management and climate modelling;
- permafrost (extent/fraction and topography/deformation monitoring) important for operational activities (transport, construction / ground movement) as well as indicator of climate change. Permafrost observation is also a strong need since permafrost includes 24% of the land in the northern hemisphere and stores massive

amounts of carbon and methane that need to be accounted for greenhouse gases monitoring according to the Paris Agreement.

According to the polar expert group, most of the products already available need to be improved in terms of resolution and time availability expecting sub-daily resolution under 5kms specially to support safe navigation. [*S3NG-T-UN-079: S3NG-T should provide topography measurements of sea ice parameters at a resolution of < 5 km] [S3NG-T-UN-080: S3NG-T should provide topography measurements of sea ice parameters at a sub-daily revisit]* Detection of small icebergs including growlers is needed when opening new routes. Monitoring of glaciers with surface elevation changes is a good indicator to assess the effects of climate change that impact directly sea level rise but also possible hydropower generation or irrigation. [*S3NG-T-UN-081: S3NG-T should provide topography measurements of glacier elevation]*

Needs identified for the Arctic are partly applicable also to monitor the Antarctic precisely in the purpose of monitoring the effects of climate change, sea ice and ice caps interactions with the oceans and sea level rise. *[S3NG-T-UN-082: S3NG-T should provide topography measurements for Antarctica]*

III.1.6 Inland Water

UN-SWD articulates the following User Needs for Inland Water.

Water products from Copernicus are new. They include inland water, wetness, snow and land ice products. Water levels are computed for 1000 lakes larger than 50 ha and intersections of major river networks. *[S3NG-T-UN-083: S3NG-T should provide topography measurements for lakes and reservoirs larger than 50 ha] [S3NG-T-UN-084: S3NG-T should provide topography measurements for major river networks] [S3NG-T-UN-085: S3NG-T should provide measurements of snow over land surfaces in support of hydrology applications] [S3NG-T-UN-086: S3NG-T should provide topography measurements for lake ice surfaces]* Lake water quality products and lake surface water temperature are produced according to the Global Lakes and Wetlands Database[31] (GLWD) and the Water Framework Directive[32]. At pan-European level, Copernicus produces water and wetness products (permanent water, temporary water, permanent wetness and temporary wetness), a water and wetness probability index and water bodies' areas covered by inland water along the year.

Snow cover has a strong influence on the Earth's radiation and energy balance. Changes in snow extent tend to amplify climate fluctuations. This phenomenon need to be well identified for the prediction of water balance, streamflow and river runoff in hydrological models used for water resource management, climate modelling and arctic/sub-arctic area monitoring. The key cryosphere parameters monitored within Copernicus are the area snow extent, snow water equivalent and lake ice extent.

[31] https://www.worldwildlife.org/pages/global-lakes-and-wetlands-database

[32] Directive 2000/60/EC of the European Parliament and of the Council of 23 October 2000 establishing a framework for Community action in the field of water policy, OJ L 327, 22.12.2000, p. 1-73.

At global level, water Essential Climate Variables are produced to report to the International Global Climate Observing System program[33] (GCOS). For climate change monitoring purposes, precipitation, relative humidity and soil moisture are monthly reported. *[S3NG-T-UN-087: S3NG-T should provide topography measurements in support of GCOS water ECV products consistent with existing time series]*

Copernicus at this stage does not provide regular information on rivers dynamics and especially on river runoff and overall hydrological dynamics, nor on under water systems. *[S3NG-T-UN-088: S3NG-T should provide water surface elevation of river catchments] [S3NG-T-UN-089: S3NG-T should support monitoring hydrological dynamics (river flow and lake storage) of river catchments]*

The implementation of the Water Framework Directive from 2000 in an integrated way (integrating all pressures from all activities) but also the dynamic monitoring and management of water (drinking, bathing and fresh waters) are major priorities for the next decades. As such, the legal framework was completed by the Bathing Waters Directive[34], the Ground Water Directive[35] and the Directive about Discharge of Dangerous Substances[36]. In February 2019, the Commission issued a report of the implementation of the Water Framework Directive[37] that highlights achievements and remaining challenges versus the objectives established in 2000. *[S3NG-T-UN-090: S3NG-T should provide topography products in support of costal bathing waters and the Water Framework Directive]* The report shows significant improvements in knowledge and reporting on the Water Framework Directive compared to the last reporting cycle. Problems remain however as regards chemical pollution, over-abstraction of water, in particular for agriculture, and obstacles to the natural flow for rivers. In concordance, the Commission proposals for a post-2020 Common Agriculture Policy[38] promote the monitoring of water resources through the implementation of specific indicators about water quality and quantity.

The European Union has set up different mechanisms to help Member States to prevent, prepare and better fight against natural risks with the Council decision on emergency

[33] The Global Climate Observing System (GCOS) is an international programme that regularly assesses the status of global climate observations and produces guidance for its improvement co-sponsored by the World Meteorological Organization (WMO), the Intergovernmental Oceanographic Commission of UNESCO (IOC-UNESCO), the United Nations Environment Programme (UN Environment), and the International Science Council (ISC). GCOS supports the monitoring as requested by the Paris Agreement (COP21).

[34] Council Directive 98/83/EC of 3 November 1998 on the quality of water intended for human consumption, OJ L 330, 5.12.1998, p. 32–54. Directive 2006/7/EC of the European Parliament and of the Council of 15 February 2006 concerning the management of bathing water quality and repealing Directive 76/160/EEC, OJ L 64, 4.3.2006, p. 37–51.

[35] Directive 2006/118/EC of the European Parliament and of the Council of 12 December 2006 on the protection of groundwater against pollution and deterioration, OJ L 372, 27.12.2006, p. 19–31.

[36] Directive 2006/11/EC of the European Parliament and of the Council of 15 February 2006 on pollution caused by certain dangerous substances discharged into the aquatic environment of the Community, OJ L 64, 4.3.2006, p. 52–59.

[37] Report from the Commission to the European Parliament and the Council on the implementation of the Water Framework Directive (2000/60/EC) and the Floods Directive (2007/60/EC) Second River Basin Management Plans First Flood Risk Management Plans COM/2019/95 final.

[38] Proposal for a regulation of the European Parliament and of the Council establishing rules on support for strategic plans to be drawn up by Member States under the Common Agricultural Policy (CAP Strategic Plans) and financed by the European Agricultural Guarantee Fund (EAGF) and by the European Agricultural Fund for Rural Development (EAFRD) and repealing Regulation (EU) No 1305/2013 of the European Parliament and of the Council and Regulation (EU) No 1307/2013 of the European Parliament and of the Council, COM/2018/392 final. Proposal for a regulation of the European Parliament and of the Council on the financing, management and monitoring of the Common Agricultural Policy and repealing Regulation (EU) No 1306/2013 COM/2018/393 final.

support[39], the EU civil protection mechanism updated in 2019[40], the humanitarian aid legislation and the creation of a dedicated corps[41] in 2014, the Floods Directive[42], the EU forest strategy, the EU action on water scarcity and droughts and the creation of the European drought observatory[43], the EU solidarity fund for major disasters, and the Commission action plan[44] on the Sendai framework for disaster risk reduction 2015-2030. *[S3NG-T-UN-091: S3NG-T should provide inland water information in support of international disaster risk reduction such as drought]*

User community

The portfolio of Copernicus for hydrology and water is new and the user community is not yet fully identified. Major recognised users are the river basin authorities and agencies, regional and local authorities in charge of drinkable water, wastewaters, agencies in charge of agriculture, emergency services and hydro-meteorological administrations. It also includes private actors of the hydro-energy sector or the water transport. Communities working along the coastline where inland waters connect with the seas are also relevant.

Evolving Needs

The UN_NOTE recalls that water level measurements and requirements must be expressed systematically for:

- rivers and channels (floods, discharge, hydro-power, waterways) and
- lakes and reservoirs (hydro-power/energy, floods, irrigation, artificial snow, droughts)

From that perspective, in particular the spatial (xyz) resolution is key.

[S3NG-T-UN-092: S3NG-T should provide inland water topography products in support of management of rivers and channels, floods, discharge, hydro-power, and waterways]

From the UN_SWD, policy needs are:

Following interviews from the community and a dedicated workshop on Copernicus for water held in 2018 (cf. 7.2) more products are needed for the implementation of the Water Framework Directive on natural water retention measures, detection of illegal water abstraction, implementation and control of river basin management plans:

- water quality and water levels (quantity) not only on major lakes, but also in smaller reservoirs and rivers at much finer scale (catchment scale); *[S3NG-T-UN-093:*

[39] Council Regulation (EU) 2016/369 of 15 March 2016 on the provision of emergency support within the Union OJ L 70, 16.3.2016.

[40] Decision (EU) 2019/420 of the European Parliament and of the Council of 13 March 2019 amending Decision No 1313/2013/EU on a Union Civil Protection Mechanism, OJ L 77I, 20.3.2019, p. 1–15.

[41] Regulation (EU) No 375/2014 of the European Parliament and of the Council of 3 April 2014 establishing the European Voluntary Humanitarian Aid Corps ('EU Aid Volunteers initiative'), OJ L 122, 24.4.2014, p. 1–17.

[42] Directive 2007/60/EC of the European Parliament and of the Council of 23 October 2007 on the assessment and management of flood risks, OJ L 288, 6.11.2007, p. 27–34.

[43] http://edo.jrc.ec.europa.eu/edov2/php/index.php?id=1000

[44] Commission Staff Working Document Action Plan on the Sendai Framework for Disaster Risk Reduction 2015-2030 a disaster risk-informed approach for all EU policies, SWD/2016/205 final/2.

S3NG-T should provide topography measurements of water surface elevation for lakes scales smaller than 50 ha] [S3NG-T-UN-094: S3NG-T should provide topography measurements of water surface elevation over reservoirs] [S3NG-T-UN-095: S3NG-T should provide topography measurements of water surface elevation over small rivers]

- water dynamic monitoring and fluxes such as river runoff, interfaces with seas and oceans to understand interactions between inland waters, seas and land component (e.g. to be used for nutrient pollution alert systems, flood prevention and flood risk management); *[S3NG-T-UN-096: S3NG-T should provide topography measurements of water surface elevation with sufficient fidelity to monitor the target (river, lake, reservoir, dynamics]*
- information to monitor additional sources of water such as ground water and aquifers.

The understanding of the hydrological cycle, including the evapotranspiration process and the soil moisture/soil water balance, monitored through timely observations and eventually forecasts, is needed for many applications from agriculture to disaster mitigation or food security and climate. Hydrological models to calculate hydrological fluxes for small streams or entire river basins in connection with sea could be a significant progress that could benefit several Copernicus data and information services requiring hydrological dynamics (climate, ocean, emergency, land) and many users from different sectors of applications. *[S3NG-T-UN-097: S3NG-T should provide topography measurements of water surface elevation to support hydrological modelling for climate, emergency and land applications]*

More information on the hydrological processes could ensure best water use practices related to irrigation monitoring and forecasting, hydrological planning and modelling for river basin governance, risk management including in urban areas, *[S3NG-T-UN-098: S3NG-T should provide topography measurements of water surface elevation to support hydrological modelling for agriculture support and urban/local planning]* development of inland fisheries and aquaculture, monitoring of the quality of bathing waters and drinking water, evaluation of hydro morphological alterations and pressures in European rivers, lakes, transitional and coastal waters.

For agricultural policy applications, key variables will be evapotranspiration estimates and relevant information for irrigation monitoring. The expected time and spatial resolutions needed are yearly and seasonal maps based on daily to weekly information and a 5-20 m pixel resolution to go for 1 ha minimum mapping unit. *[S3NG-T-UN-099: S3NG-T should provide topography measurements of water surface elevation to support hydrological modelling for agriculture at seasonal and yearly periods] [S3NG-T-UN-100: S3NG-T should provide topography measurements of water surface elevation for 1 ha minimum mapping unit]* These applications could provide data related to the use of water in agriculture for the production of indicators required by the CAP proposal. The requirements for downstream applications like irrigation management advice are more demanding in terms of frequency and faster delivery time.

For all potential snow/iced areas, new accurate and timely information on the cryosphere like snow depth, wet snow, snow melt timeline including past and future variations, ice sheet topography and elevation changes, permafrost and seasonally frozen ground monitoring are also needed especially in the frame of arctic monitoring.

In order to better address water use and especially changes in water and cryosphere resources, (e.g. for agriculture, inland aquaculture, disaster mitigation and climate risks like prevalence of pluvial floods due to climate change), water-related forecasts and water-related climate records need to be produced in addition to Copernicus existing observed products. *[S3NG-T-UN-101: S3NG-T should provide topography measurements in support of water resources in the cryosphere as climate records]*

The inclusion of this information in the Water Information System for Europe[45] (WISE) is also needed."

III.1.7 Emergency management

The European Commission **UN-NOTE** provides the following User needs in support to emergency management mainly for flood and drought monitoring of rivers, lakes and reservoir, and storm surges.

The emergency requirements in terms of topography are the following and can be grouped into three categories:

- for observation assimilation into the hydrological model used for the flood and drought early warning and monitoring component :
    - water level measurements and its translation into river discharges for improved predictions;
    - lakes and reservoir water level measurements and its translation into lake and reservoir volume to improve hydrological prediction skill of the flood and drought early warning component;
- for generating anomaly indices for the drought early warning and monitoring component
    - lake and reservoir water level measurements as long time series;
- For assimilation into storm surge forecasting system:
    - water level at coast, SWH at coast, mean wave period, mean wave direction, wave length.

[45] The Water Information System for Europe (WISE) is a partnership between the European Commission (Directorate-General for Environment, Joint Research Centre and Eurostat) and the European Environment Agency providing a web-portal entry to water related information ranging from inland waters to marine providing input to thematic assessments in the context of EU water related policies for water professionals and scientists with access to reference documents and thematic data.

Application	Variable	Required Horizontal Resolution	Required time Resolution	Required spatial Coverage	Policy context	User community
Flood and drought early warning and monitoring of rivers, lakes and reservoirs	water level,discharge and lake/reservoir volume	River widths of >10m	daily hourly for small rivers weekly for drought	Global and Europe	- Council Regulation (EU) 2016/369 of 15 March 2016 on the provision of emergency support within the Union OJ L 70, 16.3.2016. - Decision (EU) 2019/420 of the European Parliament and of the Council of 13 March 2019 amending Decision No 1313/2013/EU on a Union Civil Protection Mechanism, OJ L 77I, 20.3.2019, p. 1–15. - Directive 2007/60/EC of the European Parliament and of the Council of 23 October 2007 on the assessment and management of flood risks, OJ L 288, 6.11.2007, p. 27–34. - European drought observatory - http://edo.jrc.ec.europa.eu/edov2/php/index.php?id=1000 - J19 Commission Staff Working Document Action Plan on the Sendai Framework for Disaster Risk Reduction 2015-2030 a disaster risk-informed approach for all EU policies, SWD/2016/205 final/2 - United Nations, International Strategy for Disaster Reduction, General Assembly, Sixtieth session, Agenda item 52 (c), 05-49930, Resolution adopted by the General Assembly on 22 December 2005 [on the report of the Second Committee (A/60/488/Add.3)] 60/195, 2 March 2006, see https://undocs.org/A/RES/60/195. - Communication from the Commission to the European Parliament, the Council, the European Economic and Social Committee and the Committee of the Regions The post 2015 Hyogo Framework for Action: Managing risks to achieve resilience, COM/2014/0216 final.	Copernicus emergency service, DG ECHO, drought observatory of JRC, civil protection Disaster Risk Management Knowledge Centre, rescEU Consistency with existing time series requested
storm surge forecasting	water level at coast SWH at coast mean wave period mean wave direction wave length	1/4° for open ocean, 22.5 km 1m at coast	daily for open ocean 6 hours to hourly for near shore	global Europe	- Directive 2014/89/EU of the European Parliament and of the Council of 23 July 2014 establishing a framework for maritime spatial planning, OJ L 257, 28.8.2014, p. 135–145 - Directive 2008/56/EC of the European Parliament and of the Council of 17 June 2008, establishing a framework for community action in the field of marine environmental policy (Marine Strategy Framework Directive), OJ L 164, 25.6.2008, p. 19–40 - report from the Commission to the European Parliament and the Council on the implementation of the Water Framework Directive (2000/I1860/EC) and the Floods	Copernicus emergency service, DG ECHO, civil protection Consistency with existing time series requested

					Directive (2007/60/EC, Second River Basin Management Plans, First Flood Risk Management Plans and recommendations in Annex, COM/2019/95 final.	

[S3NG-T-UN-102: S3NG-T should provide topography measurements of water surface elevation for rivers >10m in width]

[S3NG-T-UN-103: S3NG-T should provide topography measurements of water surface elevation with daily revisit]

[S3NG-T-UN-104: S3NG-T should provide topography measurements of water surface elevation with hourly revisit for small rivers]

[S3NG-T-UN-104: S3NG-T should provide topography measurements of water surface elevation with weekly revisit for drought monitoring]

[S3NG-T-UN-106: S3NG-T should provide topography measurements of water surface elevation with global coverage]

III.1.8 Adaptation to Climate Change

UN-SWD articulates the following User Needs for adaptation to Climate Change.

Copernicus delivers relevant information on land use and land use change that can support the development of climate mitigation and climate adaptation strategies at European, national, regional level. At local level, some information is also available but could deserve additional developments either at Copernicus level or at national level. *[S3NG-T-UN-107: S3NG-T should provide topography measurements for climate monitoring, ocean, polar and inland, at national to regional scale]*

To support planning and long-term decision-making, climate records of the past and seasonal forecasts are available for the atmosphere and the marine areas. Access to historical data and information on land use is less developed. However, archives of historical Earth Observation data become accessible. Climate projections are available mainly for describing the behaviour of the Earth system (air land, water) for decades to come to help developing scenarios. *[S3NG-T-UN-108: S3NG-T should provide topography measurements in support of seasonal forecasting]*

Policy context

Adaptation to climate change is increasingly important to protect lives and assets, e.g. anticipating the adverse effects of climate change and taking appropriate action to prevent or minimise the damage they can cause, or taking advantage of opportunities that may arise. Adaptation strategies are needed at all levels of administration and across populations, economic sectors and regions within Europe, but due to the varying severity and nature of climate impacts between regions in Europe, most adaptation initiatives and strategies have to be developed at regional or local levels. *[S3NG-T-UN-109: S3NG-T should provide topography measurements to support regional to local climate adaptation strategies]*

Following the adoption of the European Union's climate and energy package in 2008, the European Commission launched the Covenant of Mayors, to endorse and support the efforts deployed by local authorities in the implementation of sustainable energy policies. In 2014, the European Commission launched the Mayors Adapt initiative. Based on the same principles as the Covenant of Mayors, this sister initiative was focusing on adaptation to climate change. In 2015, the Covenant of Mayors and Mayors Adapt initiatives officially merged into the EU Covenant of Mayors for Climate and Energy. The signatories of the EU Covenant of Mayors for Climate and Energy commit to reduce their CO2 emissions (and possibly other GHG) and to adopt a joint approach to tackling mitigation and adaptation to climate change. They commit to prepare and implement a sustainable energy and climate action plan (SECAP) with the target year of 2030 for emission reduction. SECAPs include an assessment of the geographical, demographical and energy local context, a baseline CO2 emission inventory (BEI) referring to a specific base year, a climate risks and vulnerability assessment, a clear identification of the emissions reduction target, a climate change adaptation goal and the actions planned together with periods, assigned responsibilities and estimated impacts and costs. In 2016, the European Commission supported the creation of the Global Covenant of Mayors for Climate and Energy at international scale.

User community

Copernicus could provide the necessary data for local authorities to fill in the SECAP template, in accordance with the accompanying reporting guidelines and notably for the fields related to assessing risks and vulnerabilities to climate change, monitoring and evaluating implemented adaptation measures, with the help of the adaptation indicators proposed in the template. The data provided by Copernicus could also support local authorities in their reporting to the European Commission (every two years after having submitted the SECAP or a similar relevant strategy or plan for local authorities not being part of the Covenant of Mayors). *[S3NG-T-UN-110: S3NG-T should provide topography measurements yearly to support sustainable energy and climate action plan (SECAP) reporting]*

Evolving needs

Climate reanalyses, seasonal or decadal forecasts and long-term projections could be thus provided at global, continental level so that national and regional authorities in charge of climate assessment at national and regional and/or local scales can develop relevant information to their adaptation and mitigation strategies with multi-scale consistencies. *[S3NG-T-UN-111: S3NG-T should provide topography measurements in support of seasonal, decadal forecasts and climate projections] [S3NG-T-UN-112: S3NG-T should provide topography measurements to monitor changes in topography in support of climate prediction]*

Copernicus climate data could also support the climate vulnerability and risk assessments of new investment projects, existing assets in the built environment, networks (e.g. transport, communication, energy), and nature-based solutions. Furthermore, Copernicus could provide climate data corresponding to the climate and weather variables that are relevant vis-à-vis the Eurocodes used for structural engineering (including the national annexes to the Eurocodes).

Adapting to climate change requires data and information from all Earth system components: the atmosphere, the land and the cryosphere and oceans. Both reference time series (data demonstrating of changes and trends) *[S3NG-T-UN-113: S3NG-T should provide topography measurements in support of reference time series measurements for climate trend analysis]* and climate change indicators *[S3NG-T-UN-114: S3NG-T should provide topography measurements in support climate change indicators]* are thus necessary either composite or covering the specific economic sectors impacted by European and national policies for economic and ecological sectors and services such as water, energy, agriculture, insurance, health, infrastructure, tourism, biodiversity, land use (e.g. soil sealing, imperviousness, erosion, carbon uptake, etc.). While expectations for long-term climate data records and long-term projections are similar for global international purposes and local adaptation strategies, the geospatial resolution can significantly vary to fit regional and local actions. In order to support local authorities, products need to be downscaled in resolution to cover around 80% of the local authorities' needs. *[S3NG-T-UN-115: S3NG-T should provide topography measurements in support climate change adaptation at national scale to regional/local scale]* Methodologies, core data, and information ready-to-use to build data at the city level for cities to undertake climate risks and vulnerability assessments and monitor changes could be most useful.

Copernicus could help geo-locate people vulnerable to climate change consequences (e.g. heatwaves, floods), notably concentrated in specific hotspots (e.g. districts, nurseries / educational establishments / elderly residences). It could be useful to understand, monitor and reduce the foreseen increasing impacts on vulnerable groups (e.g. low-income, elderly, young, foreigners not understanding the national language, people with poor health, etc.).

Relevant Copernicus data and information services could be made available as already initiated to users through the Climate-ADAPT platform in all areas of the current and future EU adaptation strategy. Climate-ADAPT is the strategies' main channel to disseminate information on adaptation to national and local actors. Complementarity with other EU knowledge platforms (such as the Disaster Risk Management Knowledge Centre or the European Forest Fire Information System, EFFIS) and with the growing number of national adaptation platforms will be important in this context.

III.1.9 Pollution at sea

UN-SWD articulates the following User Needs for Pollution at Sea.

Under Copernicus, significant efforts have been made and implemented by the European Maritime Safety Agency (EMSA) to fight against intentional or accidental oil pollution. The Copernicus portfolio is one of the best examples of what can be achieved worldwide in terms of space-based solutions for oil detection and pollution management. Oil pollution is fully integrated operationally with maritime surveillance. *[S3NG-T-UN-116: S3NG-T should provide topography measurements (e.g. wind, waves, currents, sea state), in support of oil and other pollution events over the ocean]*

Fighting against plastics or chemical pollution is much more complex and this is not yet developed in Copernicus with the available satellite resolutions and services capacities. Preliminary water quality products are available daily however to detect some chemical content and organic matters at sea (e.g. nitrates, iron, phosphates).

Policy context

The number of policies related to pollution at sea is quite substantial both at international and European level with:

- the United Nations Convention on the Law of the Sea (UNCLOS), Safety Of Life At Sea (SOLAS) and MARPOL conventions;
- the EU strategy for plastics;
- the Waste Directive;
- the circular economy package;
- the ‘International Ocean Governance’ Communication from November 2016;
- the Erika III package;
- the Port Reception Facilities Directive (and its proposal for revision);
- the Sulphur Directive;
- the Regulation on the monitoring, reporting and verification of carbon dioxide emissions from maritime transport;

Working documents on marine litter are also important to consider such as the guidance on monitoring of marine litter in the European seas, and thematic reports on sources of litter and on riverine litter monitoring Pollutants to be tracked are:

- oil and gas pollution from offshore activities including heavy fuel;
- pollutions due to the maritime transport (bilge and ballast waters, oil pollution and leakages, black carbon, CO2 and sulphur pollution from vessels and possible pollution from hazmat transports of goods);
- chemical pollution (e.g. nitrates, black carbon, methane, ammonium, nitrates, heavy metals) coming from land and possibly affecting aquaculture, tourist areas or marine protected areas;
- persistent-organic pollutants;
- radioactivity, invasive species (e.g. from ballast water), heat (e.g. from cooling water), dumped ammunitions, waste dumping;
- major pollution caused by floating plastics, micro plastics and debris from ships accidents or mining activities.

User communities

Actors dealing with ocean pollution are mainly public institutions in charge of the ocean good environmental status of their coasts and territorial waters, but also foundations and associations specially invested in fighting against plastics. To some extent land tenants such as farmers, cities identified as sources of pollution can also be potential users. The research institutes play an active role to support public knowledge-based decision-making.

Evolving needs

From the above list of pollutants to be tracked for regulation purposes, still a lot are not addressed: gas pollution, bilge and ballast waters, black carbon, sulphur, hazmat pollution, methane, heavy metals, waste dumping, most of micro plastics, or invasive species. Since they cannot be simply observed, they need to be deduced and modelled from proxy information provided by observations. When they diffuse or drift quickly in the oceans, diluting making them difficult to catch, their spread has to be modelled. *[S3NG-T-UN-117: S3NG-T should provide topography measurements including waves and ocean surface currents in support of marine plastic debris, bilge waters, invasive species, and other pollutant tracking]*

To help, more systematic real-time observation of pollution at finer scale is needed especially in the case of coastal pollution or in areas of high traffic.

Building upon the EU CleanSeaNet system, operated in EMSA for oil pollution detection and alert mechanism to coastal states, it is also important to integrate and coordinate all sources of information for decision-making:

- near real-time detection of pollution by satellite; *[S3NG-T-UN-118: S3NG-T should provide topography measurements including waves, currents in support of marine pollution tracking in Near Real time 3 hours]*
- ship position from traffic monitoring systems at least for ship-based pollution (the union maritime information and exchange system - SafeSeaNet);
- alerting system and;
- manned or unmanned aerial means from coastal states for verification, identification of polluters and prosecution.

Pollution control also needs the implementation of pollution drift forecasts for each type of sources and components, to establish if pollution will be dispersed in the air over the surface or at sea, to identify possibly the origin and the possible polluter (vessel at the source, chemicals from the coast, beached oil, etc.). *[S3NG-T-UN-119: S3NG-T should provide topography measurements in support of pollution drift forecasts]*

Monitoring EU flagged vessels for pollution control with regular random sampling over areas where EU flagged vessels are present could be performed to detect slicks, identify refuelling at sea and identify polluters subject to a port state control inspection.

In the event of emergencies at sea or potential pollution that threat the maritime environment, EMSA and national services need environmental information in real-time and forecasted, such as high-resolution wind, waves, temperature, salinity and currents ocean products, to be complemented with other sources of information (like automated identification systems and vessel monitoring systems), with a large systematic coverage of waters to be monitored. [*S3NG-T-UN-120: S3NG-T should provide topography measurements in support of the European Maritime Safety Agency (EMSA) integrated maritime services]*

An emergency support service including early warning alert of pollution and support during response operations is already in place based on satellite services and correlation with these other data sources, through the CleanSeaNet service, for EU and neighbourhood countries, and it is extensively based on Sentinel data that is central for its continuity. Consulted users have suggested that the extension of such service for third countries that shown interest could be considered.

For most of chemical pollutions listed in the regulations, significant improvements are needed to better assess water quality, chemical content, optical properties monitoring, land-sea and rivers-sea interactions, combined with currents modelling (surface, in-depth and vertical transport) to tackle the issue of marine litter identification and concentration forecasts.

Chemical pollutions of CO2, NOx (NO+NO2), SO2 and particulate matter (PM2.5) in the air emitted by vessels are also part of gases to monitor and need the monitoring eventually of the troposphere for all major shipping routes, including possibly at vessel scale. Atmospheric composition, aerosols, dust concentration will need to be observed or assessed at finer scale than current atmospheric composition monitored in Copernicus, to be also linked to the potential pollutant source. For some types of pollution (e.g. radioactive), needs are not mature yet and would probably need significant model developments and validation before operational use and official reporting. Promising experiences have already taken place in some Member States in monitoring sulphur emissions along major shipping routes through remotely piloted aircrafts (RPAS) which could complement the satellite imagery and provide this additional evidence ship by ship, to be shared with responsible authorities (e.g. port state control).

III.1.10 Maritime transport, navigation and safety

UN-SWD articulates the following User Needs for Maritime transport, Navigation and Safety.

Copernicus operates a comprehensive maritime surveillance service. In parallel, ocean information is produced to describe the marine environmental conditions for safe sea

shipping: 10 days forecasts up to seasonal forecasts or climate records for long-term planning.

Policy context

Safety at sea is regulated by the international Convention for the Safety of Life at Sea. Many EU regulations (on passenger ship safety, port reception facilities, safe loading and unloading of bulk carriers, safety of offshore oil and gas operations, EU arctic policy, hazardous and noxious substances carried by ships) reinforce its application in the EU. *[S3NG-T-UN-121: S3NG-T should provide topography measurements in support of maritime operations]* The European Maritime Safety Agency has been created to implement and control compliance with these regulations.

User community

Copernicus data and information products are both used by the maritime authorities: coast guards, maritime rescue coordination centre, citizen sailors but also routing services operated by the private sector. *[S3NG-T-UN-122: S3NG-T should provide topography measurements including in support of maritime safety]*

Evolving needs

For the community, the continuity of current meteorological and ocean information services is necessary to support maritime navigation and safety. This contributes to search and rescue and safer route planning or route optimisation (e.g. for. time-to-arrival estimate, fuel consumption, comfort of cruise). *[S3NG-T-UN-123: S3NG-T should provide topography measurements including in support of ship routing]*

Ship operators need increased geospatial resolution with sub-mesoscale ocean dynamics to keep improving transport operations. It is combined with met-ocean conditions (meteorological conditions over the oceans and ocean state). *[S3NG-T-UN-124: S3NG-T should provide sea state and wind speed over the ocean in support of shipping for application with meteorological products]*

Maritime emergency operations need fastest response information and met-ocean information when either a vessel or its crew are in serious distress. In terms of maritime safety and security, Copernicus is integrated in the operations of the European Maritime Safety Agency (EMSA). EMSA needs real-time identification of the vessels, debris and / or potential pollution around the area of the emergency to provide for fast, safe and appropriate response to incidents at sea where the picture may be changing by the hour.

The maritime rescue coordination centres in the EU and EMSA expect more data and information from Copernicus for detection of a missing target, oil spills, local dangers and their drift forecast (e.g. life raft or person, lost container, small vessels or their wakes, icebergs, debris of diverse nature) including to support distress in third countries. *[S3NG-T-UN-125: S3NG-T should provide topography measurements to support surface drift forecasting for maritime safety]*

Maritime surveillance becomes also significantly important in the Arctic (e.g. northern east passage) with the ship traffic, fishing, and transport increasing in this area because of the climate change impacts and reduced ice. Safety services need more sea-ice and met-ocean information and forecasts with a resolved resolution compatible of small icebergs detection (including leads and polynyas), iceberg drift forecast, merged with small vessel

tracking. *[S3NG-T-UN-126: S3NG-T should provide topography measurements (e.g. sea ice thickness, sea state, ocean topography, wind speed) in support of maritime safety in the Arctic Ocean]*

To act quickly, fast access to satellite resources (minutes to hours before the acquisition) and quasi real time delivery of information, is needed with routine monitoring of prioritised areas chosen with operational actors. *[S3NG-T-UN-127: S3NG-T should provide topography measurements in support of maritime emergency operations with a timeliness of ≤3 hours]*

Maintaining an up-to-date map of all activities and vessels at sea is important for sea operations and safety. To improve this mapping, additional radiofrequency detection capabilities using space capacities (e.g. VHF, satellite phone, GSM or maritime radar) could greatly improve the maritime situation awareness to better detect vessels at sea (including sailing boats and small boats) that are not subject to equipment by regulation with certified mandatory reporting systems. Moreover, EMSA and rescue centres need correlation of the satellite-based information detecting effective vessels at sea and their position with information gathered from the vessel reporting systems (provided by certified systems such as automated identification systems and managed by EMSA through the SafeSeaNet information system across the EU Member States) to establish the baseline of monitoring safety at sea.

Finally, assets that allow very high-resolution observation (such as high-altitude platforms or Remote-Piloted Aircraft Systems), in combination with satellite monitoring, could greatly improve maritime domain awareness both for safety and security purposes.

UN-NOTE articulates the following User needs from the Copernicus maritime surveillance service for this domain.

In reference to the set of “maritime” requirements for the Sentinel NG topographic mission, there was a compilation of requirements that may be relevant to the Copernicus Maritime Surveillance service (CMS). These include information on new or additional observational products needed for search & rescue, sea surface pollution and maritime safety (e.g. for vessel navigation/routing) purposes.

[S3NG-T-UN-128: S3NG-T should provide new/additional type of observational products that are needed for search and rescue operations, sea surface pollution and vessel navigation/routing purpose including synergy with other satellite data]

CMS uses Sentinel-1 SAR imagery for oil spill pollution and extracts as ancillary data wind and swell data. However, the service does not have access to satellite observations at shorter wavelengths in the range of ~50m and one recommendation is to acquire remote sensing observations of the 2D directional spectrum for waves period ranging between 2s-10s and capture the large temporal variability of these waves. *[S3NG-T-UN-129: S3NG-T should provide new products of the directional wave spectrum for wavelengths of >50 m, wave period ranging between 2s-10s and capture the large temporal variability of these waves including synergy with other satellite data]*

This wind sea directional wave spectrum is useful to estimate the Stokes drift and thereafter perform drift forecasting modelling for search & rescue, sea surface pollution (important for modelling marine litter circulation) and vessel navigation/routing purposes. To be noted that, as for all CMS requirements, low latency / NRT delivery is important for

this type of product. *[S3NG-T-UN-130: S3NG-T should provide measurements of Stokes drift on the ocean surface to support EMSA search and rescue, marine litter monitoring, and surface ocean pollution monitoring, including synergy with other satellite data]*

One additional recommendation is to wave observations for the whole of the European sea basin and other areas of European interest (e.g. overseas territories). Here it can be beneficial to improve Sentinel1 A/B coverage of swell data, as European seas are currently not covered by Wave Mode since Sentinel 1 uses IWS/EWS mode for “maritime” applications. To be noted that for EMSA’s CleanSeaNet service it is fundamental that Sentinel-1 continues to provide IWS/EWS over European waters and this take priority over the Wave Mode. *[S3NG-T-UN-131: S3NG-T should provide measurements of swell waves on the ocean surface]*

This requirement would potential entail having another mission (potentially a Sentinel NG mission if realistic, feasible and affordable) to provide equivalent Wave Mode observations over Europe.

NB from Commission:

These requirements do not pre-empt any choice of technologies or Sentinel missions (part or not part of the topography mission), since the CMS is mainly using the Sentinel1 mission.

EMSA reflects that, if there a new mission would be considered to deliver the products described (equivalent Wave Mode observations over Europe to Sentinel1 and evolution, if realistic, feasible and affordable), EMSA would use it, as a positive contribution to the use cases described.

UN-NOTE articulates the following additional User needs for maritime services:

EMSA, as a Copernicus user agency and as part of their Integrated Maritime Services, currently uses existing CMEMS wave forecast products for display, but not within any drift models yet. EMSA’s understanding is that new wave observational products can help the further development of search & rescue, sea surface pollution (oil and chemicals) and vessel navigation/routing drifting model services, both close to shore and in open seas.

EMSA coordinates the Integrated Maritime Services (IMS) Correspondence Expert Group on Drift Modelling and also has in-house oil and chemical spills modelling software. EMSA does not run operational drifting models yet, but is planning to develop a service for Search & Rescue in the mid-term. For sea surface pollution, EMSA uses data from both CMEMS as well as wind data from ECMWF meteorological service to run oil & chemical forecast models. The Agency is also looking at the need for additional products to support the operational decision-making process of mobilising and deploying oil pollution response equipment and resources in response to pollution incidents at sea (and to evaluate their efficiency during operation), as well as to enhance marine litter circulation modelling. *[S3NG-T-UN-132: S3NG-T should support drift modelling on the ocean surface to support the EMSA Integrated Maritime Services correspondence expert group on drift modelling]*

III.2 CMEMS Requirements for Future Satellite Observations

CMEMS (2017) articulates the following User Needs:

The analysis of present/future user requirements drive CMEMS service evolution that, in turn, leads to revised specification for the upstream satellite observations. User requirements (e.g. observing the ocean currents at 1 km resolution with a 10% accuracy) do not translate directly into satellite observation requirements. They must go through the added value chain of the service. Use of satellites for data collection and location and for navigation and security issues (AIS) are not considered here. Those are very important uses of satellite technology but CMEMS is not (or barely) a prescriber for these applications.

CMEMS requirements for future satellite observations are thus based on an analysis of the most important satellite observations required to improve/constrain future CMEMS products and services. Continuity of the present Copernicus satellite observing system should be first guaranteed as this is mandatory for maintaining the CMEMS service. *[S3NG-T-UN-133: S3NG-T should guarantee the continuity of Sentinel-3 products]*

This holds, in particular, for the Sentinel 6 altimeter reference mission and the two satellite constellation of Sentinel 3 (altimetry, Sea Surface Temperature and Ocean Colour) and Sentinel 1 (SAR). This satellite observing system must, moreover, be complemented by an adequate and sustained in-situ observing system.

Note also that the very fine scale observations provided by the two satellite constellation of Sentinel 2 provide highly valuable potential information for the CMEMS and its coastal applications. Improvement of CMEMS offer is, however, required to better serve existing users and to anticipate future needs. The main areas of improvements (see also previous section) are:

1. Improved space/time resolution to better monitor and forecast the ocean at fine scale and to improve the monitoring of the coastal zone. *[S3NG-T-UN-134: S3NG-T should improve the space and time resolution of topography measurements compared to baseline continuity of Sentinel-3 products to address the coastal zone]*
2. Better monitoring of biogeochemical state of ocean.
3. Better monitoring of the rapidly changing polar regions. *[S3NG-T-UN-135: S3NG-T should provide topography measurements to better monitor the rapidly changing polar regions compared to baseline continuity of Sentinel-3 products]*

This will require major evolution of satellite observing capabilities. When moving to higher resolution, it will be fundamental to constrain CMEMS models with new observations. *[S3NG-T-UN-136: S3NG-T should provide new topography measurements to constrain CMEMS models]* The most important satellite-based observation is sea surface height (SSH) from altimetry. The SSH is an integral of the ocean interior properties and is a strong constraint for inferring the 4D ocean circulation through data assimilation. *[S3NG-T-UN-137: S3NG-T should provide enhanced performance of sea surface height measurements (the most important satellite observation for CMEMS) compared to Sentinel-3]* Multiple nadir altimeters (at least 4 altimeters) are required (this was required 10 year ago) to adequately represent ocean eddies and associated currents in models. *[S3NG-T-UN-138: S3NG-T should include multiple nadir altimeters flying in constellation to adequately represent ocean eddies and associated geostrophic currents in models]*

Much higher space/time resolution (e.g. 50 km / 5 days) will be needed in the post 2025 time period. *[S3NG-T-UN-139: S3NG-T should provide topography products with a*

horizontal gridded resolution of ≤50 km and a temporal resolution of ≤5 days] This can be achieved through a combination of swath altimetry (to be demonstrated with the SWOT mission to be launched in 2021) with nadir SAR altimetry.

Satellite requirements for the GMES/Copernicus Marine Service have been detailed in the GMES Marine Core Service (MCS) implementation group report (Ryder, 2007) based on the recommendations of the GMES MCS Space Working Group (Le Traon et al., 2006). The nomenclature has been appended with [Copernicus] to add clarity since the requirements are only marginally met by Copernicus today and remain valid.

General recommendations:

1. Continuity of observation is crucial. This is particularly critical around 2010 when data gaps could occur for several of the most critical observations. Decisions for developing the first of the GMES [Copernicus] satellites must then be taken most urgently.
2. It is more critical to establish satellite series for sustainable service availability than to try optimizing the specifications and designing for any one satellite and its instruments, if the latter leads to expensive, non-renewable satellites. Establishing satellite series should lead to significantly lower production costs. *[S3NG-T-UN-140: S3NG-T should provide a series of satellites as a sustainable service] [S3NG-T-UN-141: S3NG-T should avoid expensive, non-renewable satellites but focus on a satellite series that should lead to significantly lower production costs]*
3. GMES [Copernicus] should allow for research and technological developments. In particular, the possibility of embarking new instruments with the potential to meet GMES [Copernicus] needs should be considered. Wide Swath altimetry and geostationary ocean colour are the two most important new technology developments that will benefit the GMES MCS [Copernicus CMEMS] in the long run.

Specific recommendations:

1. The Jason series (high accuracy altimeter system for climate applications and as a reference for other missions) is an essential and critical component of the GMES [Copernicus] satellite programme for MCS [CMEMS]. *[S3NG-T-UN-142: S3NG-T should use the Sentinel-6 reference altimeter to homogenise topography measurements]* Planning of Jason-3 must be a priority for GMES [CMEMS].
2. The MCS [CMEMS] requires a high resolution altimeter system with at least three altimeters in addition to the Jason series. Sentinel-3 should include a constellation of two satellites, flying simultaneously, providing adequate coverage and operational robustness. *[S3NG-T-UN-143: A minimum of two satellites should be available in the S3NG-T].* Instrumentation costs for S3 should be reduced as much as possible to allow for a two satellite system.
3. Compared to the present design of S3 instrumentation, the priority for Sea Surface Temperature is for high accuracy dual view measurements. The large swath requirement has a much lower priority, in particular (but not only), if S3 is a two satellite system. As far as Ocean Colour is concerned, a sensor having a similar spectral resolution to MERIS is essential to meet the important shelf and coastal ocean water quality measurement requirements. The use of a SeaWiFS type of

instrument (reduced number of channels) would serve only the minimum operational requirements for the open ocean.

4. SAR data (Sentinel 1) are required for oil spill detection and sea ice monitoring. This is clearly a European core service that should be considered as part of the MCS [CMEMS]. The requirement is for at least one and preferably two SAR missions in addition to the other non-European missions (e.g. Radarsat).
5. Access to other European and non-European (e.g. NPOESS, RADARSAT) satellite data in real time is fundamental for the MCS [CMEMS].
6. Ground segment requirements will be addressed in a specific report/note. The main recommendation is likely to be that the GMES ground segment should develop strong interfaces with EUMETSAT Ocean&Sea Ice SAF and with the MCS satellite Thematic Assembly Centres (TACs).

CMEMS Recommendations For Polar And Sea Ice Monitoring:

- Continuation and improvement of the sea ice thickness time series from CryoSat-2. [*S3NG-T-UN-144: S3NG-T should provide measurements of sea ice thickness]* This is required both for climate and operational sea ice monitoring activities (including assimilation in sea ice models).
- Continuation of the altimetry sampling over the ocean in Polar Regions to constrain ocean models through data assimilation (e.g. for improved ocean currents). *[S3NG-T-UN-145: S3NG-T should provide continuity of Sentinel-3 topography measurements over polar regions]*
- Reliable retrieval of sea level in the leads to reach the retrieval accuracy required to monitor Climate Change. *[S3NG-T-UN-146: S3NG-T should provide measurements of sea level in the sea ice leads to reach the retrieval accuracy required to monitor Climate Change.]*
- Continuation of SMOS like observations of thin sea ice below 0.5 m.
- Sustainable operation of medium-resolution (5-10 km) multi-frequency and -polarization passive microwave observations of SST, sea ice lead fraction and sea ice concentration, area and extent. [*S3NG-T-UN-147: S3NG-T should provide measurements of sea ice lead fraction]* [*S3NG-T-UN-148: S3NG-T should provide measurements of sea ice concentration]* [*S3NG-T-UN-149: S3NG-T should provide measurements of sea ice parameters using a radar altimeter and a microwave radiometer (required for tropospheric wet path delay correction of the altimeter measurements) within the altimeter footprint (at a resolution of 5-10 km)]*
- Automated production of ice chart-like products from a combination of SAR data and other data (e.g. bi-static SAR, passive microwave, multi-frequency SAR).
- Reliable retrieval of ocean colour in the marginal ice zone.

III.3 C3S requirements for climate series

UN-NOTE articulates the following User Needs for the Copernicus climate change services in terms of climate records.

The requirements for C3S given by ECMWF have been consolidated based on the requirements presented during the first ad-hoc expert group meeting by CNRS on climate science needs, and by Met Office about waves:

- Scientific requirements for S6-NG: Benoit Meyssignac (CNRS/LEGOS), after discussions with P.Bonnefond, J.Willis and C.Watson with inputs from R.de Conto, A.Ribes, A.Slangen, K.Richter, M.Ablain, P.Prandi, R.Jugier, A.Guerou, A.Blazquez, S.Labroue, T.Guinle, N.Picot, J.Benveniste, E.Obligis, Briefing for ESA Copernicus Next Generation Topography Constellation (ad-hoc) Expert Group Meeting, 17-18 Feb. 2020.
- User requirements for satellite observations of wave spectra and currents – an operational modelling perspective: Andy Saulter (Met Office), Surge and Wave Modelling Team, Briefing for ESA Copernicus Next Generation Topography Constellation (ad-hoc) Expert Group Meeting, 17-18 Feb. 2020.

C3S team endorses the requirements presented for climate science are relevant also for C3S. C3S however emphasizes that this may not reflect needs for operational ocean data assimilation, where the focus would need to be different: regional sea-level and uncertainty for sea-level instead of trend. For such requirements, C3S will follow requirements established by CMEMS for coastal and data assimilation in general.

Additional requirements would be:

- the need for an up-to-date land-ocean mask (especially in coastal regions where sand islands can move or build by humans)
- A good bathymetry data (especially crucial for shallow waters or near underwater ocean bed rise).

Requirements for wave products as presented by Met-Office reflect C3S needs. Expected performances for C3S should be:

- Return frequency order 2 days or less
- Spectral sensor resolves wavelengths from less than 40m (~5 seconds wave period in deep water) to up to 600m (~20 secs);;
- Along track sampling at least as per present generation instruments;
- Swath capability, samples up to +/-100km across track – improved spatial sampling per pass;
- Certified significant wave height range: 0.1 – 15m;
- Collocation with wind/surface stress and surface current measurements;
- Coastal sampling capability of at least within 2km of coastline and 10m water depth.

NB: If a wave ECV is part of GCOS, C3S does not plan to develop such ECV the next MFF timeframe.

III.4 European Commission Copernicus Level 2 Product and Performance Needs for S3NG-T in the 2030-2050 timeframe

The **UN-COPURD** articulates S3NG-T product performance user needs in Table III.4.1.

Table III.4.1 S3NG-T product performance user needs derived from EC User Needs documentation.

UR-ID	Requirement Description	Source	Copernicus User	Coverage	Spatial Resolution (km)	Temporal Resolution (Days)	Delivery timeliness	Uncertainty	Stability
S3NG-T-UN-P01	Sea Surface Height (Global Ocean)	UN-COPURD	CMEMS, C3S, CAMS, CGLMS, EMSA	Global ocean	≤50 gridded	≤ 15 (g: ≤ 5)	NTC	≤4 cm (g:≤2 cm)	≤(TBC)
S3NG-T-UN-P02	Sea Surface Height (Global Ocean)	CMEMS (2017)	CMEMS, C3S, CAMS, CGLMS, EMSA	Global ocean	≤50 gridded	≤ 5	NTC	≤4 cm (g:≤2 cm)	≤(TBC)
S3NG-T-UN-P03	Sea Surface Height (SSH) - 50 km, 15 days (C3S REQ UR-C3S-152)	UN-COPURD	C3S	Global ocean	≤50 grid	≤10	≤10	≤4 cm (g:≤1 cm) (global mean) over a grid mesh of 50-100 km	< 0.3 mm/yr (global mean)
S3NG-T-UN-P04	Sea Surface Height (Coastal Ocean)	UN-COPURD	CMEMS, C3S, CAMS, CGLMS, EMSA	Coastal ocean	≤50 grid	≤10	NTC	≤4 cm (g:≤2 cm)	≤(TBC)
S3NG-T-UN-P05	Sea Surface Height (Coastal Ocean)	UN-COPURD	CMEMS, C3S, CAMS, CGLMS, EMSA	Regional Coastal ocean	≤10 (g:≤5)	≤1 (g:≤0.5)	NTC	≤3 cm (g:≤2 cm)	≤(TBC)
S3NG-T-UN-P06	Global sea level (SSH)	UN-NOTE	CMEMS, C3S, CAMS, CGLMS, EMSA	Global Ocean	≤50 grid	≤10	≤60	≤0.2 cm at annual tome scales	< 0.1 mm/yr <0.05mm/yr^2

									over more than a decade
S3NG-T-UN-P07	Global sea level (SSH, GCOS-154, C3S REQ: UR-C3S-45)	C3S(2020)	CMEMS, C3S, CAMS, CGLMS, EMSA	Global Ocean	≤50	≤10	≤10	≤0.4 cm (g:≤0.2 cm) (global mean); 1cm over a grid mesh of 50 - 100 km	< 0.3 mm/yr (global mean)
S3NG-T-UN-P08	Regional sea level (SSH)	UN-NOTE	CMEMS, C3S, CAMS, CGLMS, EMSA	Global Ocean	≤100 (g:≤50)	≤10	≤60	≤1cm over a grid mesh of 50 - 100 km	< 0.5 mm/yr over more than a decade
S3NG-T-UN-P09	Regional sea level (SSH GCOS-154)	C3S(2020)	CMEMS, C3S, CAMS, CGLMS, EMSA	Global Ocean	≤100 (g:≤50)	≤10	≤60	≤1cm over a grid mesh of 50 - 100 km	< 0.5 mm/yr over more than a decade
S3NG-T-UN-P10	Regional sea level (SSH GCOS-154C3S REQ UR-C3S-46)	C3S(2020)	CMEMS, C3S, CAMS, CGLMS, EMSA	Global Ocean	≤25	≤7	≤7	≤1cm over a grid mesh of 50 - 100 km	< 1 mm/yr (for a grid mesh of 50 - 100km)
S3NG-T-UN-P11	Significant Wave Height (Hs)	UN-NOTE	CMEMS, C3S, CAMS, CGLMS, EMSA	Global Ocean	≤1	≤1	(TBC)	≤5 cm	≤(TBC)
S3NG-T-UN-P12	Significant Wave Height (Hs)	UN-NOTE	CMEMS, C3S, CAMS, CGLMS, EMSA	Global Ocean	≤10	≤1	(TBC)	≤10 cm	≤(TBC)
S3NG-T-UN-P13	Significant Wave Height (Hs)	UN-NOTE	CMEMS, C3S, CAMS, CGLMS, EMSA	Regional Ocean	≤5 (g:≤1)	≤3 hour (g:≤1 hour)	NRT3H	≤5 cm	≤(TBC)
S3NG-T-UN-P14	Significant Wave Height (Hs)	UN-NOTE	CMEMS, C3S, CAMS,	Global Ocean	≤5 (g:≤1)	≤3 hour (g:≤1 hour)	NRT3H	≤5 cm	≤(TBC)

			CGLMS, EMSA						
S3NG-T-UN-P15	Significant Wave Height (Hs, GCOS-154) (C3S REQ. UR-C3S-44)	C3S(2020)	CMEMS, C3S, CAMS, CGLMS,	Global and Coastal Ocean	≤25	≤3 hour	NRT3H	≤10 cm	≤5c m [year?]
S3NG-T-UN-P16	Directional Wave Energy Spectrum	UN-NOTE	CMEMS, C3S, CAMS, CGLMS, EMSA	Global; Costal Regional	≤1 km (g: ≤50 m Coastal regions	≤1 hour (g:≤ 0.5 hour)	NRT1H	≤0.1 m^2/Hz	≤(TBC)
S3NG-T-UN-P17	Wave direction - 0.5 - 1 h	UN-NOTE	CMEMS, C3S, CAMS, CGLMS, EMSA	Global; Costal Regional	≤5	≤1 hour (g:≤ 0.5 hour)	NRT1H	≤0.05 s	≤(TBC)
S3NG-T-UN-P18	Wave direction - 24 h	UN-NOTE	CMEMS, C3S, CAMS, CGLMS, EMSA	Global; Costal Regional	≤1	≤1	NRT3H	≤0.05 s	≤(TBC)
S3NG-T-UN-P19	Wave period (Tp, Tm01, Tm02) - 0.5 - 1 h	UN-NOTE	CMEMS, C3S, CAMS, CGLMS, EMSA	Global; Costal Regional	≤5	≤1 hour (g: 0.5 hour)	NRT3H	≤0.05 s	≤(TBC)
S3NG-T-UN-P20	Wave period (Tp, Tm01, Tm02) - 24 h	UN-NOTE	CMEMS, C3S, CAMS, CGLMS, EMSA	Global; Costal Regional	≤ 1	≤1	NRT3H	≤0.05 s	≤(TBC)
S3NG-T-UN-P21	Wind speed over the ocean at 10m height (U10)	UN-NOTE	CMEMS, C3S, CAMS, CGLMS, EMSA	Coastal and Global	≤5	≤1 hour	NRT1H	≤ 2 m/s	≤(TBC)
S3NG-T-UN-P22	Wind direction over the ocean at 10m height (U10)	UN-NOTE	CMEMS, C3S, CAMS, CGLMS, EMSA	Global	≤5	≤1 hour	NRT1H	≤5°	≤(TBC)
S3NG-T-UN-P23	Surface Water Elevation over Rivers	UN-COPURD	CMEMS, C3S, CAMS, CGLMS, EMSA	Global	Rivers ≥100m width (g:≥50 m)	≤1	NRT3H	≤10 cm (g:≤5 cm)	≤(TBC)

S3NG-T-UN-P24	Surface Water Elevation over Rivers	UN-NOTE	CMEMS, C3S, CAMS, CGLMS, EMSA	Global	Rivers ≥100m width	≤1	NRT3H	≤10 cm	≤(TBC)
S3NG-T-UN-P25	Surface Water Elevation over Lakes and reservoirs	UN-COPURD	CMEMS, C3S, CAMS, CGLMS, EMSA	Global	Lakes ≥ 1 km²	≤1	NRT3H	≤10 cm (g:≤5 cm)	≤(TBC)
S3NG-T-UN-P26	Surface Water Elevation over Lakes	UN-NOTE	CMEMS, C3S, CAMS, CGLMS, EMSA	Continental coverage	≥1	≤1	NRT3H	≤3 cm	≤(TBC)
S3NG-T-UN-P27	Surface Water Elevation over Lakes	UN-NOTE	CMEMS, C3S, CAMS, CGLMS, EMSA	Europe	≥0.5	≤0.5	NRT3H	≤50 cm	≤(TBC)
S3NG-T-UN-P28	Surface Water Elevation over Lakes	UN-NOTE	CMEMS, C3S, CAMS, CGLMS, EMSA	Global	100 km grid	≤1 month	NTC	≤10 cm	≤(TBC)
S3NG-T-UN-P29	Lake Level (GCOS-154 requirement, C3S REQ. UR-C3S-64)	UN-COPUN	C3S	Lake level of all lakes in the Global Terrestrial Network for Lakes (GTN-L)	N/A	≤1 month	≤1 month	≤50 cm	≤10 cm
S3NG-T-UN-P30	Water extent	UN-NOTE	CMEMS, C3S, CAMS, CGLMS,	Continental	≤0.2	≤1	NRT3H	10 % (relative) 5% (for 70 largest lakes)	≤(TBC)
S3NG-T-UN-P31	Water extent	UN-NOTE	CMEMS, C3S, CAMS, CGLMS,	Continental	≤0.1	≤30	NTC	10 % (relative) 5% (for 70 largest lakes)	≤(TBC)
S3NG-T-UN-P32	Sea Ice Thickness	UN-NOTE	CMEMS, C3S, CAMS, CGLMS, EMSA	Ocean coverage	≤25	≤30	NTC	≤0.1 cm	≤(TBC)

S3NG-T-UN-P33	Sea Ice Thickness	UN-NOTE	CMEMS, C3S, CAMS, CGLMS, EMSA	Regional coverage	≤0.1	≤1	NTC	≤ 1 cm	≤(TBC)
S3NG-T-UN-P34	Sea ice type	UN-NOTE	CMEMS, C3S, CAMS, CGLMS, EMSA	Ocean coverage	≤1 km (g: 100 m) for shipping and search and rescue <10 m (g: ≤3m) in highly infested ice regions	≤1	NRT3H	≤(TBC) % false rate in classification	≤(TBC)
S3NG-T-UN-P35	Snow cover on sea ice	UN-NOTE	CMEMS, C3S, CAMS, CGLMS, EMSA	Ocean coverage	≤0.5 (g:≤ 0.1 on complex terrain)	≤1	NRT3H	≤5 cm	≤(TBC)
S3NG-T-UN-P36	Ice Sheets and Shelves drift	UN-NOTE	C3S, CAMS, CGLMS,	Continental	≤ 0.1 (g:≤0.02)m	≤30	NTC	≤0.1 m	≤(TBC)
S3NG-T-UN-P37	Ice Sheets and Shelves elevation data	UN-NOTE	C3S, CAMS, CGLMS,	Continental	≤0.1	≤30	NTC	≤0.1 m/yr	≤(TBC)
S3NG-T-UN-P38	Ice Sheets elevation data	UN-NOTE	C3S, CAMS, CGLMS,	Continental	≤0.1	≤30	NTC	≤10 cm	≤(TBC)
S3NG-T-UN-P39	Ice Sheets surface elevation change (GCOS-154 requirement, C3S REQ UR-C3S-53)	UN-COPUN	C3S,	Continental	≤0.1	≤30	≤30 days	0.1 m/yr	0.1 m/yr
S3NG-T-UN-P40	Glacier area extent	UN-NOTE	C3S, CAMS, CGLMS,	Continental	≤0.03 (g:≤ 0.015 m)	1 year (at the end of the ablation season)	NTC	< 5%	≤(TBC)

S3NG-T-UN-P41	Glacier elevation data - High-Res	UN-NOTE	C3S, CAMS, CGLMS,	Continental	≤0.3 (g: ≤0.2)	1 year	NTC	≤10 cm	≤(TBC)
S3NG-T-UN-P42	Glacier elevation data - Medium-Res	UN-NOTE	C3S, CAMS, CGLMS,	Continental	≤0.1 (g:≤0.03)	10 years	NTC	≤1 m	≤(TBC)
S3NG-T-UN-P43	Lake ice cover	UN-NOTE	C3S, CAMS, CGLMS,	Continental	≤0.3	≤1	NRT3H	≤0.1	≤(TBC)
S3NG-T-UN-P44	Lake ice thickness	UN-NOTE	C3S, CAMS, CGLMS,	Continental	≤0.1	1 month	NTC	≤2 cm (g:≤1 cm)	≤(TBC)
S3NG-T-UN-P45	Permafrost Active Layer Thickness	UN-NOTE	C3S, CAMS, CGLMS,	Continental	Sites for bio-climate zones	24 h - 1 week	NTC/ STC	≤2 cm	≤(TBC)
S3NG-T-UN-P46	Sea Ice Area	UN-NOTE	CMEMS, C3S, CAMS, CGLMS, EMSA	Global; Regional	≤1 km (g:≤0.1 for shipping and search and rescue, ≤0.03 in highly infested ice regions)	≤1 (g: ≤ 3 h in highly infested ice regions)	NRT3H/ STC	≤5%	≤(TBC)
S3NG-T-UN-P47	Sea Ice Concentration - 1 week	UN-NOTE	CMEMS, C3S, CAMS, CGLMS, EMSA	Ocean	≤15 (g:≤10)	≤1 week	NTC	≤5%	≤(TBC)
S3NG-T-UN-P48	Sea Ice Concentration - 24 h	UN-NOTE	CMEMS, C3S, CAMS, CGLMS, EMSA	Global; Regional	≤1 km (g:≤0.1 for shipping and search and rescue, ≤0.03 in highly	≤1 (g: ≤ 3 h in highly infested ice regions)	NRT3H/ STC	≤5%	≤(TBC)

					infested ice regions)				
S3NG-T-UN-P49	Sea Ice Drift - 1 week	UN-NOTE	CMEMS, C3S, CAMS, CGLMS, EMSA	Ocean	≤5	≤1 week	NTC	≤1 km/day	≤(TBC)
S3NG-T-UN-P50	Sea Ice Drift - 24 h	UN-NOTE	CMEMS, C3S, CAMS, CGLMS, EMSA	Global; Regional	≤2 (g: ≤1)	≤1	NRT3H/ STC	≤(TBC)	≤(TBC)
S3NG-T-UN-P51	Sea Ice Extent/Edge - 1 week	UN-NOTE	CMEMS, C3S, CAMS, CGLMS, EMSA	Ocean	≤5 (g:≤1)	≤1 week	NTC	≤1 km	≤(TBC)
S3NG-T-UN-P52	Sea Ice Extent/Edge - 24 h	UN-NOTE	CMEMS, C3S, CAMS, CGLMS, EMSA	Global; Regional	≤1 km (g:≤0.1 for shipping and search and rescue, ≤0.03 in highly infested ice regions)	≤1 (g: ≤ 3 h in highly infested ice regions)	NRT3H/ STC	≤0.0	≤(TBC)
S3NG-T-UN-P53	Snow area extent High-Resolution 10-20 m, 3 days	UN-NOTE	CMEMS, C3S, CAMS, CGLMS, EMSA	Continental	≤0.02 (g:≤0.01)	≤3	STC/ NTC	≤(TBC)	≤(TBC)
S3NG-T-UN-P54	Snow area extent Medium-Res 1 km	UN-NOTE	CMEMS, C3S, CAMS, CGLMS, EMSA	Continental	≤1 (g: ≤0.1 in complex terrain)	≤1	NRT3H/ STC	5% (max error of ommission and commission in snow area); location accuracy: better than 1/3 IFOV with target IFOV 100 m in complex terrain; 1km elsewhere	≤(TBC)

S3NG-T-UN-P55	Snow area extent Medium-Res 500 m	UN-NOTE	CMEMS, C3S, CAMS, CGLMS, EMSA	Continental	≤0.5 (g:0.1 m in complex terrain)	≤1	NRT3H/ STC	≤5%	≤(TBC)
S3NG-T-UN-P56	Snow Depth	UN-NOTE	CMEMS, C3S, CAMS, CGLMS, EMSA	Continental	≤1 (g:≤0.1 in complex terrain)	≤1	NRT3H/ STC	≤10 mm	≤(TBC)
S3NG-T-UN-P57	Snow Water Equivalent High-Res	UN-NOTE	CMEMS, C3S, CAMS, CGLMS, EMSA	Continental	≤0.02 (g:≤0.01)	≤3	SRTC/ NTC	≤(TBC)	≤(TBC)
S3NG-T-UN-P58	Snow Water Equivalent High-Res	UN-NOTE	CMEMS, C3S, CAMS, CGLMS, EMSA	EU	≤0.1 m	≤3	SRTC/ NTC	≤0 mm	≤(TBC)
S3NG-T-UN-P59	Snow Water Equivalent Low-Res 1 km	UN-NOTE	CMEMS, C3S, CAMS, CGLMS, EMSA	Continental	≤1	≤1	NRT3H/ STC	≤10 mm	≤(TBC)
S3NG-T-UN-P60	Geoid determination	UN-NOTE	CMEMS, C3S, CAMS, CGLMS, EMSA	Global	≤100	≤1 year	NTC	≤0.5 cm (g:≤0.1cm)	≤(TBC)
S3NG-T-UN-P61	Mean and Time Variable Gravity Field (covering Polar regions)	UN-NOTE	CMEMS, C3S, CAMS, CGLMS, EMSA	Continental	≤50	≤30	NTC	≤10 km^3/yr	≤(TBC)
S3NG-T-UN-P62	Bathymetry (Water depth in shallow waters)	UN-NOTE	CMEMS, C3S, CAMS, CGLMS, EMSA	Coastal	≤0.03 (g:≤0.01)	≤1 month (to be verified)	NTC	≤10 % (g:≤5%(TBC))	≤(TBC)
S3NG-T-UN-P63	Bathymetry	UN-NOTE	CMEMS, C3S, CAMS, CGLMS, EMSA	EU Coastal	≤0.05	NTC on demand	NTC	≤(TBC)	≤(TBC)

APPENDIX IV S3NG-T REQUIREMENTS TRACEABILITY MATRIX.

The user needs identified in this section of the MRD have been derived from documents provided by the European Commission for that purpose. The user needs derived are the basis for traceability to enhancements of the S3NG-T mission beyond strict continuity of in-flight Sentinel-3 performance established in Table 2.4-1.

Table IV.1 links the S3NG-T Copernicus User Needs to the mission requirements.

Table IV.1 Traceability matrix between European commission Copernicus User Needs and the Sentinel-3 Next Generation Topography (S3NG-T) Mission Requirements

User Need ID	EC User Need	User Need ID Source	S3NG-T MRD Requirement(s)
S3NG-T-UN-001	S3NG-T should provide ocean observations to support the development of the GES indicators with consistent time series over time: sea level, wave height, ocean circulation	SWD (2019) Ares(2020)1823662 - 30/03/2020	MRD-1520, MRD-1590. Ocean circulation can be computed from SSH
S3NG-T-UN-002	S3NG-T should provide ocean products at regional and coastal scales to support national reporting including connectivity between rivers and ocean	SWD (2019) Ares(2020)1823662 - 30/03/2020	MRD-030, MRD-040, MRD-1740
S3NG-T-UN-003	S3NG-T should provide estimates of ocean circulation and Total Surface Current Velocity that together with models, would monitor the source, ocean transport, degradation and fate of floating marine plastic debris.	SWD (2019) Ares(2020)1823662 - 30/03/2020	Geostrophic velocities can be computed from SSH MRD-1520,
S3NG-T-UN-004	S3NG-T should maintain and improve satellite altimetry measurements to better understand the ocean at global scale to support the 6 topics of IOG: pollution, climate, blue economy, security, fisheries, marine protected areas	SWD (2019) Ares(2020)1823662 - 30/03/2020	

S3NG-T-UN-005	S3NG-T should enhance global observations (performance and sampling) of ocean topography measurements and contribute to climate change monitoring	SWD (2019) Ares(2020)1823662 - 30/03/2020	MRD-590
S3NG-T-UN-006	S3NG-T including S6 NG-T should contribute to the continuity of ocean climate records	SWD (2019) Ares(2020)1823662 - 30/03/2020	MRD-360, MRD-370, MRD-380, MRD-1540
S3NG-T-UN-007	The duration of the S3NG-T missions should be of sufficient duration to confidently establish and monitor future ocean changes by contributing to the GCOS and SDG reporting	SWD (2019) Ares(2020)1823662 - 30/03/2020	MRD-320
S3NG-T-UN-008	S3NG-T data products should be made available to operational applications user communities, scientific user communities and commercial user communities	SWD (2019) Ares(2020)1823662 - 30/03/2020	MRD-1240, MRD-1330, MRD-1660,
S3NG-T-UN-009	The S3NG-T should increase the resolution of topography observations in time and space to address maritime spatial planning at coast, implementation of the 11 GES indicators at coast, ship routing in complementarity to meteorological services	SWD (2019) Ares(2020)1823662 - 30/03/2020	MRD-1590
S3NG-T-UN-010	S3NG-T should provide sufficient density, revisit and coverage sampling to support ocean models at a horizontal resolution of 1/36° globally	SWD (2019) Ares(2020)1823662 - 30/03/2020	MRD-1590
S3NG-T-UN-011	S3NG-T should provide sufficient density, revisit and coverage sampling to support ocean models at a horizontal resolution of 1/72° regionally	SWD (2019) Ares(2020)1823662 - 30/03/2020	MRD-1590
S3NG-T-UN-012	S3NG-T should provide measurements of sea-ice, waves and winds in closed and marginal seas	SWD (2019) Ares(2020)1823662 - 30/03/2020	MRD-030, MRD-1620, MRD-1630, MRD-1640, MRD-1690, MRD-1700, MRD-1710, MRD-1850, MRD-1880, MRD-1890, MRD-1950

S3NG-T-UN-013	S3NG-T should enhance measurements in the coastal ocean	SWD (2019) Ares(2020)1823662 - 30/03/2020	MRD-030, MRD-040, MRD-1740
S3NG-T-UN-014	S3NG-T should provide uncertainty estimates in all products	SWD (2019) Ares(2020)1823662 - 30/03/2020	MRD-1220, MRD-1290, MRD-1300
S3NG-T-UN-015	S3NG-T should provide topography measurements of ocean state (i.e. sea surface height, sea level, wind, waves, ocean currents etc) in support of the biological ocean component	SWD (2019) Ares(2020)1823662 - 30/03/2020	MRD-1520, MRD-11530, MRD-1620, MRD-1630, MRD-1640, MRD-1690, MRD-1700, MRD-1710, MRD-1850, MRD-1880, MRD-1890,
S3NG-T-UN-016	S3NG-T should provide measurements to monitor sea ice conditions and changes	SWD (2019) Ares(2020)1823662 - 30/03/2020	MRD-1880, MRD-1890,
S3NG-T-UN-017	S3NG-T should provide topography measurements to monitor continental ice condition and changes	SWD (2019) Ares(2020)1823662 - 30/03/2020	MRD-1970
S3NG-T-UN-018	S3NG-T should provide topography measurements to measure glacier conditions and changes	SWD (2019) Ares(2020)1823662 - 30/03/2020	MRD-1970
S3NG-T-UN-019	S3NG-T should provide measurements to monitor land-ice/snow and sea-ice interface/snow conditions and changes	SWD (2019) Ares(2020)1823662 - 30/03/2020	MRD-1900, MRD-1910, MRD-1920, MRD-1920, MRD-1930, MRD-1940,
S3NG-T-UN-020	S3NG-T should provide measurements with a delivery timeliness to support applications in the polar regions in near real time for short-term forecasts and climate scales	SWD (2019) Ares(2020)1823662 - 30/03/2020	MRD-470

S3NG-T-UN-021	S3NG-T should provide measurements tailored to Copernicus Services for integration with models	SWD (2019) Ares(2020)1823662 - 30/03/2020	MRD-1220, MRD-1290, MRD-1300
S3NG-T-UN-022	S3NG-T should ensure that the definition of the coastal zone will include a limit of 24 nautical miles (50 km) offshore	SWD (2019) Ares(2020)1823662 - 30/03/2020	MRD-030
S3NG-T-UN-023	S3NG-T should provide measurements with improved performance compared to Sentinel-3 over the coastal ocean	SWD (2019) Ares(2020)1823662 - 30/03/2020	Table 7.5.1.1-1 and MRD-1470 to MRD-1590
S3NG-T-UN-024	S3NG-T should provide estimates of river discharge into the coastal ocean	SWD (2019) Ares(2020)1823662 - 30/03/2020	MRD-1765
S3NG-T-UN-025	S3NG-T should provide measurements of storm surge monitoring	SWD (2019) Ares(2020)1823662 - 30/03/2020	
S3NG-T-UN-026	S3NG-T should provide measurements in support of flood mapping and management	SWD (2019) Ares(2020)1823662 - 30/03/2020	MRD-1760
S3NG-T-UN-027	S3NG-T should provide products in support of coastal erosion monitoring and management	SWD (2019) Ares(2020)1823662 - 30/03/2020	MRD-1620, MRD1630, MRD-1640
S3NG-T-UN-028	S3NG-T should provide measurements of sea level rise	SWD (2019) Ares(2020)1823662 - 30/03/2020	
S3NG-T-UN-029	S3NG-T should ensure that the definition of the coastal zone will include a limit of 12 nautical miles offshore	SWD (2019) Ares(2020)1823662 - 30/03/2020	MRD-030
S3NG-T-UN-030	S3NG-T should provide topography measurements in support of coastal ocean modelling	SWD (2019) Ares(2020)1823662 - 30/03/2020	MRD-1520, MRD-11530, MRD-1620, MRD-1630, MRD-1640, MRD-

			1690, MRD-1700, MRD-1710,
S3NG-T-UN-031	S3NG-T should recognize definitions of transitional waters (according to the nomenclature of Water Framework Directive), coastal waters (according to the nomenclature of Water Framework Directive) and to marine waters	SWD (2019) Ares(2020)1823662 - 30/03/2020	MRD-040
S3NG-T-UN-032	S3NG-T should ensure consistency between land and ocean products	SWD (2019) Ares(2020)1823662 - 30/03/2020	
S3NG-T-UN-033	S3NG-T should provide measurements to observe coastal sub-mesoscale dynamics	SWD (2019) Ares(2020)1823662 - 30/03/2020	MRD-1520, MRD-11530, MRD-1620, MRD-1630, MRD-1640, MRD-1690, MRD-1700, MRD-1710,
S3NG-T-UN-034	S3NG-T should provide hydrological inputs (e.g. discharge estimates) to the coastal ocean from rivers, estuaries and ice melt	SWD (2019) Ares(2020)1823662 - 30/03/2020	MRD-1760, MRD1765
S3NG-T-UN-035	S3NG-T should provide estimates of bathymetry in the coastal ocean	SWD (2019) Ares(2020)1823662 - 30/03/2020	
S3NG-T-UN-036	S3NG-T should provide topography measurements to support climate adaptation applications in the coastal zone	SWD (2019) Ares(2020)1823662 - 30/03/2020	MRD-1520, MRD-11530, MRD-1620, MRD-1630, MRD-1640, MRD-1690, MRD-1700, MRD-1710,
S3NG-T-UN-037	S3NG-T should provide topography measurements in support of biogeochemical ocean forecasts (e.g. sea state, winds, ocean currents)	SWD (2019) Ares(2020)1823662 - 30/03/2020	MRD-1520, MRD-11530, MRD-1620, MRD-1630, MRD-1640, MRD-

			1690, MRD-1700, MRD-1710,
S3NG-T-UN-038	S3NG-T should provide ocean products at global scale and regional scale for EU policy implementation, support to Regional Fisheries Management Organisations (RFMO), at coastal scale to support aquaculture	SWD (2019) Ares(2020)1823662 - 30/03/2020	MRD-1520, MRD-11530, MRD-1620, MRD-1630, MRD-1640, MRD-1690, MRD-1700, MRD-1710,
S3NG-T-UN-039	S3NG-T should support policy implementation by European Fisheries Control Agency (EFCA) and EU Member States sustainable fisheries management and reporting	SWD (2019) Ares(2020)1823662 - 30/03/2020	
S3NG-T-UN-040	S3NG-T ocean products (e.g. geostrophic currents, waves, winds) should be available to support industrial and coastal fisheries	SWD (2019) Ares(2020)1823662 - 30/03/2020	
S3NG-T-UN-041	S3NG-T should provide topography measurements in support of fisheries applications	SWD (2019) Ares(2020)1823662 - 30/03/2020	MRD-1520, MRD-11530, MRD-1620, MRD-1630, MRD-1640, MRD-1690, MRD-1700, MRD-1710,
S3NG-T-UN-042	S3NG-T should provide topography measurements in support of seasonal and annual fish stock assessment	SWD (2019) Ares(2020)1823662 - 30/03/2020	MRD-1520, MRD-11530, MRD-1620, MRD-1630, MRD-1640, MRD-1690, MRD-1700, MRD-1710,
S3NG-T-UN-043	S3NG-T should provide topography measurements in support of long-term climate impacts on fisheries (e.g. sea level rise, ocean currents)	SWD (2019) Ares(2020)1823662 - 30/03/2020	MRD-1520, MRD-11530, MRD-1620, MRD-1630, MRD-1640, MRD-1690, MRD-1700, MRD-1710,

S3NG-T-UN-044	S3NG-T should provide topography measurements at different time scales :near real time, daily to monthly and climate scales	SWD (2019) Ares(2020)1823662 - 30/03/2020	MRD-1520, MRD-11530, MRD-1620, MRD-1630, MRD-1640, MRD-1690, MRD-1700, MRD-1710,
S3NG-T-UN-045	S3NG-T should provide topography measurements to support model based products for fisheries applications	SWD (2019) Ares(2020)1823662 - 30/03/2020	MRD-1520, MRD-11530, MRD-1620, MRD-1630, MRD-1640, MRD-1690, MRD-1700, MRD-1710,
S3NG-T-UN-046	S3NG-T should provide topography measurements (e.g. wind, wave SSH, ocean currents) in support of monitoring suspended sediments	SWD (2019) Ares(2020)1823662 - 30/03/2020	MRD-1520, MRD-11530, MRD-1620, MRD-1630, MRD-1640, MRD-1690, MRD-1700, MRD-1710,
S3NG-T-UN-047	S3NG-T should provide river discharge measurements aquaculture activities in the coastal ocean activities	SWD (2019) Ares(2020)1823662 - 30/03/2020	MRD-1520, MRD-11530, MRD-1620, MRD-1630, MRD-1640, MRD-1690, MRD-1700, MRD-1710,
S3NG-T-UN-048	S3NG-T should provide topography measurements close to shore area	SWD (2019) Ares(2020)1823662 - 30/03/2020	MRD-030
S3NG-T-UN-049:	S3NG-T should provide topography measurements in support of fisheries and aquaculture in the pan-European context including the exclusive economic zones of European Member states	SWD (2019) Ares(2020)1823662 - 30/03/2020	MRD-1520, MRD-11530, MRD-1620, MRD-1630, MRD-1640, MRD-

			1690, MRD-1700, MRD-1710,
S3NG-T-UN-050	S3NG-T should provide measurements in support of aquaculture and fisheries spatial planning	SWD (2019) Ares(2020)1823662 - 30/03/2020	MRD-1520, MRD-11530, MRD-1620, MRD-1630, MRD-1640, MRD-1690, MRD-1700, MRD-1710,
S3NG-T-UN-051	S3NG-T should provide topography measurements of waves, winds and ocean surface currents to support applications in energy, maritime transport, marine environmental monitoring.	SWD (2019) Ares(2020)1823662 - 30/03/2020	MRD-1520, MRD-11530, MRD-1620, MRD-1630, MRD-1640, MRD-1690, MRD-1700, MRD-1710,
S3NG-T-UN-052	S3NG-T should provide consistent information from the open ocean to the coastal ocean	SWD (2019) Ares(2020)1823662 - 30/03/2020	MRD-1440, MRD-1530
S3NG-T-UN-053	S3NG-T should provide measurements in support of sub-mesoscale dynamics	SWD (2019) Ares(2020)1823662 - 30/03/2020	MRD-1520, MRD-11530, MRD-1620, MRD-1630, MRD-1640, MRD-1690, MRD-1700, MRD-1710,
S3NG-T-UN-054	S3NG-T should provide measurements in support of vertical mixing and diffusivity in the ocean	SWD (2019) Ares(2020)1823662 - 30/03/2020	
S3NG-T-UN-055	S3NG-T should provide topography information on the interactions between inland waters, estuaries and costal ocean	SWD (2019) Ares(2020)1823662 - 30/03/2020	

S3NG-T-UN-056	S3NG-T should provide information on sea ice and continental ice	SWD (2019) Ares(2020)1823662 - 30/03/2020	to MRD-1970
S3NG-T-UN-057	S3NG-T should provide new products (e.g. wave, wind and current) in real time in support of oil spill pollution	SWD (2019) Ares(2020)1823662 - 30/03/2020	MRD-1650, MRD-1670, MRD-1680, MRD-1690, MRD-1700, MRD-1710, MRD-1720, MRD-1730
S3NG-T-UN-058	S3NG-T should provide information on sea-ice over the Arctic	SWD (2019) Ares(2020)1823662 - 30/03/2020	MRD-1770 to MRD-1970
S3NG-T-UN-059	S3NG-T should provide topography measurements of lake surface ice	SWD (2019) Ares(2020)1823662 - 30/03/2020	MRD-790
S3NG-T-UN-060	S3NG-T should provide measurements of snow cover and snow parameters	SWD (2019) Ares(2020)1823662 - 30/03/2020	MRD-1900, MRD-1910, MRD-1920, MRD-1920, MRD-1930, MRD-1940,
S3NG-T-UN-061	S3NG-T should provide measurements to support ECV for sea ice and glaciers	SWD (2019) Ares(2020)1823662 - 30/03/2020	
S3NG-T-UN-062	S3NG-T should provide measurements to support ECV for glaciers	SWD (2019) Ares(2020)1823662 - 30/03/2020	
S3NG-T-UN-063	S3NG-T should provide topography products in support of Arctic maritime safety	SWD (2019) Ares(2020)1823662 - 30/03/2020	
S3NG-T-UN-064	S3NG-T should provide topography measurements of seasonal snow cover	SWD (2019) Ares(2020)1823662 - 30/03/2020	MRD-1900, MRD-1910, MRD-1920,

			MRD-1920, MRD-1930, MRD-1940,
S3NG-T-UN-065	S3NG-T should provide topography measurements of sea ice thickness	SWD (2019) Ares(2020)1823662 - 30/03/2020	MRD-1800
S3NG-T-UN-066	S3NG-T should provide topography measurements of sea ice concentration	SWD (2019) Ares(2020)1823662 - 30/03/2020	MRD-1950
S3NG-T-UN-067	S3NG-T should provide topography measurements of sea ice [thickness] distribution	SWD (2019) Ares(2020)1823662 - 30/03/2020	MRD-1850
S3NG-T-UN-068	S3NG-T should provide topography measurements of icebergs	SWD (2019) Ares(2020)1823662 - 30/03/2020	MRD-1860, MRD-1870
S3NG-T-UN-069	S3NG-T should provide topography measurements of ice sheet elevation	SWD (2019) Ares(2020)1823662 - 30/03/2020	MRD-1960, MRD-1970
S3NG-T-UN-070	S3NG-T should provide topography measurements of glacier elevation	SWD (2019) Ares(2020)1823662 - 30/03/2020	MRD-1960, MRD-1970
S3NG-T-UN-071	S3NG-T should provide topography measurements to support ice mass balance estimates	SWD (2019) Ares(2020)1823662 - 30/03/2020	MRD-1960, MRD-1970
S3NG-T-UN-072	S3NG-T should provide topography measurements of ice sheet mass change estimates	SWD (2019) Ares(2020)1823662 - 30/03/2020	MRD-1960, MRD-1970
S3NG-T-UN-073	S3NG-T should provide topography measurements of sea level rise	SWD (2019) Ares(2020)1823662 - 30/03/2020	

S3NG-T-UN-074	S3NG-T should provide topography measurements of sea level in polar regions	SWD (2019) Ares(2020)1823662 - 30/03/2020	MRD-1530, MRD-1840
S3NG-T-UN-075	S3NG-T should provide topography measurements of sea level anomalies in polar regions	SWD (2019) Ares(2020)1823662 - 30/03/2020	MRD-1840
S3NG-T-UN-076	S3NG-T should provide topography measurements of ocean currents in polar regions	SWD (2019) Ares(2020)1823662 - 30/03/2020	MRD-1840 – currents derived from SSH.
S3NG-T-UN-077	S3NG-T should provide topography measurements of significant wave height in polar regions	SWD (2019) Ares(2020)1823662 - 30/03/2020	MRD-1620, MRD-1630, MRD-1640
S3NG-T-UN-078	S3NG-T should provide topography estimates of river discharge in polar regions	SWD (2019) Ares(2020)1823662 - 30/03/2020	MRD-1765
S3NG-T-UN-079	S3NG-T should provide topography measurements of sea ice parameters at a resolution of < 5 km	SWD (2019) Ares(2020)1823662 - 30/03/2020	MRD-1790, MRD-1800, MRD-1810, MRD-1820 , MRD-1850
S3NG-T-UN-080	S3NG-T should provide topography measurements of sea ice parameters at a sub-daily revisit	SWD (2019) Ares(2020)1823662 - 30/03/2020	MRD-590, MRD-1770
S3NG-T-UN-081	S3NG-T should provide topography measurements of glacier elevation	SWD (2019) Ares(2020)1823662 - 30/03/2020	MRD-1790
S3NG-T-UN-082	S3NG-T should provide topography measurements of sea ice in Antarctica	SWD (2019) Ares(2020)1823662 - 30/03/2020	MRD-1770

S3NG-T-UN-083	S3NG-T should provide topography measurements for lakes larger than 50 ha	SWD (2019) Ares(2020)1823662 - 30/03/2020	MRD-040
S3NG-T-UN-084	S3NG-T should provide topography measurements for major river networks	SWD (2019) Ares(2020)1823662 - 30/03/2020	MRD-040
S3NG-T-UN-085	S3NG-T should provide measurements of snow over land surfaces in support of hydrology applications	SWD (2019) Ares(2020)1823662 - 30/03/2020	MRD-1900, MRD-1910, MRD-1920, MRD-1920, MRD-1930, MRD-1940,
S3NG-T-UN-086	S3NG-T should provide topography measurements of lake ice surfaces	SWD (2019) Ares(2020)1823662 - 30/03/2020	MRD-040, MRD-800
S3NG-T-UN-087	S3NG-T should provide topography measurements in support of GCOS water ECV products consistent with existing time series	SWD (2019) Ares(2020)1823662 - 30/03/2020	MRD-1760
S3NG-T-UN-088	S3NG-T should provide water surface elevation of river catchments	SWD (2019) Ares(2020)1823662 - 30/03/2020	
S3NG-T-UN-089	S3NG-T should support monitoring hydrological dynamics (river flow and lake storage) of river catchments	SWD (2019) Ares(2020)1823662 - 30/03/2020	MRD-1760, MRD-1765
S3NG-T-UN-090	S3NG-T should provide topography products in support of costal bathing waters and the Water Framework Directive	SWD (2019) Ares(2020)1823662 - 30/03/2020	MRD-030, MRD-1530
S3NG-T-UN-091	S3NG-T should provide inland water information in support of international disaster risk reduction such as drought	SWD (2019) Ares(2020)1823662 - 30/03/2020	MRD-040, MRD-1760, MRD-1765

S3NG-T-UN-092	S3NG-T should provide inland water topography products in support of management of rivers and channels, floods, discharge, hydro-power, and waterways	SWD (2019) Ares(2020)1823662 - 30/03/2020	MRD-040, MRD-1760, MRD-1765
S3NG-T-UN-093	S3NG-T should provide topography measurements of water surface elevation for lakes scales smaller than 50 ha	SWD (2019) Ares(2020)1823662 - 30/03/2020	MRD-040
S3NG-T-UN-094	S3NG-T should provide topography measurements of water surface elevation over reservoirs	SWD (2019) Ares(2020)1823662 - 30/03/2020	MRD-040
S3NG-T-UN-095	S3NG-T should provide topography measurements of water surface elevation over small rivers	SWD (2019) Ares(2020)1823662 - 30/03/2020	MRD-040
S3NG-T-UN-096	S3NG-T should provide topography measurements of water surface elevation with sufficient fidelity to monitor the target (river, lake, reservoir) dynamics	SWD (2019) Ares(2020)1823662 - 30/03/2020	MRD-040, MRD-1760,
S3NG-T-UN-097	S3NG-T should provide topography measurements of water surface elevation to support hydrological modelling for climate, emergency and land applications	SWD (2019) Ares(2020)1823662 - 30/03/2020	MRD-040, MRD-1760,
S3NG-T-UN-098	S3NG-T should provide topography measurements of water surface elevation to support hydrological modelling for agriculture support and urban/local planning	SWD (2019) Ares(2020)1823662 - 30/03/2020	MRD-040, MRD-1760,
S3NG-T-UN-099	S3NG-T should provide topography measurements of water surface elevation to support hydrological modelling for agriculture at seasonal and yearly periods	SWD (2019) Ares(2020)1823662 - 30/03/2020	MRD-040, MRD-1760,
S3NG-T-UN-100	S3NG-T should provide topography measurements of water surface elevation for 1 ha minimum mapping unit	SWD (2019) Ares(2020)1823662 - 30/03/2020	MRD-040, MRD-1760,
S3NG-T-UN-101	S3NG-T should provide topography measurements in support of water resources in the cryosphere as climate records	SWD (2019) Ares(2020)1823662 - 30/03/2020	

S3NG-T-UN-102	S3NG-T should provide topography measurements of water surface elevation for rivers >10m in width	UN-NOTE	MRD-040, MRD-1760,
S3NG-T-UN-103	S3NG-T should provide topography measurements of water surface elevation with daily revisit	UN-NOTE	MRD-040, MRD-590, MRD-1760,
S3NG-T-UN-104	S3NG-T should provide topography measurements of water surface elevation with hourly revisit for small rivers	UN-NOTE	MRD-590
S3NG-T-UN-105	S3NG-T should provide topography measurements of water surface elevation with weekly revisit for drought monitoring	UN-NOTE	MRD-040, MRD-590, MRD-1760,
S3NG-T-UN-106	S3NG-T should provide topography measurements of water surface elevation with global coverage	UN-NOTE	MRD-040
S3NG-T-UN-107	S3NG-T should provide topography measurements for climate monitoring, ocean, polar and inland, at national to regional scale	SWD (2019) Ares(2020)1823662 - 30/03/2020	MRD-360, MRD-370, MRD-380, MRD-830, MRD-850, MRD-1090, MRD-1540
S3NG-T-UN-108	S3NG-T should provide topography measurements in support of seasonal forecasting	SWD (2019) Ares(2020)1823662 - 30/03/2020	MRD-1520, MRD-11530, MRD-1620, MRD-1630, MRD-1640, MRD-1690, MRD-1700, MRD-1710,
S3NG-T-UN-109	S3NG-T should provide topography measurements to support regional to local climate adaptation strategies	SWD (2019) Ares(2020)1823662 - 30/03/2020	MRD-1520, MRD-11530, MRD-1620, MRD-1630, MRD-1640, MRD-1690, MRD-1700, MRD-1710,
S3NG-T-UN-110	S3NG-T should provide topography measurements yearly to support sustainable energy and climate action plan (SECAP) reporting.	SWD (2019) Ares(2020)1823662 - 30/03/2020	MRD-1520, MRD-11530, MRD-1620, MRD-1630, MRD-1640, MRD-

			1690, MRD-1700, MRD-1710,
S3NG-T-UN-111	S3NG-T should provide topography measurements in support of seasonal, decadal forecasts and climate projections	SWD (2019) Ares(2020)1823662 - 30/03/2020	MRD-360, MRD-370, MRD-380, MRD-830, MRD-850, MRD-1090, MRD-1540
S3NG-T-UN-112	S3NG-T should provide topography measurements to monitor changes in in topography in support of climate prediction	SWD (2019) Ares(2020)1823662 - 30/03/2020	MRD-360, MRD-370, MRD-380, MRD-830, MRD-850, MRD-1090, MRD-1540
S3NG-T-UN-113	S3NG-T should provide topography measurements in support of reference time series measurements for climate trend analysis	SWD (2019) Ares(2020)1823662 - 30/03/2020	MRD-360, MRD-370, MRD-380, MRD-830, MRD-850, MRD-1090, MRD-1540
S3NG-T-UN-114	S3NG-T should provide topography measurements in support climate change indicators	SWD (2019) Ares(2020)1823662 - 30/03/2020	MRD-360, MRD-370, MRD-380, MRD-830, MRD-850, MRD-1090, MRD-1540
S3NG-T-UN-115	S3NG-T should provide topography measurements in support climate change adaptation at national scale to regional/local scale	SWD (2019) Ares(2020)1823662 - 30/03/2020	MRD-1520, MRD-11530, MRD-1620, MRD-1630, MRD-1640, MRD-1690, MRD-1700, MRD-1710,
S3NG-T-UN-116	S3NG-T should provide topography measurements (e.g. wind, waves, currents, sea state), in support of oil and other pollution events over the ocean	SWD (2019) Ares(2020)1823662 - 30/03/2020	MRD-1520, MRD-11530, MRD-1620, MRD-1630, MRD-1640, MRD-

			1690, MRD-1700, MRD-1710,
S3NG-T-UN-117	S3NG-T should provide topography measurements including waves and ocean surface currents in support of marine plastic debris, bilge waters, invasive species, and other pollutant tracking	SWD (2019) Ares(2020)1823662 - 30/03/2020	MRD-1520, MRD-11530, MRD-1620, MRD-1630, MRD-1640, MRD-1650, MRD-1660, MRD-1690, MRD-1700, MRD-1710
S3NG-T-UN-118	S3NG-T should provide topography measurements including waves, currents in support of marine pollution tracking in Near Real time 3 hours	SWD (2019) Ares(2020)1823662 - 30/03/2020	MRD-1520, MRD-11530, MRD-1620, MRD-1630, MRD-1640, MRD-1650, MRD-1660, MRD-1690, MRD-1700, MRD-1710
S3NG-T-UN-119	S3NG-T should provide topography measurements in support of pollution drift forecasts	SWD (2019) Ares(2020)1823662 - 30/03/2020	MRD-1520, MRD-11530, MRD-1620, MRD-1630, MRD-1640, MRD-1650, MRD-1660, MRD-1690, MRD-1700, MRD-1710,
S3NG-T-UN-120	S3NG-T should provide topography measurements in support of the European Maritime Safety Agency (EMSA) integrated maritime services	SWD (2019) Ares(2020)1823662 - 30/03/2020	MRD-1520, MRD-11530, MRD-1620, MRD-1630, MRD-1640, MRD-1650, MRD-1660, MRD-1690, MRD-1700, MRD-1710,

S3NG-T-UN-121	S3NG-T should provide topography measurements in support of maritime operations	SWD (2019) Ares(2020)1823662 - 30/03/2020	MRD-1520, MRD-11530, MRD-1620, MRD-1630, MRD-1640, MRD-1650, MRD-1660, MRD-1690, MRD-1700, MRD-1710,
S3NG-T-UN-122	S3NG-T should provide topography measurements including in support of maritime safety	SWD (2019) Ares(2020)1823662 - 30/03/2020	MRD-1520, MRD-11530, MRD-1620, MRD-1630, MRD-1640, MRD-1650, MRD-1660, MRD-1690, MRD-1700, MRD-1710,
S3NG-T-UN-123	S3NG-T should provide topography measurements including in support of ship routing	SWD (2019) Ares(2020)1823662 - 30/03/2020	MRD-1520, MRD-11530, MRD-1620, MRD-1630, MRD-1640, MRD-1650, MRD-1660, MRD-1690, MRD-1700, MRD-1710, MRD-1790, MRD-1800, MRD-1810, MRD-1820 , MRD-1850
S3NG-T-UN-124	S3NG-T should provide sea state and wind speed over the ocean in support of shipping for application with meteorological products	SWD (2019) Ares(2020)1823662 - 30/03/2020	MRD-1680, MRD-1700, MRD-1710, MRD-1720, MRD-1730
S3NG-T-UN-125	S3NG-T should provide topography measurements to support surface drift forecasting for maritime safety	SWD (2019) Ares(2020)1823662 - 30/03/2020	MRD-1520, MRD-11530, MRD-1620, MRD-1630, MRD-1640, MRD-1650, MRD-1660,

			MRD-1690, MRD-1700, MRD-1710, MRD-1790, MRD-1800, MRD-1810, MRD-1820 , MRD-1850
S3NG-T-UN-126	S3NG-T should provide topography measurements (e.g. sea ice thickness, sea state, ocean topography, wind speed) in support of maritime safety in the Arctic Ocean	SWD (2019) Ares(2020)1823662 - 30/03/2020	MRD-1520, MRD-11530, MRD-1620, MRD-1630, MRD-1640, MRD-1650, MRD-1660, MRD-1690, MRD-1700, MRD-1710, MRD-1790, MRD-1800, MRD-1810, MRD-1820 , MRD-1850
S3NG-T-UN-127	S3NG-T should provide topography measurements in support of maritime emergency operations with a timeliness of ≤3 hours	SWD (2019) Ares(2020)1823662 - 30/03/2020	MRD-1520, MRD-11530, MRD-1620, MRD-1630, MRD-1640, MRD-1650, MRD-1660, MRD-1690, MRD-1700, MRD-1710, MRD-1790, MRD-1800, MRD-1810, MRD-1820 , MRD-1850
S3NG-T-UN-128	S3NG-T should provide new/additional type of observational products that are needed for search and rescue operations, sea surface pollution and vessel navigation/routing purpose including synergy with other satellite data	UN-NOTE	MRD-1650, MRD-1660, MRD-1690, MRD-1700, MRD-1710
S3NG-T-UN-129	S3NG-T should provide new products of the directional wave spectrum for wavelengths of >50 m, wave period ranging between	UN-NOTE	MRD-1650, MRD-1660, MRD-1690,

	2s-10s and capture the large temporal variability of these waves including synergy with other satellite data		MRD-1700, MRD-1710
S3NG-T-UN-130	S3NG-T should provide measurements of Stokes drift on the ocean surface to support EMSA search and rescue, marine litter monitoring, and surface ocean pollution monitoring, including synergy with other satellite data	UN-NOTE	MRD-1650, MRD-1660, MRD-1690, MRD-1700, MRD-1710
S3NG-T-UN-131	S3NG-T should provide measurements of the swell waves on the ocean surface	UN-NOTE	MRD-1650, MRD-1660, MRD-1690, MRD-1700, MRD-1710
S3NG-T-UN-132	S3NG-T should support drift modelling on the ocean surface to support the EMSA Integrated Maritime Services correspondence expert group on drift modelling	CMEMS (2017)	MRD-1520, MRD-11530, MRD-1620, MRD-1630, MRD-1640, MRD-1650, MRD-1660, MRD-1690, MRD-1700, MRD-1710, MRD-1790, MRD-1800, MRD-1810, MRD-1820 , MRD-1850
S3NG-T-UN-133	S3NG-T should guarantee the continuity of Sentinel-3 products	CMEMS (2017)	All MRD Requirements
S3NG-T-UN-134	S3NG-T should improve the space and time resolution of topography measurements compared to baseline continuity of Sentinel-3 products	CMEMS (2017)	MRD-590
S3NG-T-UN-135	S3NG-T should provide topography measurements to better monitor the rapidly changing polar regions compared to baseline continuity of Sentinel-3 products	CMEMS (2017)	MRD-590,
S3NG-T-UN-136	S3NG-T should provide new topography measurements to constrain CMEMS models	CMEMS (2017)	MRD-1650, MRD-1660, MRD-1690,

			MRD-1700, MRD-1710
S3NG-T-UN-137	S3NG-T should provide enhanced performance of sea surface height measurements (the most important satellite observation for CMEMS) compared to Sentinel-3	CMEMS (2017)	MRD-1470, MRD-1480, MRD-14, 90, MRD-1500, MRD-1520, MRD-1530, MRD-1540,
S3NG-T-UN-138	S3NG-T should include multiple nadir altimeters flying in constellation to adequately represent ocean eddies and associated geostrophic currents in models	CMEMS (2017)	
S3NG-T-UN-139	S3NG-T should provide topography products with a horizontal gridded resolution of ≤50 km and a temporal resolution of ≤5 days]	CMEMS (2017)	MRD-590
S3NG-T-UN-140	S3NG-T should provide a series of satellites as a sustainable service	CMEMS (2017)	
S3NG-T-UN-141	S3NG-T should avoid expensive, non-renewable satellites but focus on a satellite series that should lead to significantly lower production costs	CMEMS (2017)	
S3NG-T-UN-142	S3NG-T should use the Sentinel-6 reference altimeter to homogenise topography measurements	CMEMS (2017)	MRD-590
S3NG-T-UN-143	A minimum of two satellites should be available in the S3NG-T	CMEMS (2017)	
S3NG-T-UN-144	S3NG-T should provide measurements of sea ice thickness	CMEMS (2017)	MRD-1770
S3NG-T-UN-145	S3NG-T should provide continuity of Sentinel-3 topography measurements over polar regions	CMEMS (2017)	MRD-1800
S3NG-T-UN-146	S3NG-T should provide measurements of sea level in the sea ice leads to reach the retrieval accuracy required to monitor Climate Change.	CMEMS (2017)	MRD-1800
S3NG-T-UN-147	S3NG-T should provide measurements of sea ice lead fraction	CMEMS (2017)	
S3NG-T-UN-148	S3NG-T should provide measurements of sea ice concentration	CMEMS (2017)	MRD-1590

S3NG-T-UN-149	S3NG-T should provide measurements of sea ice parameters using a radar altimeter and a microwave radiometer (required for tropospheric wet path delay correction of the altimeter measurements) within the altimeter footprint (at a resolution of 5-10 km)	CMEMS (2017)	
S3NG-T-UN-150	S3NG-T should address the product needs described in Table 14.2.1	UN-COPURD, UN-NOTE, C3S(2020), CMEMS(2017)	All Requirements

APPENDIX V TECHNICAL SUMMARY OF THE SENTINEL-3 TOPOGRAPHY MISSION

The Copernicus Sentinel-3 mission, part of the first generation of Copernicus satellites, is designed to ensure the long-term collection and operational delivery of high-quality measurements to Copernicus ocean, land, and atmospheric services. Mission Requirements are set out in the Sentinel-3 Mission Requirements Traceability Document (MRTD, Donlon, 2011). A full description of the Sentinel-3 Mission is provided in *Donlon et al.* (2016)

Sentinel-3 is designed to monitor the global environment through measurements that will also be used to constrain and drive global-local numerical prediction models in support of Global Monitoring for Environment and Security (GMES, now called Copernicus) user needs.

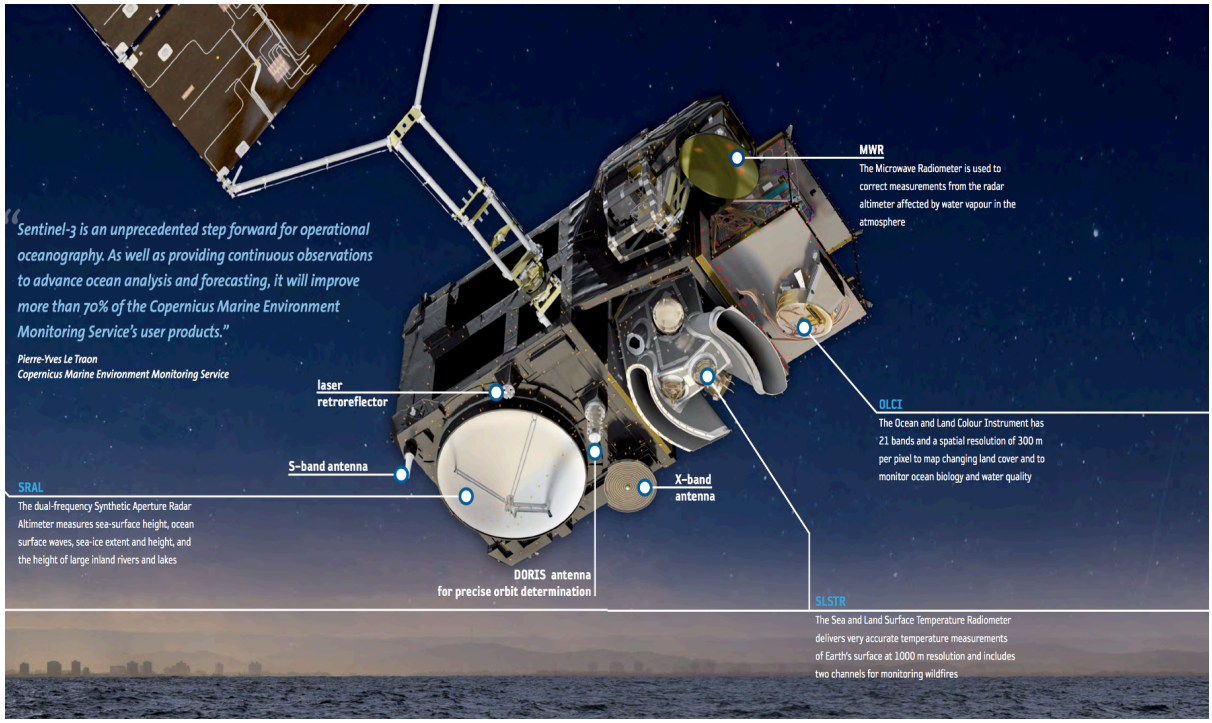

Figure V-1 The Copernicus Sentinel-3 Mission identifying key features of the mission payload.

The aim of the Sentinel-3 (Donlon, 2011) mission is:

> ***To provide continuity of ENVISAT type measurement capability in Europe to determine sea, ice and land surface topography, temperature, ocean and land surface radiance/reflectance, and atmospheric measurements with high accuracy, timely delivery and in a sustained operational manner for GMES users.***

Sentinel-3 is based on the heritage of demonstrated European measurement techniques, platform design, instrument design, and data processing systems that are required features to ensure a robust mission design in an operational system such as Copernicus (as opposed to scientific explorer missions that are designed to pioneer new measurement techniques and technologies to explore new parameters of interest

in pursuit of scientific knowledge). There are two primary mission components hosted on the same satellite platform:

- A Sentinel-3 topography mission providing altimetry measurements,
- A Sentinel-3 optical mission providing visible and infrared measurements simultaneously and contemporaneous with the topography mission (that is not discussed further in this MRD).

Sentinel-3 altimetry contributes to global climate Observing System (GCOS, 2016) climate monitoring activities via direct contributions to monitoring ocean mesoscale dynamics, ocean waves, ice mass balance, sea ice variability, river and lake stage heights and sea level ECV. The mission addressed measurement stability as a design feature for each Sentinel-3 instrument to ensure that long-term stability is maintained and accurately known throughout their entire mission lifetime through careful calibration and validation operations.

While the Sentinel-3 optical mission is not discussed further in this MRD it must be noted that it brings an enormous benefit because optical sensors together with an altimeter, viewing the same area of the ocean, at the same time, allows unprecedented synergy. In particular, the interpretation and positioning of SRAL along-track altimeter data within the context of the mesoscale circulation field of the ocean. This has been fully exploited in Copernicus applications of quasi-geostrophy (e.g. Rio et al, 2016), bringing improved estimates of geostrophic ocean currents and ocean dynamics. In addition, the collocated and contemporaneous multi-sensor measurements are also beneficial for multi-variate ocean data assimilation models.

Sentinel-3 Primary Objective-4 is dedicated to altimetry and forms the basis for the S3NG-T baseline continuity mission:

> *Sentinel-3 shall provide, in a NRT operational and timely manner, a generalised suite of high-level primary geophysical products with a consistent quality, a very high level of availability (>95%), high accuracy and reliability and in a sustained operational manner for GMES users. Products shall include as priority:*
>
> - *Global coverage Sea Surface Topography (SSH) for ocean and coastal areas,*
> - *Enhanced resolution SSH products in the Coastal Zones and sea ice regions,*
> - *Global coverage Ocean Surface Wind Speed measurements,*
> - *Global coverage Significant Wave Height measurement,*
> - *Ice products (e.g., ice surface topography, extent, concentration).*

Sentinel-3 Secondary Objective-6 is including altimetry measurements over river and lake targets:

> *Sentinel-3 shall provide in an operational and timely manner, a generalised suite of high-level secondary geophysical products with a consistent quality, a very high level of availability (>95%), high accuracy and reliability and in a sustained operational manner for GMES users. Products shall include as priority:*
>
> - *Inland water (lakes and rivers) surface height data(now elevated to a Primary Mission Objective for S3NG-T).*

To achieve the mission aim and objectives, the Sentinel-3 satellite carries the following topography payload instruments:

- A dual-frequency SAR radar altimeter (SRAL), derived from elements of ENVISAT RA-2, CryoSat SAR Interferometric radar altimeter (SIRAL) and Jason-2/Poseidon-3 heritage called the SAR Radar ALtimeter (SRAL) instrument.
- A Microwave Radiometer (MWR) instrument, which supports the SRAL to achieve the overall altimeter mission performance by providing the wet tropospheric correction derived from ENVISAT MWR heritage.
- A Precise Orbit Determination (POD) package including a Global Navigation Satellite Systems (GNSS) instrument, a Doppler Orbit determination and Radio-positioning Integrated on Satellite (DORIS) instrument (e.g. Auriol et al., 2010) and a Laser retro-reflector (LRR).

Each Sentinel-3 satellite is a low Earth-orbit moderate size satellite compatible with small launchers including Vega and Rokot. The satellite layout is driven by the need to provide a large face viewing cold-space for thermal control and, a modular design for payload accommodation and simplified management of all on-board interfaces. In order to satisfy the demanding sampling, coverage and revisit requirements, the Sentinel-3 mission is designed as a constellation of two identical satellites on-orbit at the same time. The complete mission includes a series of four satellites (Sentinel-3A, B, C and D) each having 7-year lifetime and consumables for 12 years, to operate over a 20-year period. During full operations two identical satellites will be maintained in the same orbit plane with a phase delay of 140°.

Sentinel-3A was launched on 16 February 2016 from Plesetsk, Russia using a Rockot launcher. The SRAL and MWR instruments were switched-on 1 March and 29 February 2016 respectively. On 12 April 2016, after six weeks of acquisition in LRM mode, Sentinel-3A SRAL was switched to SAR mode and has operated in SAR mode continuously and over all surfaces (the first altimetry mission to use this mode at global scale). After 5 months of commissioning, routine operations started in July 2016.

Sentinel-3B was launched on the 25 April 2018 from Plesetsk, Russia using a Rockot launcher. On 8 May 2018 the SRAL instrument was switched-on. On 6 of June 2018 Sentinel-3B reached a tandem configuration 30 seconds ahead Sentinel-3A orbit. During 4 months of tandem flight, different configurations were defined to assess the Sentinel-3B instrument performances and to improve our understanding of SAR vs LRM measurement modes. In particular, Sentinel-3B acquisition was switched between Closed Loop (CL) and Open Loop (OL) mode. On 16th October 2018 Sentinel-3B reach its final orbit position which was at a phase angle of 140° apart from the Sentinel-3A ground track. Sentinel-3C and Sentinel-3D are foreseen for launch in the 2023-2026 time frame as replacements for the A and B units providing baseline continuity until the 2035+ timeframe.

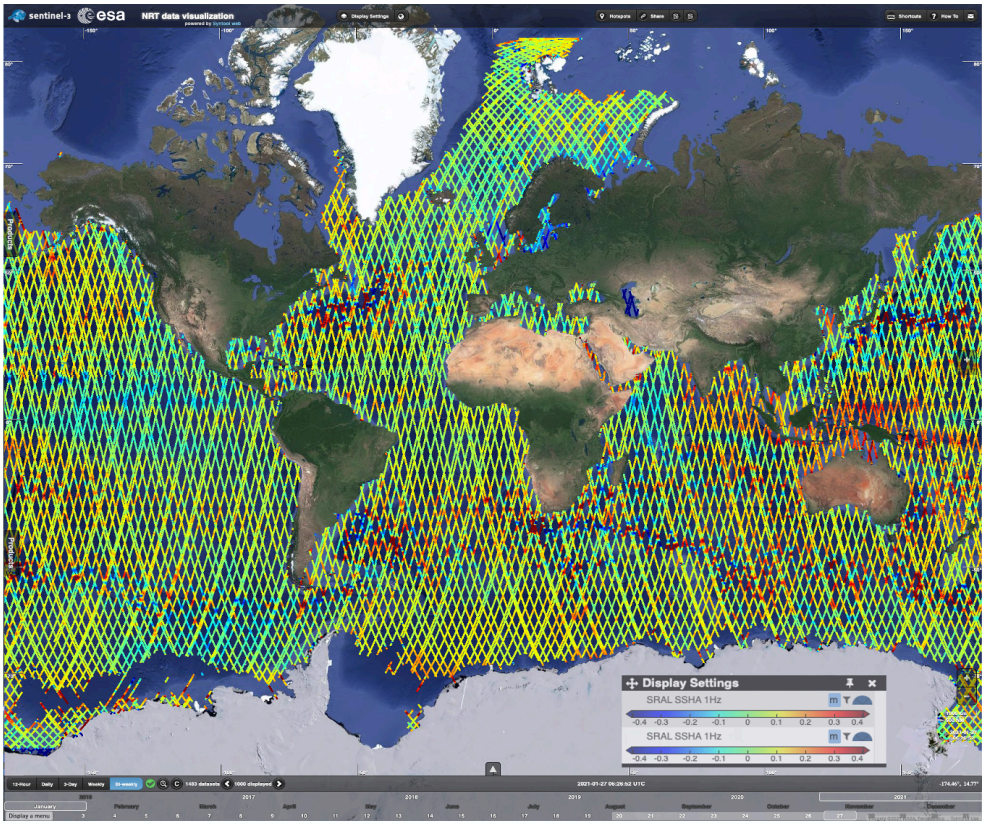

Figure V-2 Sea Surface Height Anomaly (SSHA) at 1 Hz sampling coverage of Sentinel-3A and Sentinel-3B ground tracks for a 2-week period in January 2021.

Three levels of timeliness are required for Sentinel-3 topography products within Copernicus depending on the specific application:

- Near-Real-Time 3-hour (NRT3H) products, delivered to users in less than 3 hours after acquisition of data by the sensor,
- Short time critical (STC) products, delivered to users in less than 48 hours after the acquisition that include improved orbit ephemeris data and,
- Non-time critical (NTC) products delivered not later than 1 month after acquisition that include final orbit ephemeris data.

Originally, the Sentinel-3 Mission was developed with Sentinel-3A and Sentinel-3B placed at 180° phase relative to each other in the same orbit plane. The impact of this planning resulted in a non-uniform spacing of Sentinel-3A and Sentinel-3B ground tracks. After 4 days, ground tracks would not be uniformly interleaved but close together (~57km) resulting in highly correlated measurements. In other locations large (~600 km) areas remained un-observed. Considering the characteristic time and space scales of mesoscale ocean circulation (5-10 days, 50-500 km) this was far from optimal. To improve ocean topography sampling with minimal impact on the optical mission the relative orbit phase was modified to a 140° relative satellite phasing as explained in Donlon (2015b). In this configuration, the impact of a second satellite altimeter is significantly improved for CMEMS since ocean mesoscale features are now better sampled at the 4-day sub-cycle of the Sentinel-3 orbit. This configuration remains the baseline for a two-satellite constellation as shown in Figure V-2.

V.1 Sentinel-3 SAR Radar Altimeter (SRAL)

The Sentinel-3 Radar Altimeter (SRAL) instrument (Le Roy et al, 2009) is a fully redundant dual-frequency (Ku and C-band) nadir-looking radar altimeter that employs Synthetic Aperture Radar (SAR) closed-burst altimetry technologies (e.g., Raney, 1995) inherited from the CryoSat (Wingham, 1999) mission. SRAL acquires topography data over all types of surfaces covered by the Sentinel-3 mission (ocean, coastal areas, sea ice, ice sheets, ice margins, in-land waters). Key design elements of the SRAL instrument are provided in Table V.1-1 that includes the following sub-systems:

- A dual-frequency (Ku/C band) near nadir pointing antenna of 1.2 m diameter with a focal length 0.43 m mounted on the Earth pointing face of the satellite,
- Delay Doppler synthetic aperture radar (SAR) capability in Ku-band, conventional low-resolution (LRM) mode for C-band,
- A Radio Frequency Unit (RFU) comprised of solid-state power amplifiers in Ku and C bands, diplexers used to route signals in the transmit or receive chains, a signal demodulation and “de-ramp” system, and gain controlled amplifiers to slave the echo level.
- A Digital Processing Unit (DPU) that manages all communication interfaces between the satellite platform (telemetry and tele-commands), a chirp generator, full sequencing of the instrument, received signal sampling and all elements of the required for tracking.
- Two identical DPU and RFU systems mounted inside the satellite platform provide cold redundancy.

Table V.1-1. Technical characteristics of the Sentinel-3 SAR Radar Altimeter (SRAL) instrument.

Parameter	Ku band	C band
Frequency	13.575 GHz	5.41 GHz
Bandwidth	350 MHz (320 used)	320 MHz (290 used)
Antenna footprint	18.2 km	48.4 km
Radius of 1st resolution cell	823 m	865 m
Low Resolution Mode (LRM) Pulse repetition frequency (PRF)	1924 Hz	274.8 Hz
LRM Tracking Modes	Closed loop and Open loop	
Synthetic Aperture Radar (SAR) mode		
SAR (PRF)	17825 Hz	
SAR along track resolution	291 m (Orbit height 795 km) – 306 m (Orbit height 833 km)	
SAR across track resolution	> 2km depending on Hs	
Doppler bandwidth	15055 Hz	
Tracking modes	Closed loop and Open loop	
Antenna size	1.2 m diameter, focal length 0.43 m	

SRAL transmits pulses alternatively at Ku-Band main frequency for altimeter range measurements complemented by a C-Band frequency that is used to correct range delay errors due to the varying density of electrons in the ionosphere (e.g., Lorell et al, 1982). The dry troposphere range delay is determined with sufficient accuracy using meteorological data and models (e.g., Fu and Cazenave, 2001). However, wet troposphere range delay is more challenging and must be corrected using dedicated microwave radiometer measurements to achieve the required altimetry accuracy. The SAR altimeter is used to generate high-resolution (~300 m) along-track measurements over all surface that are particularly beneficial to maximize information retrieval over variable terrain surfaces such as sea/ice and sea/land transitions in coastal areas or over inland water areas that are challenging for conventional pulse limited altimeter systems. In this mode, patterns of 64 coherent Ku-band pulses are emitted in a burst (PRF of 18 kHz) surrounded by 2 C-Band pulses to provide ionospheric bias correction. After de-ramping and digital filtering, the echo received from each pulse is sampled on 128 complex points and sent directly to ground without any on-board processing or further accumulation. SAR processing on-ground then enhances the azimuth (along-track) resolution of the altimeter for each burst of pulses.

To facilitate autonomous operations, traditional, autonomous closed-loop tracking of range and gain may be used where the altimeter range window is autonomously positioned based on-board NRT analysis of previous SRAL waveforms (Le Roy et al, 2009). Alternatively, an open-loop tracking mode is available where the altimeter range window is positioned using a-priori knowledge of the surface height stored on-board the instrument in a one-dimensional along-track Digital Elevation Model (DEM) stored as an on board Open Loop Tracking Command (OLTC) database. This mode facilitates acquisition over rough terrain and ensures continuous acquisitions across sea/land sea/ice transition zones. A key advantage of open-loop tracking is that data loss typical of conventional closed-loop tracking due to mode switching and loss of track during transitions or over variable terrain are minimised.

Two SRAL calibration modes are available that are used to monitor the flight configuration of the instrument and in ground processing. One mode calibrates the internal range and azimuth impulse responses in C and Ku Band and a second mode calibrates the gain profile of the range window by averaging thermal noise measured at each C and Ku-Band antenna port. Table 2.4-1 provides the baseline performance for the Sentinel-3 SRAL.

V.2 Sentinel-3 Microwave Radiometer (MWR)

To accurately monitor ocean parameters, satellite altimeter measurements require an accurate determination of wet tropospheric Path Delay (ZWD) over a range of 0-40 cm. The water vapour content within the troposphere exhibits large spatial and temporal variability which is difficult to model commensurate with the space and time resolution of the altimeter measurement. Instead, dedicated microwave radiometer instruments are used to correct altimeter radar pulses for this effect. Sentinel-3 includes a Microwave Radiometer to provide measurements that can be used to determine the ZWD and correct the SRAL altimeter measurements.

Table V.2-1. Technical characteristics of the Sentinel-3 MicroWave noise-injection Radiometer (MWR) instrument specification.

Parameter	K band	Ka band
Centre frequency	23.8 GHz	36.5 GHz
Bandwidth	200 MHz	200 MHz
Integration time 0.15 s +/-5%. (typical)	152.88 ms	152.88 ms
Polarization	linear	linear
Main antenna (reflector) size (projected diameter)	0.6	
Beam footprint on ground	20 km ±≤ 10 %	
Calibration	Noise injection Dicke radiometer configuration with a separate sky horn viewing deep space (cold reference @50% and 100% noise injection). Dedicated instrument calibration temperature sensors.	
Noise Figure (@ 25ºC)	< 4.4 dB (main path)	< 5.1 dB (main path)
Radiometric sensitivity	0.29 K (main path, NIR mode)	0.34 K (main path, NIR mode)
Radiometric uncertainty between150 K and 313 K	< 3 K	< 3 K
Radiometric lifetime stability	0.6 K	0.6 K

The Sentinel-3 Microwave Radiometer (MWR) is a dual frequency Noise Injection Radiometer (NIR) developed from the ENVISAT MWR instruments (Bergadà et al, 2010). The main specifications of the MWR are provided in Table V.2-1. The design aim is to determine a wet troposphere correction for SRAL with typical accuracy of 1.4 cm. The MWR is sensitive to the amount of water vapour and liquid water content in the atmosphere over a ~20 km footprint coincident with the SRAL nadir point. A channel at 23.8 GHz is used for tropospheric water vapour determination and a channel at 36.5 GHz provides information on non-precipitating clouds. During in-orbit calibration, the MWR uses well characterised cold space noise measured using a dedicated feed viewing coast space and the Dicke load. Fixed amounts (50% and 100%) of noise are injected on top of the cold space signal to calibrate the power of the noise diode and the receiver gain. In addition, periodic short views are made between calibration measurements using the standard NIR operation to monitor the stability of the instrument. To avoid possible electro-magnetic interference from SRAL, the MWR design includes a blanking signal to synchronise its measurement cycle to SRAL and optimise the measurement integration time. The radiometric sensitivity of the MWR is designed to provide brightness temperatures <0.4 K with a stability <0.6 K, and absolute accuracy <3 K over a brightness temperature range of 150-313 K (Bergadà et al, 2010). Frery et al (2020) report the performance of the Sentinel-3 MWR.

In terms of S3A/B/C/D the Copernicus priority is for continuity of performance using channels at 23.8 GHz and 36GHz (TBC due to 5G networks – a better solution with improved ITU protection may be at 31GHz).

APPENDIX VI SYNERGIES AND INTERNATIONAL CONTEXT

VI.1 Altimeter Missions

Europe has gained a lead role in the topographic component of the operational ocean observing system and its associated technology. For the reference mission, these efforts are implemented in a cooperation scheme among EUMETSAT, ESA, France and the United States (both NASA and NOAA). It is proposed to extend this highly successful cooperation scheme to the future phases, including confirming the respective operation roles for the various missions. No significant commercial initiatives exist in this domain. Copernicus is assumed to continue to play the lead role.

It is to be assumed that the reference ocean altimeter measurements provided today by Sentinel-6 A/B (continuation of the Jason series) will be ensured. The planned launch date of Sentinel-6B is 2025 with a nominal lifetime of 5.5 years. Considering that one year overlap with its successor is required to ensure accurate cross-calibration, the new system will need to be ready for launch in the 2029/2030 timeframe.

For monitoring the surface elevation of polar ice sheets, glaciers, snow the CRISTAL mission is considered to fulfil this role as an enhanced operational follow-on to the CryoSat-2 Ku-band altimetry mission as part of the Copernicus Expansion. The baseline continuity Sentinel-3 measurements will complement CRISTAL measurements as Sentinel-3 complements CryoSat-2 today as explained by Lawrence et al. (2019).

A summary of contemporary and future satellite altimeter missions used for operational ocean applications is provided in Table VI.1-1, which is derived from the extensive information provided within the World Meteorological Organisation (WMO Observing Systems Capability analysis and Review Tool (OSCAR, https://www.wmo-sat.info/oscar/).

Table VI.1-1. Summary of contemporary (2021) and future satellite altimeter missions used for operational ocean applications (from the World Meteorological Organisation Observing systems Capability analysis and Review Tool (OSCAR, https://www.wmo-sat.info/oscar/).

Acronym	Full name	Altimeter Frequency and sampling	Radiometer Frequency	Orbit and sampling characteristics	Space Agency	Satellites	Usage from	Usage to
S3	Sentinel-3	C-band (LRM) Ku-band (SAR closed loop)	23.8 GHz 36.5 GHz	Polar sun-synchronous, up to 82.5°N and 82.5°S 27 day repeat cycle	Copernicus (ESA, EUMETSAT)	Sentinel-3A Sentinel-3B Sentinel-3C Sentinel-3D	2016 2018 (2023) (2025)	2026 2028 2032+ 2034+
S6	Sentinel-6	C-band (LRM) Ku-band (SAR open loop)	18.7GHz 23.8 GHz 36.5 GHz	Non sun-synchronous up to 66°N and 66°S	Copernicus (ESA, EUMETSAT, NOAA, NASA)	Sentinel-6A Sentinel-6B	2020 2025	2027 2032

				10 day repeat cycle				
CS2	CryoSat-2	Ku-band SAR interferometer	None	Non sun-synchronous up to 88°N and 66°S 369 day repeat cycle	ESA	CryoSat-2	2010	
J2	OSTM/Jason-2	C- and Ku-band LRM nadir radar altimeter	18.7GHz 23.8 GHz 36.5 GHz	Non sun-synchronous up to 66°N and 66°S 10 day repeat cycle	NASA, CNES, NOAA, EUMETSAT	Jason-2	2008	2019
J3	Jason-3	C- and Ku-band LRM nadir pointing radar altimeter	18.7GHz 23.8 GHz 36.5 GHz	Non sun-synchronous up to 66°N and 66°S 10 day repeat cycle	NASA, CNES, NOAA, EUMETSAT	Jason-3	2016	
AKA	SARAL/AltiKa	Ka-band LRM nadir pointing radar altimeter	35.75 GHz 23.8 GHz	Sun synchronous 35 day repeat inclination 98.538º	ISRO CNES	Saral	2013	
HY2	HaiYang	C- and Ku-band LRM nadir pointing radar altimeter	6.6 GHz 10.7 GHz 18.7 GHz 23.8 GHz 37.0 GHz	Sun synchronous, inclination 99.3º 963 km, 14-day repeat	CAST/ NSOAS	HY-2B HY-2C HY-2D HY-2E HY-2F HY-2G HY-2H	2018 2020 2021+ 2023+ 2024+ 2025+ 2025+	
CRI	CRISTAL	Ku and Ka-band SAR interferometer	18.7GHz 23.8 GHz 36.5 GHz	Non sun synchronous	ESA	CRISTAL-A CRISTAL-B	2028+	

VI.2 Missions Relevant to Ocean Wave Measurements

Existing capabilities are those of the Sentinel series, specifically the C-band SAR wave mode on Sentinel-1; and Delay Doppler Radar Altimeter on Sentinel-3. Three main product types are derived from these instruments: significant wave height (Hs) from altimeters and long wavelength swell wave spectra (2DWVSPEC) from SAR imaging.

For measuring directional wave spectrum, the Chinese/French Oceanography Satellite (CFOSAT) SWIM instrument provides an excellent in-flight demonstration of a mission

concept to derive this parameter, (e.g. CFOSAT/SWIM, Hauser et al, 2020). The current Copernicus constellation is made of a dual-satellite constellation (A and B units) for Sentinel-1 (providing swell spectral information to a wavelength >150m) and Sentiel-3 (providing Hs. The C and D units are planned to provide operational continuity up to the 2030s CFOSAT/SWIM data re now being used in the CMEMS Wave TAC in support of wave model development but there is no research mission or operational follow on-mission at present.

The concept was further elaborated during ESA Earth Explorer-9 and was extended to provide a capability to retrieve Total Surface Current Velocity (TSCV) in support of Marine Debris monitoring and further understanding of ocean-atmosphere exchange of CO2, ship routing and ocean model developments amongst other applications (ESA, 2019). Such a concept was further studied during the ESA S3NG-T Phase-0 activities to provide an electronically steered (as opposed to a mechanically rotating) antenna. A SWIM/SKIM concept could satisfy the European Commission and EMSA User Need for directional wave spectrum measurements.

Sentinel-1/NG wave mode products could provide improved products to address some of these aspects.

At writing sources of satellite wave information are summarized in Table VI.2-1.

Table VI.2-1. Sources of satellite wave information and mission characteristics used within Copernicus (as of 2020).

Mission	Instrument	Primary variable	Operating modes	Operating Frequency	Data period	Repeat cycle (Days)	Orbit altitude (km)	Orbit inclination (°)
CryoSat-2	SIRAL	Hs along track	LRM/SAR	Ku	2010-Ongoing	369	Non sun-synchronous circular 717	92
SARAL	AltiKa	Hs along track	LRM	Ka	2013-Ongoing	35	Sun-synchronous 800	98.55
JASON-3	Poseidon-3B	Hs along track	LRM	Ku	2016-Ongoing	10	Non sun-synchronous circular 1336	66
Sentinel-3A	SARAL	Hs along track	SAR (LRM capability)	Ku	2016-Ongoing	27	Sun-synchronous 800	98.65
Sentinel-3B	SARAL	Hs along track	SAR (LRM capability)	Ku	2018-Ongoing	27	Sun-synchronous 800	98.65
Sentinel-6 Michael Freilich	Posiedon-4	Hs along track	Simultaneous SAR and LRM interleaved	Ku	2020-Ongoing	10	Non sun-synchronous circular 1336	66
CFOSAT	SWIM	Wave Spectrum	Wave scatterometer	Ku	2018-ongoing	13	Sun-synchronous near-circular 519	97
Sentinel-1A	C-SAR	Swell spectrum (long-	SAR Imager	C	2014-ongoing	12	near-polar, sun-synchronous	98.18

		wavelength limited)					693	
Sentinel-1C	C-SAR	Swell spectrum (long-wavelength limited)	SAR Imager	C	2024-ongoing	12	near-polar, sun-synchronous 693	98.18
HaiYang HY2 (several launches TBC)	HY-2B HY-2C HY-2D HY-2E HY-2F HY-2G HY-2H	Hs along track	LRM nadir pointing radar altimeter	C- and Ku	2018 2020 2021+ 2023+ 2024+ 2025+ 2025+	14	Sun synchronous, i 963 km	99.3
Other third party missions	TBD	TBD	TBD	TBD	TBD	TBD	TBD	TBD

Table VI.2-2 summarizes characteristics of the wave variables delivered from the Sentinel missions. Pertinent additional details are that;

- In a number of practical applications, 1Hz and 20Hz measurements of significant wave height are further quality controlled and smoothed in order to fit more consistently with scales of contemporary numerical models (Abdalla et al., 2013; Bohlinger et al., 2019). However, this usage of the data is reflective of the generally open ocean application of satellite data, where wave fields are normally evolved over large spatial areas. Conversely, for coastal zone applications, existing along-track resolution is likely to be a limiting factor.
- Repeat cycle and resulting revisit times need to be considered not only for the specific mission, but also in context of other operational data sources. In short, most users will consider multiple sources of data and may be more concerned with collective revisit times for a particular area rather than for a particular instrument. Although repeat cycle is quoted at 28 days in the table below, the combined 4-day sub-cycle of Sentinel-3A and 3B will achieve ground track separation at the equator varying between 57 and 614km. The Sentinel-1 repeat cycle is 12 days, but the two-satellite constellation leads to a revisit time of 3 days at the equator.
- Coverage is global up to high latitude limits set by the orbit inclination (data up to approximately 82 degrees North/South for Sentinel-3 Surface Topography). Constraints regarding the distance to coast at which robust measurements can be made (offshore of 5-20km depending on coastal morphology), combined with revisit times may further reduce the in-practise utility of data in certain coastal seas and channels.
- Availability of Sentinel-1A and 1B L3/L4 spectral data through CMEMS is presently limited to post-processed swell partitions only (http://marine.copernicus.eu/documents/QUID/CMEMS-WAV-QUID-014-002.pdf). This is a post-processed (L3) product rather than a direct output from the

Sentinel C-SAR. There is ongoing scientific development of spectral wave products from S1 TOPS modes that will be included in CMEMS wave portfolio when mature.

- Although not a mission with an official wave output product, Sentinel-2 has also shown potential to provide wave spectra measurement from wave patterns seen in high-resolution visible imagery (Kudryatsev et al., 2017) and may lead to an additional source of operational wave data in future (in cloud-free regions).

Table VI.2-2 Wave variables delivered by Copernicus and operating synergy missions.

Variable	Mission	Timeliness	Precision and quoted accuracy (1Hz)	Along-track sampling	Repeat Cycle	Spatial coverage
Significant wave height	S3/SRAL	NRT (3hours), STC, NTC	4% (=8cm @ 2m)	1-20Hz	27 days	[-81.5, +81.5]
	S6/POS4	NRT (3hours), STC, NTC	15 cm plus 5% of SWH for 0.5 to 8 m range	1-20Hz	10 days	[-66; +66]
	J3/POS3B	NRT (3hours), STC, NTC	?	1-20Hz	10 days	[-66; +66]
	SARAL/ AltiKa	NRT (3hours), STC, NTC	?	1-40Hz	35 days	[-82, +82]
	CryoSat-2	NRT (3hours), STC, NTC	?	1-20Hz	369 days	[-88,+88]
2D swell wave spectra	Sentinel-1	NRT (3 hours)	?	20x20km, at 100km intervals	12 days	Global
2D wind and swell wave spectra	CFOSAT/ SWIM	NRT (3 hours)	SWH: 10% or 50cm Spectra: 10% wavelength; 15% direction; 15-20% energy	70x90km	13-days	[-80,+80]

APPENDIX VII S3NG-T PRELIMINARY SYSTEM CONCEPTS AND CHARATERISTICS

VII.1 S3NG-T system characteristics

The S3NG-T mission is dedicated to guaranteeing baseline continuity of existing Copernicus Sentinel-3 nadir-altimeter measurements in the 2035-2050 time-frame while enhancing measurement performance. Since the current sentinel-3 constellation of nadir altimeter largely under samples the ocean, a main area of improvements is to improve altimeter sampling at global scales to better monitor and forecast the ocean at fine scale and to improve monitoring of the coastal zone. For S3NG-T a number of options are available for potential implementation. Regardless of technical solution (i.e. nadir-pointing or swath interferometer mission), a coordinated constellation of spacecraft is required to provide enhanced continuity to the Sentinel-3 Mission to meet the ≤5days, ≤50km enhanced baseline goal sampling requirements provided by CMEMS. Such a constellation requires a reference that allows each mission to be used in synergy without bias discrepancies and for the S3NG-T mission, the reference is Copernicus Sentinel-6, which is designed exactly for this purpose. The operational topography measurements required by Copernicus Services must met using a Constellation of satellite altimeters in synergy. Additional third-party altimeter missions may also provide additional data although their launch or access to their data cannot be guaranteed.

Based on the S3NG-T Phase-0, Phase-A activities and other studies conducted by ESA possible scenarios to implement S3NG-T include the following:

Scenario-1: Replacement of Sentinel-3C and Sentinel-3D using a constellation of 2-*n* nadir-pointing altimeters.

Potential options for this scenario could include the following.

Enhanced performance continuity of Sentinel-3 would be assured by flying two satellites of the CRISTAL design as replacements for Sentinel-3C and Sentinel-3D. The CRISTAL Ka/Ku-band altimeter technology (designed for ice and ocean applications) would bring enhanced performance over all target surfaces. The CRISTAL satellite design can accommodate sun-synchronous and non-sun synchronous orbits. Re-use of the CRISTAL design would likely lead to reduced costs and technical development. The CRISTAL Phase B2 study is on-going at this time.

CMEMS are a primary user of altimeter sea state measurements and have now assumed European responsibility for wave forecasting and directional wave spectra are required for high-resolution ocean-atmosphere coupled models making this an attractive solution. This leads to an alternative approach, using an optimised CFOSAT/SWIM type concept as replacements for Sentinel-3C and Sentinel-3D. This solution would provide nadir SAR altimetry measurements, and to support secondary S3NG-T objectives, directional wave spectrum estimates. An ESA Phase-0 Concurrent Design Facility (CDF) study considered several variants of a conically scanning wave scatterometer including an electronically steered solution.

Alternatively, a constellation of small satellites (with operational reliability and longevity i.e. not nano/cubesats) deploying nadir-pointing altimeters could replace Sentinel-3C and Sentinel-3D and significantly enhance both time and space sampling requirements. Enhanced performance fully-focussed SAR altimetry and digital technologies (developed for Sentinel-6) would bring improved performance compared to Sentinel-3. Several studies have been conducted in the past that highlighted the benefit and approach (e.g. GANDER (Allen, 2001), WITTEX (Raney and Porter, 2001). 10-12 small-satellite altimeters would be required to fly in constellation, coordinated with the Sentinel-6 reference altimeter (to guarantee inter-satellite calibration and long-term stability). An ESA Phase-0 Concurrent Design Facility (CDF) study has determined that small satellites using a single antenna design with fully-focussed SAR technology and a dual-frequency microwave radiometer sharing the same antenna reflector appears feasible bringing improved performance compared to Sentinel-3 in-flight performance. 6 small satellites are compatible with a single VEGA launch. Thus, a constellation of 10-12 mini-altimeter satellites is feasible using two launchers. Furthermore, this solution offers flexibility and scalability since a single launch could satisfy both S3NG-T baseline continuity and enhanced continuity requirements alone. However, the ground segment concept would need to be fully elaborated. The solution also addresses the recent request of the European commission to consider the use of small satellite constellations.

Scenario-2: Implementation of 2..*n* swath altimeter including a nadir altimeter

The NASA/CNES Surface Water Ocean Topography (SWOT) mission (Desai et al, 2018, Wagner et al, 2021) is expected demonstrate, for the first time, actual in-flight capability of an InSAR technique over inland waters and ocean surfaces. This concept also includes a nadir altimeter. An assumed launch in 2022/23 followed by and extensive Phase-E1 of at least 1 year is planned. Commissioning will include a 6-month period in which SWOT will operate in a 1-day repeat orbit to optimize the system knowledge followed by a 6-month period to optimize geophysical retrievals. Thus, we may expect first data in public no earlier than 2024/25. SWOT will pilot new suite of explorer type ‘snapshot’ image products serving ocean and inland water users with an exact revisit every 21 days (with a sub-cycle at ~10 days) once the satellite has been commissioned.

A dedicated Phase-0 CDF study considered the ESA Swath Altimeter for Operational Oceanography (SAOO) design with different combinations of payload to implement a swath altimeter solution including a nadir altimeter, a multi-beam, multi-frequency microwave radiometer and an optional a dedicated Hs directional spectra measurement capability. Depending on the final concept design, since the swath is relatively narrow (60+60km either side of nadir) a number of swath satellites will be required to meet the ≤5days, ≤50 km wavelength enhanced baseline goal requirements provided by the European Commission. In addition, depending on the payload design and data processing performed, a capability to generate wave directional spectra over part of the swath is possible. A single satellite solution appears feasible with a dedicated VEGA launch implying multiple launches.

Scenario-3: Hybrid approach.

> Combinations of different approaches could be used to meet S3NG-T requirements. A combination of nadir-pointing and swath altimetry could be optimised to meet sampling, coverage and performance for SSH and Hs. A wave scatterometer or enhanced processing of swath altimeter measurements could be used to satisfy Directional Wave Spectrum User Needs. A staggered development could be adopted allowing all of the lessons learned from NASA/CNES SWOT in orbit results to be pulled through into an optimised European swath altimeter design that could be launched at an appropriate time. Such an approach offers the most flexible and ultimately the best solution to meet Copernicus User Needs.

In conclusion, continuity of Sentinel-3 measurements can be guaranteed using a number of different approaches. User needs provided by the European Commission for enhanced continuity for ocean and hydrology services require significantly enhanced sampling capability to meet the ≤50km wavelength, ≤5 days requirement. A variety of technical solutions of different technology, coverage, sampling, calibration stability system complexity and size are potential candidates for implementation of the S3NG-T mission

Following the S3NG-T Preliminary Concept Review (PCR) in August 2022, the decision was reached to implement the mission as a constellation of two large spacecrafts carrying a next generation nadir-looking synthetic aperture radar (SAR) altimeter that will provide the baseline continuity with the current S3 constellation, and an across-track wide swath interferometer that will provide the required enhanced sampling capabilities. This decision was confirmed at the Mission Gate Review (MGR), held at the end of Q1 2024, where inputs from the phase A/B1 intermediate System Requirements Review (ISRR) and additional analyses benefiting from the inflight experience of SWOT mission were considered to determine whether the selected mission concept was fit for purpose to meet the S3NG-T mission requirements as gathered in this MRD.

VII.2 S3NG-T measurement approaches

Modern SAR nadir-pointing altimeter signals are coherently processed, i.e. unfocussed SAR processing 300 m resolution along-track, to perform multi-looking operations to reduce uncorrelated speckle noise. At nadir, the measured Delay-Doppler maps are dominated by wind-roughened quasi-specular facets distributed along the moving long wave profiles, locally associated to the peak wind sea and remote swell events. Accordingly, SAR nadir-pointing altimeter signals integrate the joint statistical characteristics of slowly varying long waves, i.e. surface elevation, slopes, velocities, with rapidly varying short wind-roughened scales, i.e. surface elevation and slope variances and time-coherency. In particular, slope variances associated to short scales are known to be unevenly distributed along the long wave profiles, i.e. areo-hydrodynamical modulations, lead to a systematic indetermination of the precise mean sea surface height. Sea state bias correction strategies have been developed to address this issue that remain one of the largest sources of uncertainty.

Under light to moderate wind conditions, constructive velocity bunching phenomena can further occur (i.e. Alpers et al., 1981), leading to image swell systems traveling near and along the altimeter track e.g. Boy et al, 2016, Moreau et al., 2018, Egido and Smith, 2019, Reale et al, 2020. Combined with the areo-hydrodynamical modulations, signals associated with these phenomena occur under low wind conditions in presence of along-track swell systems that can be extracted and applied. For sea surface height estimation, such signals mut be accounted for in the data processing if large biases are to be avoided.

To perform sea surface height estimations over a larger swath, SAR across-track interferometry is now considered (see Bai et al. (2020) for a recent review of the technique). During airborne experimental campaigns, the technique has been demonstrated to estimate the distribution of sea surface wave elevations (e.g. Shultz-Stellenflath and Lehner, 2001). At near-nadir configuration, the technique can provide sea surface height estimates after proper spatial averaging to eliminate sea surface elevation contributions. Comparable to nadir configurations, the measured Delay-Doppler maps will be largely dominated by wind-roughened quasi-specular facets distributed along the moving long wave profiles. A comparable systematic indetermination of the precise sea surface mean height remains. Some peculiar up-wind, down- asymmetries for the short scale slope distributions may further alter the interpretation of these measurements for differing antenna-to-wind azimuth configurations. In addition, front face wave/swell, back face wave/swell and along wave/swell crests for wave groups for differing antenna-to-wind azimuth configurations add to data interpretation challenges.

To the expected velocity bunching phenomena, an additional range bunching effect will occur under steep sea conditions, mainly traveling in the across-track directions (e.g. combined velocity and layover effects Chapron et al. 2001). While complicating the proper range determination, these effects may be helpful to determine sea state proxies within the measurement swath.

To the best current knowledge, in the absence of contemporaneous and co-located measurements, bias corrections are statistically determined using a combination of altimeter estimates (intensity NRCS, significant wave height) possibly complemented using numerical wave model outputs (orbital and slope variance estimates).

APPENDIX VIII ALTIMETER ORBIT CONSIDERATIONS FOR MEASURING TIDES

The choice of the altimeter orbit determines the observability of the different ocean tidal constituents. In sun-synchronous orbit (SSO) satellites, all solar lines in the tidal spectrum are not accessible because the orbital plane is in phase with the sun. Thus, the S2 constituent is frozen in the orbit (i.e. the satellite always observes exactly the same phase of that tidal component) so it cannot be determined. Sun-synchronous satellites cannot disentangle aliasing of the K1 tide and the annual sea level variation. For these constituents, an ocean tide model based on the non-SSO reference altimeter time series (TOPEX/Poseidon, Jason-/2/3 and Sentinel-6) together with other oceanographic data can be used. This is an important element of satellite altimetry measurement - one approach is explained by Lindsley (2011) and further examples are provided by Parke et al. (1987).

A non-SSO orbit offers a preferable solution to enable tidal phenomena to be studied but it induces a greater level of technical complexity to a mission (e.g. Parke et al., (1987). Because of the very fast variability of mesoscale phenomena or the effect of local/regional atmospheric pressure variations, temporal sampling offered by satellite altimetry (nadir or swath based solutions) induces an aliasing of the associated sea level variation measurements towards longer apparent time scales. In a sun synchronous orbit this is true for the remaining non-solar lines in the tidal spectrum. Conversely, the lifespan of a single mission is sometimes too short to capture and properly calibrate the lowest frequencies of natural variability. The need to address for these effects leads to two specific requirements the altimetry constellation system:

- The tidal signal is made up of several components of known frequencies. Aliasing is deterministic in this case, and for each component the apparent frequency is known. To ensure efficient correction, it is necessary that the aliased frequencies are (1) high enough so that spectral analysis can isolate main tidal constituents, (2) that aliased frequencies for two different constituents do not overlap, and (3) that the aliased frequencies do not fall into critical time scales, such as seasonal signal. This leads to specific, sometimes quite severe constraints on the orbit parameters. In contrast, if the auxiliary corrections based on model output/measurements are accurate enough with respect to the application, these aliasing constraints on the orbit can be accommodated (e.g. a SSO that includes tidal aliasing is acceptable for ocean forecasting using along-track data together with the use of tidal models).
- Level 2 products include SSH observed by the altimeter (i.e. including ocean/pole tidal signal and high frequency components), and the geophysical corrections that can be applied to remove the aliased contribution from the long-time-scale signal or the calibration of slowly evolving errors to properly observe slow changes of small amplitude.

Today, the largest errors in our state-of-the-art barotropic tidal models are in coastal regions and at higher-latitudes, that are not well covered by the non-SSO of the T/P-Jason series (Stammer et al., 2014) now maintained by Copernicus Sentinel-6. We expect major improvements of the 2D observation of the barotropic tide in the open ocean and coastal regions, with the future SWOT mission (2022-2025). The SWOT

mission has ana nominal phase orbit inclination of 77.6° at an altitude of 891 km and a 21-day repeat cycle. This allows observations to be made up to 78° in latitude across a narrow 120 km swath at a resolution of 250m (posting) and 2 km grid-cell resolution. SWOT's non-sun-synchronous orbit has been specifically designed to observe the main tidal constituents after 3 year. mission lifetime in its nominal orbit phase.

SWOT observations will also improve our understanding of the phase-locked (coherent) internal tides and provide the first 2D observations of the interaction for the internal tide with the changing ocean circulation. Internal baroclinic tides and internal gravity waves are less well known or predictable (Ray and Zaron, 2016; Savage et al., 2017, Arbic et al, 2018). Work is progressing to understand how and where internal tides are generated, but the location of their 2D pathways or dissipation regions remains an important scientific question. The interaction of the internal tide with the ocean circulation and currents has been shown to be complex, with ocean currents refracting and dissipating the internal tide (Ponte and Klein, 2015). During 2022-2025, the SWOT science mission observations will be used to improve coherent internal tide models up to 78° in latitude.

In principle, SWOT observations will allow us to reprocess all past altimetry missions using improved corrections for many coastal and high-latitude barotropic ocean tides and coherent internal tides. SWOT and other along-track nadir altimeter data will be used to tune and improve tide models to allow us to predict future barotropic tides and coherent internal tides for all future missions, including the S3-NGT series in 2030+.

Incoherent non-phase-locked internal tides cannot be observed via harmonic analysis of altimeter data, even for data on non-sun-synchronous orbits designed to resolve the tides. The tide community is currently working on techniques to identify and separate the incoherent internal tide (Zhao, 2019; Zaron, 2017) using 2D reconstructed fields from along-track altimeter data and 2D SWOT swath observations. We expect that these techniques will be refined over the next 5 years with SWOT, and that they will be available for the S3-NG-T in 2030+.

The expected improvements in the modelling of ocean barotropic tides and ocean coherent internal tides after the SWOT period (2022-2025) reduces the requirement for a non-SSO for altimeter mission data after 2025, including the S3NG-T series.

APPENDIX IX ALTIMETER LEVEL 2 PERFORMANCE SPECIFICATION

Level 2 performance can be specified for a given instrument with specific sampling characteristics and multiple measurements obtained from a ***coordinated*** constellation of altimeters working in synergy (e.g. as a minimum Sentinel-3NG and Sentinel-6NG, and potentially CRISTAL). A constellation of satellite altimetry instruments of different design, with different orbits and sampling characteristics results in very different ability to resolve the mesoscale ocean structure in order to constrain ocean models and to monitor the ocean dynamics than is available today. Ignoring the potential of staring geostationary missions capable of sub-hourly temporal resolution (that do not yet exist), there is no single satellite measurement solution that addresses all of these aspects. Thus, a compromise is required based on the most important contributions and choices that impact the time-space sampling characteristics of satellite altimetry. These include:

- **Space and time variability of the mesoscale ocean signal** has to be correctly sampled. Oceanic processes at fine scales from ~30 to 150 km are characterized by temporal variability of days to weeks (Figure 5.8.1.1). Ageostrophic sub-mesoscale signals (i.e. <~30km) have very small scales and very rapid timescales of hours to days. Tides and internal tides are also ageostrophic, with rapid evolution (hours) but spanning a wide space-scale range (few km to basin-scales for barotropic tides). The Nyquist sampling to resolve 50-100 km wavelength is 50-25 km. With a limited number of uncoordinated conventional nadir-pointing altimeters, this is already a challenge in the along-track direction due to instrument noise and wave/swell effects (fundamental components of any radar measurement over the sea surface), but is a significant challenge in the cross track direction due to the narrow footprint of a nadir-pointing altimeter. Single-pass cross-track InSAR techniques (e.g. Rodriguez et al., 1992) holds potential to provide ‘snapshot’ images of the SSH field over ~120 km with an order of magnitude lower noise than conventional altimetry that can resolve scales to 15-40 km in two dimensions. In order to correctly resolve the time variability such information is required at very frequent time intervals commensurate with the rapid evolution and short lifecycle of smaller-scale features (Figure IX-1). These aspects imply a revisit time commensurate with the translation speed of ocean mesoscale features. However, at such high resolution, the impact of sea state becomes a challenge for the interpretation of SSH as demonstrated by SAR nadir altimeters (e.g. Boy et al, 2016, Moreau et al., 2018, Egido and Smith, 2019, Reale et al, 2020). In fact a new definition of SSH and its representation may eventually be required to fully account for the impact of sea state at high spatial resolution.

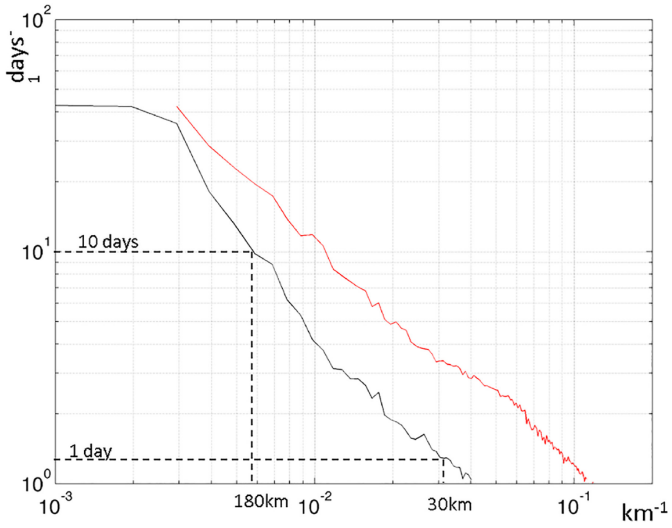

Figure IX-1. Example time-space decorrelation in the North Atlantic. Black curve: decorrelation time as a function of wavelength (shown in inverse log scale, per day and/km, respectively) estimated from an MITGCM simulation in the North Atlantic. Red curve: Decorrelation time when we subtract the 1-layer Quasi-Geostrophic evolution (From Morrow et al, 2019, Credits: NASA-JPL).

- **Random uncertainties (noise) and systematic uncertainties in the measurement** must be commensurate with the relative strength of the signal to be sampled. These are dominated by swell and wind wave effects (typically combined in Hs estimates based on normalised radar cross section measurements) that are themselves influenced by ocean surface dynamics.
- **A sampling plan must be derived to ensure sufficient distinction between superimposed signals of interest** (e.g. barotropic and internal tidal components are superimposed in mesoscale sea surface height signals, seasonal and longer variability, and short-time scale effects such as sea state variability – particularly in the coastal ocean – is a notable challenge.).

The ocean is turbulent with a strong cascade of energy between the large scales, the energetic mesoscales, and down to the smaller, sub-mesoscales. This turbulent energy cascade varies regionally, seasonally and on multi-annual time-scales leading to a large range of wavelengths and periods that do not scale in a linear manner– especially at smaller ageostrophic scales. Clearly, not all SSH expressions of ocean surface dynamics can be measured since their surface vertical and spatial extent is beneath the SNR and sampling characteristics of current altimeter technologies. Notably, mesoscale features currently resolved with a limited number of nadir altimeters range in amplitude between a few mm to ~50 cm with a median value based on Jason satellites of ~7 cm (e.g. Dibarboure et al. 2012; Dibarboure et al 2014).

One approach to optimisation of ocean topography sampling is to derive an average global ocean spectrum of sea surface height based on either under sampled altimetry measurements or ocean model data (e.g. Desai et al, 2018). The along-track SSH wavenumber Power Spectral Density (PSD) estimation is an efficient way to analyse the result of the direct and indirect energy cascades between large-scale, mesoscale, and sub-mesoscale dynamics (Dufau et al. 2016, Vegara et al., 2019). In this approach,

the SSH error spectrum assumes a constant white noise contribution that dominates at small wavelengths, and a correlated noise contribution, that dominates at longer wavelengths, representing residual geophysical uncertainty (related to the sampling characteristics of the measurement (LRM or fully focused SAR technologies and sampling), altimeter performance uncertainties (e.g. ionospheric path delay, wet and dry tropospheric path delay, sea state bias, mean sea surface, precise orbit determination, satellite attitude knowledge, centre of gravity variation and thermoelastic satellite distortion, radar antenna distortion, random errors, etc) and the characteristics of the mesoscale SSH signals themselves onto which the highly dynamic sea state (wind sea and swell) is superimposed). Such a spectrum provides an estimate of '1-D mesoscale resolution capability' (the smallest wavelength that can be observed from the along-track altimeter observations having a signal-to-noise ratio greater than unity) for a given altimeter can be used to tailor requirements for altimetry sampling. This quantity varies seasonally and geographically depending on the spectral slope and the varying noise level.

Figure IX-2(a) shows sea level height anomaly (SLA) spectra computed for the Sentinel-3 SRAL using data posted at 80 Hz (Level 1a full resolution product), 20 Hz (operational processor) and data computed at 20Hz based on 80Hz input using a window=4 rolling average. High-frequency signals from wind sea and swell waves together with sub-mesoscale processes complicate the interpretation of the resulting altimeter derived spectra (which are quite different) depending on how the data are processed (for example, Vergara et al (2019) use only 1 Hz estimates fro Sentinel-3). Rieu et al (2021) demonstrate that it is necessary to process data with a high posting rate (40-80 Hz) to avoid the spectral aliasing that occurs at 20 Hz that creates long-wavelength errors. Further processing can then be optimized to extract the signals of interest (e.g. Egido et al., 2020) to reduce the level of the measurement noise. Additional sources of uncertainty may arise due to the estimates of altimeter noise level that needs to be handled with care since Any overestimation of the instrument error, once subtracted, could potentially induce an underestimation of the spectral slope values (Vergara et al. 2019). Figure IX-2(b) shows the mean global SLA spectrum from Sentinel-3 SAR acquisitions for standard operational processing at 20 Hz (red), full-instrument resolution products 80 Hz (black) and optimally filtered 80Hz data at 20 Hz (blue). Variance is reduced for the blue spectrum with respect to the red one, up to wavelength of 100 km and the noise floor is significantly lowered (Rieu et al, 2021). This implies that better performance can be attained when high frequency sampling is available to users on ground.

A good SNR is needed for an altimeter to properly describe the ocean topography at the chosen operating point for the ocean features of interest. If the instrument noise (ε) is too high with respect to the amplitude of the signal of interest, it becomes difficult or impossible to observe the features of interest. Since average signal amplitudes vary with average wavelength (shown in the spectrum in Figure 5.8.1-2(b) right), tolerable instrument errors can be linked to scales of ocean dynamics. This implies that a high SNR is required for the S3NG-T altimeter range measurements.

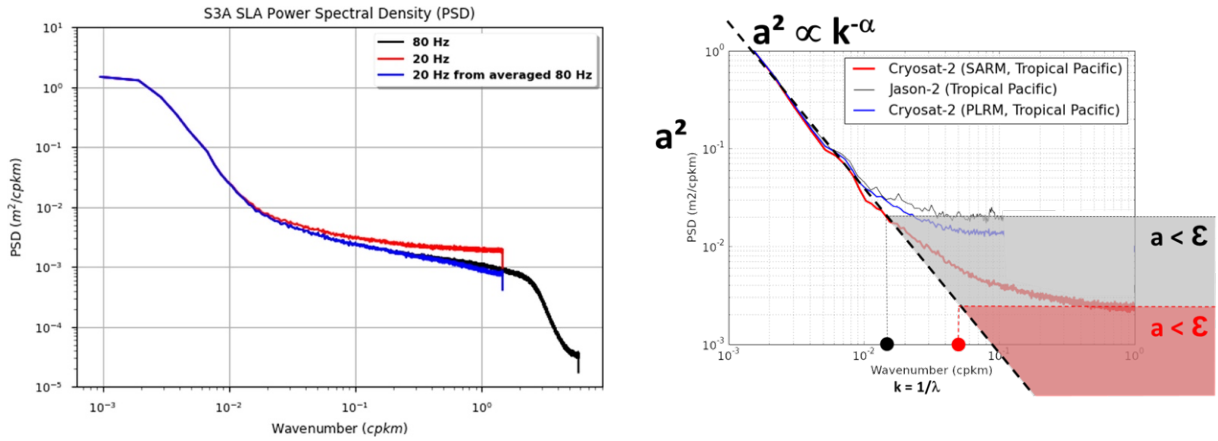

Figure IX-2 (a) Mean S3A SLA spectrum at 20 Hz (red), at 80 Hz (blue) and at 20 Hz after rolling average over four 80 Hz samples (black). (From Rieu et al 2021). (b) Power spectral density of the sea level anomaly from Jason-2 (black) CryoSat-2 (red) in the Tropical Pacific region where CryoSat-2 is operated in delay-Doppler mode (SAR). Derived from Dibarboure et al. (2014).

The ESA Satellite Altimetry for Operational Oceanography (SAOO) Phase-0 study (ESA, 2019) defined an error specification in the form of a spectral envelope to refine / relax sampling requirements according to the spatial scale considered and to identify critical scales for each error source (Desai et al, 2019). This allowed a statistical interpretation of the requirements to be fully specified for mean ocean conditions based on available measurements (largely Jason altimeter data). Using this approach, uncertainties can be specified for all scales and all periods with a probability derived from an ensemble of observations (e.g. 68%). Thus, uncertainties can be specified so that they are met only 50% of the time (i.e. a temporal interpretation). The SSH error spectrum *E(f)* in the ESA SAOO Phase-0 study (ESA, 2019) was specified as a function of the spatial wavenumber, *f*, defined for wavelengths ranging from 50 to 1000 km:

$$E(f) = K_{pl} + 0.00125\, f^{-2}\ [\text{cm}^2/\text{cycle/km}]\ 50\ \text{km} < \lambda < 1{,}000\ \text{km}$$

The expected SSH error variance in the wavelength interval [λ_{min}, λ_{max}] is then given by the integral of E(f):

$$\langle(\delta h^2)\rangle = \int_{1/\lambda_{max}}^{1/\lambda_{min}} \mathrm{E}(f)\, df$$

E(f) consists of a constant white noise contribution K_{pl}, which dominates at small wavelengths, and a correlated noise contribution, which dominates at longer wavelengths, representing residual geophysical errors, orbit and attitude restitution errors. The lower value that is specified for the random noise floor K_{pl}, the smaller features can be observed. This approach ensures that instrument noise is not the limiting factor of the measurement. The sea surface height error spectrum can be calculated over as the across-track average of the along-track spectra computed at different across-track locations over a swath for Hs ≤ 2 m. The nominal 'one-ocean' requirement is to set K_{pl} ≤ 4 cm^2/cycle/k with a goal requirement is to have K_{pl} = 2 cm^2/cycle/km.

However, a drawback of this approach is that it ignores the regional geographical distribution of strong ocean features (e.g. Quilfen et al. 2021) and does not fully capture properly temporal variability including seasonal variations of SSH or important extreme ocean events that lie outside the spectral envelope related to storms such as storm surge and upper ocean mixing, and sea states as monitored by todays altimetry satellites (e.g. Hanafin et al. 2012) ocean circulation (e.g. Stewart et al., 2021) and ensemble prediction of SSH (e.g. Close et al., 2020). Extreme ocean events are important features to resolve in the context of ocean modelling and forecasting. Although the complete time-space spectral analysis of the ocean characteristics are not available at this time, the ESA SAOO approach has generated a global analysis of SSH spectral slopes using 7-months of LRM data from Jason-2, CryoSat-2 (both in Ku-band) and new Ka-band SARAL/AltiKa (Dufau et al. 2016). AltiKa provides lower noise data than the Ku-band altimeters because of a larger 40 Hz Ka-band emitting frequency, its wider bandwidth, lower orbit, increased Pulse Repetition Frequency, reduced antenna size and beam width.

This analysis is also useful to identify oceanic regions where residual tidal signals affect specific altimeter SSH measurements with varying intensity (e.g. M2 and S2 tidal aliasing frequencies for the Sentinel-6 orbits at 140 km wavelength and ~62 daytime period), for example due to errors in the baroclinic tides or the uncorrected internal tides. Seasonality of the SSH spectral slopes has been revealed by observations in the Gulf Stream, Kuroshio and subtropical countercurrents highlighting more intense winter activity. Spectral analysis of altimeter 1 Hz noise level (rms) estimated from mean SSH wavenumber spectrum is also possible revealing that SSH noise characteristics vary in space and in time, in close relation with the wave /swell variations. Internal tides can perturb the spectral slope estimates based on a linear fit within the mesoscale range of the along-track spectrum and thus limit the correct estimation of the mesoscale resolution capability of altimetry missions in certain regions. As we start to resolve smaller-scale structures < 200 km, all altimetry missions will encounter difficulties in separating the smaller mesoscale and sub-mesoscale signals from the internal tides with energy at similar spatial scales.

The NASA/CNES SWOT mission will provide a great opportunity to observe and understand barotropic and internal tides and the ocean energy cascade over scales from 50-200 km and < 15 days that are not well resolved with today's uncoordinated altimeter constellation, including the dynamics of mesoscale and sub-mesoscales processes and their interactions with internal tides. This legacy will be extremely useful for the S3NG-T and effort must be made to ensure lessons learned from SWOT are pulled through into the S3NG-T. The challenge is in calculating geostrophic velocities from the altimetric SSH (and the derived vorticity or ocean strain), in the presence of a strong ageostrophic internal tide field and correctly separating the different dynamics.

APPENDIX X FIDUCIAL REFERENCE MEASUREMENTS

X.1 Calibration and Validation of Altimetry Missions

CEOS define Calibration as: “the process of quantitatively defining a system’s responses to known, controlled signal inputs”. Calibration includes aspects of the measurement system which need to be addressed in the generation of all level 1b data products. Since level 1b algorithms and associated products take care of the conversion from the instruments’ measurement quantities (engineering units) into standard physical (SI) units, they may be addressed by many techniques. Examples of calibration are the compensation for internal path delay in computing the apparent echo range, phase or power measurement from an altimeter, or compensating for gain and linearity in generating brightness temperature as measured by a microwave radiometer. Calibration parameters are applied during the generation of the level 1b data products. Pre-launch estimates will be available (and initially used) but, as far as possible, improved estimates need to be established in-orbit. Furthermore, the uncertainty associated with these calibration parameters will be characterised in-orbit.

Validation is “the process of assessing, by independent means, the quality (uncertainty) of the data products derived from those system outputs” (CEOS definition). Validation, typically focusses on Level-Level 2 data products after conversion of instrument measurements into geophysical quantities. Validation results in the end-to-end characterisation of the uncertainty of geophysical parameters (SSH, Hs and wind speed) derived from the calibrated altimeter echoes (which are termed retrieval errors) and in the ground processing system and algorithms that are implemented. Validation is a core component of a satellite mission (and should be planned for accordingly) starting at the moment satellite instrument data begin to flow until the end of the mission. Without adequate validation, the geophysical retrieval methods, algorithms, and geophysical parameters derived from satellite measurements cannot be used with confidence and the return on investment for the satellite mission is reduced. In addition, meaningful uncertainty estimates cannot be provided to users. Once on-orbit, the uncertainty characteristics of (a) the satellite instruments (i.e. altimeter, microwave radiometers, GNSS, etc.) established during pre-launch laboratory calibration and characterisation activities and (b) the end-to-end instrument measurements (e.g. microwave brightness temperature, radar power and backscatter) from which geophysical measurements (e.g. SSH) are retrieved, can only be assessed via independent calibration and validation activities. The primary activities relevant to the validation of satellite altimeter measurements include:

- Quantify, using independent measurements, the performance and validity of the algorithms used in the satellite geophysical retrieval of SSH/SSHA, Hs and σ^0/U10,
- Monitor any degradation or change of specific satellite instrument performance (and therefore geophysical product uncertainty) across the entire mission lifetime,
- Provide an independent reference data set that can be used to bridge between different satellite missions,

- Provide an independent reference data set to develop and test new satellite retrieval algorithms,

If ground-based measurements are to be credibly used for satellite validation activities, particularly for assessments of climate data record stability (e.g. Cancet et al., 2013), then they must be obtained contemporaneously and co-located with satellite measurements and be accurate and precise. In 1995 at the 20th Conference Generale des Poids et Mesures (BIPM, 1995), a recommendation was made that:

‘‘those responsible for studies of Earth resources, the environment, human well-being and related issues ensure that measurements made within their programs are in terms of well-characterized SI units so that they are reliable in the long term, are comparable world-wide and are linked to other areas of science and technology through the world’s measurement system established and maintained under the Convention du Metre’’.

This lays the foundation to relate satellite measurements to Systeme International d’Unites (SI) standards. This recommendation is the basis for producing Climate Data Records as by following it, measurements from different satellite and ground-based sources, taken over a period of time, can be combined in a meaningful manner (e.g. Hollmann et al., 2013). For this purpose, the concept of Fiducial Reference Measurements (FRM) has been established (Donlon et al., 2015) as:

“The suite of independent ground measurements that provide the maximum Return On Investment (ROI) for a satellite mission by delivering, to users, the required confidence in data products, in the form of independent validation results and satellite measurement uncertainty estimation, over the entire end-to-end duration of a satellite mission.”

FRM are required to determine the on-orbit uncertainty characteristics of satellite geophysical measurements via independent validation activities. Establishing an uncertainty budget for FRM is a fundamental step that drives a better understanding of the various components of FRM uncertainty. If reliable and well-defined uncertainties can be provided, then these measurements can uniquely provide an SI traceable measurement on a per-measurement basis when matched to satellite measurements – without the need for many observations to reduce the random error (as in the case of altimeter measurements referenced to a transponder, for example).

The regular calibration and validation in an absolute (i.e. using an independent reference data set) and relative (i.e. mission-to-mission cross- and inter-comparisons) of the global altimeter constellation underpins the quality of the [multi-]mission data set. Historically, several complementary techniques in geographically diverse settings have been used in parallel to calibrate SSH. These have resulted in complementary techniques for the calibration of satellite altimeters (e.g. Bonnefond et al., 2011, 2018) including the use of the global tide gauge network to provide a relative calibration and the use of dedicated in-situ permanent calibration sites to provide an absolute calibration. They can be classified as:

1. **Relative Indirect:** Measurements from high-quality tide gauges are processed to determine regional and global long-term (seasonal) trends in sea level variation that can be compared to the estimates of SSH derived from satellite altimeters. This allows the drift in altimeter bias to be estimated with accuracy commensurate with typical altimeter mission requirements (e.g. Mitchum, 1998). Tide gauge

calibration has become an essential ingredient for developing the long-term sea-level record from altimetry. One of the limiting error sources in this technique, whether it is performed at dedicated calibration sites or using the global network is the uncertainty in measuring vertical land motion.

2. **Relative Direct:** Crossover analysis between reference altimeters and other missions (e.g. Ablain et al., 2010). The comparison between different altimetry missions flying together is used to monitor the relative performance of a specific mission with reference to other "reference" missions and to the collective altimeter data record composed of all altimeter data sets. It provides a large number of inter-comparisons allowing the efficient long-term monitoring of specific instrument measurements. Monitoring of all altimeter and radiometer parameters, performance assessment, geophysical evaluation, and cross-calibration with different mission measurements is possible. However, the approach does not provide an absolute calibration of mission data. For this independent in situ fiducial reference measurements are required.

3. **Absolute Direct:** Fully instrumented fiducial reference measurements are used to monitor absolute sea-level at permanent altimeter calibration facilities that are located offshore (e.g. the NASA Harvest site (Fu and Haines ¿et al? 2013, Haines et al., 2020). Other measurements may include tide gauges, GNSS, a DORIS beacon, meteorological sensors, wave-height sensors, airborne campaigns for gravity and sea-surface topography, water-vapour radiometry, solar atmospheric spectrometry, GNSS buoys, altimeter transponder, Satellite Laser Ranging, etc. The mean sea level and the earth's tectonic deformation field in the region have also been determined accurately. A standardized methodology using sea-surface measurements for the estimation of the altimeter bias of Jason satellites has been followed by the four permanent calibration sites of NASA Harvest platform (Haines et al., 2020), Corsica (Bonnefond et al., 2010, Cancet et al 2010), Bass Strait (Watson et al. 2011) and Gavdos (Pavlis et al 2004, Mertikas et al., 2011, Mertikas et al., 2019).

4. **Absolute Indirect:** Fully instrumented fiducial reference measurements (as for the absolute direct methods) are used to monitor absolute sea-level at permanent altimeter calibration facilities that are located ***away*** from the sea surface. Measurements are then transferred to sea level by accurate levelling and precise geoid models (e.g. Mertikas et al., 2015, Mertikas et al., 2010b, Mertikas et al., 2011, Bonnefond et al., 2011; 2018, Cancet et al., 2010, Watson et al., 2011). Dedicated microwave transponders are typically deployed as an independent technique for satellite altimeter's calibration. The principle of a transponder is to receive, amplify and retransmit, with minimal distortion, a satellite radar altimeter pulse. The transponder signal is recorded on-board the satellite. The measure of the pulse's two-way travel-time yields the range between satellite and transponder. This range is then adjusted for the propagation delays (i.e., dry and wet troposphere, ionosphere) and for the geophysical corrections (i.e., solid Earth, ocean and loading tides).

Transponders and corner reflectors are FRMs for altimetry as they allow verification of

s^0, range, datation, interferometry geometry among other parameters. These are mandatory for Cal/Val activities and cross-calibration of missions. Both transponders and corner reflectors need to be supported by accurate positioning (with FRM standard uncertainty) information, using GNSS and other positioning systems (e.g. DORIS beacon). Additionally, a collocated radiometer is also desired to derive the wet tropospheric delay during transponder calibrations in addition to the GNSS-derived delays.

As part of the Permanent Facility for Altimeter Calibration (PFAC) located in Crete, Greece (Mertikas et al., 2018, 2019), the a Ku-band transponder is supported by in-situ reference systems (GNSS reference points). A second transponder located on Gavdos Island, Western Crete, has been installed as part of the ESA Sentinel-6 calibration and validation activities. It is notable that a single Sentinel-3A and Sentinel-3B transponder pass over the PFAC during the Sentinel-3 tandem phase established a bias difference of just 1.5cm between the two altimeters. The PFAC is maintained operationally.

The global tide-gauge network provides a reliable means to determine the stability of altimeter sea-surface height measurement. A global network of tide gauges is available but are rarely found along a satellite ground track and not all are directly collocated with GNSS or DORIS systems that provide information on vertical land motion. Nevertheless, a comparison between satellite estimates of sea level and the tide gauge network (Valladeau et al., 2012) facilitates:

- detection of drifts or jumps in the altimeter mean sea level;
- estimation of improvement in altimeter SSH provided by new altimeter data processing and instruments;
- detection of anomalies within other in-situ datasets.

Dedicated tide gauge facilities are maintained to FRM standards at the Senetosa Cape, Corsica calibration/validation site (e.g. Bonnefond et al., 2018) which has monitored the performance of all altimeter missions occupying the reference orbit. This site has recently been extended to include a new location at Ajaccio.

The TOPEX/Poseidon-Jason time series provides 27 years of high quality altimetric data that have been used to monitor the global mean sea level (MSL) trend of 3.56 mm/year with an accuracy of about 0.5 mm/year. The challenge for S6-MF is to confidently connect Sentinel-6 with the time series by detecting, characterising and mitigating errors, end-to-end biases and drifts. A fundamental element is maintaining a complete uncertainty budget for each product produced from the mission and using independent FRM-quality ground measurements to validate both the problems and the mitigating solutions implemented. During the satellite commissioning phase, intensive activities will begin this process that continues for the duration of the mission and for many years afterwards – as evident from the activities of T/P and the Jason series. This is a multi-national scientific activity that is necessary to maintain and evolve the performance of the operational system.

S3NG-T opens new strategies of validating the geophysical parameters, Swath ‘2D’ data (e.g. absolute geostrophic currents derived from the absolute dynamic topography) might be compared with ground-truth total currents derived from high frequency radars.

This would allow the validation of both zonal and meridional components of the currents. Close to the coast the ageostrophic component (basically due to the wind drag and the bottom friction) must be accounted for and must be added to the altimeter derived currents. Once this is included the accuracy of altimeter data improves (especially close to the coast) as shown by Mulero et al. (2021).

Calibration and validation of altimetry measurements for inland open waters is performed with similar objectives to that for ocean. Estimating instrument noise and is an important calibration activity (Crétaux et al., 2018). Validation is performed to estimate overall uncertainty of altimetry data at a specific location, but also to compare the impact of different re-trackers and/or corrections used. The following methodology are currently used to validate radar altimetry data for WSE:

- Absolute WSE validation with dedicated temporary field campaigns or permanent in situ stations at location of virtual stations and/or along the satellite ground tracks (e.g. Crétaux et al., 2018; Pitcher et al., 2020; Quartly et al., 2020). It is typically done with GNSS measurements (on the lake/river shore or on a boat) to get absolute elevation, and potentially associated with limnigraph (or water loggers) to get long time series of WSE. Some additional measurements could also be done using weather stations, and/or ADCP instrument. This type of measurement allows to compute absolute WSE to estimate altimetry-derive absolute WSE uncertainty and estimate measurement bias for the observed lake or river reach.
- Relative WSE validation could be done using existing in situ stage gage network, installed not specifically to validate altimetry data (Biancamaria et al., 2018; Quarly et al., 2020; Nielsen et al., 2020; Kittel et al., 2021). These in situ gages are generally not below the satellite ground tracks and therefore absolute WSE validation cannot be done, at least for rivers. The river slope induces a bias and gage level are not necessarily levelled. Besides, because of potential change in river bathymetry, WSE dynamic could be naturally different between the virtual station and in situ gage locations, which could be wrongly interpreted as altimetry uncertainty.
- Indirect validation can also be done, especially over big lakes, at cross-over locations, like for the ocean.

For phenology and signal characteristics assessment, some potential airborne campaign might be needed (e.g. Pitcher et al., 2020). Finally, it should be noted that in case of new measurements (river slope for example) additional validation instruments will be needed (JPL Internal Document, 2018).

X.2 The Importance of Uncertainty Budgets

Climate data records are required to have a comprehensive uncertainty budget. An uncertainty estimate allows a data set to be used with confidence: without such an estimate of uncertainty, measurements cannot be compared, either among themselves or with standards reference values. All measurements are imperfect and have errors that can be of a random nature (i.e. “popcorn” noise on microwave radiometer channels) or of a systematic nature (e.g. incorrect characterization of an altimeter point

target response). Increasing the number of measurements can reduce random errors through computation of statistical averages that reduce the random uncertainty component. Systematic errors can only be corrected using an appropriate correction factor. Clearly all recognised systematic errors must be corrected and random errors reduced if a reliable and accurate measurement is to be obtained from any instrument - either on the ground or in space.

Uncertainties arise due to many aspects that can be generally grouped into the following primary categories:

- **Instrument measurement uncertainty**: those relating to instrument hardware,
- **Retrieval/algorithm uncertainty:** those relating to derived quantities,
- **Application uncertainty:** those relating to a specific application.
- **Unknown:** those uncertainties that are “unknown”.

For each category standard practice requires an uncertainty budget to be derived including all aspects leading to a quantification of a root-sum-square (RSS) estimate of uncertainty. This is a challenging exercise but nevertheless, for climate and satellite validation activities, it is a requirement.

Establishing an uncertainty budget for FRM is a fundamental step that drives a better understanding of the various components of FRM uncertainty: quite often an instrument engineer will learn much about an instrument and its fitness for purpose by attempting the derivation of a full instrument uncertainty budget – potentially leading to innovation and improvement in design. But the real driver is to remember that, if reliable and well-defined uncertainties can be provided with each FRM field radiometer, then these measurements can uniquely provide an SI traceable measurement *on a per-measurement basis when matched to satellite measurements – without the need for many observations to reduce the random error* (as in the case of altimeter measurements referenced to a transponder, for example).

APPENDIX XI RAW DATA ACQUISITION MASK EXAMPLE

Title:	Detailed description and location of S3NG-T Raw_Data_Acquisition_Mask (TBC).	
Version:	0.1 (stating point to be updated for Hydrology)	
Map of preliminary Raw_Data_Acquisition_Mask box locations (TBC)	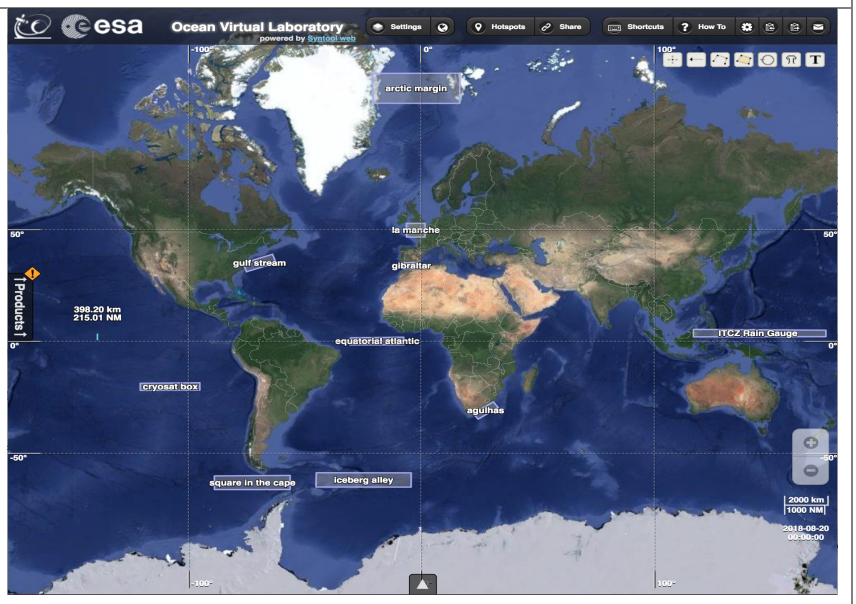	
Description	The S3NG-T raw acquisition mask definition specifies and justifies the location of specific areas where systematic RAW data acquisitions are requested to support the optimisation and understanding of OBP once S3NG-T is on orbit. A maximum of up to 1 minute (TBC) within any location of any orbit is assumed The order and timing of data takes within the cycle is left open for trade-off analysis by industry where the constraints of specific hardware solutions and data downlink can be optimised. The order and timing of specific data takes over each raw acquisition mask area must be optimised over the orbit cycle to ensure, as much as possible, that an equal number of data takes are available over each box.	
Region Identifier	**Coordinates**	**Selection rationale**
1_Agulhas	POLYGON((22.44 -34.961, 31.13 -29.940, 33.21 -32.439, 24.60 -37.356, 22.45 -34.961))	**Strong persistent currents** Optimisation of OBP close to coast An ocean Virtual Laboratory that is well studied and well characterised
2_ Arctic_Margins (Fram Strait)	POLYGON((-20.96 79.828, 16.70 79.835, 16.670 76.68, -20.96 76.70, -20.96 79.828))	**Marginal Ice Zone** Optimisation of OBP in the Marginal Ice Zone
3_CryoSat-2 Box	POLYGON(	**Quiet ocean region**

	(-120.50 -21.293, -94.909 -21.023, -94.909 -24.55, -120.50 -24.55, -120.50 -21.023))	Studied by CryoSat-2, Sentinel-3 Jason altimeters for intercomparisons Optimisation of OBP in weak ocean current region
4_Equatorial_Atlantic	POLYGON((-7.27 -1.880, -7.27 2.066, -30.212 1.880, -30.212 -1.924, -7.27 -1.880))	**Strong vertical shear in the upper 10-20m of the ocean** Optimisation of OBP for Delta-K in vertical shear region
5_ Strait of Gibraltar	POLYGON((-7.35 37.600, -0.76 37.648, -0.76 35.047, -7.35 34.966, -7.35 37.648))	**Region of large persistent internal waves and heavy ship traffic.** Optimisation of OBP with internal waves present Optimisation of OBP with ships present
6_ Gulf_Stream	POLYGON((-74.87 33.781, -76.39 37.390, -63.69 40.974, -62.18 37.5119, -74.87 33.781))	**Strong and extensive western boundary current influencing European Region.** Optimisation of OBP in strong mesoscale flows
7_SKIM_Square_the_Cape	POLYGON((-88.68 -57.017, -56.16 -56.897, -56.16 -60.673, -88.68 -60.673, -88.68 -57.017))	**Region of very strong wind and large sea state conditions.** Optimisation of OBP in very strong winds and large sea state conditions
8_ Iceberg_Alley	POLYGON((-45.00 -56.121, - 45.00 -60.021, -4.175 -60.042, -4.175 -56.121 -45.00 -56.121))	**Region of persistent icebergs** Optimisation of OBP in the presence of icebergs
9_ICTZ_Rain_Gauge	POLYGON((173.93 2.328, 173.93 5.669, 117.078 6.1141, 117.078 2.195, 173.93 2.328))	**Region of very strong and persistent precipitation** Optimisation of OBP in very strong precipitation conditions.
10_ La_Manche	POLYGON((1.83 51.956, -6.20 51.949, -6.20 47.344, 1.83 47.344, 1.83 51.956))	**Region of strong tidal conditions** Optimisation of OBP in strong tidal currents
11_ AmazonRiver;	POLYGON ((-62.4700136429303 -1.77328651204468,-61.1949695749018 -2.90573530014703,-61.5312007191258 -3.28235763925355,-63.1352940295273 -3.52950197450324,-63.1810353276959 -4.17914869000069,-61.92426223444 -4.31604815771176,-61.8930808299278 -4.33835534648083,-61.8608185646241 -4.33943636824589,-60.8697169630956 -	**Wide river re**ach with tributaries, impacted by vegetation

	3.72925166844123,-59.956516044413 - 3.63767052770653,-59.9354758960655 - 3.63848126811071,-58.6354363974876 - 3.74171563978357,-58.6144389501604 - 3.74254482511862,-57.759522327391 - 3.11470264417791,-57.7486078675777 - 3.10463061210122,-58.0240147270841 - 2.60096403786131,-58.4473739665081 - 2.95160569472506,-59.3151927770408 - 2.86518333761441,-60.6348892789196 - 2.43432359183891,-61.6353232184463 - 0.302876910236014,-61.8999448581998 - 0.138625407233868,-62.215798829958 - 0.977656749852458,-63.3445720524029 - 0.195749500160337,-63.6569945913718 - 0.706610266021788,-62.4700136429303 - 1.77328651204468));	
12_ Garonne	POLYGON ((0.275903929245398 44.1742802498682,0.292469124360273 44.1727689102618,0.706448498629964 44.0762201724722,1.21518056052166 43.7564385485005,1.28097258247667 43.5259193507827,1.28264361278383 43.5143991302432,1.27993475687705 43.5054505293051,0.585262863969427 43.0861180604776,1.0668264605525 42.9483206361533,1.24896599067907 42.9699949995757,1.33798115657269 43.2970174396992,1.57465437215364 43.5453100395654,1.25198526022827 44.1076674964334,0.062084845168557 44.6110795970126,-0.052756804604855 44.4903736322351,0.275903929245398 44.1742802498682))	**Medium to narrow river reach**
13_ Issykkul	POLYGON ((76.1043262153571 42.2298771232124 0,77.1189366738362 42.0635907000604 0,78.4495180366021 42.4256266978697 0,78.472698850665 42.4260493134674 0,78.3727605937795 42.8474078459191 0,76.0542977393522 42.5126348155946 0,76.1043262153571 42.2298771232124 0))	**Large lake** (lake Issykkul with long tradition of altimetry cal/val)
14_ PAD	POLYGON ((-112.899475359232 58.1202622496296,-110.471201513055 58.2270906809678,-110.661702216472 59.1606102460582,-113.012990666839 59.0467614062538,-112.899475359232 58.1202622496296))	**Arctic lake** (Lake Claire, part of Athabasca lake and very small lakes) with artic rivers
15_Hydrology5	TBD	**River with complex surrounding terrain (mountains)**
16_Hydrology6	TBD	**River with complex surrounding terrain (vegetation)**
17_Hydrology7	TBD	**Lake with complex surrounding terrain (mountains)**

18_Hydrology8	TBD	**Lake with complex surrounding terrain (vegetation)**

APPENDIX XII LIST OF ACRONYMS

(A)ATSR	Advanced Along Track Scanning Radiometer [of ESA]
3CS	Copernicus Climate Change Service
AHEG	Ad Hoc Expert Group
AIV	Assembly, Integration and Verification
ALT	Altimeter
AMOC	Atlantic Meridional Overturning Circulation
AMSR	Advanced Microwave Scanning Radiometer [of JAXA]
AOCS	Attitude and Orbit Control Subsystem
APC	Antenna Pattern correction
APKE	Absolute Pointing Knowledge Error
ARA	Absolute Radiometric Accuracy
ASCAT	Advanced Scatterometer [of MetOp]
AVHRR	Advanced Very High Resolution Radiometer [of NOAA]
BEC	Barcelona Expert Center
BOL	Beginning Of Life
BUFR	Binary Universal Form for the Representation of meteorological data
CAMS	Copernicus Atmospheric Monitoring Service
CCDB	Characterisation and Calibration Database
CCI	Climate Change Initiative [of ESA]
CCSDS	Consultative Committee for Space Data Systems
CDR	Climate Data Record
CEMS	Copernicus Emergency Management Service
CEOS	Committee on Earth Observation Satellites
CFOV	Composite Field Of View [gridding scheme]
CGMS	Coordination Group for Meteorological Satellites
CIMR	Copernicus Imaging Microwave Radiometer
CMEMS	Copernicus Marine Environment Monitoring Service
CNES	Centre National d'Etudes Spatiales
COP	Conference of the Parties [of IPCC]
CPOD	Copernicus POD Service
CSC	Copernicus Space Component
dB	deciBel [unit]
DIB	Drop In Bucket [processing scheme]
DMI	Danish Meteorological Institute
DMSP	Defense Meteorological Satellite Program

EC	European Commission
ECMWF	European Centre for Medium Range Weather Forecasting
ECSS	European Cooperation for Space Standardization
EEA	European Environment Agency
ENSO	El Nino Southern Oscillation
EOL	End Of Life
EPS-SG	EUMETSAT Polar System Second Generation
ESA	European Space Agency
EU	European Union
EUMETSAT	European Organisation for the Exploitation of Meteorological Satellites
FOS	Flight Operations Segment
FOV	Field Of View
FWHM	Full Width at Half Maximum
FYI	First Year Ice
G	Goal
GCOM	Global Climate Observation Mission [of JAXA]
GCOS	Global Climate Observing System
GMI	Global Monitoring Imager [of JAXA]
GNSS	Global Navigation Satellite System
GPP	Ground Processor Prototype
GS	Ground Segment
GTS	Global Telecommunications System
HEO	Highly elliptic Orbit
HF	High Frequency
HKTM	House Keeping Telemetry
HPCM	High Priority Copernicus Mission
HR	High Resolution
Hs	Significant Wave Height
IFOV	Instantaneous Field Of View
IOD	Indian Ocean Dipole
IPCC	International Panel for Climate Change
IR	Infrared
IST	Ice Surface Temperature (also Sea Ice Surface Temperature SIST)
ITU	International Telecommunications Union
IWS	Interferometric Wide Swath [radar mode of Sentinel;-1]
JAXA	Japan Aerospace Exploration Agency

LEO	Low Earth Orbit
LEOP	Launch and Early Orbit Phase
LF	Low Frequency
LR	Low Resolution
LRM	Low Resolution Mode
LST	Land Surface Temperature
LTS	Long Term Scenario
LWP	Liquid Water Path
MAG	Mission Advisory Group
MERIS	MEedium-spectral Resolution Imaging Spectrometer [of ESA]
MFC	Modelling and Forecast Centre [of CMEMS]
MIZ	Marginal Ice Zone
MLST	Mean Local Solar Time
MODIS	MODerate resolution Imaging Spectrometer [of NASA]
MOE	Medium Orbit Ephemeris
MRD	Mission Requirement Document
MWI	Microwave Imager [of MetOp-SG(B)]
MWR	Microwave Radiometer
MYI	Multi Year Ice
NASA	National Aeronautics and Space Administration [of the USA]
NCEP	National Centers for Environmental Prediction
NEMO	Nucleus for European Modelling of the Ocean
NEΔT	Noise Equivalent difference Temperature
NIR	Near Infrared
NOAA	National Oceanic and Atmospheric Administration
NRT	Near Real Time, see more specific definitions of NRT1H and NRT3H
NRT3H	Near Real time 3 hour
NSIDC	National Snow and Ice Data Center [of the USA]
NTC	Non Time Critical
NWP	Numerical Weather Prediction
OI	Optimal Interpolation
OPSI	Observation Performance Simulator
OSCAR	Observing Systems Capability analysis and Review Tool [of WMO]
OSISAF	Ocean and Sea Ice Satellite Applications Facility [of EUMETSAT]
OSTST	Ocean Surface Topography Science Team
OTS	Off-The-Shelf

OW	Open Water
OZA	Observation Zenith Angle
PBEO	Program Board for Earth Observations [of ESA]
PCP	Precipitation
PDGS	Payload Data Ground Segment
PEG	Polar Expert Group [of the EC]
PL	Polar Low
POD	Precise Orbit Determination
POE	Precise Orbit Ephemeris
PSF	Point Spread Function
QMS	Quality Management system
RF	Radio Frequency
RFC	Radio Frequency Compatibility
RFI	Radio Frequency Interference
RPKE	Relative Pointing Knowledge Error
S3NG-T	Sentinel-3 Next Generation topography [Mission of Copernicus]
SAR	Synthetic Aperture Radar
SD	1. Standard Deviation 2. Snow Depth
SI	1. Sea Ice. 2. Systeme Internationale [of meterology units]
SIC	Sea Ice Concentration
SID	Sea Ice Drift
SIE	Sea Ice Extent
SIR	Scatterometer Image Reconstruction [algorithm]
SIST	Sea Ice Surface Temperature SIST
SIT	Sea Ice Thickness
SM	Soil Moisture
SMAP	Soil Moisture Active Passive [mission of NASA]
SMOS	Soil Moisture and Ocean Salinity [mission of ESA]
SNR	Signal to Noise Ratio
SPF	Single Point Failure
SRD	System Requirements Document
SSD	1. Spatial Sampling Distance 2. Sea Surface Density
SSH	Sea Surface Height
SSHA	Sea Surface Height Anomaly
SSM/I	Special Sensor Microwave Imager [of DMSP]
SSP	Sub Satellite Point

SSS	Sea Surface Salinity
SST	Sea Surface Temperature
STC	Short Time Critical
SWE	Snow Water Equivalent
TBC	To Be Confirmed
TBD	To Be Defined (by ESA)
TBS	To Be Specified
TC	TeleCommand
TCWV	Total Column Water Vapour
TEC	Total Electron Content
TIR	Thermal Infrared
TM	TeleMetry
TMI	TRIMM Microwave Imager
TOA	Top Of Atmosphere
TRIMM	Tropical Rainfall Imaging Microwave Radiometer [of JAXA]
TRP	Temperature Reference Point
URD	User Requirements Document
VEGA	Vettore Europeo di Generazione Avanzata
VIS	Visible wavelength
WIGOS	WMO Integrated Global Observing System
WMO	World Meteorological Organisation
WS	Wind Speed
WSE	Water Surface Elevation
WVC	Water Vapour Content

[End of Document]